Stratigraphy and Structure in the Neoarchaean of the Kalgoorlie district, Australia: Critical Controls on Greenstone-hosted Gold Deposits

Thesis submitted by

Gerard Ignatius TRIPP B.Sc. (UTS), M.Sc. (Curtin)

in January 2013

for the degree of Doctor of Philosophy
in the School of Earth and Environmental Sciences
James Cook University

STATEMENT OF ACCESS

I, the undersigned, author of this work, understand that James Cook University will make this thesis available for use within the University Library and, via the Australian Digital Theses network, for use elsewhere.

I understand that, as an unpublished work, a thesis has significant protection under the Copyright Act and; I do not wish to place any further restriction on access to this work.

Signature

26/10/2013
Date

STATEMENT OF SOURCES

DECLARATION

I declare that this thesis is my own work and has not been submitted in any form for another degree or diploma at any university or other institution of tertiary education. Information derived from the published or unpublished work of others has been acknowledged in the text and a list of references is given.

Signature

26/10/2015
Date

STATEMENT ON THE CONTRIBUTION OF OTHERS INCLUDING FINANCIAL AND EDITORIAL HELP

Funding for this project was provided by Barrick Gold of Australia Limited including analytical costs for petrography, geochronology, geochemical analyses, and all other associated logistical costs including travel and paid study leave. Additional funding for selected geochronology was provided by the Australian Government funded Predictive Mineral Discovery Co-operative Research Centre (as noted in the text).

The project was primarily supervised by Prof. T. Blenkinsop of James Cook University and Prof. H. Poulsen ex. Queens University, Ontario, who provided all editorial assistance and provided guidance on the project direction and coaching in the field. Additional guidance and support was provided by Dr. T. Kemp of James Cook University; Dr. R Tosdal of UBC; Dr. J. Wooden of Stanford University; Dr. K Sircombe of Geoscience Australia; and Dr. R. Weinberg of Monash University.

Assistance was provided by Dr. R. Tosdal and Dr. J. Wooden for geochronological analysis on the SHRIMP-RG at Stanford University, San Francisco for analytical work under a commercial arrangement with Barrick.

Collaborations with numerous Placer Dome / Barrick colleagues involved over the period of the research are presented in detail in Section 1.4 - 'Author contributions to the work presented'. The project was variably associated with research groups in the Australian Government funded pmdCRC, AMIRA funded P718; P680; P763; and MERIWA project M376.

Acknowledgements

To Jodene, Madison and Claudia thank you for tolerating an absent husband and father, and sincere gratitude for putting up with me being ‘absent’ even when I was there.

Thanks to Barrick for supporting and funding this work, in particular Barrick AusPac Vice President of Exploration Robbie Rowe for approving a generous study assistance package and encouragement to complete the project. Chief Geologists Dr. Francois Robert, Dr. Craig McEwan and Rex Brommecker approved, supported and encouraged the completion of this work.

Sincere thanks to Professor Tom Blenkinsop for helping me to get through the truly testing experience of a part-time PhD. It was a privilege to be supervised by a world leader in structural geology. My thanks for being a mentor, an able task master and a friend. Our fruitful discussions on Archaean geology, tectonics and deformation, and African geology taught me many valuable lessons and provided a clear direction for the project.

Thanks to Professor Howard Poulsen, who provided the best field training a geologist working in the Archaean could hope to get from one of the world's most knowledgeable and experienced geologists on Neoarchaean rocks and mineral deposits. Thanks for teaching the value of getting basic observations right and making them count, and for demonstrating the intrinsic value of the work of the pioneering geologists who got out on the ground, made observations, and wrote reports that (remarkably) we must still refer to for the key geological relationships.

Professor Richard Tosdal was a force in pushing this thesis to completion by taking a personal interest in getting the zircon geochronology on track, which included collecting my zircons from UBC in Vancouver on his own time, meeting me in San Francisco at his family’s house, and giving me a week of his allocated time on the Stanford University SHRIMP-RG with Dr. Joe Wooden. Significant parts of this work would not have been done without that kindness and support and he has my sincerest thanks.

Thanks to John Dobe for friendship, encouragement, and countless conversations; his unique ability to show one how to find ‘the relevant’ for mineral discovery, and filter out ‘the irrelevant’; and for using his software to deform my sketches to show just how complex the rocks are after a couple of unconformities and deformations.

Mike Christie (Placer Dome) approved, supported and encouraged this project, and provided enthusiasm and guidance to get the job done. Chief Geologist Greg Hall (Placer Dome) ultimately approved this project with a prescient warning: “be careful what you wish for Gerard, you just might get it”. My thanks for being one of the more insightful, kind and friendly people I have met.

Dr. Doug Mason provided support via contracted petrography of rocks in the general area, but mostly from his friendship, enthusiasm and unfailingly professional responses to many queries particularly related to Neoarchaean rocks in North Mara, Tanzania.

My thanks go to Dr. Martin Van Kranendonk and Dr. Warren Hamilton for lengthy email discussions on several topics, principal of which was the application of arc-accretion and subduction to the Archaean. Dr. Hamilton provided a wealth of information from his personal field experiences and voluminous research over a long and illustrious career.

Colleagues from the erstwhile Placer Dome and Barrick were integral to the work presented here, particularly Dr Jamie Rogers with whom I spent over two years in a Toyota Landcruiser driving hundreds of kilometres in the Eastern Goldfields of WA and working out how to do Archaean geology. Field work, mapping, core-logging, discussions, and technical / analytical work were done (in no particular order) with David Boyd, Kevin Joyce, Carl Young, Marcus Willson, Rob Henderson, Michael Outhwaite, Sarah Millin, Craig Peuschel, Heath Dalla-Costa, Claire Hillyard, Darren Allingham, Gary Snow, Dr. Brett Davis, Dr. John Beeson, Jon Standing, John Crossing, Dave Archer, Wade Evans, Dr. Trevor Beardsmore, Louis Gauthier, Dr Kevin Cassidy, Ned Howard, David Nixon, Rohan Hine, Yuri Dobrotin, Andrew Barker, and Dr. Rick Squire.

Abstract

The remarkably prodigious gold endowment of the Neoarchaean was controlled by specific characters of the stratigraphy, structural geology, and geochemistry of greenstone belts. This study attempts to synthesise stratigraphic, structural and geochronological data to understand the geology of the Kalgoorlie greenstones, and by representing those data on maps to assess the controls on major gold deposits. Voluminous, previously unavailable regional - scale data sets from exploration and mining provide new insights into the controls on gold deposits in the north Kalgoorlie district of the Eastern Goldfields Province (EGP) in Western Australia.

The end of mafic volcanism is constrained by a new U-Pb SHRIMP age determination for the Golden Mile Dolerite at 2685±4 Ma (host to the largest Archaean greenstone gold deposit). This new age determination indicates a possible three million year time gap between the intrusion of the Golden Mile Dolerite (>2681 Ma) and overlying Lakewood dacite volcanics (<2678 Ma), allowing for the possibility that the Golden Mile dolerite was a high-level intrusion at the Upper Basalt / Black Flag Group interface.

The stratigraphy of post Upper Basalt rocks, including three newly defined formations, is separated on the basis of this work into four units from oldest to youngest: 'Talbot formation'; White Flag Formation; 'Gibson-Honman formation' (~2675 Ma); and 'Gidji Lake formation' (~2660 Ma). Gibson-Honman formation includes felsic volcanic rocks at Gibson-Honman Rock, Lakewood dacitic volcanics, and Perkolilli rhyolitic volcanics. Gidji Lake formation includes felsic volcaniclastic rocks at Gidji, Binduli Porphyry Conglomerate and Grave Dam Grit at Kanowna. The stratigraphy includes unconformities between White Flag Formation and Talbot formation (locally), and between Gibson-Honman and Gidji Lake formations. The Panglo member in the Kanowna district is interpreted as a correlative of the Kurrawang Formation, and represents a major change to the district stratigraphy that identifies late, unconformable clastic sequences in the vicinity of the Kanowna Belle gold deposit.

Five major deformation events are separated into pre-Kurrawang and post-Kurrawang deformation episodes, which record a change from early extension to bulk contraction, with the latter including syn-orogenic clastic sedimentation. Major map scale F1 folds are located at Kanowna and the Golden Mile in a restricted distribution that may reflect typically poor preservation of D1 fabrics. Localised syn-orogenic extension resulted in the deposition of linear fault-controlled, late clastic sedimentary sequences at <2650 Ma (Kurrawang, Panglo), unconformably overlying F2 folded rocks. The deposition of those sequences marks the onset of penetrative deformation over a relatively short time interval (~2650 – 2639 Ma). A regionally pervasive S3 foliation transects F1 and F2 fold axial planes. The S3 foliation trends uniformly over the district, and is axial planar to F3 folds with inclined axial planes in the late clastic sequences. The maximum age of the regional S3 foliation is constrained by the <2650 Ma rocks that are folded

and foliated by it, and a minimum age at 2639±3 Ma from Lode-Au veins that were synchronous with and overprinting the regional foliation.

The Zuleika Shear Zone marks a domain boundary that juxtaposes crustal blocks with minor stratigraphic differences and thickness of sequences, yet the blocks do not have significantly different deformation intensity or metamorphic grade. Fault bounded domains in the Kalgoorlie Terrane were therefore not diverse crustal blocks amalgamated by strike slip or accretion, but were more likely subjacent depocentres, possibly half-grabens, bounded by early extensional faults such as the Zuleika Shear Zone and Bardoc Tectonic Zone.

Geological sequences of the Yindarlgooda Dome show no major differences in lithotectonic assemblages, stratigraphic sequence, or age, from sequences in the adjacent Boorara Domain. On this basis, the allocation of 'terrane boundary' status to the Mount Monger Fault as separating a western back-arc (Kalgoorlie Terrane) from an eastern accreted volcanic arc (Gindalbie Terrane) is suspect, and casts doubt on the application of subduction / arc-accretion models to greenstones of the southern EGP. Models that propose rifting of a pre- ~2700 Ma greenstone basement may be better analogues for the tectonic setting of the Kalgoorlie greenstones.

At a regional scale, major gold districts in the EGP have spatial and temporal relationships with unconformable, late clastic sedimentary sequences that mark areas of thick greenstone preservation. There is diversity of mineralisation styles and settings in the largest gold deposits, including early syn-volcanic hydrothermal alteration and mineralisation systems, and late-tectonic, vein hosted lode-Au deposits. High-level mineralisation styles were developed early in the formation of the greenstone belts with spatially coincident, late-tectonic mineralisation, indicating persistent mineral systems at fixed locations throughout several uplift and deformation cycles. That persistence suggests fundamental structural controls.

Structural controls on the different mineralisation styles include early-formed disseminated sulphide replacement mineralisation (e.g. Binduli) deformed and cut by late, syn-tectonic lode-Au vein style mineralisation (e.g. Binduli; Kundana). The Binduli district is spatially associated with the ~2664 Ma Binduli Porphyry Conglomerate unconformity that is interpreted to separate the Gibson-Honman and Gidji Lake formations. Kanowna Belle gold deposit is hosted in hypabyssal porphyritic rocks that have a spatial association with a ~2660 Ma unconformity at the base of the Grave Dam sequence (Gidji Lake formation). Unconformable sedimentary and volcaniclastic rocks of the Gidji Lake formation (~2660 Ma) are present in the vicinity of the eastern margin of the world class Mount Charlotte / Fimiston gold camp. This spatial association of major gold deposits with rocks located above an unconformity internal to the Black Flag Formation is a new understanding of the critical controls on Neoarchaean gold deposits and is a key criterion for area selection in exploration.

Contents

List of Figures

List of Tables

1 Introduction

1.1 Background

Archaean cratons are distributed on all major continents as disconnected segments of the earliest crust. They range in age from Hadean (>4.0 Ga) to Neoarchaean (2.8 - 2.5 Ga), and collectively account for nearly one third of Earth history (Fig 1.1). The Neoarchaean is recognised as a period of major crustal growth and is marked by voluminous Neoarchaean (~2700 - 2500 Ma) granite-greenstone terranes contained within larger Archaean cratons (Condie 2000; Rino et al. 2004; Shirey et al. 2008). Several major greenstone gold provinces are distinguished by abundant world-class gold deposits (Fig. 1.1) including the Eastern Goldfields Province (EGP) of Western Australia (Fig. 1.2), which contains 10 world class gold deposits and many hundreds of smaller deposits and gold occurrences (>126 million ounces endowment; Groves et al. 2003; Robert et al. 2005).

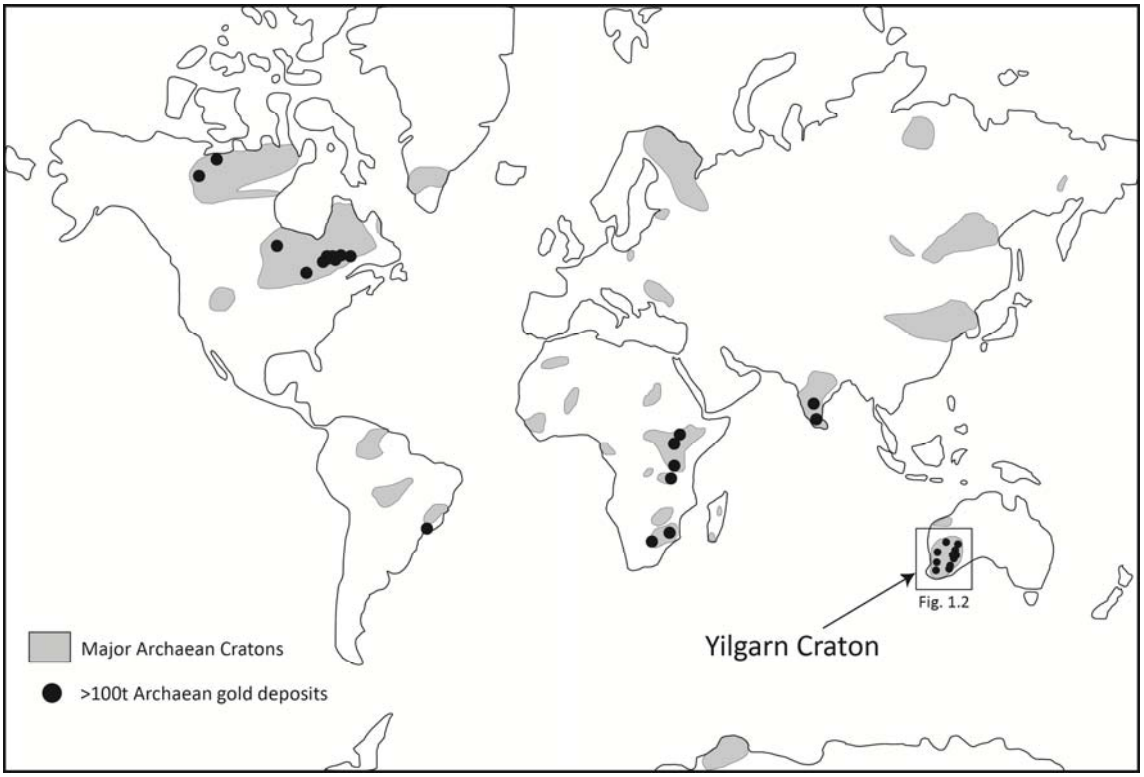

Figure 1.1 — Global distribution of Archaean cratons (from Condie, 1997), with location of major gold provinces indicated by >100t Au world-class gold deposits.

Greenstone gold terranes in the EGP of Western Australia, the Abitibi Belt of Canada, the Lake Victoria Goldfields of Tanzania (LVGF) and the Eastern Dharwar Craton of India share similarities in terms of rock assemblages, geological history and (broadly) the timing of gold mineralisation (Robert et al. 2005; Robert et al. 2007; Poulsen 2010); hence, understanding geological and structural controls of gold mineralisation in the Eastern Goldfields Province of Western Australia has wide application. Similar geological histories between Neoarchaean

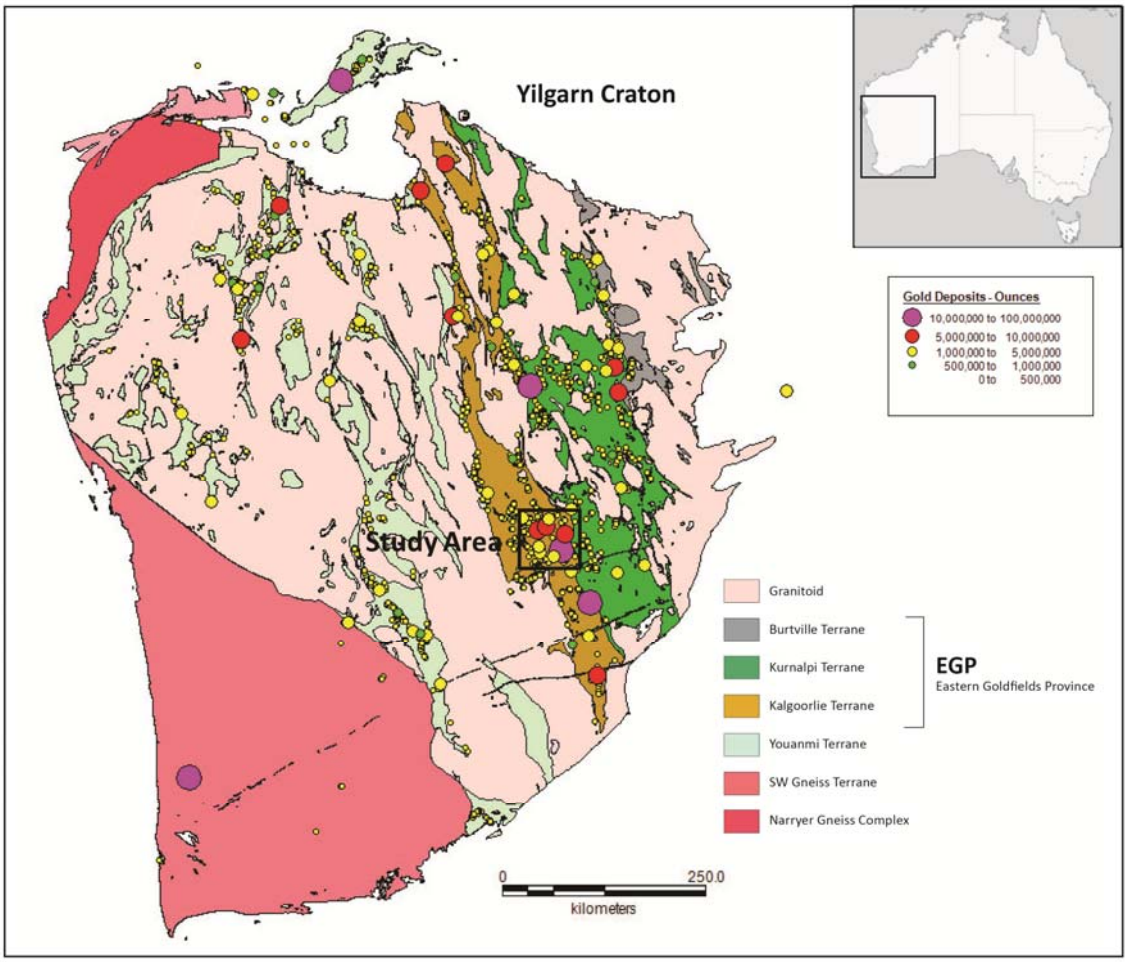

Figure 1.2 — Geological Survey of Western Australia (GSWA) terrane map of the Yilgarn Craton and granite-greenstone terranes of the Eastern Goldfields Province, with major gold deposits and location of the study area.

granite-greenstone terranes include the onset of orogeny marked by a change from early volcanism to clastic sedimentation above unconformities, followed closely by granitic intrusion, deformation, and metamorphism (Robert et al. 2005). A late penetrative deformation and metamorphism overprinted the greenstone segments, and obscured the relations between previously contiguous blocks and/or juxtaposed sections of the stratigraphy.

Some aspects of Neoarchaean geology (2700 - 2500 Ma) in the EGP remain unresolved including: the correlation of fault bounded lithostratigraphic packages in deeply weathered regions, the timing and genesis of gold deposits with respect to volcanism and deformation, and the relative roles of crustal shortening and/or density-driven processes in deformation. These three aspects are closely linked given that (1) large, Neoarchaean gold deposits have a demonstrated spatial association with rocks that mark a change from volcanism to clastic sedimentation at the onset of orogenesis (Robert et al. 2005), (2) mineralisation styles vary with geotectonic setting generally (Groves and Bierlein 2007), and (3) in nearly all cases gold deposits are closely associated with deformational structures (e.g. ‘lode - gold deposits’; Groves et al. 2003).

This spatial association of large gold deposits with rocks that mark a change from volcanism to clastic sedimentation, necessitates a clear understanding of the stratigraphy and deformation history of Neoarchaean greenstone belts to assist mineral exploration. For practical exploration, maps showing the distribution of formations with structural geometry and accurate stratigraphic columns are key inputs.

Over the period 2002 - 2010, multi-disciplinary research projects including AMIRA (Australian Mineral Industry Research Association), pmdCRC (Predictive Mineral Discovery Co-operative Research Centre), and MERIWA (Minerals and Energy Research Institute of Western Australia) greatly advanced knowledge of the stratigraphy and deformation history in the EGP of Western Australia. These studies included detailed lithostratigraphic mapping, provenance studies of detrital zircons, and direct age analysis of mineralisation – refining a framework of state-wide geological mapping by the Geological Survey of Western Australia (GSWA). The work here builds upon those studies, and in some parts was undertaken in conjunction with AMIRA, and pmdCRC research projects.

Gold mineralisation controls

Gold deposits in the north Kalgoorlie district include the world's largest Archaean greenstone gold deposit (Golden Mile - including Fimiston, Mount Percy and Mount Charlotte). Gold endowment for the district exceeds 100 million ounces Au (production + resources + reserves) with about 75 million ounces Au endowment contained within the Golden Mile series of deposits, ~5 million ounces Au in the Kanowna Belle gold deposit, with the remainder in several 1-2 million ounce lode gold deposits and many hundreds of small deposits and occurrences (Weinberg et al. 2005; Vielreicher et al. 2010). Gold deposits are hosted by a range of rock types in the greenstone sequences including iron-rich mafic igneous rocks (dolerite / basalt), iron-rich sedimentary rocks (including banded iron formation - BIF), and felsic to intermediate porphyry stocks and dikes (Robert et al. 2005).

A generalised classification of 'orogenic lode-gold deposits' has been applied to the major occurrences of mineralisation in the north Kalgoorlie district (Groves et al. 2003, and references therein). The orogenic classification implies the gold deposits are located proximal to crustal scale faults, which controlled igneous intrusions and late clastic sedimentary rocks; and that the deposits contain dominantly Au-only quartz-carbonate vein mineralisation within faults and shear zones related to late-tectonic deformation of the greenstones. Two key factors required for an 'orogenic' classification of gold deposits are that they are (1) epigenetic (i.e. post-dating formation of the host rock sequences), and (2) formed in a continuum of crustal environments: epizonal (<6 km depth), mesozonal (6-12 km depth) and hypozonal (>12 km) (Gebre-Mariam et al. 1993; 1995). For vein-hosted and vein stockwork deposits, textural relationships and structural timing of gold mineralisation are primarily used to determine an 'epigenetic'

categorisation of the lode-gold deposits, whereas crustal depth of formation is determined from a combination of vein textures and fluid inclusion studies. Textures of mineralised veins, their internal deformation and cross-cutting relations with wallrock foliations and fabrics provide critical tests of timing with respect to greenstone formation and later greenstone deformation (e.g. Robert and Poulsen 2001). Other mineralisation styles common in greenstone settings (Au - base metal veins, disseminated sulphide replacement, and intrusion hosted stockwork-disseminated styles) are more ambiguous in their timing.

A clear link exists between the locations of some Archaean greenstone-hosted gold deposits and coarse clastic sedimentary rocks deposited above unconformities as demonstrated in the Abitibi of Canada (e.g. Colvine et al. 1984; Poulsen et al. 2000; Robert et al. 2005). The link has not been as widely emphasised in the EGP, but in several areas major gold deposits are proximal to, or within, unconformable late-clastic sedimentary rocks (Fig. 1.3; Wallaby gold deposit, Sunrise Dam, Lawlers; Fig. 1.4). Unconformity-bounded polymictic conglomerate sequences mark a major change in greenstone development from volcanism to clastic sedimentation at or after the onset of orogenesis (cf. Robert et al. 2005). They also form boundaries in the sedimentary record that identify episodes of tectonic uplift and provide constraints on the deformation and mineralisation history. Large gold deposits proximal to major unconformities as documented in the Abitibi and the EGP have also recently been observed in the Lake Victoria Gold Fields (LVGF) of Tanzania (Tripp et al. 2007c unpublished data) and in the Dharwar Craton of India (Poulsen 2010).

Stratigraphic relationships of the Kalgoorlie Neoarchaean

In the north Kalgoorlie district of the EGP, a series of fault-bounded, granite-greenstone domains were interpreted as part of a ‘Kalgoorlie Terrane’ (Swager et al. 1990; Cassidy et al 2006). The ‘greenstones’ in each domain comprise: ultramafic volcanic and intrusive rocks; tholeiitic and high-Mg volcanic and intrusive rocks; intermediate - felsic volcanic and volcaniclastic rocks; and volcanogenic clastic sedimentary rocks (Swager et al. 1990). Rare, disconnected segments of late, unconformable clastic sedimentary rocks are present as elongate synclinal remnants preserved in the footwalls of major faults. The fault-bounded domains contain differences in the detail of rock associations from one domain to the next, but the general pattern of early ultramafic-mafic volcanic rocks overlain by intermediate-felsic volcanic and sedimentary rocks is consistent (Swager et al. 1990).

Differences in the thickness of sequences, volume of co-magmatic intrusive rocks and particularly the provenance of felsic volcaniclastic rocks between domains may reflect changes in intra-basinal sources and/or hinterland provenance of fault-separated basins, or alternatively, the domains could be interpreted as disconnected segments amalgamated during transpressional

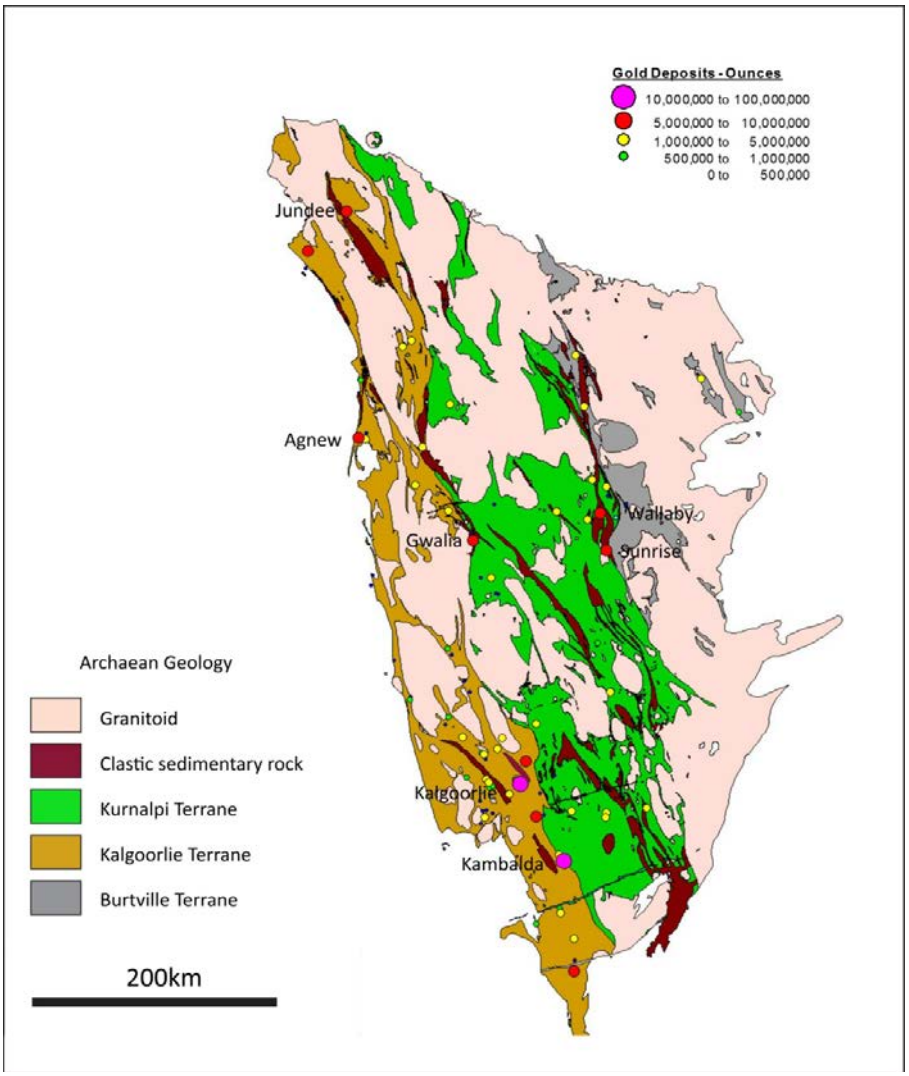

Figure 1.3 — Distribution of granite-greenstone terranes, clastic sedimentary rocks and major gold deposits in the Eastern Goldfields Province of Western Australia (GSWA).

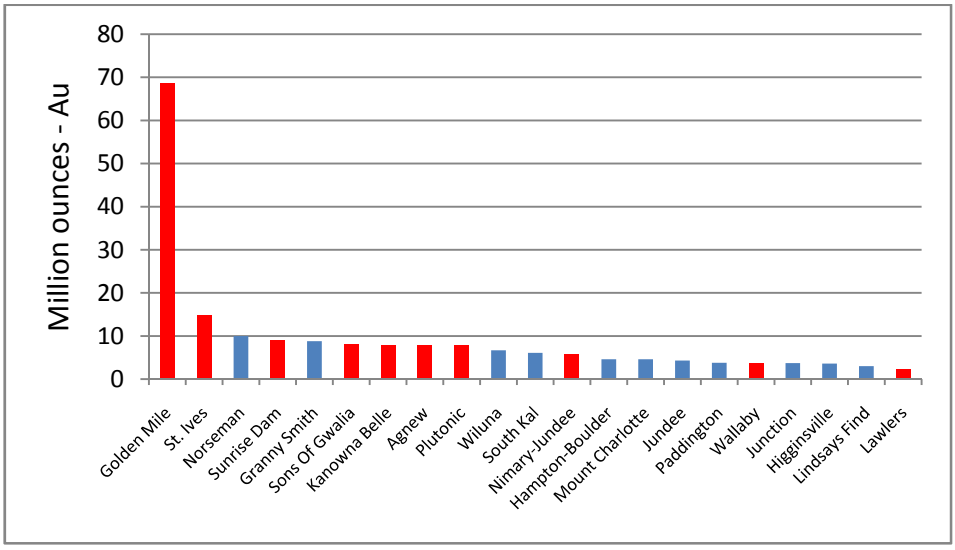

Figure 1.4 - Endowment graph of major gold deposits of the EGP. Deposits with spatially associated clastic sedimentary rocks coloured red (Barrick Gold unpublished data compilation 2010).

deformation. Lithostratigraphic and chronostratigraphic correlation of rock assemblages across the domain - bounding faults is therefore critical to assessing whether the greenstones represent autochthonous assemblages or diverse crustal blocks. This question is of interest to understanding Archaean geology generally, but is of primacy to mineral explorers given the close association of large gold deposits and Cu-Au deposits with major tectonic boundaries and magmatic belts in Phanerozoic terranes (Goldfarb et al. 2005; Groves and Bierlein 2007).

Localised intermediate and felsic volcanic packages are typical of the sequences that post-date ultramafic-mafic volcanism, but pre-date late clastic sedimentation; and spatial / genetic relationships of felsic volcanic rocks with high-level porphyritic intrusions and mineralisation are of particular interest to exploration (Robert 2001; Duuring et al. 2007). The tectonic style that led to uplift and deposition of the volcanic / volcaniclastic rocks, and late epiclastic sequences (i.e. strike-slip; extensional; contractional) is widely debated in the literature (e.g. Swager 1997; Barley et al. 2008; Krapez et al. 2000; Blewett et al. 2010; Czarnota et al. 2010).

Tectonic style in the Kalgoorlie district

Greenstone terranes in the EGP form narrow linear belts of volcano-sedimentary rocks interspersed with elongate granitoid batholiths and plutons, which are separated by major faults and shear zones. The linear trend of the greenstone belts with elongated granitoid intrusions is a regional-scale fabric, visible in regional geophysical images, that appears to reflect abundant widespread intrusion in the presence of horizontally directed stresses. In Western Australia the characteristic fabric of the Neoarchaean EGP contrasts with the Palaeo-Meso Archaean Pilbara Block where (in the latter) greenstones are separated by circular-shaped felsic intrusions with no preferred long axis or belt-wide flattening fabric (Van Kranendonk et al. 2002). These differences have been used to infer secular changes in the tectonic style of the Archaean from early vertical to later horizontal tectonic processes (see references in Van Kranendonk 2007; 2010).

The relative roles of crustal shortening and density driven processes in deformation are principal inputs to the debate about Archaean greenstone evolution and tectonics. A higher proportion of radiogenic isotopes (U, Th, K) in the crust and mantle before 2.5 Ga suggests that mantle heat production was up to three times greater than at present (e.g. Martin 1986; Pollack 1997); or 100º to 300º C hotter than present (Christensen 1985; Richter 1985) and may have influenced the thermal and rheological structure of the Archaean lithosphere. Two end-member deformation styles in the Archaean: (1) dome-and-keel, and (2) linear upright fold belts, provide evidence of variations in the strength of the Archaean crust, with diapiric deformation of the continental crust in terranes older than 2.9 Ga in the Pilbara and Dharwar Cratons, and long-linear upright fault/fold belts with elongate batholithic intrusions in terranes younger than 2.8 Ga (Condie and Benn 2006).

For the Neoarchaean of the EGP, varied tectonic scenarios have been applied as reviewed in Chapter 2, with most authors interpreting vertical tectonics in response to mantle plumes, horizontal tectonics (rifting, subduction), or mixed plume and plate models. Characteristic linear greenstone geometries separated by major transpressional faults have influenced some authors to interpret the deformation of the greenstone belts as a result of subduction and arc-accretion applying a Phanerozoic-style plate tectonic interpretation (Barley et al. 1987; Barley et al. 2002; Barley et al. 2008; Krapez and Barley 2008) – also evident in many papers at the recent 5th International Archaean Symposium (see papers in Tyler and Knox-Robinson 2010). Several authors present notable arguments against uniformitarian plate tectonic models for the Neoarchaean and the early Archaean (e.g. Hamilton 2010; Stern 2008); hence, issues of Archaean tectonic style have no consensus and remain unresolved despite the conclusions of many papers from the recent 2010 5th Archaean Symposium held in Perth, Western Australia (e.g. Percival 2010; Stevens et al. 2010; Van Kranendonk 2010; see also Condie and Kroner 2008; Foley 2008; Polat et al. 2008; Shirey et al. 2008; Wyman et al. 2008).

Central to the debate about tectonic models is the process of greenstone formation, and whether vertical tectonics, rifting, or arc accretion were involved in the formation of the environments that led to voluminous mafic and ultramafic volcanism, and that were followed by felsic volcanism and sedimentation in spatially restricted basins. A change to late clastic sedimentation is of particular interest since in the EGP, this event marks the end of volcanism and the onset of major *penetrative* deformation phases (Robert et al. 2005). Controls on the deposition and preservation of late clastic sequences have important implications for the style of tectonics and particularly the location of major gold deposits (Robert et al. 2005).

Whether plate tectonics operated in the Archaean is important for understanding early Earth history, and is vigorously debated in the recent literature (Chapter 2), but in terms of gold mineralisation and exploration the issue is crucial. The application of gold deposit genetic models has advanced from early unifying models that placed Archaean mineralisation as unique (metamorphic model, continuum model) to later analyses that include Archaean gold deposits in a broader geotectonic spectrum of mineralisation styles including syn-volcanic and magmatic hydrothermal styles (e.g. Robert et al. 2005; Chapter 7). If Phanerozoic-style plate subduction / arc-accretion tectonics operated in the Archaean, linear belts of accreted volcanic island arcs with intrusion-related, high-level epithermal precious-metal and porphyry Cu-Au deposits would be expected. Archaean mineral deposits do not conform to the expected metal associations, alteration zonations, spatial distributions and numbers that are characteristic of Phanerozoic terranes. Few Archaean deposits have been interpreted as porphyry and epithermal deposits (Goldie et al. 1979; Barley 1982; deLaeter and Martyn 1986; Cameron and Hattori 1987; Duuring et al. 2007), but for some of those deposits, there is still debate about their classifications and metal associations. Pro- plate-tectonic authors (e.g. Begg et al. 2010) explain

the paucity of porphyry-associated deposits as a lack of preservation of deposits formed in the upper 1-6 km of the crust. The dominance of epithermal and porphyry deposits in Cainozoic-aged sequences globally is usually interpreted in those terms (e.g. Seedorff et al. 2005; Hutchinson 1987). In contrast, the presence of high-level, Au-rich VMS deposits overlain by unconformable fluvial-alluvial sedimentary sequences in some Archaean terranes indicates that at least locally, preservation is not at issue.

1.2 Aims and objectives

Critical questions for the Neoarchaean include: (1) why that period was such an extraordinary episode of gold mineralisation in greenstone-hosted gold deposits, and (2) what were the specific geological and tectonic controls that influenced Neoarchaean metallogenesis. The main aim of this thesis is to identify the key controls on world-class, greenstone-hosted gold deposits of the Neoarchaean in Kalgoorlie, Western Australia. Fundamental inputs to address that aim include advancing the understanding of the stratigraphic and structural history of the Kalgoorlie greenstones, and the timing and nature of gold mineralising events in the study area, and the tectonic style of the Neoarchaean.

Structural history is addressed here in the context of the greenstone stratigraphy, recognising that stratigraphy and structural geology are fundamentally interrelated in tectonics (e.g. DeSitter 1956). Concurrent studies of stratigraphy and structural geology provide an understanding of the major geological episodes, and hint at possible tectonic settings for greenstone belts in the Neoarchaean.

Specific objectives to address the aims are:

1. Defining major stratigraphic formations and attempting correlations across the fault-bounded greenstone domains, supported by field mapping and geological observations.
2. Geochronological determinations of specific lithological units to constrain mapped lithostratigraphic sequences and uplift events.
3. Assessment of the kinematic nature and significance of faults that bound greenstone domains and terranes, in particular the gold mineralised Zuleika Shear Zone
4. Develop a structural history of the Kalgoorlie district based on stratigraphic distribution of greenstones, field observations of regional deformation fabrics (folds, major shear zones and faults) and new interpretations of crustal-scale seismic data and potential field data (gravity and aeromagnetics)
5. Detailed mapping and paragenetic studies of the Kundana and Binduli ore systems to identify timing criteria between contrasting gold mineralisation styles within a regional stratigraphic and structural framework.

6. Reconstruction of the major geological events, with a consideration of the tectonic style of the greenstone sequences, and possible implications for metallogenic evolution and mineral exploration.

1.3 Study area

The study area covers a ~50 km x 50 km region in the north Kalgoorlie district comprising detailed local study areas and mining districts at Kanowna, Mt Pleasant, Kundana, Gidji, and Binduli (Fig. 1.5). Apart from a prodigious gold endowment, the study area has abundant data available from exploration drilling, mine openings and geophysical data.

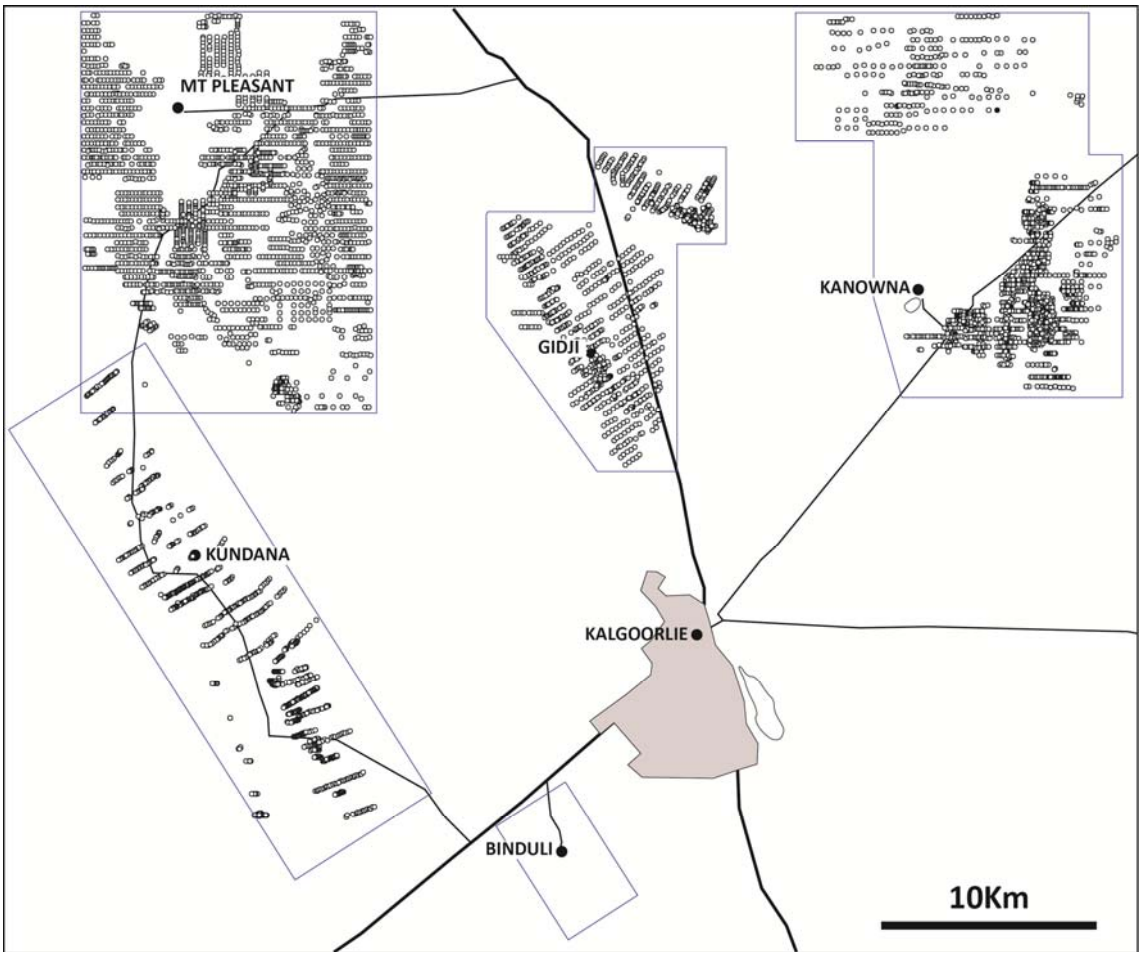

Figure 1.5 — Location of the study area in the north Kalgoorlie district with boxes showing detailed 1:10,000 scale mapping areas, and collar locations of some of the 6982 regional RAB, AC and RC drill holes re-logged and sampled in Placer/Barrick campaigns (all areas re-logged by the author and Dr. J. Rogers with some contributions from the following colleagues: *Mount Pleasant* — D. Boyd, C. Fairall, P. Smith, G. Allen; *Gidji* — C. Hillyard, D. Allingham, J. Standing; *Kundana* — M. Willson, A. Aaltonen, S. Halley; *Kanowna* — K. Joyce, C. Young, M. Willson, K. Montgomery, C. Large). The map does not include diamond drill holes re-logged in detailed campaigns for stratigraphy and geochronology (included on maps in later sections).

The north Kalgoorlie district is composed of several fault-bounded greenstone domains, including some of the least metamorphosed and deformed rocks in the Norseman-Wiluna Greenstone Belt - as such the prefix ‘meta’ will be omitted from rock names used throughout

the thesis, but the presence of lower-to-upper greenschist facies metamorphism is ubiquitous, with localised middle amphibolite-facies-grade rocks in the vicinity of intrusions. A coincidence of geologic preservation and a highly gold-endowed area provides a unique opportunity to understand Archaean geological processes and environments, greenstone belt construction, and controls on the formation of gold deposits.

1.4 Author contributions to the work presented

The studies documented in this thesis cover a range of field and analytical techniques with multi-disciplinary inputs. It is important to note that the contribution of the author in each of these areas is primarily one of field mapping and documentation at regional and mine scales; but including a significant proportion of analytical work comprising petrography, geochemistry and geochronology; and in some cases providing field constrained samples with regional context for contracted analytical work.

For the stratigraphic mapping outlined in Chapter 3, the bulk of the work was accomplished by the author and Dr. J. Rogers over a two year period of mapping, and drill hole re-logging and sampling (Fig. 1.5). A further three-month period included detailed re-logging of 16 km of diamond core, selected by the author and actively logged as part of a team of six geologists. The analysis and reporting of these results is the work of the author and Prof. H. Poulsen of Queen's University, Ontario, with some input from the members of that team - reported in Tripp et al. (2007a unpublished data) and published in Tripp et al. (2007b). Parts of that report are included in this thesis.

Selection of key stratigraphic units for SHRIMP U-Pb analysis of zircons was an outcome of the work done by the drill core re-logging team, the author, and Prof. H. Poulsen. Physical collection of those samples was done in the field with the assistance of Prof. J. Mortensen of University of British Columbia (UBC) to obtain the best samples for analysis. Prof. Mortensen separated the zircons at UBC, under contract to Barrick Gold. Analysis of zircons from those key stratigraphic units was done by the author on the SHRIMP-RG at Stanford University, San Francisco, under the guidance of Dr. R. Tosdal and Dr. J. Wooden, and was funded by Barrick.

A range of samples from the district were collected by the author with Placer Dome/Barrick colleagues and Dr. K. Cassidy of Geoscience Australia, and are reported in Chapter 4. Those samples were given field context by the mapping of the author and Dr. J. Rogers, and were provided to Dr. K. Sircombe of Geoscience Australia for analysis under funding provided by the pmdCRC research consortium. One sample lacking from the previous data sets was collected with field context by the author and provided to Dr. R. Squire who analysed the sample on the Curtin University SHRIMP, and reported the results under contract to Barrick. The analysis results are reported here and fully attributed to Dr. Squire's work.

Paragenetic studies of the Kundana and Binduli gold deposits by the author resulted in key samples that could benefit from further analytical work, but which was outside the scope of this thesis given the regional scope of the project. Those samples were selected and documented by the author and delivered to Dr. S. Hagemann for fluid inclusion analysis of the Kundana mineralisation, and to Dr. D. Mason for LA-ICPMS analysis of complex pyrites from the Centurion gold deposit at Binduli. Both of those analytical projects were delivered under contract to Barrick. The results are presented here in the context of the field relationships determined by the author, but fully referenced to the sources of the analyses. Detailed structural and paragenetic constraints on the Kundana mines were provided to Dr. N. Vielreicher who collected samples from the Rubicon deposits for SHRIMP U-Pb analysis of hydrothermal phosphates. The AMIRA P680 project requested field-constrained and documented samples for analysis, and since the paragenesis and fluid inclusion work at Kundana was completed in this study, data and samples were provided by Placer/Barrick as a sponsor of that project. The results of Dr. Vielreicher's analyses are presented to add valuable geochronological constraints to the field mapping and paragenetic studies at Kundana.

In summary, the key contributions of the author to the thesis include extensive field mapping and exploration drill hole re-logging, stratigraphic mapping, geochemical data analysis, structural mapping and analysis, petrography and geochronology.

1.5 Methods

In 2005, a major campaign conducted by Placer Dome Inc. compiled the collective work and databases of the previous forty years in north Kalgoorlie, by exploration and mining companies, government geological surveys, and universities. This effort produced a detailed MAPINFO-GIS lithological map of the study area (Chapter 3). A regional scale 3-dimensional (3D) GOCAD computer model of the north Kalgoorlie district was constructed from the lithological map, as well as thirteen ~100km long crustal sections. Depth projections of the geology interpreted from mapped structural data were verified with gravity forward-modelling along the line of sections incorporating detailed interpretation of several crustal-scale seismic lines. A regional 3-D gravity model of the same area used a UBC geophysical inversion code, to assess the sub-greenstone structure of the district. This work was done by a team of geologists, geophysicists and computer modellers; the author's contributions being mainly in the interpretation and construction of crustal sections and maps from personal and compiled field data, and supervising the production of 3-dimensional models.

Following the regional 3-D modelling of Kalgoorlie, six areas were selected for more detailed work at 1:10,000 scale included field mapping, drill hole re-logging, bottom-of-hole (BOH) multi-element geochemistry and portable infrared mineral analyser (PIMA) analysis of

white mica reflectance. These campaigns resulted in 1:10,000 scale revised geological maps with serial cross-sections and 3-D GOCAD computer models.

The 2-D lithological map of Kalgoorlie normally functions as a base layer for mineral exploration and is progressively refined and updated as new drilling and mapping progresses, but it lacks critical insights of stratigraphy, formation order and correlation. A major step in revealing the distribution and correct sequence of stratigraphic successions is creating an accurate geological map of the various formations. In 2006, Barrick Gold of Australia revised the regional geological map and produced a stratigraphic interpretation and correlation of coarse clastic rocks for the district. The geological campaigns produced an improved understanding of the geological history, and the data from those campaigns form of the basis of this research. Further details on research methods are listed below.

1.5.1 Field methods (lithostratigraphy)

Western Australia is mapped by the GSWA (Geological Survey of Western Australia) at 1:250,000 scale. Geological maps at 1:100,000 scale were produced systematically for the Norseman-Wiluna Greenstone belt among other areas in the state of Western Australia. A large portion of the north Kalgoorlie district was re-mapped at 1:10,000 scale by Crossing (2003), and the Kanowna district at 1:2,000 scale by Archibald (1993). Field mapping for this research was targeted at specific formations, localities and contacts that display relationships key to the stratigraphic and structural history (Chapter 3). These local scale areas are combined with detailed mapping of isolated outcrops that are typical of the generally poor exposure in the north Kalgoorlie District.

Isolated outcrop observations are linked with bottom-of-hole observations of rock-type in Rotary Air Blast (RAB), Aircore (AC) and Reverse Circulation (RC) exploration drilling. Uniform spatial coverage with exploration drill holes is typical, with a large proportion of holes drilled through the weathered profile to semi-fresh rock. The broad, uniform drill data were used with disparate outcrops and abandoned mine exposures for geological map compilation. Historical exploration drill holes were re-logged in the field on a pre-determined grid usually at 200 m spaced centres along 400 m spaced drill lines (Fig. 1.5). The material available for inspection is centimetre-sized rock chips, which was assessed for lithology, alteration and deformation and sampled for multi-element geochemistry.

Diamond core holes were descriptively logged with emphasis on the coarse clastic sedimentary and volcanic rocks (conglomerate/breccia). Details of the logging process and descriptive data are located in graphic drill logs in the Appendices. Data were recorded for both diamond drill holes and outcrops, with outcrop pavements measured in a linear fashion normal to the strike of bedding where possible.

1.5.2 SHRIMP geochronology (chronostratigraphy)

Principal stratigraphic units and intrusions were identified as requiring better age control and were selected for analysis to validate lithostratigraphic interpretations made on the basis of observational data and cross-cutting relationships. Two rounds of SHRIMP (Sensitive High Resolution Ion Microprobe) U-Pb zircon analysis were completed. The first round of analyses included collection of eighty-one samples resulting in fifteen attempted, and nine successful age determinations. A further round of fifteen samples was identified with the intention of applying the TIMS (Thermal Ion Mass Spectrometry) analysis method to achieve levels of precision not possible by ion microprobe methods. On inspection of the separated zircons, the complexity of internal zircon structure and morphology effectively ruled out the applicability of the TIMS method and the decision was taken to attempt SHRIMP analysis on those samples (Chapter 4).

Precision in geochronological determinations, and the resultant ±errors leave room for interpretation depending on the type of unit analysed (e.g. detrital zircon populations vs. igneous crystallisation ages). In a strict reading of the mean age and its error range, it is apparent that the actual age could reside anywhere within the analytical error range. However, in a detailed study of detrital zircons from across the Eastern Goldfields Province Krapez et al. (2000) state that for provenance studies "it is logical to consider that a maximum depositional age must be younger than the statistical limits placed on the age of the youngest source (i.e. the minimum age of the youngest age distribution). This takes consideration of an expected time period between the crystallisation age of the youngest source, and the uplift, erosion and deposition of the sedimentary unit being analysed.

In this thesis, a shorthand method of taking the depositional age of the unit as younger than the mean age minus the minimum error is a useful way to bracket events, particularly in Neoarchaean rocks where the analytical error is larger than in younger rocks (±5-10 Myr), and where field relationships and geochronology show that several major geological events occur within ~10 Myr, as for the key unconformities, deformation and mineralisation events in the Kalgoorlie greenstones.

1.5.3 Regional structural analysis and conventions

Regional structural data are compiled from numerous data sources including personal observations over a broad area by the author. Additional sources include GSWA 1:100,000 Series map sheets; 1:10,000 geological mapping of Crossing, (2003) and data from 1:2,000 mapping of Archibald (1993) at Kanowna. The data sets provided mostly orientation data on bedding, foliation and in some instances sedimentary younging directions and lineations. These data were combined with new observations and structural measurements to compile regional-scale maps of foliation trajectory, bedding trends and younging directions to interpret the regional fold geometry. Outcrop-scale mapping provided inputs into this interpretation, noting

bedding, fabric, and younging orientations; and where possible oriented thin sections were collected to properly assess bedding / cleavage relationships and for structural cross-cutting relationships of foliations.

In this thesis structural orientation data will be presented with a dip and dip-azimuth convention: planar structures will be presented as dip/dip direction (e.g. a plane dipping at 45 degrees towards an azimuth of 135 degrees will be notated 45º/135º); lineations will be notated as plunge/plunge direction (e.g. a lineation that plunges at 45 degrees towards an azimuth of 135 degrees will be notated 45º/135º). The dip / dip-azimuth notation systems for planar and linear structures are used since they provide unique orientations and avoid the potential confusion of 'Left / Right hand rule' notation systems. For structures where a reading had to be estimated from a distance (e.g. mine shafts) strike/dip/dip-quadrant notation is used.

Way-up indicators in this thesis use the 'inverted Y' convention (Borradaile 1976), in which the stem of the 'Y' points to the stratigraphic top. Using this convention, if the top of this page was the stratigraphic top, the symbol would be presented as: ⅄.

1.5.4 Detailed paragenetic/structural studies of mineralisation

Lode-gold vein deposits at Kundana were studied collectively to assess the detailed mineral paragenesis with drill core and mine mapping. The veins were characterised into generations by common characteristics including: vein thickness, texture, morphology, vein fill mineralogy, alteration mineralogy, orientation, wallrock structure and cross-cutting relationships. Core observations were supported with mapping in underground and open-cut mines, detailed mapping of the Rubicon deposit and petrographic / mineragraphic description of the main vein types.

Selected drill holes and outcrops from the Binduli deposits were assessed to gain insights into the unique relationships between early/late mineralisation styles and structural cross-cutting relationships that are present at the Binduli mining centre. This work was supported by geochemical analysis, with details as described in Chapter 7.

1.5.5 Three-dimensional geological modelling

Three-dimensional geological modelling formed a large part of the base data for this project. The regional field data collected (described in Section 1.4) were used to create new geological maps for six 1:10,000 scale map sheets. Hand-drawn serial cross-sections and longitudinal sections were constructed for each of these map sheets by the author and Dr. J. Rogers. These sections were used to create 3D GOCAD computer models.

A regional 1:100,000 scale 3D geology computer model was constructed by the same methods, with +100 km scale hand-drawn cross-sections and longitudinal sections. This was a team-based effort by the author, Dr. J. Beeson, M. Willson, D. Archer, W. Edgar, and Dr. S.

Halley, with computer support from F. Davidson. Digitising and forward modelling of inverted gravity data along the lines of section were used to constrain the depth interpretation of geological formations by I. Neillson.

1.5.6 Geophysical data analysis (aeromagnetics, ground gravity, seismic)

Regional-scale geophysical data sets were used to assist correlations across poorly exposed areas. The north Kalgoorlie district has voluminous data sets, which were used to support the work outlined here. Interpreted regional-scale images include aeromagnetics, processed with the total magnetic intensity reduced-to pole (RTP); first vertical derivatives of the RTP; ground gravity data collected on 200 x 400 m spaced centres; and several regional scale seismic lines (Goleby 1993).

Selected sections of the regional seismic lines were reprocessed by the Curtin University facility in Perth WA, and new 'micro-seis' lines were shot across the Kanowna project. Various parts of those lines have been interpreted for this study in an attempt to project surface field data and constrain serial cross-section interpretations.

1.6 Thesis outline

Background material outlining the scope of work and the personal contribution of the author to multi-disciplinary team-based geological work are listed in Chapter 1. Reviews of previous literature and work on the north Kalgoorlie district are documented in Chapter 2.

Detailed descriptive work on the major post- Upper Basalt sedimentary and volcanic formations, with new data leading to a revised, interpreted lithostratigraphy of the Kalgoorlie district is presented in Chapter 3. Chapter 4 contains the results of SHRIMP U-Pb analyses of zircons including field location data and geological constraints that justify sample selection for analysis for the major formations. This chapter also assesses the stratigraphic interpretations in Chapter 3 in light of the interpreted ages.

Detailed information on domain boundary faults is presented in Chapter 5 using the Zuleika Shear Zone as a prime example. This includes an assessment of the role of major faults as domain and terrane boundaries. Regional and local structural data and a revised structural history for the study area are presented in Chapter 6; those data outline a deformation event history of the study area, with attempts to correlate against published deformation schemes.

Chapter 7 presents detailed ore systems research on the Kundana and Binduli gold deposits, and data from other deposit styles in the region, to demonstrate areal and temporal distribution of Archaean gold deposits. This chapter also demonstrates the place of gold styles/events within the deformation scheme outlined in Chapter 6.

Possible geotectonic settings for the Kalgoorlie district are discussed in Chapter 8 on the basis of the work presented here. Given the small study area size in relation to major litho-

tectonic belts in the Eastern Goldfields Province, these inferences are naturally speculative, but provide information about whether a contribution can be made to large-scale tectonic interpretations by mesoscopic geological data. Conclusions of the thesis are presented in Chapter 9. Supporting data sets are collected in the Appendices.

2 Literature review

Archaean rocks in the Kalgoorlie district form part of the Kalgoorlie Terrane of Swager et al. (1990), a fault-bounded sequence of volcanic, sedimentary and intrusive rocks of ultramafic to felsic compositions. Internal subdivision of the Kalgoorlie Terrane into six domains bounded by major shear zones highlights an elongate, sinuous geometry of the greenstone domains (Fig. 2.1). Stratigraphic sections vary among domains, which contain complete or partial sections of a total sequence (Fig. 2.2a, b). The general sequence has been subdivided on stratigraphic position, composition and geochronology into three broad classes: mafic volcanic; felsic volcaniclastic; and epiclastic rocks (Fig. 2.2a, b).

The following descriptions will focus on the Coolgardie, Ora Banda, Boorara and Kambalda Domains in the Kalgoorlie gold district. Full descriptions of the lithological distribution in each domain are given in Swager et al. (1990) and Morris (1993).

2.1 Stratigraphy

Neoarchaean basin development with extrusion of mafic and ultramafic volcanic rocks at ca. 2710 Ma suggests rifting of a basement that may be represented by earlier granite-greenstone assemblages in marginal areas of the Eastern Goldfields Province e.g. 2930±4 Ma rhyolite at Norseman (Nelson 1995); 2750±8 Ma granodiorite that intruded greenstones at Jasper Hills, Leonora; and 2817±6 Ma sedimentary rocks in the Sons of Gwalia mine (Baggott 2006; see also Chapter 8). Sedimentation and felsic-intermediate volcanism followed the mafic-ultramafic volcanism for ~30 million years from 2690 - 2660 Ma. A final phase of interpreted extension produced clastic sedimentary basins that contain polymictic conglomerate indicating un-roofing of the granite-greenstone terrane (Swager 1997).

2.1.1 Mafic-ultramafic volcanism

Mafic-ultramafic volcanic rocks include three internal stratigraphic subdivisions of Lower Basalt unit; Ultramafic unit; and Upper Basalt unit. The sequence: mafic volcanic rocks - ultramafic rocks - mafic volcanic rocks - felsic volcaniclastic rocks, is a typical section for determining broad stratigraphic facing throughout the district. Members of each lithologic unit are variably developed throughout the Kalgoorlie Terrane, whereas the Upper Basalt unit is widely developed across the district, and appears to have suffered the least internal deformation compared to the other units.

The Lower Basalt unit comprises basaltic volcanic rocks and co-magmatic mafic intrusive sills that include high-Mg (komatiitic basalt) and tholeiitic compositions. In the Ora Banda Domain, basaltic volcanic rocks (Missouri Basalt) are intercalated with felsic sedimentary rocks indicating felsic volcanism at ‘Lower Basalt time’ or erosion of an older felsic source region. In

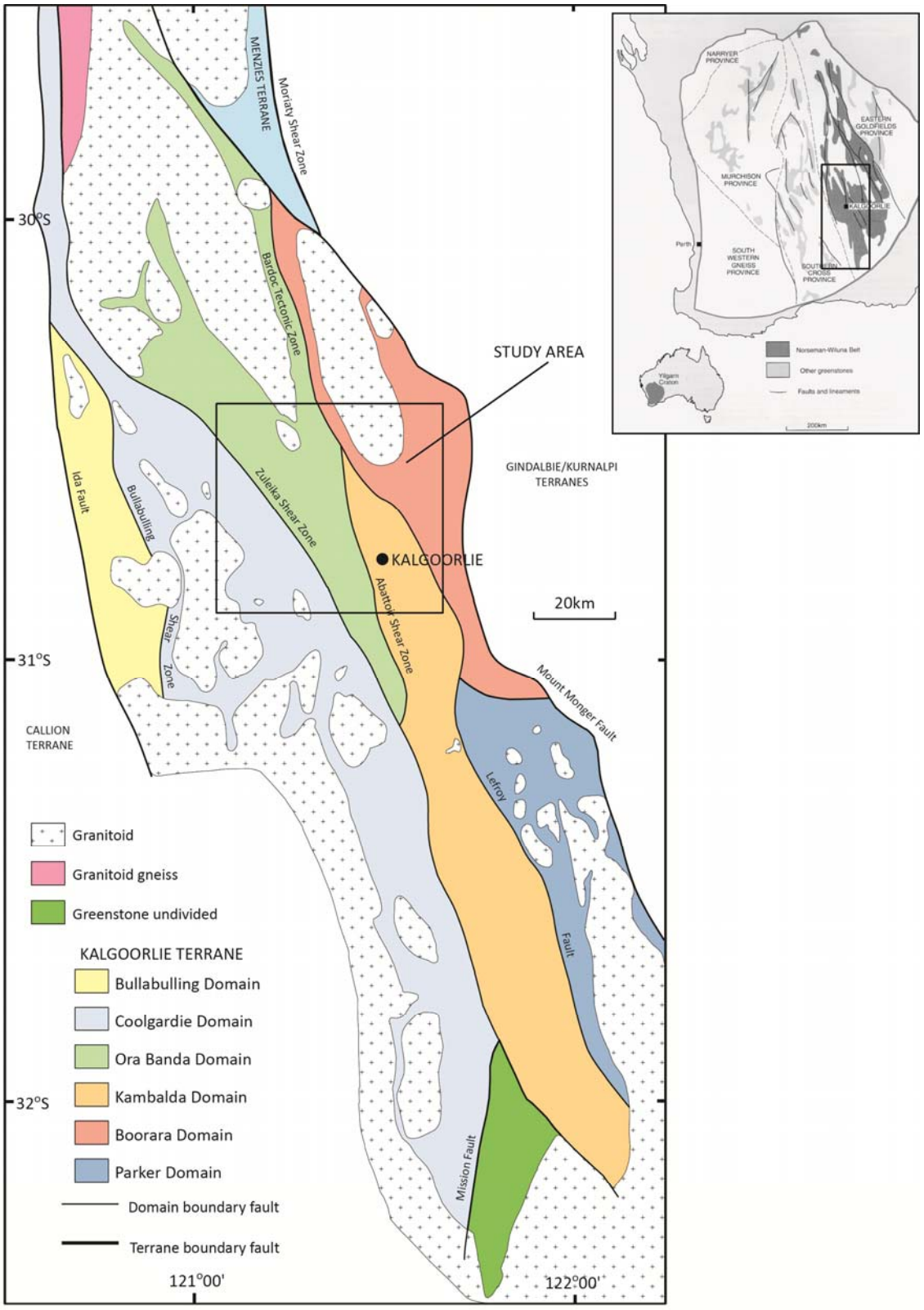

Figure 2.1 – Location map of the Kalgoorlie Terrane in the south of the Eastern Goldfields Province (inset map from Hagemann et al. 2000); and map of fault-bounded domains of the Kalgoorlie Terrane of Swager et al. (1990). Coloured bands are greenstone segments separated by major domain boundary faults.

a

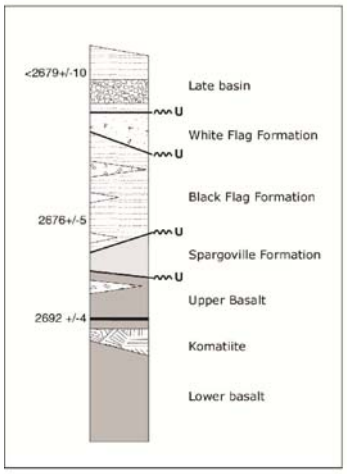

b

Kalgoorlie Regional Stratigraphy

Sequence	Designation	Formation	Unconformities
Epiclastic Sedimentary Sequence	Late Basin	Kurrawang/Merougil Formations	
Felsic Volcaniclastic Sequence	Black Flag Group	Sequence 7 Sequence 6 Sequence 5 Sequence 4	
		Sequence 3	
		Sequence 2	
		Sequence 1	
Mafic Volcanic Sequence	Upper Basalt	Paringa Basalt	
	Komatiite	Devon Consols Basalt Kambalda Komatiite	
	Lower Basalt	Lunnon Basalt	

Figure – 2.2a) Published schematic summary stratigraphic column for the Kalgoorlie Terrane (Krapez et al. 2000); b) table of major subdivisions of the Kalgoorlie stratigraphy, interpreted sequences, and interpreted unconformities (after Barley et al. 2002).

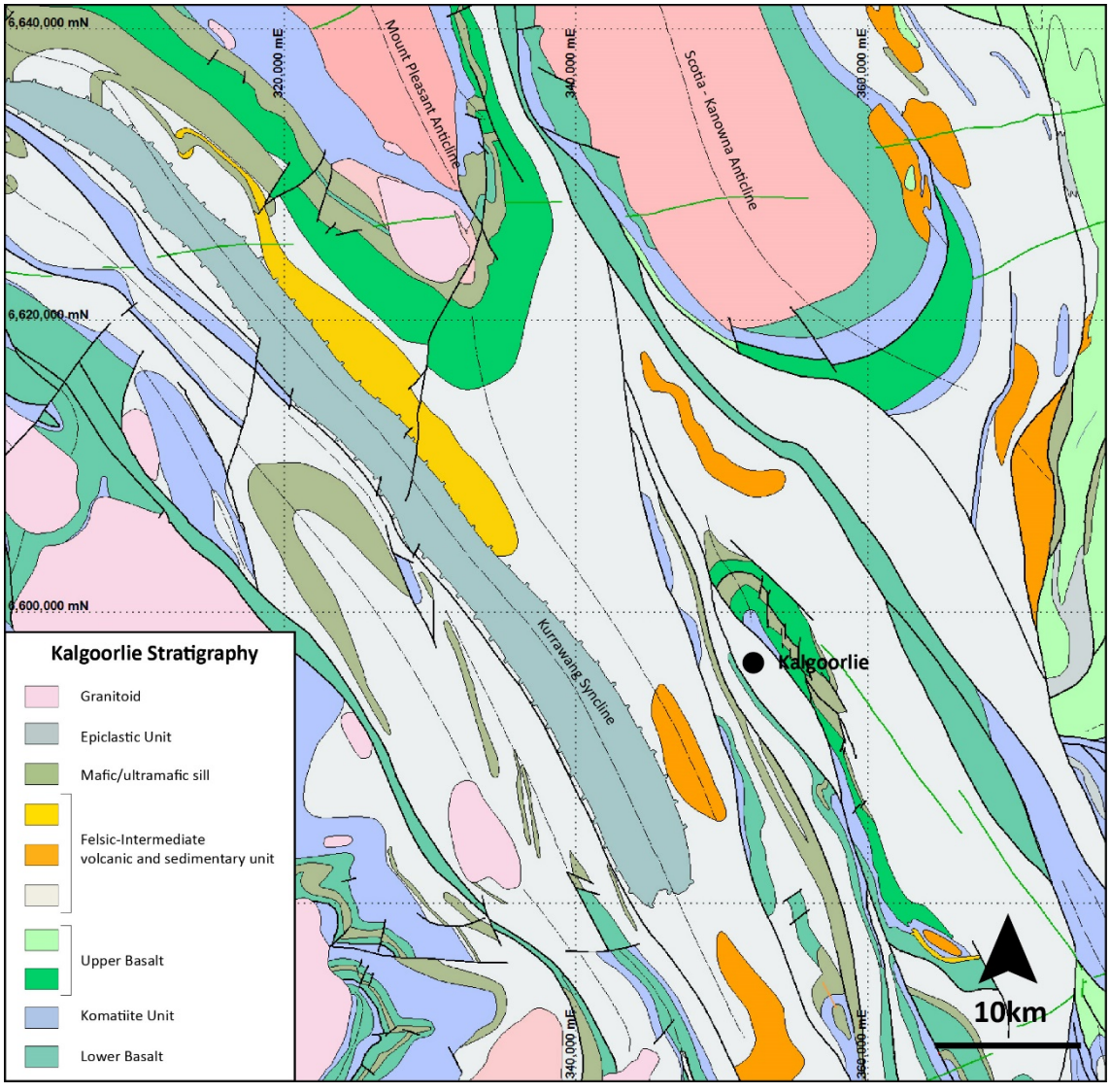

Figure 2.3 – GSWA map showing distribution of the major formations of the north Kalgoorlie district (Swager et al. 1990); this map is the most current published basement map of the district geology.

the Boorara Domain the Lower Basalt is represented by the Scotia Basalt, which is present as a sliver on the western margin of the Scotia-Kanowna dome (Fig. 2.3), and a thick succession of poorly exposed mafic volcanics on the eastern margin that is intercalated with felsic volcanic rocks (Fig. 2.3; Williams 1970).

The ultramafic unit is a regionally extensive sequence of komatiite flows and intrusions, locally with thick cumulate sections and high-Mg basalt. A general sequence for the ultramafic unit in the Ora Banda Domain is: adcumulate dunite; spinifex komatiite; high-Mg pillow basalt. The dunite is interpreted as adcumulus olivine growth at the base of a lava flow (Hill et al. 1995). In most domains the komatiite unit is a discrete component of the stratigraphic section, whereas komatiites in the Boorara Domain are co-magmatic with dacite-rhyolite volcanics and are intrusive into sedimentary rocks (Trofimovs et al. 2004; Fig. 2.3).

The Upper Basalt consists of high-Mg komatiitic to tholeiitic mafic volcanic rocks, and co-magmatic mafic-ultramafic sills. In the Ora Banda Domain, Upper Basalt comprises two tholeiitic mafic flow sequences with several layer-parallel, co-magmatic sills and interflow sedimentary rocks. Of these two mafic flow sequences the upper unit is the Victorious Basalt, a distinctive coarse plagioclase-phyric flow sequence. In the Kambalda domain the Paringa Basalt (Upper Basalt unit) consists of tholeiitic basalt and intercalated komatiitic basalt with interflow sedimentary rocks, but locally with upper plagioclase-phyric flows similar to the Victorious Basalt. Upper Basalt is absent in the Coolgardie Domain, and until recently has been considered absent in the Boorara Domain, but new unpublished work by Barrick has interpreted a thick sequence of Upper Basalt with intercalated differentiated dolerite sills that was previously correlated with Lower Basalt unit (cf. Swager et al. 1990).

Distinguishing between Upper and Lower basalts is difficult based on textural character alone since both sequences comprise pillowed flow sequences with calc-alkaline and tholeiitic to high-Mg compositions (Harrison et al. 1990; Morris 1993). Morris (1993) distinguished between the two sequences using ratios of Ti/Zr, Zr/Y and Al_2O_3/TiO_2.

2.1.2 Felsic-intermediate volcaniclastic rocks

Volcaniclastic rocks of the Black Flag Group have been subdivided into seven depositional and magmatic sequences grouped into four unconformity-bounded packages (Fig. 2.2b) which were interpreted to represent major tectonic stages of uplift/subsidence (Barley et al. 2002). The Black Flag Group in the Coolgardie Domain contrasts with the Ora Banda Domain where the former comprises turbiditic sedimentary rocks with rare andesitic volcanic rocks, whereas greater thicknesses of andesitic volcanic and volcaniclastic rocks are present in the latter. In the Ora Banda Domain the Black Flag Group comprises turbidite sedimentary rocks assigned to: a ‘Spargoville Formation’; White Flag Formation intermediate volcanics (Hunter 1993); and a poorly exposed upper sedimentary unit named ‘Black Flag Formation’

(Krapez et al. 2000). Note that Krapez et al. (2000) have interpreted their 'Black Flag Formation' to underlie the White Flag Formation (Fig. 2.2a) but that interpretation cannot be sustained in light of new results in Chapter 3.

In the Kambalda Domain, Black Flag Group rocks is composed of felsic volcanic rocks, turbiditic wacke and mudstone, and localised andesite-dacite volcanics interpreted as dome and apron assemblages with intercalated and overlying turbiditic sedimentary rocks (Hand 1998). The Black Flag Group in the Boorara Domain has significant differences to the sequences elsewhere in the Kalgoorlie Terrane with a predominance of coarse conglomerates, which suggest localised provenance, intercalated with felsic volcanic and sedimentary rocks.

The Ora Banda Domain contains well-preserved lithological units lacking the transposition and disruption of sequences characteristic of the surrounding domains. In the Ora Banda Domain, the 'Spargoville Formation' was locally dislocated from the underlying Upper Basalt unit, yet rare primary contacts are preserved. Bedding-parallel faulting has facilitated significant internal thrust stacking of the turbidites, whereas broad regional-scale upright folds deformed the surrounding Upper Basalt and White Flag Formation (Tripp et al. 2007b).

Recognition of the interpreted unconformity-bounded tectonic stages of Barley et al. (2002) in the field is hindered by poor preservation of primary contacts and extensive tectonic shortening in the sedimentary formations. The unconformities were interpreted from sequence stratigraphic concepts applied to basin analysis of the sedimentary rocks in the Kalgoorlie district (Krapez 1997). In that review Krapez (1997) advocated depositional sequence analysis as a pre-requisite for basin recognition and geotectonic setting in the Archaean of Western Australia, and suggested the interplay between tectonics and eustatic sea level change is applicable to the Archaean.

2.1.3 Late-stage epiclastic sedimentary rocks

Epiclastic sedimentary rocks are present in two main associations: (1) elongate fault-bounded, NW-SE trending synclines (e.g. Kurrawang and Merougil formations) containing rocks unconformably overlying previously folded rocks; and (2) unconformable sequences, which 'wrap' around the major granite domes. The late-stage sedimentary rocks were interpreted as fluvial to deep-marine turbidite sequences of sandstone, conglomerate and sandstone/siltstone (Krapez et al. 2000). There are many previous studies, theses and publications on the Kurrawang and Merougil Formations (Honman 1914, 1916; Glikson 1968; Bader 1994; Krapez 1997; Hand 1998; Howe 1999; Krapez et al. 2000; Fletcher et al. 2001; Godfrey 2004; Krapez and Barley 2008; Krapez and Pickard 2010; Squire et al. 2010), most of which were primarily concerned with the palaeo-depositional settings of those units.

The presence of significant components of hypabyssal porphyritic and equigranular granite clasts in the conglomerates indicates uplift and unroofing of granite batholiths (Swager

1997); whereas a lack of co-eval volcanic rocks in the late clastic sequences suggests their deposition post-dated extrusive volcanism.

Late-stage sedimentary rocks were deformed by a regional ENE-WSW contraction that included formation of a pervasive foliation, which is axial planar to folds in the late clastic sequences (Tripp et al. 2007a). However, their deposition above demonstrable angular unconformities on deformed underlying greenstones suggests that there was at least one earlier contractional deformation phase prior to the regional fabric-forming event (Tripp 2000; see also Blewett et al. 2004). The late stage sedimentary rocks therefore play a critical role in understanding the structural geological timing of the final stages of the development of the Archaean Kalgoorlie Terrane, as well as relationships with major gold deposits.

Krapez et al. (2000) described the Kalgoorlie basin (Black Flag Group) as a classic example of a deep marine intra-arc strike-slip basin, with depositional sequences representing deep marine turbidites and submarine channel complexes. Fining upward sequences with upper organic-rich shales, record condensed sections of transgressive and highstand systems tracts (Krapez 1997). Interpretations were also made for the Kurrawang and Penny Dam basins as structurally dismembered flysch deposits, and the Merougil and Jones Creek Formations were interpreted as typical molasse depositional systems of fluvio-deltaic and fluvio-lacustrine fault-bounded basins (Krapez et al. 2000; Barley et al. 2002; Krapez and Pickard 2010).

The basal contact of the Kurrawang Formation is reported widely as an unconformity (Swager et al. 1990; Witt, 1990; Weinberg et al, 2002), whereas field exposures show evidence of strain on the contacts except in relatively few examples (Chapter 3). Strong linear fault controls on the ‘basin margins’, and preservation as synclines in the footwalls of major faults, suggests that some of the late clastic sedimentary sequences are syn-orogenic fault-preserved remnants rather than in-situ ‘basins’.

2.2 Intrusion and metamorphism

Plutonic granitoid magmatism occurred over a protracted period in stages related to extensional and contractional deformation phases. A recent study (Cassidy et al. 2002) showed the presence of five distinct suites of granitoids throughout the Yilgarn Craton, three of which are volumetrically significant in the granite-greenstone terrane:

High-Ca suite tonalite-granodiorite	(60% of all granitoids) 2720 Ma – 2650 Ma
Mafic suite granodiorite	(10-15% of all granitoids) 2694 Ma – 2648 Ma
Low-Ca suite quartz monzonite	(>20% of all granitoids) 2655 Ma – 2620 Ma

The age ranges of the granitoid suites have wide spread since the data are from the entire Yilgarn Craton, however the main classes have peak ages that indicate times of most prominent

magmatism for each suite represented in the Kalgoorlie Terrane. High-Ca tonalite and granodiorite have an interpreted collisional tectonic setting; mafic suite granodiorites are interpreted as products of rift-related to arc/collisional-related syn-volcanic magmatism; and Low-Ca quartz monzonites were emplaced after most of the other suites within an inferred extensional setting.

Several studies have emphasized the critical role of Mafic and Low-Ca suite granitoids in controlling the peak distribution of metamorphic isograds (Witt 1991; Witt and Davy 1997; Mikucki and Roberts 2003). A close relationship between alteration type and metamorphic grade indicates that in many cases gold mineralization appears to have been emplaced during or after peak metamorphism (Phillips and Groves 1983; Witt 1991; Knight et al. 2000) implying a metamorphic event lasting 30-35 million years based on the inferred ages of mineralization.

Metamorphism ranges from lower greenschist to upper amphibolite facies with a distribution that lacks association with High-Ca series granitoids or major faults. The regional distribution of metamorphic facies cuts across major faults indicating no significant juxtaposition of contrasting metamorphic histories across domain and terrane boundaries. A complex timing between metamorphism and deformation is evident, however metamorphism is considered to have commenced during D2 deformation and continued until the end of D3 (Mikucki and Roberts 2003; cf. Goscombe et al. 2010).

The interaction of deformation and metamorphism in the Kalgoorlie district is complex (Mikucki and Roberts 2003; Goscombe et al. 2010). Metamorphic isograds cross major shear zones indicating that the metamorphism post-dated at least the early faults. Isograds do however conform to the distribution of Mafic and Low-Ca suite granitoid intrusions and the interaction of these intrusions with deformation events allows some broad relationships to be established. Mafic suite granites have a mean age of emplacement of about 2665 Ma and display relationships that indicate intrusion synchronous with or late within the regional folding phase of deformation (e.g. Scotia Dome, Liberty Granodiorite). The granites in some cases may have facilitated the upward doming of the greenstones (Weinberg et al. 2003). In the Kalgoorlie district, granitoid intrusions are mostly bounded by sheared greenstones, and the shear zones are also wrapped around the granite domes. Some granites apparently controlled the kinematics of the shear zones (Tripp 2002a) and may have acted as rigid bodies, which controlled the deformation. An exception to these relationships is the Scotia Dome, which appears to have a fault-controlled eastern margin, and apophyses that extend southwards across folded greenstones to be truncated at an unconformity (Chapter 5; see A0 geological map-map pocket).

Low-Ca suite granites show significant disruption of regional foliation trajectories and may crosscut regional folds. A late to post-tectonic timing of the Mungari Monzogranite was interpreted by Glikson (1971). The presence of solid state fabrics in the granitoid intrusions appears to be a poor indicator of structural timing of emplacement since all granites in the

Norseman-Wiluna belt have responded to deformation as competent bodies (Weinberg et al. 2003).

Five spatially and temporally discrete metamorphic events were defined in the Eastern Goldfields Superterrane by the pmdCRC Yilgarn project (Goscombe et al. 2009). High pressure assemblages (M1) with low geothermal gradients attained 8.7 kbar in the oldest greenstone sequences adjacent to granite domes. A rarely preserved low P (2.5-5.0 kbar) granulite event ('Ma') was interpreted to have formed in high heat flow settings within a magmatic arc. The main regional (moderate P and T) metamorphic event (M2 contractional) was interpreted as accounting for most of the available metamorphic fluid and was generated before the main gold events (suggesting it was not a major fluid source for Au). Anticlockwise P-T-t paths in an "upper plate" that exhumed older high-P assemblages in a "footwall" were interpreted as associated with a D3 extensional event (M3a extensional). A final widespread low P (~1 kbar) metamorphic event (M3b) was interpreted as producing regional scale retrogressive alteration associated with regional exhumation during D4 to D5 deformation (Goscombe et al. 2009).

2.3 Geochronology

U-Pb SHRIMP analysis of zircons has been the primary tool used to determine absolute ages of volcanic formations and detrital zircons in sedimentary rocks from the Kalgoorlie district (e.g. Nelson 1995, 1997; Krapez et al. 2000; Ross et al. 2004). Detailed CL (cathodoluminescence) and BSE (back-scattered electron) imaging by SEM (scanning electron microscope) have demonstrated complexity in Neoarchaean zircons from rocks across the Eastern Goldfields Province due to effects induced by the natural decay of U and Th, leading to Pb loss and isotopic resetting of metamict high-U/Th zircons by subsequent thermal events (e.g. Hill and Campbell, 1989; Clout 1991; Nelson 1997; Krapez et al. 2000; Ross et al. 2004). Metamictisation (radiation and decay) damages the crystal structure of zircon such that the products of radioactive decay (Pb) may be lost during later heating and recrystallisation. Other complexities include inheritance, recrystallisation of zircon, metamorphic overgrowth, alteration, and crystal defects that can be separated by several millions of years and may produce mixed ages in SIMS (Secondary Ion Mass Spectrometry) U-Pb determinations (Ross et al. 2004). To counter these effects, the SHRIMP (Sensitive High Resolution Ion Microprobe) method allows for ~20-30 µm spot determinations on selected parts of individual zircon grains, that can be selected to minimise the listed issues, and provide age data to support the documented field relationships.

Selected results of previous geochronological studies of rocks from the study area are summarized in Table 2.1. The age of the regional komatiite volcanic unit is generally interpreted from a SHRIMP U-Pb zircon age of 2708±7 Ma from felsic dacitic flow rocks interbedded with the basal komatiite unit at Kanowna (Nelson 1997), whereas the Kapai Slate

tuffaceous sedimentary rocks at the top of Devon Consols Basalt (upper member of the komatiite unit) near Kambalda, returned an age of 2692±4 Ma (Claoue-Long et al. 1988). These ages bracket komatiitic and associated mafic volcanism between 2715-2688 Ma. A SHRIMP U-Pb zircon age of 2687±5 Ma (Hill et al. 1995) determined for the Mount Pleasant Sill, which intruded interflow sedimentary rocks at the base of the Upper Basalt sequence, broadly supports the interpreted age bracket for mafic volcanism.

The age of felsic volcanism in the 'Black Flag Group' is constrained by a rhyodacite volcaniclastic sequence at Gibson-Honman Rock (2676±5 Ma; Krapez et al. 2000), and a thick sequence of mostly rhyolitic volcanic and volcaniclastic rocks at Perkolilli (2675±3 Ma; Nelson 1995). Felsic volcaniclastic rocks at Gidji are constrained by SHRIMP analyses of zircon in polymictic conglomerate-sandstone dated at 2666±6 Ma (Hand 1998); the Gidji volcaniclastic sequence may correlate with the Grave Dam sequence at Kanowna (2668±10 Ma, Ross et al. 2004). Andesitic re-sedimented volcaniclastic rocks east of Mount Charlotte have an age of 2661±3 Ma from SHRIMP U-Pb zircon analyses of a single andesite porphyry clast, interpreted as the maximum depositional age of that unit (Fletcher et al. 2001).

Late clastic sedimentation is constrained by maximum depositional ages interpreted from peaks in detrital zircon populations (Krapez et al. 2000; Kositcin et al. 2008; Krapez and Pickard 2010). The available geochronological data (Table 2.1) from the sedimentary rocks of the Kurrawang Formation indicate there are variable populations of youngest detrital grains from place to place and from different members: 2657±4 Ma from the Navajo sandstone at Binduli Mine (Fletcher et al. 2001), 2679±10 Ma from conglomerate at Lake Douglas (Krapez et al. 2000), and 2655±5 Ma (Fletcher et al. 2001). The differences are in part attributable to variation in provenance, but all are consistent with depositional ages for the Kurrawang Formation in the range of 2660-2650 Ma or less. A characteristic to the late clastic conglomerate / sandstone sequences is the presence of detrital age peaks representative of the major volcanic and intrusive episodes in the district, but also the presence of a population at >3.0 Ga suggesting the late clastic sequences sourced rocks that are older than any preserved in the Eastern Goldfields Province (Krapez et al. 2000).

Zircon SHRIMP analyses for rocks in the Kalgoorlie district overlap in age, but form three broad groups of ages at around 2710 Ma, 2690 Ma and 2660 Ma. These ages correspond with major volcanic and sedimentary events in the geological history. Mafic and ultramafic volcanism occurred at ~2710 Ma – 2690 Ma; felsic and intermediate volcanism and sedimentation ~2690 Ma – 2660 Ma; and waning felsic volcanism and epiclastic sedimentation at around 2660 Ma – 2650 Ma.

Table 2.1 - Selected SHRIMP zircon analyses reported for rocks from the Kalgoorlie district

Unit	Location	Sample #	Rock type	Zircon population mean	plus	minus	Rock age (Ma)	Comments	Source
Spargoville	Golden Ridge	E75	dacite volc	2698	6	-6	2692-2704		Krapez et al. 2000
Kanowna porphyry	Kanowna Belle	KWA-1	poprhyritic rhyolite	2676	4	-4	2672-2680	2711 inheritance	Krapez et al. 2000
Mount Shea Porphyry	Mt Shea	SHD	porphyritic rhyolite	2658	3	-3	2655-2661	2677 inheritance	Krapez et al. 2000
Kurrawang	Lake Douglas	KU-1	sandstone	2679	10	-10	<2669	2 grains<2650; 2> 3500	Krapez et al. 2000
White Flag Fm	White Flag Lake	BF-6	conglomerate matrix	2813	3	-3	<2810	1 grain 2761, 1 3480	Krapez et al. 2000
Black Flag Fm	Gibson-Honman	E179	congl clast (dacite), volc. breccia	2676	5	-5	2671-2681	1 grain 2900	Krapez et al. 2000
Black Flag Fm	Eight Mile Dam	EMD-2	sandstone	2666	6	-6	<2660	1 grain>3300, many 2740	Krapez et al. 2000
Black Flag Fm	Eight Mile Dam	EMD-10	dacite breccia?	2669	7	-7	<2662	also 2700 grains	Krapez et al. 2000
West Wall porphyry	Kanowna Belle			2676	5	-5	2671-2681	cuts Grave Dam??	Ross et al. 2004
KB porphyry	Kanowna Belle			2655	6	-6	2649-2661	includes 2683/2701 pop	Ross et al. 2004
Grave Dam	Kanowna Belle	hole 432	sandstone	2667	10	-10	<2657		Ross et al. 2004
Golden Valley	Kanowna Belle	pit	congl clast	2667	9	-9	<2658	2719 inheritance	Ross et al. 2004
HW porphyry	Kanowna Belle	felsic porphyry		2648	11	-11	2638-2659	older pop at 2675	Ross et al. 2004
Black Flag Fm	Perkolilli Hills		dacite breccia	2675	3	-3	2672-2678		Nelson, 1995
Kambalda?	Ballarat-Last Chance	104958	dacite	2708	8	-8	2700-2716		Nelson, 1995
Scotia Granite	Split Rock	93901	granodiorite	2657	5	-5	2652-2662		Nelson, 1995
Four Mile porphyry	Four Mile Hill	104967	porphyry	2613	11	-11	2602-2624		Nelson, 1995
Golden Mile Dolerite	Fimiston	?	dolerite	2675	3	-3	2672-2678	cuts Spargoville	Woods, 1997
Golden Mile Dolerite	Fimiston	?	dolerite	2680	9	9	2671-2689		Rasmussen et al. (2009)
FSP dykes	Fimiston	?	felsic porphyry	2676	1	-2	2674-2677	cuts Spargoville but post-dates Kalgoorlie anticline/syncline	Clout et al, 1990; Yeats et al. 1999; Gauthier et al. 2004a (Mortensen, TIMS)
HP dykes	Fimiston	?	int porphyry	2663	11	-11	2652-2674	xenoliths of carb veins	Gauthier et al. 2004a
Volcaniclastic Conglomerate	East of Fimiston	2000967006D	Int porphyry clast	2661	3	-3	2658-2664	White Flag Equivalent?	Fletcher et al. (2001)
Navajo sandstone	Binduli	20009967013	sandstone	2657	4	-4	<2661	In or below Kurrawang	Fletcher et al. (2001)
Oroya lamprophyre	Fimiston		lamprophyre	2642	6	-6	2636-2648		Gauthier et al. 2004a

2.4 Structural geology

2.4.1 Introduction

A review of literature on the deformation history of the study area reveals a widely used correlation of major events into contractional and extensional phases (Swager 1989; Swager et al. 1990; Vanderhor and Witt 1992; Williams and Whitaker 1993; Nguyen (1997); Swager & Nelson 1997; Blewett et al. 2004; Blewett et al. 2010; Czarnota et al. 2010; Table 2.2). A simplified deformation scheme extensively cited in the literature (Swager et al. 1990) has historically focussed on contractional deformation phases (D1-D4). Models that attempt to explain the deformation history of the greenstone sequences differ widely, including end-members that ascribe most of the architecture to early extensional deformation, and others that interpret the greenstone deformation primarily as a product of prominent regional contractions (Davis et al. 2000; Davis et al. 2010; Archibald 1979; Archibald et al. 1981; Williams & Whitaker 1993).

A common published deformation sequence for the district includes:

a) Early extensional deformation DE
b) Early contractional D1 deformation interpreted from recumbent folds and thrust repetition of stratigraphy and an inferred south-over-north transport direction (Archibald et al. 1978; Swager and Griffin 1990; Swager et al. 1990; Swager 1997).
c) D2 – an ENE-WSW directed contraction that produced thrust faults and folds. The D2 event was interpreted as the primary fabric-forming episode in the Kalgoorlie district producing a prominent NNW-SSE structural grain.
d) D3 and D4 interpreted as manifestations of the same progressive shortening with local strains that are not kinematically distinguished from D2, characterised by strain localization in 'D3' shear zones, and D4 brittle-ductile faults (e.g. Tripp and Vearncombe 2000).

The deformation of the Kalgoorlie district is part of an interrelated series of events in a broad geological history that includes sedimentary basin development; volcanism; granitoid intrusion; uplift and unconformity; deformation; metamorphism; and mineralization. A complete understanding of the geological history can only be accomplished in a framework that includes all of these parts. Extensive past and current research has produced results that address many of these issues.

Table 2.2 – Correlation of deformation schemes from Blewett et al. (2010)

Mueller et al. (1988a)	Swager (1997)	Nguyen (1997)	Blewett et al. (2004)	Miller (2006)	Blewett et al. (2010)	
	Collapse		Late De		Minor Extension	D6
D3	D4	D4	D3	D4	Dextral Strike Slip	D5
D2 D1	D3 D2	D3 D2	D3 D2b	D3 D2	Sinistral transpression	D4a D4b
	DE	DE3	D2e	D1	Extensional doming	D3
	D2		D2a		Upright folding and reverse faulting with extension	D2
	DE	DE1-2	DE		Extension with intermittent compression	D1

2.4.2 Deformation events

Several studies proposed an early phase of extension prior to regional contractional deformations (Archibald et al. 1981; Hammond and Nisbet 1992; Williams and Whittaker 1993; Oversby 1994; Passchier 1994; Swager 1997; Swager and Nelson 1997; Brown et al 1999; Blewett 2005; Blewett et al. 2010). Some authors recognised the early extension as being related to basin formation (Martyn 1987; Hammond and Nisbet 1992; Passchier 1994) whereas

others focussed primarily on extensional greenstone *deformation*. Many of these studies infer extensional deformation related to greenstones sliding off granite dome complexes with stacking and repetition of sequence.

The extension vector for the earliest basin formation is unknown, but is generally inferred from observations in the southern flanks of elongate NNW-trending domes. This has resulted in interpreted extension vectors of NNW-SSE with top to the SSE movement during rifting (Hammond and Nisbet, 1992) or gneissic core complex uplift (Williams and Whittaker, 1993; Swager and Nelson 1997; Figure 2.4).

Contractional D1 deformation has been described widely over the Eastern Goldfields Province by Archibald et al. 1978; Archibald 1979; Platt 1980; Martyn 1987; Swager and Griffin 1990; Hammond and Nisbet 1992; Swager 1989; Swager 1997; Swager et al. 1990; Myers 1993; Williams and Whittaker 1993; Passchier 1994; Stewart 1998; Chen et al. 2001; Witt 2001; Davis 2002; Weinberg et al. 2003; Bateman et al. 2001a; Blewett 2005; and Czarnota et al. 2010. A majority of authors report south-over-north thrust transport and variably developed recumbent folding, with a few notable exceptions in which D1 is presented as an east over west directed shortening for the Golden Mile (Swager 1989; Bateman et al. 2001a). Furthermore, Swager (1997) suggested this E-W thrusting might be an early phase of D2 ENE-WSW shortening.

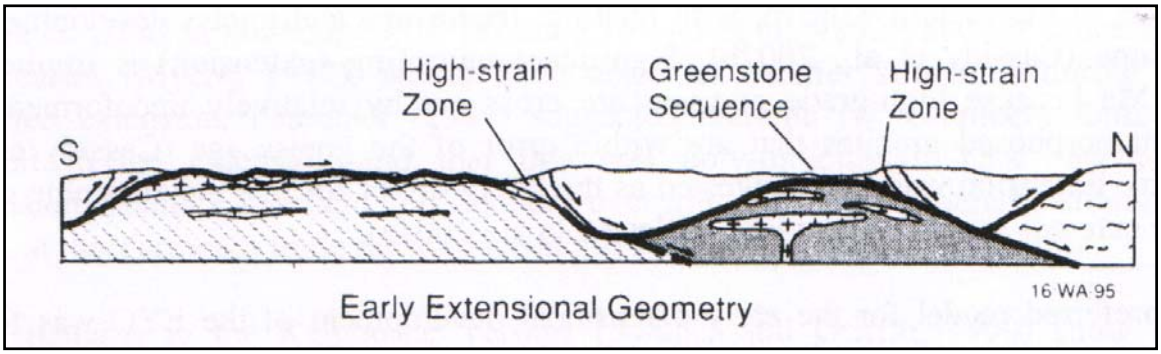

Figure 2.4 – Extensional deformation from gneissic core complex uplift (Williams and Whitaker 1993).

Basin inversion was accompanied by the earliest contractional deformation with some shortening, but not significant crustal thickening (Swager 1997). Structures interpreted as D1 are commonly preserved in the hinge areas of regional D2 domes.

The kinematics of the earliest contraction (D1) is not well constrained since the resultant structures are poorly exposed and subject to reactivation. Exposures of early structures generally contain evidence of movement consistent with latest ENE-WSW contraction, whereas their control on the distribution of greenstone stratigraphy reveals an early history (e.g. Shamrock Fault in the Boorara Domain). For this reason interpretation of D1 transport directions are problematic. Despite these difficulties, south-over-north thrusting with accompanying recumbent folding is widely reported in the literature and most authors make reference to a

critical paper by Swager and Griffin (1990) that presented D1 deformation of the Kambalda dome (Fig. 2.5; Fig 2.6). In that paper the authors state "…no definite D1 movement direction has yet been established". The basis of the conclusion of south-to-north thrusting was an interpretation of a thrust duplex south of Kambalda. However, Swager and Griffin (1990) conceded that the south-to-north movement depends on the Foster, Tramways and Republican faults could be interpreted as frontal ramps, and proposed an equally likely interpretation of those faults as lateral ramps in an E-W directed thrust duplex, similar to an interpretation made for an F1 fold at the Golden Mile in Kalgoorlie (Swager 1989).

The south-to-north D1 transport has been consistently cited from the Swager and Griffin (1990) paper, whereas the kinematics of D1 structures in other studies is generally not documented due to poor exposure. In instances where the kinematics of D1 is known (e.g. Davis et al. 2000), the documented localities again are found on the southern side of granite domes coincident with regional F2 fold axes, where granite intrusion was a potential influence in reverse faulting and stacking, and on the observed fabric styles and kinematics.

Possible alternatives for D1 stratigraphic repetition include: (1) a south-over-north event restricted to the southern Kambalda domain, hence not a 'regional' deformation event, or (2) regional D1 deformation via ENE-WSW directed shortening, producing recumbent folding and thrust repetition. This latter possibility negates the need for a major switch in tectonic shortening vectors early in the deformation history and would imply that recumbent folding and thrusting was an early phase of the major fabric forming ENE-WSW orogeny. Several other features may be explained by such an interpretation including early pre-fabric F2 folding of the greenstones that sit beneath late-stage basins, and it provides a less complicated interpretation of the tectonic setting of late clastic basins (cf. Blewett et al. 2004).

Goleby et al. (1993) interpreted abrupt truncation of reflectors, that were interpreted as regional fold limbs in seismic data, as evidence of regional E-W extension. They also interpreted reflections as stacked sequences truncated in the middle crust. Interpreted 'roll-over anticlines' were thought to become the pre-cursor to regional D2 folds with deposition of clastic basins into roll-over anticlines that were subsequently folded and stacked by D2 (e.g. Swager 1997).

The main phase of deformation in the Kalgoorlie district was an ENE-WSW directed contractional deformation that produced regional-scale folds and a pervasive, upright planar foliation (Swager et al. 1990; Swager 1989; Swager and Griffin 1990; Hammond and Nisbet 1992; Witt 2001; Davis 2002; Weinberg et al. 2003). Some new thrusts were developed in D2, which was broadly synchronous with granitoid intrusions that domed into regional anticlines. The D2 event produced a strong NNW-SSE trending structural grain, evident in greenstone belt distribution and aeromagnetic imagery. Folds (F2) dominate the regional patterns of greenstone distribution, and are variously truncated by high angle unconformities and shear zones or have

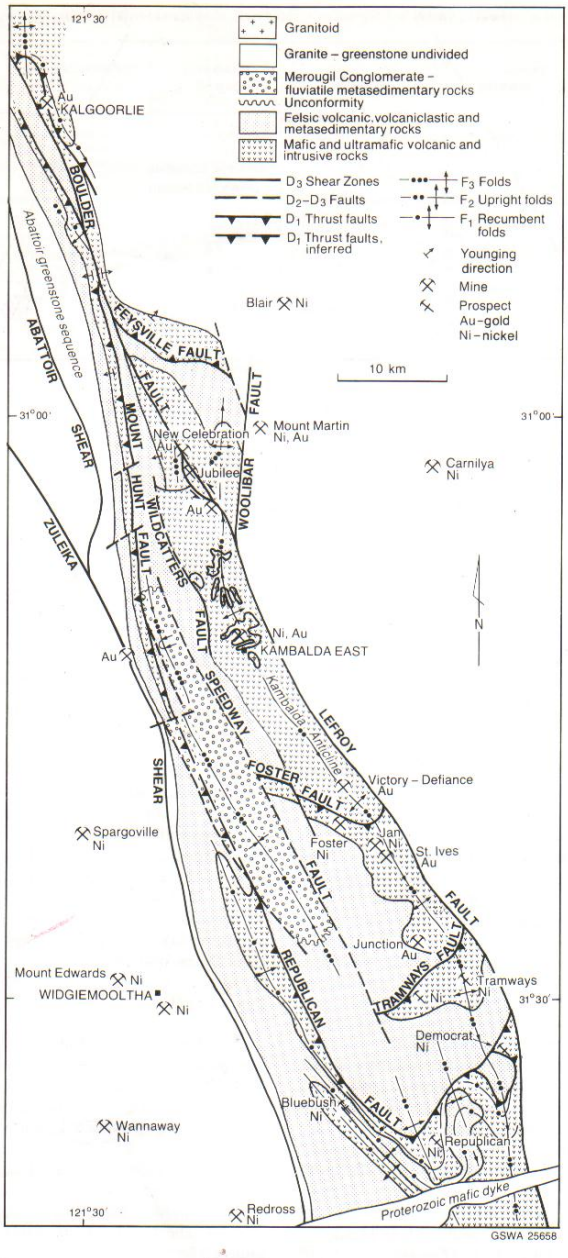

Figure 2.5– Geology and structural of the Kambalda – Tramways corridor (from Swager and Griffin, 1990).

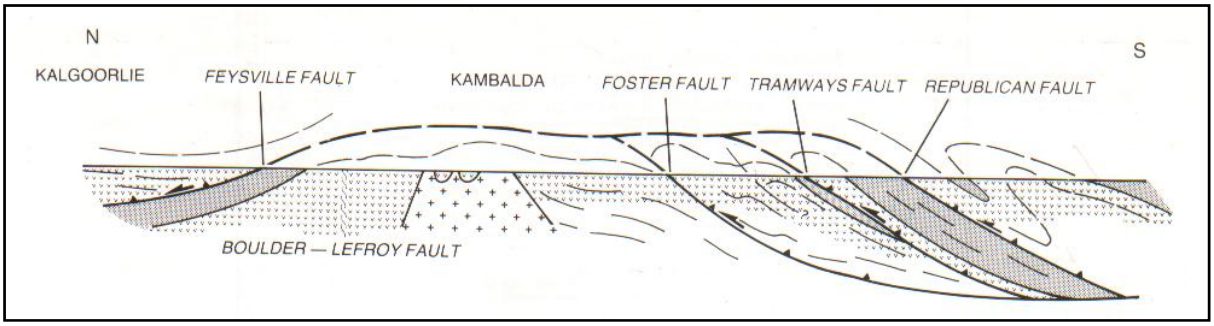

Figure 2.6 – Longitudinal section along the trace of the Kambalda Anticline (from Swager and Griffin, 1990).

attenuated limbs entrained parallel to sheared granitoid margins. Note that new data in Chapter 6 result in a re-organisation of the deformation chronology (S2 / S3 etc.) based on new observations and interpretations of cross-cutting and pervasive foliations.

Evidence for a late- to post-D2 sub-vertical shortening during post-orogenic collapse is rare but compelling, and includes sub-horizontal folds with flat axial plane foliations in the hanging wall of the Ida Fault at the Iguana mine (Davis and Maidens 2003; Fig. 2.7; Weinberg and van der Borgh 2008; and G. Tripp unpublished data). Swager and Nelson (1997) interpreted a late stage extension as facilitating the uplift and emplacement of granite-gneiss domes in the South Laverton Tectonic Zone.

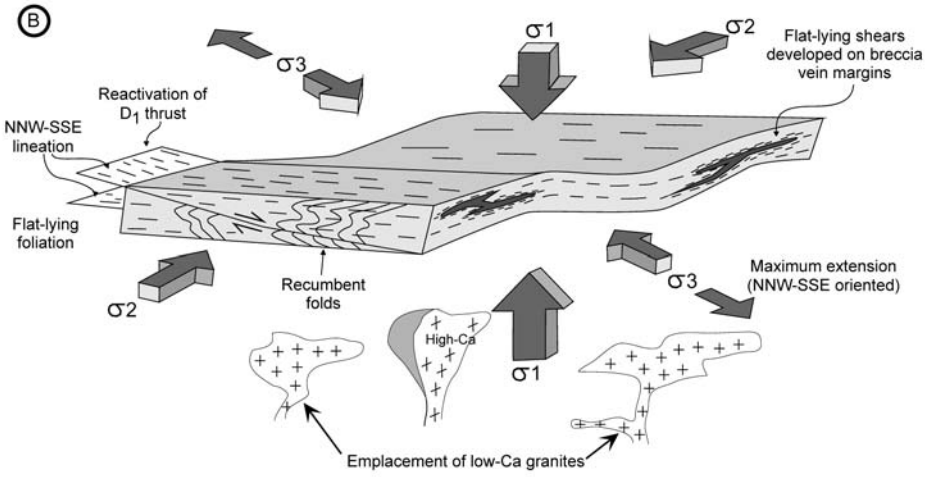

Figure 2.7 – late gravitational collapse model for the Eastern Goldfields Province (Davis and Maidens, 2003).

Deformation phase D3 was documented as a regional sinistral ductile-shearing event that produced ductile shear zones up to hundreds of kilometres long (e.g. Mueller and Harris 1987; Mueller et al. 1988); however, evidence for *major* strike-slip deformation is lacking in the study area with the exception of the Kunanalling Shear Zone (Swager 1994). Many 'D3' shear zones could be ascribed to D2 since the D3 phase is in essence a continuation of D2 kinematically and temporally, whereas the control of those shear zones on greenstone distribution suggests an earlier timing than D3 (Chapter 5). Ascribing all NNW-SSE trending shear zones to a separate 'D3' oversimplifies a situation where pre-existing D1 transfer faults, D1 thrusts and D2 thrusts may have been reactivated and/or become the foci of later strain accumulation. Shear zones newly formed during D2 may include NNW-SSE and N-S trending structures with dextral kinematics. Fabric studies of the Zuleika Shear Zone (Chapter 5) indicate changing displacement vectors and kinematic modes along the strike of the shear zone; hence, ascribing a

'D3' timing and sinistral wrenching movement sense along all interpreted shear zones may not be accurate.

The final phase of regional contraction was a faulting event usually called 'late' since many early structures are crosscut and offset by these faults, particularly the foliated Kurrawang Formation. This faulting event was characterised by Tripp and Vearncombe (2004) as a domain-wide fault network consisting of synchronous faults in three principal orientations NE-SW, N-S and E-W. Some dextral D2 shear zones may have been reactivated during this event, but D4 was interpreted as co-axial with D2 and may be the result of an increasing strain rate or exhumation at the end of a protracted regional shortening phase (Tripp and Vearncombe 2004).

A recent innovative approach to the latest deformations was taken by Micklethwaite and Cox (2004), and Micklethwaite (2007). Those authors mapped the displacement profiles of the major faults (e.g. Black Flag Fault) in detail and interpreted rupture terminations as coincident with zones of zero displacement on the faults. Damage zones were modelled using a USGS (United States Geological Survey) programme 'Coulomb', which is generally applied to neo-tectonic earthquake mitigation efforts on the San Andreas Fault, where well/bore overflow indicates active fluid movement at rupture terminations in recent earthquake events particularly on the Hayward Fault segment, San Francisco. Earthquake magnitudes for inferred Archaean faulting events were interpreted from displacement profiles, and the Coulomb programme predicted areas of fault damage and fluid-flow related to fault orientation, kinematics and magnitude. The results of that research indicated coincidence of damage zones with areas of known high-density faulting and quartz veining in the Mount Pleasant gold district. The presumed aftershock activity of the damage zone matched well with the textural characteristics of gold lodes in the Mount Pleasant gold deposits (i.e. multi-stage hydrothermal breccia, laminated fault hosted quartz veins etc.).

2.4.3 Kinematic interpretations

Kinematic analyses of D2 folding are generally considered in the context of ENE-WSW shortening (Swager 1997); subsequent shearing (D3) and faulting (D4) events display evidence for *later* development during a consistently oriented ENE-WSW contraction (Tripp and Vearncombe 2004). In contrast, several studies have inferred stress switches between these events based on assumptions about the interpreted sinistral nature of 'D3' shear zones and the interpreted dextral nature of D4, from detailed mapping in granite dome pavements and localised gold mines. Recent work by Blewett et al. (2004) suggested the D2 phase of contraction consisted of four separate pulses of shortening with switches in 'stress axes' from E-W to NW-SE, to NE-SW, and back to E-W. These events are timed prior to a NNW-SSE shortening that folded the upright foliation 'S2' and tilted regional folds to both north and south plunges. A further 5 shortening events with separate 'stress axes' were also inferred (Fig. 2.8).

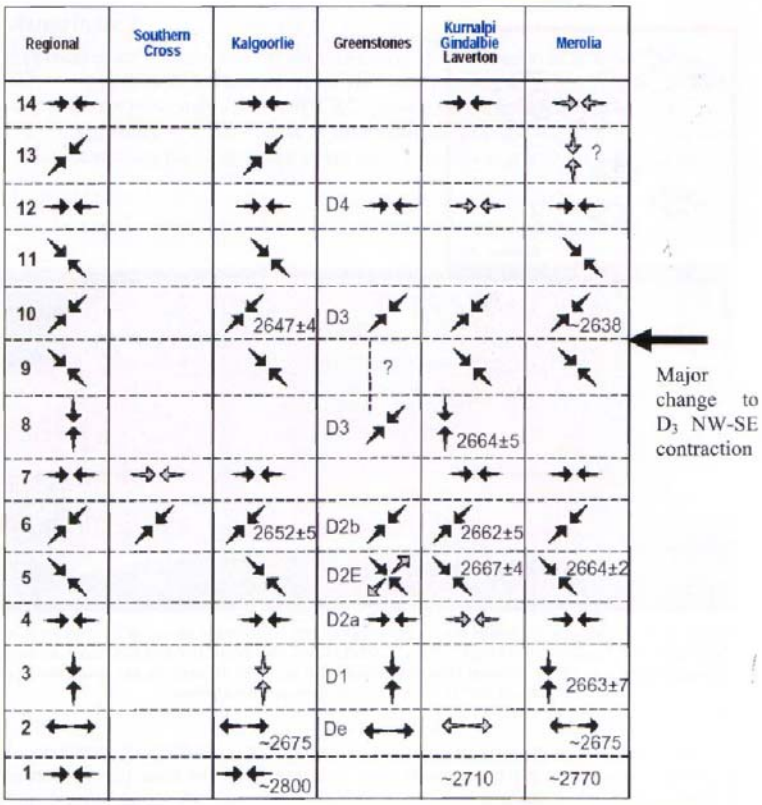

Figure 6-15: Main NW-SE D_3 contractional change occurs just before Low-Ca magmatism in granites (Blewett et al., 2004a).

Figure 2.8 – Interpreted multiple switching of stress axes across terranes of the Eastern Goldfields Province (Blewett, 2005)

The published interpretation of switches in shortening directions uses some data from ductile rock fabrics, and hydrothermal vein deposits that were not formed by instantaneous brittle deformations, and alternatively may have resulted from accumulated strain over a period of time, potentially with rotation of pre-existing fabrics. In that respect, interpretations of stress axes from ductile finite strains are suspect. Detailed kinematic work on regional ductile shear zones demonstrates widely variable kinematics within the same shear zone (Eisenlohr et al. 1989; Passchier 1994; Libby et al. 1990; Vearncombe 1998; Tripp 2002b; Chapter 5), which can be explained by (1) reorientation of finite strain axes in the presence of rheological contrast, (2) changes in orientation of a shear zone, or (3) transpression with a high ratio of pure shear to simple shear (Blenkinsop 2004; Tripp and Vearncombe 2004). Brittle-ductile faults in the study area have three principal orientations with mutual crosscutting between the three principal fault groups, and a consistent interpreted axis of shortening; hence the kinematic data used to constrain 'stress switches' need to be cautiously evaluated for deformation style, crosscutting relationships, and the potential influence of hydrothermal fluid pressure in controlling localised vein development. Variable orientations and magnitudes of stresses are characteristic of the seismic cycle (Sibson 1977), and are independent of longer term, regional stress changes, which

may add significant complexity to the interpretation of palaeo-stresses, particularly from 'brittle' structures.

2.4.4 Domain boundary faults

Major faults in the Kalgoorlie district are described as separating tectonostratigraphic domains (Swager et al. 1990; Morris 1993; Swager 1997; Weinberg et al. 2003). The definition of domains in the early literature was based on contrasting geological, structural and metamorphic histories with inferred vertical crustal movements (e.g. Swager et al. 1990). However, recent studies and compilations of metamorphic data by Witt (1993), Mikucki and Roberts (2004) and Goscombe et al. (2010) demonstrate that metamorphic isograds crosscut some regional scale ductile shear zones and domain boundaries, whereas isograds are systematically arranged around late stage Mafic and Low-Ca plutonic intrusions that postdate the majority of greenstone belt construction. The concept of domain boundaries is therefore primarily an issue of stratigraphy (Swager et al. 1990) and the presence or absence of units described in Section 2.1 is the main discriminator of domain boundaries.

Domain boundaries are indicators of a pre-contractional distribution of greenstones and they may represent the positions of original extensional structures during basin formation. Several of those structures demarcate major thickness variations in various stratigraphic units across their boundaries (e.g. Zuleika Shear Zone; Bardoc Tectonic Zone; Bullabulling Shear Zone; Mount Monger Fault; Boulder Fault) and these may be used to attempt stratigraphic reconstruction. Thickness variations in volcanic rocks can be explained by palaeo-topography and proximity to source, eruption style as a function of composition (felsic vs. mafic), or stratigraphic growth during extensional faulting.

Domain boundaries are generally considered to be high strain zones, but this relationship is not universal. The 'Kanowna Shear Zone' is an often cited 'high strain zone', which new mapping demonstrates as an unconformity lacking high strain or tectonic interleaving (Standing 2004a). Original extensional faults are not necessarily reactivated during inversion and may retain relationships produced during original extensional deformation (McClay 2002). In some instances the interpretation of domain boundaries may have relied on strain arguments rather than demonstrable stratigraphic change.

2.5 Geodynamic interpretations

2.5.1 Long standing controversy

A gradual change in the interpretation of Archaean tectonics has occurred starting in the early 1970's, through 1980's and to the present day, ranging from early authors cautious about projecting a uniformitarian approach from the present to the Archaean, to modern publications

that show a much greater acceptance of plate tectonics throughout earth history and the beginning of plate tectonics as early as 3.85 Ga.

A consensus at the 1975 Penrose Conference on 'Pre-Mesozoic Tectonics' determined "...Archaean global tectonics were radically different from Mesozoic-Cainozoic plate tectonics..." (Dewey and Spall, 1975), but that basal komatiites represent ocean floor with island arcs built upon the komatiitic oceanic crust in microplate tectonic settings (Goodwin and Annhaeuser - referenced in Dewey and Spall, 1975). For the Proterozoic, arguments were offered in favour of plate tectonics (e.g. West African aulacogen), but there were also arguments against, including the interlacing Pan African belts where geology and palaeomagnetic studies implied structural coherence of cratonic blocks (Shackleton and Wood - referenced in Dewey and Spall, 1975; see also Kroner 1977, 1979). The nature and recognition of sutures that mark the existence of former oceans were considered key arguments (Dewey 1977).

A review paper by Gee et al. (1981) from the Second International Archaean Symposium (Glover and Groves 1981) considered that "Diapiric movement of granitic substrate, with compensatory sinking of greenstone sequences, must be considered as the most important deformation mechanism in the Yilgarn Block", and that "Density inversion is seen as the main tectonic driving force". Giles (1981) in the same volume reviewed field evidence for calc-alkaline volcanism (andesites) throughout the Eastern Goldfields Province and concluded that the distribution of low-volume calc-alkaline rocks in discrete isolated centres rather than arcs argued against a subduction origin for those rocks, despite requirements for hydrous melting of the upper mantle in their petrogenesis. Park (1981) considered that the widespread horizontal structure of high-grade Archaean gneiss terranes was a result of gravity spreading associated with diapiric emplacement of granite plutons, and was not a result of subduction tectonic processes.

Archibald et al. (1981) concluded that "tectonic features of the terrain are not directly analogous with modern plate-tectonic settings, for example oceans or back-arc basins", but the vast volume of granitic rocks without mafic/ultramafic residues suggested a subduction-like process. It is notable that Talbot (1973) presented arguments in favour of a plate tectonic model for the Archaean, and Tarney et al. (1976) preferred a Pacific marginal basin analogy to explain the development of Archaean greenstone belts.

Since that time most Archaean workers interpret plate / plume or mixed tectonic models (e.g. Condie 1986; Card 1990; de Wit and Ashwal 1997; de Wit 1998; Percival et al. 2001; and various papers in the $4^{th}/5^{th}$ International Archaean symposia). Notably, some Archaean and Phanerozoic workers strongly object to the application of plate tectonics beyond the Neoproterozoic (Hamilton, 1998; McCall 2004; Stern 2008; Bedard 2010; Hamilton 2011). A review of abstracts from the recent 2010 global 5th International Archaean Symposium appears

to indicate a *relative consensus* of modern workers on the application of plate tectonics to the Archaean (starting as early as 3.85 Ga):

- The onset of subduction was interpreted at 3.85 Ga inferred from work on diamonds, interpreting stabilisation of continental crust from subduction processes as suggested by eclogitic sulphide inclusions in diamonds from Orapa, Zimbabwe that contain atmospheric sulphur in lithospheric materials (Shirey and Carlson 2010).
- From a worldwide TERRANECHRON database of 12,375 zircon analyses, Hf isotope data show that most magmatic rocks represented in each of the major age episodes were derived from recycled pre-existing crust and indicate extensive subduction recycling (Belousova et al. 2010).
- The orogenic evolution of the Superior Province has been interpreted as a product of plate tectonics with recognition of numerous isotopically, chronologically, and geophysically distinct continental and oceanic terranes (Percival 2010).
- For the early Archaean, steep modern style subduction is interpreted to have commenced at ~3.2 Ga when plate size may have increased as a function of planetary cooling and the development of thick protocontinental nuclei that would have helped deflect plates downward (Van Kranendonk 2010).

The case *in favour* of plate tectonics also includes broad geochemical factors that attempt to identify key rock assemblages that are present in modern settings:

- Boninites, primitive andesites and LREE enriched mafic rocks documented in the Archaean (e.g. Smithies et al. 2003; Angerer et al. 2013) are thought to represent anomalously hot supra-subduction zone conditions, and where closely associated with komatiite magmatism are considered to indicate plate settings beginning at least <3.12Ga.
- Evidence for mantle wedge interaction in modern settings is determined by the presence of sanukitoids (elevated Mg#, Ni, Cr in Tonalite-Trondhjemite-Granodiorite-TTG), metasomatised mantle wedge products, and abundant ‘arc rocks’ (e.g. Oliveira et al. 2010).
- In the Archaean, Low and High Al TTG’s (interpreted as akin to modern adakites) are partial melts of mafic lower crust, yet the tectonic setting of these rocks is non-unique and they can be interpreted as a result of plume heating of the base of crust, or slab melts (Martin 1986; Martin et al. 2005). Syn- to post-deformational mafic series intrusions are interpreted as products of melting a metasomatised mantle wedge above a subduction zone (Champion and Cassidy 2007).

- Long linear belts of mafic-ultramafic seafloor volcanic rocks and associated sedimentary rocks separated by major shear zones interpreted as crust penetrating thrusts and strike slip amalgamation structures are typical of the Neoarchaean (but note these are not demonstrably 'ophiolite' in the accepted modern sense; Hamilton 1998; Bickle et al. 1994; Moores 2002).
- Eastern Goldfields Province-wide deformation and development of syn-orogenic basins has been interpreted as a collision phase assemblage (e.g. Krapez and Barley 2008) or as a late core-complex style extensional product (Czarnota et al. 2010).

In contrast to those *'pro-plate tectonic'* interpretations, Bedard (2010) argued that modern subduction settings are unlikely to represent the tectonic settings of Archaean greenstones since Archaean TTG greenstone-granite dome-and-keel associations (e.g. Superior Province of Canada; Bedard et al. 2003) do not occur at modern convergent margins, and andesitic strato-volcanoes and fold-thrust belts, common in the modern, are atypical of Archaean terranes. Models of tectonic development for the Abitibi Belt have swung between end members of regional layer-cake stratigraphy to collages of micro-terranes (Bleeker and van Breemen 2010), but given the polyphase deformation history and geological complexity of the Abitibi Belt, those authors expect a realistic model will lie somewhere between the two extremes.

The case *against* also includes several broader arguments related to the modern characters of subduction and plate interaction, particularly those of Stern (2008) and Hamilton (1998, 2011); with the latter author's interpretations being critically appraised by McCall (2004) using his detailed mapping of the Makran Accretionary Complex in Iran:

- Key indicators of Archaean subduction are not demonstrated: ophiolite absent - defined as preserved oceanic crust with mafic-crustal rocks ending in depleted mantle rocks; blueschist is absent - defined as HP/LT exhumed silicic rocks; paired metamorphic belts are absent; broken formation melange is absent.
- Compositional analogies with Phanerozoic arcs are weak: Phanerozoic rocks are unimodal with a mafic peak, whereas Archaean 'arc rocks' are sharply bi-modal with strong mafic and felsic peaks. Archaean / Phanerozoic TTG's have significantly different geochemistry (Archaean TTG's have steeper REE patterns, less Mg, Ca; higher Si-Na-K than Phanerozoic equivalents). Phanerozoic TTG's are a minor component of modern arcs dominated by diorite and gabbro (cf. vast terrains of Archaean TTG).
- Archaean andesites are relatively uncommon compared to voluminous distribution in Phanerozoic arcs, and have lower Al, and higher Fe, FeO/Fe2O3, Mg, Ni, Cr, Co, and Zn, than modern arc andesites.

- Archaean supracrustal sequences have sub-regional continuous stratigraphy of a lithotectonic assemblage that is nowhere found in modern depositional settings.
- Archaean 'boninites' (rare in modern arcs) are lower in Si, higher in Al and heavy rare-earth elements (HREE): i.e. not modern boninites.

2.5.2 Tectonic models applied to the Neoarchaean of the EGP

Several tectonic models have been applied to the Eastern Goldfields Province on the basis of stratigraphy, geochemistry and petrogenetic interpretations of the sequences with most involving a former sialic basement (Fig. 2.9a,b,c). The proposed models include:

- Plume (vertical) tectonics (Campbell and Hill 1988)
- Ensialic Rift – Early sial (Groves and Batt 1984; Morris 1993; Swager 1997)
- Westward dipping subduction-accretion tectonics (Morris 1998; Nelson 1997; Smithies et al. 2003)
- Hybrid models (Czarnota et al. 2010)

Many of these models use mafic volcanic and felsic volcanic geochemistry for petrogenetic interpretations, with a general consensus including: plume involvement in komatiite magmatism; arc related felsic volcanic rocks; and early sialic basement (Campbell and Hill 1988; Swager 1997; Bateman et al. 2001b). For the Kalgoorlie district, Bateman et al. (2001b) envisaged mafic magmas erupted onto continental crust as indicated by the presence of 2.9-3.4 Ga xenocrystic zircons. Komatiites were considered high-T / high-P, high-melt-fraction mantle melts, whereas basalt geochemistry indicates extraction from a depleted mantle evolving from residual plagioclase to residual garnet, and suggests progressively deeper melting (Bateman et al. 2001b). In the mafic volcanic sequences there is a gradual increase in the degrees of crustal contamination to Paringa Basalt, then rapid diminution of contamination at upper levels of the mafic pile (Bateman et al. 2001b). The time gap between hot, deep-sourced high-Mg magmas and lithospheric mantle derived Black Flag gabbros and basalts was interpreted to coincide with a belt wide extensional event (responsible for widespread felsic volcanism).

Morris (1998; Fig. 2.10a,b) used the chemistry of andesites, dacites, and rhyolites of the Black Flag Group to suggest that those rocks resulted from melting of a mafic protolith, siting similar chemical characteristics to high-Al TTD and their Cainozoic analogues (adakites). He attributed those rocks to the partial melting of a mafic protolith transformed to amphibolite or eclogite during shallow subduction. Morris's modelling suggested production of felsic volcanic rocks of the Black Flag Group required residual amphibole and garnet, where melting would have occurred at pressures of more than 10 kbar, corresponding to about 35 km depth.

Smithies et al. (2003) argued for west-dipping Archaean 'flat subduction' whereby TTG was produced as the lower part of a thickened crust, once melted, leaving an eclogitic residue with an upwelling mantle that provided a heat source for more TTG and a basalt source for

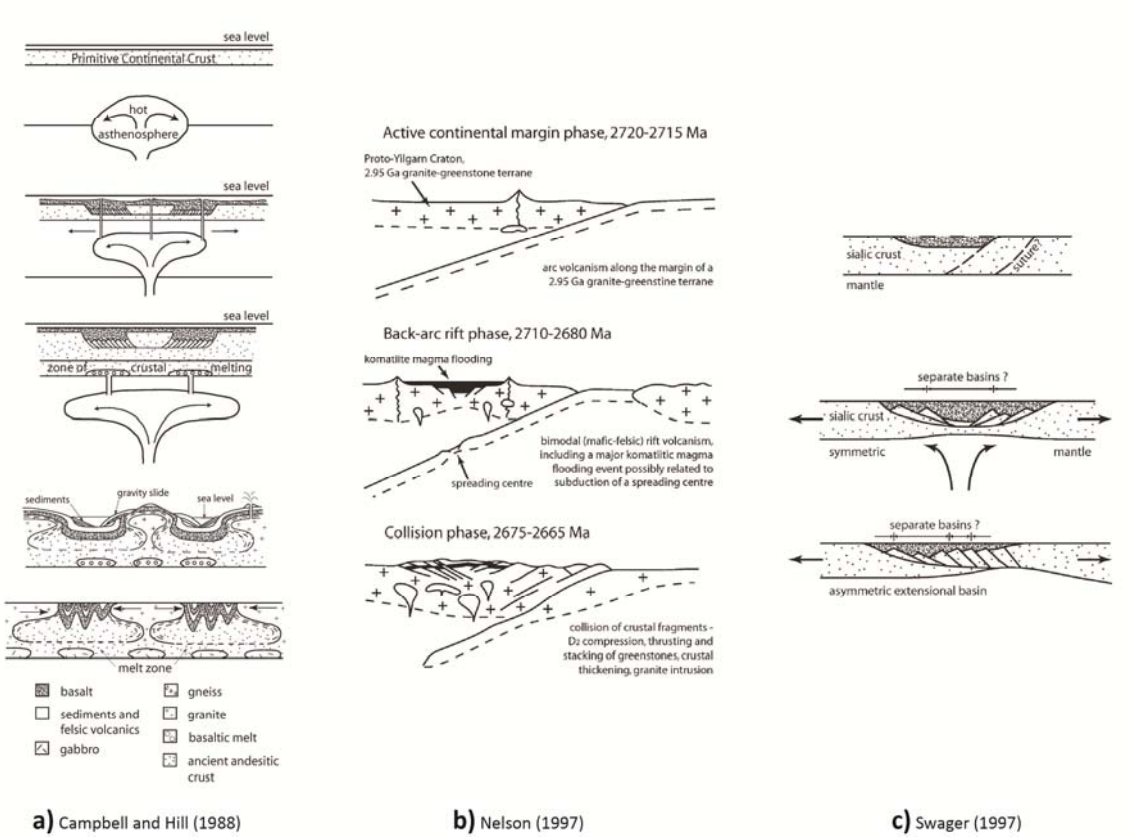

Figure 2.9 – Various tectonic models applied to the Eastern Goldfields province, a) Mantle plume interacts with primitive continental crust (Campbell and Hill, 1998); b) Active compressional setting with, subduction related rifting, back-arc supra crustals, and continental collision (Nelson, 1997); c) Microcontinental fragments amalgamate to form sialic crust, extensional rift basins form depocentres for volcanics in an ensialic rift (Swager, 1997). Figures modified from Trofimovs (2003).

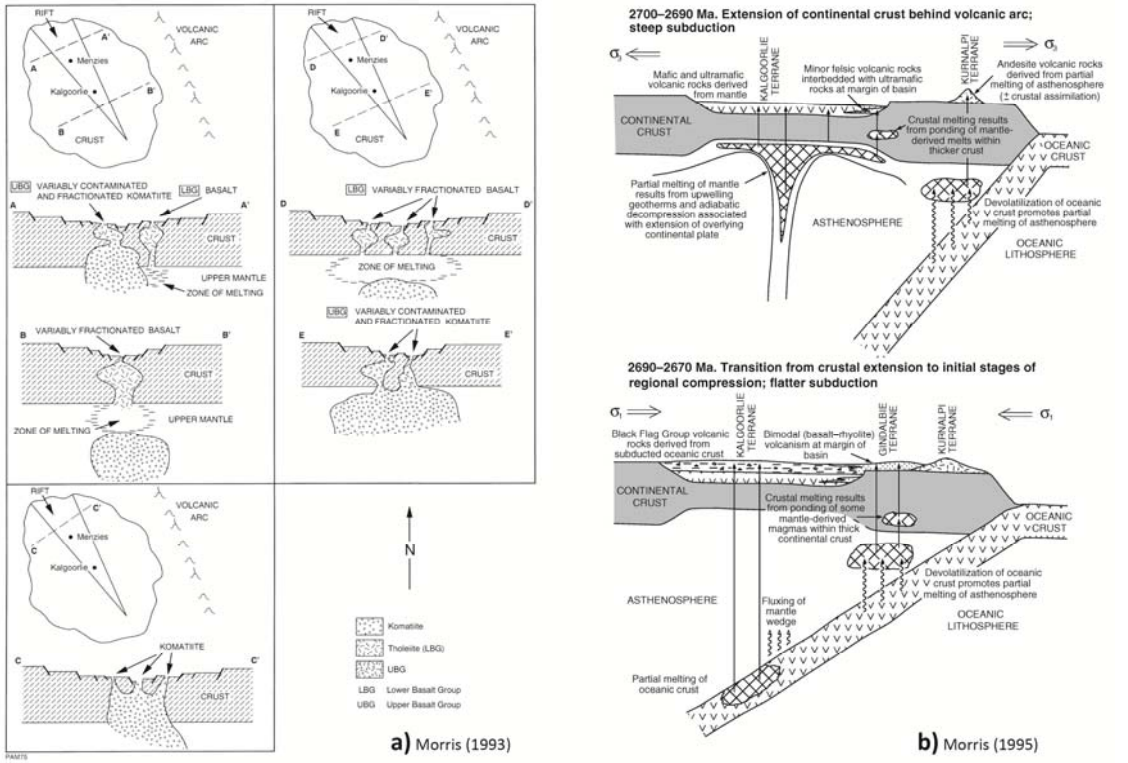

Figure 2.10 – Tectonic models for the Menzies-Norseman belt proposed by Morris (1993; 1998) on the basis of petrogenetic interpretations of mafic and felsic volcanic rocks

supracrustal rocks (Fig. 2.11a). Czarnota et al. (2010) also favoured westward-dipping subduction (Fig. 2.11b), with slab melting in response to shallow subduction over a thermal mantle anomaly and "high-Ca granitoids derived from slab melting, interacting with the lower crust in a 'MASH' zone" (MASH: granite Mixing, Assimilation, Storage and Hybridization), where the melts acquired an evolved Sm-Nd signature and formed a dense eclogitic lower crust (Czarnota et al. 2010).

Plume models are generally accepted as involved in the production of at least the ultramafic and mafic magmas by most authors, but some suggest *all* magmatism and later deformation is a response to plume tectonics (e.g. Campbell and Hill 1988). Many authors end with some variation of a plate-tectonic model including:

- Steep slab / shallow slab (Nelson 1997; Smithies et al. 2003)
- Oceanic crust outboard to the east (lower plate; Morris 1998; Nelson 1997; Smithies et al 2003; Czarnota et al. 2010)
- Tectonic mode switching (extension to compression; Blewett et al. 2010; Czarnota et al. 2010)

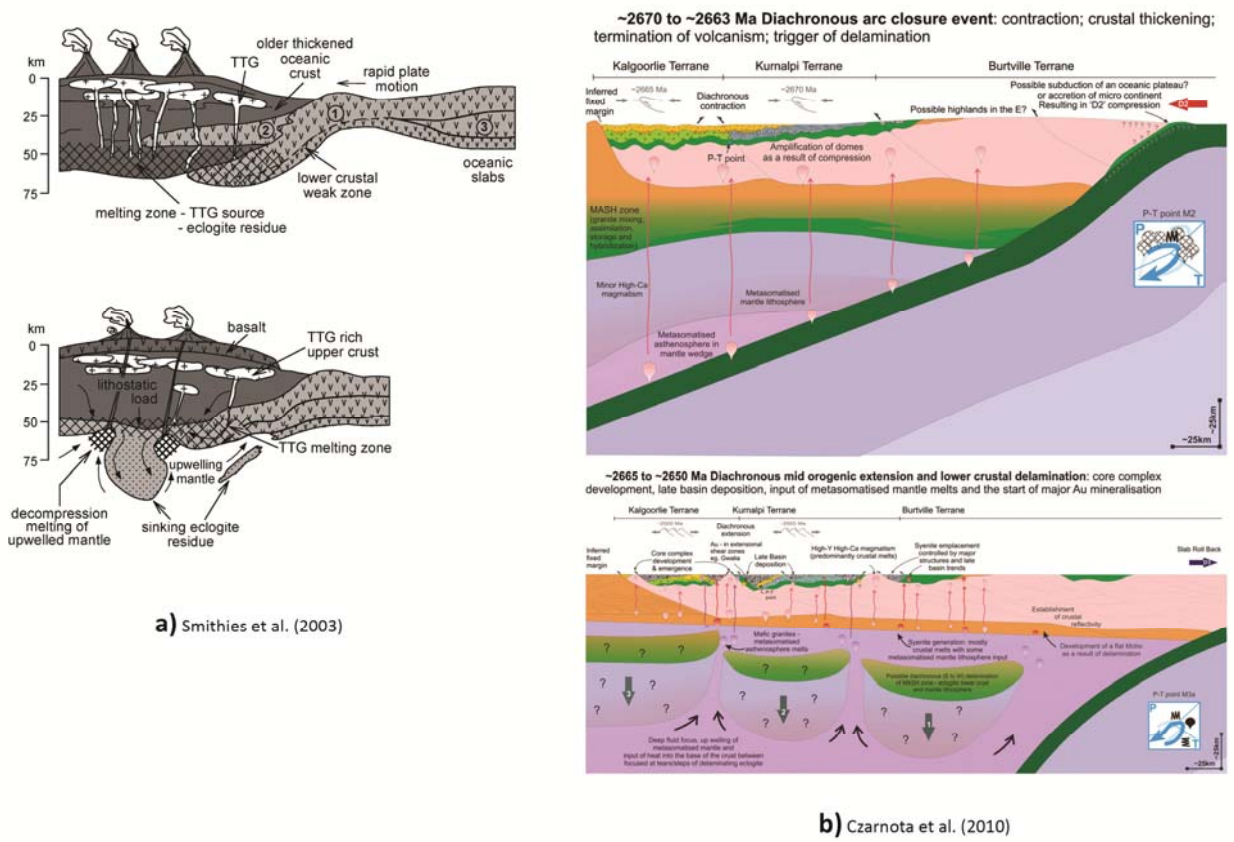

Figure 2.11 – Tectonic models applied to the Eastern Goldfields Province, a) Archaean 'flat subduction' in which TTG, produced as lower part of thickened crust, melts leaving eclogite residue, upwelling mantle provides heat source for more TTG and basalt source for supracrustals; b) Westward-dipping subduction zone, with slab melting in response to shallow subduction over a thermal mantle anomaly – with "high-Ca granites derived from slab melting.

- Late collision or subduction of seamounts to explain contractional deformation (Nelson 1997; Czarnota et al. 2010)
- Ensialic rift models (non-specified far-field contractional agents; Morris 1993; Swager 1997)
- Extension only models – volcanism / deformation / mineralisation (Hammond and Nisbet 1992; Williams and Whitaker 1993)

Analogy with modern settings for the late siliciclastic sequences was made by Krapez and Barley (2008), who interpreted those rocks as remnants of linear basins produced by subsidence between intra-terrane faults, similar to graben and half-graben in the Western Anatolian province of Turkey (Fig. 2.12). Linear subsidence zones were interpreted as developed adjacent to strike-slip, oblique-slip, or normal-slip faults, in a tectonic setting similar to a projected collision between the Phillipine Archipelago and continental crust of the South China Sea. An 'orogenic architecture' similar to the accreted superterranes of the Canadian Cordillera was interpreted for the Burtville, Kalgoorlie, Gindalbie and Kurnalpi terranes of the Eastern Goldfields Province (Krapez and Barley, 2008).

2.5.3 Evidence from isotopic studies

On the basis of neodymium isotopic data, volcano-sedimentary sequences across the Eastern Goldfields Province were interpreted as marginal arcs by Cassidy et al. (2006), as opposed to intra-oceanic island arcs. They further speculated that the tectonic setting was characterised by recycling of >3.0-2.8 Ga crust along a complex convergent margin: the coincident addition of newly generated crust and recycling of >3.05 Ga crust were interpreted from hafnium isotopic data, with interpretation of dominantly continental margin signatures and magmatic recycling of older arc crust (Cassidy et al. 2006). These techniques were used to interpret tectonostratigraphic terranes of a single arc / back-arc system that was dismembered and reassembled by accretionary tectonics (Cassidy et al. 2006; also Krapez et al. 2000; Barley et al. 2002).

A review of existing isotopic data for the Yilgarn Craton was presented by Wyche et al. (2012), who concluded the data support the presence of an ancient crustal block in the eastern part of the Southern Cross Domain, and that craton-wide isotopic data indicate focussed contemporaneous addition of juvenile crust in the Eastern Goldfields and Murchison Domains. The Sm-Nd and Lu-Hf data show that local, newly-generated crust in the Murchison was coeval with crust generated in the Eastern Goldfields Province (Wyche et al. 2012; Cassidy et al. 2002; Ivanic et al. 2010); and that these were possibly affected by coeval magmatic events i.e. craton-wide magmatism <3.0Ga simultaneously affected all terranes (Van Kranendonk and Ivanic 2009). Wyche et al. (2012) interpret contemporaneous stratigraphic successions across the Yilgarn as products of the same large scale events.

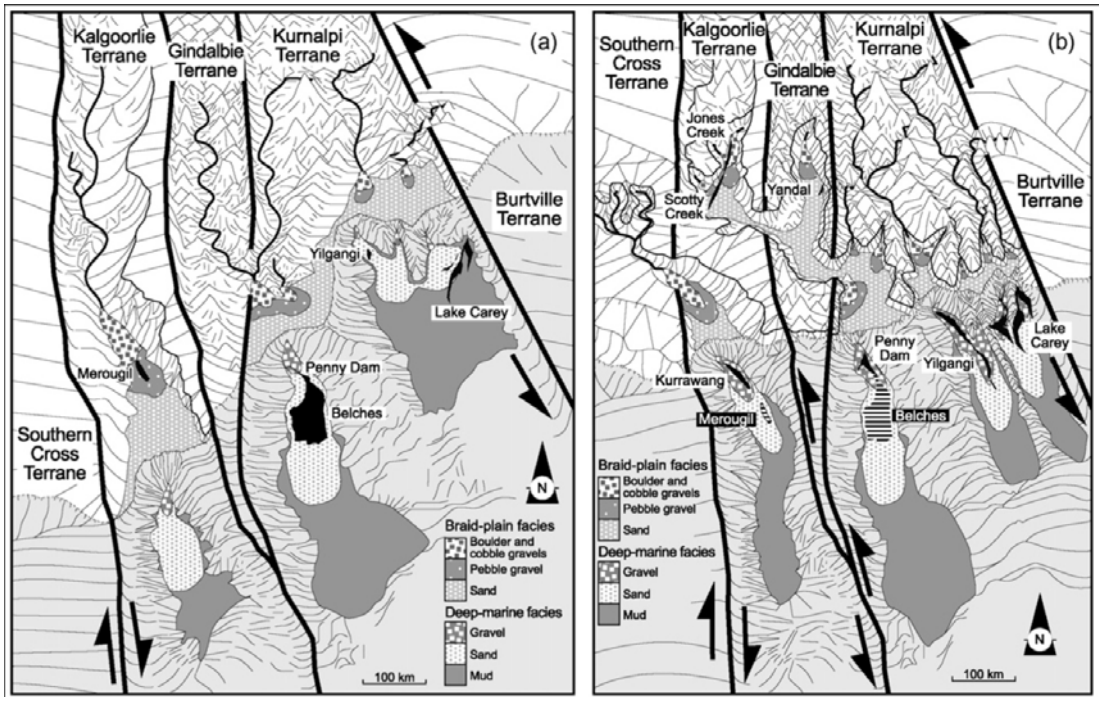

Figure 2.12 – Palaeo-environmental reconstruction of late-stage basins in linear subsidence zones between intra-terrane faults (Krapez and Barley 2008).

On the basis of common histories between the Youanmi Terrane and Eastern Goldfields Province, interpreted from isotopic data, Wyche et al. (2012) conclude that "the older parts of the Eastern Goldfields Superterrane do not represent an amalgamation of terranes that were exotic to the proto-Yilgarn craton"; furthermore, they state that consistent spatial distribution patterns of young crust are not requisite to the interpretation of allochthonous terranes; and that due to their degrees of isotopic similarity, adjacent 'terranes' in the Eastern Goldfields Province may never have been significantly separate entities, and are not necessarily the products of arc accretion of exotic fragments. Their preferred interpretation is that a widely recognised ~2800 Ma magmatic event may have initiated rifting of early formed components of the Eastern Goldfields Province (Wyche et al. 2012).

Similar conclusions to those of Wyche et al. (2012) were reached by Barnes et al. (2012) who took to task several points of the arc-accretion hypothesis advanced for the Eastern Goldfields Province and wider Yilgarn Craton. The latter authors were particularly concerned with geochemistry and the issue of scale in the subduction / arc-accretion models advanced by Barley et al. (2008) and Czarnota et al. (2010), which in those papers are orders of magnitude smaller that what is required in plume magmatism, interpreted as responsible for the formation of large igneous provinces. The Czarnota et al. (2010) interpretation of plume heads impinging on arc settings was also marked as problematic and recognised to have fundamental differences to modern examples of hot spot tracks interacting with arc systems.

In terms of lithotectonic assemblages Barnes et al. (2010) concluded there is no evidence anywhere in the Eastern Goldfields Province for basaltic rocks with characteristic island arc

basalt signatures (Nb-depleted, low-Ni, low-Cr). Furthermore they state that andesites in the Kurnalpi Terrane are not necessarily products of subduction, nor in fact are they exclusive to arc settings generally (references in Barnes et al. 2012); and that the low-Th basalt populations (Morris 1993) from the adjacent Kalgoorlie 'terrane' (interpreted back-arc) and Kurnalpi 'terrane' (interpreted arc), are essentially indistinguishable from one another.

2.6 Gold mineralization

Gold rich ore deposits are sub-divided into distinctive model types listed in Table 2.3 as a series of 'deposit clans' (Poulsen et al. 2000; Robert and Poulsen 1997; Robert et al. 2007) providing a substantial genetic framework for the interpretation of gold deposit settings ranging in age from Archaean through Phanerozoic (Fig. 2.13). This concept was advanced by Robert et al. (2007) with detailed description and global examples of major gold deposits from each clan.

Neoarchaean greenstone-hosted gold deposits were previously interpreted with unifying models for Archaean mineralisation processes i.e. the metamorphic replacement model (Phillips and Groves 1993); the crustal continuum model (Groves 1993; Gebre-Mariam et al. 1993, 1995); intrusion-related models (Durring et al. 2007) and an all encompassing designation of Neoarchaean deposits, the 'orogenic' model (Goldfarb et al. 2001; Groves et al. 2000; Groves et al. 2003). Neoarchaean greenstone-hosted gold deposits are generally described as 'orogenic lode-gold' deposits emphasising a synchronous-to-late timing of gold mineralisation with respect to major deformation events, and hence, a close association in space and time with orogenesis. Critically, and controversially, 'orogenic' is used by some authors to imply a convergent margin setting related to subduction (Groves et al. 2003; Goldfarb et al. 2001). Other distinguishing characteristics of this clan are listed in Table 2.4.

Robert et al. (2007) further subdivided the orogenic clan by host sequence into greenstone-hosted deposits; turbidite-hosted veins; and BIF-hosted (Banded Iron Formation; Table 2.3). For Neoarchaean gold deposits, recent studies have emphasised the presence of additional deposit styles including some that are atypical for the 'orogenic' clan (including modified Cu-Au-Mo porphyry; volcanic associated Zn-Pb-Ag-Au massive sulphide; Zn-Pb-Ag-Au or Ba-Au-Mo-Hg submarine epithermal systems; Groves et al. 2003); and other anomalous styles that suggest some ambiguity in the simple 'orogenic' designation for Archaean deposits (e.g. the 'anomalous low-sulphidation alkalic' designation for the Fimiston, Golden Mile deposit by Jensen and Barton, 2000; and the 'porphyry style' Carosue Dam deposit by Witt and Hammond, 2008). Attempts to organise Archaean greenstone-hosted deposits into a broader framework with younger mineral systems is a relatively recent development, and highlights the relationships of mineralisation, tectonic setting, crustal depth and association with magmatism.

A voluminous literature on Archaean gold deposits in the Eastern Goldfields Province, and particularly Kalgoorlie, shows much focus on descriptive documentation of isolated

Table 2.3 - Major gold deposit clans (extract from Robert et al. 2007)

Clan	Deposit Type	Key Features of Ore-Forming Environments (Regional Scale)
Orogenic	Greenstone-hosted deposits	- Volcanic- or sediment-dominated greenstone belts; Crustal-scale shear zone; Conglomeratic rocks
	Turbidite-hosted veins	- Folded turbidite sequence; Granitic intrusions - Crustal-scale faults; Greenschist grade
	BIF-hosted	- Volcanic- or sediment-dominated greenstone belts containing thick iron formations; Folded and metamorphosed
Reduced Intrusion Related	Sediment Hosted Intrusion Related	- Faulted and folded reduced siliciclastic sequences; Granitic intrusions; Crustal-scale faults
	Intrusion-Hosted Mesozonal	- Reduced siliciclastic sequences; Belts of moderately reduced intrusions; Common association with W-Sn belts
	Intrusion-Hosted Epizonal	- Reduced siliciclastic sequences; Belts of moderately reduced intrusions; Common association with W-Sn and/or Sb belts
Carlin		- Faulted and folded miogeoclinal sequences; Slope-facies lithologies (silty carbonate); Felsic magmatism
Oxidized Intrusion Related	Au-rich Porphyry	- Calc-alkaline to alkaline magmatic arcs; Regional arc-parallel fault; Coeval volcanic cover not abundant
	High (intermediate) sulphidation epithermal	- Calc-alkaline to alkaline arcs andesitic to dacitic arcs; Regional arc-parallel fault; Preserved volcanic cover
	Low sulphidation epithermal Alkalic	- Extensional settings related to island arcs and rifts; Alkaline magmatic belts; Regional faults
Other	Low sulphidation epithermal Subalkalic	- Intra-arc to back-arc, rift-related extensional settings; Subaerial bimodal volcanic suites (basalt-rhyolite)
	Au-rich VMS	- Rifted arcs and incipient back-arcs; greenstone belts; Mafic-felsic submarine volcanics
	Paleoplacer	-Very mature sediments in cratonic sedimentary basin; Foreland or back-arc basins

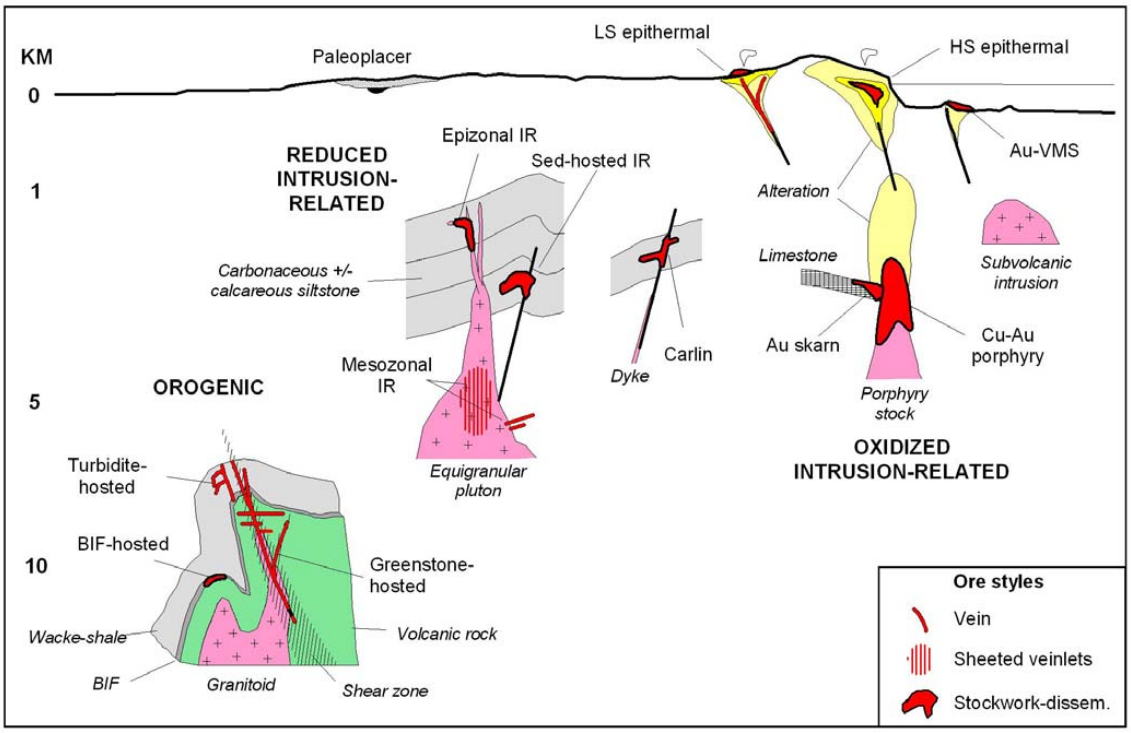

Figure 2.13 – Schematic compilation cross-section of major gold deposit styles indicating crustal depth of formation against a logarithmic depth scale (from Robert et al. 2007; modified from Poulsen et al. 2000)

Table 2.4 – Defining characteristics of gold-only deposits in the Orogenic Clan (from Groves et al. 2003)

Host rocks	Extensive greenschist to lower amphibolite facies host rocks
Timing	Localised in the latter part of the deformation / metamorphic history of the hosting terrane
	Ores are developed syn-kinematic with at least one stage of penetrative deformation
Geometry	Vertical dimensions of 1-2km with only subtle vertical metal zoning and strong lateral zonation of wallrock alteration with addition of K, As, Sb, LILE CO_2 and S
	Strong structural control
Ore style	Quartz-carbonate veins are ubiquitous and commonly gold-bearing, or in many systems gold is in sulphidised high Fe/Fe+Mg+Ca wall rocks
	Wallrock alteration varies from sericite-carbonate-pyrite at high crustal levels through biotite-carbonate-pyrite to biotite-amphibole-pyrrhotite and biotite/phlogopite-diopside-pyrrhotite at deeper crustal levels
Fluid chemistry	Metal association: Au-Ag ± As ± B ± Bi ± Sb ± Te ± W, with high bulk Au/Ag ratios
	Only slight enrichments of Cu, Mo, Pb, Sn and Zn
	Deposited from low salinity, near-neutral, H_20-$C0_2$ ± N_2 fluids that transported Au as a reduced sulphur complex
	Variable S and C isotope ratios that varied with redox state of the fluid between $H_2S/S0_4$ and $C0_2/CH_4$ buffers

deposits and broader gold camps; with interpretations of metal sources, precipitation mechanisms, fluid composition, and transport and trap processes (see many papers in compilation volumes by Ho and Groves 1987; including Ho 1987; Ho and Groves 1988; and Ho et al. 1990). Timing of gold mineralisation, as based on absolute ages of mineralisation by direct dating of ore components, has produced wide ranges in ages suggesting a protracted (50 Myr) gold mineralisation 'event' (e.g. Vielreicher et al. 2010; Bateman and Hagemann 2004).

Of the 'unifying models' previously cited, the crustal continuum model of Groves (1993) came the closest to accounting for differing crustal levels and fluid sources that can be interpreted from the textural and chemical features of Archaean gold deposits. That model envisaged a coherent genetic group of variable deposit styles developed over a 15 km crustal profile at PT conditions ranging from 180ºC at < 1 kbar, to 700ºC at 5 kbar (Groves 1993; Table 2.4).

Gold mineralization in the Eastern Goldfields Province has ubiquitous structural control. Localised deformation zones define hosting structures and gold ore shoots, with intimate kinematic controls on the geometry of ore. Most gold deposits are hosted by low-displacement faults and fault networks that facilitated high-magnitude fluid flow and provided dilational precipitation sites (Vearncombe et al. 1989). Fault perturbations: strike changes, dip changes, dilational jogs, restrictional bends, and fault-fault intersections influenced the magnitudes of

fluid flow and the location of ore precipitation sites (Tripp and Vearncombe 2004). The type and geometry of an ore shoot is a function of the deformation style (ductile vs. brittle) and the relative components of pure and simple shear in the deformation (Blenkinsop 2004).

The localisation of gold deposits in late, low-displacement faults is generally used to demonstrate a late-tectonic timing for gold deposition (Tripp and Vearncombe 2004). However this relationship is not universal and there are some deposits in the north Kalgoorlie district that have suffered significant deformation post dating ore-emplacement (e.g. Wendy Gully; Fimiston; Kanowna Belle; Binduli). At the Golden Mile, Bateman et al. (2001a) reported the Fimiston lodes as being the result of an early D1 deformation later folded by D2 (see also counter arguments in Gauthier et al. 2004a). The Kanowna Belle gold deposit is a multi-stage vein system with pre- to syn-ore, and post-ore veins that allows a tight definition of the vein paragenesis, where the ore-stage was interpreted as synchronous with D2 (Aaltonen 1997; Davis et al. 2000). The Kundana lodes show evidence of thrusting prior to vein emplacement, reverse dextral oblique-slip during vein emplacement, and sinistral reverse deformation of the veins during mineralization (Chapter 7). Crosscutting relationships of vein stages with regional penetrative fabrics may provide a relative timing constraint between gold mineralization and deformation across the district.

2.7 Summary

The geological, structural and metamorphic histories of the Kalgoorlie Terrane were developed over ~90 Ma in the Neoarchaean. Structural and geochronological analyses are obscured by complex geological relationships and reactivation of structures; hence, further definition of the structural history and validation with field data and geochronology are required. Understanding the enigmatic Neoarchaean geological history and remarkable mineral endowment of Neoarchaean terranes are strong justifications for continued research in these areas.

Early extensional structures in the basin-forming phase of the Kalgoorlie Terrane may have reactivated during later contraction, and those early structures can be traced by using map patterns and stratigraphic distributions of the greenstones. The late clastic basins remain important time markers in the deformation history and need to be properly timed with respect to the regional penetrative fabric and pre-basin deformation of the greenstone substrate. A better understanding of the deformation sequence is a critical input into the controls of gold mineralization and the interpretation of the Neoarchaean tectonic setting. The following chapters attempt to address these issues.

There is still division of opinion as to whether subduction and arc-accretion plate tectonics applies to the Archaean, but there are compelling arguments against that hypothesis. In some instances there is inconsistent application of logic arguments e.g. subduction/accretion

indicators present = support for plate tectonics, or subduction/accretion indicators missing ≠ support for plate tectonics. For some authors a lack of subduction/accretion indicators does not detract from their insistence that plate tectonics operated in the Neoarchaean. In such cases, model-supporting geochemical data is preferentially favoured, whereas a lack of field evidence is not considered to detract from the validity of applying modern tectonics to the Archaean. Since plate tectonic models include many tenets demonstrable in the modern, but lacking from the ancient, identifying subduction as a valid Archaean process remains problematic. This controversy will probably remain unless fundamental definitive characters of Archaean plate tectonics can be identified. In the absence of such evidence it appears that other tectonic models (e.g. rifting) are equally applicable to the geological development of the Neoarchaean Eastern Goldfields Province.

3 Lithostratigraphy of domains in the north Kalgoorlie district

3.1 Introduction

The study area contains Late Archaean meta-volcanic and meta-sedimentary rocks that were divided into four fault-bounded domains from west to east: Coolgardie Domain, Ora Banda Domain, Kambalda Domain and Boorara Domain (Swager et al. 1990). Intervening NNW-SSE striking shear zones (Zuleika, Abattoir and Bardoc shear zones) mark the domain boundaries (see Fig. 2.1; Fig. 3.1; Swager et al. 1990). Ora Banda Domain is recognised as having the most complete stratigraphic column, with widespread preservation of primary textures and unit contacts; whereas the other three domains contain partial sections of the 'regional stratigraphy' outlined by Swager et al. (1990). The Boorara Domain is notable for an early komatiite-dacite association that is lithologically distinct from similar-aged sequences in the other domains. A generalised regional stratigraphy for the Kalgoorlie Terrane of Swager et al. (1990) comprises from oldest to youngest: mafic volcanic rocks (Lower Basalt Unit); ultramafic volcanic rocks (Komatiite Unit, including high-Mg basalt); mafic volcanic rocks (Upper Basalt Unit); intermediate to felsic volcanic and sedimentary rocks (Felsic Volcanic and Sedimentary Unit); and epiclastic sedimentary rocks (Polymictic Conglomerate Unit).

Mafic and ultramafic volcanic units are well understood, they are documented in significant detail in all domains (Hunter 1993; Morris 1993; Witt 1990; Ahmat 1995a,b), and are portrayed as regionally-correlated formations on geological maps - those rocks are not covered in detail in this thesis. The upper intermediate-felsic volcanic and sedimentary units have been documented with local lithostratigraphic sections (Morris 1998; Taylor 1984; Hand 1998; Krapez et al. 2000; Brown et al. 2001; Squire et al. 2010), but unlike the mafic volcanic sequences, no regional correlation of formations for the felsic sequences has been presented on maps. Those units are the focus of new data presented here.

Extensive cover sequences of transported sediments, in-situ soils, laterite and lake clays limit exposure, preventing correlation between small disconnected outcrops. A relatively subdued aeromagnetic response of felsic rocks in the upper units compared with mafic and ultramafic rocks also impedes interpretation - the latter having generally higher magnetite contents that enhance an ability to interpret strike extensions under cover from aeromagnetic images. A GIS map area of 1805 km^2 selected from the GSWA KALGOORLIE 1:250,000 map sheet contains 368 km^2 of outcrop for a calculated 20.4% exposure. This figure is about twice that normally quoted for the Kalgoorlie district, but includes rocks of highly variable quality from fresh rock to highly clay-weathered saprolite rubble; hence 20.4% is probably an overestimate of acceptably identifiable rock. Given limited outcrop, the best aid to correlation is bottom-of-hole lithological and lithogeochemical mapping from RAB and AIRCORE exploration drill holes, which are distributed broadly over the north Kalgoorlie district, and

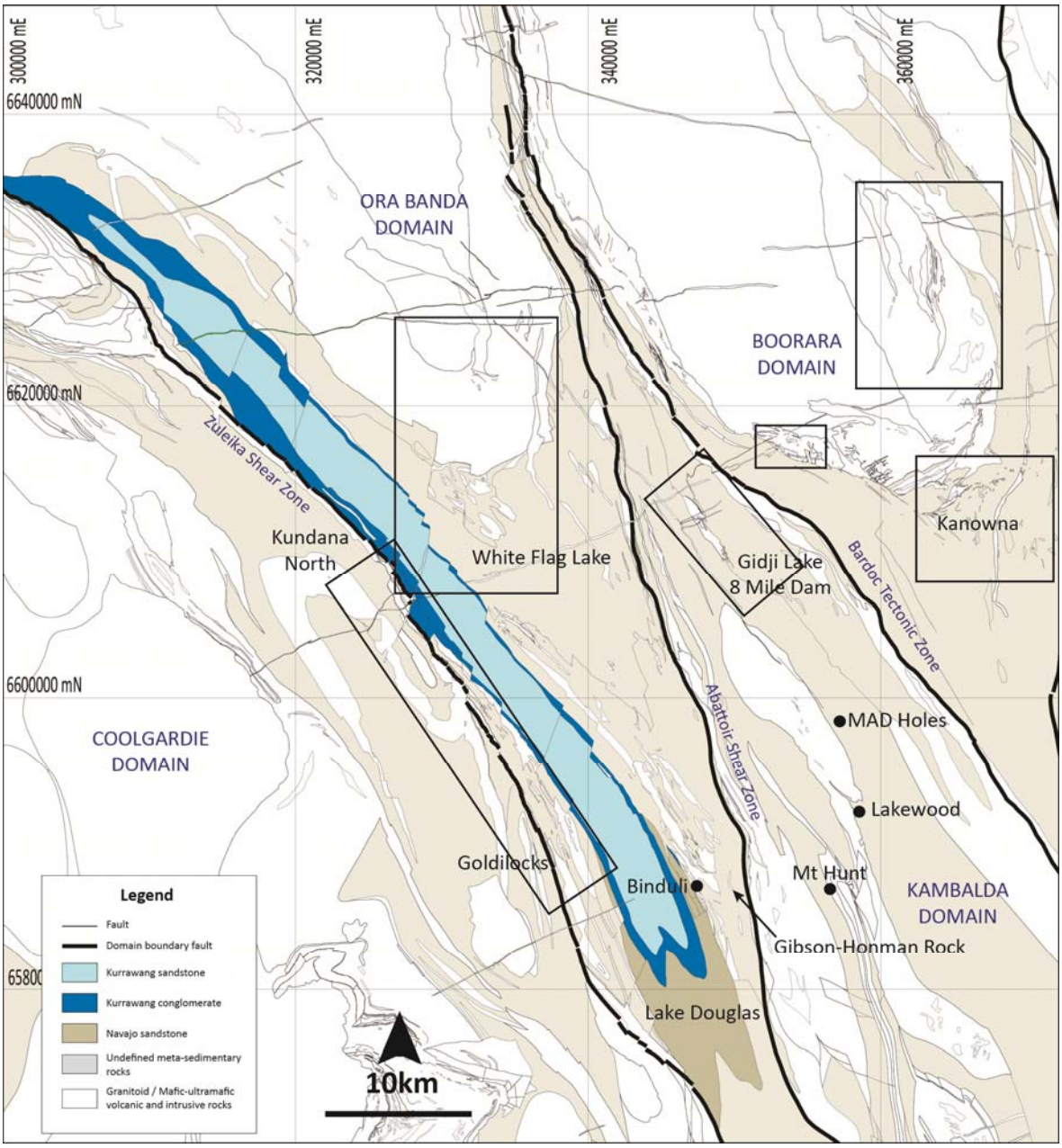

Figure 3.1 – Study area for this project with boxes highlighting areas of detailed work on a map showing the domains of the Kalgoorlie Terrane separated by the major domain boundary faults. The Kurrawang Formation is highlighted in the centre of the map. See Figure 1.5 and the A0 Map - map pocket, for detailed location of drill holes and outcrops mapped in this study. All grid coordinates in this thesis are UTM co-ordinates given in 'GDA' (Geodetic Datum of Australia 1994; equivalent to Map Grid of Australia Zone 51J).

are used here to produce 1:10,000 scale basement interpretation maps for selected areas, in addition to outcrops and selected deep diamond drill holes, used to characterise the formations.

3.1.1 Rationale for this work

Correlating mappable units into formations is the primary goal of this chapter, to provide an understanding of the stratigraphy and constraints on the structural geology as reflected at a map scale. Currently the Barrick geology map of the north Kalgoorlie district is a highly detailed 'lithological map' that represents the combined work of >30 years by numerous companies from industry and some research groups (Fig. 3.2). The geology map combines outcrop and bottom-of-hole lithology observations, augmented by regional-scale aeromagnetic and gravity surveys and multi-element lithogeochemistry.

A very high-density of information (>480,000 drillholes) results in high confidence in the distribution of lithologies, whereas there is much less confidence in how the mapped lithological units correlate with recognised stratigraphic formations. A key aspect of this thesis is the production of a preliminary regional 'formation map' that shows the areal distribution of units correlated by sequence, lithology and age presented at the end of Chapter 3 (see Fig. 3.77).

In the Kalgoorlie district, rocks younger than the Upper Basalt have been assigned to the Felsic Volcanic and Sedimentary Unit (Black Flag Group), and the Polymictic Conglomerate Unit (Kurrawang Formation; Swager et al. 1990). The Black Flag Group has been studied by several authors in the past, who produced a range of stratigraphic columns including: the Black Flag and White Flag Series' of Talbot (1934), Forman (1937) and Forman (1953); the Black Flag Beds of Woodall (1965) and Travis et al. (1971); the Gundockerta Group of Gemuts and Theron (1975) and Williams (1976); the Black Flag Beds Unit IIIA and IIIB of Keats (1987); and the Spargoville and White Flag Formations of Hunter (1993); see Table 3.1 (Map Pocket).

Recently Krapez et al. (2000) proposed a revised stratigraphic order for the Black Flag Group with a lower Spargoville Sequence, and an upper Kalgoorlie sequence comprising a 'Black Flag Formation' overlain by White Flag Formation (see Fig. 2.2a). It is unclear whether Krapez et al. (2000) include the Spargoville Formation of Hunter (1993) with the upper part of their "Spargoville Sequence" or with the lower part of their "Black Flag Formation": from their description "volcaniclastic and epiclastic turbidites, with intervening condensed sections of carbonaceous shales" it would appear to be included with the Black Flag Formation. Given this uncertainty, those rocks will be dealt with initially as 'sedimentary rocks overlying Upper Basalt'.

This chapter is organised into five major sections to document and interpret the stratigraphy of felsic volcanic and sedimentary rocks overlying the Upper Basalt Unit: in the Ora Banda Domain (Section 3.2); Coolgardie Domain (Section 3.3); Kambalda Domain (Section 3.4) and Boorara Domain (Section 3.5).

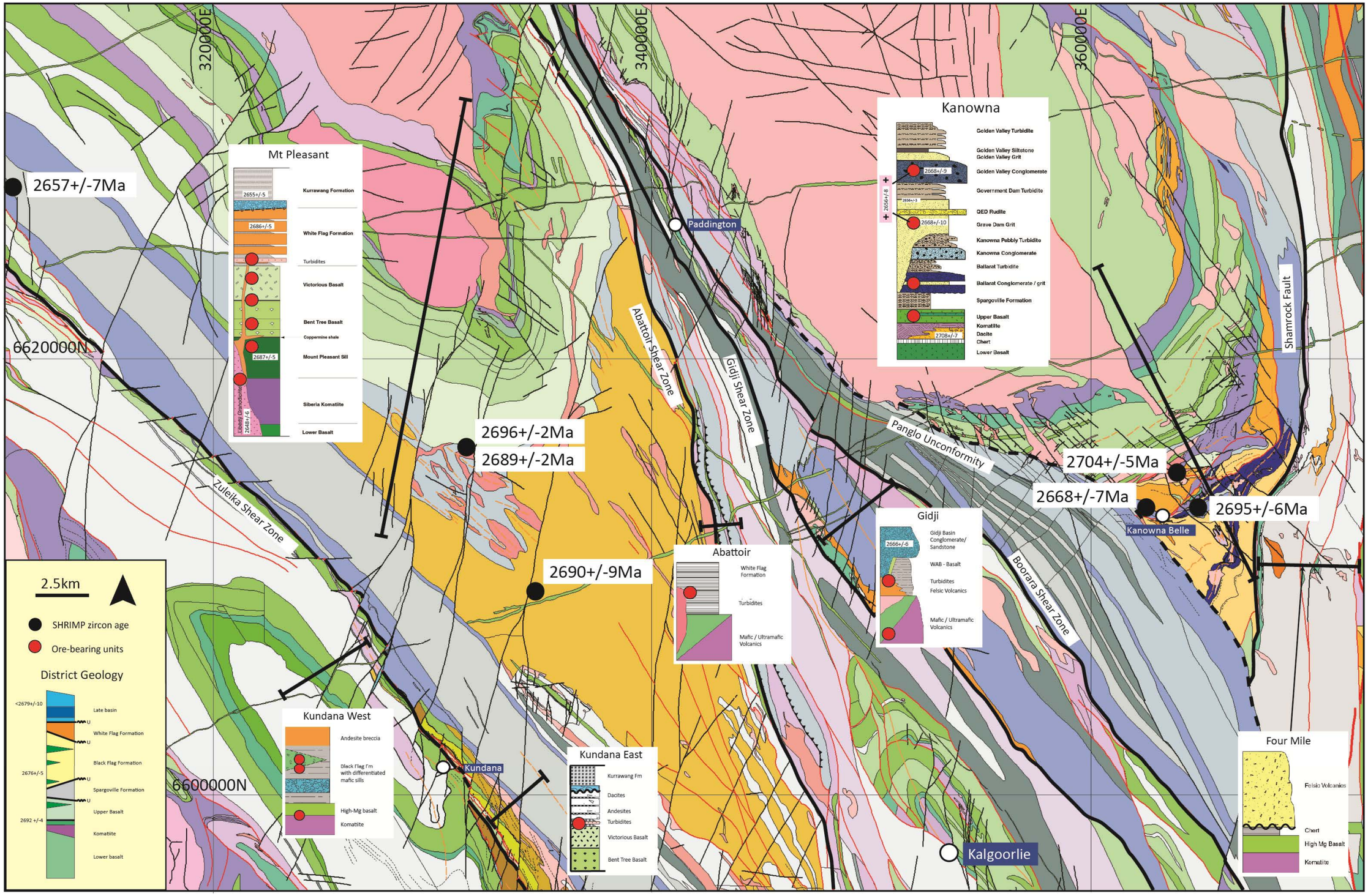

Figure 3.2 –Basement interpretation lithological map of the north Kalgoorlie district, with local selected lithostratigraphic columns for the section lines marked in black. The legend is generalised, see A0 map (in pocket) for details of lithological units.

A summary of major formations and key criteria to discriminate the formations is presented in Section 3.7. The approach here uses field data from key outcrops, selected bottom-of-hole RAB and AIRCORE drill holes and lithofacies mapping from >16 km of diamond drill core. Since the Ora Banda Domain preserves the most complete stratigraphic sequence, it will be documented first, followed by limited information from the Coolgardie Domain immediately west of the Zuleika Shear Zone; selected outcrops in the Kambalda Domain; and finally the Boorara Domain, which contains the bulk of detailed work on the various unique sedimentary formations in that area.

Sedimentology, contact relationships, structural geology, and interpretations are documented in a systematic manner for each unit. Mapping and analytical data are summarised in graphical form with representative plans, or cross-sections, stratigraphic columns and photographs of the typical exposures for each formation. Stratigraphic columns are presented in summary view for each formation as composite columns compiled from outcrops and drill holes selected to provide a summary description of each formation. It should be noted that these are compiled from disconnected exposures and, at best, are an estimate of the structure and composition of the formations in poorly exposed areas. The graphic sections are designed to give a snapshot view of each formation rather than a detailed lithofacies interpretation. Detailed recording of the nature of the lower contact and internal structure of each bed is provided in the drill logs in the Appendices. The various formations are presented in order of decreasing age.

3.2 Ora Banda Domain

Rocks in the Ora Banda Domain show a near complete stratigraphic sequence from Lower Basalt Unit to the unconformable Polymictic Conglomerate Unit (Fig. 3.3). Major gaps in volcanism appear to be recorded by condensed section mudstones and black shales as interflow units, or as thick sections of volcanic-derived, feldspathic turbiditic sandstones and shales. Figure 3.3 is a schematic summary map of the entire Ora Banda Domain from Lower Basalt Unit at the base of the section (north) to the uppermost unnamed felsic volcanic rocks at the intersection of the Zuleika and Abattoir shear zones south of Kalgoorlie. The stratigraphy is well-constrained up to the Binduli sequence, but south of Binduli the relationships are obscured due to minimal exposure, and are inferred from map patterns and minor reconnaissance of exploration drill holes.

3.2.1 Sedimentary rocks overlying Upper Basalt unit

Introduction

Sedimentary rocks overlying Upper Basalt Unit (SUB) in the Ora Banda Domain are variably exposed over a 12 km x 6 km area to the northwest of Kalgoorlie (Fig.3.3). These rocks were first documented as ‘Black Flag Series’ (Talbot 1934, Table 3.1-map pocket). The formation comprises sandstone, siltstone and minor shale with an estimated total thickness of 1000 m-1500

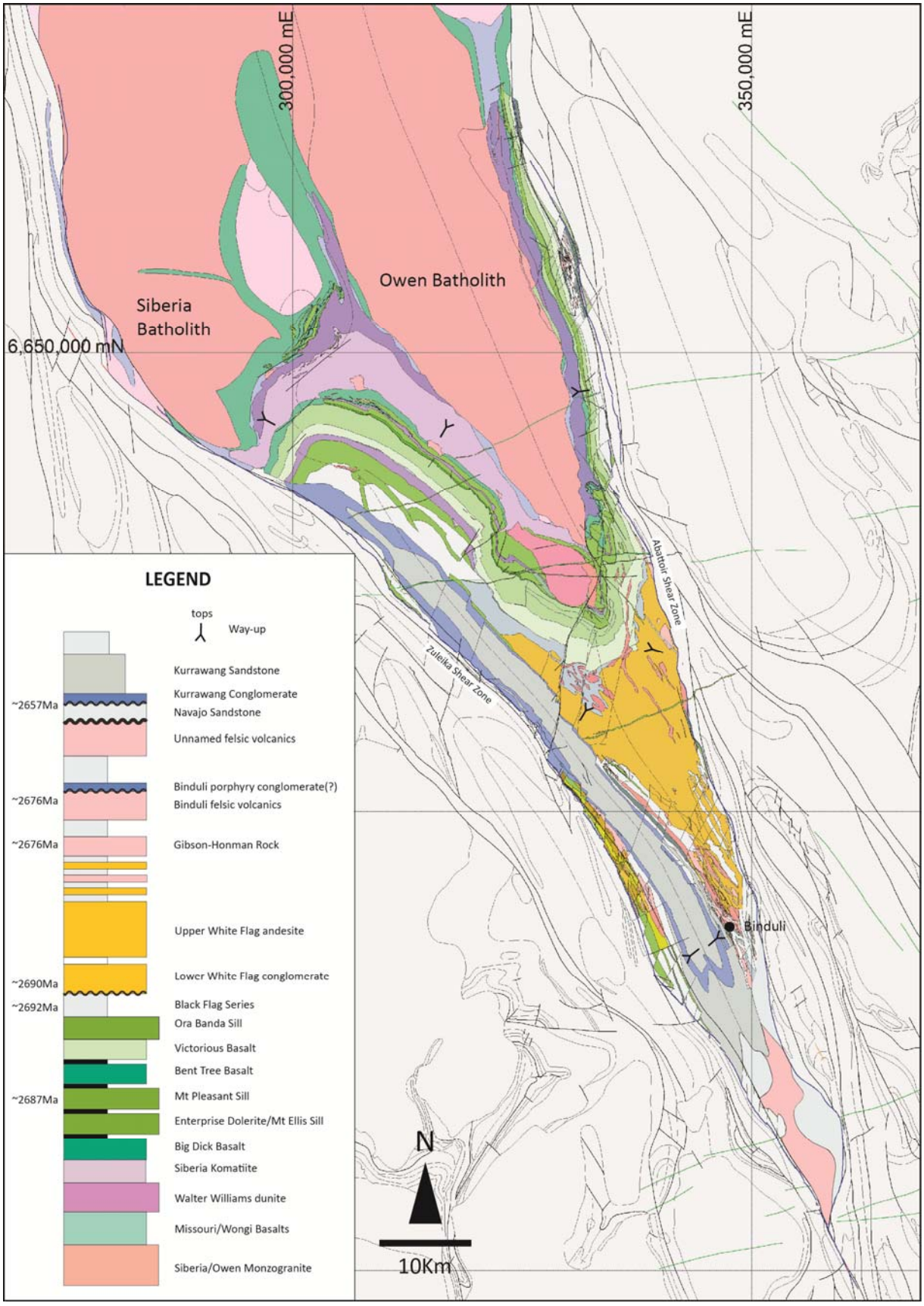

Figure 3.3 – Ora Banda Domain geology and stratigraphy (see Chapter 4 for details of geochronology).

m (Hand 1998; Hunter 1993). Intense local deformation and tectonic thickening prevent the construction of a stratigraphic column, and thickness calculations are likely to significantly overestimate the true thickness of the unit. The SUB in the Ora Banda Domain lacks intercalated volcanics, but was intruded by hornblende-feldspar porphyry dykes and sills. To avoid confusion of nomenclature between the original 'Black Flag Series' and upper and lower Black Flag formations, a new term 'Talbot formation' is proposed later in this chapter and in Chapter 4 to refer to sedimentary rocks overlying the Upper Basalt.

Contact relationships

The basal contact of the SUB (Fig. 3.4) is preserved in a small breakaway at 329000E-6618500N. This rare, but excellent, exposure displays a normal depositional contact between Victorious Basalt and SUB, whereas elsewhere the contact is faulted with no preservation of primary relationships.

Upper SUB is locally unconformable to transitional with the lower conglomeratic part of the overlying White Flag Formation. A sharp structural contact between folded sandstones and overlying block/bomb andesite breccia is located 5 km SW of Mount Pleasant, whereas at White Flag Lake the contact is not exposed. In drill holes, feldspathic sandstones give way to outcropping, well-rounded andesitic boulder conglomerate over ~70 m, suggesting an unconformity at least locally (Section 3.2.2).

A gradational contact with intercalated, fine-medium-grained quartzo-feldspathic sandstone, andesitic conglomerate and breccia of the White Flag Formation was intersected in drill hole URD073 at Kundana south. A similar gradational relationship was documented by Hunter (1993), and was demonstrated from coarsening of upper units of the SUB with a gradual provenance change from felsic to intermediate composition from whole-rock XRF analysis (Hand 1998).

Description

Plane-bedded sandstone, siltstone (Fig. 3.5a, b) and minor shale dominates the SUB, which lacks coarse clastic rocks with the exception of rare localised intra-formational sedimentary breccia (Fig 3.5c). Sandstone and siltstone form thin-bedded (0.1-0.5 m) strike-continuous parallel beds in areas lacking intense folding and thrusting, however most exposures are folded at a kilometre scale, with more intense zones of shearing and detachment developed locally at a metre scale (Section 5.7.1.2), and locally parasitic folding at outcrop scales (Fig. 3.5d).

Plane bedded sandstone, siltstone and shale units have ubiquitous internal sedimentary structures (Fig. 3.5 a, c, e) including graded bedding, water escape structures soft-sediment deformation, and scour and loading structures. The mudstones are typically silicified in outcrop producing a weathering phenomenon colloquially known as 'regolith chert'. The so-called

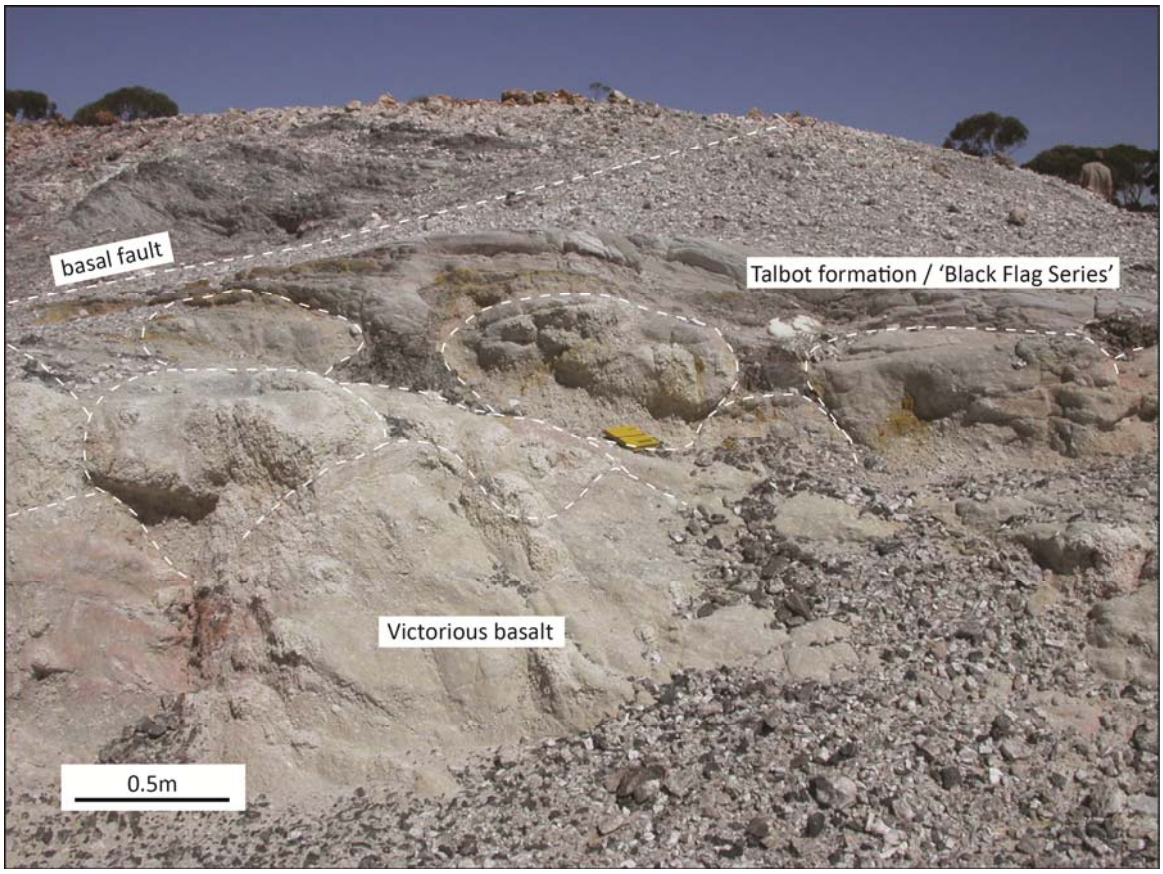

Figure 3.4 – Outcrop photograph showing sandstone and shale draped over the top of, and deposited into spaces between basalt pillows (view to southwest; yellow notebook for scale; GDA: 329005E; 6618533N).

'cherts' form resistant ridges of parallel silica layers that preserve load casts on their upper surface from soft sediment slumping of overlying sandstone layers (providing a way-up indicator). The silicification indurated the shale/mudstone such that with advanced weathering, surrounding sandstone beds were eroded leaving sheet-like protrusions of silicified mudstone.

Typically, coarse-grained sandstones grade upwards to fine-grained siltstones, with locally carbonaceous mudstone tops up to several 10's of centimetres thick (Figure 3.5e). Rare thick, coarse sandstone beds are present and form locally relevant marker units that elucidate the structure. Sandstone beds contain primary volcanic quartz crystals and twinned plagioclase feldspar indicating a dacitic source. In thin section, the sandstones are composed of medium-grained to very coarse to sand-sized (1-2 mm) clasts comprising sub-angular to sub-rounded broken plagioclase crystals (85%) with <5% sub-rounded quartz grains in a finely intermixed silt-sized matrix of feldspar and quartz (Fig. 3.5f, g). A dominantly quartzo-feldspathic composition of the sandstones / siltstones suggests reworking of a felsic volcanic source.

The presence of sandstone grading into shale represents Ta-b divisions of the Bouma sequence (Hand 1998), and the entire package was interpreted by Hand (1998) as a deep-water turbidite succession deposited in a submarine fan setting. Rare cross-bedded sandstone was

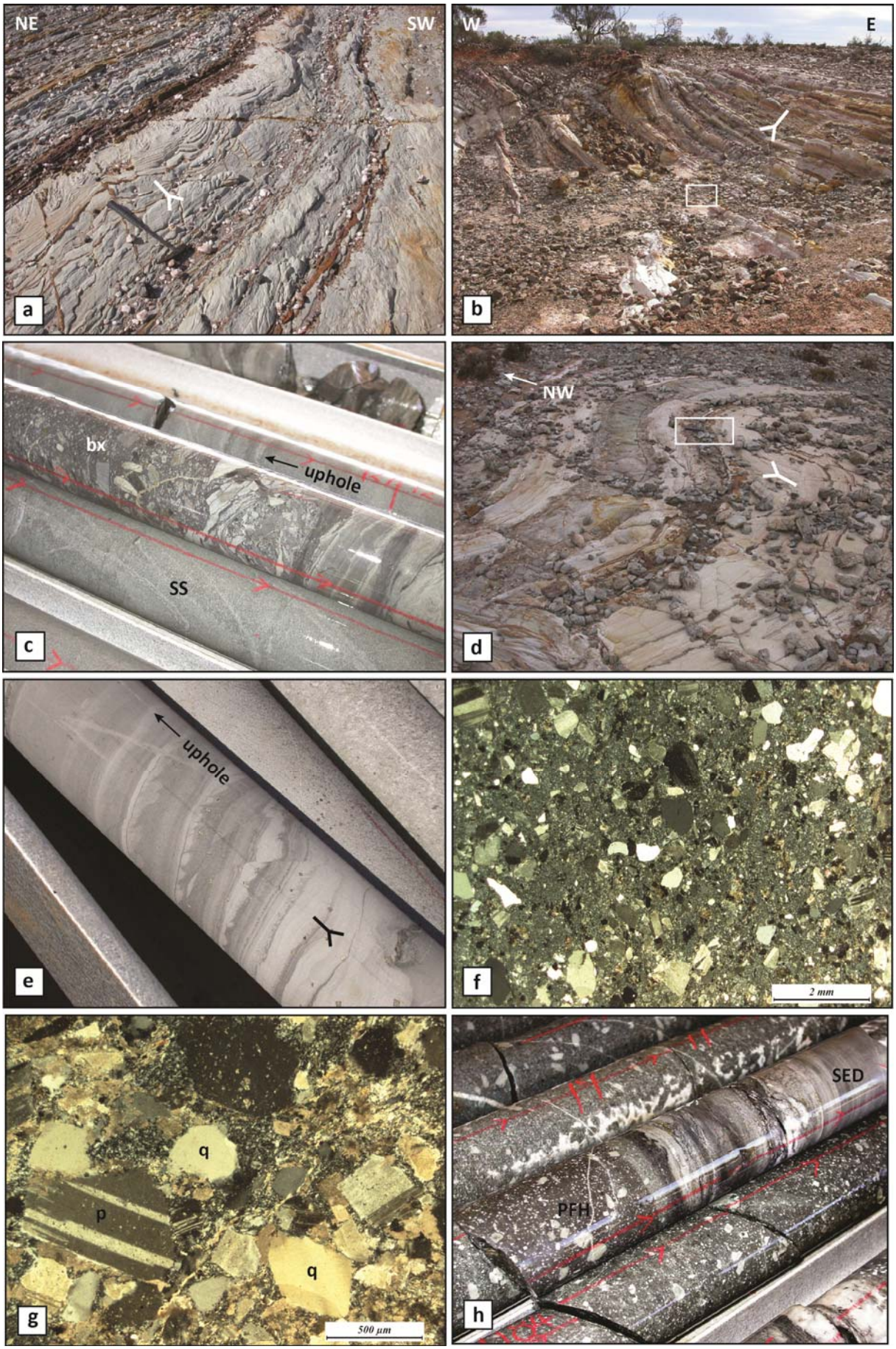

Figure 3.5

Captions for Figure 3.5 - Sedimentary rocks overlying Upper Basalt (Black Flag Series / Talbot formation)

a) Soft sediment deformation structures in plane-bedded sandstone/siltstone. Truncated convolute lamination and bedding-confined slump structures indicate way-up to the east. White Flag Lake (GDA: 331303E; 6614828N). Hammer for scale.

b) Plane-bedded sandstone siltstone at White Flag Lake (GDA: 331911E; 6612728N). Bedding in spotted sandstone and shale layers oriented 30°/028° with minor disruption on faults at low angle to bedding. Truncated convolute laminations indicate way-up to the east. Hammer for scale (white box)

c) Intraformational sedimentary breccia in Talbot formation rocks from drill hole THD001 125.2-125.9 m (GDA: 331202E; 6615692N). The breccia is composed of angular mudstone, bedded siltstone and fine-grained sandstone fragments in a fine-grained argillaceous matrix. Fragmentation is developed in a band roughly parallel to the bedding / core axis angle, but similar breccia zones occur as tabular 'pebble-dykes' that cross the bedding at a high angle in the Golden Funnel gold mine. NQ drill core 50 mm diameter.

d) Folded plane-bedded sandstone/siltstone/shale at White Flag Lake (GDA: 332007E; 6612703N). The sequence is locally downward facing at this locality with open fold axes plunging to the NW at 58°/312°, whereas the sequence is younging to the SE. Hammer for scale (white box).

e) Flame structure in Talbot formation sandstone/mudstone indicating uphole younging– NATDD003 194.2 m. NQ drill core 50 mm diameter.

f) XPL (cross polarised, transmitted light) Photomicrograph of quartz-rich coarse sandstone in drill hole NVDD001 155.5 m (GDA: 333725E; 6610479N) drilled close to the upper contact of the Talbot formation with overlying White Flag Formation andesitic volcaniclastic rocks, on White Flag Lake. Sub-rounded to sub-angular strain-free quartz and plagioclase grains are dominant, with a minor component of angular grains and biotite flakes in a fine-grained quartzofeldspathic silty matrix. Feldspars are locally altered by patchy dull calcite and sericite. Rare remnants of volcanic quartz and feldspathic composition in matrix supported sandstone indicate a fairly immature sedimentary product of rapidly deposited turbiditic rocks.

g) XPL photomicrograph of feldspar-rich coarse sandstone in drill hole NVDD001 136 m. Coarse-grained framework-supported sandstone composed of sub-angular twinned plagioclase and weakly strained quartz grains, with a minor matrix component. Abundant dull carbonate-sericite alteration overprints the fine siltstone matrix (p – plagioclase; q – quartz).

h) Strained intrusive contact of microdiorite porphyry intruded parallel to bedding in Talbot formation turbiditic sandstone / mudstone. Microdiorite magmas intruded the stratigraphy primarily as sills, but local examples of dykes cutting the bedding are also observed. Minor shearing at the contact has localised Au-sulphide mineralisation with carbonate and sericite alteration. Drill Hole THD001 184.1 m. NQ drill core 50 mm diameter.

interpreted as Tc divisions within the Bouma sequence (Hand 1998), with a north to south palaeocurrent direction. Plane bedded, non-erosive sandstone beds with rare interbedded mudrock in the SUB indicates deposition on submarine fan lobes, whereas coalesced sandstone beds with erosional contacts represent braided channel deposits in proximal sections of a suprafan lobe (Hand 1998).

The SUB was intruded by porphyritic microdiorite sills that have similar intermediate geochemistry to the overlying White Flag Formation and may be sub-volcanic remnants of that volcanic event (Fig. 3.6). Porphyritic microdiorite sills have distinctive 5-10 mm plagioclase laths and euhedral hornblende set in a granular groundmass of intergrown feldspar and biotite crystals. Hornblende phenocrysts are completely replaced by randomly oriented mats of hydrothermal / metamorphic(?) biotite, and chlorite aligned along cleavage traces.

The coarsely plagioclase porphyritic texture of the microdiorite sills may be confused with superficially similar textures in the plagioclase glomero-porphyritic Victorious Basalt, but the latter is distinguished by its glassy groundmass, subhedral plagioclase phenocryst clusters, a lack of any significant mafic phenocrysts, and well-developed volcanic features (pillow margins, hyaloclastite breccia, interflow sedimentary rocks). The two porphyritic rock types are encountered in a zone of intrusions located between the Black Flag and Royal Standard Faults.

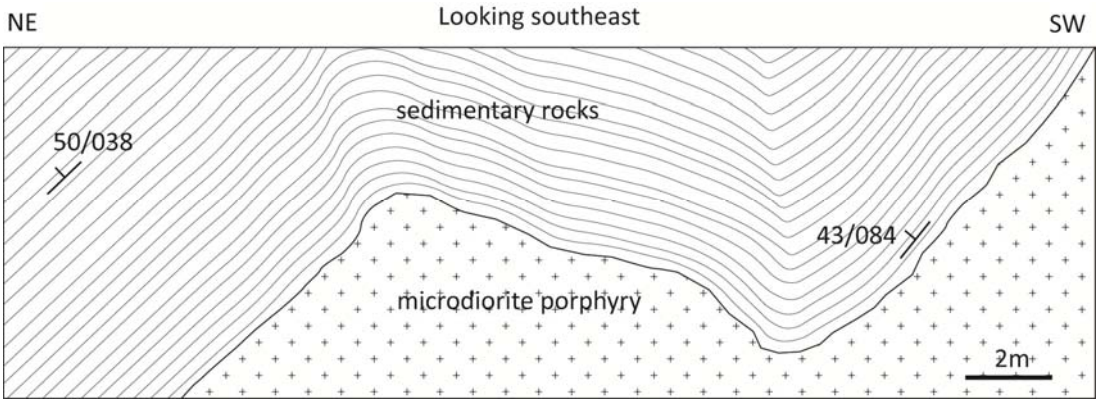

Figure 3.6 – Trench wall map of microdiorite porphyry sill intruded into turbiditic sedimentary rocks at GDA: 330812E; 6614929N. The two rock types are folded at a mesoscopic scale, and similar relationships are observed at a map scale.

Structural geology

Sedimentary rocks of the SUB are extensively folded (Fig. 3.5 b, d) and thrusted (Section 6.6.1) resulting in a significant tectonic thickening of the formation. The thickest parts of the SUB occur at the culmination of the Mount Pleasant Anticline, with structural thickening and disharmonic folding accommodated by a 10 m-wide basal detachment fault (e.g. Fig 3.4; see also Section 6.6.1.2). Sandstone and siltstone turbidites are folded at metre to kilometre scales, with ramp anticlines separated by locally developed detachment zones, and characterised by intense shearing, and locally, re-folded folds (Section 6.6.1). A penetrative foliation appears locally axial

planar to the folds, but does not overprint the basal detachment fault suggesting that some movement occurred post-folding. Porphyritic microdiorite sills intruded parallel to bedding and were folded with the sedimentary rocks (Fig. 3.5h; Fig. 3.6), and locally with dykes cross-cutting the wallrocks.

Interpretation and correlation

The rocks overlying Upper Basalt Unit in the Ora Banda Domain are dominated by below-wave-base, fine-grained turbiditic sedimentary rocks with no significant coarse clastic or volcanic units. This association is typical in the Ora Banda and Boorara domains (as is significant thicknesses of Upper Basalt mafic volcanic rocks), but the sedimentary rocks overlying Upper Basalt Unit in other domains (Kambalda domain, Coolgardie domain) also contain coarse clastic and intercalated volcanic rocks. On this basis it appears unlikely that the sedimentary rocks south of Mount Pleasant can be correlated with the thick sections of volcanic and coarse clastic rocks documented elsewhere as Spargoville Formation (Hunter 1993). A thin black shale unit at the Upper Basalt contact documented in the Kambalda Domain and elsewhere (e.g. Hunter 1993; Keats 1987; Travis et al. 1971) may be a possible correlative of the sedimentary rocks south of Mount Pleasant.

3.2.2 White Flag Formation (WFF)

Introduction

The White Flag Formation (WFF) in the Ora Banda Domain covers a 17 km x 27 km area to the northwest of Kalgoorlie. Outcrop is limited to a 13 km x 3.5 km area near White Flag Lake to the south of Mount Pleasant including a near-complete lake section (Fig. 3.3, 3.7). Extensive exploration drilling has mapped the unit farther to the south. The WFF, with a total estimated thickness of 3600 m, comprises a lower unit of andesitic conglomerate with thin sandstone interbeds including rare andesite sills (1200 m), and an upper unit of coarse intermediate composition volcanic breccia and peperite with abundant sandstone interbeds and andesitic sills (2400 m). Detailed descriptive data were collected from one diamond drill hole and the stratigraphic column segment (Fig. 3.8) was measured from an exposure along the edge of White Flag Lake.

Contact relationships

The basal WFF conglomerate is transitional to locally unconformable with the underlying Talbot formation sedimentary rocks. The lower contact is not exposed in the White Flag Lake area, but drill hole NATDD012 intersected a basal 5 m zone of quartz-calcite network veins with some cataclasite in contact with underlying shale and sandstone (also see Section 3.2.1 for details of the lower contact). At the southern edge of the outcrop on White Flag Lake, the WFF is in

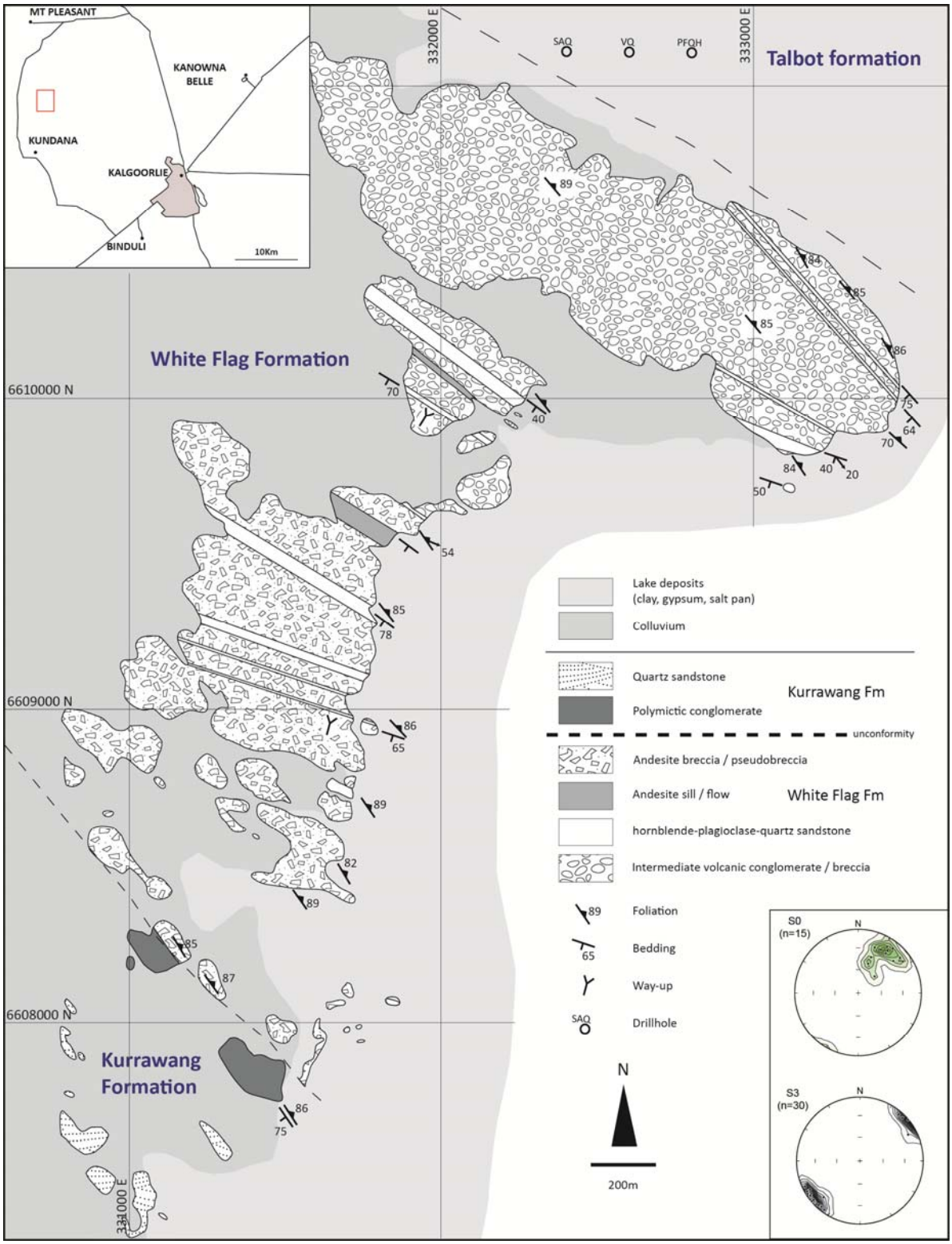

Figure 3.7 – Geological map of type section through the White Flag Formation, White Flag Lake. A thick sequence of basal andesitic conglomerate, at the top right, has a relatively sharp transition in grainsize and clast shapes with upper units dominated by volcaniclastic andesite breccia, and rare peperite. Lower and upper units are interbedded with fine-grained quartz-hornblende-plagioclase sandstones, and pebble breccia layers. The Upper contact in the lake section is unconformable with overlying Kurrawang Formation conglomerate and sandstone. Note the angular discordance between bedding in the andesites and the Kurrawang unconformity. All structural data in this thesis are presented as equal area, lower hemisphere projections. Drill hole labels: SAQ – quartz sandstone; VQ – vein quartz; PFQH – hornblende-quartz-feldspar porphyry. Outcrop shapes modified from Barrick GIS (Crossing, 2003).

unconformable contact with Kurrawang Formation conglomerate (Fig. 3.7); however, this contact is not the top of the WFF. The upper WFF contact is also not exposed, but is interpreted from aeromagnetics where a distinct change in magnetic intensity response marks a transition from WFF to the overlying rocks of the Binduli sequence. Drill hole intersections show a mixed zone of dacitic and andesitic rocks, whereas diamond drill core from the Goldilocks area (Fig. 3.1) indicates a sharp contact between hornblende-bearing White Flag Formation andesite and a transitional zone of intercalated andesite/dacite dominated felsic volcanic rocks interpreted as a lower Binduli sequence (Fig 3.1; Section 3.2.3).

Description

The WFF displays broad-scale stratification throughout, with sandstone beds spaced at about 50-200 m (Fig. 3.7). Beds have broadly continuous thickness along strike with sandstone interbeds separating thick, massive and disorganised beds of volcanic breccia and conglomerate (Fig. 3.8). Breccia and conglomerate in the WFF have a mean grainsize of 105 mm with geometric means up to 130 mm. Locally the formation contains clasts up to 1.5 m diameter (Fig. 3.9d). The rocks are dominantly matrix supported (Fig. 3.9a) with lithic sandstone matrices, but some sections are clast supported locally (Fig. 3.9b). Coarse clastic units are moderately to poorly sorted, composed of sub-angular to angular, elongate lithic andesite fragments (Fig. 3.9g). Bed forms are massive and lacking any internal organisation, with the exception of lower conglomeratic units that show upward-fining sections in coarse boulder conglomerate beds of ~10 m thickness (Fig. 3.9d).

Clasts are dominantly porphyritic and of intermediate composition with 87% hornblende-feldspar porphyry clasts, with the remaining 13% made up of mafic volcanic clasts (Fig. 3.8). In the lower conglomerate unit, the composition of the clasts is dominantly intermediate; however, a much greater variety of intermediate porphyry types is mixed with various minor mafic fragments including coarse gabbroic rocks, and microdiorite porphyry clasts akin to the sills and dykes that intruded the underlying Talbot formation rocks. Upper breccia units have restricted fragment populations composed of cobble and boulder sized angular andesite breccia clasts, including amygdaloidal andesite lava.

Interbedded sedimentary rocks in the lower conglomeratic unit comprise 5-10 m-thick plane-bedded, fine-grained, graded, ripple-laminated sandstones and siltstones composed of very fine-grained angular crystal fragments of feldspar and hornblende and quartz (Fig. 3.9f, g; Fig 3.10a), or thin plane-bedded pebbly sandstones. The sandstones locally have rare, primary soft sediment deformation structures (convolute lamination), and scour and fill structures indicating way-up to the southwest. Sedimentary interbeds in the upper volcanic part of the White Flag Formation comprise 10-50 m-thick units of plane-bedded pebbly sandstone/siltstone beds that are generally coarser grained than the lower interbedded sandstones and siltstones.

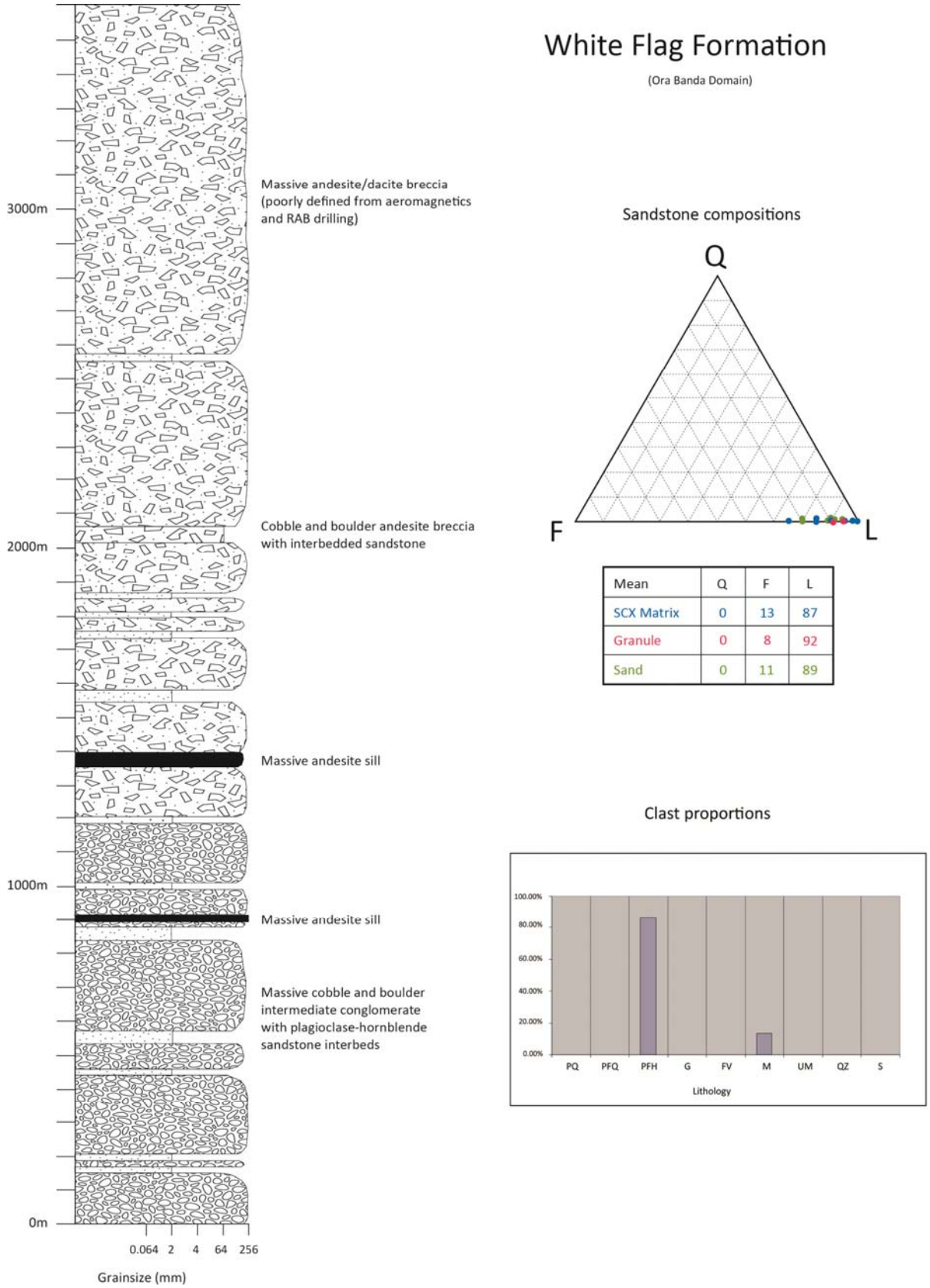

Figure 3.8 – Partial stratigraphic column of the White Flag Formation measured from the section along White Flag Lake. Quartz-Feldspar-Lithic (QFL) proportions and clast proportions are taken from drill hole NATDD012 (GDA: 329070E; 6614961N) . QFL data are coloured according to the table of mean values. SCX refers to conglomerate or breccia-sized clastics. PQ – quartz porphyry; PFQ – quartz feldspar porphyry; PFH –hornblende-feldspar porphyry ± quartz; G – granite; FV – felsic volcanic; M – mafic volcanic; UM – ultramafic; QZ – quartz; S – sedimentary

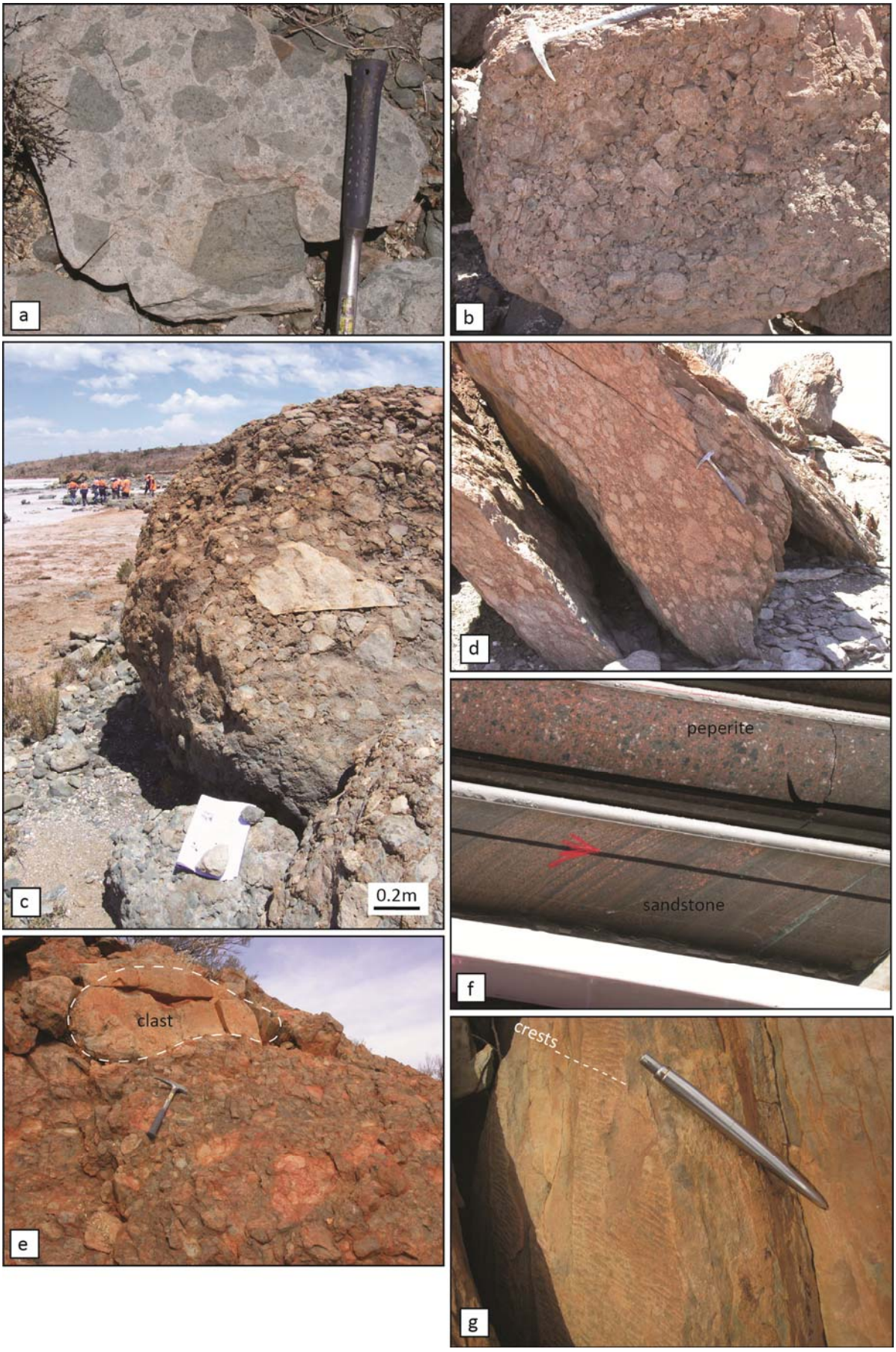

Figure 3.9

Captions for Figure 3.9 - White Flag Formation conglomerate, breccia and sandstone.

a) Matrix-supported andesite breccia from the upper parts of the sequence at White Flag Lake (GDA: 331706E; 6608679N). Fragments are angular, ranging from pebble to boulder size composed chiefly of coherent hornblende andesite and set in a fine-grained sandstone matrix of feldspar-hornblende crystal and lithic debris. The degree of support changes from a dominant clast framework support in restricted planar thick units, to matrix supported debris-flow style deposits. Hammer for scale.

b) Clast-supported, lithic tuff composed of sub-angular to sub-round fragments of coherent, vesicular andesite tightly packed into a framework of variable grainsize up to lapilli. Locally preserved contact textures suggest the clasts were hot and partially plastic upon deposition. The interclast porosity may be a primary feature of the rocks, whereas drill core intersections of similar rocks generally show a calcite-epidote ± tourmaline hydrothermal void fill assemblage. White Flag Lake (GDA: 331786E; 6608944N). Hammer for scale.

c) Poorly sorted, juvenile andesite boulder breccia composed of large, angular to sub-angular and sub-rounded clasts of coherent, hornblende-plagioclase porphyritic and amygdaloidal andesite. Locally the clasts have irregular cuspate forms reminiscent of primary lava fragments, whereas others show advanced rounding and comminution of particles. White Flag Lake (GDA: 331955E; 6609648N).

d) Weakly developed layering in poorly sorted angular andesite boulder breccia. A moderately developed foliation is present about parallel to the hammer handle (block not in-situ). White Flag Lake (GDA: 331741E; 6609101N).

e) Volcanic conglomerate on White Flag Lake headland (GDA: 333205E; 6610409N). The conglomerate is composed of coherent, porphyritic clasts of andesitic composition and rare fragments of gabbro to pyroxenite composition. Well-rounded poorly sorted conglomeratic rocks are typical of the lower sequences of the White Flag Formation, which in this exposure contains a single rounded fragment ~1.5 m long.

f) Coarse-grained volcaniclastic sandstone from drill hole NATDD012 111.2-111.6 m. Fine plane bedded sandstones within coherent and peperitic units are dominantly composed feldspar and hornblende crystals and crystal fragments, glassy remnants and porphyritic lava wisps. The sandstones locally have sharp depositional contacts with adjacent pebble breccia beds or show normal grading.

g) Outcrop photograph of in-situ ripple laminated sandstone from a 10-15 m thick sandstone unit interbedded with thick conglomeratic units of the lower White Flag Formation. The ripples are not widely developed, but indicate a tractional depositional environment. Local soft-sediment deformation features include truncated convolute laminations in graded sandstone beds. The presence of these units in conglomeratic rocks of the lower WFF suggests a possible fluvial to shallow marginal-marine depositional environment during the initial stages of the White Flag Formation volcanism. White Flag Lake (GDA: 333156E; 6609822N).

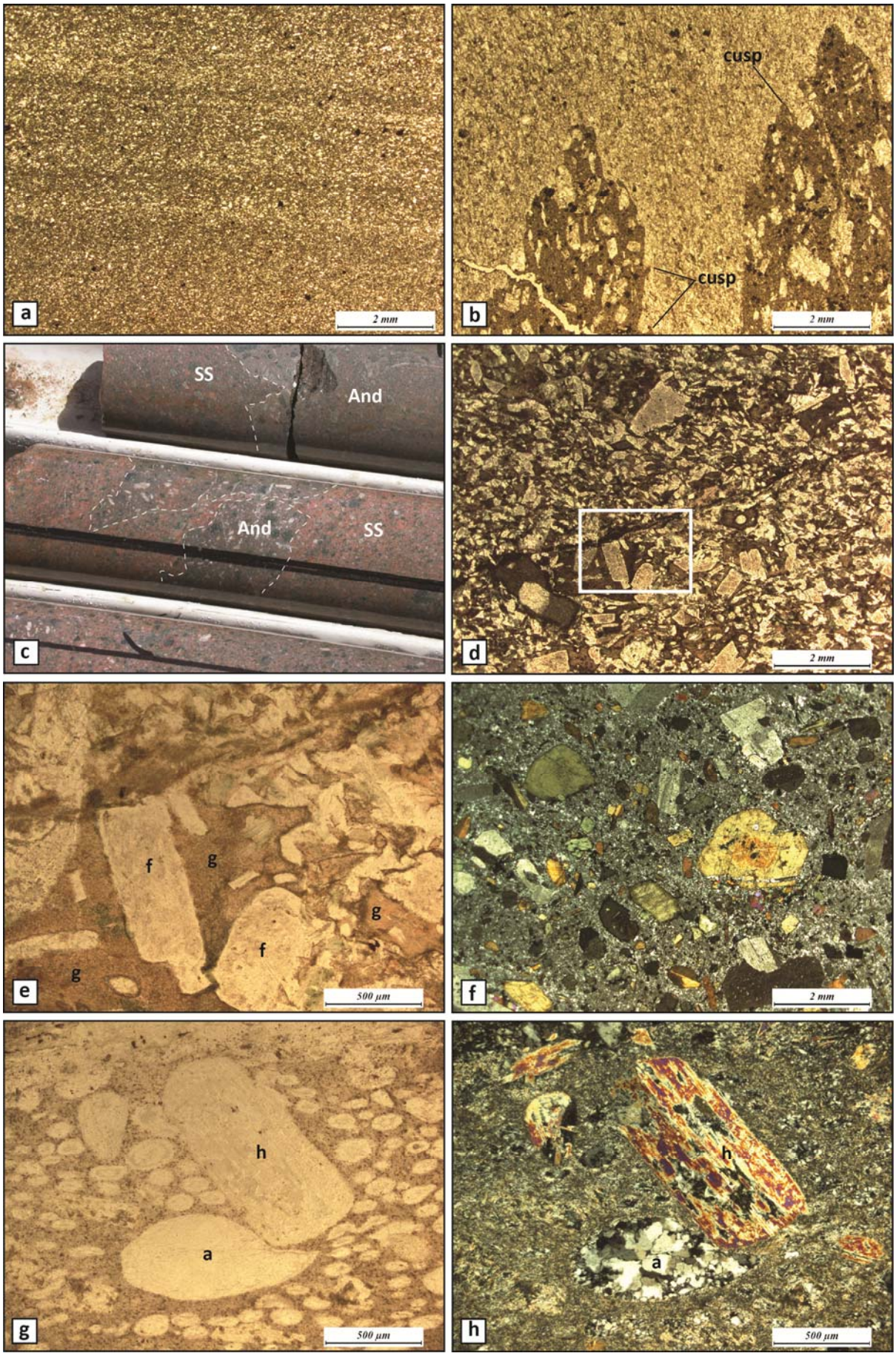
a
2 mm
b
cusp
cusp
2 mm
c
SS
And
And
SS
d
2 mm
e
f
g
g
f
g
500 µm
f
2 mm
g
h
a
500 µm
h
h
a
500 µm

Figure 3.10

Captions for Figure 3.10 - White Flag Formation volcanics photomicrographs

a) PPL (plane polarised transmitted light) photomicrograph of ripple laminated sandstone from interbedded sandstone and volcaniclastic conglomerate on White Flag Lake headland (GDA: 333156E; 6609822N). The fine-grained sandstone beds are dominantly composed of sub-angular feldspar and hornblende crystals, and less than 5% rounded quartz grains, in a very fine-grained silt matrix of similar composition to the sand component.

b) PPL photomicrograph of andesite volcanic breccia / peperite White Flag Lake island (GDA: 331822E; 6608069N). Fragments of hornblende andesite lava are distributed in volcaniclastic sandstone matrix, but locally have with wispy cuspate re-entrants at the margins of the lobes. The sandstone composition is intermediate, composed primarily of strongly carbonate-sericite altered plagioclase and hornblende crystal fragments. Andesite fragments are strongly saussuritised (zoisite-carbonate-chlorite).

c) Fluidal andesite peperite mixture of amygdaloidal andesite lava rocks intruded into in pebble-breccia to bedded sandstone facies. The sedimentary rocks are locally fine-grained, plane-bedded volcaniclastic sandstone with sharp contacts. Coherent andesite lava lobes have irregular wispy contacts; bedding in the sandstones trends at 50/216 - NATDD012 109.7 m (GDA: 329070E; 6614961N).

d) PPL photomicrograph of fluidal andesite peperite in coarse-grained volcaniclastic sandstone. The slide is of a fine-grained layer in a coarse tuffaceous interbed within pebble to cobble volcanic breccia units. Peperitic textures at a fine scale include fine hematite(?) altered glass sections enclosing feldspars and ragged acicular amphibole microlites. Parts of the rock appear to retain evidence of glass shards within a moderate to poorly sorted crystal tuff. NATDD012. (GDA: 329070E; 6614961N).

e) PPL photomicrograph of the view marked with a white box in (d) showing the medium pinkish-brown glass enclosing crystals of albitised plagioclase; the glass is locally amygdaloidal and forms a groundmass to the crystal-rich tuff that in hand-specimen shows plane-bedded sedimentary structure.

f) XPL photomicrograph of microdiorite porphyry clast in volcaniclastic conglomerate. The clast is composed of plagioclase, euhedral hornblende and minor anhedral epidote in a fine-grained groundmass with remnant microlitic flow texture and granular feldspar. White Flag Lake (GDA: 333205E; 6609694N).

g) XPL photomicrograph of amygdaloidal porphyritic andesite clast in an outcrop of White Flag Formation, flattened block and bomb volcaniclastic andesitic breccia. The outcrop shows evidence of tectonic flattening perpendicular to a well developed anastomosing foliation in matrix sandstones. (GDA: 328356E-6613121N).

h) XPL photomicrograph of the view in (g).Internal fabrics in the amygdales show evidence of strain with sutured grain boundaries of undulose quartz grains and zoisite-chlorite alteration, whereas a hornblende crystal appears to have impinged at the edge of the large amygdale when the rock was in a plastic state; a=amygdale; h=hornblende

Peperite in the upper units (Fig. 3.9f) is composed of coherent andesite lobes with fragmented margins, mixed with lithic sandstone and grit composed of feldspar and hornblende (Fig. 3.10 b,c). Thin sections of the peperite show juvenile volcanic lava fragments with euhedral feldspar and hornblende crystals in a glassy trachytic groundmass (Fig. 3.10d, e). The lava fragments have irregular wispy margins interspersed with ('flaming' into) surrounding lithic sandstone debris.

In thin section the andesites show a range of volcanic textures including coherent andesite porphyry with euhedral crystals of plagioclase and hornblende set in a felted matrix of fine plagioclase laths and interstitial glassy groundmass (Fig. 3.10f), to amygdaloidal lava rocks composed of plagioclase and hornblende phenocrysts with quartz-filled, round amygdales in a fine glassy groundmass, with zoisite-chlorite alteration (Fig. 3.10g,h). In many instances the groundmass contains murky saussuritised and chlorite-altered material that appears to preserve broken angular shard geometries, and possibly devitrification textures. The breccias contain sub-angular lithic fragments of porphyritic andesite in matrices dominated by angular broken lithic and crystal fragments. A sample from drill hole WTD2 ~2.5 km south of the mapped andesites, drilled into the transitional upper zone, is primarily dacitic in composition with 15-20% quartz intergrown with feldspar and rare chlorite-altered remnant hornblende, indicating an upwards transition to more felsic compositions (as lower Binduli sequence becomes dominant).

Structural geology

Volcaniclastic and sedimentary rocks of the WFF are some of the least deformed rocks in the Kalgoorlie district. The unit is folded into regional scale upright folds, but lacks mesoscopic-scale folding or any evidence of thrust repetition. With the exception of local faults and zones of strain localisation, the WFF contains a single, weak to moderate NNW-SSE striking disjunctive cleavage. Conglomerate and breccia clasts are stretched and deformed into elongate shapes only in the highest strain zones. The broad outcropping section on White Flag Lake appears to show a conformable, moderately southwest-dipping sequence of intermediate conglomerate and volcanic rocks, with strain localised by the finer grained units (pebble breccia or sandstones).

Interpretation and correlation

The WFF in the Ora Banda Domain shows clear relationships with surrounding formations: the WFF lies stratigraphically above the 'sedimentary rocks overlying Upper Basalt' and is overlain by intermediate-felsic volcanic rocks of the Binduli sequence. Whole-rock XRF analysis (Hand 1998) and descriptive observations in this study suggest a locally unconformable transition from underlying sedimentary rocks into the overlying WFF. This stratigraphic order is different to that proposed by Krapez et al. (2000; Table 3.1-map pocket), who interpreted the WFF to lie unconformably above a 'Black Flag Formation' in which they included rocks of the Binduli and

Gibson-Honman Rock areas. Samples for geochronology to resolve this issue are documented in Chapter 4.

Rounded pebble-to-boulder conglomerate in the lower section of the White Flag Formation suggests the unit was emergent in the initial stages of volcanism with reworking of volcanic breccias in a near-shore environment. This is supported by fine-grained quartz-hornblende-plagioclase sandstones with ripple-laminated textures (Fig. 3.9h). The upper section of dominantly angular, primary volcanic / volcaniclastic / peperitic rocks with interbedded fine-grained, graded sandstones and andesite sills suggests the majority of the unit was deposited as apron breccias proximal to submarine andesitic lava dome complexes.

3.2.3 Black Flag Formation (BFF)

Introduction

Despite uncertainties in published stratigraphic positions of the White Flag and Black Flag Formations of Krapez et al. (2000), the 'Black Flag Formation' terminology will be continued here since it accounts for large sections of the Felsic Volcanic and Sedimentary Unit (Black Flag Group) of Swager et al. (1990). Note that in the following sections 'Black Flag Formation' refers to rocks in the Ora Banda Domain overlying White Flag Formation.

The Black Flag Formation is here informally subdivided into: lower Black Flag formation (BFl), and upper Black Flag formation (BFu). Lower Black Flag formation is known mostly from drill holes, over 15 km x 8 km to the northwest of Kalgoorlie and is folded around the Mt Pleasant Anticline. Upper Black Flag formation is exposed in the Binduli mining district and in drill holes and outcrops to the south of that area (Fig. 3.1; Fig. 3.3; Fig. 3.11).

In the Ora Banda Domain, the entire Black Flag Formation is variably exposed for about 45 km south from the contact with White Flag Formation (interpreted from aeromagnetic imagery), to its southernmost extent at the juncture of the Abattoir and Zuleika Shear Zones (Fig. 3.3). Folding and deformation prevent an estimation of the true thickness of the unit, but it is likely to exceed 3000 m (see below). The nature of the BFu is poorly known and its distribution is compiled from government geological survey maps, reconnaissance drill-hole logs and aeromagnetic imagery.

Contact relationships

Lower units of the BFl overlie the White Flag Formation for 13 km along a NW-strike, but the contact is known only in exploration drill holes at Kundana South. The upper contact of the BFu is not exposed and the southern extent of the unit is marked by its intersection with the Zuleika and Abattoir shear zones (Fig. 3.3).

The contact between the lower and upper members is interpreted to lie above felsic rhyodacitic volcanic rocks at Gibson-Honman Rock east of Binduli, and at the base of a

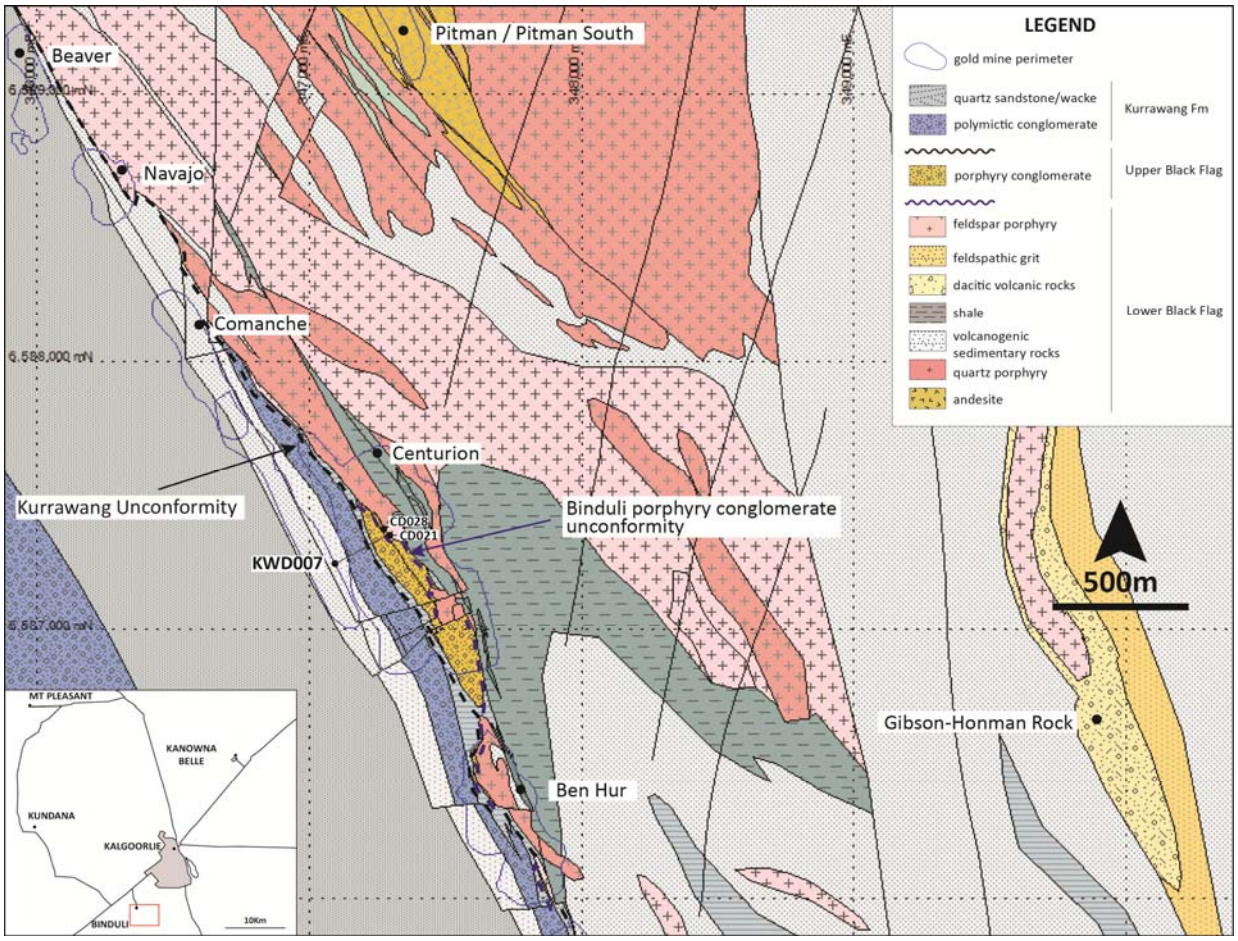

Figure 3.11 – Barrick GIS geology map of the Binduli area (Crossing 2003) significantly edited from new work in this study, with location of key unconformities, mine outlines, drill holes, and the Gibson-Honman Rock outcrop - addressed in this section.

distinctive porphyry conglomerate unit, termed 'Binduli porphyry conglomerate', in the Centurion and Ben Hur gold mines at the Binduli mining centre (Fig 3.11). This contact was a locus of intrusion by crowded-feldspar porphyry sills and dykes in the mines at Binduli (Centurion Porphyry). At Gibson-Honman Rock, felsic volcanic rocks and porphyritic intrusions overlie coarse-grained lithic grit to the west of the outcrop, which passes downward into sandstone and shale of the BFl (Fig. 3.12). The BFl/BFu contact is interpreted to lie stratigraphically above this sequence. Unfortunately exposure in this area is not extensive and uncertainties in the distribution of the Binduli porphyry conglomerate unconformity remain.

Two possibilities exist: (1) the Binduli porphyry conglomerate is a lower part of the Kurrawang Formation with very restricted provenance strongly skewed by the rocks that were ripped-up into the depositing units, or (2) the Binduli porphyry conglomerate was deposited above an unconformity boundary within the Black Flag Formation. Given the strongly siliciclastic/polymictic nature of the Navajo Sandstone and Kurrawang Formation, and that

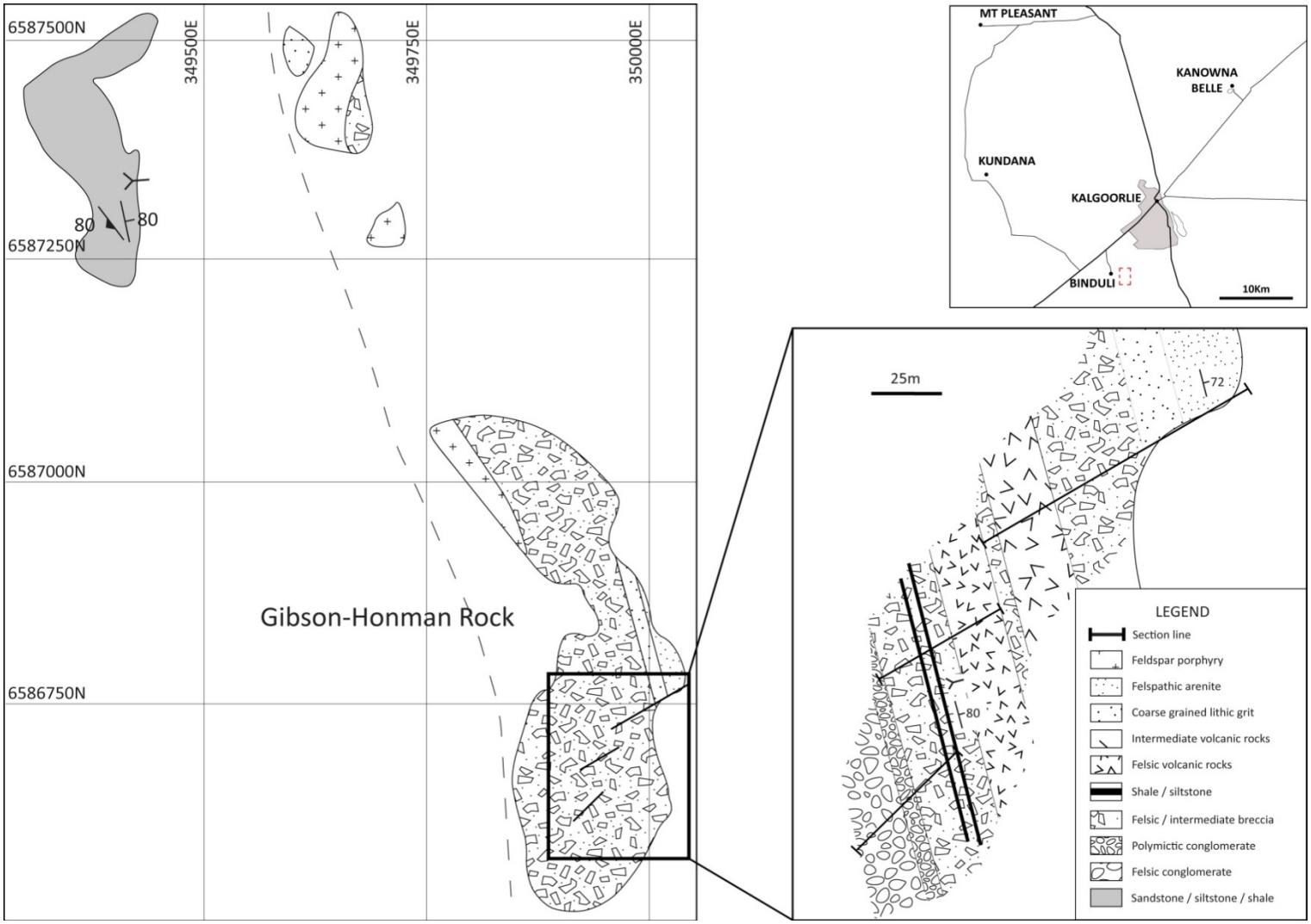

Figure 3.12 – Outcrop map of the Binduli east area – with detailed section through Gibson-Honman Rock. Outcrop shapes modified from Barrick GIS (Crossing, 2003); see Figure 3.11 for location.

those units unconformably overlie the Binduli porphyry conglomerate, the base of the latter is considered to mark an internal unconformity within the Black Flag Formation.

Description (Binduli)

At Binduli (Fig. 3.11), lower Black Flag formation (BFl) comprises a zone of intercalated andesite / dacite with interbedded sandstone, siltstone and carbonaceous shale, which is extensively intruded by feldspar porphyry, quartz-feldspar porphyry, and minor dolerite. The BFl includes shale and sandstone (Fig. 3.13a) to the east of the Binduli mining centre, and porphyry-clast dominated conglomerate, exposed in the Pitman mine. Massive structureless sandstone units are interbedded with highly deformed carbonaceous shale in areas close to porphyry intrusions, whereas locations away from the intrusions display well-preserved plane-bedded sandstone and siltstone interbeds with minor shale horizons. A total estimated thickness of 2700 m is calculated from the interpreted structure and outcrop extent of the BFl unit.

Lower Black Flag formation (BFl) also includes felsic volcanic rocks and associated breccia and conglomerate overlain by sandstone and shale. The best outcrop exposure of these rocks is at Gibson-Honman Rock where dacitic and rhyolitic volcanic rocks were described by Morris (1995) as 3-4 m lava lobes with weak flow banding, surrounded by thick breccia units of the same composition. The breccia units (Fig. 3.12; Fig. 3.13b,c, d) grade into coherent felsic porphyritic rocks and may represent proximal apron breccias around felsic domes, whereas some of the breccia units contain a significant component of sub-rounded debris indicating minor reworking of the volcaniclastic clasts. In thin section the breccias are composed of sub-round dacitic clasts set in a coarse sandstone matrix of angular crystal and lithic fragments (Fig 3.13e, f).

Intermediate porphyritic rocks are also present as dykes or sills with some hornblende-bearing intermediate material observed in the breccia zones (Fig. 3.12). Thin shale-siltstone beds are found between breccia units that have strike persistence over 20-50 m and are parallel to bedding in feldspathic sandstone units at the eastern edge of the outcrop. The breccia zones are stratiform and the larger shale lenses are not exotic fragments or shale rafts (Fig. 3.12; cf. Morris 1995), however some fragments of shale are present in the breccias (Fig 3.13g, h). Rocks to the east and south of Gibson-Honman Rock include coarse feldspathic and quartzose sandstone (Fig. 3.11) and abundant siltstone and shale that are poorly exposed, but identified from exploration drill holes.

Several diamond drill holes from the Centurion gold mine contain intersections of the uppermost units of the lower Black Flag formation (CD26; CD27; CD28; CD29 - See Chapter 7). The sequence contains intercalated felsic, dacitic volcanic rocks with peperitic contacts against a sequence that includes finely laminated siltstone, sandstone and mudstone locally with

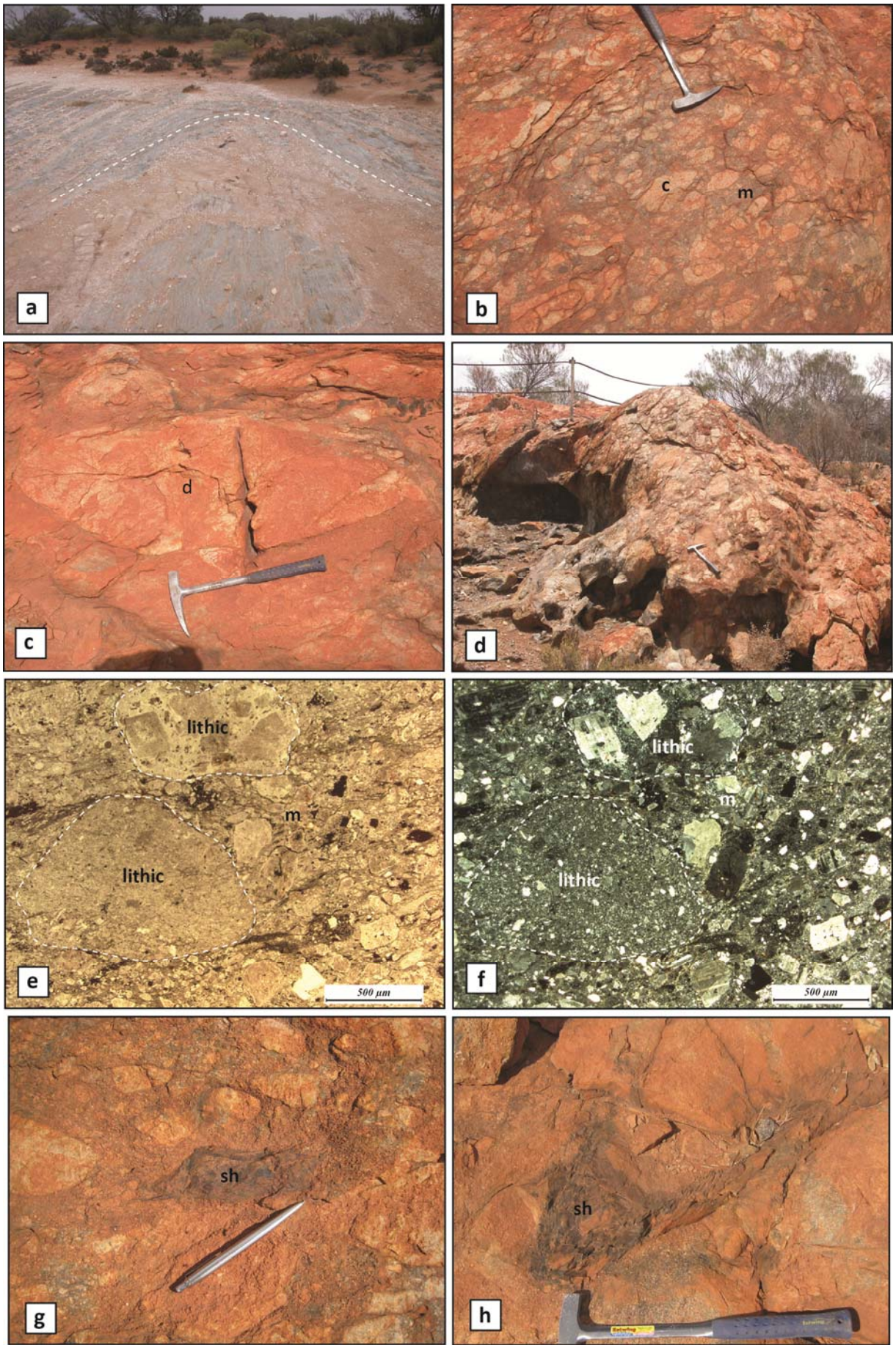
a
b
c
m
c
d
d
lithic
m
lithic
e
500 µm
lithic
m
lithic
f
500 µm
sh
g
sh
h

Figure 3.13

Captions for Figure 3.13 - Lower Black Flag formation sandstone/shale and felsic breccia.

a) Lake pavement outcrops of folded shale and siltstone with a strong axial planar cleavage. Plunge in unknown due to the flat exposure, view to the north-west, Binduli (GDA: 348996E; 6587137N).

b) Oligomictic, matrix supported dacite breccia composed of coherent dacite clasts loosely packed in a crystal-lithic rich matrix of similar composition to the clastic component, including abundant stark white feldspar crystals and crystal fragments, and sub-round dacitic lithic fragments, Gibson-Honman Rock (GDA: 349938E; 6586697N); c=clast; m=matrix.

c) Coherent dacite boulder in poorly sorted volcaniclastic breccia. The boulder measures ~1 m in the long axis but has been tectonically flattened perpendicular to the clast long axis, which is sub-parallel to a weakly developed disjunctive foliation, Gibson-Honman Rock (GDA: 349938E; 6586697N).

d) Poorly sorted oligomictic dacite boulder breccia. The rock is primarily matrix supported suggesting deposition as a mass flow, in thick structureless tabular volcaniclastic deposits. This outcrop is interbedded with thin shale beds in a sequence that grades laterally into coherent rhyodacite without a sharp boundary, suggesting these are proximal volcaniclastic deposits. Gibson-Honman Rock (GDA: 349970E; 6586544N); d=dacite clast.

e) PPL photomicrograph of dacite and quartzo-feldspathic sandstone clast-rich breccia in a quartzo-feldspathic and lithic volcaniclastic sandstone matrix. Sub-rounded porphyritic dacite clasts, have euhedral plagioclase crystals set in a fine felsitic groundmass - the matrix is composed of broken sub-round to sub-angular crystal fragments of quartz and plagioclase with late euhedral alteration (metamorphic?) biotite in cleavages and crystal pressure shadows. Late red hematite overprints the rock in fractures and cleavage planes. Gibson-Honman Rock (GDA: 349938E; 6586606N); m=matrix.

f) XPL photomicrograph of (e) displaying moderate murky chlorite alteration of the matrix and albitic alteration of feldspars; m=matrix.

g) Outcrop 600 m NNE of the Centurion gold mine with black mudstone clasts in weathered oligomictic volcaniclastic conglomerate. The felsic conglomerate clasts are composed of feldspar porphyry (Centurion Porphyry) with euhedral plagioclase in a white groundmass of plagioclase and quartz(?) – Binduli (GDA: 347420E; 6588190N); sh=shale.

h) Same outcrop as (e) with coarse breccia facies to coherent dacitic volcanic rocks intercalated with fine black mudstone bands, very similar to the Gibson-Honman Rock sequence. The black shale units in this example are restricted to small inter-clast ‘hinges’ which may reflect primary consolidation of the units, or structural overprinting; sh=shale.

intraformational sedimentary breccia (See Section 7.4.2 for details). Beds of fine pebbly felsic grit are dominated by quartz and feldspar grains with lithic fragments, angular mudstone chips and clasts of sulphide replaced mudstone - these are interbedded with thick sections of sulphide replaced mudstone and fine-grained quartz-rich siltstone / mudstone. Rocks interpreted as peperite in the Centurion drill cores contain a mixture of coherent facies quartz-feldspar dacitic volcanic rocks, intermixed with fine mudstones and with wispy intrusive contacts of the dacite against the mudstone, in zones up to 2 m wide.

Outcrops of porphyritic rocks east of the Centurion gold mine at Binduli have very similar characteristics to the sequence at Gibson-Honman Rock with coarse, fragmental dacitic volcaniclastic rocks that contain dacitic porphyry clasts set in a matrix of identical composition to the clasts with fragments and intercalations of fine black mudstone. Intermixing of sedimentary and volcanic rocks, which are locally brecciated, suggests a setting marginal to a sub-marine felsic lava dome complex (Crossing 2001). The rocks from Centurion are tentatively correlated with similar units at Gibson-Honman Rock.

Upper Black Flag formation (BFu) at Binduli, comprises a distinct porphyry conglomerate unit overlain by a thick sequence of deep-water-deposited shale and sandstone that extends to the south of the Binduli mining centre, with uppermost felsic volcanic rocks located west of the New Celebration Mining Centre on GSWA maps (Fig. 3.11; Fig. 3.3). The Binduli porphyry conglomerate (Fig. 3.14a-d) is a massive, poorly sorted deposit with variable contact relationships ranging from sharp basal unconformable contacts with underlying mudstone (CD28) to irregular contacts with rip-up clasts of sulphide replaced mudstone at the base of the unit (CD21; KWD007). The upper contacts were not observed in the drill core examined, but were documented as conformable with overlying sandstone and siltstone units (Croesus mine closure report). The interpretation of conformity at the upper contact is at odds with the map scale distribution, which shows a sharp contact with the overlying unconformable Navajo Sandstone and conglomerate units, and may have been interpreted from parallel bedding trends.

Conglomerate beds comprise clasts of pebble to boulder sized, pink, and altered porphyry clasts (85-95%) that are sub-rounded to sub-angular in a feldspar (±quartz) fine-grained groundmass; finely banded, weakly pyrite-replaced angular mudstone fragments (~1%); strongly sulphide replaced angular mudstone clasts (1-2%); light-coloured felsic clasts that appear similar to felsic rocks in peperitic contact with underlying mudstone (1-2%; host to Eastern Contact Mineralisation at Binduli-ECM), and rare chert and quartzite. The conglomerate is mostly clast supported with <10% matrix composed of fragmented feldspars and lithics, and is diffusely bedded with rare 0.2-0.5 m-thick drill intersections of coarse grit to pebble conglomerate interbeds composed of weakly polymictic clasts with the same composition as the conglomerate. Locally the clasts are well-rounded (CD28), but the dominant clast morphology is sub-rounded to sub-angular. In drill hole CD21 the porphyry conglomerate

contains 5-10% mudstone/siltstone pebbles and some dark-brown strongly carbonate and magnetite-altered pebbles that have remnant porphyritic texture. Generally high strain in the conglomerate is represented by strong flattening of the clasts. In drill holes at Centurion gold mine, the porphyry conglomerate unconformably overlies lower Black Flag formation sulphide-replaced siltstone/mudstone and contains rip-up clasts of this underlying unit immediately overlying the contact (Fig. 3.14 e, f).

In thin section the conglomerate matrix comprises: angular fragments of euhedral feldspar, embayed volcanic quartz, porphyritic lithic fragments and angular wispy mudstone fragments in a very fine-grained sand-silt sized mass of quartz and feldspar (Fig. 3.14g, h). A strong foliation overprints the unit expressed as a preferred alignment of clasts, crystal fragments and matrix groundmass, with spaced seams of biotite and sericite micas.

Description (Kundana South)

The stratigraphic sequence in the Kundana South area, 6.5 km south of the Kundana mining centre, dips and faces to the northeast and includes most units in the regional Kalgoorlie stratigraphy above and including the Upper Basalt (Fig. 3.15). Rocks on the western margin are separated from sedimentary rocks of the Coolgardie Domain by the Zuleika Shear Zone, which is mapped as a 10-15 m wide zone of intense carbonation and deformation in drill holes from the Frog's Leg deposit and in deep drill holes elsewhere (e.g. at the Strzelecki mine see Chapter 5, Fig. 5.2 and Fig. 5.3). Data for the interpretation in Figure 3.15 include: 15 diamond drill holes; geological mapping of the Rubicon gold mine; diamond drill holes at Atlantis and Hornet prospects; several hundred RAB and AIRCORE bottom-of-hole rock chips in the southern area (which is typified by abundant lake clays and dune sands with few surface exposures); and published geological maps of the Frog's Leg area.

The Upper Basalt unit is exposed in the Rubicon gold mine comprising massive-pillowed Bent Tree Basalt and plagioclase-phyric Victorious Basalt separated by a thin discontinuous horizon of carbonaceous shale (Chapter 7). This sequence continues south to the Frog's Leg deposit, but appears to pinch out against the Zuleika Shear Zone at a short distance to the southeast of the Frog's Leg Mine (Fig. 3.15). Bent Tree Basalt and Victorious Basalt are units of the Upper Basalt Formation mapped in the Ora Banda and Mt Pleasant districts, and continue north of Goldilocks into the Kundana mining camp. Primary textures are locally well-preserved with strongly localised zones of intense shearing and flattening.

Fine-grained sandstone and siltstone overlying Upper Basalt in the Rubicon mine and nearby drill holes are correlated with the Talbot formation. The lowermost division is the Centenary Shale, which forms a continuous unit, generally 1.5 m thick and locally up to 10 m thick. The shale is a carbonaceous mudstone that is replaced by disseminated arsenopyrite, pyrrhotite and biotite with extensive quartz-sulphide vein emplacement, and chlorite alteration

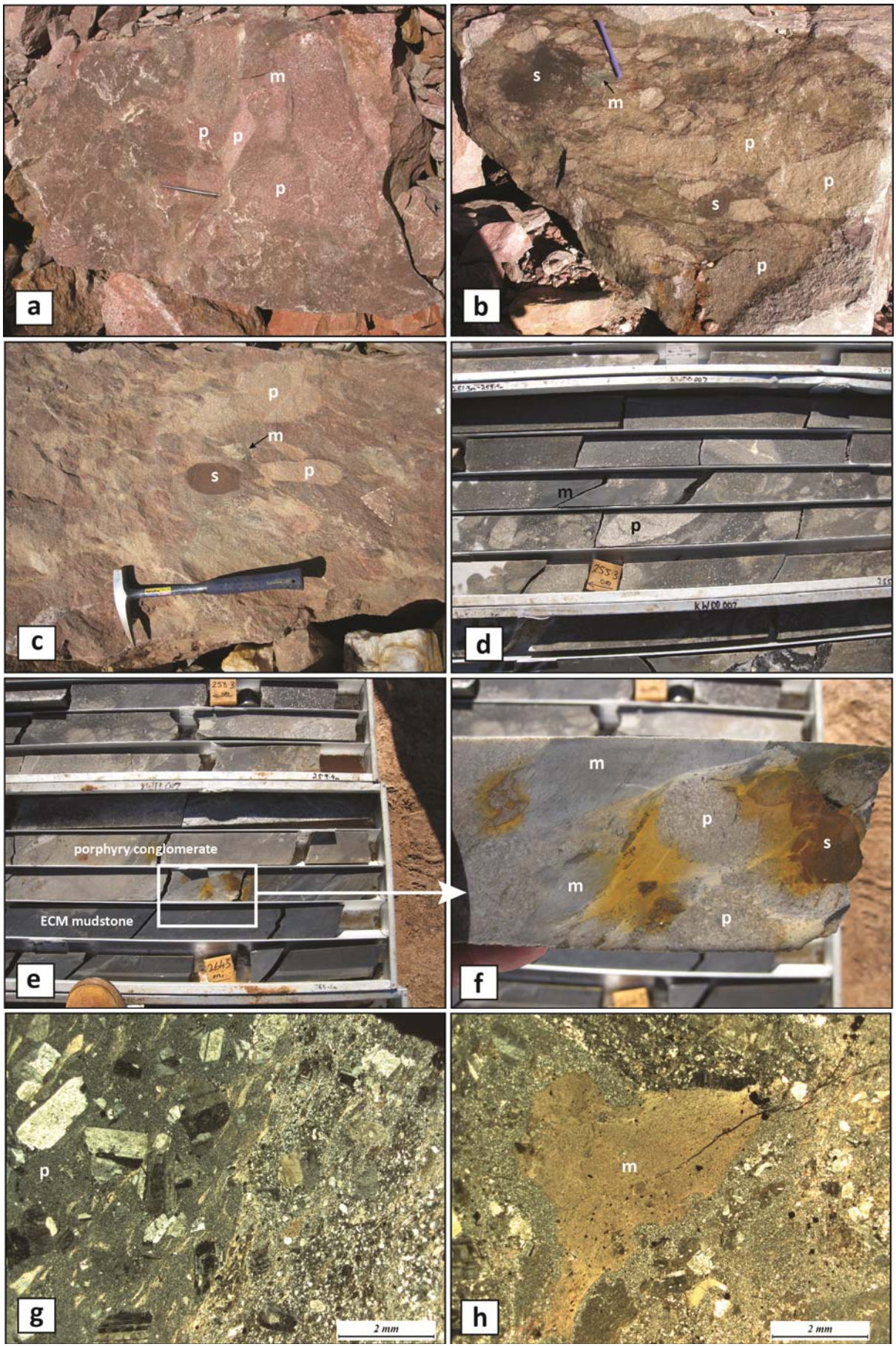
a
m
p
p
p
b
s
m
p
p
s
p
c
p
m
s
p
d
m
p
e
porphyry conglomerate
ECM mudstone
f
m
p
s
m
p
g
p
2 mm
h
m
2 mm

Figure 3.14

Captions for Figure 3.14 – Binduli porphyry conglomerate

a), b), c): Binduli porphyry conglomerate showing sub-rounded clasts dominated by crowded, aphanitic-groundmass feldspar porphyry, subordinate clasts of dark sulphide-replaced mudstone, and weakly sulphidised, bedded mudstone in a clast-supported, poorly-sorted conglomerate. The conglomerate has a moderate tectonic flattening, with a spaced disjunctive cleavage. Clasts of almost totally sulphide replaced mudstone, and others with only weak pyrite mineralisation concur with similar units in the ECM basement of the porphyry conglomerate that were probable sources during erosion. In similar fashion the Centurion Porphyry, a crowded aphanitic groundmass porphyry, is locally overlain by the unconformable Binduli porphyry conglomerate which contains a majority of clasts of near identical composition to the Centurion Porphyry in the substrate. Samples from Centurion gold mine at Binduli (GDA: 347350E; 6587250N); s=sulphide replaced mudstone; m=mudstone; p=porphyry.

d) Porphyry clast conglomerate with small sections of mudstone clasts and locally mudstone matrix KWDD007 – 250 m (GDA: 347110E; 6587256N); m=mudstone matrix.

e) Lower unconformable contact of Binduli porphyry conglomerate against underlying ECM (Eastern Contact Mineralisation) mudstone. The contact zone is a mixture of porphyry and mudstone clasts locally with massive sulphide fragments (f).

f) Close up of mudstone rip-up clasts above interpreted unconformity in (e).

g) XPL photomicrograph of dacite porphyry clast (left) with matrix to conglomerate. The dacite contains broken euhedral plagioclase phenocrysts and weakly undulose embayed volcanic quartz phenocrysts in a fine glassy groundmass of microcrystalline quartz and feldspar. The matrix comprises angular, broken feldspar and quartz crystals, and small lithic fragments (Centurion gold mine at Binduli; GDA: 347350E; 6587250N); p=porphyry clast.

h) XPL photomicrograph of mudstone clast in the Binduli porphyry conglomerate with wispy angular morphology, with angular and broken volcanic quartz and feldspar in the conglomerate matrix (Centurion gold mine at Binduli; GDA: 347350E; 6587250N); m=mudstone clast.

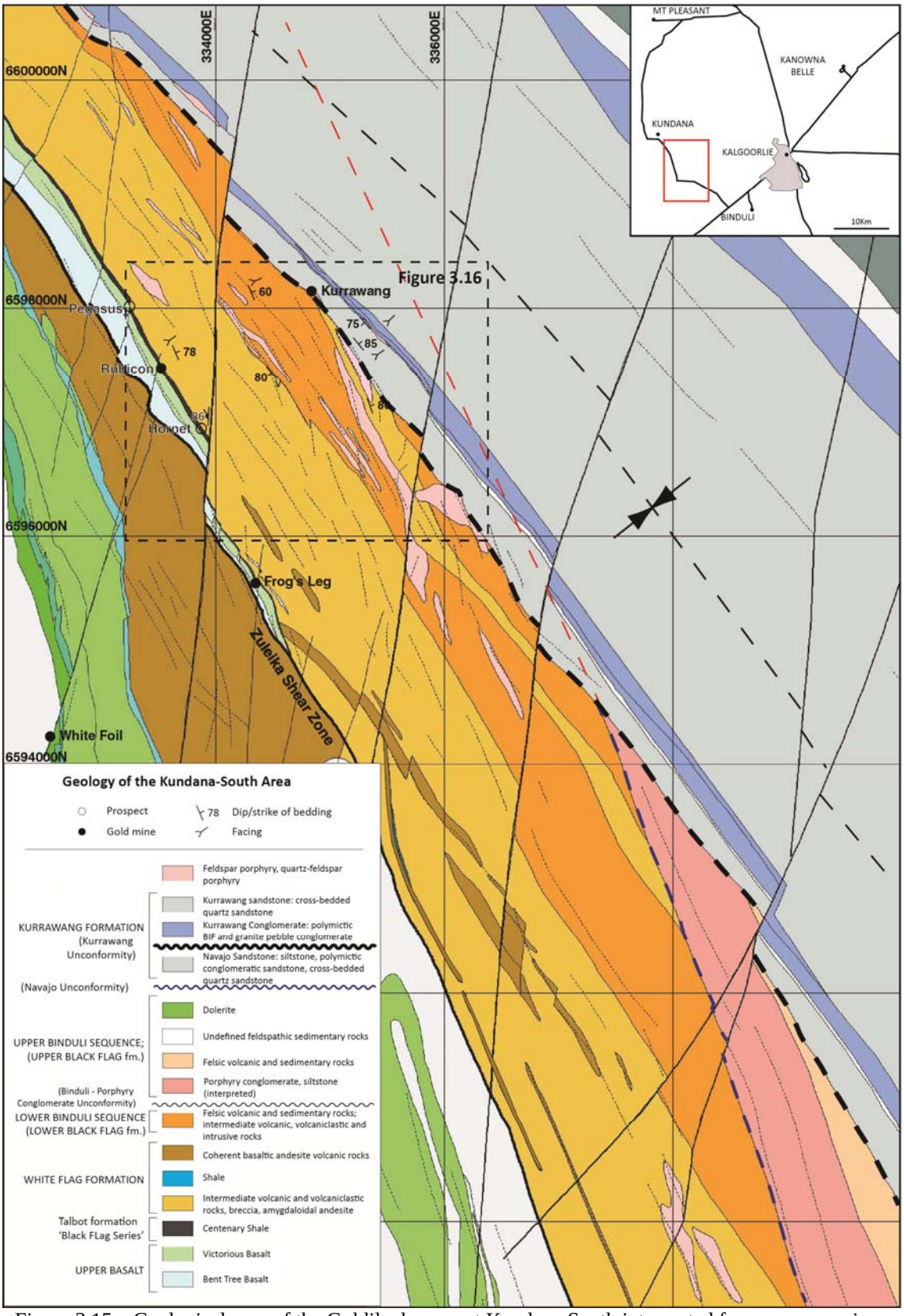

Figure 3.15 – Geological map of the Goldilocks area at Kundana South interpreted from new mapping and drill holes logged in this study, showing a sliver of Ora Banda Domain stratigraphy between the western unconformable margin of the Kurrawang Formation and the Zuleika Shear Zone. The red dashed line marks an interpreted extension of the Binduli stratigraphy underneath the Kurrawang Formation. Dashed black box marks the Goldilocks project area (Fig. 3.16).

in the vicinity of the veins. Talbot formation rocks at Rubicon include fine-grained psammopelites, quartz-chlorite and quartz-biotite schists that are interpreted as relicts of original finely-bedded turbidites, and polymictic conglomeratic sandstone, forming a band several metres thick on the eastern side of the Centenary Shale (Fig. 3.17a,b). In some areas primary textures are preserved with graded bedding and scour-and-fill structures. The fine-grained rocks also have interbedded crystal-rich tuffaceous sandstones with plagioclase-hornblende-biotite composition, in gradational contact with the psammopelites, allowing for a conformable progression with overlying White Flag intermediate volcanic rocks.

A thick section of intermediate volcanic rocks with intercalated sedimentary horizons sits conformably above the Talbot formation at the Goldilocks project (Fig. 3.16; Fig. 3.17a-h). The rocks are correlated with White Flag Formation since they display similar textures and layering to andesitic volcanics outcropping on the edge of White Flag Lake (Fig. 3.17c, d, e). The sequence includes: coarse volcanic breccia with angular clasts of hornblende-phyric vesicular lava and andesite porphyry in a matrix of andesite dominated lithic grit and feldspathic sandstone (Fig. 3.17b, c); fine to medium-grained feldspathic sandstone (Fig. 3.17g); conglomeratic zones with rounded clasts of intermediate composition (Fig. 3.17h); and rare finely-bedded siltstone interbeds.

Several layers of coherent andesitic volcanic rocks have been recorded in previous drill holes and in some cases classified as 'mafic'. These units are basaltic andesites that form prominent magnetic features defining an internal layering within the unit (Fig. 3.15). The basal contact of the White Flag Formation appears gradational with Talbot formation sandstones in drill hole URD073, whereas the upper contact appears to be sharp in contact with felsic dominated volcanic and sedimentary rocks (lower Binduli sequence?) to the east (Fig. 3.15; Fig. 3.16). Deformation of the unit is weak to moderate with good preservation of primary volcanic textures. Thick sections of amygdaloidal andesite lava are intercalated with volcanic breccia and sandstone, indicating the primary volcanic nature of the package (Fig. 3.17 d).

A ~600 m thick package of felsic volcanic and sedimentary rocks with intercalated intermediate volcanics overlies the White Flag Formation and is tentatively correlated with the lower Binduli sequence (lower Black Flag formation). In the Goldilocks project area, the presence of amygdaloidal intermediate volcanic rocks internal to the felsic succession (Fig. 3.17 e,f) may indicate that the White Flag Formation has a transitional contact with the overlying Binduli sequence. This relationship is also suggested by the map pattern distribution of intermediate and felsic volcanic rocks in the Binduli mine corridor (confirmed in drill holes).

The transitional unit contains thick sections of felsic breccia and conglomerate (Fig. 3.18a) with interbedded feldspathic sandstone. Abundant feldspar porphyries were intruded as sills into finely bedded sandstone-siltstone sequences with sharp intrusive contacts (Fig. 3.18b). Primary felsic volcanic rocks include amygdaloidal felsic lavas with hyaloclastite intercalated

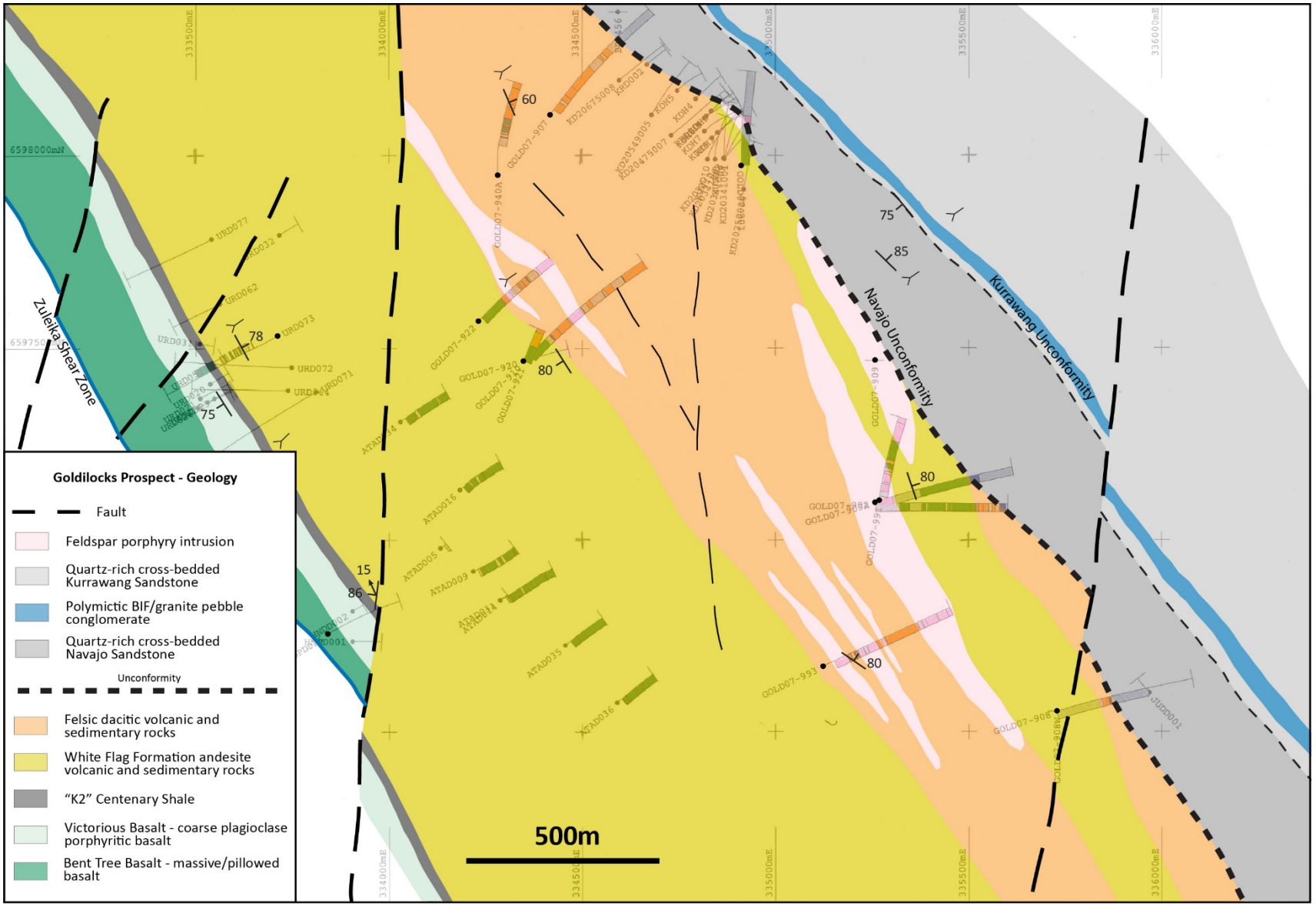

Figure 3.16 – Interpreted geology from re-logged diamond drill holes at the Kundana-south Goldilocks project (detailed drill hole logs in Appendix). Re-logged holes display lithology hachure, and have a bold black circle marking the collar position.

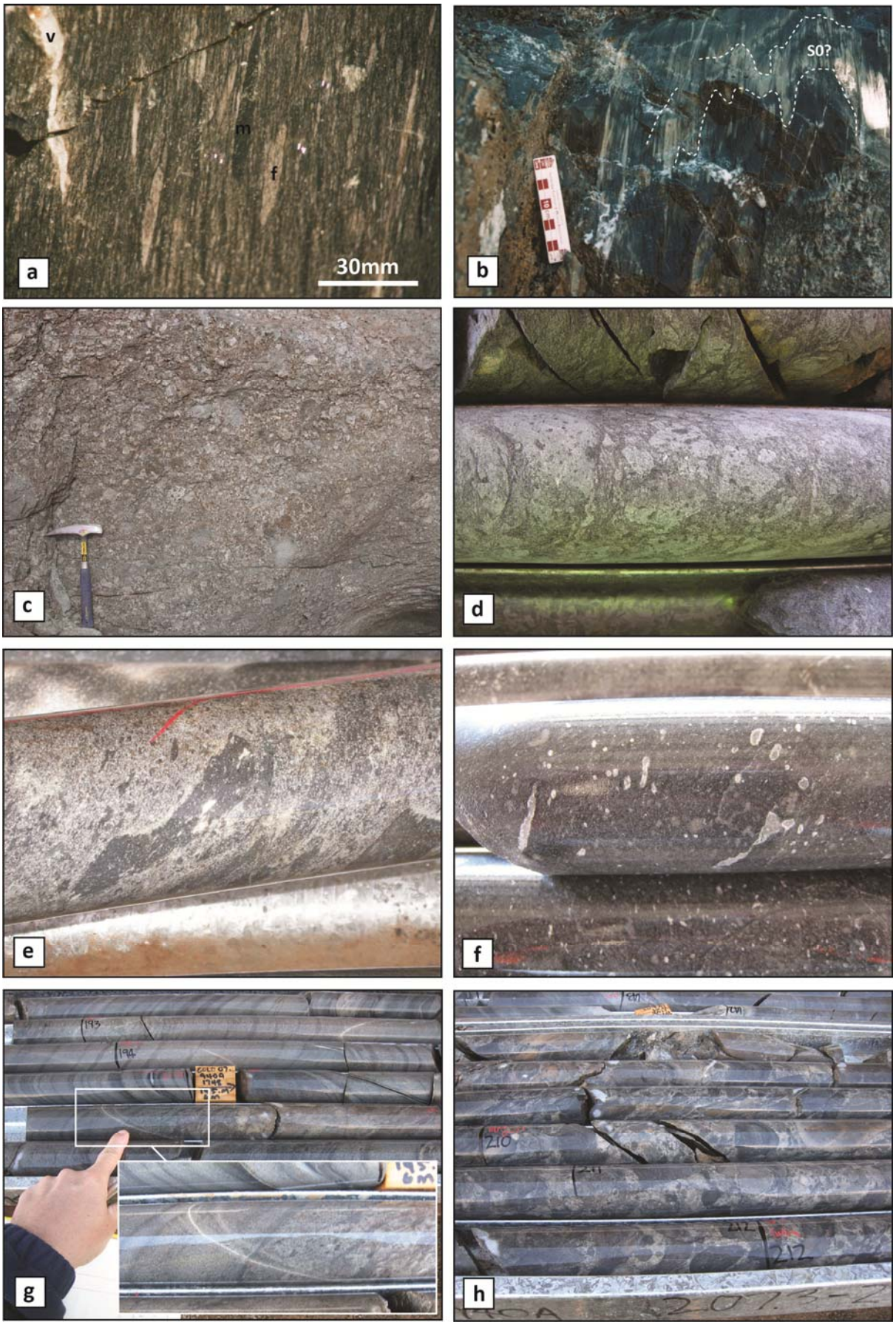

Figure 3.17

Captions for Figure 3.17

a) Talbot formation polymictic conglomeratic sandstone. The unit sits stratigraphically above a strike continuous carbonaceous shale unit 'Centenary Shale', which is the first sedimentary sequence located conformably above the Upper Basalt in the Kundana mining centre. The Talbot formation in this area is a relatively thin unit with strong flattening strain and a rapid gradation up-section with overlying White Flag Formation intermediate volcanic rocks. Clasts of felsic to intermediate volcanic rock and dark mudstone are set in a coarse sand sized matrix of crystals and lithic fragments. The clasts shapes may have been sub-angular, but the flattening obscures primary textures. Rubicon gold mine, Kundana (GDA: 333550E; 6597450N).

b) Mine wall photograph of fine-grained psammopelite (quartz-chlorite and quartz-biotite schist), which are probable relicts of original finely bedded turbidites with rare horizons of black shale. In some areas primary textures are preserved with graded bedding, scour-and-fill structures, and interbedded crystal-rich tuffaceous volcaniclastic rocks with plagioclase-hornblende composition. The tuffaceous rocks are polymictic and gradational in contact with the psammopelites, indicating a probable sedimentary origin. Viewed with a hand-lens, multiple penetrative foliations display very little angular discordance, but are cut and reoriented by S_3 shear bands, which also displace fold limbs in S0. Talbot formation, Rubicon gold mine (GDA: 333550E; 6597450N).

c) Poorly sorted lapilli breccia from the White Flag Formation on White Flag Lake (GDA: 331777E-6608928N), for comparison with near identical rocks intersected in drill holes from the Goldilocks area (d).

d) Oligomictic poorly-sorted andesitic volcanic breccia composed of angular clasts of coherent hornblende andesite set in a poorly sorted matrix of sand to pebble sized lithic fragments of identical composition to the clasts; and crystal fragments. Some clasts have very juvenile shapes indicating these are proximal deposits. Goldilocks, Kundana south; drill hole GOLD07-921 63.2 m (GDA: 334348E; 6597467N). Drill cores 50 mm diameter.

e) Crystalline to fragmental and feldspar-phyric andesitic volcanic breccia, with abundant angular to fluidal clasts of coherent amygdaloidal andesite. The unit has a gradational upper contact against fine-medium-grained biotite altered feldspathic sandstone. White Flag Formation; drill hole URD073 - 233 m; Rubicon gold mine, Kundana (GDA: 333709E; 6597533N). Drill cores 50 mm diameter.

f) Coherent amygdaloidal andesite lava rocks; Goldilocks, Kundana south; drill hole GOLD07-909 390 m (GDA: 335257E; 6597467N). Drill cores 50 mm diameter.

g) Interbedded feldspathic sandstone and conglomerate. Sharp bedding contact between coarse and fine units; Goldilocks, Kundana south; drill hole GOLD07-940A 195.6 m (GDA: 334281E; 6597949N). Drill cores 50 mm diameter.

h) Intermediate conglomerate (weakly polymictic) dominantly composed of sub-round porphyritic hornblende andesite clasts; Goldilocks, Kundana south; drill hole GOLD07-940A 210 m (GDA: 334281E; 6597949N). Drill cores 50 mm diameter.

with fine-grained sandstone beds (Fig. 3.18c), and peperitic contacts of coherent feldspar porphyry volcanic units, where there is an apparent relationship of intrusion into unconsolidated sediments (Fig. 3.18d,e). Porphyritic volcanic rocks in drill hole GOLD07-903 also display brittle deformation with siltstone infilling between fractures and clasts of the consolidated porphyry contained within the siltstone (Fig. 3.18f).

A significant proportion of the sequence consists of massive, structureless sections of fine-medium-grained feldspathic rock, and there is considerable difficulty in distinguishing the rocks as either porphyritic intrusive or sedimentary arkose (Fig. 3.19a,b). In drill hole PDDD004 south of Goldilocks, sections of this rock type up to 10's of metres thick are separated by narrow fine-grained zones that may have been original sandstones. The sandstones grade into conglomerate and felsic volcanic apron breccias around a coherent felsic volcanic package with marginal hyaloclastite (Fig. 3.18c,d).

The sequence contains several minor sections of intermediate breccia/conglomerate and volcanic rocks, and one thick section that appears as a mappable unit (Fig. 3.15), allowing for the possibility that the Binduli sequence and White Flag Formation may be conformable. On Figure 3.15 the rocks labelled "Lower Binduli Sequence" are distinguished by a dominantly hornblende-absent composition in felsic volcanic and sedimentary rocks, whereas the underlying White Flag rocks are dominated by intermediate hornblende-bearing volcanic and sedimentary rocks. This relationship appears to hold along strike and the contact has been placed on that basis. An abundance of feldspar porphyry intrusions also seems to indicate a change at the contact of this sequence.

A correlation with the rocks at Binduli seems reasonable given that similar stratigraphy and field relationships have been mapped in drill holes from the Centurion mine, with peperitic intrusions of dacite volcanic rocks interpreted as submarine lava dome facies, and hypabyssal porphyritic rocks intruded into a package of feldspathic sandstone, siltstone and shale. Similar rocks are also documented at Gibson-Honman rock.

A particular difficulty in the Goldilocks and Binduli areas is distinguishing syn-volcanic porphyritic intrusions and lava flows from later felsic intrusions. The distinction, although difficult, is important if there is alteration and mineralisation related to the later intrusions. Several zones of intense magnetite alteration were observed in the drill core and are obvious on the aeromagnetics as a broad aeromagnetic high anomaly in the Goldilocks area. This anomaly appears to be located in an area where felsic porphyritic intrusions are identified in drill holes. Some of this anomaly may also be a primary signal from magnetite-rich portions of the White Flag Formation (Fig. 3.20).

Figure 3.18 - Typical examples of lower Black Flag formation rocks correlated with the Binduli sequence in Kundana South drill core (50 mm diameter). a) Angular felsic breccia/conglomerate, with cuspate volcanic clasts, GOLD07-921 160 m - GDA: 334348E; 6597467N; b) Sharp intrusive contact of porphyry with bedded sandstone, GOLD07-993 222.2 m - GDA: 335122E; 6596670N; c) Amygdaloidal crystal-rich volcanic hyaloclastite, GOLD07-993 446 m, d) Peperitic margins of feldspathic volcanic rock, GOLD07-907 220 m - GDA: 334416E; 6598105N, identical to rocks recorded at Binduli by Doyle (1999); e) Peperitic margins of feldspathic volcanic rock, GOLD07-907 220 m, f) Fractured feldspar porphyry with infilling by siltstone GOLD07-903 - GDA: 334912E; 6597974N. Drill cores have 50 m diameter.

Figure 3.19 - Lower Black Flag formation rocks in Kundana South drill core (50 mm diameter). a) Structureless feldspathic tuffaceous rocks PDDD004 65 m; b) Structureless feldspathic tuffaceous rocks GOLD07-991 ~60 m – GDA: 335268E; 6597103N; c) Marginal dacite hyaloclastite in sandstone siltstone at the edge of a package of coherent dacitic volcanics PDDD004 294.5 m; d) Coherent dacite/rhyodacite volcanic rock PDDD004 325 m.

Structural geology

Deformation in the lower Talbot formation sedimentary rocks is similar to the styles observed in the sedimentary rocks overlying Upper Basalt south of Mt Pleasant with zones of open to tight upright folds alternating with zones of intense shortening that display isoclinal folding and shearing. The sequence at Binduli is folded into a south-plunging isoclinal syncline-anticline pair as indicated by structural and facing data, which contrasts with the NNW-plunging Kurrawang syncline to the west across the Kurrawang unconformity. A shear zone (Centurion Fault) also separates the two major fold structures (Fig. 3.11). In all locations the folds are upright with variable fold plunges to the NW or SE. At Kundana South there is widespread preservation of primary rock fabrics and contact relationships. Shear zones are localised on major contacts between rocks of variable strength, and within weak siltstone units.

A significant pre-Kurrawang unconformity is interpreted from drill holes and aeromagnetic data on the south-eastern portion of the geological map in Figure 3.15. A highly magnetic unit shows strong angular truncation of the Kundana South sequence in aeromagnetic images and is correlated with a similar unit along the western margin of the Kurrawang

Syncline that trends directly along strike from the Binduli porphyry conglomerate unconformity (Fig.3.20).

In the Centurion gold mine at Binduli, the Binduli porphyry conglomerate unconformably overlies a sequence of intercalated felsic volcanic rocks and fine laminated siltstone/mudstone (host to Binduli Eastern Contact Mineralisation-ECM) that was intruded by the Centurion porphyry: a crowded aphanitic groundmass feldspar porphyritic intrusion. The unconformity is interpreted from the similarity of clast compositions to the units in the substrate: i.e. characteristic clast compositions dominated by crowded feldspar porphyritic rocks and rare siltstone/mudstone clasts. Added to this is the observation that the Binduli ECM-host mudstone displays strong sulphide replacement, as do clasts of this same rock in the overlying Binduli porphyry conglomerate (Chapter 7).

Several other units with superficial similarities to the Binduli porphyry conglomerate were intersected in the Kundana south diamond drill holes, and observed in outcrops in the Binduli mining camp (Pitman gold mine; Fig. 3.11).

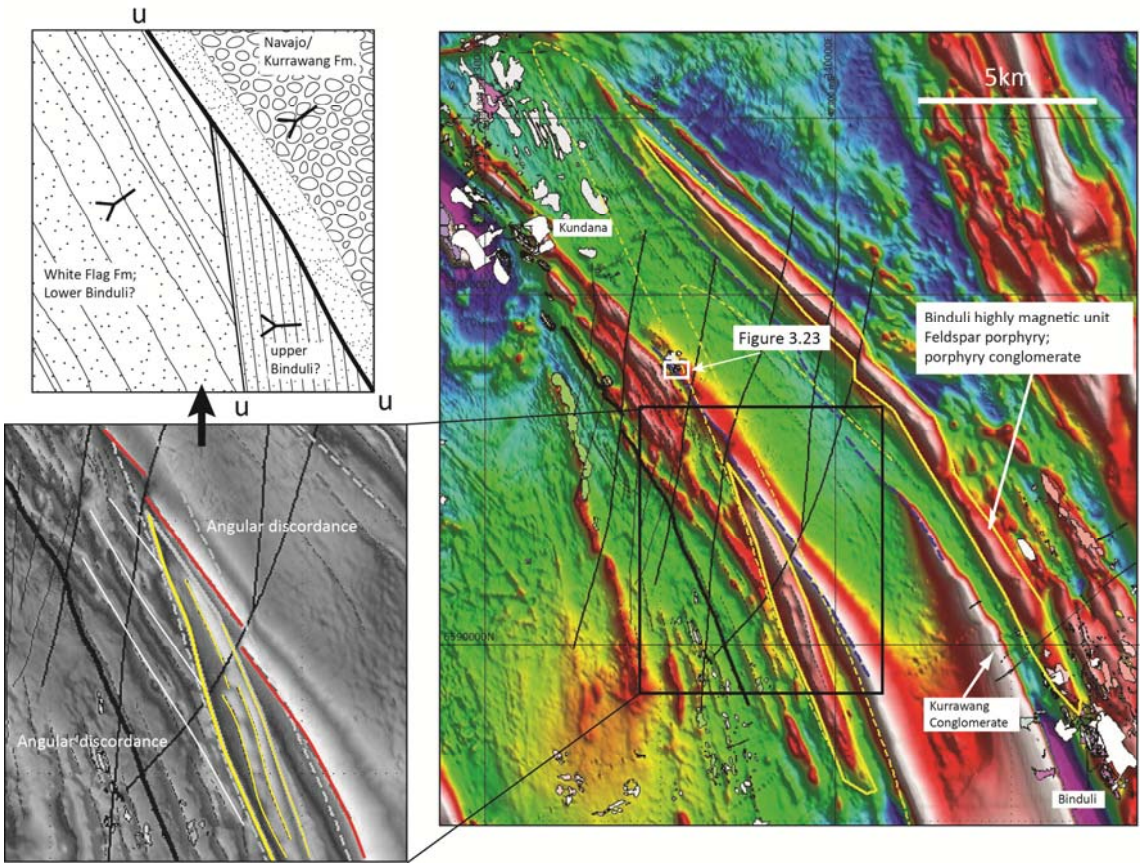

Figure 3.20 – Annotated images of aeromagnetic data (total magnetic intensity, reduced to pole) of the Kundana to Binduli area with outcrop polygons overlain on the coloured image. Highly magnetic unit at Binduli appears to be folded (pre-Kurrawang), re-emerging in the Kundana South area. There is a clear angular discordance between the highly magnetic unit and underlying rocks, and between the Navajo/Kurrawang sequence and all underlying rocks to the west.

The Binduli porphyry conglomerate exposed in the Centurion gold mine at Binduli unconformably cuts underlying felsic volcanic rocks, which have textures suggestive of sub-marine lava dome facies similar to Gibson-Honman Rock; hence, this contact is considered to mark a time boundary between the lower and upper Black Flag formations. It should be noted that the exposure of this unconformity is restricted to the Centurion gold mine and diamond drill holes, and further data is required improve the understanding of this contact (Fig 3.11).

The appearance of Ora Banda Domain sequences on the western side of the Kurrawang Syncline with angular unconformable contact suggests a possibility that the Ora Banda stratigraphy was folded prior to the deposition of the Kurrawang Formation. A further issue is the much reduced thicknesses in an otherwise complete stratigraphy, which suggests the possibility of fault-controlled growth sequences (discussed in Chapter 5) or potentially structural thinning of the sequence.

Interpretation and correlation

Separation of the Black Flag Formation into upper and lower divisions is justified by the presence of a distinctive porphyry conglomerate unit located about halfway up the sequence at Binduli (Fig. 3.14a-d). The porphyry conglomerate unit at Binduli indicates a significant change from intercalated andesite-dacite volcanic rocks and deep-water deposited sandstone/siltstone and shale in the lower Black Flag formation. This contact is interpreted as an unconformity internal to the Black Flag Formation, and is cross-cut by the unconformable base of the Navajo Sandstone at the location of the Binduli gold mines.

The age of the Black Flag Formation in the Ora Banda Domain is open to question. A U-Pb zircon SHRIMP age of 2676±5 Ma for clasts taken from dacite breccia at Gibson-Honman Rock was reported by Krapez et al. (2000) and interpreted to be the igneous age of volcanic eruption most probably between 2671 Ma and 2681 Ma. The age was calculated from eight concordant zircons selected from a larger data set, but analyses of two older grains at approximately 2900 and 3300 Ma were also reported. Barley et al. (2002), influenced by the presence of the older grains, reinterpreted the breccias to be volcanogenic sedimentary rocks and recalculated a new age of 2669±8 Ma from a selection of 11 of the most concordant analyses, implying an age of deposition less than 2661 Ma. Both ages are consistent with the inferred stratigraphic position of the section at Gibson-Honman Rock in this study. A third interpretation, however, is that the older analyses are from inherited xenocrysts in an igneous rock, and that the age of the dacite at Gibson-Honman Rock is bracketed between 2661 and 2677 Ma using the recalculated value of Barley et al. (2002). This is consistent with the suggestion that the rock is volcanic in origin. Since the dacite at Gibson-Honman rock occurs at a relatively high level in the stratigraphic column, this would allow for the possibility that lower members were deposited at around 2680 Ma, and their superposition on the White Flag Lake

rocks. An upper limit on the ages of the Black Flag strata in Binduli mining centre is provided by U-Pb zircon analyses in the range of 2664-2670 Ma for a feldspar porphyry body cutting the section at the Centurion pit (Fig 3.11, Fig 3.21).

Sedimentary rocks in the Kundana mining district have uncertain contact relationships and could be interpreted as part of the Coolgardie Domain despite their location east of the mapped Zuleika Shear Zone. A 500 m-thick section of Upper Basalt is exposed between the Zuleika Shear Zone and the Kurrawang Formation at Kundana, and appears to represent a condensed section of Victorious and Bent Tree Basalt. The 500 m-thick section at Kundana is contrasted with a 3.1 km-thick section of the same stratigraphy in the Ora Banda Domain, which is a significant thickness change, and may represent a growth sequence or a tectonically thinned stratigraphic sequence. Well-preserved primary volcanic textures, and strike continuity argue against tectonic thinning, but if this thickness change represents a growth sequence, another major fault must be located to the east of Kundana, possibly below the Kurrawang Formation or at the eastern contact of that unit.

Other shear zones to the east of the nominal Zuleika Shear Zone may be a part of the same regional domain boundary fault, with the section of Ora Banda stratigraphy at Kundana forming a disconnected tectonic sliver. With the available data, it appears the Ora Banda Domain formations were folded under the Kurrawang Formation prior to uplift and unconformity, but the possibility that early faults controlled primary thickness variations cannot be ruled out.

3.2.4 Kurrawang Formation (KUF)

Introduction

The Kurrawang Formation (KUF) is variably exposed over a 78 km x 4 km area to the west and northwest of Kalgoorlie (Fig. 3.3). The formation comprises four major subdivisions from bottom to top: trough cross-bedded quartz sandstone with pebbly quartz-sandstone and polymictic conglomerate, ~250 m thick (Navajo Sandstone); polymictic conglomerate and minor quartz-lithic sandstone, ~460 m thick (Kurrawang Conglomerate); trough cross-bedded quartz-sandstone with rare siltstone interbeds, ~1250 m thick; and plane-bedded sandstone and siltstone, ~290 m thick (Kurrawang Sandstone); for an estimated total thickness of 2250 m. Note that Glikson (1971) provided estimates of 600 m, 700 m and 1200 m (inclusive of upper sandstone/siltstone), respectively, for similar units. The KUF lacks intercalated volcanics, but its contact was intruded by hornblende-feldspar porphyry dykes and sills along the south-western and south-eastern margins. The revised stratigraphic column (see Fig. 3.24) is significantly modified from Krapez (1996) and Barley et al. (2002), but is based on the lithostratigraphic column presented in Krapez et al. (2008a). Two drill holes and several outcrop sections were used to determine the detailed characteristics of the KUF.

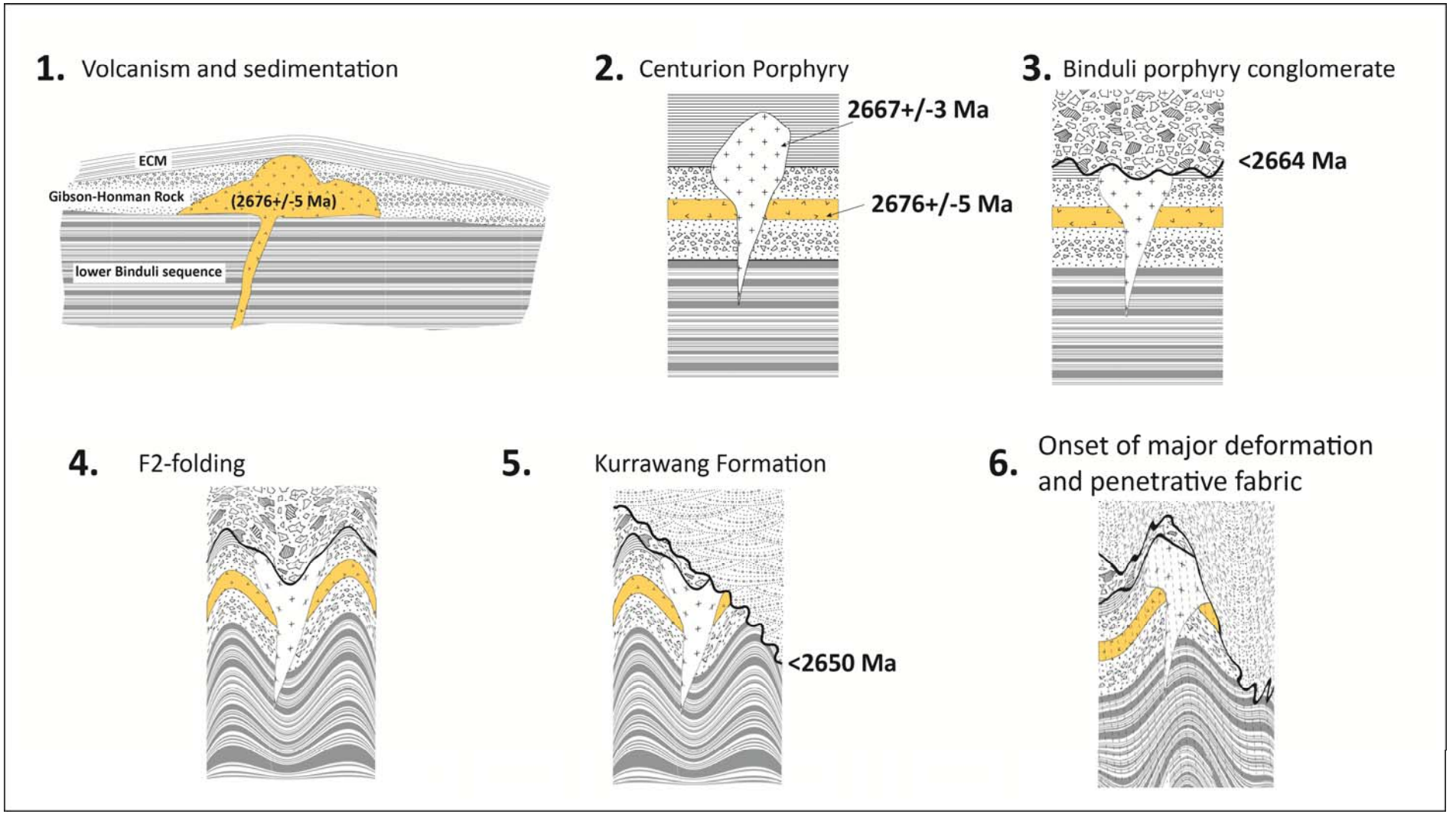

Figure 3.21 – Schematic geological and age relationships of the Gibson-Honman Rock and Binduli sequence.

Contact relationships

A majority of exposures of the lower contact of the KUF in drill holes and outcrops shows a deformed contact against underlying formations with a ~5 m wide shear zone in diamond drill holes near the Kurrawang gold mine. The boundary is usually sharp with no significant tectonic inter-layering and suggests the relationship of a sheared unconformity rather than a major structural disruption. The shearing appears to be localised with variable intensity along strike and this may be controlled by orientation changes of the contact. However, several of the Kundana South drill holes show the lower contact of the Navajo Sandstone (lowest unit of the KUF) is an undeformed unconformity against underlying rocks and appears as a sharp planar boundary.

Angular discordance between bedding in the KUF and underlying formations is demonstrable on a kilometre scale (Fig. 3.3). The eastern margin of the KUF is in contact with all formations from Siberia Komatiite (oldest) to the upper Black Flag formation at the top of the underlying sequence. The upper contact of the KUF forms the uppermost boundary of the Archaean against Cainozoic sedimentary rocks.

At Kundana south, a major unconformity between the Navajo Sandstone and underlying units to the west (Fig. 3.16) was intersected in seven diamond drill holes and is characterised by a major change in rock type from intermediate-felsic volcanic rocks, to quartz-rich, cross-bedded sandstone-siltstone with polymictic pebble lags and scours. Strikes of bedding measured from the Navajo Sandstone and those measured from the underlying rocks are sub-parallel, but there is angular discordance between the dips of bedding in both units (Fig. 3.16). At a map-scale, the angular discordance is well demonstrated by map patterns and aeromagnetic images (Fig. 3.20). The unconformity at the base of the Navajo Sandstone is also exposed in mines and drill holes in the Binduli mining centre: in diamond drill hole KWDD007 at 178.5 m down hole, where the contact is sharp over 1-2 cm. Matrix material from the porphyry conglomerate was ripped up and mixed with the overlying quartz-rich Navajo sandstone, and there is a mild foliation imposed over the contact (Fig. 3.22).

A minor unconformity internal to the Kurrawang Formation (between Kurrawang Conglomerate and underlying Navajo Sandstone) was mapped in breakaway salt lake / clay pan exposures south of the Kurrawang Gold mine (Fig. 3.23). The outcrop shows angular unconformity between thick, tabular, cross-bedded quartz sandstone including minor conglomerate (Navajo Sandstone), and polymictic BIF-granite-porphyry pebble conglomerate and sandstone (Kurrawang Conglomerate). In map pattern there is minor angular discordance between the units in the southern closure of the Kurrawang Syncline, which is confirmed by the outcrop and displayed schematically in Figure 3.24.

Description

The lowest unit of the KUF is the Navajo Sandstone exposed at the Binduli mining centre and in drill holes from the Kundana south area. Navajo Sandstone (Fig. 3.23 and Fig. 3.25 a, b) is characterised by trough cross-bedded sandstone with interbedded pebbly sandstone and conglomerate, and is interpreted as a fluvial sequence (Krapez et al. 2008a). Navajo Sandstone outcrops in type section at Binduli, with previous map-scale interpretations showing the unit as restricted to the southernmost closure of the Kurrawang Syncline (Krapez et al. 2008a). Recent drilling demonstrates that the Navajo Sandstone is present at Kundana south with a thickness of about 300 m, and probably continues to the north of the Kundana mining centre. The Navajo Sandstone typically comprises thickly-bedded (~0.5 m) trough cross-bedded quartz sandstone and wacke, with local gravel lags and thick sections of siltstone.

Conglomerate units (Fig. 3.25c,d,e) in the Kurrawang Conglomerate are dominated by poorly sorted, rounded and elongate, plutonic, volcanic and sedimentary debris, characterised by diffuse bedding of <5-10 m mean thickness, with individual beds up to 16 m thick. Internal sandstone units are plane bedded on a decimetre scale. The mean clast size of the conglomerate is ~84 mm with geometric means up to 147 mm, and rare clasts up to 1.5 m diameter. Conglomerate beds are matrix or clast supported (Clast-to-matrix ratio, C/M = 0.5), with a lithic-wacke matrix (Q:F:L = 12:6:82). The conglomerate contains interbedded sandstone units that have a slightly broader spread of Q:F:L compositions (23:10:67; Fig. 3.24), but also comprise coarse-grained sandstones with a dominant component of angular feldspar grains (Fig. 3.24). Conglomerate beds are polymictic with a broad range of clast types (Fig. 3.24). The unit on average is characterised by abundant mafic volcanic clasts (41%); banded iron formation, chert and quartz vein pebbles (22%); quartz-hornblende-feldspar porphyry (15%); sedimentary (13%) and granitic clasts (8%).

Kurrawang Conglomerate has been mapped from geophysics mostly by its distinctive high-intensity magnetic signature on aeromagnetic images as a thick unit of polymictic conglomerate, whereas outcrops show the highly magnetic signature is produced by a thin conglomerate layer <15 m thick. The unit has abundant pebbles of iron formation and ferruginous chert with the Fe-rich layers replaced by hydrothermal magnetite; there is also an assortment of rounded granite and porphyry pebbles. Conglomerate bands are interbedded with minor lithic sandstone and siltstone.

Clast proportions of conglomerate beds appear strongly skewed by the local composition of the ripped-up substrate: observed in several sections along the strike of the Kurrawang Formation. Outcrops at the Blister Dam area, in the northernmost part of the unit adjacent to the Siberia Monzogranite, have a dominant granitoid component in the conglomerate, whereas outcrops at the edge of White Flag Lake in contact with White Flag Formation have a predominance of andesite and lithic-sandstone clasts. At north Kundana where the Kurrawang

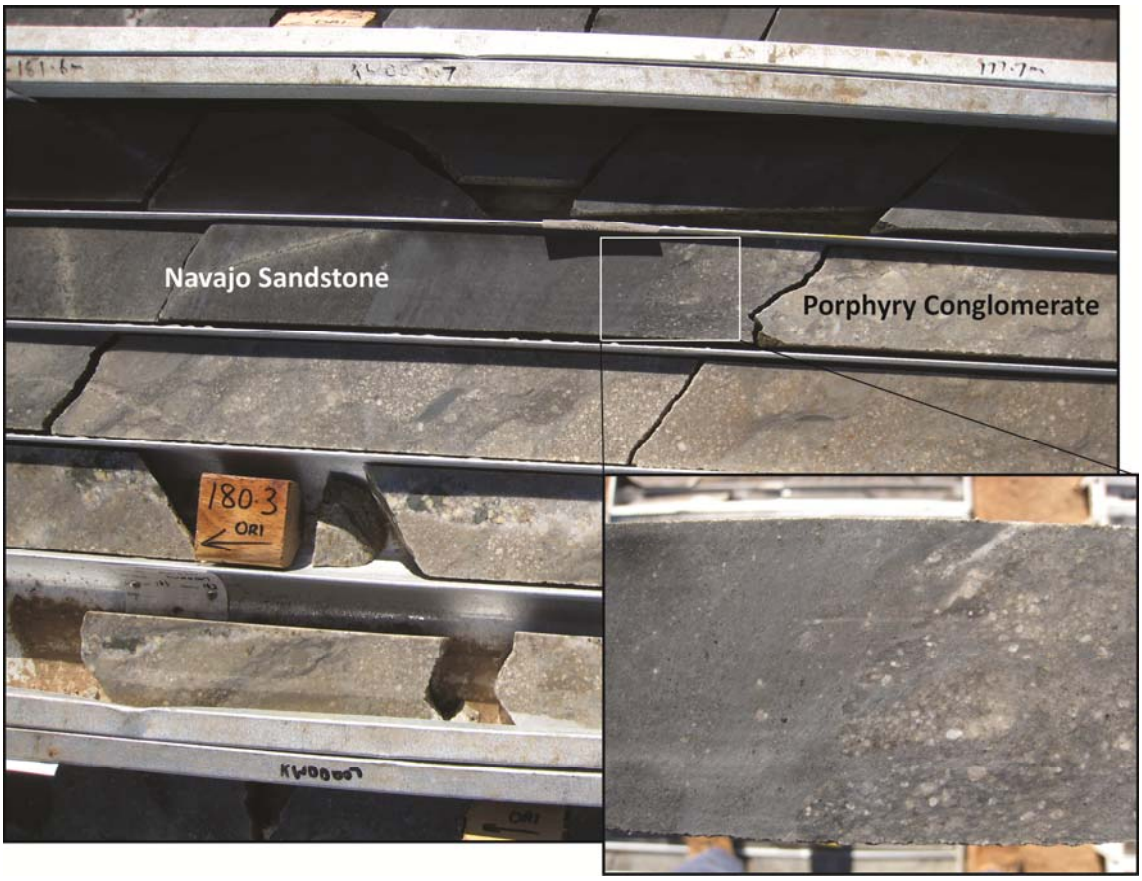

Figure 3.22 – Navajo sandstone unconformity at the Centurion mine, Binduli. Drill hole KWDD007-178.5 m, drilled at 60/050, GDA: 347110E; 6587256N, down-hole direction is from top left to bottom right. The two units have a relatively sharp unconformable contact lacking intercalation or gradation between sequences, with minor rip-up of the underlying Binduli porphyry conglomerate.

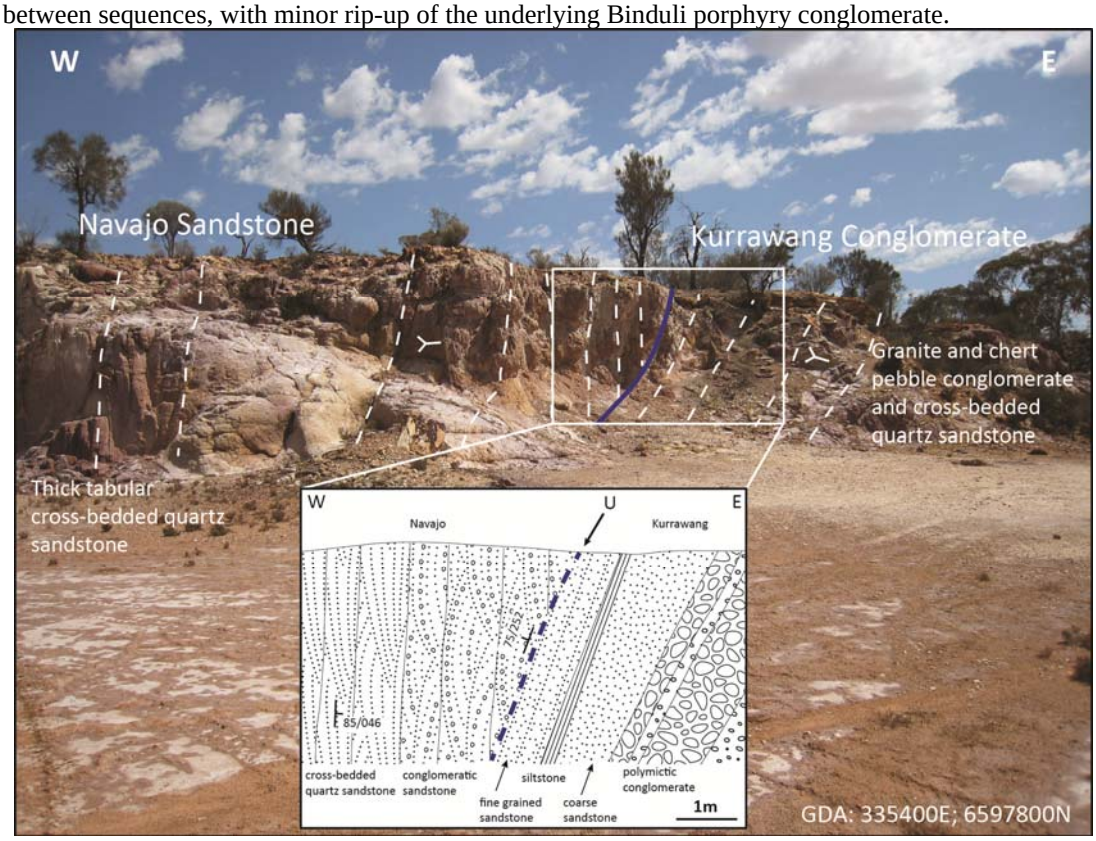

Figure 3.23 – Outcrop of east-tilted angular unconformity between Kurrawang Conglomerate and underlying Navajo Sandstone at Kundana south (U = unconformity). See Figure 3.20 for location.

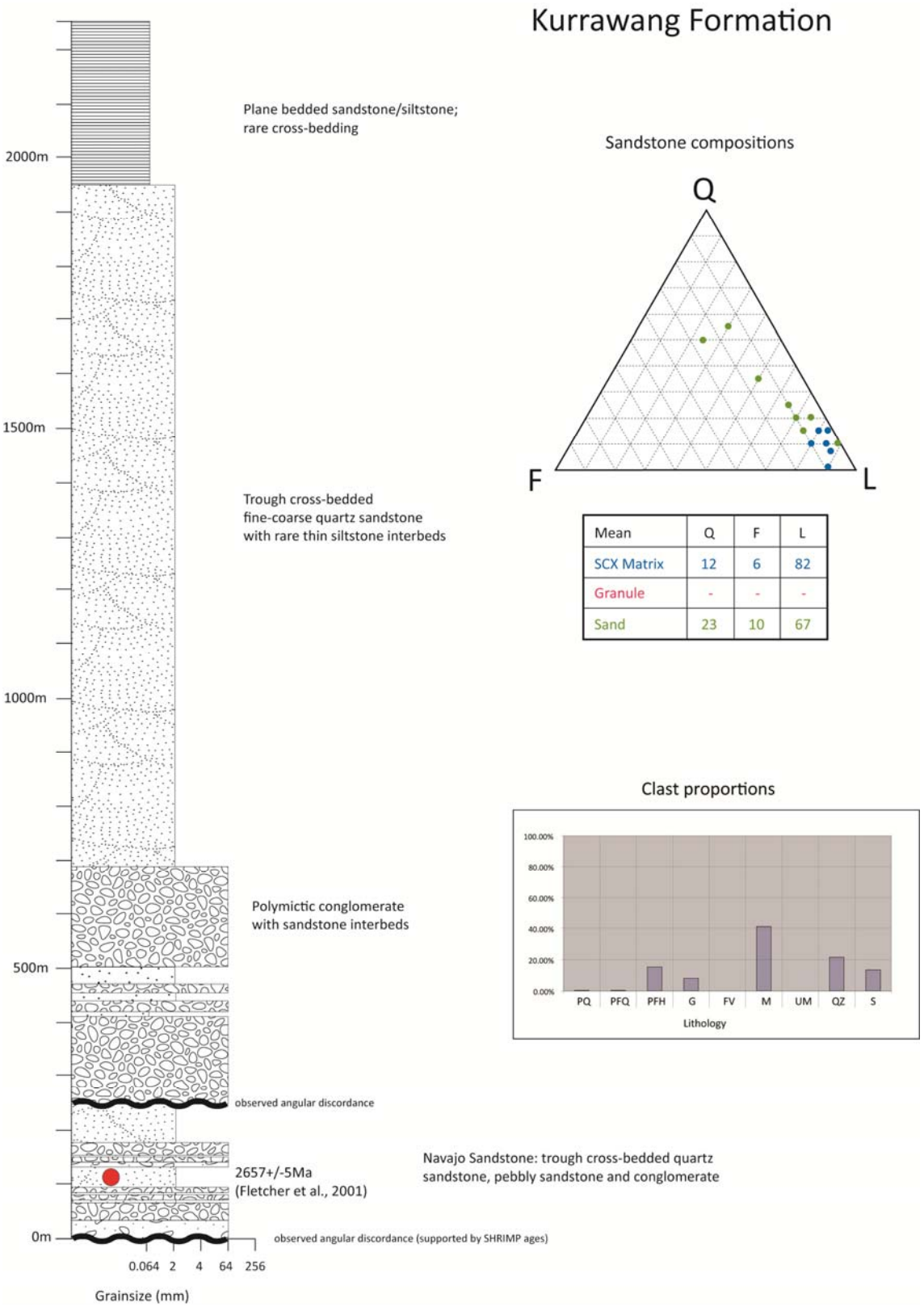

Figure 3.24 – Composite stratigraphic column of the Kurrawang Formation modified from Krapez (1996), and Barley et al. (2002). QFL data from this study are coloured according to the table of mean values in the Appendices. SCX refers to conglomerate or breccia-sized clastics. PQ – quartz porphyry; PFQ – quartz-feldspar porphyry; PFH – hornblende-feldspar porphyry ± quartz; G – granite; FV – felsic volcanic; M – mafic volcanic; UM – ultramafic; QZ – quartz; S – sedimentary. Note that Kurrawang sandstones comprise dominantly quartz-rich wacke, which is not reflected by the presented QFL compositions that were recorded from sandstone interbeds in the lowermost conglomerate units.

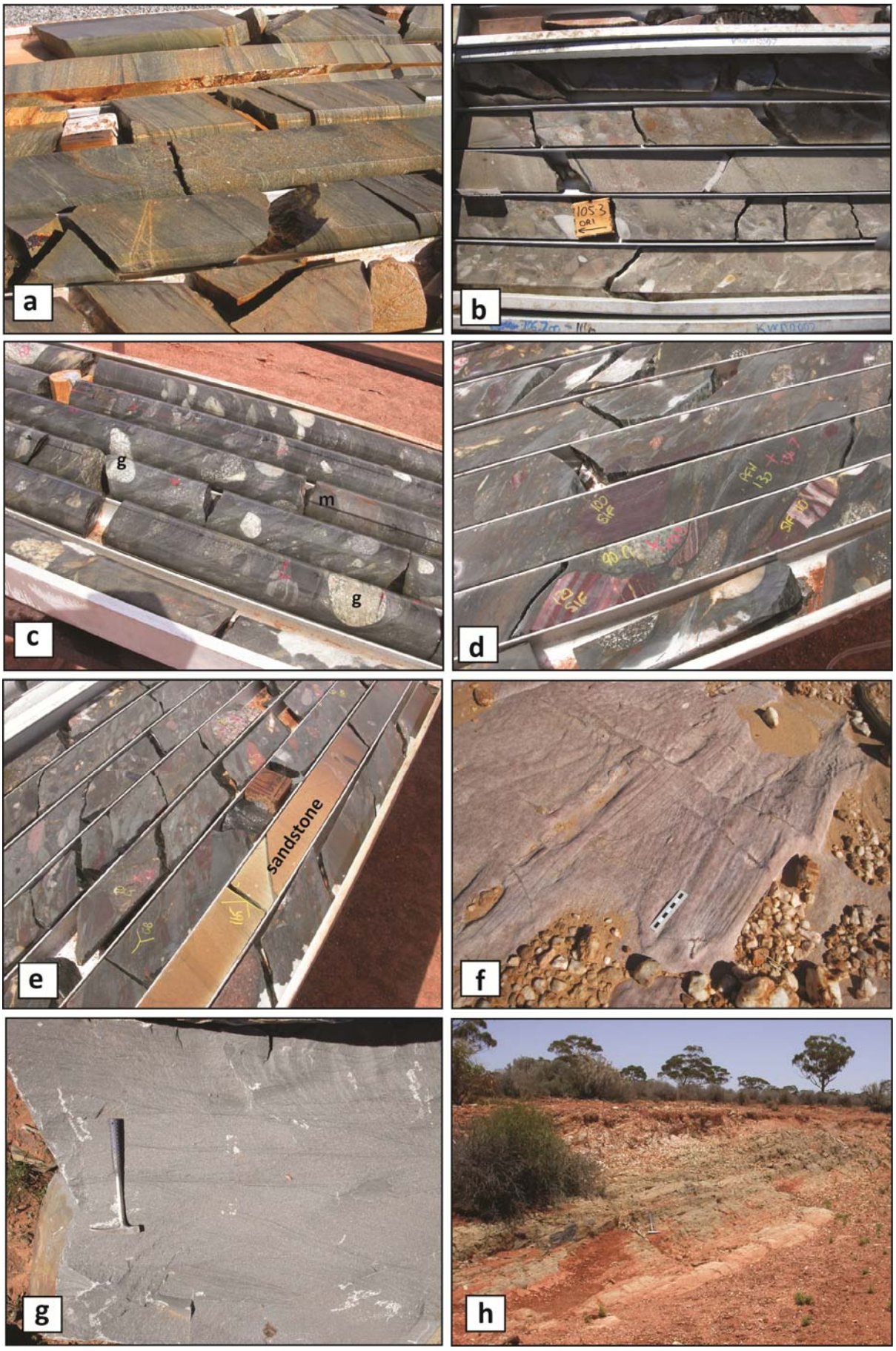

Figure 3.25

Figure 3.25 - Kurrawang Formation conglomerate and sandstone.

a) Cross-bedded polymictic, pebbly quartz sandstone. Cross-bedding, flame structures and scours indicate up-hole younging. Sandstones in this drill intersection of the Navajo member are composed of quartz and feldspar in equal proportions, with minor lithics (not included in the QFL data presented). The sequence contains some coarse-grained sandstone with pebble layers and fine siltstones. (Navajo Sandstone, Beaver gold mine – drill hole BVD001 43.0 m; GDA: 346483E; 6588097N).

b) Cross-bedded Navajo Sandstone with polymictic conglomerate. Beds of polymictic conglomerate, 2-3 m thick, are composed of sub-rounded to sub-angular, and locally well-rounded, clasts of quartzite; sedimentary rock; porphyry; and rare banded chert clasts in clast-supported, massive beds with a quartzolithic sandstone matrix. The conglomerate beds are interspersed with cross-bedded quartzolithic sandstone with cm-scale pebble lags at bed contacts. (Centurion gold mine – drill hole KWD007 105 m; GDA: 347109E; 6587256N).

c) Polymictic conglomerate, with average clast size <64 mm, dominated by mafic volcanic and hornblende-feldspar porphyry clasts. Matrix sandstones have a Q:F:L of 1:9:90. Conglomerate beds are moderately sorted of ~5 m average thickness. White, weakly deformed equigranular granitoid clasts (~5%) stand out amongst a polymictic clast assemblage including Fe-rich chert, mafic volcanic and quartzite clasts. The rock has a strong disjunctive biotite foliation wrapping the clasts (Kurrawang Conglomerate – Brown Dam prospect, drill hole LWD001 97 m; GDA: 304206E; 6632892N).

d) Mafic volcanic and sedimentary rock clast-dominated polymictic conglomerate. Brick red banded iron formation and Fe-rich chert clasts (~5%) stand out with extensive flattening and deformation of the clasts, wrapped by a pervasive matrix foliation. Clast to matrix ratio = 0.5 (Kurrawang Conglomerate – Kundana north, drill hole RCD001 136.5 m; GDA: 327637E; 6608157N).

e) Quartzofeldspathic sandstone interbed with gradational contacts in an up-hole younging sequence of polymictic conglomerate. The sandstone is well sorted, with a true thickness of about 0.3 m, and Q:F:L ratios of 50:26:24 (Kurrawang Conglomerate – Kundana north, drill hole RCD001 165 m GDA: 327637E; 6608157N).

f) Thickly bedded, tabular cross-bedded quartz sandstone from outcrop near the centre of the Kurrawang Syncline. The rock is strongly weathered, but primary textural remnants indicate a westward younging, upright sequence of fluviatile coarse quartz-sandstones with local polymictic gravel lags, and rare internal siltstone beds (Kurrawang Formation; see Figure 3.26; GDA: 329169E; 6608924N).

g) Cross bedded quartz sandstone/wacke dominated by fine-grained angular, ragged quartz and feldspar grains in a very fine quartzofeldspathic siltstone matrix. Fine euhedral brown biotite flakes form a moderate foliation parallel to a weak long-axis alignment of quartz grains. Euhedral biotite flakes overprint an earlier very fine-grained amorphous matrix chlorite, indicating a possible later metamorphic origin for the biotite (upper sandstone unit, Kurrawang Formation – 7 Mile quarry; GDA: 344925E; 6586350N).

h) Rare creek exposure of plane bedded fine-grained sandstone/siltstone in the upper parts of the Kurrawang Formation. The outcrop is several tens of metres east of the Kurrawang Syncline fold axis; fine-grained graded sandstone/siltstone units and scours indicate westward younging in the outcrop. This unit is the same sequence in the south western part of the exposure on Figure 3.26 (upper sandstone unit, Kurrawang Formation; GDA: 327662E; 6610593N).

conglomerate is in sheared contact with Coolgardie Domain mafic and felsic rocks, the conglomerate has a high proportion of coarse dolerite, quartzite, and quartz vein pebbles. Likewise polymictic conglomerate in the Navajo Sandstone at Binduli is dominated by a component of dacitic porphyry pebbles (first recognised by Honman 1914).

The upper Kurrawang Sandstone comprises a section of thickly-bedded (0.3-0.8 m), trough cross-bedded quartz sandstone (Fig. 3.24, Fig. 3.26) with polymictic pebble lags and scour channels, rare siltstone interbeds, and a thin upper unit of plane-bedded, parallel sandstone and siltstone beds with a minor mudstone component (Fig. 3.25h, Fig. 3.26). An outcrop exposure of the upper units of the Kurrawang Sandstone, west of White Flag Lake (Fig. 3.26), shows a broad, continuous sequence of thick cross-bedded units with a ~25 m transitional contact with overlying fine-grained sandstone and siltstone. A rare creek exposure of this same unit (Fig. 3.25h) comprises a sequence of fine-grained plane-bedded sandstone, siltstone and minor shale turbidites locally with scour and fill structures and rip-up clasts of mudstone indicating west younging of the sequence.

This siltstone unit is the uppermost preserved unit of the Kurrawang Formation (Fig. 3.26) and is demonstrated as being very close to the major Kurrawang Syncline fold axis in a creek traverse from 327687E-6610071N to 327888E-6610301N where the rocks show a younging reversal from east-younging, coarse-grained sandstone and fine siltstones with graded-bedding and basal pebble scours, to west-younging very fine-grained siltstone and shale with graded bedding in cyclic turbidites. Crucially, this exposure and the breakaway outcrop depicted in Figure 3.26 demonstrate that the upper siltstone component of the Kurrawang Formation is not a thick sequence, and a best estimate of the thickness of that unit is ~290 m.

In thin section the Kurrawang sandstone/wacke is composed of ~80% grains of strain-free quartz with some remnant euhedral crystal shapes suggesting volcanic precursor grains (Fig. 3.27a, b). The majority of quartz grains are sub-angular to sub-rounded with a sub-population of very angular grains (Fig. 3.27a-d). Minor components include twinned, fragmented albitic plagioclase and lithic fragments in a fine-grained silt-sized quartzo-feldspathic matrix, and rare recrystallised plutonic quartz fragments (Fig 3.27c, d). The matrix is commonly strained with disjunctive biotite and chlorite folia wrapping long-axis-aligned detrital quartz, feldspar and lithic grains (Fig. 3.27d). In some low-strain examples, weakly-strained biotite flakes are randomly arranged through the wacke matrix (Fig. 3.27f).

Structural geology

The Kurrawang Conglomerate contains a strongly developed NNW-trending foliation defined by metamorphic biotite and chlorite that has affected both clasts and matrix minerals in the unit. Mafic, ultramafic, sedimentary and vein clasts are stretched and deformed with a variably plunging stretching lineation throughout the KUF, whereas rigid granite and porphyry

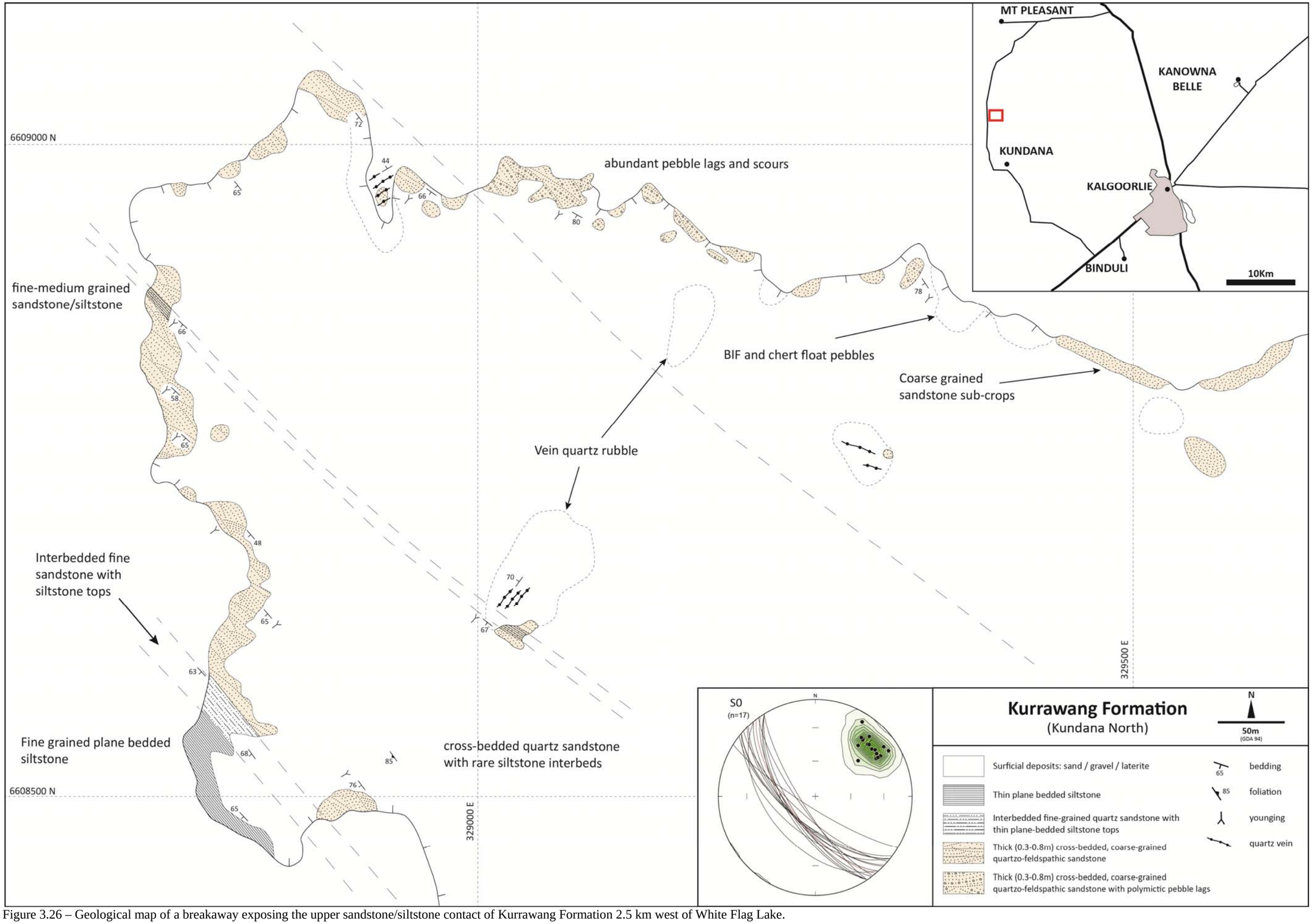

Figure 3.26 – Geological map of a breakaway exposing the upper sandstone/siltstone contact of Kurrawang Formation 2.5 km west of White Flag Lake.

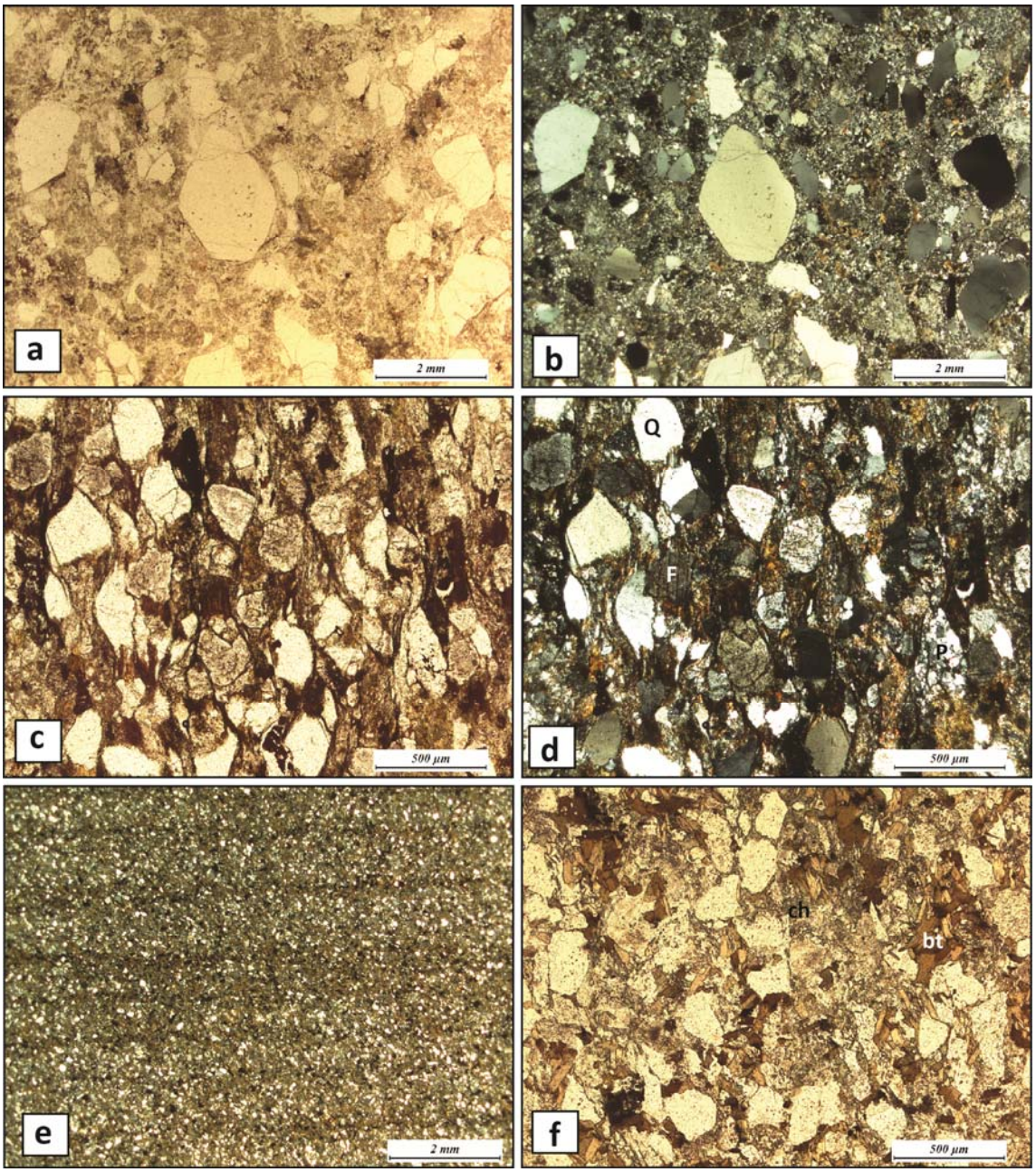

Figure 3.27 – a) and b) PPL and XPL photomicrographs of Kurrawang sandstone showing relatively strain free angular, subhedral volcanic quartz grains with little or no matrix fabric development (WMC road cut sample GDA: 341954E; 6585331N); c) and d) PPL and XPL photomicrographs of coarse-grained Kurrawang sandstone with strongly developed matrix biotite fabric wrapping and forming pressure shadow beards on sub-angular quartz – 'Q', and twinned feldspar grains – 'F'. Note a grain of plutonic recrystallised quartz in the bottom right marked 'P' (Mount Pleasant southwest; GDA: 327479E; 6611829N); e) XPL photomicrograph of plane-bedded fine-grained quartz wacke (Mount Pleasant south; GDA: 327636E; 6610628N); f) PPL photomicrograph of Kurrawang sandstone with euhedral platy metamorphic biotite 'bt' forming a weakly aligned matrix foliation that overprints earlier matrix chlorite 'ch' (7-Mile quarry outcrop sample; GDA: 344924E; 6586351N).

pebbles were less affected by the deformation. Conglomerate pebbles in clast supported sections show evidence of significant pressure solution on contacts parallel to the pervasive foliation, and well-developed pressure shadow beards composed of biotite and quartz. Quartz forms long, linear rod shaped aggregates that wrap the clasts. The gross structure of the unit is a NNW-SSE

trending syncline with a variably plunging fold axis along strike. Rare outcrop sections show parasitic folds on the limbs of the major syncline (Fig. 3.28). Late kink folds trending NE-SW are developed sporadically in thinly bedded sections and in the most intensely deformed zones.

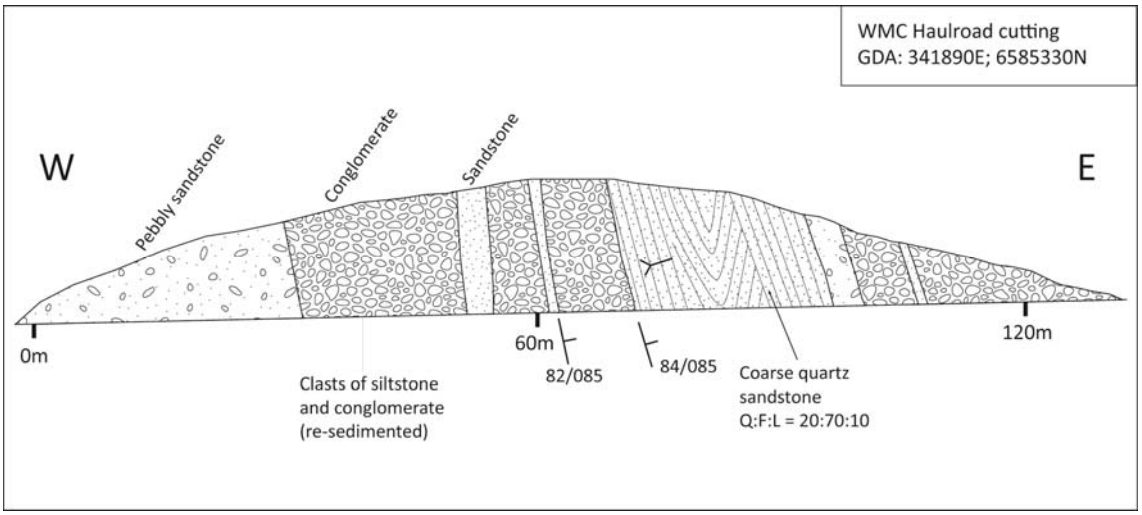

Figure 3.28 - Geological section of a road cut through the western limb of the Kurrawang Syncline displaying various litho-types including sandstone, pebbly sandstone and polymictic conglomerate

Interpretation and correlation

The KUF is one of the youngest Archaean formations in the Kalgoorlie district and is similar in age and character to the Merougil Formation at Kambalda. The lower Navajo Sandstone fluvial sequence was interpreted to be unconformably overlain by the Kurrawang conglomerate (Krapez 1996) and that relationship is confirmed here. Kurrawang conglomerates in the middle of the sequence give way to a thick section of trough cross-bedded Kurrawang sandstone with similar lithofacies to the lower Navajo fluvial sequence. This thick section was interpreted as proximal turbidite rocks resembling high-terrace deposits by Krapez (1996) with a significant deepening of the basin recorded by a change in the lithofacies from fluvial to submarine fan deposits. Krapez et al. (2008) also mapped a section of the upper Kurrawang sandstone as including abundant ‘S-Type’ (trough cross-bedded sandstone) turbidites and ‘M-type’ (mudstone) turbidites. Their interpreted lithofacies are taken from outcrops in the southern most part of the Kurrawang Formation. Critical to their interpretation is that the Kurrawang conglomerates represent submarine density flows that grade upwards into turbidites.

The outcrops at Kundana south and west of White Flag Lake mapped in this study show the upper units of the Kurrawang are thick, tabular-bedded, quartz rich cross-bedded pebbly sandstones, with rare thin (1-5 m) interbedded siltstone layers, similar to the Navajo sandstone and sandstones in the Merougil Formation, whereas the upper turbidite unit, comprising siltstone and mudstone, is a minor component. Some doubt remains about the interpretation of a major change in depositional environment (basin deepening) post-dating the deposition of the Kurrawang Conglomerate as proposed by Krapez and Hand (2008).

The available geochronological data from the sedimentary rocks of the Kurrawang Formation indicate there are variable populations of youngest detrital grains from place to place and from different members: 2657±4 Ma from the Navajo sandstone at Binduli Mine (Fletcher et al 2001); 2679±10 Ma from conglomerate at Lake Douglas (Krapez et al. 2000); 2655±5 Ma and 2657±7 Ma from sandstone west of the Ora Banda area (Chapter 4.). The differences are in part attributable to variation in provenance, but all are consistent with depositional ages for the Kurrawang Formation in the range of 2660-2650 Ma or less.

The age data support the observed lithostratigraphic order and the idea of a depositional contact (unconformable) at the base of the Kurrawang Formation (Navajo Sandstone). An unconformable contact in Figure 3.23 at the base of Kurrawang c*onglomerate* represents a minor internal contact within the Kurrawang Formation, which may be related to a minor uplift event, or simply normal faulting, whereas the unconformity at the base of the Navajo Sandstone represents a major time break, with significant folding of the underlying rocks prior to the deposition of the Navajo Sandstone at ~2652 Ma (Fig.3.3).

The other major unconformity lower in the sequence appears to be between intercalated White Flag Formation (2690±9 Ma) / lower Binduli felsic volcanic rocks; and the upper Binduli Sequence, which has a postulated age of deposition of <2664 Ma from the interpretation that the porphyry conglomerate at Binduli contains clasts of the Centurion Porphyry and underlying mudstone units (Fig. 3.21). The Centurion Porphyry at Binduli has a U-Pb SHRIMP zircon crystallisation age of 2667±3 Ma (Fletcher et al. 2001). The two major unconformities can be generalised as occurring at about ~2660 Ma and ~2650 Ma (highlighted in blue in Figure 3.29a,b).

3.3 Coolgardie Domain (Kundana, Kundana-north)

Rocks younger than the mafic and ultramafic volcanics are not well understood in the Coolgardie Domain due to poor exposure. Minor areas of outcrop are located in the Kundana mining centre; at Cutters Ridge; and in the vicinity of the Mungari Monzogranite, where the rocks are strongly deformed and metamorphosed (Glikson 1971a). This has resulted in geological maps portraying rocks younger than the Upper Basalt as a single group (Fig. 3.30), however there is undoubtedly a more complex stratigraphy including many of the regional stratigraphic units, as suggested by rare exploration drill hole intersections away from the mines and outcrops.

The boundary between Coolgardie and Ora Banda Domains is taken at the location of the Zuleika Shear Zone, a 10-15 m wide zone of high strain with tectonic interleaving of adjacent wallrocks (Chapter 5). This assumption agrees with most previously published accounts of the

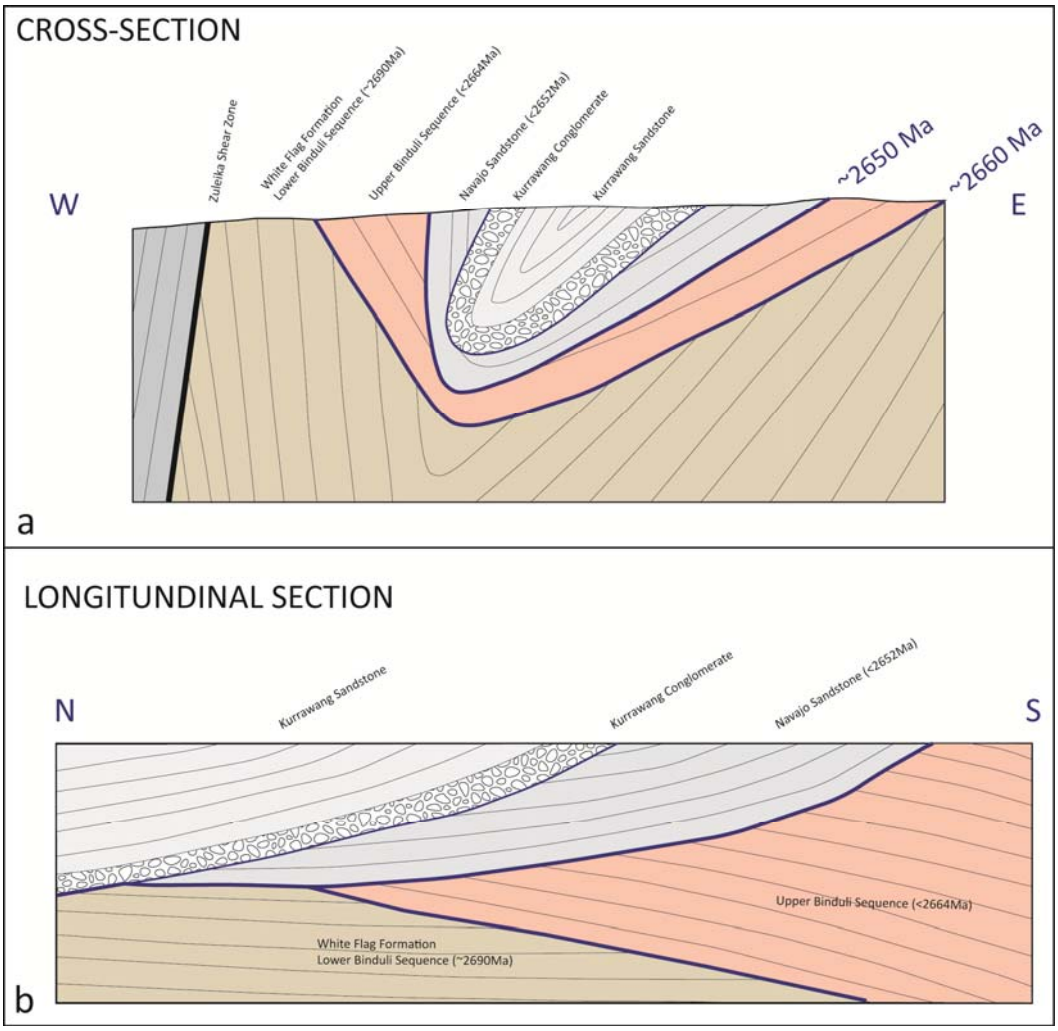

Figure 3.29 – a, Schematic cross-section and, b) longitudinal section showing the gross structure and relationships of major formations in the Kundana South area. Unconformities highlighted in blue.

district, particularly Swager et al. (1990). Whereas most authors place the boundary on this basis, there are no published descriptions of the structure and kinematics of the shear zone, which is mostly interpreted from a sharp, visible linear break on aeromagnetic images. Details of the Zuleika Shear Zone are presented in Chapter 5.

The stratigraphy of the Coolgardie Domain was documented by Standing and Castleden (2002, Table 3.1-map pocket) from unit in the vicinity of the Coolgardie mining district, which show a thick, complex sequence of mafic and ultramafic volcanic rocks and intrusive mafic sills with interspersed sedimentary rocks (Table 3.1). Notably, the area mapped by Standing and Castleden (2002) is separated from the Kundana area by the Kunanalling Shear Zone (KNS; Fig 3.30), with significant differences in stratigraphy that may indicate that there is a separate 'Kunanalling Domain' bounded to the west by the KNS and to the east by the Zuleika Shear Zone. In particular is a lack of thick mafic-ultramafic volcanic sequences in the Kundana area compared with Coolgardie. Differences between the stratigraphy in the immediate Kundana area and the remainder of the Coolgardie Domain are also indicated by regional gravity data that

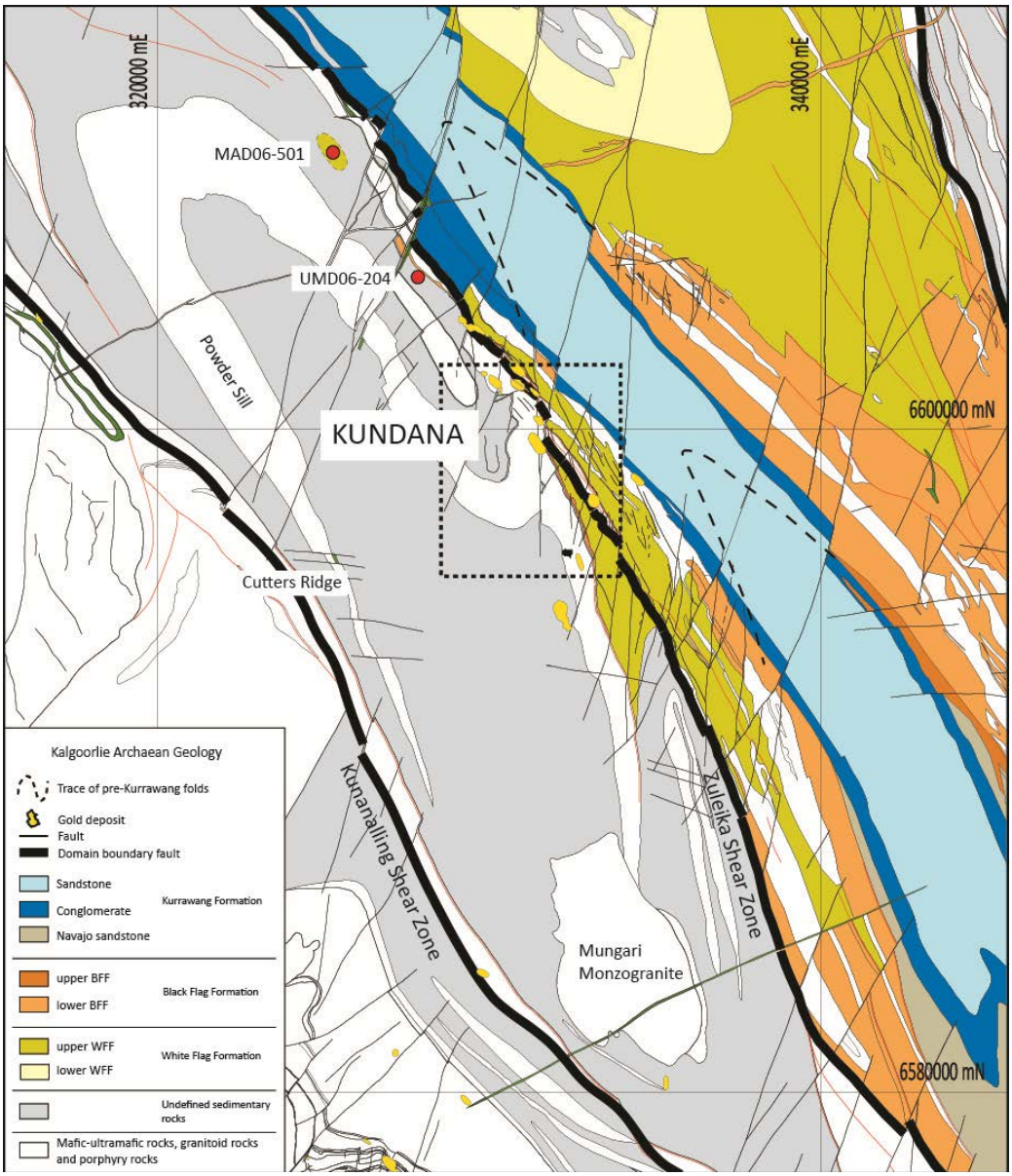

Figure 3.30 – Map of the White Flag Formation in the Coolgardie Domain and location of drill hole MAD06-501 and UMD06-204. Dashed lines show the location of interpreted pre-Kurrawang folded contact traces; dashed box shows the location of Figure 3.29.

show very little high-density crust in a long linear belt from Kundana and to the north-west, compared to the stratigraphy at Coolgardie, where a linear belt of high gravity is interpreted as greenstones along the margins of granitoid batholiths (Calooli, Bali, Dunnsville intrusions;later presented in Chapter 6 - Fig. 6.4). This discussion will focus on rocks in the immediate Kundana area.

White Flag Formation is the only recognisable formation observed in the Kundana area: no examples of rocks ascribable to the Black Flag Formation were observed in this study; however the sequence of sedimentary rocks surrounding White Flag Formation intermediate volcaniclastic rocks on Figure 3.30 is generally considered to be part of a generic ‘Black Flag Group’. Locally, Kurrawang Formation rocks were structurally emplaced as deformed, metre-

scale, fault-bounded slivers along the Zuleika Shear Zone in the Kundana mining centre, but offer no stratigraphic information due to their deformed and disconnected nature.

3.3.1 Rocks overlying ultramafic volcanics

Introduction

Sedimentary rocks are ubiquitous to the west of the Zuleika Shear Zone, but are generally poorly exposed. To the north of the Kundana mining centre, sedimentary rocks are in direct contact with ultramafic rocks with a thin carbonaceous shale layer at the contact. The ultramafic rocks are correlated with the Hampton Ultramafic rocks from Coolgardie (D. Archer written communication), but in the Kundana area form only a small aerially restricted body in the core of the Kundana Anticline (Fig. 3.31). Slivers of sedimentary rocks are exposed in several of the open pit gold mines at Kundana and in broad areas in RAB and AIRCORE drill holes, but in general are highly strained and lack any mappable internal organisation. High degrees of strain and locally low-middle-amphibolite facies metamorphism are present in rocks on both sides of the Zuleika Shear Zone. indicating that the Zuleika Shear Zone doesn't mark a major change in geological history. Changes in metamorphic facies across a 'Mungari' shear zone was suggested by the work of Glikson (1971), but his work reported andalusite, cordierite and garnet in muscovite-biotite schists in the thermal aureole of the Mungari Monzogranite (Fig 3.30). Elevated metamorphic grades in the vicinity of intrusions include the presence of garnet with coarse amphiboles in some meta-mafic intrusions (White Foil), and ubiquitous recrystallisation of shear zones to coarse randomly oriented actinolite in meta-mafic and meta-ultramafic rocks.

Description

Typical sedimentary rock types in the Kundana area include sandstone, siltstone and shale locally interbedded with oligomictic and polymictic conglomerate (Fig. 3.32a,b). Plane-bedded sandstone comprises fine to coarse-grained feldspathic units that grade upwards into siltstone. A distinctive coarse-grained, feldspar-rich sandstone is recognised regionally throughout the sedimentary rocks in the northwest of Kalgoorlie at Paradigm (39 km NW of Kundana), in the Kundana mining centre, and as far south as Kambalda (‘feldspar granule breccia’ of Squire and Cas 2006). Coarse clastic units include volcaniclastic porphyry breccia intersected in drill holes to the north of Kundana and interbedded polymictic and oligomictic conglomerate / breccia in the Kundana mining centre.

Structural geology

In general, sedimentary rocks at Kundana display higher strain than typical gently folded, plane-bedded sedimentary rocks in the Ora Banda Domain, which may be due to the location of the Kundana mines close to the Zuleika Shear Zone. The rocks were also metamorphosed to

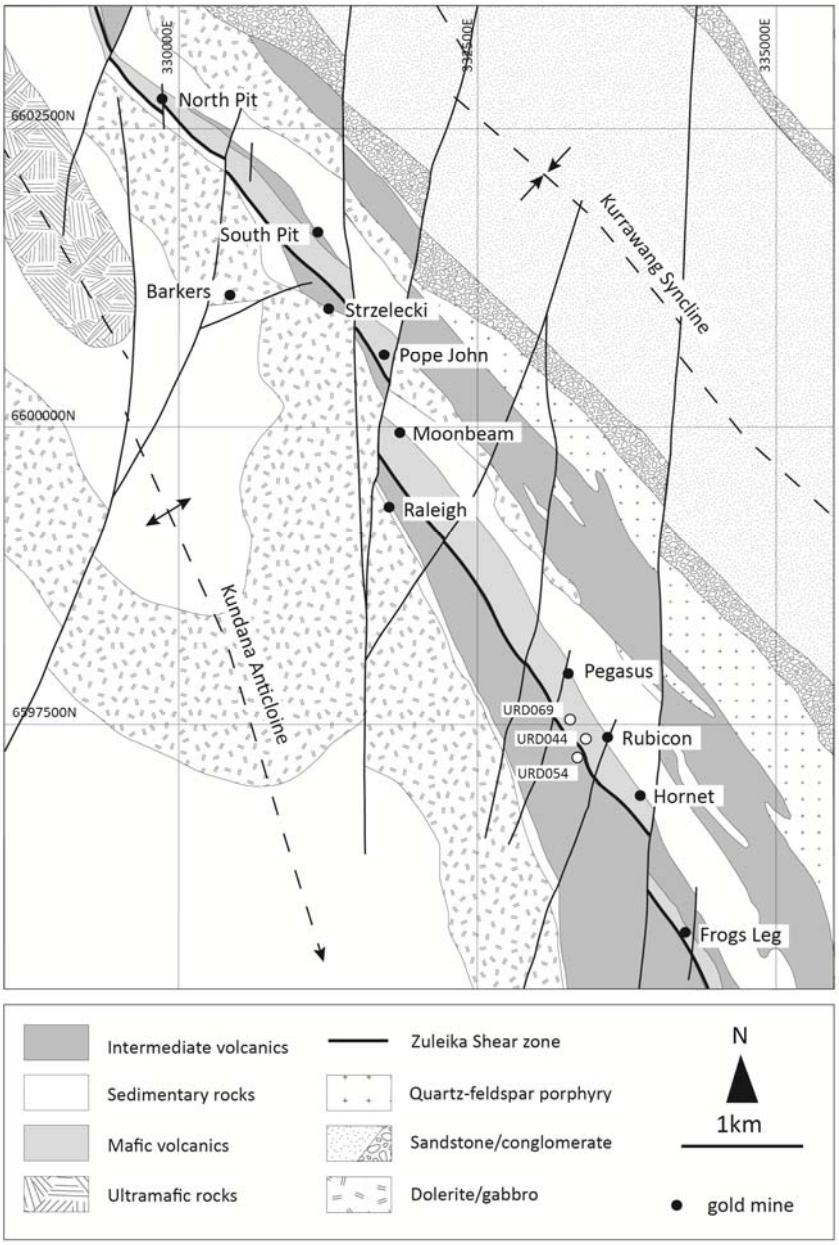

Figure 3.31– Geology of the Kundana mining centre with location of the gold mines, produced from geophysics, pre-existing maps and extensive re-logging of exploration drill holes.

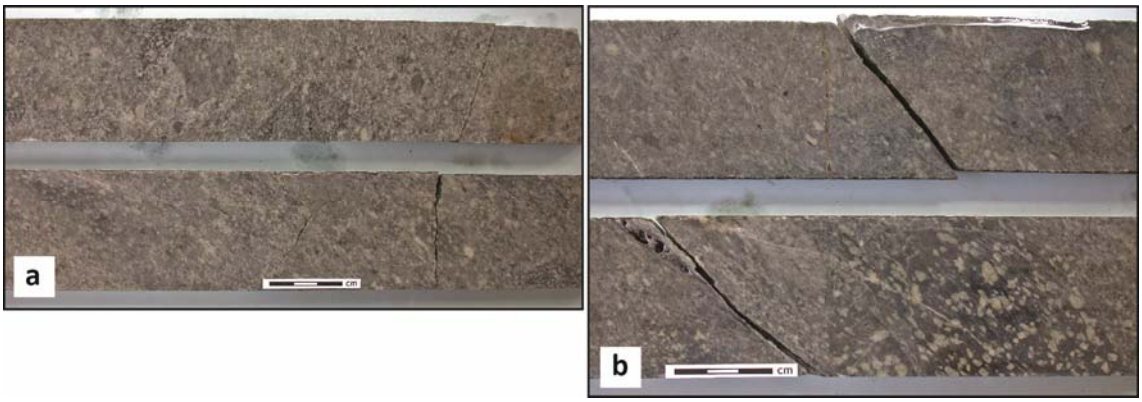

Figure 3.32 - Examples of felsic volcanic / sedimentary rocks in the Kundana north area. a) Sericite-carbonate-biotite altered meta-volcaniclastic breccia, UMD06-202 113.0-113.6 m photo from Mason (2006), b) Albite-sericite-carbonate-biotite altered meta-dacitic volcaniclastic breccia, UMD06-204 161.0-161.5 m photo from Mason (2006).

upper greenschist / lower amphibolite facies. At Kundana the sequence dips steeply west, but faces east and is therefore structurally overturned. Pavements of less deformed sedimentary rocks are located east of Cutters Ridge (Fig. 3.30). At north Kundana the degree of strain and alteration makes the recognition of primary rock types difficult, however rare sections of drill core show some textures dominated by porphyry breccia and conglomerate (Fig 3.32a,b), indicating these rocks have (at least) textural affinities with the lower Black Flag formation as described at Kundana south.

Interpretation and correlation

Sedimentary rocks in the Kundana area show similarities to the lower Black Flag formation in the Ora Banda Domain. Strain is higher in the Kundana rocks compared with the Ora Banda Domain; hence, any correlation is uncertain at best and would require detailed trace element geochemistry to advance the stratigraphic understanding.

A reduction in section thickness of the Upper Basalt from about 3.0 km to 0.5 km (discussed in Section 3.2.3) cannot be explained by tectonic thinning alone, given local preservation of broad tracts of relatively undeformed rock. The presence of an extensional growth fault to the east of Kundana is a possibility, as is the presence of anastomosing shear zones surrounding undeformed tectonic slivers.

3.3.2 White Flag Formation (WFF)

Introduction

White Flag Formation (WFF) is extensively exposed in mines and drill holes in the Kundana mining centre, but is relatively scarce elsewhere in the Coolgardie Domain. The majority of the area coloured as ‘sedimentary rocks overlying Upper Basalt’ may contain WFF that has been unidentified to date (see Figure. 3.30 for location of drillholes).

Description

One drill hole (MAD06-501) was logged to gain detailed information on the WFF in the Coolgardie Domain. Drill hole MAD06-501 was drilled internal to the WFF; hence, the contact relationships and the relative position of the hole within the formation are unknown.

Conglomerate / breccia units in the WFF are dominated by moderately sorted, sub-angular and elongate, intermediate volcanic debris, characterised by diffuse bedding of >5 m mean thickness with individual beds up to 35 m thick (Fig. 3.33, Fig. 3.34b, c). Internal sandstone units are plane bedded on a decimetre scale (Fig. 3.34a).

The mean clast size of conglomerate / breccia in the WFF is ~150 mm with geometric means of the ten largest observed clasts up to 292 mm, and rare clasts up to 0.8 m diameter. Conglomerate beds are clast supported (C/M ratio: 0.7), with a lithic-wacke matrix (Q:F:L =

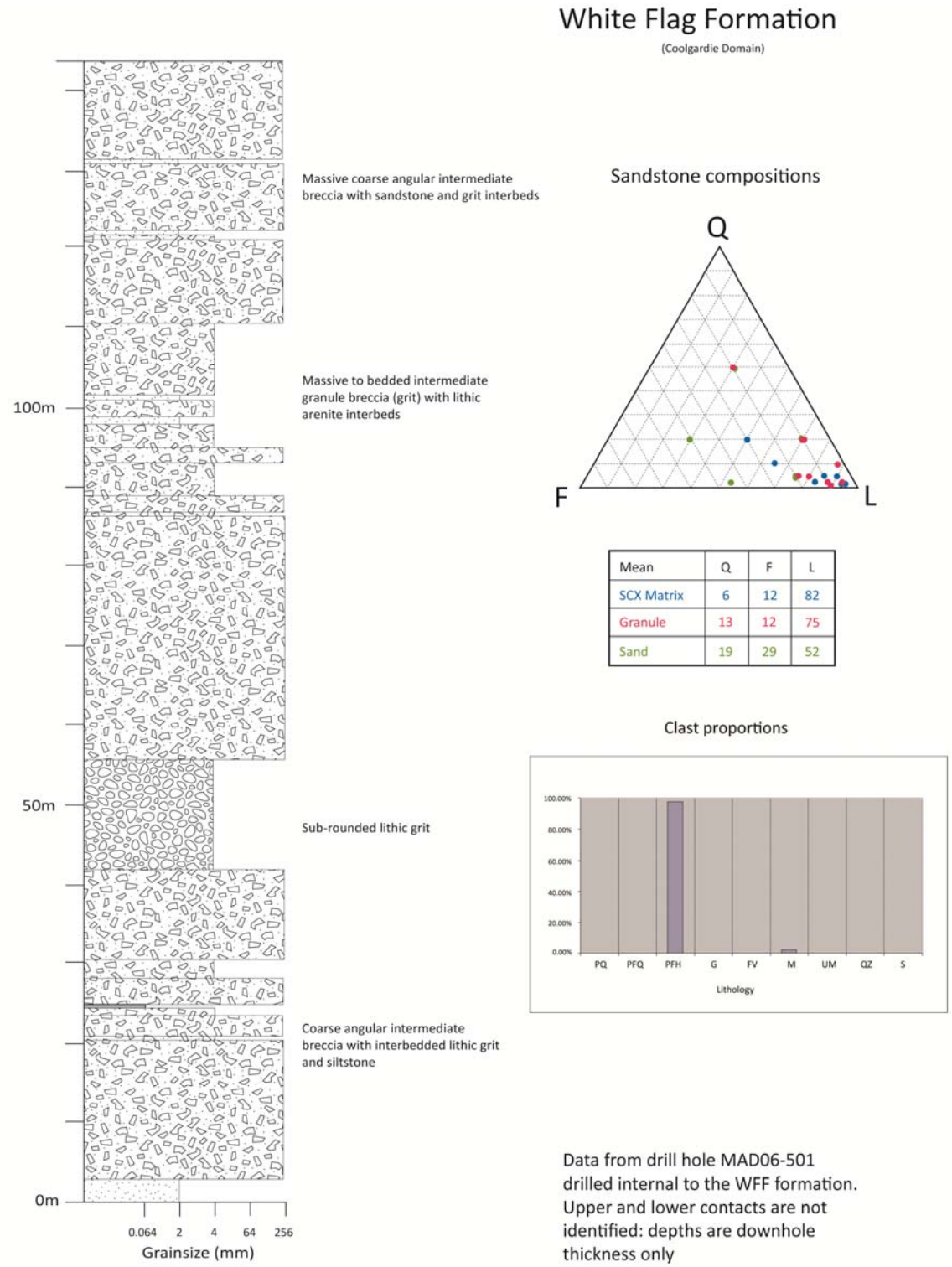

Figure 3.33 – Drill hole section with clast and matrix information for White Flag Formation in the Coolgardie Domain. QFL data are coloured according to the table of mean values. SCX refers to conglomerate or breccia-sized clastics. PQ – quartz porphyry; PFQ – quartz feldspar porphyry; PFH – hornblende-feldspar porphyry ± quartz; G – granite; FV – felsic volcanic; M – mafic volcanic; UM – ultramafic; QZ – quartz; S – sedimentary.

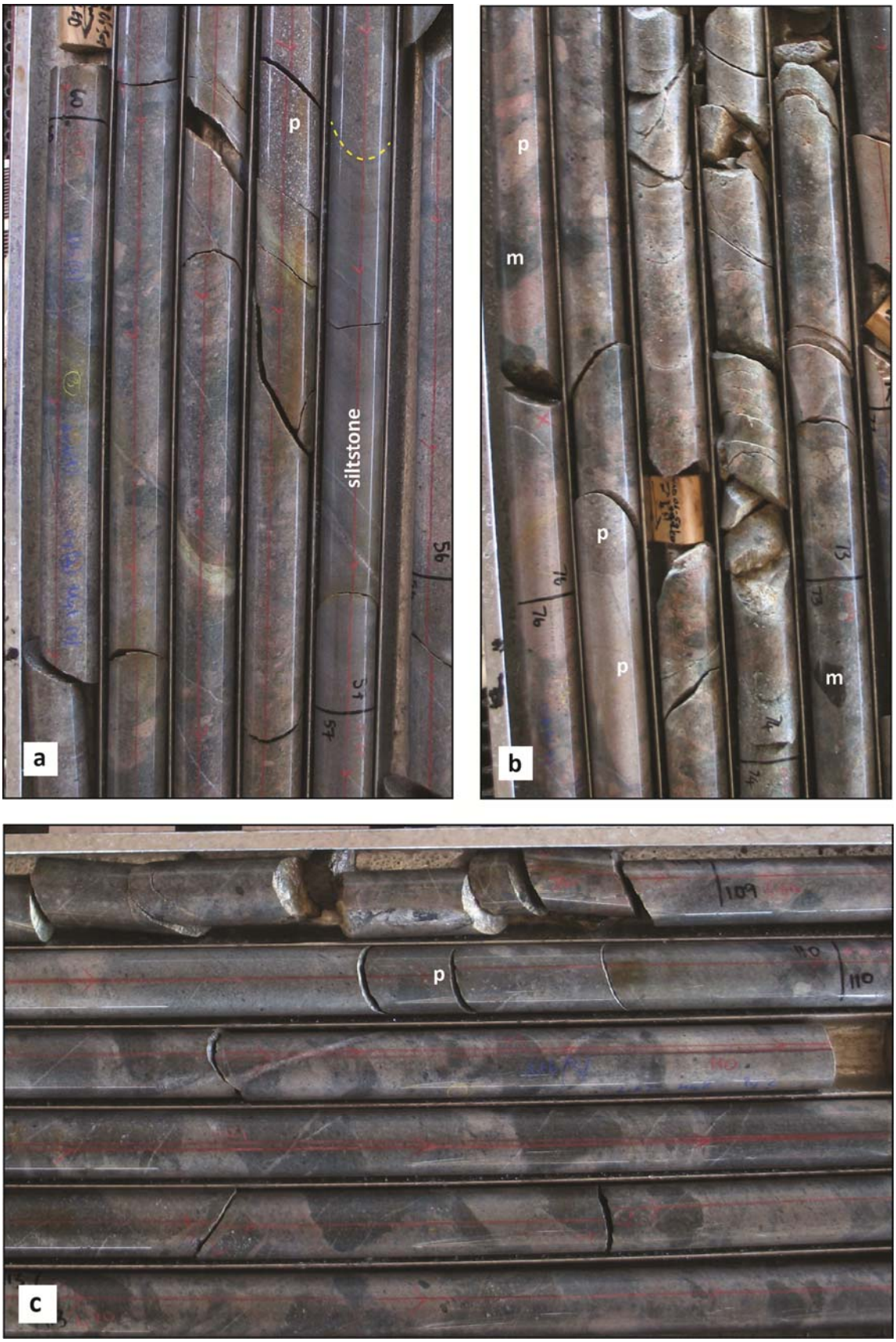

Figure 3.34 – Photos of White Flag Formation from drill hole MAD06-501. a) Siltstone/sandstone at 57 m interbedded with andesite boulder breccia, b) Sub-angular to sub-rounded andesite porphyry breccia, c) Sub-angular breccia composed of andesite porphyry and mafic volcanic clasts. 50 mm core diameter.

6:12:82) (Fig. 3.33). The conglomerate contains interbedded fine-grained units that have a broader spread of Q:F:L compositions (19:29:52; Fig. 3.18a), varying from fine-grained sandstone to siltstone. Conglomerate / breccia in the WFF is essentially oligomictic with a restricted range of clast types (Fig. 3.33). The unit on average is characterised by abundant intermediate hornblende-feldspar porphyry clasts (98%); with the remainder represented by 2% mafic volcanic clasts (Fig. 3.17) similar to the White Flag Lake exposures in the Ora Banda Domain.

Sandstone and siltstone interbeds display plane bedding and graded bedding in thin units between otherwise thick massive sections of breccia. Conglomerate and breccia units have mostly diffuse gradational contacts and are identified primarily by marked grainsize changes. The WFF intersected in MAD06-501 is mostly undeformed except for a slight flattening of the clasts, whereas WFF in the Kundana mining centre is characterised by localised intense foliation and flattening.

Interpretation and correlation

White Flag Formation intermediate rocks are generally considered to be scarce or not developed in the Coolgardie Domain away from the Kundana mining centre, but recent drilling demonstrates that some areas currently thought to contain only turbiditic sedimentary rocks, may contain a more complex stratigraphic sequence. Abundant sedimentary rock is located above the section intersected by MAD06-501, and may indicate that a significant thickness of Black Flag Formation also exists in the Coolgardie Domain. If so, this has significance for the location of internal Black Flag unconformities and possibly for exploration targeting away from the structurally-focussed Kundana gold deposits.

3.3.3 Black Flag Formation / Kurrawang Formation

Black Flag and Kurrawang Formation rocks as defined in Sections 3.2.3 and 3.2.4, have not been identified to date in the Coolgardie Domain. The gross distribution of lithologies, west of the Zuleika Shear Zone in the Kundana south district suggests that sedimentary rocks with mafic dolerite intrusions (potentially correlated with Black Flag Formation) start at the southern end of the Kundana mining centre and continue southwards to the end of the Kurrawang Syncline. This succession is poorly understood and may contain upper Black Flag formation rocks as well as the interpreted unconformity between BFl and BFu.

3.4 Kambalda Domain

In the Kambalda Domain, rocks examined at Mt Hunt and Lakewood are commonly assigned to the 'Spargoville Formation' or a general ‘Black Flag Group’ (Woodall 1965, Table 3.1-map pocket; Krapez and Hand 2008), whereas the rocks examined at Gidji Lake and Mount

Charlotte-east have previously been included in the Black Flag Formation of Krapez et al. (2000).

The White Flag Formation has not been identified in the Kambalda Domain to date, but drill holes east of Mount Charlotte intersected rocks that display striking similarities to the WFF from the Ora Banda Domain with coherent andesitic volcanic rocks intercalated with intermediate conglomerate and sandstone. Recent SHRIMP analysis, however, has ruled out correlation of those rocks with the WFF and the unit is therefore included here with the upper Black Flag formation based on field relationships and previous geochronology.

3.4.1 Sedimentary rocks overlying Upper Basalt unit

Introduction

Rocks overlying the Paringa Basalt (Upper Basalt unit) at Mt Hunt were examined in this study (Fig. 3.35), but detailed lithofacies mapping is available in Hand (1998) for pavements outcropping to the east of the Kalgoorlie-Kambalda highway; that work is not repeated here. Two deep drill holes from historic Western Mining Corporation exploration at Lakewood, south of the Golden Mile (Fig. 3.35), were examined at the Geological Survey of Western Australia core library, and used in conjunction with published information by Travis et al. (1971), Hand (1998) and Morris (1995) to evaluate the nature of the rocks overlying Upper Basalt. Current map interpretations of the post-upper basalt stratigraphy in the Kambalda Domain are vague and show little delineation of formations or units within a large area of rocks coloured grey on Figure 3.35; but notably these rocks are ascribed to the Spargoville Formation (SPF). The few exposures examined in this study have shown that some subdivision is possible; yet widely-separated exposures preclude any definite correlation or map pattern analysis of members, and raise questions as to the correctness of assigning these rocks to the SPF.

Contact relationships

The contact of the Black Flag Group against underlying rocks is exposed in drill holes at Lakewood and outcrops at Hannan's Lake (Mount Hunt). Most workers regard the lowermost part of the section to constitute rocks of the Spargoville Formation. The nature of the basal SPF contact with the top of the Golden Mile Dolerite (Golden Mile Dolerite) has been contentious (e.g. Tomich 1974; 1976; Golding 1985; cf. Travis et al. 1971; Keats 1987; see also Krapez and Hand 2008). The contention is based upon whether the Golden Mile Dolerite is a shallow sub-volcanic sill that intruded the contact between Paringa Basalt and overlying sedimentary rocks, or whether it represents an extrusive mafic volcanic sequence that pre dates the SPF because rounded clasts of dolerite are found in the conglomeratic rocks immediately overlying the Golden Mile Dolerite (Golding 1985; see also Krapez and Hand 2008). Erosion of an extrusive sequence was ruled out by Keats (1987) and Barley et al. (2002) on the basis of field

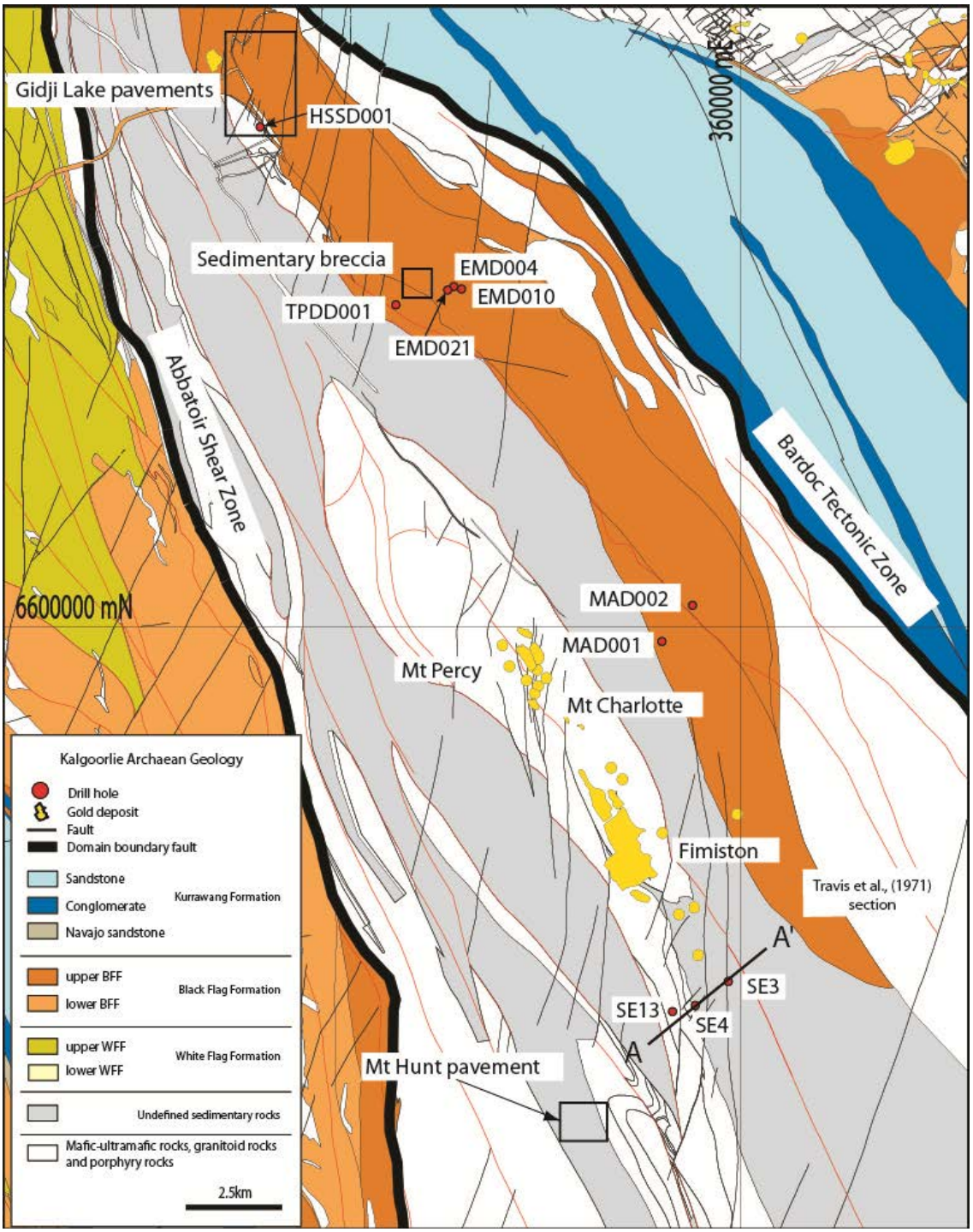

Figure 3.35 – Distribution of formations in the Kambalda Domain with locations of mapping areas and drill holes logged in this study. Mafic volcanic, ultramafic volcanic and felsic intrusions – are blank areas for the purpose of highlighting the sedimentary formations. See Fig. 3.37 for section A-A'.

relationships, with the former citing field observations by Travis et al. (1971), whereas the latter stated that the dolerite clasts in the overlying conglomerate are distinctly different to the Golden Mile Dolerite.

In this study, observations at the GMD contact in underground drives from the Chaffers Mine are obscured by late intrusions in contact with shales (Fig. 3.36a). In drill hole SE4 however, an intrusive relationship is confirmed between GMD and the overlying shales, where apophyses of dolerite with marginal breccias have intruded thinly bedded sedimentary rocks. The upper contact of the sedimentary rocks has not been established in the Lakewood area.

Description (Mount Hunt)

Sedimentary rocks overlying Upper Basalt are exposed in a small 250 m x 250 m pavement to the west of the Kalgoorlie-Kambalda highway near Mount Hunt (Fig. 3.35). A large area of well exposed basalt (Paringa Basalt) is located on the eastern side of the highway, but the contact between basalt and overlying sedimentary rocks is covered by the road. A small outcrop immediately west of the highway, and within ~20 m of the contact, contains polymictic conglomerate at the base of the sequence with clasts of basalt, quartz porphyry, granite and hornblende porphyry, overlain by fine-grained sandstone and siltstone. The remainder of the exposure comprises interbedded sandstone, siltstone and shale. Locally the rocks are folded with minor areas that are downward facing.

Sandstone/siltstone is plane bedded with well-defined normal grading and scoured bases that indicate overall westward facing of the sequence. Further west, the section contains mudstone and shale interbedded with thin units of massive sandstone. The upper parts of the section have a thickening upward and coarsening upward trend (Hand 1998). The succession at Mount Hunt was interpreted by Hand (1998) as characteristic of main channel deposits within a proximal submarine fan environment, and with evidence of a significant felsic volcanic input.

Description (Lakewood)

Drill holes SE3 and SE4 were logged from the Lakewood area south of the Golden Mile (Fig. 3.36b-h). The holes were interpreted to intersect a folded sequence as depicted by Travis et al. (1971) (Fig. 3.37). Several authors (Clout et al. 1990; Morris 1998; Hand 1998) have since disagreed with aspects of the structural interpretation of Travis et al. (1971) particularly the portrayed ductile nature of the deformation. Those later authors interpreted brittle, rotated fault blocks to account for the distribution of units. The identification of a sequence of volcanic and sedimentary rocks with newly recognised marker units by this study (Fig. 3.37) has largely confirmed and enhanced the original interpretation of Travis et al. (1971).

Sedimentary and dacitic volcanic rocks at Lakewood structurally overlie the Golden Mile Dolerite in a sequence of deep-water-deposited sedimentary rocks interspersed with felsic

Figure 3.36

Figure 3.36 – Sedimentary rocks overlying Upper Basalt – Kambalda Domain

a) Intrusive contact with carbonaceous shale on the western margin of the 'Golden Mile Fault'. The carbonaceous shale unit is a prominent subvertical zone in the walls of the Fimiston Superpit that separates the eastern and western lode systems and marks the faulted Kalgoorlie syncline: a major fold in the Golden Mile Dolerite. Strong alteration and deformation obscure rock textures, but the exposure was confirmed as hornblende porphyry at the upper contact of the Golden Mile Dolerite with overlying Black Flag Beds (Gauthier 2004b). The carbonaceous shale unit was intruded extensively by quartz-feldspar porphyry dykes and sills, and is very strongly sheared with crenulation lineations pitching 35S in a 345/90 shear fabric. Locally bedding is preserved with way-up to the east. Local mixing of the two rock types may indicate intrusion was into unconsolidated sediments (Chaffers 20-Level cross drive, Fimiston, Golden Mile).

b) Intercalated zone of mixed felsic volcaniclastic rocks and fine mudstone and carbonaceous shale. A felsic breccia unit with a gradational upper contact is highlighted. The breccia unit forms a prominent marker that confirms the fold interpretation of Travis et al. (1971) in Figure 3.37 (WMC drill hole SE3 4060ft; GDA: 358937E; 6590357N).

c) Close up of felsic breccia marker from (b). The marker unit is composed of sub-angular lithic fragments of rhyodacite porphyry and broken quartz and feldspar crystals (WMC drill hole SE3 4422ft).

d) Talbot formation intraformational breccia composed of angular fragments of felsic rocks, sandstone and mudstone chips in a fine-grained sandstone matrix (WMC drill hole SE3 1745ft).

e) Polyphase folding in coarse angular quartz grit with fine-grained interbeds. The drill core shows refolding of early isoclinal folds with bedding-parallel fold axial planes (WMC drill hole SE4 4426ft, GDA: 358497E; 6590057N).

f) Oligomictic dacite volcanic breccia composed primarily of highly angular to jigsaw fit dacite fragments in a lithic and crystal matrix of the same rock. Note strong, brown Fe-carbonate and sericite alteration (WMC drill hole SE3 435ft).

g) Coherent dacite and hyaloclastite composed of jigsaw-fit dacitic breccia at the margin of a coherent dacite, flow-banded lava lobe (WMC drill hole SE3 600ft).

h) Flow banded coherent dacite (WMC drill hole SE3 1020ft).

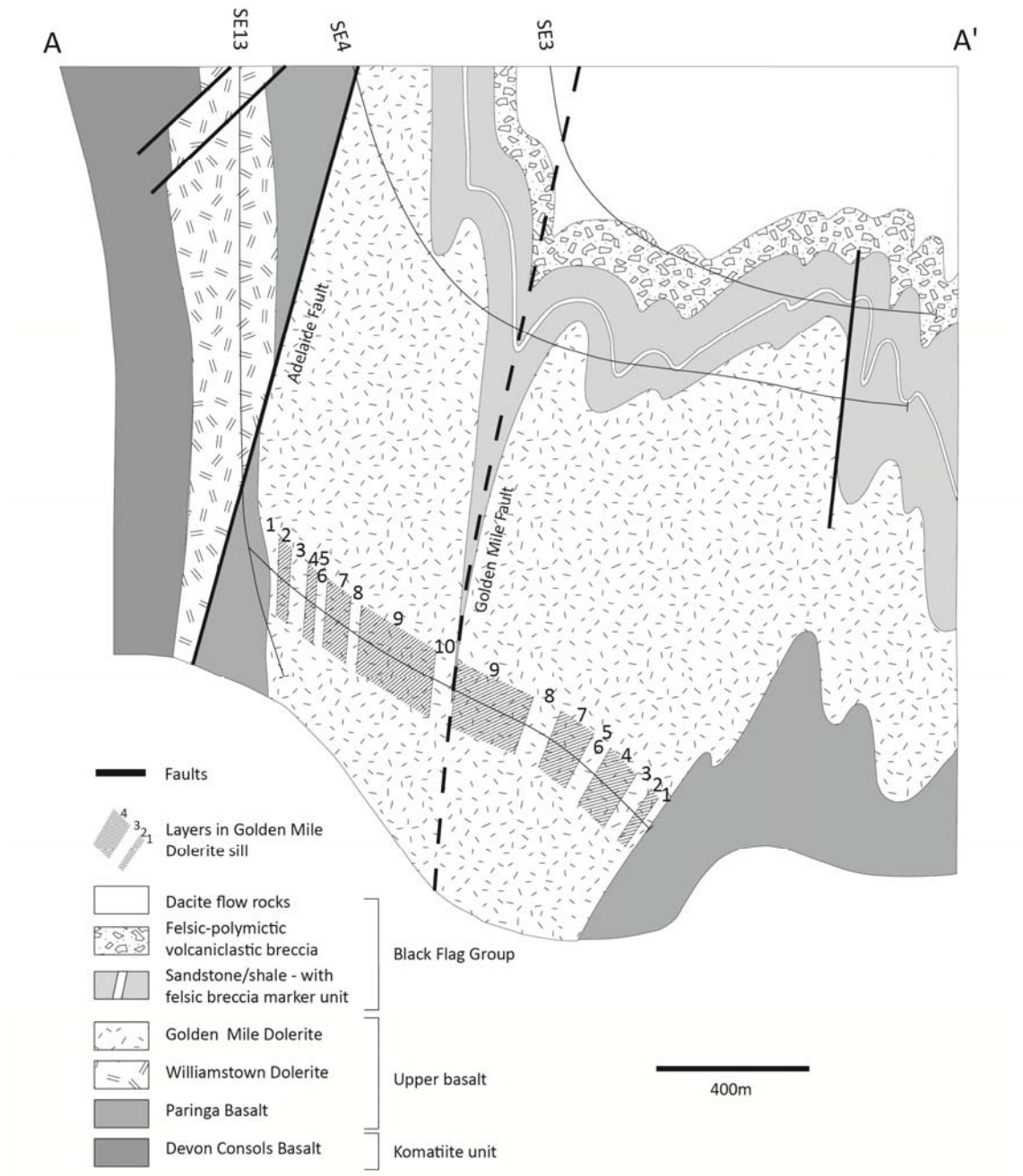

Figure 3.37 – Cross section A-A' through the south of the Kalgoorlie greenstone belt modified from Travis et al. (1971) using re-logging data from drill holes SE3 and SE4. Location of cross section is displayed on Figure 3.35. Strong drill hole deviation is confirmed by variation in the core-axis angles of a pervasive foliation, with depth in the drillholes.

volcanic and volcaniclastic rocks, overlain by dacitic volcanic and volcaniclastic rocks. Sedimentary rocks above the Golden Mile Dolerite comprise thinly-bedded sandstone / siltstone / mudstone units (Fig. 3.36a, b) with a wide range of sand : silt ratios from 1:1 to 1:30 in normally graded beds (Morris 1998). Medium-grained feldspathic sandstones are similar to rocks from the Kundana south area, and are interbedded with coarse-grained pebbly sandstone that contains clasts of felsic rocks and shale similar to Figures 3.17a and b (Fig. 3.36d).

An internal marker unit of felsic breccia is present in the sedimentary rocks that overlie the Golden Mile Dolerite (Fig. 3.36b, c) and this marker unit has been used to confirm the stratigraphic and structural interpretation of Travis et al. (1971). The unit is composed of angular clasts of dacitic (Fig. 3.36c), characterised by stark white feldspar phenocrysts and feldspathic patches in an altered groundmass. A gradational upper contact with overlying sandstone / carbonaceous shale (Fig. 3.36b) indicates that the unit represents an influx of felsic volcanic material to the depocentre, which was followed immediately by continued deep water sedimentation. The lower sedimentary rocks are overlain by felsic volcanic and volcaniclastic rocks. Volcanic breccia beds contain disorganised, clast-supported oligomictic breccia composed mostly of dacitic fragments locally gradational with jigsaw breccia (Fig. 3.36f, g). Some polymictic breccia is present with variable amounts of sandstone matrix. Coherent dacite lava is variably porphyritic to massive with prominent flow banding and local brecciation (Fig. 3.36h). The lower margin of the upper coherent dacite facies is gradational into oligomictic proximal dacite breccia (Fig. 3.36g).

Structural geology

Mesoscopic folding and transposition is a characteristic of the sandstone / carbonaceous shale units in the sedimentary rocks with refolded folds developed locally (Fig. 3.36e). This apparently intense deformation is in direct contrast with felsic volcanic rocks and volcaniclastic breccias that are relatively undeformed. The apparent strong localisation of strain in weak laminated phyllosilicate-rich rocks is typical of deformation styles throughout the Kalgoorlie district. Upright folding of the stratigraphy has produced a major syncline with minor folds on the limbs as depicted by the Travis et al. (1971) section (Fig. 3.37). The recognition of a felsic volcaniclastic breccia marker layer within the sandstone / shale that is intersected several times throughout the drill holes confirms the interpreted folded structure.

Interpretation and correlation

Rocks assigned to the Spargoville Formation in the Kambalda Domain contain a significant dacitic volcanic component, which is similar to Spargoville Formation as documented at the type locality (Hunter 1993; Brown et al. 2001). These are distinct however, from sedimentary rocks at Mount Pleasant (Ora Banda Domain) that lack any volcanics, but were also correlated with Spargoville Formation by Hunter (1993). Dacitic rocks at Widgiemooltha were interpreted as ‘Spargoville Formation’ with an interpreted age of deposition at 2686±3 Ma (but also including significantly younger concordant age determinations; Krapez et al 2000). Dacitic volcanic rocks at the Golden Ridge mine, also assigned to Spargoville Formation, returned an interpreted age of deposition at 2698±6 Ma. The Widgiemooltha and Golden Ridge rocks are within error of the bracketed age of deposition for

sedimentary rocks overlying Upper Basalt at Mount Pleasant, but are significantly older than new SHRIMP determinations for the dacitic volcanic sequence at the Golden Mile (Chapter 4).

The presence of deep-water-deposited sandstone and shale at the base of SPF is a characteristic common to all domains, yet there is considerable variability in the volume of dacitic volcanic components, even in the Kambalda Domain. For example, there are no sections of dacitic volcanic rock at Mount Hunt comparable to those in the same apparent stratigraphic position as recognised in the Lakewood drill holes. The variations could be explained by facies variations in the same lithostratigraphic unit or the possibility the sections are not strictly correlative.

In comparison to sequences from the Ora Banda Domain, the stratigraphic section at Lakewood also resembles part of the lower Black Flag formation at Binduli, where dacitic volcanic rocks (Gibson-Honman rock) are underlain by black mudstone and sandstone. Geochronology of the dacitic rocks from the Lakeview section is targeted to resolve this problem (Chapter 4).

3.4.2 Black Flag Formation (BFF)

Rocks in the Kambalda Domain assigned to the Black Flag Formation of Krapez et al. (2000) are represented in a 30 km x 3 km elongate belt to the east of Kalgoorlie (Fig. 3.35). The belt of BFF overlies ultramafic and mafic volcanic rocks on both western and eastern margins indicating the presence of a gently south-plunging fold: the Gidji Syncline. Black Flag Formation rocks are separated from underlying sedimentary rocks by the steeply west-dipping Gidji fault.

The broad belt of rocks west of Gidji Lake area depicted as Spargoville Formation on Figure 3.35 is a poorly exposed sequence of sandstone / shale turbidites dismembered by faults and shear zones. This sequence is allocated to SPF since no rocks of BFF affinity have been identified in that area to date. Exposures studied to the east of the Gidji fault include: outcrops on the edge of Gidji Lake; drill holes from the Eight Mile Dam resource area; a small pavement labelled 'sedimentary breccia' on Figure 3.35; and drill holes TPDD001 and MAD01/02.

Gidji felsic unit (Upper Black Flag formation)

The Gidji succession comprises a sequence of felsic volcanic rocks with interbedded conglomerate and siltstone, and extensive hornblende-feldspar porphyry dykes and sills. The known strike extent (11 km) southwest of Gidji Lake may represent only a small portion of the unit in the Kambalda Domain. Detailed studies of the Gidji felsic unit were completed by Taylor (1984) and Hand (1998).

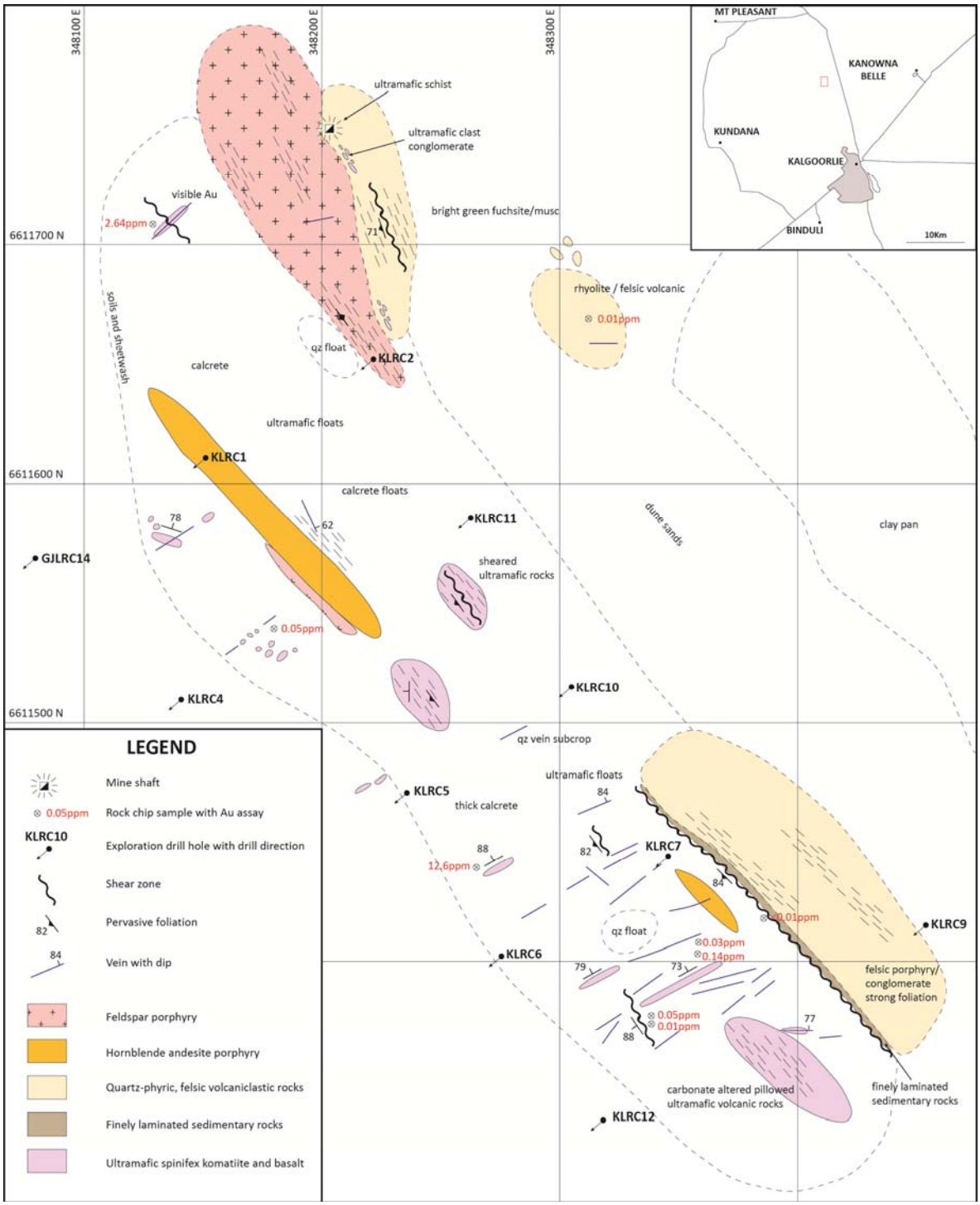

Figure 3.38 – Outcrop geology of the Gidji Hill area showing contact relationships between spinifex komatiite lava rocks and the overlying Gidji Felsic unit volcanic and sedimentary rocks.

Contact relationships

The basal contact of the Gidji felsic unit is locally erosional onto underlying ultramafic komatiite and komatiitic basalt (Fig 3.38). Clasts of ultramafic rocks are present in the lowermost beds of the felsic unit in southern outcrops (Fig. 3.38), whereas the northernmost contact of the unit is intercalated laterally with sandstone and siltstone where the felsic volcanic rocks die out (Fig. 3.35). The upper contact of the Gidji felsic unit is an erosional unconformity

with the overlying Gidji conglomerate in the south (near TPDD001 on Fig. 3.35), whereas in the north the Gidji felsic unit is overlain by a thin amygdaloidal basalt (Gidji mafic volcanic) unit that appears to have been extruded after erosion of the sequence and close to age of deposition of the Gidji conglomerate, with common peperitic textures between basalt and volcaniclastic sedimentary rocks observed in drill holes from the Eight Mile Dam prospect. The basalt at Gidji is similar to a basaltic flow unit that underlies the Golden Valley felsic unit in the footwall of Kanowna Belle.

Description

The Gidji felsic unit is a poorly exposed sequence comprising lower polymictic conglomerate and breccia intruded by hornblende-feldspar porphyry (Fig 3.39a, b), and overlain by dacite-rhyolite volcanic breccia (Fig. 3.39c, d) with interbedded mudstone and sandstone units (Fig. 3.39e, g, h). This upper volcaniclastic sequence is also intruded by andesitic hornblende-feldspar porphyry sills and dykes.

Polymictic conglomerate and breccia contain fragments of felsic lava, quartz-phyric rhyolite, mafic volcanics and hornblende-feldspar porphyry. The clasts vary from sub-angular to sub-rounded in massive disorganised, clast-supported units. Felsic volcanic rocks (Fig. 3.39d) include strongly-altered oligomictic rhyolite breccia. The breccia is composed of crystalline and glassy fragments that have a flattened angular morphology, with an irregular fluidal aspect suggesting that the morphology may reflect primary volcanic textures. Crystalline fragments are composed of carbonate, quartz and chlorite with minor biotite; glassy fragments are very fine-grained and totally altered to sericite.

The matrix of the breccia is quartz-rich, fine-grained siliceous material. Hornblende-feldspar porphyry in the Gidji felsic volcanic unit contains elongate, euhedral hornblende and minor feldspar crystals in a fine groundmass of intermediate composition with carbonate filled amygdales.

Interbedded sandstone/mudstone units are thin continuous beds intercalated with the volcanic breccias. The sedimentary rocks display abundant cross-bedding and soft-sediment deformation features (Fig. 3.39e, h) including sedimentary breccia locally (Fig. 3.35; Fig. 3.39g).

Structural geology

Felsic volcanic rocks at Gidji are folded and extensively sheared proximal to the Gidji fault (Fig. 3.39f). Local examples of downward-facing folds are encountered, possibly indicating an earlier phase of deformation, but this relationship is not universal or widely developed, and appears localised in underlying Talbot formation sedimentary rocks. The rocks of the Gidji felsic unit are generally northeast dipping, but younging to the southwest. At depth

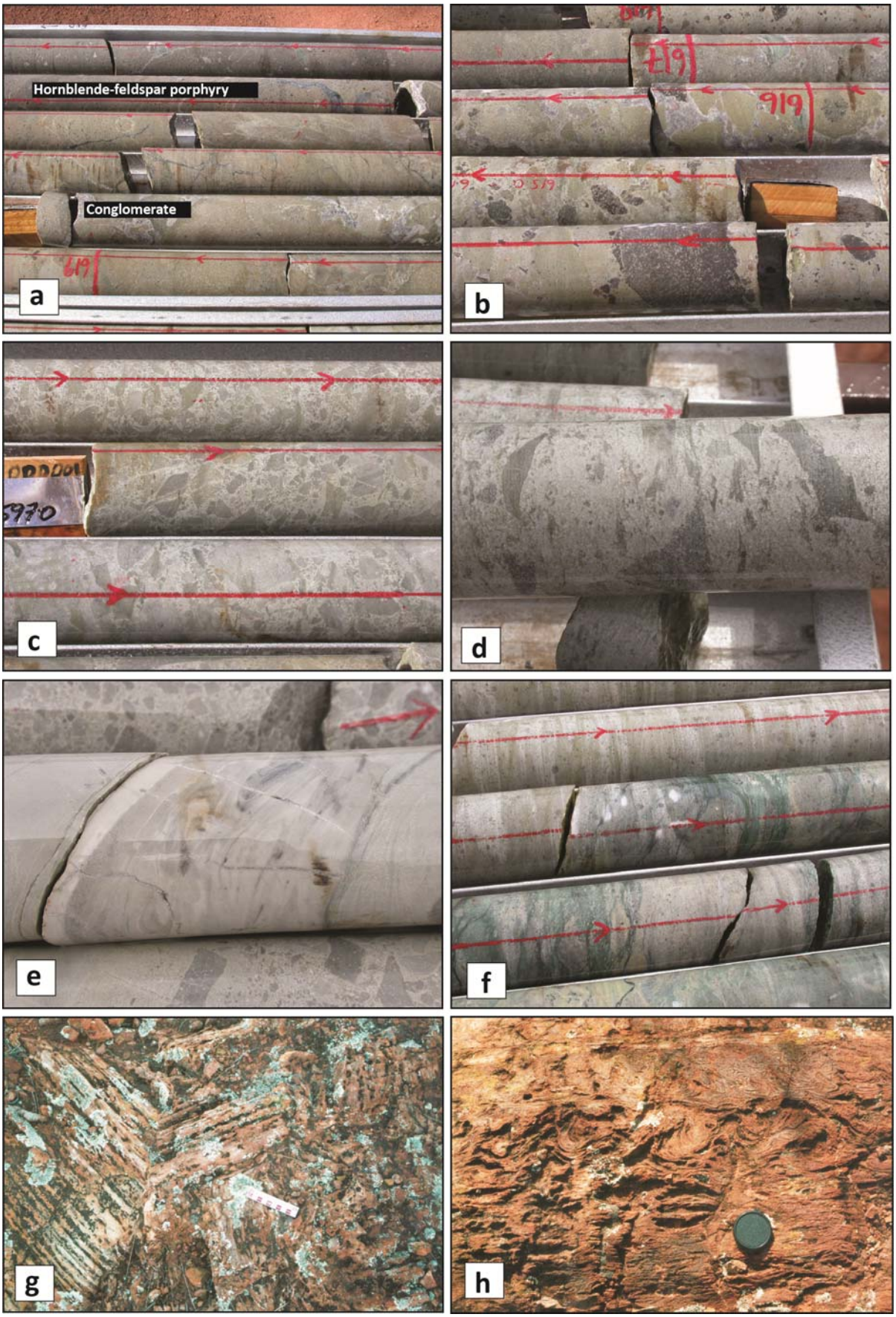

Figure 3.39

Figure 3.39 – Upper Black Flag formation – Kambalda Domain,

a) Hornblende-biotite-feldspar porphyry intrusion into basal polymictic conglomerate. The intrusion is pink-coloured from abundant carbonate in the groundmass, locally vesicular with xenoliths of microcrystalline igneous rock (Gidji Teepookana Prospect, drill hole TPDD001 619 m; GDA: 350889E; 6608326N). Drill cores have 50 mm diameter.

b) Polymictic conglomerate/breccia basal unit to the Gidji Felsic sequence. The unit contains angular to sub-angular fragments of felsic lava rocks, porphyry, finely bedded sedimentary rocks, quartz-eye rhyolite, and mafic volcanic rocks; all with intense pale green sericite-carbonate alteration , TPDD001 616 m,

c) Volcaniclastic breccia with crystalline and glassy felsic volcanic clasts and rare clasts of fine-grained felsic rock (sedimentary?). The unit is a proximal volcanic deposit with highly angular cuspate rhyolite fragments, in a fine-grained matrix of quartz eyes and feldspar crystal fragments. All clasts have a sub-parallel plane of flattening that may represent an original plane of compaction(?). Intense sericitic alteration has obscured much of the primary texture. (Gidji Teepookana Prospect, drill hole TPDD001 697 m).

d) Close-up photograph of the unit in (c) showing angular, cuspate glassy rhyolite fragments in oligomictic breccia (Gidji Teepookana Prospect, drill hole TPDD001 440 m),

e) Mudstone interbed in felsic volcanic breccia. The mudstones have abundant sedimentary structures that indicate up hole (westward) younging, which matches with outcrops of similar units (g an h) (Gidji Teepookana Prospect, drill hole TPDD001 545.5 m).

f) Sheared zone within in rhyolite breccia with seams of fuchsite mica alteration. The fuchsite may represent fragments of ultramafic rock in a brecciated quartz-eye rhyolite sequence. Fuchsitic micas form a foliation that wraps broken, angular and flattened clasts of mineralised rock (Gidji Teepookana Prospect, drill hole TPDD001 435 m).

g) Breccia composed of cross-bedded mudstone and sandstone blocks, The individual blocks are highly angular and arranged clast-to-clast with little or no matrix or cement. The breccia occupies a channel of broken formation, whereas bedding is regular and steeply dipping adjacent to this site (GDA: 351548E; 6608267N).

h) Cross-bedding and soft-sediment deformation structures in sandstone/mudstone beds from one of the blocks in (g). Other areas on the same outcrop have regular bedding with local symmetrical ripples in fine-grained sandstones that indicate westward facing of the unit. This unit corresponds with the mudstone beds drilled in TPDD001 a few hundred metres to the north west (GDA: 351548E; 6608267N).

the sequence forms the western limb of an overturned syncline, with steeply-dipping beds compared to a moderate to shallow west-dipping cleavage.

Interpretation and correlation

The Gidji felsic unit is a volcaniclastic package of rhyolite to dacite volcanic breccia with interbedded sandstone, mudstone and shale. The sequence unconformably overlies ultramafic rocks that are bounded to the west by the Gidji fault, hence the felsic volcanics potentially could be correlated with (1) the Spargoville Formation, (2) the lower Black Flag formation, or (3) the Golden Valley felsic unit, which at Kanowna, is considered to be part of the upper Black Flag formation (see below). The sequence here is in lateral contact with sandstone/shale to the northwest of the Gidji Syncline, which may be part of the Spargoville Formation, but the exact relationship between these units is unclear. The top of the unit is well defined where it is unconformably overlain by sedimentary rocks of the Gidji conglomerate to the east. The age relationships of the unit are investigated further by geochronology in Chapter 4.

Gidji Lake conglomerate (upper Black Flag formation)

The Gidji Lake conglomerate (GLc) is variably exposed over an 18 km x 2.5 km area to the northeast of Kalgoorlie with the best exposures located on the shore of Gidji Lake (Fig. 3.35; 3.40). The formation comprises massive-pebbly sandstone ~550 m thick; conglomerate ~200 m thick; sandstone/shale ~80 m thick; and sandstone/siltstone ~270 m, with an estimated total thickness of 1100 m. The GLc locally contains intercalated felsic volcaniclastic rocks in the uppermost parts of the stratigraphy, and was intruded by hornblende-feldspar porphyry dykes and sills along the south-western margin. Two diamond drill holes and several outcrop sections were used to determine the detailed sedimentology of the GLc.

Contact relationships

The lower contact of the GLc exposed in drill hole HSSD001 (Fig. 3.35; Fig. 3.40) is sharp and erosional against underlying amygdaloidal basalt; whereas in drill hole EMD021 (Fig 3.35) from the Eight Mile Dam area, the lower amygdaloidal basalt has a peperitic contact with intermixing of the two rock types over 1-2 m. A coeval relationship is suggested by the northern closure of the GLc syncline in map pattern (Fig. 3.35; Fig. 3.40) where the two sub-parallel units track around the closure of the Gidji syncline. The western margin of the GLc cuts across an irregular sequence that includes ultramafic, mafic, felsic volcanic and sedimentary rocks. That sequence is interpreted to represent the ultramafic volcanic to upper Black Flag Group portion of the regional stratigraphy and the GLc lower contact is therefore interpreted as an erosional unconformity internal to the Black Flag Group. The GLc is the youngest sequence in the Gidji district and the upper contact is not present.

Description

Sedimentary breccia and conglomerate in the GLc have a mean clast size of ~60 mm with geometric means up to 189 mm. Beds are clast or matrix supported (C/M ratio: 0.5) and have a lithic-wacke matrix with Q:F:L = 42:10:48 (Fig. 3.41). Coarse clastic units in the GLc are dominated by moderately sorted, sub-rounded to sub-angular and elongate volcanic debris, characterised by planar to diffuse bedding of ~1 m mean thickness. The internal structure of the beds is generally planar stratified with scoured contacts and grain size grading.

Conglomerate and sedimentary breccia (Fig. 3.42a ,b, e, f) in the GLc are polymictic, characterised by abundant sedimentary clasts (46%), quartz-hornblende-feldspar porphyry (23%), and felsic volcanic (11%) clasts; with minor amounts (20%) of quartz-feldspar porphyry, ultramafic, granitic and vein clasts (Fig. 3.41). Rhyodacitic volcaniclastic breccia (Fig. 3.41g, h) in the upper GLc contains sub-angular and elongate felsic volcanic clasts (up to 98%) with 2% sedimentary clasts in a lithic-rich matrix.

A large proportion of the GLc is composed of feldspathic and lithic wacke, and granule-sized sedimentary rocks (Fig 3.41; Fig 3.42c-e). Granule sized rocks are characterised by a dominant quartz component (Q:F:L = 46:12:42), whereas the sand sized rocks are dominated by lithics (Q:F:L = 39:11:50) (Fig. 3.41).

Structural geology

The GLc contains a strongly developed NNW fabric that has affected both clasts and matrix minerals. Ultramafic and sedimentary clasts are elongate with a shallow southeast-plunging stretching lineation throughout the GLc, parallel to a bedding/foliation intersection lineation. Competent porphyry and sedimentary grit pebbles are less affected by the deformation and retain approximately spherical shapes.

The GLc occupies a NNW-SSE trending syncline that plunges on average to the southeast at ~20 degrees, whereas field evidence (Fig. 3.40) suggests steeper fold axis plunges in its northern part, suggesting the possibility of a curved fold hinge. The western limb of the syncline is slightly overturned to the east with steep bedding on its western limb and a moderately west dipping cleavage (Fig 3.40). Overturning of the western fold limb is more pronounced in the vicinity of the Eight Mile Dam gold resource. Structural and facing data combined with cross-sectional reconstruction, assuming constant bed thickness, demonstrate that the syncline is right-way-up with a moderately west-dipping axial plane. Geometric reconstruction suggests that the GLc syncline extends to ~2 km depth.

Interpretation and correlation

The GLc is one of the youngest Archaean formations in the Kalgoorlie district with a maximum depositional age within error of the Kurrawang Formation in the Ora Banda Domain,

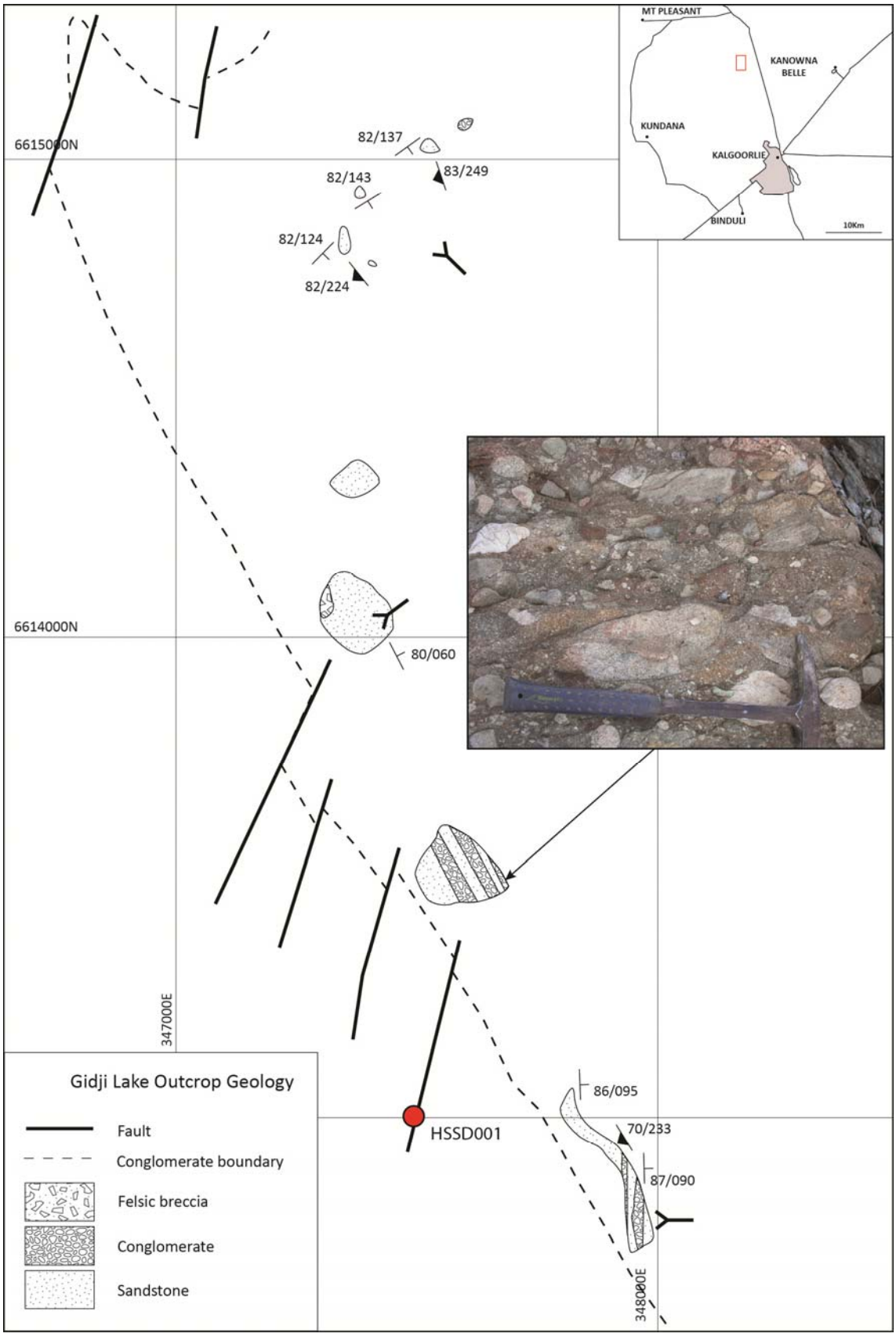

Figure 3.40 – Outcrop map of the Gidji Lake conglomerate, demonstrating the northern closure of the southeast-plunging Gidji Syncline; dashed margin taken from basement interpretation map compiled from re-logged RAB and AIRCORE drill holes.

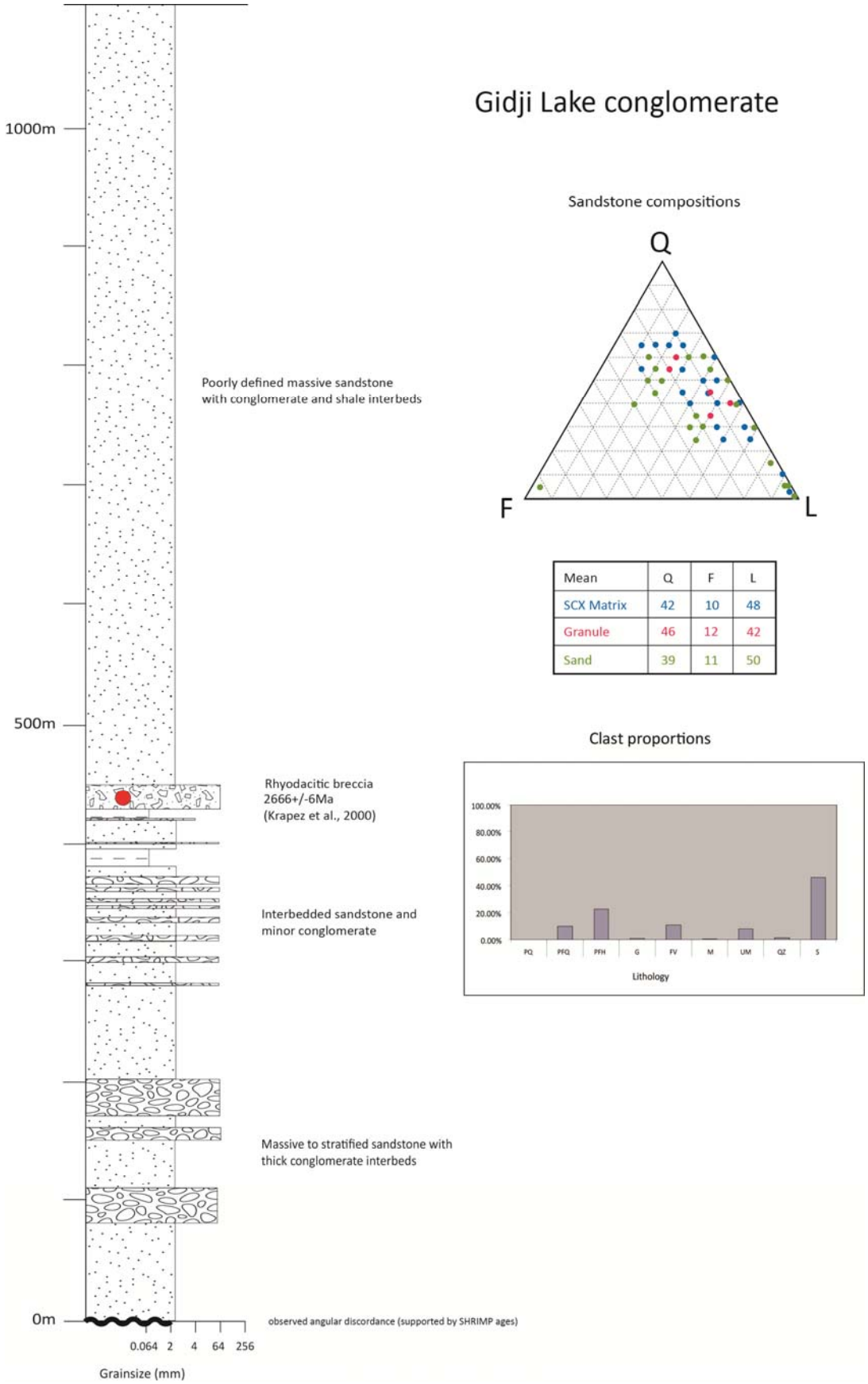

Figure 3.41 – Composite stratigraphic column of the Gidji Lake formation. QFL data are coloured according to the table of mean values. SCX refers to conglomerate or breccia-sized clastics. PQ – quartz porphyry; PFQ – quartz feldspar porphyry; PFH – hornblende-feldspar porphyry ± quartz; G – granite; FV – felsic volcanic; M – mafic volcanic; UM – ultramafic; QZ – quartz; S - sedimentary

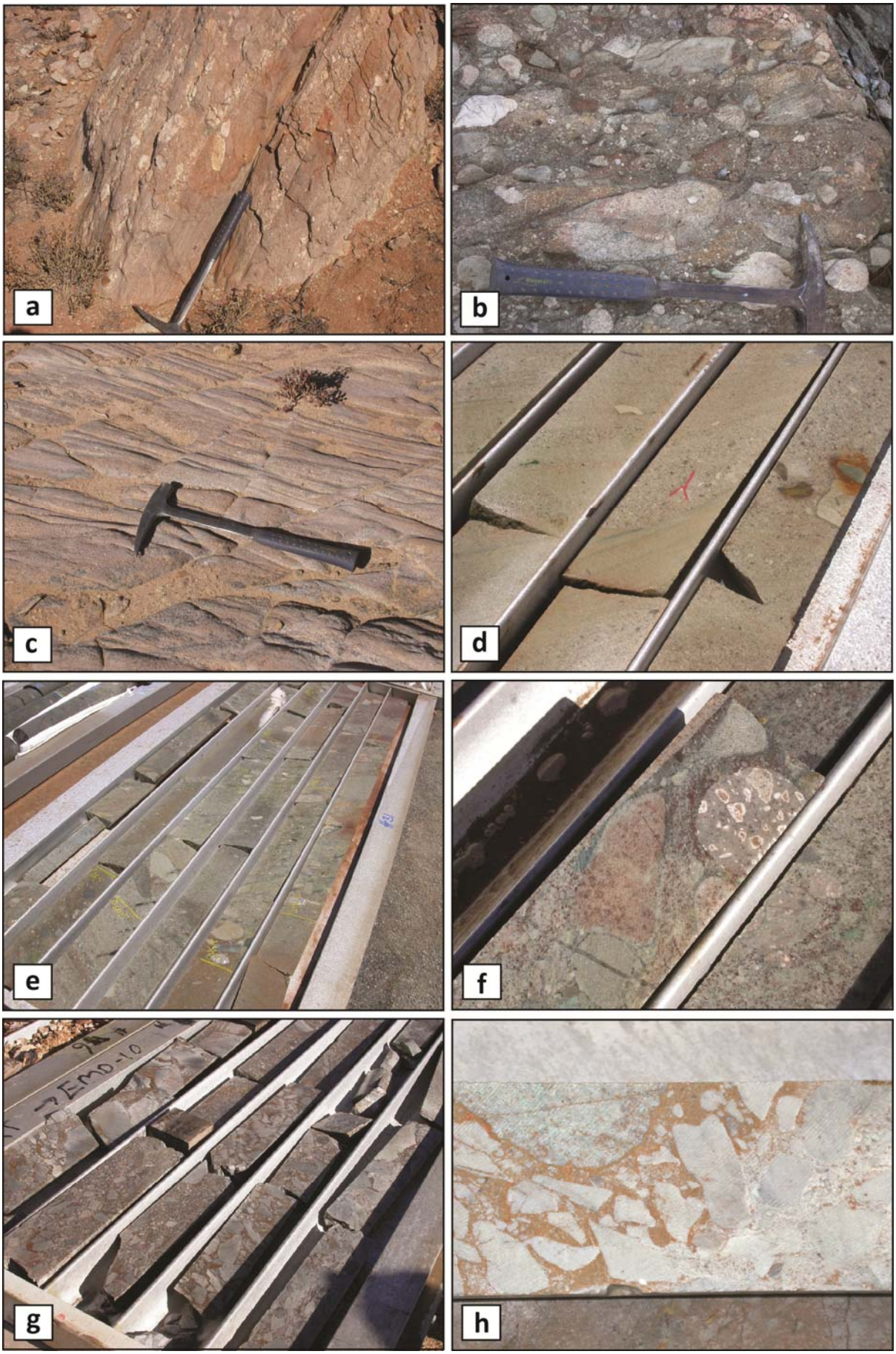

Figure 3.42

Figure 3.42 – Gidji Lake conglomerate and sandstone

a) Planar bedded conglomeratic quartz sandstone from the southern outcrop in Figure 3.40. Thick sequences of thinly bedded, quartz rich sandstones with local conglomeratic layers dip steeply east. Way-up is to the east as indicated by graded bedding and scoured conglomeratic bases of beds. The sandstone contains coarse, sub-rounded to sub-angular grains of translucent quartz, feldspars and polymictic lithic fragments. Steep east-dipping bedding is overprinted by steep to moderate west-dipping foliation, which indicated the western limb of the Gidji Syncline is slightly overturned (Gidji Lake; GDA: 347937E; 6612867N).

b) Polymictic pebble to cobble, matrix-supported conglomerate, composed of rounded and flattened pebbles of felsic volcanic rock, with rare ultramafic, granitoid and chert clasts in a coarse sand – granule matrix. Strong brown carbonate alteration overprints the matrix sands (Gidji Lake; GDA: 347640E; 6613450N).

c) Steeply east-dipping, cross-bedded quartz sandstone within the Gidji Conglomerate sequence. Way-up is to the east – (Gidji Lake; GDA: 347830E; 6612990N).

d) Drill core from the Eight Mile Dam resource area with intersections through plane bedded quartz rich conglomeratic sandstone of the Gidji Conglomerate sequence. Strong light green coloured sericite alteration is pervasive throughout the core. The hole was drilled at -60/090. Way-up is down hole as indicated by grading and scoured bases (Eight Mile Dam; EMD4 152.4 m; GDA: 352506E; 6608780N).

e) Polymictic conglomeratic sandstone characterised by scattered well rounded clasts within a matrix supported plane bedded quartz rich sandstone sequence. (Eight Mile Dam; EMD4 245 m).

f) Well rounded pebble conglomerate showing an example of spherical coarsely porphyritic felsic clasts (Eight Mile Dam; EMD10 245 m; GDA: 352744E; 6608830N).

g) Felsic volcanic, matrix supported rhyodacite breccia unit internal to the Gidji Conglomerate sequence. The unit is composed of abundant fine-grained, to locally porphyritic felsic volcanic clasts in a coarse-grained sand-granule matrix of crystals and lithic fragment. Strong Fe-carbonate overprints the groundmass of the breccia. The is the unit analyses by Hand (1998) that returned a SHRIMP U-Pb age of 2666±6 Ma (Eight Mile Dam; EMD10 80 m)

h) Close up of rhyodacite breccia showing the presence of rare exotic fragments that may be porphyritic intrusive rocks in the top left of the image, and the strong Fe-carbonate alteration of the groundmass (Eight Mile Dam; EMD10 80 m).

or with the Grave Dam / Golden Valley members in the Boorara Domain. The GLc is relatively quartz rich when compared to other conglomerates in the district, and is distinct in its clast proportions with dominant sedimentary and quartz-hornblende-feldspar porphyry components. The unit is mostly plane bedded with episodes of quiescent sedimentation (shales) followed by influxes of proximal felsic volcanic debris.

Mt Charlotte east intermediate rocks (Gidji conglomerate - Upper Black Flag formation)

Two drill holes MAD01 and MAD02 (Fig. 3.35) located north-east of the Mount Charlotte gold mine, intersected a distinct intermediate conglomerate unit that has superficial similarities to the White Flag Formation of the Ora Banda Domain. The drill holes intersected the upper and lower contacts of the unit giving a near complete section (Fig. 3.43). The unit has a distinct intermediate composition with a volcanic age of 2661±3 Ma (Fletcher et al. 2001), which is interpreted as a maximum depositional age, and suggests deposition of the conglomerate after ~2658 Ma. The stratigraphic position of the unit is uncertain, but given the location of the unit and its age, it appears to be part of the Black Flag Formation. The age of the unit and its relationship with the Gidji conglomerate suggest that it may be correlated with upper Black Flag formation.

Contact relationships

Drill hole MAD01 intersected the basal contact of the intermediate conglomerate unit, whereas MAD02 intersected the top contact (Fig. 3.43). The upper contact is sharp, depositional suggesting that the intermediate conglomerate is part of a normal stratigraphic column, whereas the lower contact juxtaposes relatively undeformed intermediate conglomerate against strongly folded and deformed sandstone and siltstone, and may thus represent an erosional unconformity.

Description

Breccia and conglomerate in the MAD drill holes have a mean clast size of ~72 mm with geometric means up to 206 mm. Beds are clast supported (C/M ratio: 0.6) and have a lithic-wacke matrix with Q:F:L = 1:24:75 (Fig. 3.43). Coarse clastic units in the MAD holes are dominated by moderately to poorly sorted, sub-angular to angular and elongate andesite porphyry debris, characterised by planar to diffuse bedding of ~0.6 m mean thickness. The internal structure of the beds is generally planar stratified with cross-bedding and rare grain size grading.

Conglomerate and breccia (Fig. 3.44a, b, e, f) in the MAD holes are mainly oligomictic, characterised by hornblende-feldspar porphyry clasts (94%) and lesser (6%) sedimentary clasts (Fig. 3.43). Rare rounded exotic mafic clasts composed of coarse-grained amphibolite are present (Fig. 3.44b), as are rare felsic volcanic clasts (Fig. 3.44c).

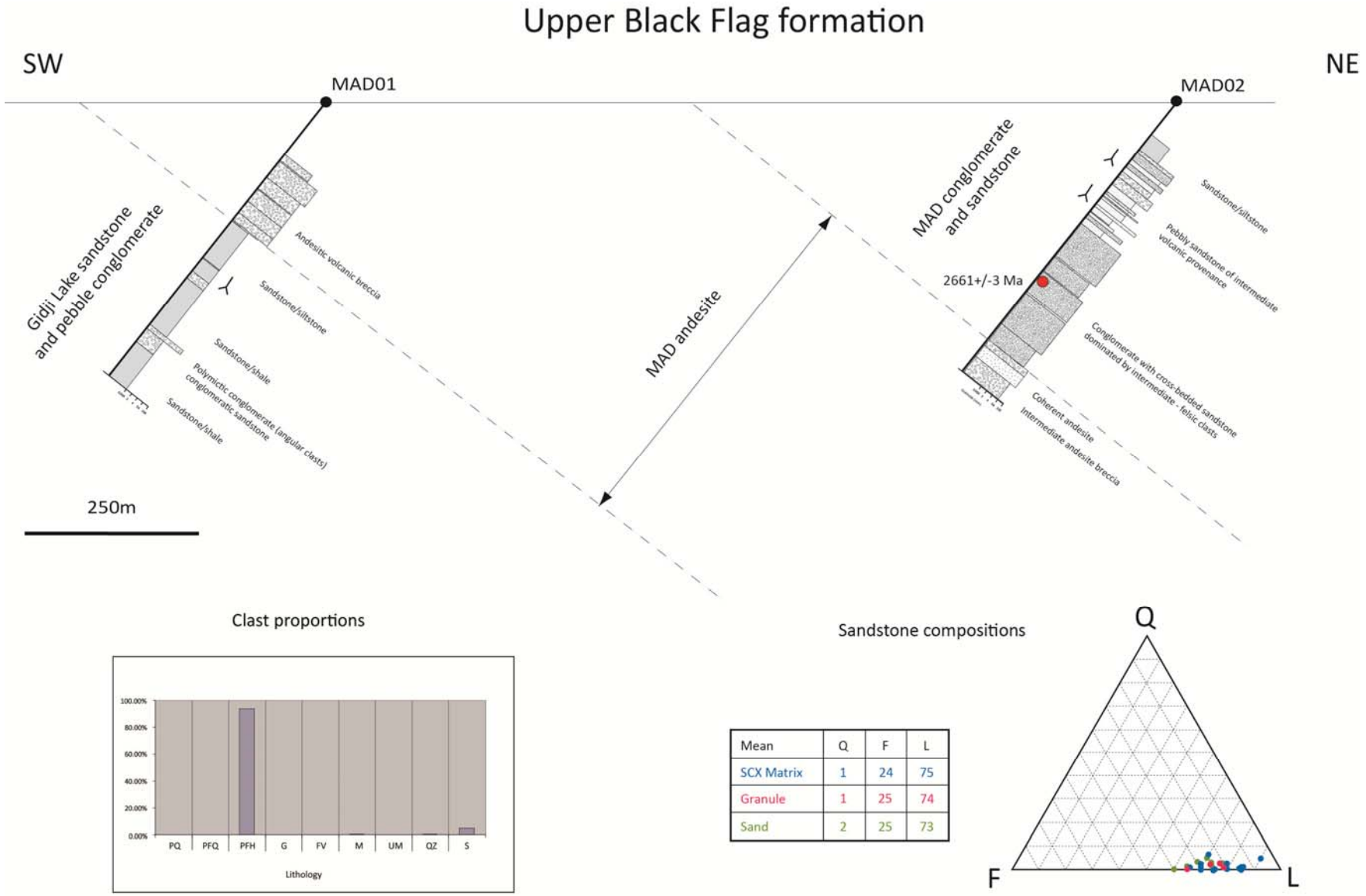

Figure 3.43 - Cross section through drill holes MAD01 and MAD02 with diagrams showing clast proportions and QFL ratios for the andesitic part of the section.QFL data are coloured according to the table of mean values. SCX refers to conglomerate or breccia-sized clastics. PQ – quartz porphyry; PFQ – quartz feldspar porphyry; PFH – hornblende-feldspar porphyry ± quartz; G – granite; FV – felsic volcanic; M – mafic volcanic; UM – ultramafic; QZ – quartz; S - sedimentary

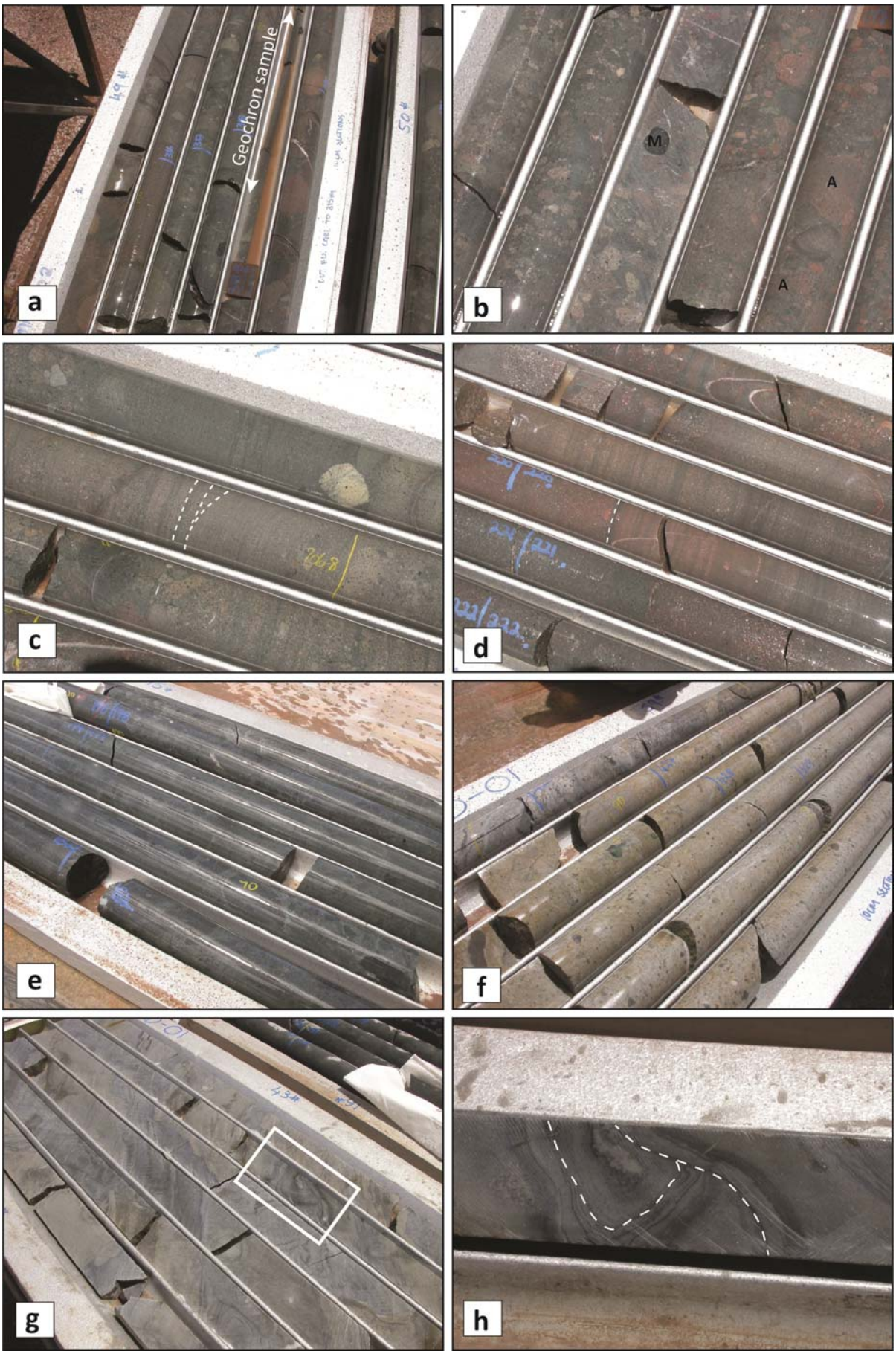

Figure 3.44

Figure 3.44– Upper Black Flag formation intermediate conglomerate,

a) Intermediate composition pebble to boulder, clast supported, poorly sorted conglomerate. A clast of hornblende-feldspar porphyry from this unit was analysed by Fletcher et al. (2001) and returned SHRIMP U-Pb analysis of 2661±3 Ma. The location of the sampled clast is marked by the 1/8 core section (Mount Charlotte east; MAD02 318 m; GDA: 358797E; 6600485N).

b) Pebble to cobble andesite dominated conglomerate band with rare mafic clasts. Sub-rounded clasts of variably sericite and hematite altered andesite are predominantly clast supported. (Mount Charlotte east; MAD02 322.5 m).

c) Fine to medium-grained cross-bedded, intermediate crystal-lithic sandstone, interbedded with andesite dominated conglomerate and conglomeratic sandstone. Cross-bedding is common throughout the more clastic parts of the MAD holes and may indicate a fluvial environment of deposition given the scale and character of the cross beds (Mount Charlotte east; MAD02 209 m).

d) Cross-bedded intermediate sandstone as for (c). (Mount Charlotte east; MAD02 220 m).

e) Strongly chlorite altered and silicified intermediate breccia/conglomerate. The unit is part of an intermediate volcanic package that in places contains coherent volcanic breccias and possible hyaloclastites. The clasts are obscured by alteration, but show some evidence of rounding, and are set in coarse clastic matrix sandstone. (Mount Charlotte east; MAD01 180 m; GDA: 357993E; 6599572N).

f) Felsic dominated polymictic, granule breccia in contact with sandstone below intermediate breccia. Sub-angular clasts in the unit (30%) are dominated by felsic to intermediate porphyry clasts in a lithic dominated matrix sandstone. (Mount Charlotte east; MAD01 430 m).

g) Deformed sandstone/siltstone turbidites stratigraphically below the andesite dominated volcanic units further up in the drill hole. The sandstone/siltstone sequence is interpreted as the upper part of the Gidji Conglomerate sequence outcropping to the north, which also contains shales and siltstone in the sequence (Mount Charlotte east; MAD01 330 m).

h) Small scale fault-bend fold in fine-grained sandstone/siltstone from (g). (Mount Charlotte east; MAD01 330 m).

A small proportion of the intermediate rocks in the MAD hole is composed of lithic wacke, and granule-sized sedimentary rocks (Fig 3.43). Cross-bedded granule and sand-sized rocks vary little from the matrix compositions of breccia and conglomerate in the same stratigraphic sequence (Fig. 3.43). The unit also contains a section of intermediate andesitic volcanic rocks, including volcanic breccia and coherent andesite (Fig. 3.43).

Structural geology

The intermediate volcaniclastic rocks in MAD01 and MAD02 show very little evidence of deformation, whereas the sandstone and siltstone rocks stratigraphically above and below are intensely deformed (Fig. 3.44g, h) - likely reflecting primary rheological contrasts. Cross-bedded lithic sandstones are common throughout the lower sections of MAD02 (Fig. 3.44c, d) indicating that the sequence is east-dipping and upward younging (Fig. 3.43).

Interpretation and correlation

Intermediate rocks in drill holes to the north-east of Mount Charlotte gold mine display lithological similarities to the White Flag Formation in the Ora Banda Domain. However, significant differences include a lack of a *dominant* juvenile volcanic component, the presence of cross-bedded sandstones (lacking in the WFF), and a precise SHRIMP analysis of zircons from a hornblende-feldspar porphyry clast of 2661±3 Ma (Fletcher et al. 2001) compared to an age from the WFF of 2690±9 Ma (Sircombe et al. 2007).

The rocks in MAD01 and MAD02 were intersected along strike of the Gidji conglomerate, and while displaying several differences to that unit, the MAD sequence could also be correlated with upper Black Flag formation on the basis of stratigraphic position and age. One possibility is that these rocks represent the uppermost part of the Black Flag Formation (of Krapez et al. 2000) in that the section faces upward to the east, towards the trace of the Gidji syncline, implying that they in turn are the youngest rocks in the syncline. The abundance of hornblende-feldspar porphyry clasts in this unit may indicate erosion of intrusions of that composition, examples of which are present at Fimiston, 5 km to the southwest.

3.5 Boorara Domain

Sedimentary formations in the Boorara Domain have remained enigmatic as to their proper location in the stratigraphy of Kalgoorlie. A general consensus has been to assign these rocks to the 'Black Flag Group', but a prodigious volume of conglomerate of apparently localised provenance has prevented any regional correlations. Barley et al. (2002) assigned some of the Boorara Domain formations to sequences identified in the other domains on the basis of lithofacies associations, but the proper sequence of the units is uncertain in the case of several of the Kanowna members.

This section describes six units in the Boorara domain in the vicinity of the Kanowna mining centre (Fig. 3.45). The units are assigned as informal members of the regional formations based on descriptive and geochronological criteria as: sedimentary rocks overlying the Upper Basalt unit; upper (BFu) and lower (BFl) divisions of the Black Flag Formation; and Kurrawang Formation (KUF).

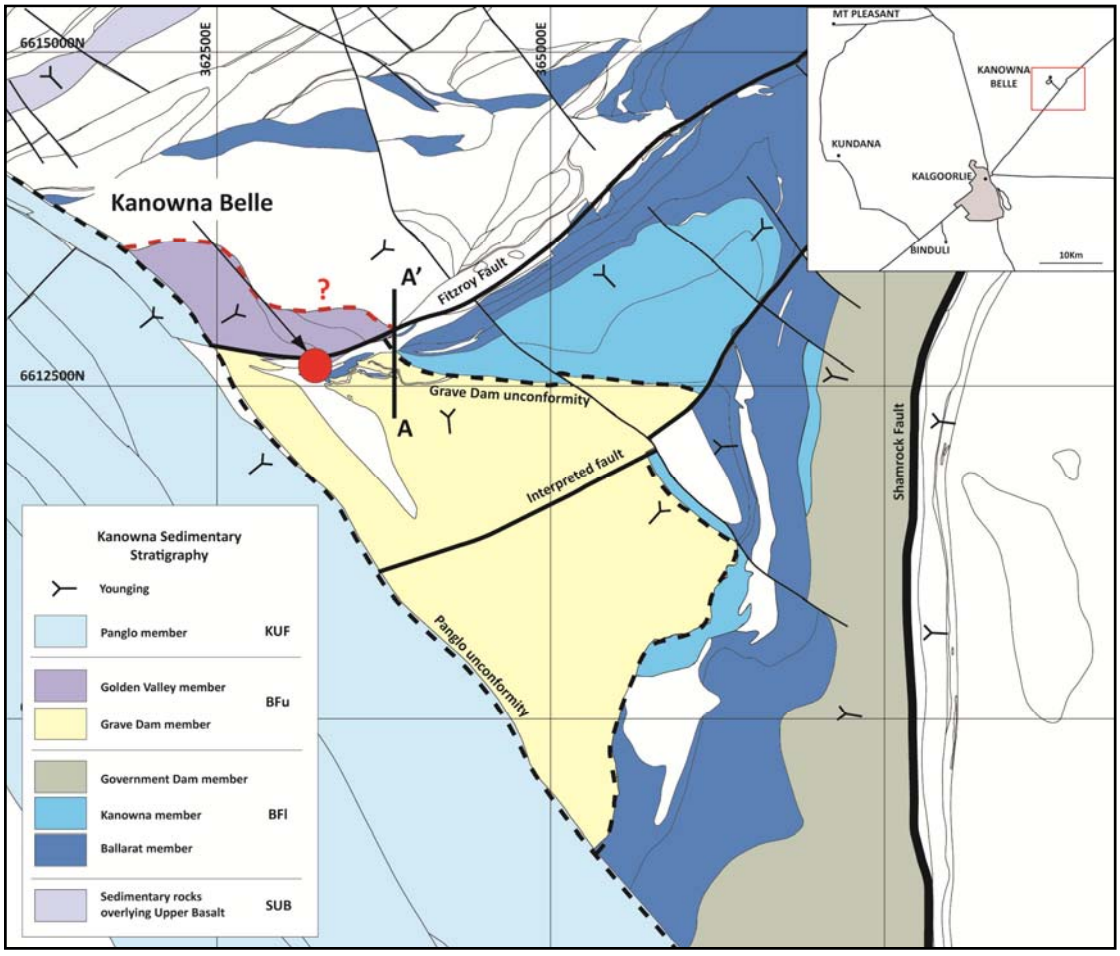

Figure 3.45 – Map of the sedimentary formations in the Kanowna district. White areas contain mafic/ultramafic volcanic rocks, intrusive rocks and other formations not addressed by this study. The white unit north of the Fitzroy Fault is Robinson's Komatiite, white units south of the Fitzroy Fault are porphyry intrusions.

3.5.1 Sedimentary rocks overlying Upper basalt (SUB)

Sedimentary rocks overlying the Upper Basalt Unit (SUB) are known from drill holes to the north of Kanowna Belle in a 7 km x 0.3 km band striking NE-SW (Fig. 3.45). The unit contains mostly plane bedded, fine-grained sandstone and siltstone with no coarse clastic component. Bedding in the sandstone dips moderately to the south and the sequence is south younging and upright. These rocks have previously been assigned to the Spargoville Formation primarily based on their stratigraphic position above the Upper Basalt, but may be better correlated with the Talbot formation at Mount Pleasant.

Drill hole intersections of the lower contact of SUB show a primary intrusive contact where dolerite sills intruded the base of SUB contact, with a similar relationship to the Golden Mile Dolerite at Kalgoorlie. The upper contact was intruded by dacite porphyry.

In the northeast, the SUB sedimentary band appears to be continuous with highly deformed sedimentary rocks that lie in contact with the Robinson's Komatiite, however this remains a significant uncertainty. A discontinuity between the two sedimentary units is probable since the north-western contact of the komatiite has intruded sedimentary rocks at its contact and the komatiite/sedimentary sequence is younging to the northwest. The two sedimentary units are unlikely to be the same formation and may be juxtaposed by faulting and folding.

3.5.2 Ballarat member - uncertain stratigraphic position (lower Black Flag formation?)

The Ballarat member (BAM) is variably exposed in a faulted and folded sequence over 8 km x 1.5 km to the east and northeast of Kanowna Belle (Fig. 3.46). The unit comprises a lower conglomerate/grit sequence (Ballarat grit), a middle conglomerate sequence (Ballarat conglomerate) and an upper pebbly sandstone sequence (Ballarat sandstone) for an estimated total thickness of ~500 m. Significant variability in thickness and facies along strike makes this an approximate value only. Detailed stratigraphy of the BAM was determined from sixteen drill holes (Fig. 3.47), and only few outcrop exposures which are generally of poor quality. The graphic drill hole logs presented in Figure 3.48 are from two separate holes chosen as a guide to the character of each subdivision within the member rather than a composite stratigraphic column.

Contact relationships

A range of relationships with the surrounding rock formations is encountered at the margins of the BAM. Map patterns show a faulted lower contact with underlying ultramafic rocks of the Robinson's Komatiite (coloured white on Fig. 3.46). The faulting appears to cut bedding in the BAM with internal Ballarat grit/Ballarat conglomerate contacts truncated by the fault at a low angle. In drill hole GVD50, a sharp depositional contact of Ballarat conglomerate on Ballarat grit is located ~5 m from a sheared, mixed zone of grit and ultramafic rock with sheared slivers of Ballarat conglomerate totally contained within the ultramafic unit. A strongly sheared Ballarat conglomerate / ultramafic rock contact is present also in GVD46. Locally, angular contact relationships are preserved between Ballarat grit and the underlying Komatiite (Fig 3.49h) or between Ballarat conglomerate and the underlying Komatiite, indicating an unconformable lower contact.

Internal unit contacts within the BAM (Ballarat grit / conglomerate / sandstone) are gradational indicating a continuous depositional sequence (Fig. 3.49f). The upper contact of the BAM with lower units of the overlying Kanowna conglomerate is also gradational and can only

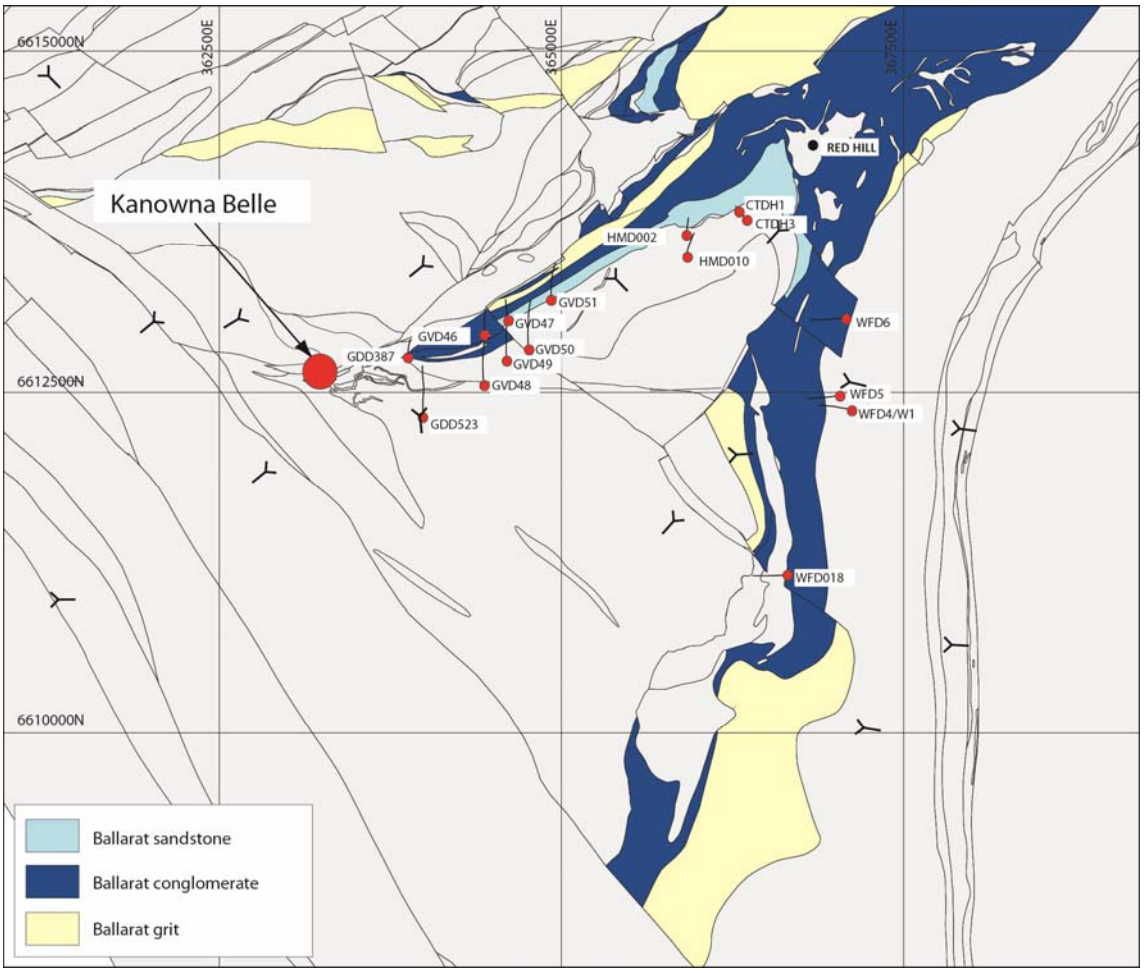

Figure 3.46 – Distribution of the Ballarat member and locations of drill holes used to assess the detailed geology (see Appendix for detailed logs)

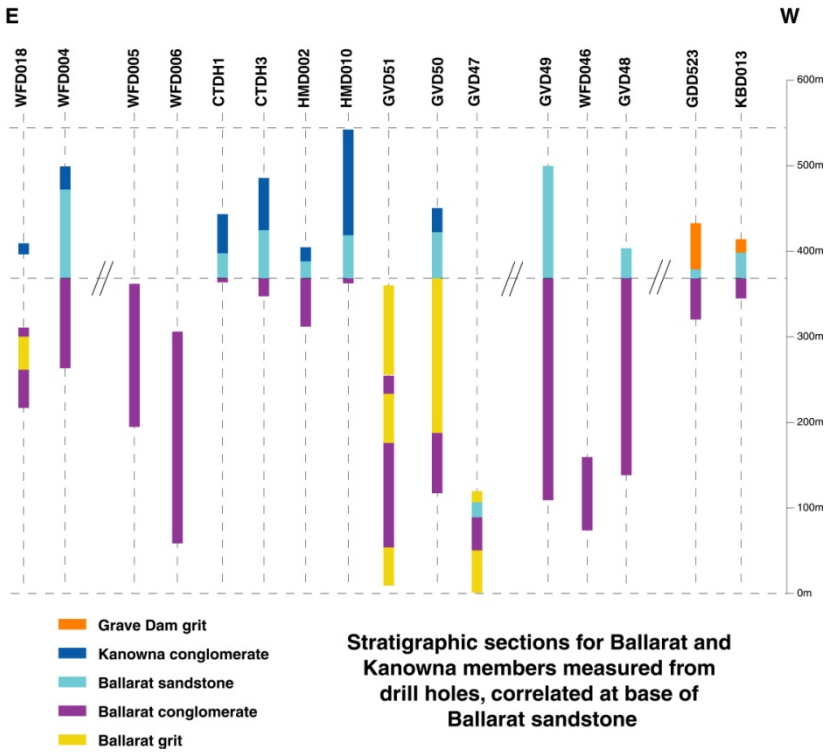

Figure 3.47 – Drill holes re-logged in this study intersecting the Ballarat and Kanowna members, correlated at the base of Ballarat sandstone.

Ballarat member

GVD49

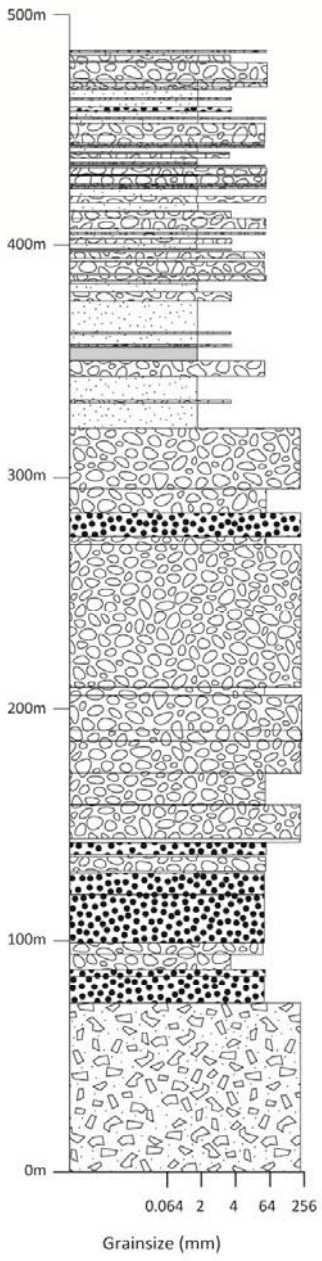

Ballarat sandstone:
Lithic arenite with polymictic pebble interbeds

Ballarat conglomerate:
Massive gradational units of polymictic boulder conglomerate and mafic/ultramafic conglomerate

Sub-angular polymictic conglomerate

GVD51

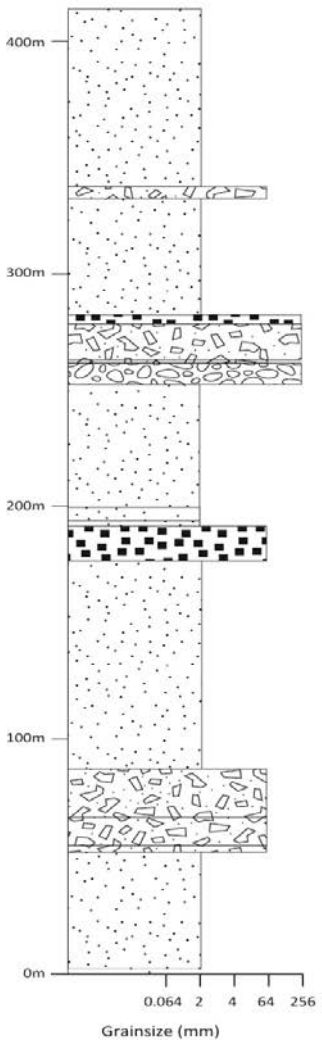

Ballarat grit:
massive beds of granule-sized quartz-rich felsic sandstone with rare interbeds of mafic conglomerate and felsic volcaniclastic breccia

Ballarat sandstone

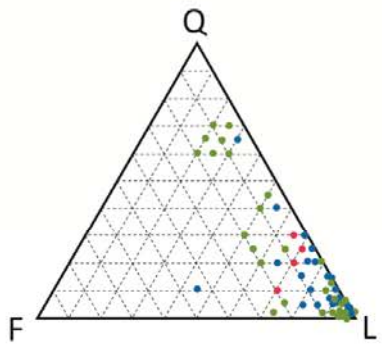

Clast proportions

Mean	Q	F	L
SCX Matrix	9	4	87
Granule	21	12	67
Sand	18	7	75

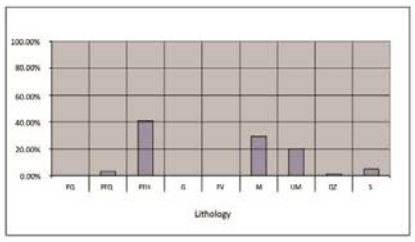

Ballarat conglomerate

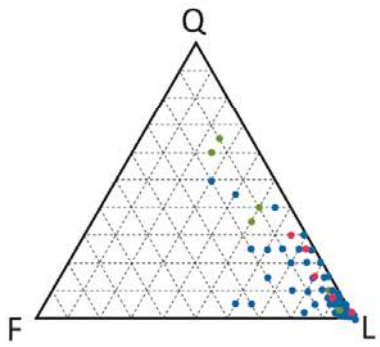

Clast proportions

Mean	Q	F	L
SCX Matrix	7	3	90
Granule	14	4	82
Sand	14	4	82

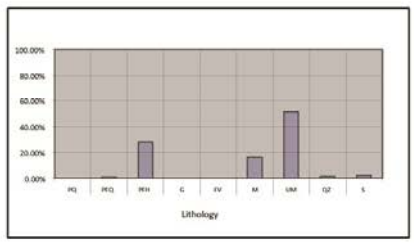

Ballarat grit

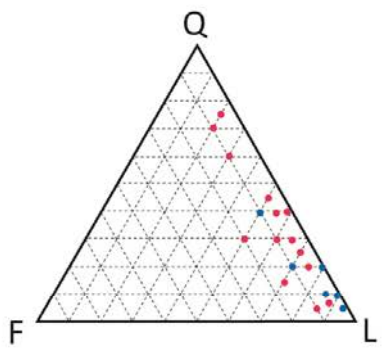

Clast proportions

Mean	Q	F	L
SCX Matrix	18	4	78
Granule	33	8	59
Sand	8	5	87

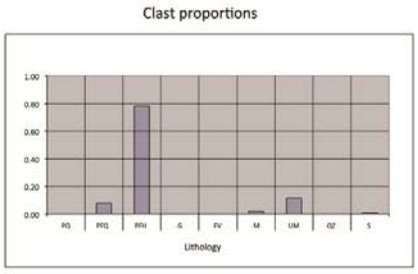

Figure 3.48 – Stratigraphic columns with clast and matrix information for the Ballarat member. QFL data are coloured according to the table of mean values. SCX refers to conglomerate or breccia-sized clastics. PQ – quartz porphyry; PFQ – quartz feldspar porphyry; PFH – hornblende-feldspar porphyry ± quartz; G – granite; FV – felsic volcanic; M – mafic volcanic; UM – ultramafic; QZ – quartz; S – sedimentary.

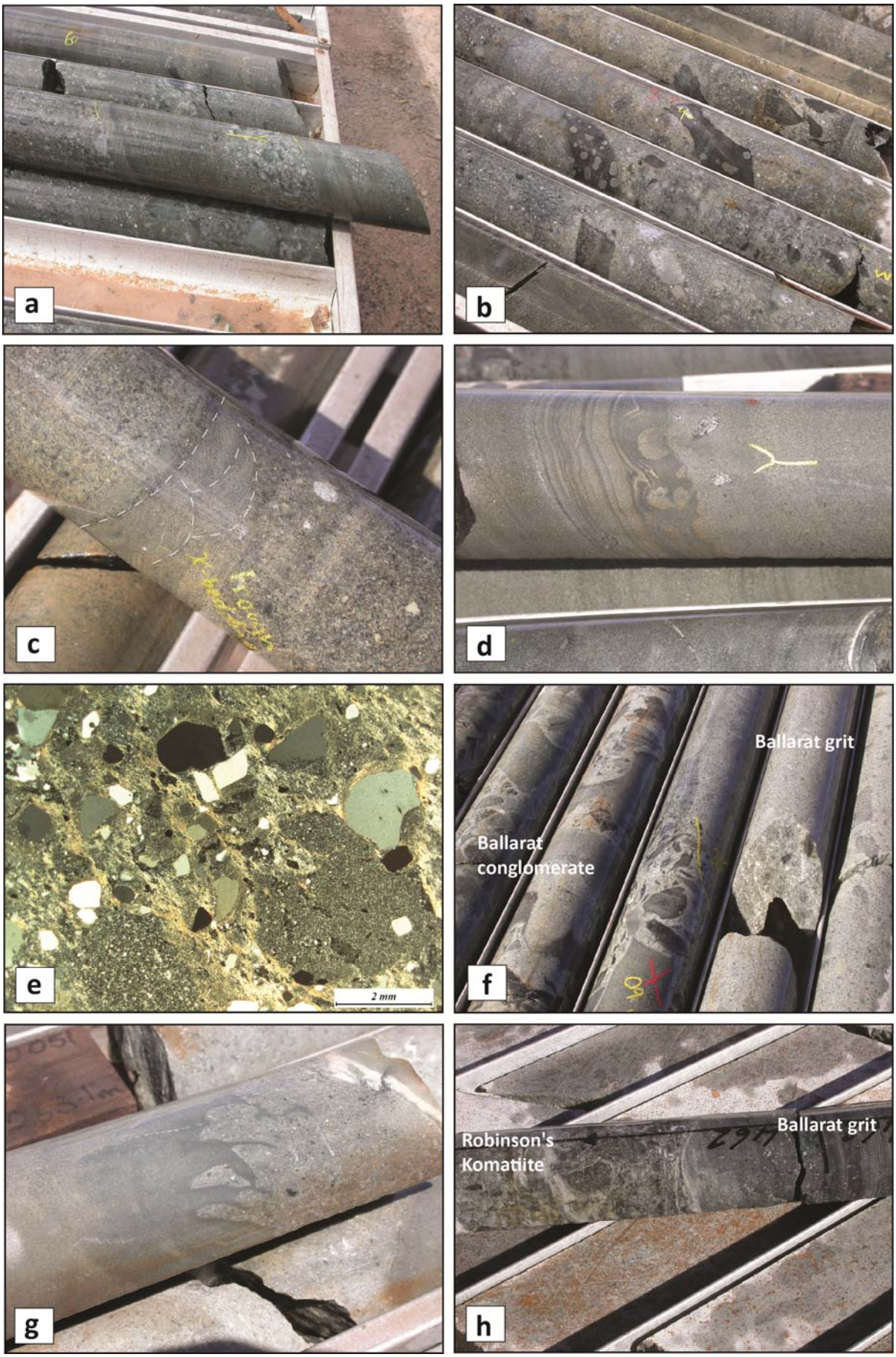
a
b
c
d
e
2 mm
f
Ballarat grit
Ballarat
conglomerate
g
h
Robinson's
Komatiite
Ballarat grit

Figure 3.49

Figure 3.49 – Ballarat sandstone and Ballarat grit

a) Uphole younging graded-bedding in Ballarat pebbly sandstone. The unit contains pebble-cobble layers dominated by hornblende-feldspar porphyry clasts (60%) and mafic-ultramafic volcanic clasts (30%) in a lithic dominated sandstone matrix (GDD523 477.3 m; GDA: 363993E; 6612323N).

b) Ballarat pebbly sandstone with variolitic basalt clasts. The basalt clasts are highly angular with cuspate forms within a matrix-supported, mafic pebble dominated conglomeratic sandstone (GDD523 484 m).

c) Fine scale trough cross-bedding in fine-grained Ballarat sandstone interbed. The fine-grained sandstone is interbedded with coarse lithic grits and granule breccia with Q:F:L of 3:1:96. Way-up is to the left, up hole (GVD49 98.1 m; GDA: 364600E; 6612736N).

d) Up hole facing flame structure and sand slumps in fine-grained lithic dominated Ballarat sandstone with up to 20% quartz (GVD49 245 m).

e) XPL photomicrograph of Ballarat felsic grit. The rock is dominated by sub-rounded, fine-grained porphyritic rhyolite clasts and monocrystalline, euhedral volcanic quartz grains that are angular and fragmented with some evidence of resorption textures, in a very fine strongly sericitised groundmass (GVD50 607.5; GDA: 364759E; 6612809N).

f) Gradational contact between Ballarat conglomerate and Ballarat felsic grit. Mafic and ultramafic clast conglomerate gives way to a dominantly felsic volcaniclastic grit indicating a gradation of sources over 10-20cm. The grit package is dominantly volcanic derived volcaniclastic rock and indicated that the depocentre for the Ballarat member was swamped with felsic volcanic debris (GVD51 285.4 m; GDA: 364926E; 6613186N).

g) Up hole facing flame structure in siltstone interbed, Ballarat grit (GVD51 263.1 m).

h) Sharp depositional contact between Ballarat grit and komatiite indicates a possibility for the Ballarat sequence to have draped an uneven substrate, since the Ballarat grit is present as a felsic unit within the Ballarat ultramafic clast conglomerate (GVD51 462 m).

be determined by a change in sedimentary provenance marked by a reduction in ultramafic clasts, and the introduction of a much greater variety of source rocks including distinctive white granitoid clasts (Squire 2006) and sedimentary rock clasts in the Kanowna conglomerate.

Description (Ballarat grit)

The Ballarat grit comprises massive, disorganised beds of granule-sized, quartz-rich felsic grit with rare interbeds of mafic conglomerate and felsic volcaniclastic breccia (Fig. 3.48). Granule-sized sedimentary rocks make up the largest proportion of the unit (Fig. 3.49e) characterised by matrix supported (C/M ratio: 0.2) well-sorted beds with sub-angular, spherical clasts of dominantly felsic composition. The grit is quartz-rich, but mainly lithic on average (Q:F:L = 33:8:59) (Fig. 3.48). A minor coarse clastic component of the Ballarat grit comprises hornblende-feldspar porphyry (78%), quartz-feldspar porphyry (8%) and 13% mafic and ultramafic clasts with a minor component of sedimentary clasts (1%). Rare fine-grained interbeds of siltstone display soft sediment deformation and dewatering structures (Fig. 3.49g).

Description (Ballarat conglomerate)

Ballarat conglomerate (Fig. 3.50a-h) is characterised by poorly sorted, sub-rounded and elongated clasts dominated by ultramafic rocks, with diffuse bedding of about 8 m mean bed thickness, and individual beds up to 80 m thick. Internal sandstone and siltstone units are rare and plane bedded on a decimetre scale (Fig. 3.50h). The mean clast size of conglomerate / breccia in the BAM is ~92 mm with geometric means up to 265 mm. Conglomerate/breccia beds are clast supported (C/M ratio: 0.63) with a lithic-wacke matrix (Q:F:L = 7:3:90). Ballarat conglomerate is polymictic with a range of clast types (Fig. 3.48): the unit is characterised by abundant ultramafic (51%); hornblende-feldspar porphyry and quartz-feldspar porphyry (29%); mafic volcanic (16%); sedimentary (2%) and quartz vein clasts (1%).

Description (Ballarat sandstone)

The upper part of the BAM (Fig. 3.48) is a thinly-bedded sequence of lithic arenite with polymictic pebble horizons (Ballarat sandstone). The unit is gradational with the underlying Ballarat conglomerate and is characterised by normally-graded beds with scoured contacts (Fig. 3.49a) of 2.5 m mean thickness and individual beds up to 18 m thick. Sand-sized rocks in the Ballarat sandstone are lithic arenites (Q:F:L = 18:7:75) with some quartz arenite (Fig. 3.48). Sandstones are composed of sub-rounded, elongate grains of lithics and quartz, in well-sorted beds with planar to diffuse morphology. Sedimentary structures in the Ballarat sandstone include rare cross-bedding (Fig. 3.49c) and dewatering structures with sandstone / mudstone slump structures (Fig. 3.49d).

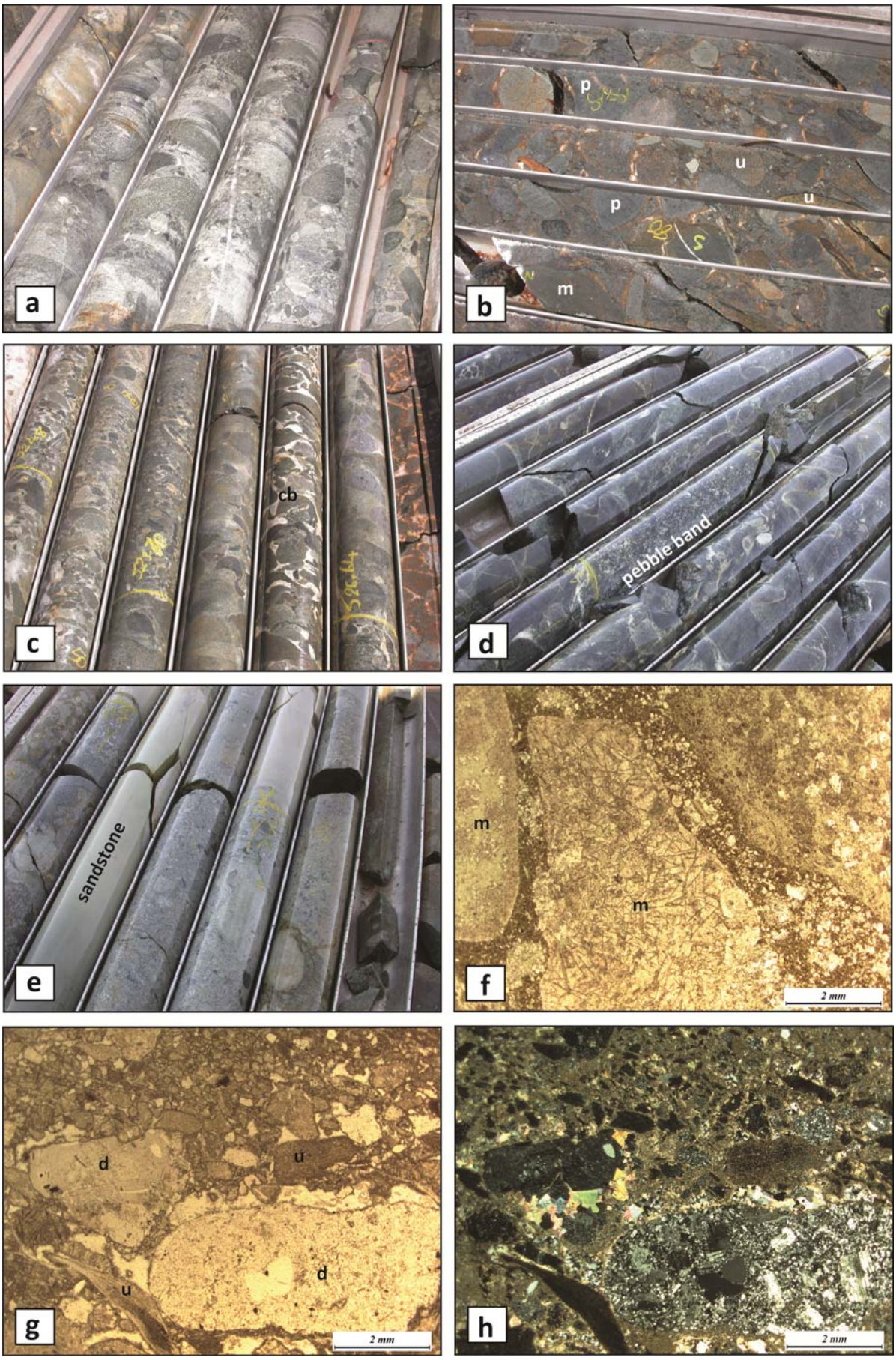

Figure 3.50

Figure 3.50 – Ballarat conglomerate member,

a) Ultramafic and hornblende-feldspar porphyry clast conglomerate, dominated by 80% mafic and ultramafic volcanic clasts in a clast supported arrangement within a lithic sandstone matrix. The conglomerates and massive disorganised beds of pebble to cobble fragments (GVD46 193 m; GDA: 364438E; 6612918N).

b) Clast supported conglomerate composed of mafic volcanic, ultramafic and porphyry. Clasts are well-rounded with a moderate degree of flattening. Strong carbonate and locally fuchsite alteration overprints the conglomerate and matrix (GVD46 209.5 m).

c) Ultramafic clast conglomerate with crustiform carbonate matrix (GVD50 524 m; GDA: 364760E; 6612809N).

d) Conglomerate bedding defined by pebble band with 75% mafic and ultramafic volcanic clasts, and 25% hornblende-feldspar porphyry clasts. Rare zones of fine-grained granule to pebble conglomerate with gradational contacts define broad massive disorganised beds within the conglomerate (WFD6 215.5 m; GDA: 367069E; 6613039N).

e) Rare sandstone and siltstone interbeds in Ballarat conglomerate. Very well sorted fine-grained lithic sandstone with uphole younging indicated by grading and scours (WFD6 100.2 m).

f) PPL photomicrograph of Spinifex ultramafic komatiite clast (centre) and mafic volcanic clasts in a coarse sand matrix (GVD48 285.5 m; GDA: 364437E; 6612547N).

g) PPL photomicrograph of matrix supported Ballarat conglomerate. Ultramafic clasts (u) are small and form much of the coarse matrix granule breccia / sandstone; large clasts of crystalline porphyritic dacite (d) are well rounded with phenocrysts of twinned feldspar, quartz and minor ferromagnesians in a fine-grained crystalline groundmass (WFD6 112.2 m).

h) XPL photomicrograph of view in (g); the rock has abundant chlorite and murky saussurite alteration of the matrix with minor euhedral calcite rimming the dacite clasts (WFD6 112.2 m).

Thin conglomerate interbeds are clast or matrix supported (C/M ratio: 0.52) and have mean clast sizes of 53 mm with geometric means up to 165 mm, which is significantly less than clast sizes observed in the underlying Ballarat conglomerate, and indicates an overall upwards fining sequence. The proportions of clasts are also different with a greater amount of hornblende-feldspar porphyry (41%) and a lesser amount of mafic and ultramafic volcanic clasts (49%). A greater proportion of clasts of sedimentary rock (5%) shows a steady increase up-section that continues into the overlying Kanowna conglomerate.

Structural geology

The Ballarat member is distributed in two elongate belts: one trending northeast from Kanowna Belle gold mine and the other trending north-south to the east of Kanowna Belle (Fig. 3.46). The two belts join at Red Hill across an interpreted fault trending sub-parallel to the Fitzroy Fault at Kanowna Belle (Fig. 3.46). Way-up and bedding trends indicate that the northeast trending belt is folded into a moderately SW-plunging syncline. Across the fault, the eastern belt of BAM is younging to the east, whereas a reverse fault (White Feather fault) cuts through the centre of the belt.

Previous workers (Barrick / Placer) interpreted a younging reversal across the White Feather fault, yet no evidence of this was found from the current study. Recent drill intersections of rocks to the west of the White Feather fault indicate an upright shallow east-dipping sequence.

Moderate flattening of mafic and ultramafic clasts is typical of the BAM (Fig. 3.50d, e) locally with a strong disjunctive cleavage that wraps elongate clasts. Competent porphyry clasts have round to oval shapes, whereas the weak ultramafic clasts are streaked out parallel to the foliation and in some instances are difficult to distinguish from the matrix to the conglomerate.

Interpretation and correlation

The exact structure of the Ballarat member is unclear due to lateral facies variations and folding and faulting of the unit. Internal felsic grit units with gradational contacts against conglomerate at several levels within the BAM indicate a felsic volcanic source in addition to the ultramafic and felsic-intermediate porphyry sources present at the time of deposition. Felsic and intermediate porphyry clasts were likely sourced from hypabyssal intrusions, whereas dacitic porphyritic volcanic rocks coeval with ultramafic volcanism in the Boorara Domain (Trofimovs 2003) are also a potential source for some of these clasts. A prodigious amount of ultramafic and mafic volcanic clasts that make up the BAM distinguishes this unit from all other coarse clastic units in the Kalgoorlie district. The gradational upper contact indicates continuous deposition between Ballarat and Kanowna sequences, but separation of the two members is justified by a major change in sedimentary provenance (See below).

A confident allocation of the Ballarat member to one of the proposed subdivisions of the Black Flag Group is not possible from field data alone (BFl / BFu?). Empirically, the Ballarat member is the first sequence that sits directly above ultramafic volcanic rocks in the Kanowna district. The dominance of ultramafic volcanic, mafic volcanic and porphyry clasts suggests the Ballarat member had a restricted provenance that likely sourced nearby uplifted edifices of the lower ultramafic volcanic unit, and was deposited onto a substrate of similar composition. This relationship is suggestive of fault-controlled depocentres, whereas the restricted distribution of these unique ultramafic-clast conglomerates suggests these were not laterally extensive sub-basins.

Field relationships indicate the Ballarat member is the oldest of the conglomerate sequences in the Kanowna district. Age data from the Ballarat grit and Ballarat sandstone have been collected (Chapter 4), and at least one consistent suite of SHRIMP U-Pb analyses of zircons from intercalated felsic grits of the Ballarat member, suggests this unit occupies a stratigraphic position lower than Black Flag Formation (discussed in detail in Chapter 4).

Kanowna conglomerate member (KNC)

The Kanowna conglomerate member is located in a 2.3 km x 0.5 km belt to the east of Kanowna Belle (Fig. 3.51). Outcrop of the unit is limited, but exposures are located in the centre of the Kanowna historic town site near Warden's Hill. Drill hole intersections have demonstrated the existence of two thin units of the KNC to the south of the main exposure.

The KNC has a massive section of thick-bedded polymictic conglomerate surrounded by upper and lower zones of pebbly sandstone. An approximate true thickness of 650 m is estimated for the unit, but the majority of the upper pebbly sandstone unit is unexposed and known only from shallow exploration drill holes and sparse outcrops.

Detailed geology and structure of the unit were determined from seven diamond drill holes (Figs. 3.47, 3.51) and a few scattered outcrops. The graphic drill hole log presented in Figure 3.52 is for a single drill hole HMD010, which has the most complete section through the unit and was chosen as a guide to the character of the main conglomerate section of the KNC rather than as a composite stratigraphic column.

Contact relationships

The lower contact of the KNC is gradational with the underlying Ballarat sandstone, and is distinguished by a gradual reduction in the content of ultramafic clasts in pebble bands upwards, as described for the Ballarat member. Dividing the Ballarat and KNC units is justified on the basis of a significant provenance change that occurs up section and that the two units are mappable horizons at a mine corridor scale; the location of a contact is arbitrarily chosen on this basis.

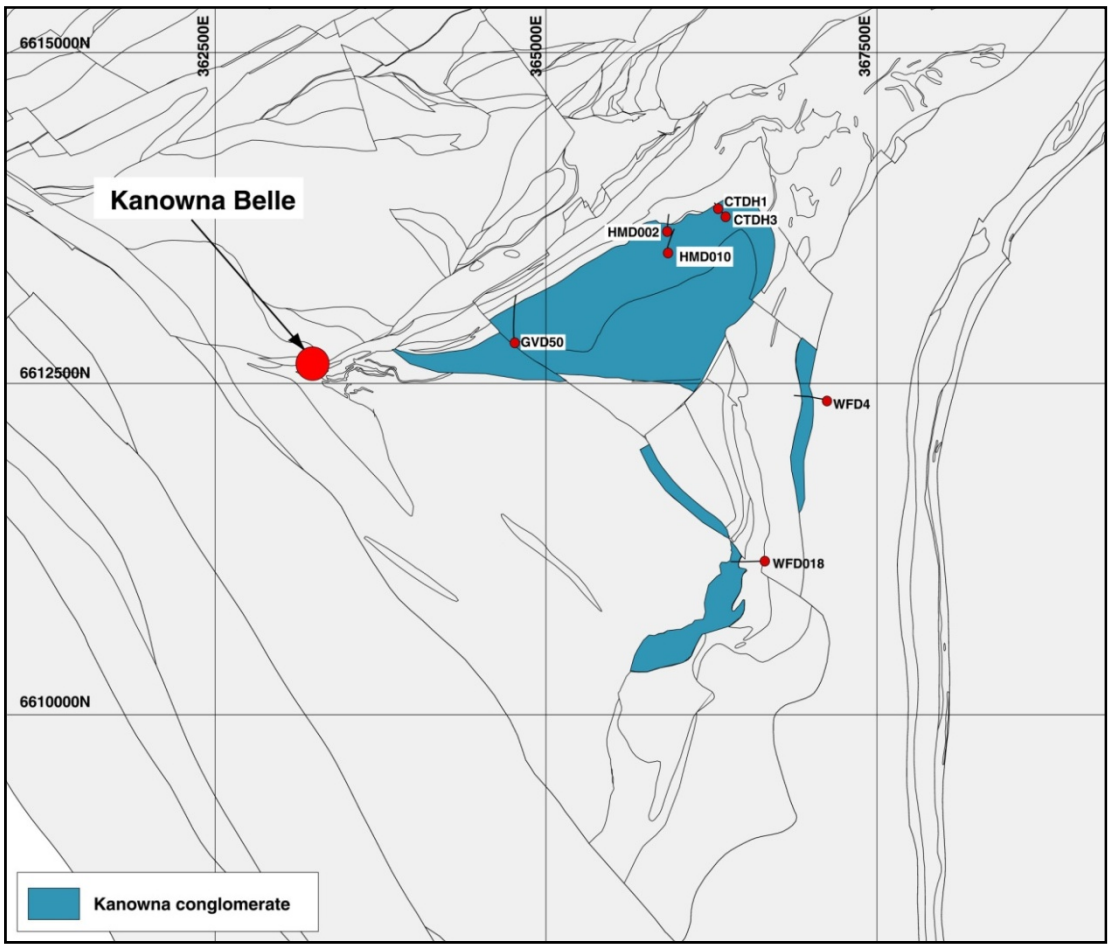

Figure 3.51 – Distribution of the Kanowna conglomerate member and locations of drill holes used to assess the detailed geology (see Appendix for detailed logs)

From a stratigraphic point of view, the two members may simply be different components of the same continuous depositional unit. The upper contact of the KNC is erosional, with the Grave Dam member unconformably overlying KNC and BAM.

Description

Kanowna conglomerate (Fig. 3.53a-h) is characterised by thick, diffusely-bedded sections of polymictic conglomerate with a mean bed thickness of 6 m and individual beds up to 58 m thick. Conglomerate beds contain well-sorted, sub-angular to sub-rounded and elongate clasts in beds that are clast or matrix supported (C/M ratio: 0.56) with a lithic-wacke matrix (Q:F:L = 9:5:86) (Fig. 3.53). The mean clast size of conglomerate/breccia in the KNC is 83 mm with geometric means up to 226 mm. The conglomerate is polymictic with a wide range of clast types including hornblende-feldspar porphyry (40%); mafic volcanic (35%); ultramafic (8%); sedimentary (7%); quartz-feldspar porphyry (6%); quartz vein and granite clasts (4%) and clasts of felsic volcanic rock (1%). Internal sandstone and siltstone units are rare and plane bedded on a decimetre scale (Fig. 3.53g).

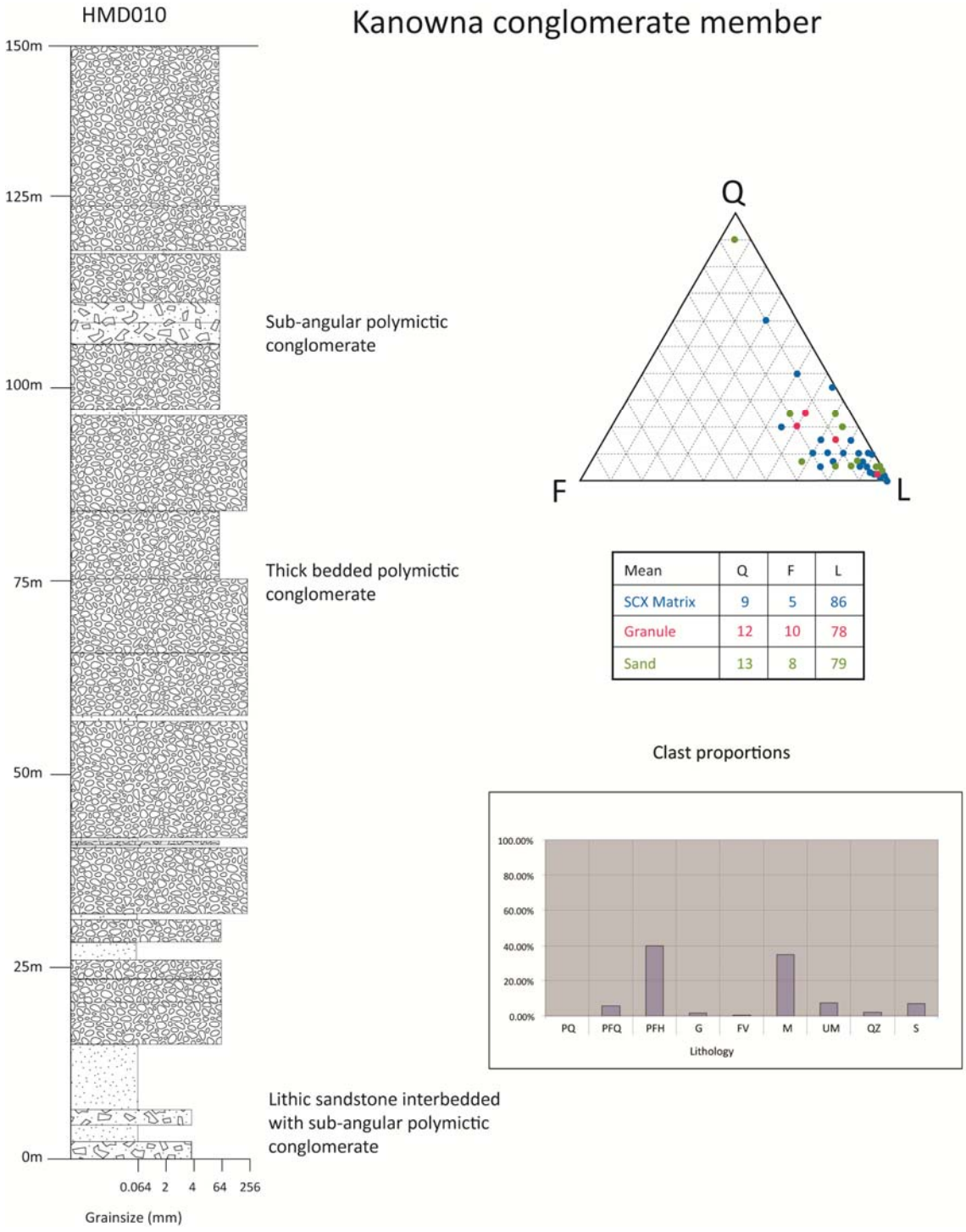

Figure 3.52 – Graphic drill log with clast and matrix information for the Kanowna conglomerate member. QFL data are coloured according to the table of mean values. SCX refers to conglomerate or breccia-sized clastics. PQ – quartz porphyry; PFQ – quartz feldspar porphyry; PFH – hornblende-feldspar porphyry ± quartz; G – granite; FV – felsic volcanic; M – mafic volcanic; UM – ultramafic; QZ – quartz; S – sedimentary.

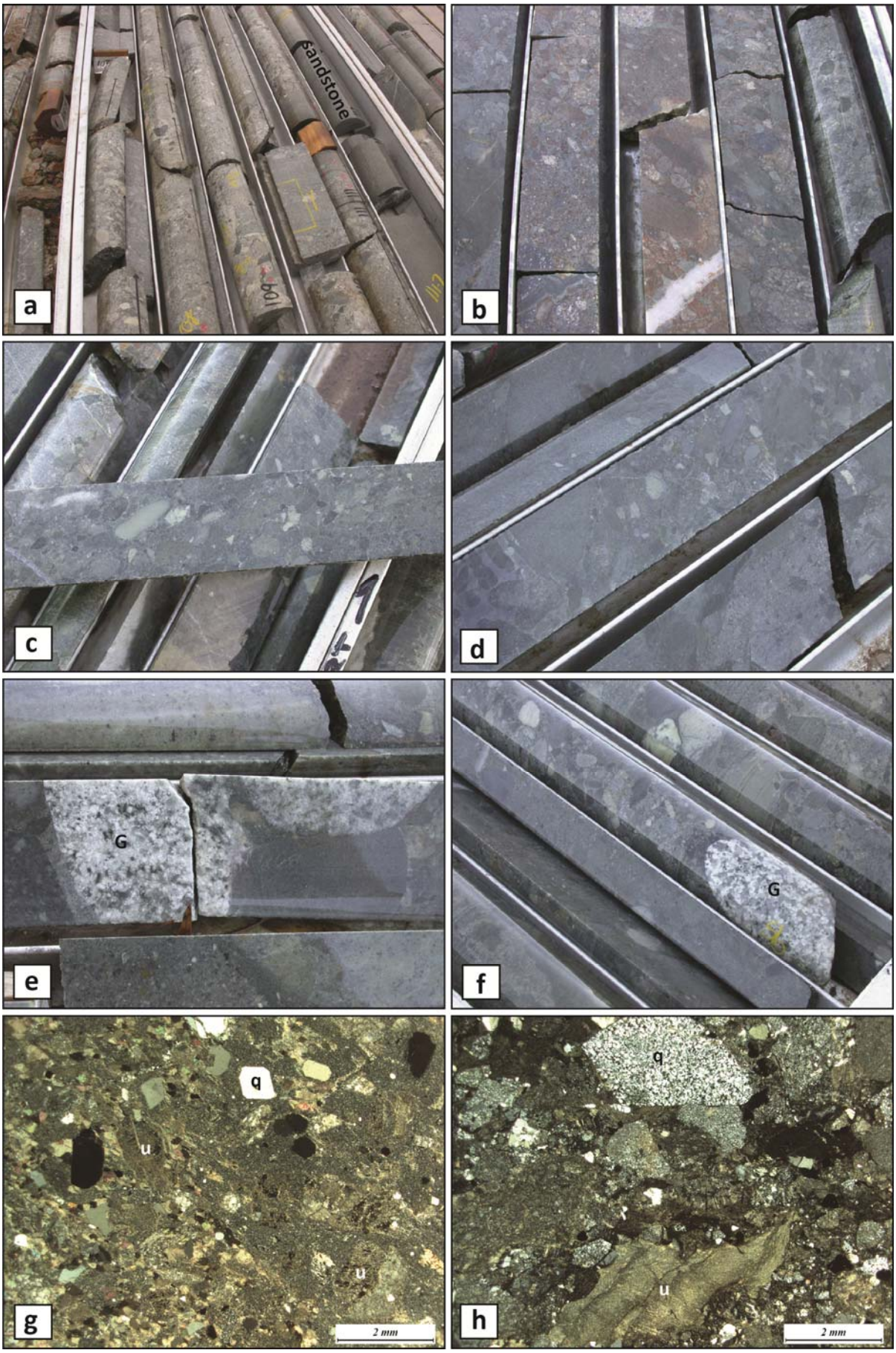

Figure 3.53

Figure 3.53 – Kanowna conglomerate member

a) Polymictic conglomerate with sandstone interbeds, facing up hole. The Kanowna Conglomerate is dominated by cobble sized well rounded mafic volcanic (65%) and hornblende-feldspar porphyry clasts, in a lithic sandstone matrix (HMD002 109 m; GDA: 365917E; 6613657N).

b) Moderately sorted, clast supported polymictic conglomerate with a greater proportion of felsic clasts (35%) in a dominantly lithic (96%) matrix (HMD010 105 m; GDA: 365916E; 6613497N).

c) Pebble band in polymictic conglomerate with gradational contacts against coarse cobble to boulder conglomerate defining gross stratification within massive bedded units. Pebbles are elongate and well rounded (HMD010 129 m).

d) Mafic clast dominated polymictic conglomerate HMD010 152.5 m,

e) Distinctive white granite clasts in polymictic conglomerate. The granite clasts typically increase in number in the upper parts of the Kanowna Conglomerate indicating an upwards gradation from the mafic dominated lower parts in gradation contact with Ballarat conglomerate to upper felsic-rich mafic conglomerate (HMD010 203.8 m).

f) Well rounded, distinctive white granite clasts in polymictic conglomerate (HMD010 207.3 m).

g) XPL photomicrograph of lithic sandstone interbed in Kanowna Conglomerate with Q:F:L ratios of 20:5:75. The sandstone is planar bedded with average 0.8 m bed thickness. Abundant lithic fragments of ultramafic volcanic (u) and mafic clasts interspersed with coarse quartz grains including monocrystalline euhedral volcanic quartz grains (q), set in a very fine mud sized cement. Local biotite and strong carbonate alteration obscure the texture of clasts (GVD50 72.1 m; GDA: 364759.E; 6612809N).

h) XPL photomicrograph of polymictic lithic sandstone with abundant coarse-grained polycrystalline, rounded quartzite clasts, and angular, wispy ultramafic clasts in a coarse sand matrix (HMD010 129.4 m).

Structural geology

The KNC is folded into a southwest-plunging syncline defined in scattered pavements that display bedding and way-up orientations. Strain throughout the unit is generally low with a weak foliation and minor elongation of the clasts (Fig. 3.53c). A sliver of KNC to the south of the main body (Fig. 3.51) trends to the north-northwest with way-up to the west in steeply dipping beds. On the eastern margin of the Ballarat member, a thin band of KNC is in gradational contact with Ballarat sandstone and younging east in moderately east-dipping beds. These small units are separated from the main body of KNC by faults.

Interpretation and correlation

The Kanowna conglomerate member is the upper part of a sequence that is continuous from the lowest sedimentary rock units deposited onto the ultramafic volcanics (Ballarat member) to the uppermost units in the district (base of Grave Dam unconformity). A conformable contact between the two members is demonstrated by gradual changes in provenance, and a physical gradation from Ballarat sandstone to Kanowna conglomerate. Similarities in geochemistry of felsic granitoid clasts in both units were cited by Squire et al. (2006) as evidence of a similar source for the two units. The KNC contains granitic clasts with distinctive geochemistry that may be used to distinguish this unit from others in the district. The equigranular felsic clasts (Fig. 3.53e, f) were identified as having affinities that closely match the HFSE (High Field Strength Elements) suite of intrusions found near Kookynie (Squire et al. 2006), which indicates that a distinct source contributed to the Kanowna conglomerate member.

The Ballarat-Kanowna package of rocks cannot be confidently correlated with the lower Black Flag formation from available field evidence. The relationship of these rocks to sedimentary rocks overlying Upper Basalt in the Boorara Domain is unknown, but an unconformable contact between the Ballarat-Kanowna sequence and ultramafic volcanics is suggested by the field relationships; allowing for the possibility that a large section of Upper Basalt, Spargoville and perhaps White Flag aged stratigraphy was eroded from this area. An alternative explanation is that these underlying units were never present, and the deposition of Ballarat and Kanowna members was controlled by syn-volcanic, or syn-sedimentary extensional faults that restricted the distribution of earlier volcanic/sedimentary formations. This uncertainty with respect to the stratigraphic position of the Ballarat-Kanowna sequence is tentatively resolved by new detrital zircon geochronology. Recent geochronology (Sircombe et al. 2007; Chapter 4) returned a zircon SHRIMP age of 2695±6 Ma for the Ballarat grit. The age was interpreted as a maximum depositional age and, if that is true, indicates that the deposition of the Ballarat member occurred after ~2689 Ma. This age is relatively old for Black Flag Formation rocks and is closer to the age of the Spargoville or White Flag Formation (e.g. Ora Banda Domain). The 2689 Ma age may represent the age of the dominant felsic volcanic

component of the Ballarat grit, with sedimentation occurring at a still younger date. This at least provides a maximum age limit on deposition of the unit; the inferred maximum depositional age of 2658 Ma for the overlying Grave Dam member (see below) provides a minimum age for the Ballarat member.

Field data (Section 3.5.3) demonstrate an angular unconformity between the Grave Dam member and underlying rocks and provide a more robust demonstration of the relationships between the formation members. A maximum depositional age for the Grave Dam member was interpreted at 2668±10 Ma from detrital zircon analyses by (Ross et al. 2004); and taking a combination of field and analytical data, it is possible to infer a break between the Ballarat-Kanowna members and the unconformably overlying Grave Dam and Golden Valley members.

Government Dam member (GDM)

The Government Dam member is a deformed sequence of plane-bedded sandstone / siltstone / conglomerate, exposed in several excellent pavements throughout the Kanowna district to the south and east of Kanowna Belle, and in exploration drill holes (Fig. 3.54). In the area of best exposure, the GDM consists of two sequences: a lower sequence of soft-sediment deformed siltstone horizons, and an upper sequence of normally-graded channelised conglomerate horizons gradational into sandstone-siltstone (Hand 1998).

The full section is not outcropping, but exploration drill holes have intersected the unit further to the south and north of the exposure at the Kanowna Government Dam. True thickness for the GDM is estimated at 1100 m, which takes into account the known extent and folding of the unit. Previous studies (Taylor 1984; Hand 1998; Trofimovs 2003) have documented the lithofacies at the Government Dam in great detail and that work is not repeated here.

Contact relationships

The GDM appears to overlie the Kanowna and Ballarat members with apparent unconformity based on map patterns and a drill hole intersection in WFD4. The contact with Kanowna conglomerate is only mildly strained, but disharmonic folding of the GDM with respect to surrounding units suggests that GDM lower contact is probably a detachment fault. The upper contact is exposed in a small breakaway at GDA: 367735E-6609696N where east-younging, cross-bedded pebbly sandstone is juxtaposed with spinifex komatiite across a 10 m-wide zone of mylonite (Shamrock Fault; Fig. 3.55). This faulted upper contact has been intersected in several diamond drill holes along strike to the north and was also recognised by Archibald (1993).

Previous studies by Taylor (1984) and Hand (1998) did not identify the faulted contact between the GDM and the komatiite to the east and these authors assumed a conformable progression, implying that the GDM stratigraphically underlies ~2700 Ma ultramafic rocks.

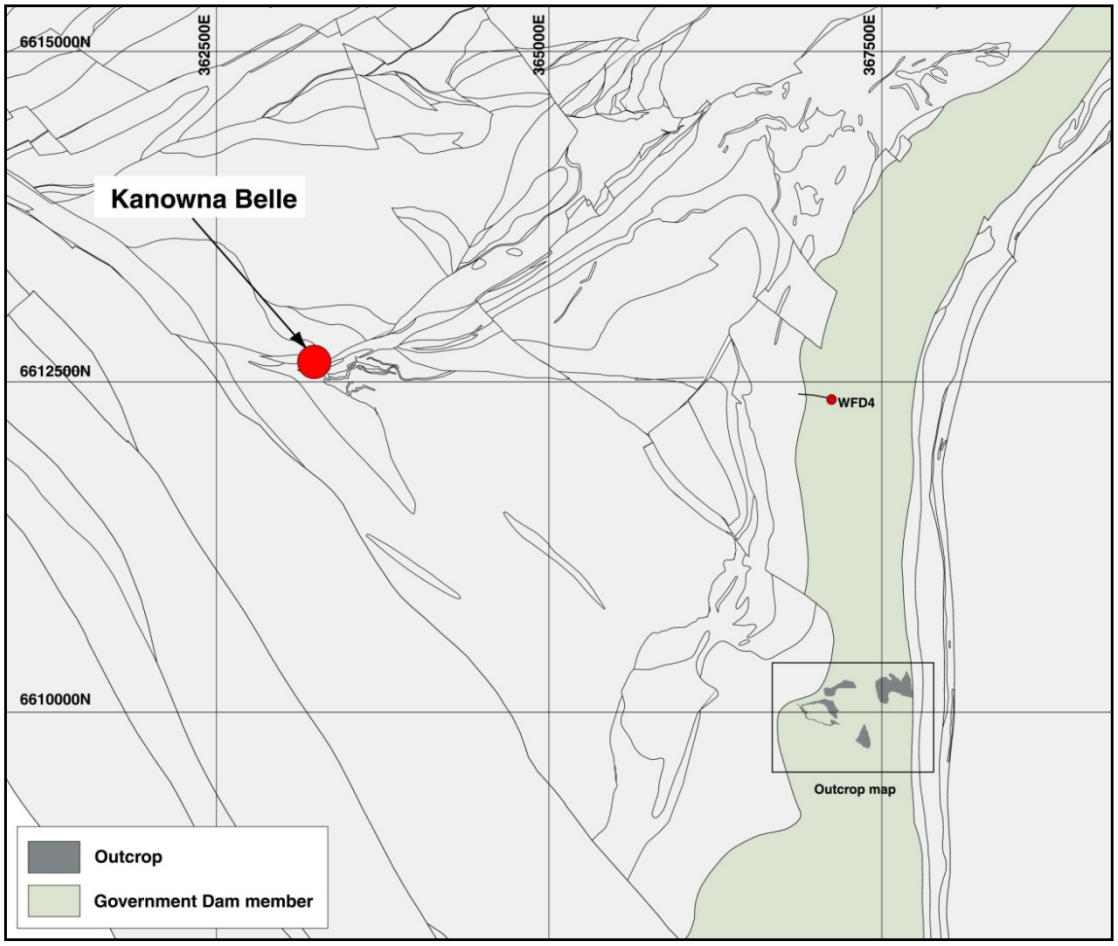

Figure 3.54 – Distribution of the Government Dam member and locations of outcrops and drill holes used to assess the detailed geology (see Appendix for drill logs)

From the field relationships this is clearly not the case, and the GDM occupies a much higher position in the stratigraphy.

Description

Lower sequences of the GDM comprise interlaminated siltstone-mudstone overlain by units of channelised dacitic conglomerate beds with alternately fining-upward (Fig. 3.56c, d) and coarsening-upward trends (Hand 1998). Fine-grained siltstone-mudstone contains post-depositional, soft-sediment deformation structures including convolute lamination, flame structures and bedding-confined slump folding (Fig. 3.56a, b, e, f). Coarse facies overlying the siltstone include deposits of erosive based, channelised dacite-clast conglomerate horizons (Fig. 3.56h) with rare ultramafic clasts that grade into lensoidal and channelised sandstone and mudstone deposits (Hand 1998; Fig. 3.56g). Conglomerate horizons are characterised by abundant gravel to pebble-sized dacite clasts with subordinate ultramafic clasts, supported by a medium- to coarse-grained sandstone matrix. Identifiable lithic grains in sandstone include quartz, felsic lithics and minor fuchsitic ultramafic clasts.

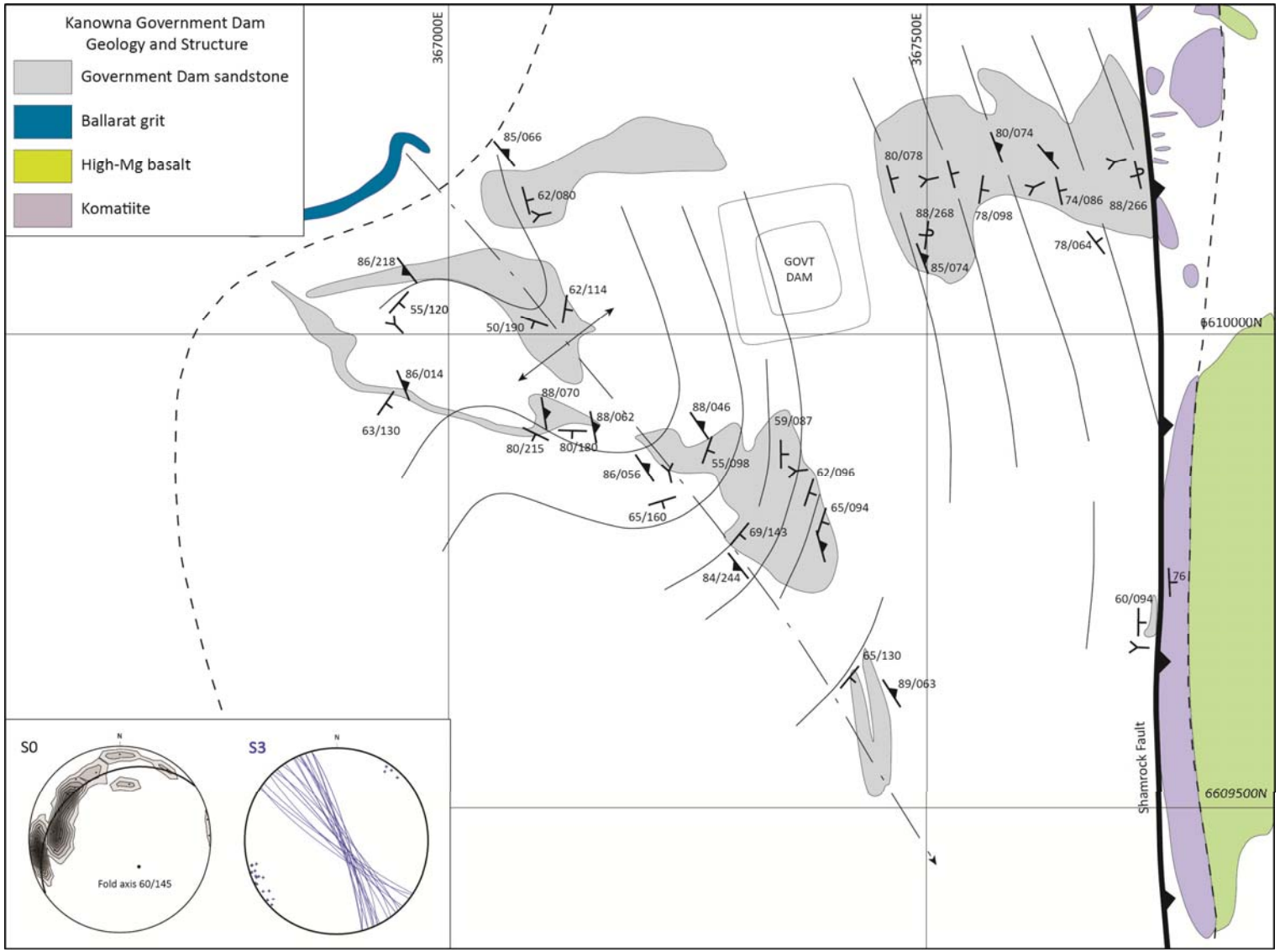

Figure 3.55– Geology and structure of the Government dam area south of Kanowna Belle mapped by the author and Dr. J. Rogers. (Outcrop shapes modified from Barrick GIS (Archibald 1993).

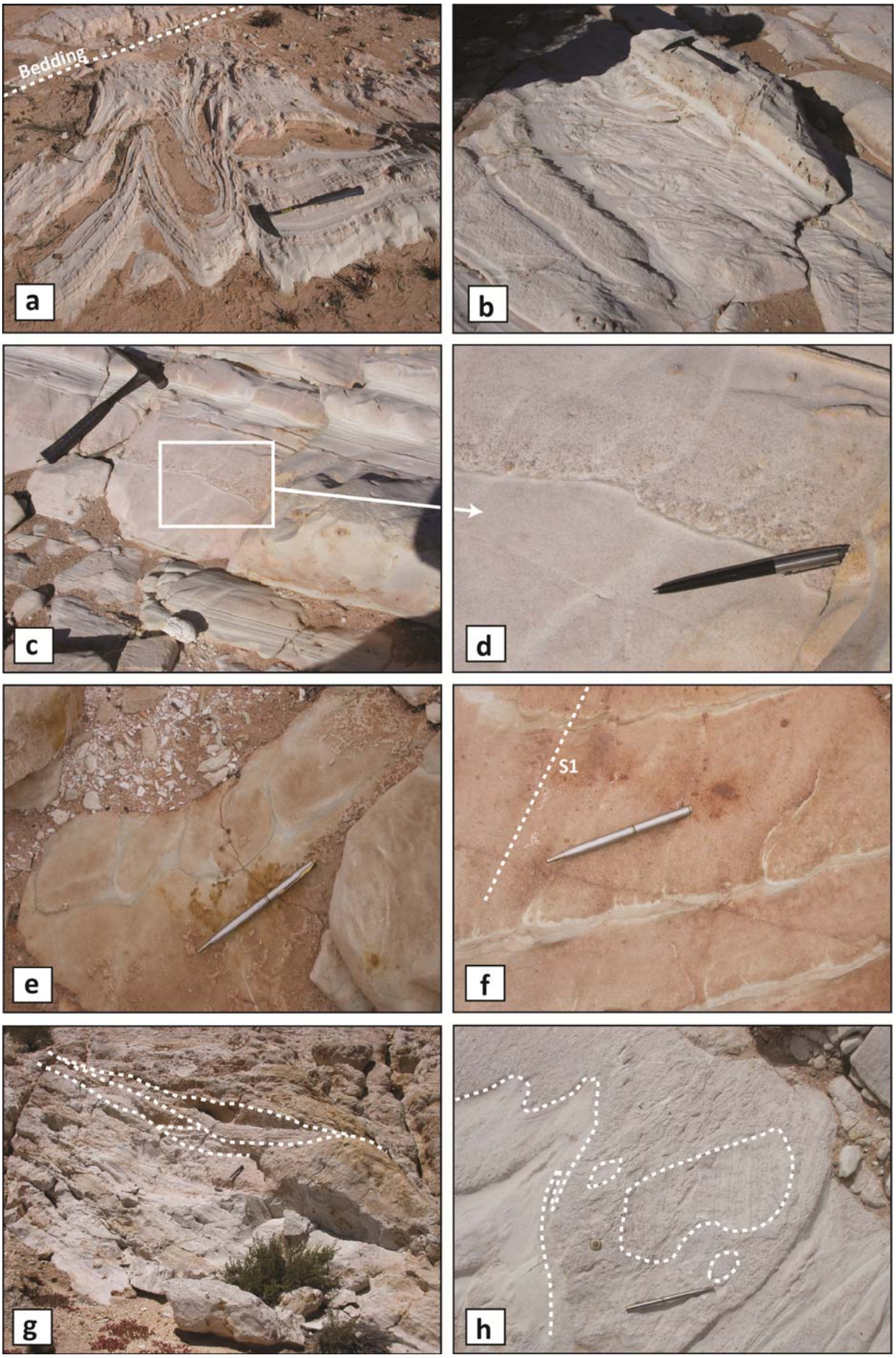

Figure 3.56

Figure 3.56 – Government Dam member sandstone, siltstone, conglomerate,

a) Metre-scale bedding-confined soft sediment deformation folds. The folds are entirely contained within fine-grained mudstone layers internal to coarse sand beds. Unusually the fold axial planes are parallel to outcrop scale tectonic fold axial planes and the regional axial planar cleavage, suggesting that some post lithification flattening and rotation may have occurred (Kanowna Government. Dam; GDA: 367292E; 6609862N).

b) Bedding confined slump folds and soft-sediment deformation in sandstone–siltstone (Kanowna Government. Dam; GDA: 367292E; 6609862N).

c) Graded bedding in plane-bedded sandstone-siltstone. Graded beds typically have coarse sand to fine gravel bases composed of dacitic pebbles and granules that grade upwards into quartz-feldspar rich sandstone (Kanowna Government Dam; GDA: 367292E; 6609862N).

d) Close up of graded bedding in (c).

e) South younging dewatering flame structures. Dark grey mudstone wisps point to the top of the photograph (Kanowna Government Dam; GDA: 367280E; 6609844N).

f) Water escape flame structure parallel to cleavage, again suggesting that some tectonic flattening and rotation may have occurred post lithification (Kanowna Government. Dam, GDA: 367280E; 6609844N).

g) East-younging channelised cross-bedded sandstone. The sandstones have coarse pebble to cobble basal gravels that grade upward to the east in bedding that dips 74/086. (Shamrock breakaway; GDA: 367644E-6610149N)

h) Large banded dacite/felsic clasts in channelised conglomerate that cuts across the generally uniform plane bedded turbidites (Kanowna Government Dam GDA: 367280E; 6609844N).

The upper sequence of coarse channelised conglomerates includes beds of dominantly felsic, rounded 2-5 cm clasts supported by a sandstone matrix with tops grading into lensoidal sandstone and mudstone horizons. This sequence fines upwards into interbedded sandstone and channelised dacitic conglomerate (Hand 1998).

Structural geology

Deformation of the GDM produced moderately southeast plunging open folds with a pervasive axial-planar foliation (Fig. 3.53). The folds are developed at a scale of several hundred metres and are disharmonic with respect to the regional folding of surrounding units, with possibly detached lower and upper contacts. The Shamrock Fault marks the upper contact.

Interpretation and correlation

The Government Dam member is interpreted to overlie the Ballarat and Kanowna members. Although it is not in contact with the Grave Dam member, the Government Dam member is assumed to be older, based on the Grave Dam member unconformably overlying the Ballarat and Kanowna members. A second possibility exists that the GDM is a time equivalent of the Grave Dam member, but this cannot be substantiated from current exposure. Samples of detrital zircons from the GDM were collected for SHRIMP analysis to attempt to resolve this issue (Section 4.6.5).

3.5.3 Black Flag formation - upper (BFu)

Grave Dam member (GDG)

The Grave Dam member (GDG) is variably exposed over a 3 km x 4 km area to the south of the Kanowna Belle gold mine (Fig. 3.57). The unit comprises thickly-bedded felsic, and locally polymictic, volcaniclastic breccia interbedded with feldspathic sandstone and polymictic conglomerate, with an estimated true thickness of ~1700 m (Fig. 3.58). The GDG was intruded by hornblende-feldspar porphyry dykes and sills and has rare intercalated mafic volcanic units of up to several metres thickness with peperitic contacts against sandstone. Five drill holes and one outcrop pavement were used to determine a summary stratigraphic column of the GDG (Fig. 3.58, Fig. 3.59).

Contact relationships

The lower contact of the GDG (Fig. 3.60g, h) is exposed in three drill holes (KBD13, GDD523, and GVD047). A thin 10cm-thick siltstone at the base of the GDG is observed in contact against Ballarat sandstone in KBD13 and GDD523, and against Ballarat conglomerate in GVD047. At a mesoscopic scale the contact is a sharp, depositional boundary with underlying Ballarat conglomerate in GVD047, but is less clear in other holes due to similarities

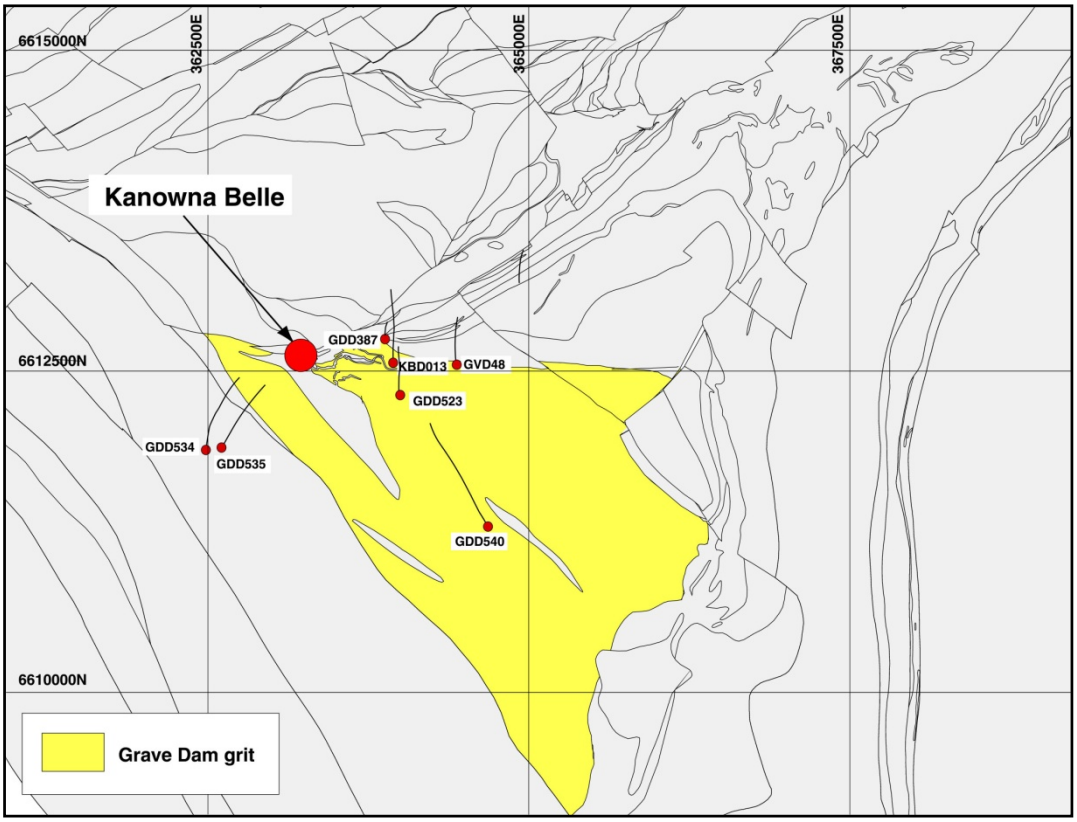

Figure 3.57 – Distribution of the Grave Dam member and locations of drill holes used to assess the detailed geology (see Appendix for detailed logs)

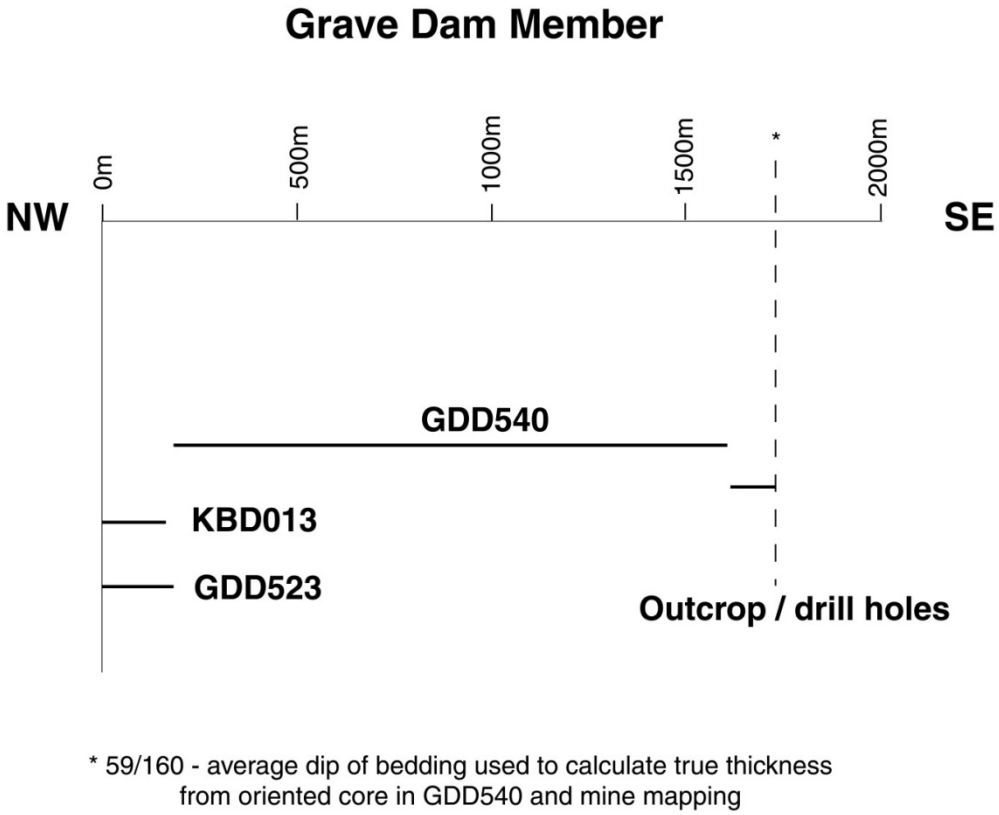

Figure 3.58 – Drill holes used to assess the detailed geology of the GDM (see Appendix for logs)

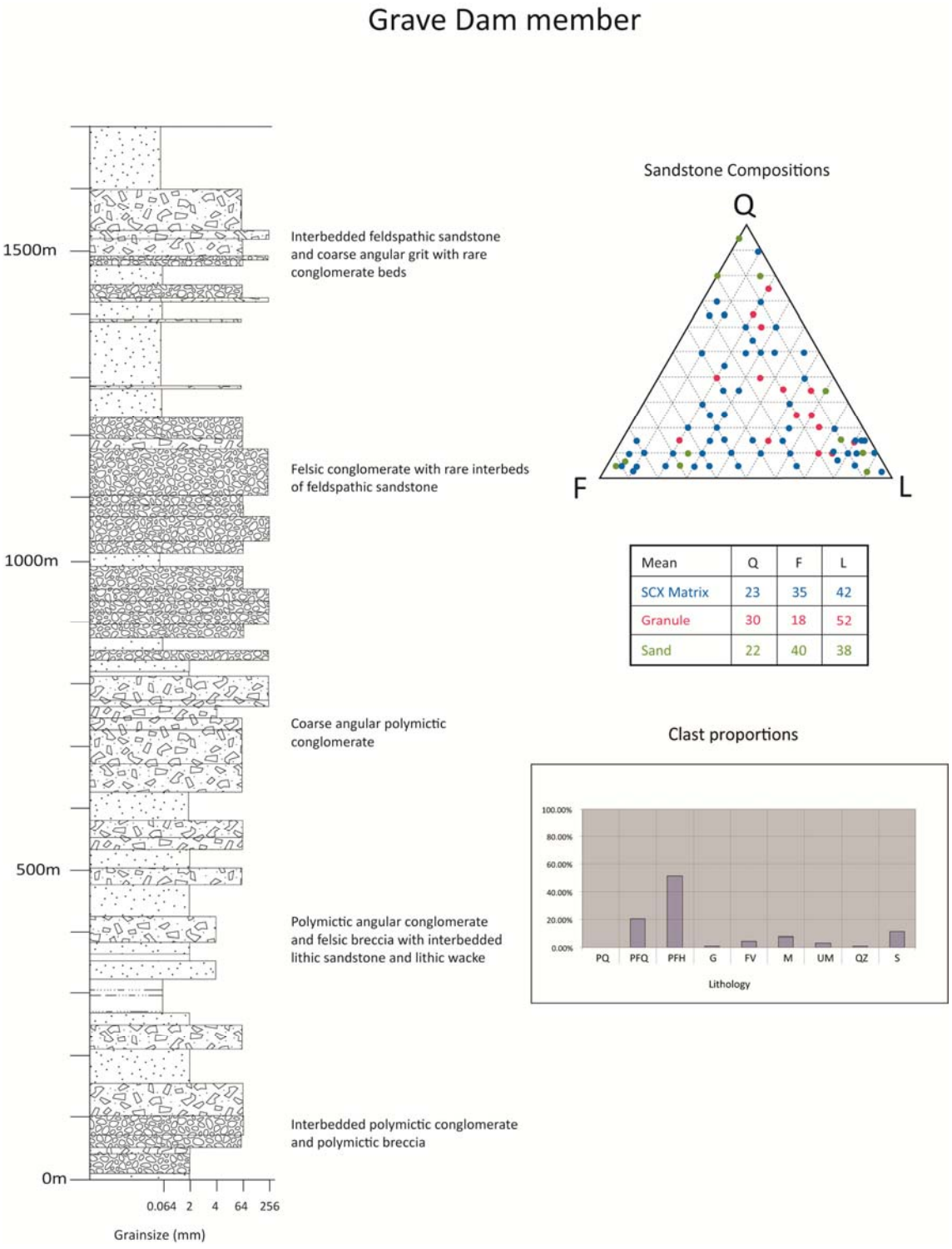

Figure 3.59 – Stratigraphic column with clast and matrix information for the Grave Dam Formation. QFL data are coloured according to the table of mean values. SCX refers to conglomerate or breccia-sized clastics. PQ – quartz porphyry; PFQ – quartz feldspar porphyry; PFH – hornblende-feldspar porphyry ± quartz; G – granite; FV – felsic volcanic; M – mafic volcanic; UM – ultramafic; QZ – quartz; S – sedimentary.

Figure 3.60

Figure 3.60 – Grave Dam member

a) Felsic, sub-angular breccia dominated by felsic volcanic clasts in a matrix supported (80%), poorly bedded volcaniclastic unit. Clasts are predominantly dacite to rhyodacite wispy and randomly distributed throughout a feldspar rich matrix with Q:F:L ratios of 10:65:25. Moderate sericite-carbonate and minor chlorite alteration obscures the texture (GDD540 130 m, GDA: 364677E; 6611298N).

b) Quartz sandstone interbed in Grave Dam grit. The composition of the clastic component of the sandstone is quartz-95%; feldspar-5%, in very well sorted, well bedded, uphole younging beds that trend 63º/161º (GDD540 965.4 m).

c) Quartz-bearing feldspathic grit in massive disorganised beds that lack obvious stratification. Up to 10% quartz is visible as the dark crystals in a light strongly sericite-carbonate altered matrix (GDD540 269 m).

d) Felsic clast, boulder cobble to boulder conglomerate dominated by dacite volcanic clasts with minor components of ultramafic volcanic and sedimentary clasts. Sub-rounded, poorly sorted clasts up to 70% are set in a feldspathic sandstone matrix. The unit broadly fines in an up hole direction (GDD540 776 m)

e) Outcrop of felsic conglomerate in abandoned mine workings showing matrix supported poorly sorted felsic volcaniclastic conglomerate composed of sub rounded – sub angular felsic clasts and rare green fuchsitic ultramafic clasts (GDA: 365664E; 6612157N).

f) Rare polymictic section of dominantly felsic conglomerate with rare red banded jasperitic clast. Clasts are up to boulder size dominated by felsic volcanic rocks set in a lithic matrix that comprises 50% of the rock. Average bed thickness of 5 m and gradational contacts with surrounding lithic sandstones (GDD540 572 m)

g) Fine-grained quartz rich siltstone at the base of the Grave Dam grit in contact with underlying Ballarat Conglomerate. The siltstone unit is seen in several drill hole intersections at the basal unconformity of the Grave Dam grit in contact with underlying formations (GVD47 123.95 m; GDA: 364614E; 661303N).

h) Fine lithic wacke unit at the base of the Grave Dam grit in contact with Ballarat conglomerate (GDD523 461.5 m; GDA: 363993E; 6612323N).

between fine-grained sedimentary rocks in both units.

In map view and cross-section, the GDG cuts sedimentary sequences to the east of Kanowna Belle and unconformably overlies those units (Figs. 3.45; 3.61) (first recognised by J. Rogers and K. Joyce - written communication). The upper contact of the GDG is interpreted from sparse outcrops and exploration drill holes to the south of Kanowna Belle, where it appears the unit is truncated by an erosional unconformable contact at the base of the Panglo member.

Description

Volcaniclastic breccia and conglomerate clasts in the GDG have a mean grain size of ~100 mm with geometric means up to 276 mm (Fig. 3.60a, d, e, f). Beds are dominantly matrix-supported (C/M ratio: 0.4) and have a lithic-wacke matrix, with roughly equal amounts of quartz, feldspar and lithics (Fig. 3.59). Coarse clastic units in the GDG are dominated by poorly to moderately sorted, sub-angular and elongate volcanic debris, characterised by planar to diffuse bedding of <10 m mean thickness, with individual beds up to 200 m thick. The internal structure of the beds is generally massive and disorganised with rare planar stratification and grain size grading (Fig. 3.60b).

Coarse clastic rocks in the GDG vary between felsic and polymictic end members. The unit is characterised by abundant quartz-hornblende-feldspar porphyry (52%), quartz-feldspar porphyry (20%), and sedimentary (11%) clasts; with minor amounts of mafic, ultramafic, felsic volcanic, and 17% granitic and vein clasts (Fig. 3.59). Polymictic breccia and conglomerate in the GDG locally contain greater amounts of sedimentary (up to 80%) and mafic/ultramafic clasts (up to 60%).

A large proportion of the GDG is composed of feldspathic and lithic wacke (Fig. 3.60b, c), and granule-sized sedimentary rocks. These units also have a roughly equal spread of Q:F:L compositions which appears to characterise the fine-grained portions of the GDG. The QFL compositions of the GDG suggest the unit is essentially unsorted with respect to sandstone compositions, and this may reflect the depositional environment of the unit, which was previously interpreted as a single, chaotic felsic volcanic eruption event (Dr. R. Cas personal communication).

Structural geology

The GDG contains a weak, to moderately developed, NNW fabric that has affected both clasts and matrix minerals. Mafic, ultramafic and sedimentary clasts are stretched and deformed, which may have influenced grain size measurements of the clastic portions. The gross structure of the Grave Dam Grit unit is a uniform, plane-bedded sequence dipping 60°/160° on average with only macroscopic folding. These data are determined from the best examples of the unit in

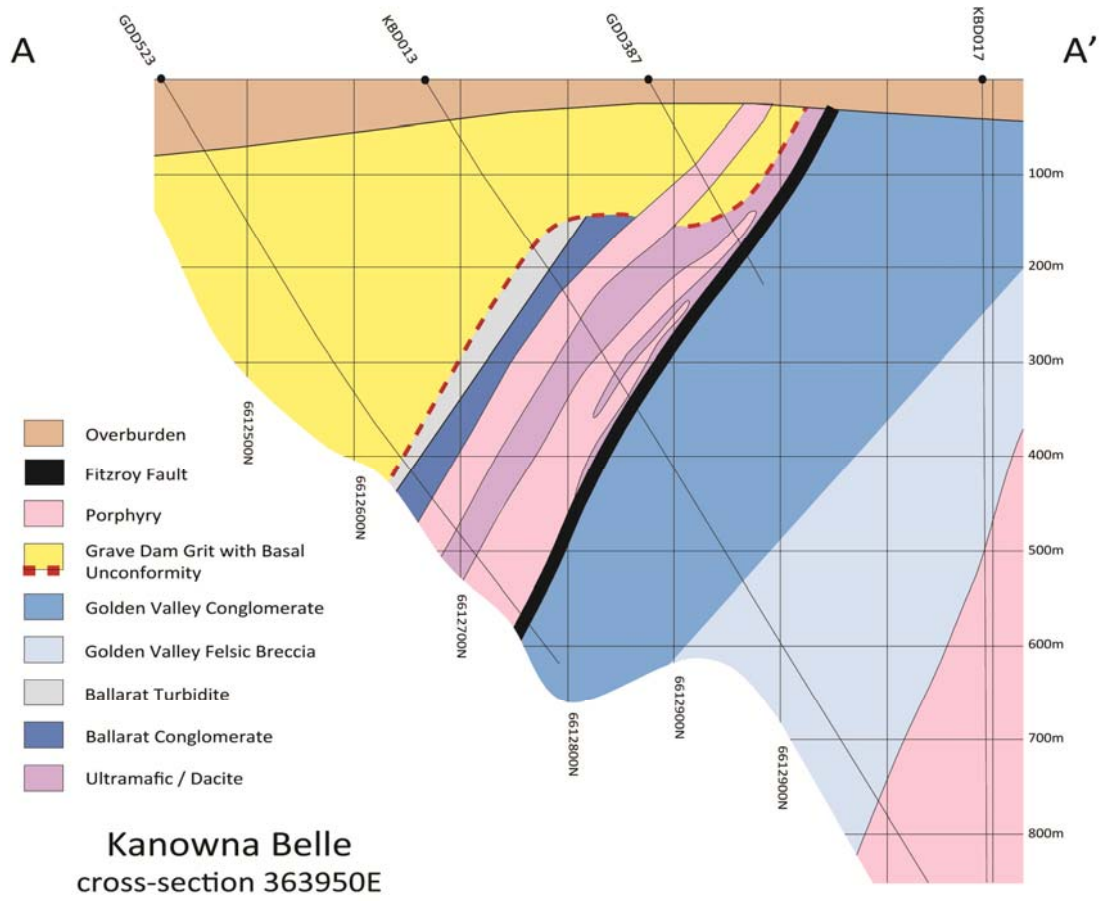

Figure 3.61 – Cross section through the Kanowna Belle mine showing the geology and location of the basal GDG unconformity (C. Pueschel; from Tripp et al. 2007a). See Figure 3.45 for location of section.

drill hole GDD540 where there is well-preserved sedimentary structure. Measurements from the drill hole are similar to the mapped exposures of the GDG in Kanowna Belle mine indicating uniform bedding over much of the stratigraphic column, but variation and folding of the bedding sequence along strike cannot be ruled out.

Interpretation and correlation

The GDG is the main rock unit in the hangingwall of the Fitzroy Fault at Kanowna Belle gold mine. The unit has been interpreted to be a lateral time equivalent of the footwall Golden Valley member, which has a maximum age of deposition of 2668±9 Ma (Ross et al. 2004). The Golden Valley member contains interbedded felsic breccia, grit and sandstone with similarities to the GDG; and the GDG contains units of polymictic conglomerate in the middle-to-upper units of the member, whereas the dominant clast lithologies are different.

Similar maximum depositional ages of hangingwall and footwall rocks in the Kanowna Belle mine may indicate that the Fitzroy Fault lacks significant thrust movement. Structural studies indicate reverse shear-sense and a 20 m-thick mylonite (Davis 1998), but there appears

to be no major disruption to stratigraphy other than a change in the orientation of bedding and juxtaposition of time equivalent units. Precise ages of the footwall and hangingwall units are unknown (only the same upper limit for both), as a result this doesn't help to resolve amounts of movement on the Fitzroy fault, normal or reverse. It is also possible that the Grave Dam member underlies the Golden Valley member; this would require a minimum displacement at least equal to the thickness of the Golden Valley member.

Lateral contacts with the underlying Kanowna and Ballarat members are unconformable, as is the western contact with the overlying Panglo member in deep diamond drill holes. If bedding continues uniformly to the west, then the contact with the overlying Panglo formation is most likely to be a high-angle unconformity.

Golden Valley member (GVC)

The Golden Valley member (GVC) covers a 2 km x 0.5 km area in the immediate footwall of the Fitzroy Fault at Kanowna Belle (Fig 3.62). Diamond drill holes and extensive open pit and underground exposures at Kanowna Belle were used to determine the detailed stratigraphic sequence of the GVC (Figs 3.62, Fig. 3.63). The GVC comprises three main units: a lower section (~350 m) of felsic grit with interbedded volcanic breccia and felsic conglomerate (Golden Valley felsic); a central section (1050 m) of thickly bedded polymictic conglomerate with interbeds of felsic conglomerate, polymictic grit and sandstone (Golden Valley conglomerate); and an upper sequence (400 m) of thinly-bedded sandstone, with thin sparse interbeds of polymictic conglomerate (Golden Valley sandstone; Fig. 3.64). The estimated true thickness of the unit is ~1800 m, but there is an unmapped section internal to the Golden Valley sandstone, and the lower contact is poorly defined; hence, the 1800 m true thickness may be a minimum estimate.

Contact relationships

The lower contact of the GVC has not been observed directly due to a poor understanding of felsic rocks in the lower part of the footwall sequence at Kanowna Belle. Previous workers have been divided in opinion on the nature of the felsic rocks and the relative proportions of volcaniclastic rocks versus felsic intrusions. Distinguishing between the two rock types has proved difficult in the past due to poor exposure and alteration. A thin basalt unit (Fig. 3.62) near the base of the sequence that represents a change between felsic volcanic / intrusive rocks and epiclastic sedimentary rocks in the lower Golden Valley felsic, may be a better candidate for the lower contact of the Golden Valley member. This basalt is in a similar stratigraphic position to the Gidji mafic volcanic unit and may be a lateral correlative of that unit.

Upper units of the GVC have been intersected in drill holes in apparent conformable contact with the Panglo member (GVD141). Bedding in the two members is sub-parallel

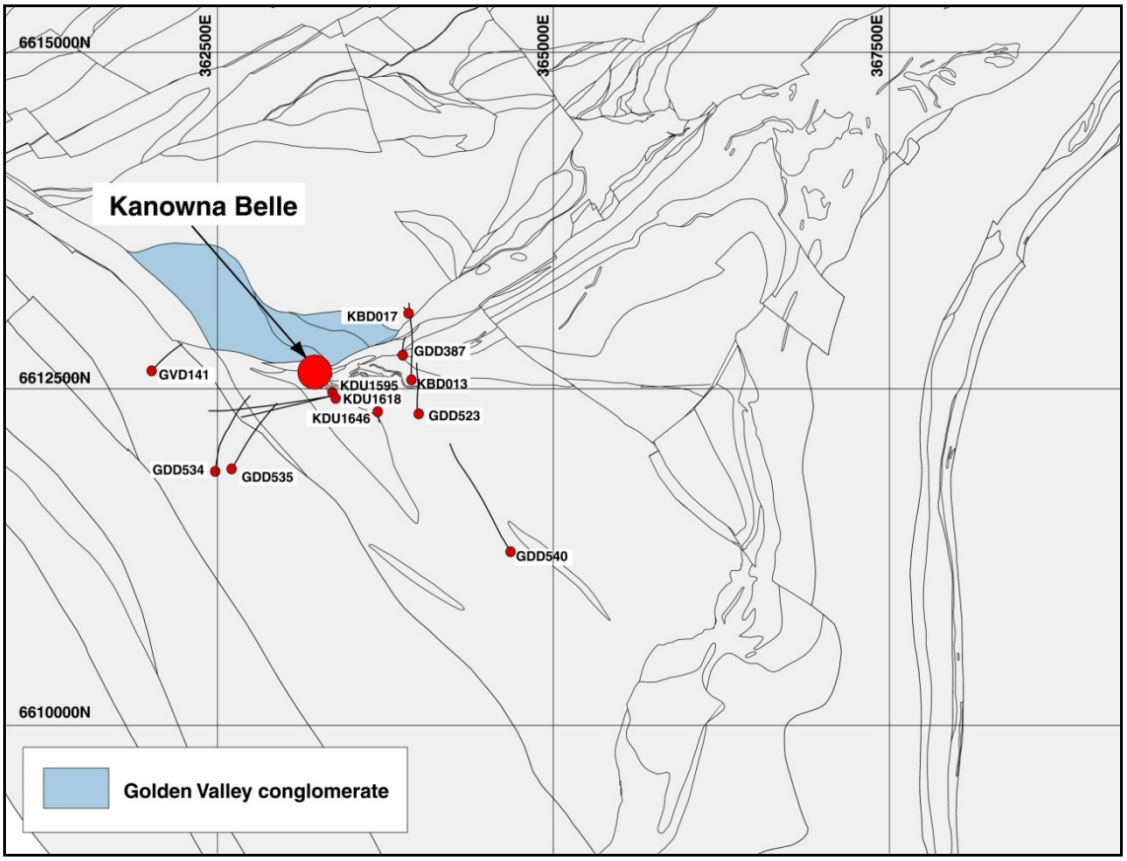

Figure 3.62– Schematic diagram showing the distribution of the GVC and relative positions of drill holes and outcrops used to determine the stratigraphic column.

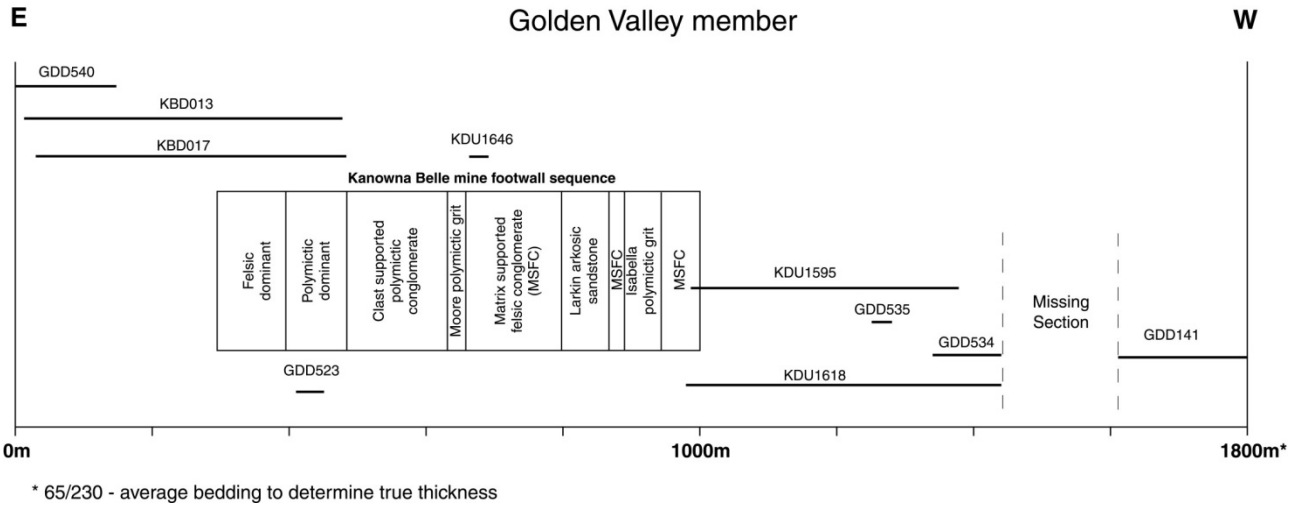

Figure 3.63 – Schematic plan of relative positions of drill holes and exposures used to determine the stratigraphic column for the Golden Valley member

Golden Valley member

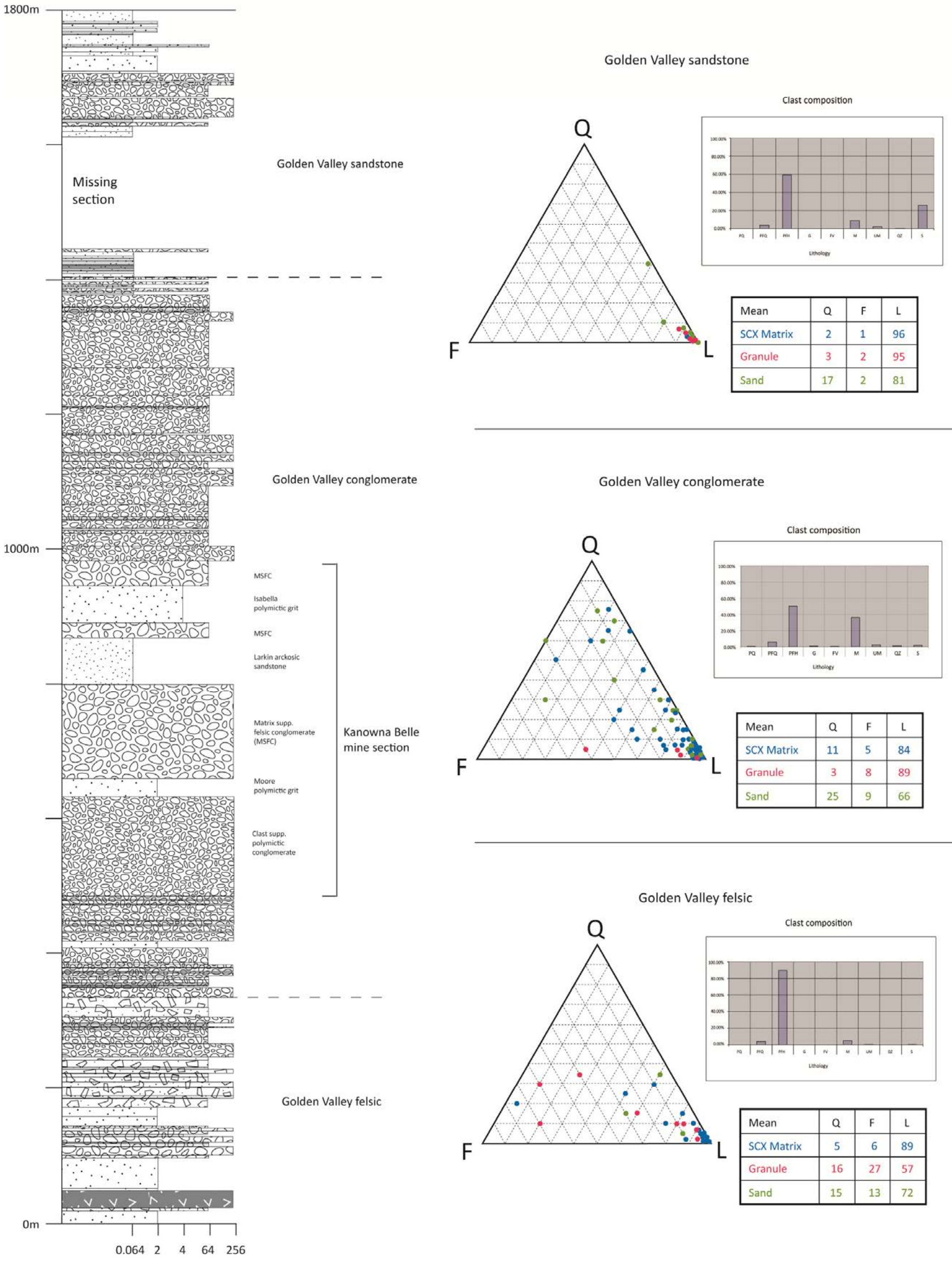

Figure 3.64– Stratigraphic column with clast and matrix information for the Golden Valley member. QFL data are coloured according to the table of mean values. SCX refers to conglomerate or breccia-sized clastics. PQ – quartz porphyry; PFQ – quartz feldspar porphyry; PFH – hornblende-feldspar porphyry ± quartz; G – granite; FV – felsic volcanic; M – mafic volcanic; UM – ultramafic; QZ – quartz; S – sedimentary. The lower grey unit with 'v' hachuring is a thin horizon of basalt that marks a change from lower dominantly felsic volcanic rocks to upper dominantly epiclastic sedimentary rocks.

locally, but at a district scale, the Panglo member is clearly cross cutting the entire section from Lower Basalt north of Kanowna to the Government Dam member in the south. The upper contact of the GVC is therefore interpreted as an erosional unconformity.

Description (Golden Valley felsic unit)

The Golden Valley felsic volcanic rocks comprise massive, disorganised beds of sand to granule-sized felsic grit with abundant interbeds of felsic conglomerate and breccia (Fig. 3.64, Fig. 3.65f, g, h). Sand and granule-sized sedimentary rocks make up the lower portion of the unit (Fig. 3.64), characterised by matrix supported (C/M ratio: 0.2), well-sorted beds with sub-angular, elongate grains. The grit is feldspar-rich in places, but lithic grit on average (Q:F:L = 16:27:57) (Fig. 3.64). A minor coarse-clastic component of the Golden Valley felsic volcanics comprises felsic volcanic breccia and felsic conglomerate beds of 25 m mean thickness (Fig. 3.65f). Conglomerate and breccia are felsic dominant with intermediate hornblende-feldspar porphyry clasts (90%), quartz-feldspar porphyry (4%) and 4% mafic clasts with a minor component of sedimentary clasts (1%).

Description (Golden Valley conglomerate)

Golden Valley conglomerate (Fig. 3.65a, c, d, e) is characterised by moderately sorted, sub-rounded and elongate clasts in thick, plane-bedded units of 17 m mean bed thickness, with individual beds up to 90 m thick. Internal sandstone and siltstone units are plane bedded on a decimetre scale with graded bedding and scoured contacts marked by basal gravel deposits (Fig. 3.65e).

The mean clast size of the conglomerate is ~120 mm with geometric means up to 264 mm. Conglomerate beds are clast or matrix supported (C/M ratio: 0.53) with lithic-wacke matrices (Q:F:L = 11:5:84). Golden Valley conglomerate is polymictic with a range of clast types (Fig. 3.64): the unit is characterised by abundant hornblende-feldspar porphyry, quartz-feldspar porphyry and quartz porphyry clasts (56%); mafic volcanic and ultramafic clasts (36%); sedimentary (2%) and quartz vein clasts (1%).

Sand-sized rocks in the Golden Valley conglomerate are quartz-rich lithic arenites (Q:F:L = 25:9:66) composed of sub-angular, elongate lithic grains in moderately sorted beds with planar to diffuse morphology. Sedimentary structures include graded bedding with scoured contacts (Fig. 3.65e) and rare cross-bedding.

Description (Golden Valley sandstone)

The upper part of the GVC (Fig. 3.64) is a thinly-bedded sequence of lithic arenite with polymictic pebble horizons (Golden Valley sandstone). The unit is gradational with the underlying Golden Valley conglomerate and is characterised by normally graded beds with

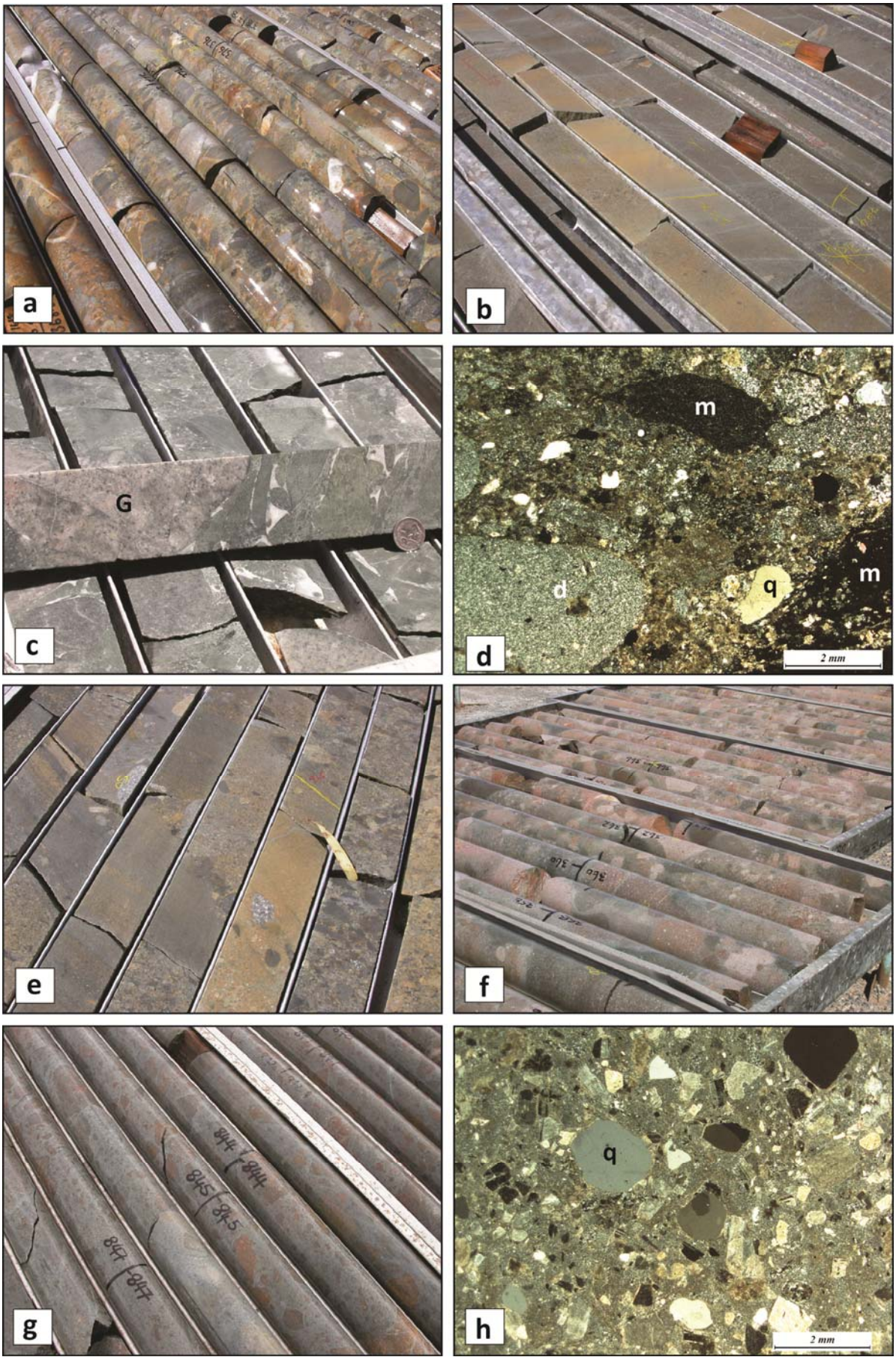

Figure 3.65

Figure 3.65 – Golden Valley conglomerate, sandstone and felsic volcaniclastic rocks

a) Polymictic conglomerate with a dominant proportion of hornblende-feldspar porphyry clasts (59%), mafic volcanic clasts (25%) and sedimentary rock clasts (10%). The conglomerate has 0.5 clast to matrix ratio and contains well rounded clasts in a lithic dominated sandstone matrix (KDU1618 374 m; GDA: 363359E; 6612448N).

b) Graded bedding in Golden Valley fine-grained sandstone. Q:F:L ratios of 5:1:94 show the dominantly lithic nature of the matrix sands and the general poor compositional maturity of the unit. Bedding on the scale of 10cm thickness dips steeply to the west and way-up is down-hole also to the west (KDU1618 764 m).

c) Golden Valley Conglomerate is distinctive for a small proportion of granite clasts in a dominantly mafic volcanic clast – dominated (70%) conglomerate. Coarse equigranular granite clasts are typical (1%), but a small proportion of porphyritic granite clasts are identical to the marginal phases of the Scotia Batholith exposed on the shores of the salt lakes north of Kanowna Belle. Variolitic basalt clasts in the conglomerate are set in a carbonate matrix where voids were available, but otherwise the pebbles and boulders are contained within a lithic sandstone matrix (KDU1618 565.5 m).

d) XPL photomicrograph of Golden Valley Conglomerate from Kanowna Belle underground with well rounded, weakly porphyritic dacites and angular, wispy mafic volcanic clasts in a strongly saussurite altered quartzolithic matrix sandstone. Monocrystalline volcanic quartz grains are rounded and angular (KDU1646 12 m; GDA: 363721E; 6612312N).

e) Gravel lags in graded sandstone beds within the Golden Valley Conglomerate. Q:F:L ratios in these beds are quartz rich 50:40:10, with prominent graded bedding and basal scours. Pebble lags are polymictic but dominated by mafic volcanic (50%) and quartz-feldspar porphyry (30%) clasts (KDU1595 80 m, GDA: 363359E; 6612449N).

f) Matrix supported felsic boulder conglomerate within the Golden Valley felsic unit, dominated by hornblende-feldspar porphyry clasts (97%) in lithic sandstone matrix (KBD17 360 m; GDA: 363903E; 6613089N).

g) Felsic matrix supported breccia dominated by angular felsic porphyritic clasts (100%) in a lithic sandstone matrix. Clasts of felsic porphyry up to boulder size (>256 mm) show strong Fe-carbonate alteration (Golden Valley felsic; KBD13 845 m; GDA: 363945E; 6612567N).

h) Quartz bearing feldspathic grit Golden Valley felsic unit. Q:F:L ratios of 10:70:20 show the feldspathic nature of the rock, which also contains monocrystalline volcanic quartz grains that are locally euhedral, in a very fine-grained siltstone matrix cement (KBD13 1132 m).

scoured contacts (Fig. 3.65b), of 6 m mean thickness and individual beds up to 28 m thick. Sand-sized rocks in the Golden Valley sandstone are lithic arenites (Q:F:L = 17:2:81) composed of sub-angular to sub-rounded, elongate grains in moderately sorted, graded beds with planar morphology.

Thin conglomerate interbeds are clast or matrix supported (C/M ratio: 0.50) and have mean clast sizes of 68 mm with geometric means up to 93 mm. The proportions of clasts are different to the Golden Valley conglomerate with a greater amount of hornblende-feldspar porphyry and quartz-feldspar porphyry (64%) and a lesser amount of mafic and ultramafic volcanic clasts (11%). A greater proportion of sedimentary rock clasts (26%) marks a significant change in provenance towards the top of the Golden Valley member.

Structural geology

Rocks in the Golden Valley member are some of the least deformed in the Kanowna district. Primary contacts and round / oval pebble shapes are preserved with only a minor fabric imposed on the rocks. The unit is dipping moderately and younging to the southwest indicating folding at broad scale, yet no mesoscopic folding has been identified.

Interpretation and correlation

The Golden Valley member is a sequence in the footwall of the Fitzroy fault, distinctly different to the hangingwall Grave Dam member. The GVC has been dated by Ross et al. (2004) with a zircon SHRIMP U/Pb age of 2668±9 Ma returned from a porphyry clast in the conglomerate indicating a maximum depositional age of 2659 Ma or less. Recent SHRIMP analyses of detrital zircons from the Golden Valley sandstone by Sircombe et al. (2007) returned an interpreted maximum depositional age of 2668±7 Ma. These ages are very close to the age reported for the Grave Dam member indicating the two units are time (if not lateral) correlatives. The relationship between the two members is unknown since they are juxtaposed across the Fitzroy Fault, but it is perhaps noteworthy that the Grave Dam member is cut by numerous felsic intrusions, whereas the Golden Valley member is not.

3.5.4 Kurrawang Formation (KUF)

Panglo conglomerate member (PAN)

The Panglo conglomerate member is exposed in a broad belt to the west of Kanowna Belle gold mine. Three diamond drill holes were used to determine the detailed nature of conglomerate at the base of the member (Figs. 3.66; 3.67), whereas the stratigraphic column (Fig. 3.68) was determined from the map distribution of lithological units as interpreted from mapping and shallow exploration drill holes.

Four main rock types are present in the PAN including polymictic conglomerate, sandstone, siltstone and carbonaceous shale. The rocks form a complex sequence (Fig. 3.68) with polymictic conglomerate horizons at the base, middle and top of the unit, which has an estimated true thickness of >3800 m. No major stratigraphy repeating thrust faults have been identified in the PAN, but deformation in the fine-grained units indicates they have been tectonically thickened, leading to an overestimate of its true thickness.

Contact relationships

The lower contact of the PAN is an extensive angular unconformity that cuts all units in the stratigraphy of the Boorara Domain from Lower Basalt to the uppermost units of the Black Flag Group. The lower contact has been interpreted by most previous workers as a major fault (the "Kanowna Shear'). Recent mapping by Standing (2004a) demonstrated an undeformed contact between conglomerate and mafic rocks in the north-western part of Figure 3.66. Several drill holes transecting the contact between conglomerate of the PAN and Golden Valley sandstone have failed to intersect any major structure at the contact. No upper contact of the PAN with younger rocks has been observed in the present study, but the uppermost part of the unit is assumed to occupy the centre of the interpreted syncline in Figure 3.66.

Description

Conglomerate at the base of the PAN (Fig. 3.69a-e) is characterised by moderately sorted, rounded and elongate clasts in thick, massive, disorganised units of 17 m mean bed thickness, with individual beds up to 56 m thick. The mean clast size of the conglomerate is ~130 mm with geometric means up to 267 mm and individual clasts up to 460 mm. Conglomerate beds are clast supported (C/M ratio: 0.62) with a lithic-wacke matrix (Q:F:L = 11:4:85). Panglo conglomerate is polymictic with a range of clast types (Fig. 3.68): the unit is characterised by abundant granitic clasts (34%), hornblende-feldspar porphyry and quartz-feldspar porphyry clasts (31%); mafic volcanic and ultramafic clasts (32%); sedimentary (2%) and quartz vein clasts (1%).

Sand-sized rocks in the Golden Valley conglomerate are quartz-rich lithic arenites (Q:F:L = 21:5:74) composed of sub-angular, spherical grains in moderately to well-sorted beds with planar morphology and decimetre scale thickness (Fig. 3.69g). Sedimentary structures include rare graded bedding.

Structural geology

Conglomerate in the PAN is only weakly deformed with minor elongation of the clasts. This contrasts with significant internal folding and transposition in the sandstone and shale units higher in the unit. A weak foliation affected the PAN, more pronounced in phyllosilicate-rich

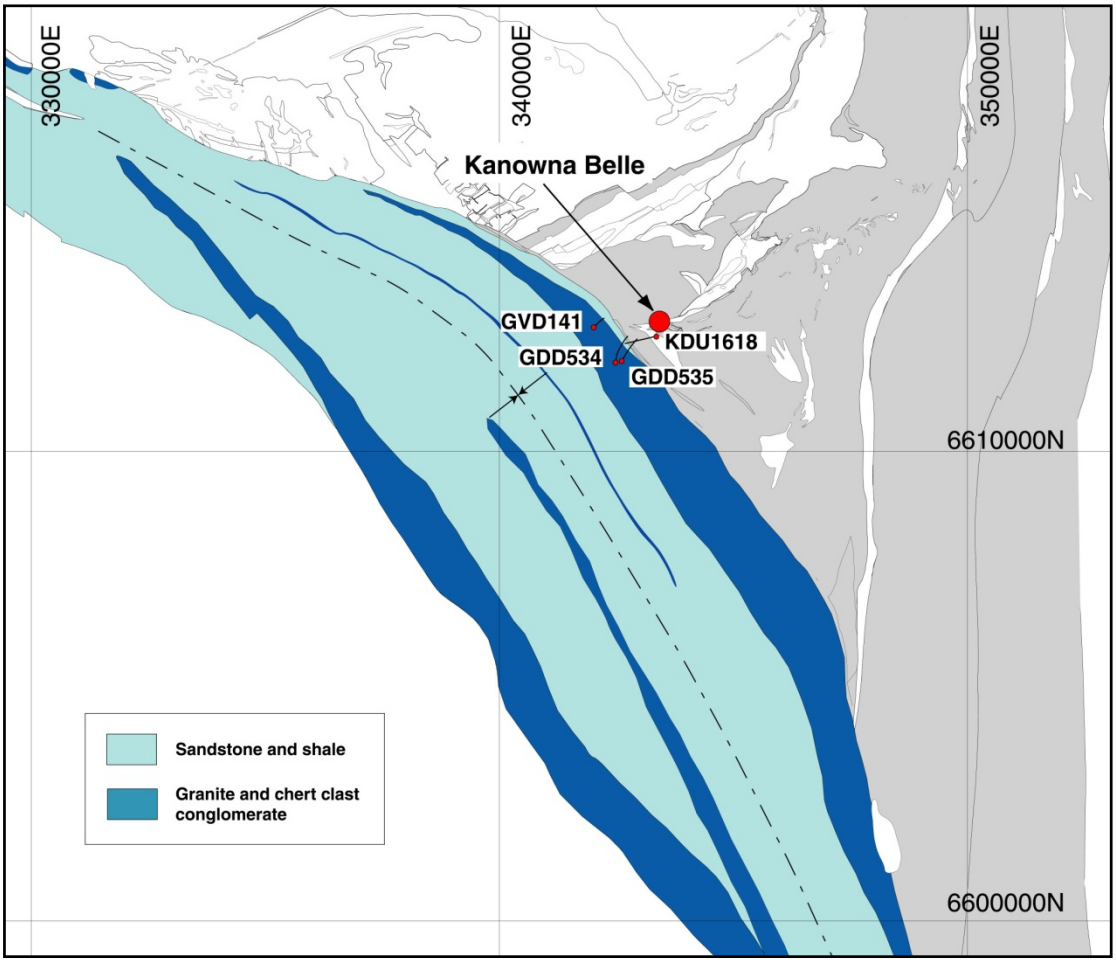

Figure 3.66 – Distribution of the Panglo conglomerate member with locations of drill holes used to assess detail of the lower conglomerate unit, and location of interpreted syncline axis

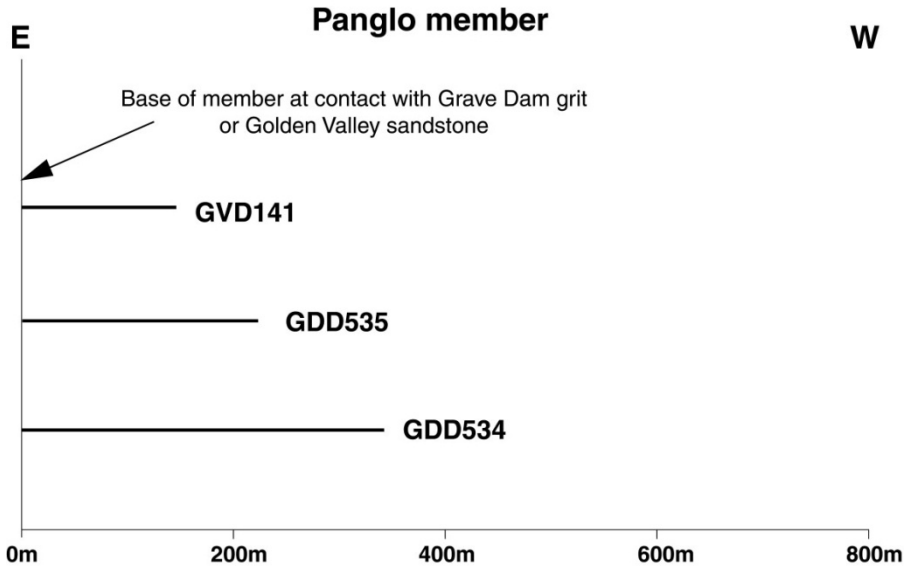

Figure 3.67 – Schematic illustration of the relative positions of drill holes used to assess the geology of the lower conglomerate units in the PAN (see Appendix for detailed logs)

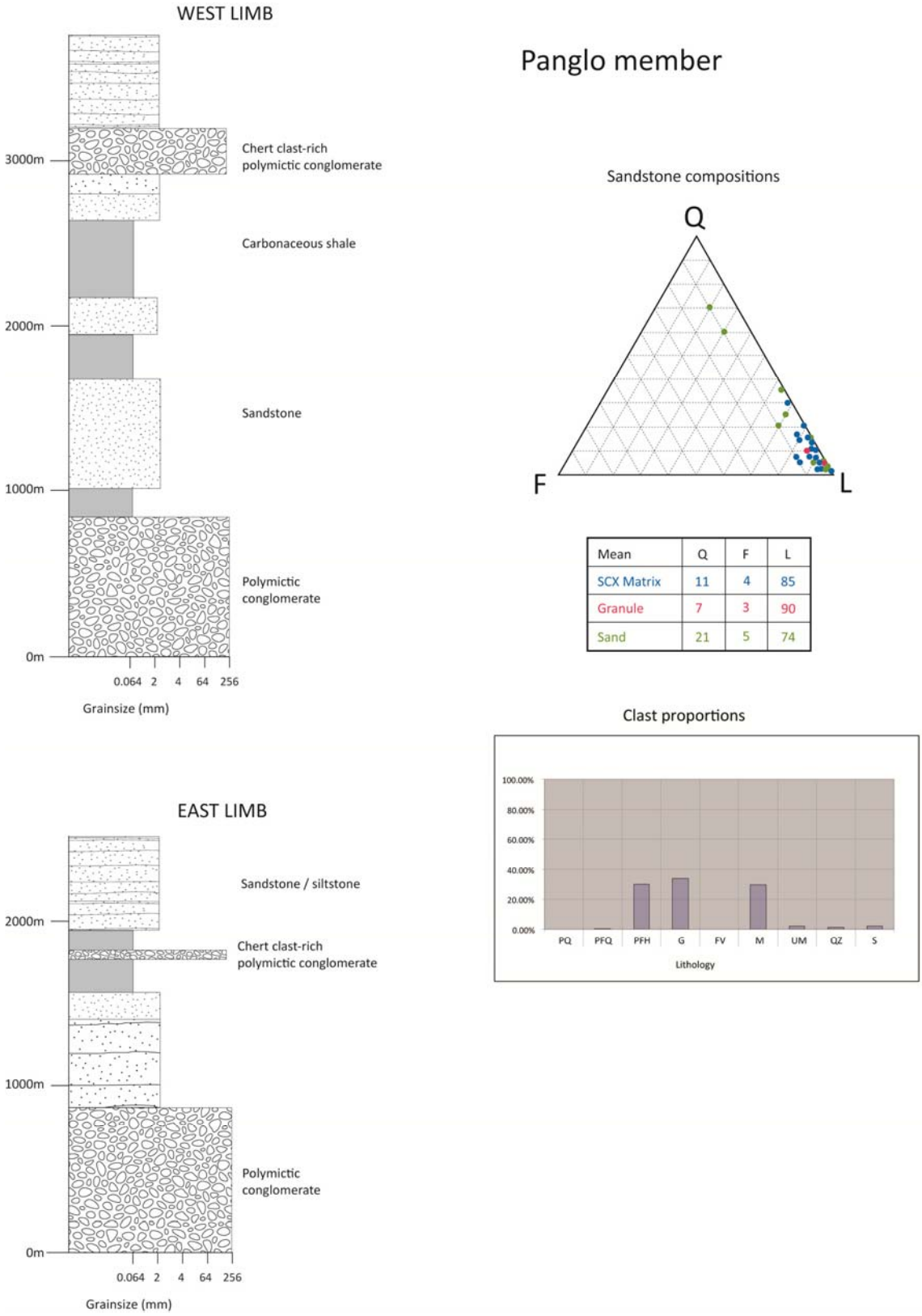

Figure 3.68 – Composite stratigraphic column for the Panglo member derived from a horizontal line of section across the unit in map view. Thicknesses are recalculated to account for the dip of bedding. QFL and clast data are from drill holes that intersect only the lowermost conglomerate unit. QFL data are coloured according to the table of mean values. SCX refers to conglomerate or breccia-sized clastics. PQ – quartz porphyry; PFQ – quartz feldspar porphyry; PFH – hornblende-feldspar porphyry ± quartz; G – granite; FV – felsic volcanic; M – mafic volcanic; UM – ultramafic; QZ – quartz; S – sedimentary.

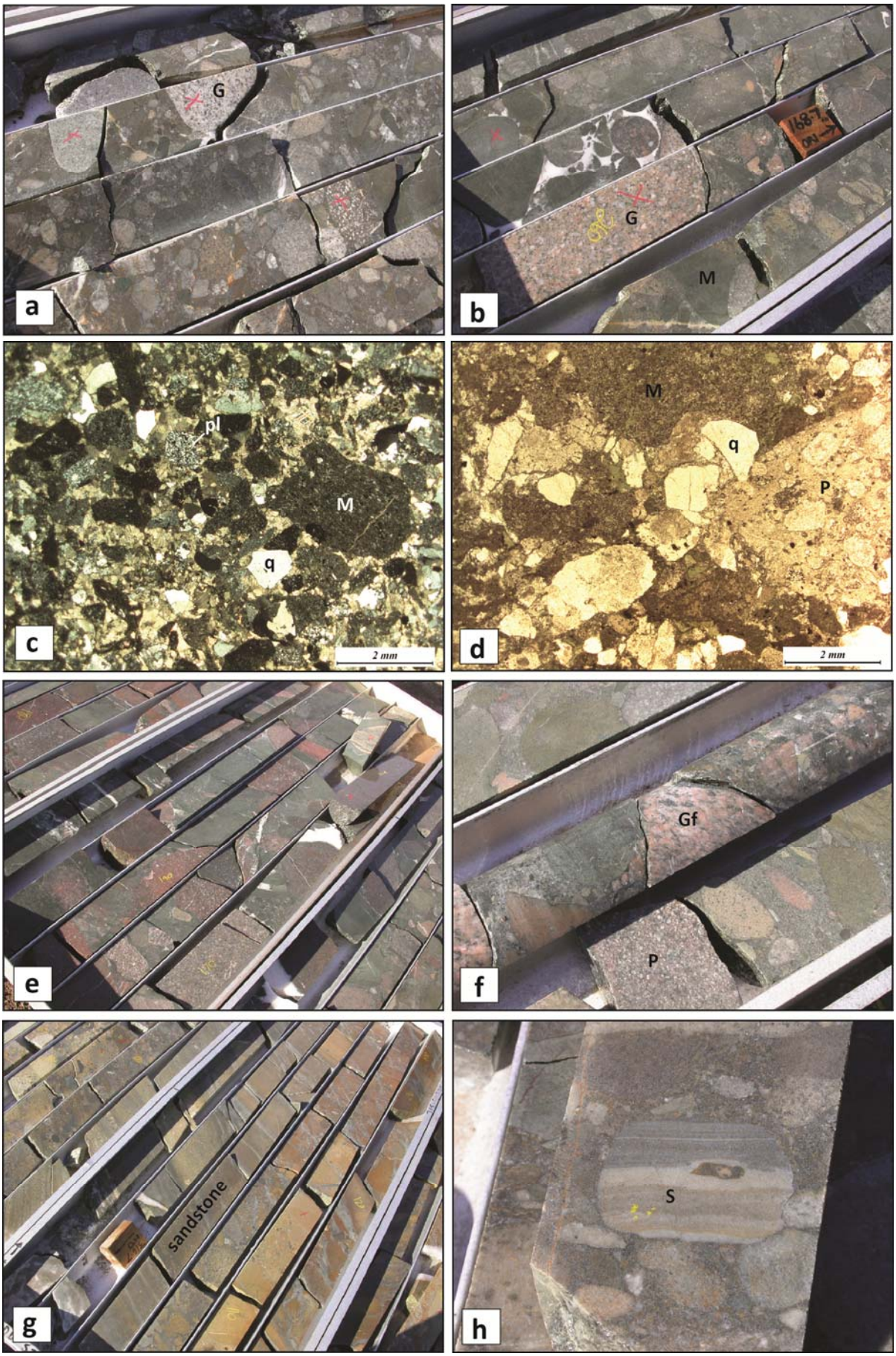

Figure 3.69

Figure 3.69– Panglo conglomerate and sandstone,

a) Polymictic, granite-clast (53%) dominated conglomerate with minor proportions of mafic (25%) and hypabyssal porphyry (20%) clasts. The clasts are well rounded cobbles-boulders in a clast supported framework (GDD535 158 m; GDA: 362611E; 6611908N).

b) Large clast of equigranular pink kfs-plag-qz granite in Panglo polymictic conglomerate. Note well rounded to spherical clasts with carbonate matrix., GDD535 168 m,

c) XPL photomicrograph of polymictic, mafic clast rich granule to pebble conglomerate. Several types of quartz fragments are visible including strain-free monocrystalline volcanic quartz (q) and rounded, polycrystalline plutonic quartz grains (pl). Pebbles of mafic volcanic rocks are sited in well-sorted, closely packed framework supported sub-angular coarse lithic sandstone (GDD535 115.7 m).

d) PPL photomicrograph showing rounded hypabyssal dacite porphyry clasts (P), mafic volcanic clasts and coarse polymictic lithic sandstone matrix. Clasts and coarse sand grains are interlocking with little of no cement (GDD535 136.6 m,)

e) Hematite altered granite clast-rich boulder conglomerate, composed of granite clasts (48%), mafic volcanic (35%) and dacite porphyry (10%) clasts in a framework supported arrangement with a lithic sandstone matrix (GDD535 255 m).

f) Foliated granite clast, showing evidence for pre-Panglo deformation. Note the lack of strain in most examples of the Panglo conglomerate (GDD535 264.5 m).

g) Fine-grained, lithic dominated sandstone interbeds in polymictic conglomerate. Bed thickness averages 0.2 m, with gravel lags and grading. Strong Fe-carbonate alteration overprints the unit evident in the yellowish brown staining from exposure to air (GDD535 317 m).

h) Bedded sedimentary rock clast (GDD535 136.4 m).

units. Significantly, conglomeratic units in the PAN contain clasts of foliated granitoid rocks, indicating that sources for the PAN included deformed basement rocks.

The PAN is folded into an elongate, NNW-SSE trending syncline as demonstrated by bedding/younging relationships and the distribution of a chert-clast conglomerate marker layer. That syncline is in the footwall of the Bardoc Tectonic Zone with a similar relationship to the Kurrawang syncline, located in the footwall of the Zuleika Shear Zone.

Interpretation and correlation

The presence of abundant granitic and chert clasts makes the PAN stand out from other members of the Kanowna district stratigraphy. Granite and porphyry clasts show diverse textural types indicating a range of sources that includes foliated granite (Fig. 3.69f). Bedded sedimentary clasts (Fig. 3.69h) and rare felsic volcanic clasts and a large proportion of mafic volcanic clasts indicates the truly polymictic nature of the PAN. The central belt of conglomerate (Fig. 3.66) is dominated by banded chert and iron formation clasts. Given the unconformable contact against most units in the Boorara Domain and the diversity of clast types, the PAN is tentatively correlated with the Kurrawang Formation.

3.5.5 Summary of Boorara Domain formations and members

The present work builds on several excellent previous studies of the rocks in the Kanowna district by Taylor (1984), Archibald (1993), Davis (1998), Hand (1998), Ross et al. (2004), Trofimovs et al. (2004); and in particular, a reinterpretation of the stratigraphy by J. Rogers and K. Joyce (presented in Tripp and Rogers 2005). This study, like that of Hand (1998), has attempted to assign the rocks of the Kanowna district to recognised formations of the Kalgoorlie Terrane, which inherently assumes that the rocks of the Boorara Domain are indeed part of that terrane.

Some distinct differences between Boorara Domain rocks and the typical Kalgoorlie Terrane section include the presence of a felsic volcanic source contemporaneous with the ~2710 Ma ultramafic volcanic rocks (Trofimovs 2003): this association is not observed in any other parts of the Kalgoorlie Terrane. Another important difference is the abundance and apparently localised provenance of conglomeratic rocks in the sequences younger than the Upper Basalt. These instances may indicate the Boorara Domain rocks were deposited in a sub-basin disconnected from the rest of the Kalgoorlie Terrane with unique local sources, albeit deposited around the same time.

Regardless of these important differences, SHRIMP geochronology (Chapter 4) demonstrates that the rocks of the Kanowna district are contemporaneous with depositional units in the Kalgoorlie Terrane if not direct lateral correlatives. For this reason the assignment of the Kanowna members to formations of the Kalgoorlie Terrane is still a valuable exercise for

understanding the relative correlation of the rock units. A revised stratigraphic column for the Kanowna district is presented in Figure 3.70, showing the distribution of mappable units, but grouped into Kalgoorlie Terrane formations, with the locations of important unconformities.

3.6 Major unconformities in the north Kalgoorlie district

3.6.1 Definition and identification of unconformities

An important advance in understanding the structural history of the north Kalgoorlie district is gained by recognising major unconformities and placing them on maps that display the distribution of formations. Unconformities are surfaces that represent time breaks during which there may have been periods of: non-deposition, uplift and erosion, folding and faulting, igneous intrusion, or a combination of these. In the north Kalgoorlie district, recognising and mapping unconformities allows for unequivocal resolution of relative structural relationships and cross-cutting relationships between events that can be demonstrated to pre- or post-date the unconformity surface. For this reason they are a preferred criterion for erecting structural histories, and provide greater confidence than structural fabric overprinting.

Given generally poor outcrop in the north Kalgoorlie district, available exposures of unconformities are not abundant, but several key unconformity surfaces have been documented in this chapter from drill core and outcrops. The presence of solid state fabrics in some of the documented examples could be interpreted as evidence of faulting rather than unconformity, but this has been carefully considered in each case using the greater distribution of formations, bedding trends and other criteria such as basal conglomerate composition and the presence of rip-up clasts. A common observation of bedding surfaces throughout the district is the presence of some degree of strain, which in general is heterogeneously distributed along strike, and leads to windows of preservation where the primary relationships are undisturbed. In many of those cases, contacts can be confidently interpreted as ‘strained primary contacts', rather than as faults or shear zones with major displacements.

3.6.2 Kurrawang unconformity (regional map patterns, Binduli, Panglo)

The Kurrawang Formation is the youngest member of the Kalgoorlie stratigraphy and was interpreted as unconformably overlying all older units by Glikson (1971) and Swager et al. (1990). A map-scale distribution of the Kurrawang Formation shows the unit cuts across most stratigraphic sequences in the Kalgoorlie district from Siberia Komatiite to Upper Black Flag formation along its eastern contact, whereas the western contact is variable: sheared along the anastomosing Zuleika Shear Zone, or in unknown contact with greenstones of the Coolgardie Domain. From this map-scale relationship alone, the eastern contact could be interpreted as a suspected unconformity, but the low degree of strain on that eastern contact is a crucial feature. A key relationship is that folds in the underlying greenstones are truncated against the eastern

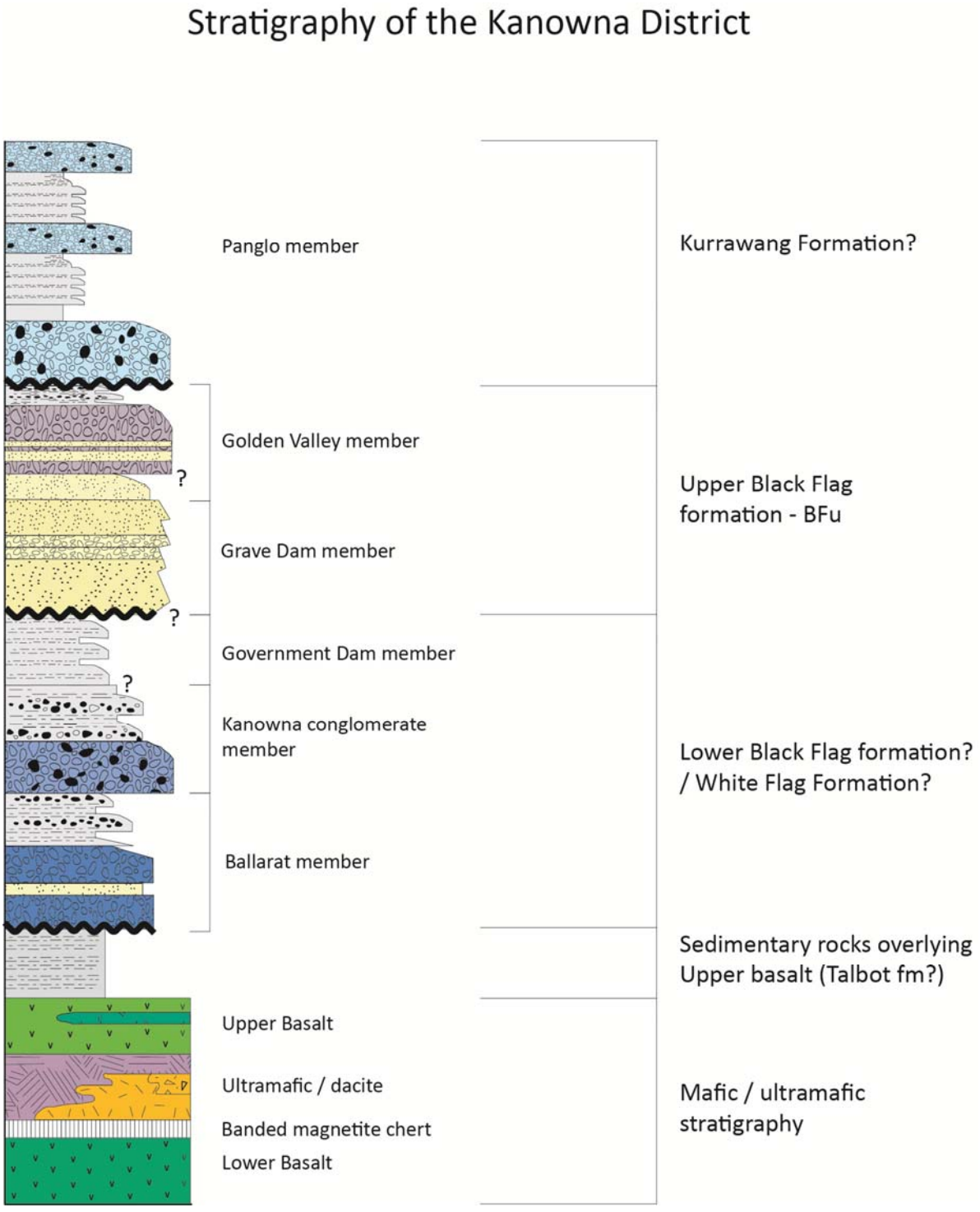

Figure 3.70 – Schematic stratigraphic column for the Kanowna district produced from the results of this study (modified from J. Rogers, K. Joyce written communication, 2005). Note the position of Government Dam member relative to Grave Dam member remains uncertain, but this is addressed in Chapter 4. The stratigraphic correlation of the Ballarat and Kanowna members are unknown from field data alone. Also the relative position of Golden Valley and Grave Dam Members is uncertain since the two units are nowhere in contact, but have similar interpreted maximum depositional ages from SHRIMP analyses. The Panglo member is placed tentatively with the Kurrawang Formation, but this will also remain somewhat uncertain in the absence of geochronology.

Kurrawang contact and, importantly, the Kurrawang Formation is not folded around the Mount Pleasant Anticline.

Few exposures of the eastern Kurrawang Formation contact are available, and these have been observed at White Flag Lake, and Binduli. The White Flag Lake exposure is laterally obscured by ~5 m of lake clays, yet the rocks on each side of the cover clays are not highly strained (Kurrawang Conglomerate to the west; White Flag andesites to the east; no interleaving of units). At this outcrop the Kurrawang Formation comprises thick conglomerate beds dominated by andesitic and sedimentary clasts and other polymictic debris, with 10 cm-wide layers and lenses of interbedded, coarse quartzo-lithic sandstone. Loose pebbles on the surface display some stretching with a south-plunging stretching lineation and axial ratios of ~4:1, but high strain is not observed. This is matched by pavements of White Flag andesitic breccia on the eastern margin of the contact, which also have some flattening, but are not highly strained. From these relationships the eastern contact of the Kurrawang Formation is interpreted as a strained unconformity rather than a major zone of shearing. In contrast, exposures of the western Kurrawang conglomerate contact at Kundana north, have pebbles that show 20:1 stretching in a highly strained matrix of sheared sandstone and foliated mica schist (Zuleika Shear Zone; see Chapter 5).

At Binduli, the lower Navajo Sandstone contact with underlying Binduli porphyry conglomerate is exposed in mines and drill holes as a sharp, weakly foliated plane, with minor rip-up clasts of the underlying unit. Similar relationships are preserved in drill holes from the Kundana south (Goldilocks) area. It is notable that C.S. Honman (1914), in detailed descriptions of the Binduli Series, debated the presence of an unconformity between the Kurrawang rocks and porphyry dominated conglomerate along the Binduli trend. Honman (1914) states: “As to the possibility of an unconformity between the gneissic sedimentary and the porphyritic series the only evidence in favour of this is the contrast in lithological character of the two series. This is, however, probably due to a difference in the conditions of sedimentation and possibly the porphyries have been subjected to greater metamorphic action. Against an unconformity is the uniformity in strike and presence of conglomerate in both series”.

Honman documented the outcrops at Binduli to try to resolve the problem, but the above quote appears to be as far he could go towards resolving the problem with outcrop data alone. He described in order from east to west:

1. Conglomerate with pebbles of slate with some porphyry pebbles on its western side, no quartz pebbles.
2. Conglomerate with slate and sandstone pebbles in a coarse sandstone matrix.
3. As Kurrawang ridge approached: conglomerate with porphyry pebbles, quartzite, coarse grit, rare slate pebbles, quartz pebbles, rounded and water worn.

4. Conglomerate with mainly porphyry pebbles and beds of feldspathic sandstone and a gneissic structure.
5. Gradual change to conglomerates with quartz and jasper pebbles, some nearly pure hematite and magnetite with occasional porphyry pebbles.

In modern terms this equates with:

1. Binduli porphyry conglomerate
2. Navajo conglomeratic sandstone
3. Navajo Conglomerate
4. Kurrawang Conglomerate
5. Kurrawang magnetic conglomerate

Critically, Honman states: "South of the dry lake country the porphyry pebble conglomerate is in closer association with the main porphyry belt than north of the lake, and bands of conglomerate can be actually traced in the massive porphyry similar to the fragmental porphyry at Binduli" – i.e. the 'porphyry pebble conglomerate' is part of an earlier sequence, rather than the Kurrawang Formation.

Modern data from the field and drill core also support the porphyry conglomerate as part of a lower sequence:

1. A porphyry conglomerate in the Fort William area about 1.5 km east of the Kurrawang/Navajo shows strikingly similarities to the porphyry-clast dominated conglomerate from recent drill holes at Binduli, albeit with a greater proportion of altered siltstone and mudstone clasts. Flattened conglomeratic rocks in the Pitman gold mine at Binduli might also be part of that sequence; hence, the Binduli porphyry conglomerate appears more laterally extensive than suggested by scant exposures in the Centurion gold mine.
2. Drill hole KWD007 at Centurion has a cm-scale sharp contact of quartz-rich cross-bedded Navajo Sandstone against Binduli porphyry conglomerate that is not interbedded. From the sedimentary characters - cross-bedded, quartz-dominant sandstones, and polymictic conglomerate in the Navajo; versus massive disorganized porphyry-dominated conglomerate with minor crystal-lithic matrix in the Binduli porphyry conglomerate, there is no sense of gradation between the sources. Therefore an unconformable Navajo Sandstone overlying Binduli porphyry conglomerate is the preferred interpretation.
3. Observations from Goldilocks, on the western side of the Kurrawang Syncline, show equally convincing unconformability between polymictic Navajo conglomerate and sandstone; and the underlying felsic breccia, volcaniclastic conglomerate, andesitic conglomerate, and siltstone that are interpreted as part of a lower Binduli sequence. Some porphyry conglomerate in the Goldilocks drill

holes has striking similarities to the Binduli porphyry conglomerate, but they are interbedded parts of a greater volcaniclastic package.

Conglomerate in the Kurrawang Formation near Binduli is dominated by porphyry pebbles, which reflects a common relationship observed in several localities on the eastern unconformable margin of the Kurrawang Formation, that the local conglomerate clast proportions appear skewed by the composition of the substrate (Section 3.2.4).

To the south of Binduli a pervasive, regionally developed, NNW-SSE striking solid-state metamorphic, biotite-muscovite foliation is axial planar to minor folds in the Kurrawang Formation, and also overprints the underlying units. This suggests that folding and foliation were imposed after the uplift and erosion events that deposited the Kurrawang Formation, and presumably, the pervasive fabric was imposed after significant burial of the Kurrawang. A further speculation is that F2 folding of the greenstones prior to deposition of the Kurrawang occurred as a high-level thickening of the sequences without the development of a penetrative axial planar foliation.

The Panglo member of the Kanowna district shows similar map-scale relationships to the Kurrawang Formation: it truncates a folded stratigraphy from Scotia Basalt (Lower Basalt Unit) to the Grave Dam member (upper Black Flag formation; Fig. 3.2; Fig. 3.66). The contact is observed in drill holes to the west of Kanowna Belle gold mine (drill hole V3; GDA: 362922E; 66118265N) where clasts of a porphyry intrusion in the Grave Dam member are observed in the basal parts of the Panglo conglomerate. Previous interpretations of a major ‘Kanowna Shear’ at this contact may relate to deformed sandstone/siltstone/shale in the central and upper parts of the Panglo member, whereas lower conglomerate units and the lower contact show remarkably low strain.

3.6.3 Upper / lower Black Flag formation unconformity (Gidji, Binduli, Kanowna)

An important unconformity is interpreted to separate lower and upper units of the Black Flag Formation. At Gidji this unconformity surface is interpreted at the base of the Gidji felsic volcanic unit, which has a thinly-bedded sandstone unit and local conglomeratic beds, which contain fragments of underlying ultramafic rocks at Gidji Hill. In this area it appears there was no development of the lower Black Flag formation as documented for the Ora Banda Domain and the Boorara Domain; however, examples of this formation are identified elsewhere in the Kambalda Domain (Section 3.4.1).

In the Ora Banda Domain an unconformity at the base of the distinctive Binduli porphyry conglomerate unit is interpreted to mark a boundary between lower and upper Black Flag formations. Despite clear unconformable relationships in the Centurion mine supported by SHRIMP U-Pb zircon analysis, the lateral distribution of this unconformity surface remains uncertain.

There are several levels in the lower Binduli stratigraphy that contain dacite-porphyry dominated conglomerate, and this is also documented in the drill holes from the Goldilocks area at Kundana south. Further information is required to properly map the lateral distribution of the Binduli porphyry conglomerate unconformity, but the contact is placed tentatively as a south-plunging anticlinal folded surface, interpreted to sit above the Gibson-Honman Rock rhyodacite and extending west into the Centurion gold mine. This interpretation accords with the gross south-plunging anticlinal fold structure of rocks in the Binduli corridor and SHRIMP U-Pb zircon analyses.

The upper Black Flag unconformity at Kanowna is placed with confidence at the base of the Grave Dam member, supported by mapped relationships in the Kanowna Belle cross-section from several drill holes, and the observation of truncated early folds in the underlying Ballarat and Kanowna members. A key observation at Kanowna is that fold axes from a folding event earlier than the Panglo unconformity trend NE-SW. This relationship is unique for the entire north Kalgoorlie district and may suggest an early, localised folding event that pre-dates the main NNW-SSE trending folds that are ubiquitous throughout the district (Chapter 6).

3.7 Review and update of stratigraphic correlations

3.7.1 Ora Banda Domain

The stratigraphic column in the Ora Banda Domain was examined in outcrop and drill core (Table 3.2). Note that in the present study, the inferred stratigraphic order of Krapez et al. (2000) is revised placing the White Flag Formation below, rather than above the Black Flag Formation. As described correctly by Forman (1937, 1953; Table 3.1-map pocket) the rocks exposed in the Black Flag mining district (the original Black Flag Series, but later termed ‘Spargoville’) are overlain by rocks of the White Flag Formation.

A normal depositional contact of the ‘Spargoville Formation’ deposited on glomero-porphyritic Victorious Basalt exposed north of White Flag Lake is unequivocal. Thick sections of intercalated andesitic / dacitic and sedimentary strata overlie the andesitic volcanic rocks of the White Flag Formation and these are assigned to a lower Black Flag formation although earlier workers included them with the White Flag Formation (Forman 1937) or with the ‘porphyrite’ division of Honman (1916; Table 3.1-map pocket).

The development of intercalated andesitic (hornblende-present) and dacitic (hornblende-absent) rocks in the Goldilocks area at Kundana south suggests a conformable progression between underlying White Flag Formation and rocks interpreted as lower Black Flag formation. This relationship however, is predicated on the assumption that the Binduli sequence was folded pre-Kurrawang and that the Kundana south section is representative of that Binduli sequence. Given the weight of descriptive evidence this assumption is reasonable, but further trace element geochemistry or geochronology is required to support the proposed interpretation.

Table 3.2 - Summary of results from the Ora Banda Domain formations

Formation	Primary data source	Secondary data source	Compositional characteristics	Textural characteristics
Kurrawang	Surface traverse; outcrop maps; ddh RCD001; LWD001	Surface traverse	Significant proportion of granitoid clasts; BIF and chert conglomerate unit higher in section	Polymictic conglomerate;>65% rounded clasts; overlain by thick section of cross-bedded sandstone, thin upper section of siltstone
Navajo sandstone member (likely belongs to Kurrawang)	ddh BVD-6, Kundana south, drill holes from Centurion mine	Surface traverse	Polymictic clasts in quartz-rich sandstone and wacke; local jaspilitic chert	Poorly to moderately sorted, massive arenite, pebbly arenite and sandy conglomerate; many angular to sub-angular clasts; cross-bedded sandstone
Upper Black Flag (Centurion porphyry conglomerate?)	ddh BVD-6; CD-28 and other holes from Centurion mine	reconnaissance logging of RAB drill holes, GSWA maps	Conglomerate with feldspar porphyry clasts; associated siltstone and black shale with upper felsic volcanic rocks	Weakly polymictic conglomerate; round to subround clasts dominant; black shale laminated
Lower Black Flag	Gibson-Honman Rock, Kundana South	drillholes from Centurion mine at Binduli	Intermixed zone of andesitic and dacitic volcanic rocks and conglomerate	Coherent volcanic rocks, peperite, conglomerate and bedded sandstone; sub-angular clasts most common
White Flag	ddh NATDD12	Outcrops at White Flag Lake	Lower boulder conglomerate and sandstone overlain by andesitic volcanic breccia	Andesite dominated conglomerate with rounded clasts;
Spargoville Fm?	Mount Pleasant outcrops,	drill holes	Wacke-mudstone	Graded beds

A 700 m thick conglomerate (White Lake meta-conglomerate of Glikson 1971; Table 3.1-map pocket) has been portrayed on several modern maps (e.g. Swager et al. 1990; Witt 1993) to mark the base of the Kurrawang Formation, but there are problems with this interpretation. Prior to those studies, Forman (1937) assigned similar rocks to a ‘Kundana Formation’, but this was revised in 1953 to include them with the Kurrawang Formation. Krapez et al. (2008) have recently proposed the name “Navajo Supersequence” for this unit, but unlike Glikson and Forman did not include it directly with the Kurrawang Formation, portraying it instead as a separate unconformity-bound unit correlated with the Merougil Formation at Kambalda.

Even taking the Navajo Sandstone into account, there remains a discrepancy between the modern definitions of the Kurrawang Formation and the original of Honman (1916). Honman (1916) showed the Kurrawang to be much more extensive south of the boundary as placed by Swager et al. (1990), whereas Glikson (1970) placed 600 metres of “lithic, quartzose and feldspathic metagreywacke” below the conglomerate. The outcrops originally mapped by Honman (1916) were re-mapped in this study confirming the presence of polymictic banded-chert pebble bearing conglomerate 2.6 km south of White Lake, as originally placed on Honman’s map (see compilation geological map - map pocket).

The Kurrawang Formation is the only formation previously identified directly with the Timiskaming of the Abitibi Belt (Honman 1916; Hewitt 1963; Glikson 1971a), possibly because of the presence of a conglomerate unit containing distinctive red jasperitic chert clasts and abundant magnetic iron-formation. This unit is also comparable to the Kavirondian of the Lake Victoria Greenstone belt in Tanzania (Shackleton 1946; Tripp et al. 2007c unpublished data); Shamvaian of the Zimbabwe Craton (Haughton 1969; Stidolph 1977; Blenkinsop et al. 1997; Hofman et al. 2002), and Palkanmardi conglomerates in the Hutti district of the Dharwar Craton, India (Poulsen 2010).

3.7.2 Coolgardie Domain

Localities at Kundana were studied in the Coolgardie domain (Fig. 3.30). The rocks in question come from diamond drill hole MAD-06-501. This hole - collared in an area portrayed on maps to be underlain by wacke and mudstone of an unknown formation, but assumed to be Spargoville Formation - intersected distinctive volcaniclastic breccia dominated by hornblende-feldspar-phyric clasts. Those rocks are tentatively correlated with the White Flag Formation in the Ora Banda Domain, but there is insufficient evidence to determine how extensive they really are. An alternative possibility is that they are correlative with the andesitic volcanic/sedimentary member of the Gidji Lake formation east of Fimiston.

3.7.3 Kambalda Domain

The rocks exposed on the shore of Gidji Lake and drill core from holes EMD4 and EMD10 at the Eight Mile Dam gold prospect were documented in this study. The sand-sized fraction in the section at Eight Mile Dam is characterised by a relatively high average percentage of quartz (approximately 40%) and more than twice that of any of the other formations studied. This is perhaps mirrored by a high proportion of quartz-porphyry, felsic volcanic and sedimentary clasts in the conglomerate. The Gidji Lake sections are notable for distinctive alternations of thick (10 to 50 m) sandy and thinner (1 m to 10 m) conglomeratic intervals: a characteristic shared by the Ballarat sandstone, Kanowna conglomerate and Golden Valley sandstone members in the Kanowna area.

The along-strike extension of the rocks at Gidji Lake gives way south-eastward to distinctive rocks that are only recorded in two drill holes MAD01 and MAD02 (Fig. 3.43). The distinguishing characteristics of these rocks are that they are essentially oligomictic and composed dominantly of hornblende-feldspar porphyry clasts with a quartz-poor, lithic to feldspathic sand-sized fraction. Clasts vary in angularity from angular to sub-round, but on average are sub-angular. Intervals of graded lithic- to feldspathic arenite allow a consistent stratigraphic way-up (eastward) to be established. Initially it was thought that oligomictic conglomerates and volcanic breccias of overall intermediate bulk composition represented

another new section of the White Flag Formation, which in the past has been regarded as restricted to its type locality. A serious difficulty with this interpretation, however, is that Fletcher et al. (2001) reported a zircon population suggesting a maximum depositional age of 2661±3 Ma, which precludes a time-equivalence with the circa 2690 Ma White Flag Formation. A better interpretation is to consider these rocks, which include cross-bedded sandstones, as the uppermost members of the Gidji Lake section (one of the youngest pre-Kurrawang units in the district), albeit with a dominantly intermediate composition.

The most abundant sedimentary rocks in the Kambalda domain appear to belong to the Spargoville Formation on published maps (Fig. 3.35), but there is considerable uncertainty about this. The rocks in question were examined in outcrop north of Kalgoorlie and near Mount Hunt (True Sons) and in drill core from drill holes SE3, SE4 in the Lakewood section south of Kalgoorlie (Fig. 3.35). A recent interpretation by Barley et al. (2002) places many of these rocks into their sequences 2, 3, 4, 5 or 6, which would equate them with the White Flag and Black Flag Formations, and hence, not the Spargoville Formation. Implicit in their interpretation is that an erosional unconformity below these rocks in the Lakewood section actually cuts down into the Golden Mile Dolerite. Unfortunately the type section for the Spargoville is not in the Kalgoorlie district and there is some uncertainty as to how correlative the Spargoville Formation rocks really are. Samples of these rocks from the Lakewood drill core were selected for SHRIMP U-Pb analysis and are reported in Chapter 4.

In the Lakewood section at Kalgoorlie, the dominant rock types structurally above the Golden Mile dolerite are wacke and mudstone, commonly as folded graded-beds similar to those encountered north of White Flag Lake. There are few coarse clastic rocks in the section, but local mud-matrix conglomerates likely represent submarine channel deposits. Higher up in the Lakewood section however, there are dacitic volcanic tuff, tuff breccia, lapilli tuff and breccia, which locally overlie the wacke-mudstone units and may represent an unrelated higher stratigraphic unit as suggested by Barley et al. (2002). The important implication of this second possibility is that the rocks at Gidji Lake / Eight Mile Dam and the inferred unconformity beneath them might extend into the Fimiston mine area, and provide stratigraphic constraints on a world-class Archaean gold deposit.

3.7.4 Boorara Domain

The Kanowna area (Fig. 3.45) received particular attention because of uncertainties in correlation of the units there with recognised formations in the Kalgoorlie district. Six informally defined conglomeratic units were studied both in drill holes primarily selected to cut the particular formation as well as those in which they were intersected incidentally, during the study of a different formation (Table 3.3). The formations are arranged in perceived upward stratigraphic order from Ballarat through Panglo.

Table 3.3 -Summary of results from the Boorara Domain formations

Formation	Member	primary data source	secondary data source	compositional characteristics	textural characteristics
Kurrawang	Panglo	GDD534,535; GVD141	KDU1618; outcrops	Significant proportion of granitoid clasts; BIF and chert conglomerate unit higher in section	Polymictic conglomerate;>65% rounded clasts
Upper Black Flag	Golden Valley	KBD17; KDU 1595 1618 1646	GDD 523, 534, 535,540; GVD141; KBD13	Feldspar-porphyry dominated	Weakly polymictic conglomerate; subround clasts dominant
Upper Black Flag	Grave Dam	GDD387, 523,540; KBD13	GDD534,535	Feldspar- and quartz-feldspar porphyry dominated; local jasperitic chert	Poorly to moderately sorted, massive arenite, pebbly arenite and sandy conglomerate; many angular to sub-angular clasts
Upper Black Flag	Government Dam	ddhWFD4, outcrop		Quartzo-feldspathic wacke	Graded beds
Lower Black Flag	Kanowna	CTDH1,3; GVD50; HMD2,10		Mainly mafic volcanic and feldspar-(hornblende) porphyry clasts	Polymictic conglomerate and bedded sandstone; sub-angular clasts most common
Lower Black Flag / White Flag	Ballarat (includes Gordons Mafic Conglomerate)	ddh GVD-46,47, 51; WFD-6,18	CTDH1,3; GDD-387,523; GVD-48,50; HMD-2,10; WFD4,4w1,5	Clast and sand population dominated by ultramafic, mafic and fsp-hornblende porphyry debris	Polymictic conglomerate with sub-rounded clasts and bedded sandstone

The clast populations in the conglomerates appear to vary from unit to unit from the ultramafic-mafic dominated Ballarat conglomerate member to the truly polymictic Panglo member and Golden Valley conglomerate member. A distinctive unit within the Kanowna section is the Grave Dam member, which, unlike the well-organised water-deposited conglomerate and sandstone in most other units, is composed of massive unsorted debris: it is distinguished by a high sand : clast ratio, by the overall angularity of clasts which are dominantly cm-sized, and by dominant quartzo-feldspathic debris. The Grave Dam member has been singled out as potentially marking an internal unconformity within the Kanowna section, overlying the Ballarat and Kanowna members, but correlated with the Golden Valley member.

The exact stratigraphic position of the Ballarat, Kanowna and Government Dam members is uncertain from a district-scale perspective. Barley et al. (2002) appear to have assigned the Ballarat/Kanowna section to their Sequence 2, whereas limited geochronological evidence suggests the Ballarat and Kanowna members could be time equivalents of the White Flag Formation. In the past these rocks have been treated as part of the Black Flag Group (Hand 1998). Some of the complications in the internal stratigraphy at Kanowna arise from offsets along the Fitzroy fault and a second probable, parallel fault to the south. The Golden Valley member is notable because it contains not only conglomerate and sandstone, but also distinctive

amygdaloidal basalt and quartz-feldspar-phyric lapilli tuff and tuff breccia. Barley et al. (2002) assigned the Golden Valley member and underlying Grave Dam member to their sequence 4, potentially equating them with the rocks in the Gidji Eight Mile Dam area and this is supported by the present study. They also viewed the rocks at Kanowna Dam (Government Dam member) to be younger yet (Sequences 5 and 6).

Perhaps the most notable sedimentary unit at Kanowna is the Panglo member. Once thought to be bounded by a 'Kanowna Shear', these remarkably undeformed conglomeratic rocks are better regarded as lying above an angular unconformity, which transgresses a folded sequence of several different units. The name of the formation comes from a location adjacent to the Panglo open pit mine to the northwest where J. Hallberg interpreted the conglomeratic rocks to represent a fault-scarp fanglomerate deposit. The Panglo sequence was also suggested as a possible correlative of the Kurrawang Formation by C. Swager (personal communication 1999). In the Kanowna area the conglomerate gives way upward to magnetic sandstone/siltstone and shale, and a distinctive, poorly exposed polymictic conglomerate containing abundant laminated chert clasts: a characteristic of the Kurrawang conglomerates elsewhere in the district.

3.7.5 Summary of sedimentological characteristics by formation

Detailed palaeo-environmental interpretations have been covered by previous studies based on lithostratigraphy (Hand 1998; Trofimovs 2003) and more speculative sequence-stratigraphic concepts, notably Barley et al. (2002), Krapez et al. (2008), Krapez and Pickard (2010), and those approaches are not attempted nor repeated here. The previous work of Hand (1998), Krapez and Hand (2008) and Krapez et al. (2008) interpreted the bulk of units in the Kalgoorlie Terrane as products of submarine fan turbidites, and gravel-rich slope apron deposits, fed by canyon-confined debris flows, and density currents.

The thrust of the present work is aimed at producing stratigraphic correlations based on identified unconformity-bounded units, where those unconformities are observable in the field; and supported by added geochronological support (Chapter 4). An ultimate goal of this work is to produce a formation map that presents equivalent formations across the north Kalgoorlie district, and allows comparison with the distribution of gold deposits - to understand the stratigraphic and structural controls that may have influenced the location of the major and world class Archaean gold mineral systems. Note that the sequence stratigraphic approach assumes unconformity based on the interpreted sequence boundaries and their speculative relationships with respect to sea-level changes related to tectonic or eustatic factors. At least one of those assumed unconformities (e.g. 'Spargoville' contact with upper basalt in the Ora Banda Domain) is demonstrated by the field evidence as a normal depositional contact with no major time break. The following is a summary and compilation of the descriptive sedimentological aspects of each formation compared across domains.

White Flag Formation

Mapped units correlated with White Flag Formation include the well-preserved lake section at White Flag Lake, diamond drill holes at Mount Pleasant, Kundana north and Kundana south. Quantitative data were collected from two drill holes (NATDD012 and MAD06-501; Fig. 3.71a). On average the White Flag Formation is characterised by clast-supported, sub angular, elongate, well-sorted conglomerate/breccia, in planar, massive disorganised beds. The clast compositions of volcaniclastic conglomerate and breccia in the drill holes show dominant components of hypabyssal hornblende-feldspar porphyry clasts with a minor mafic volcanic component (dolerite and gabbro; Fig. 3.71a). Sandstone compositions are dominantly lithic with minor feldspar, whereas the WFF in the Coolgardie Domain has a wider range of quartz and feldspar abundances in the sandstones (Fig. 3.71a).

A comparison with rocks from the Kambalda Domain, that were observed with superficial similarities to WFF (a dominant intermediate composition of the clasts; Fig. 3.71b), shows significant differences in lithological character that support the contention that the Kambalda Domain intermediate rocks are *not* correlated with the WFF: particularly since they contain a component of sedimentary debris, which is more characteristic of the Gidji conglomerate. Previous geochronology also supports a preferred correlation with the Gidji conglomerate unit (Section 3.7.3).

The field relationships at White Flag Lake, where a basal andesitic conglomerate is overlain, up section, by primary volcanic andesite breccia, sills and possibly flows, suggests the bulk provenance of these rocks was locally derived from actively erupting and eroding intermediate volcanic centres (this assertion is supported by the dominantly feldspathic-lithic composition of immature sandstones and matrices). A much reduced section of andesitic volcanic and volcaniclastic material correlated with White Flag Formation in the Kundana South area, with abundant andesitic conglomerate, may infer that these rocks are more distal to a volcanic centre compared to the proximal White Flag Lake rocks (see also Hunter 1993).

Intercalated zones of andesitic and dacitic volcanic and volcaniclastic material is suggestive of contemporaneous and adjacent, intermediate and felsic volcanic centres in the lower Black Flag formation. Note that the contact of WFF with overlying lower BFF at Goldilocks is arbitrarily placed at the base of the intercalated section; hence, the possibility exists that andesitic volcanism was continuous at least for the lower part of the stratigraphy interpreted as lower BFF.

Lower Black Flag formation

Sequences correlated with lower Black Flag formation were observed in the Kundana south area and Gibson-Honman Rock (Ora Banda Domain). No rocks correlated as lower Black Flag formation were observed from the Coolgardie domain in this study. The stratigraphic

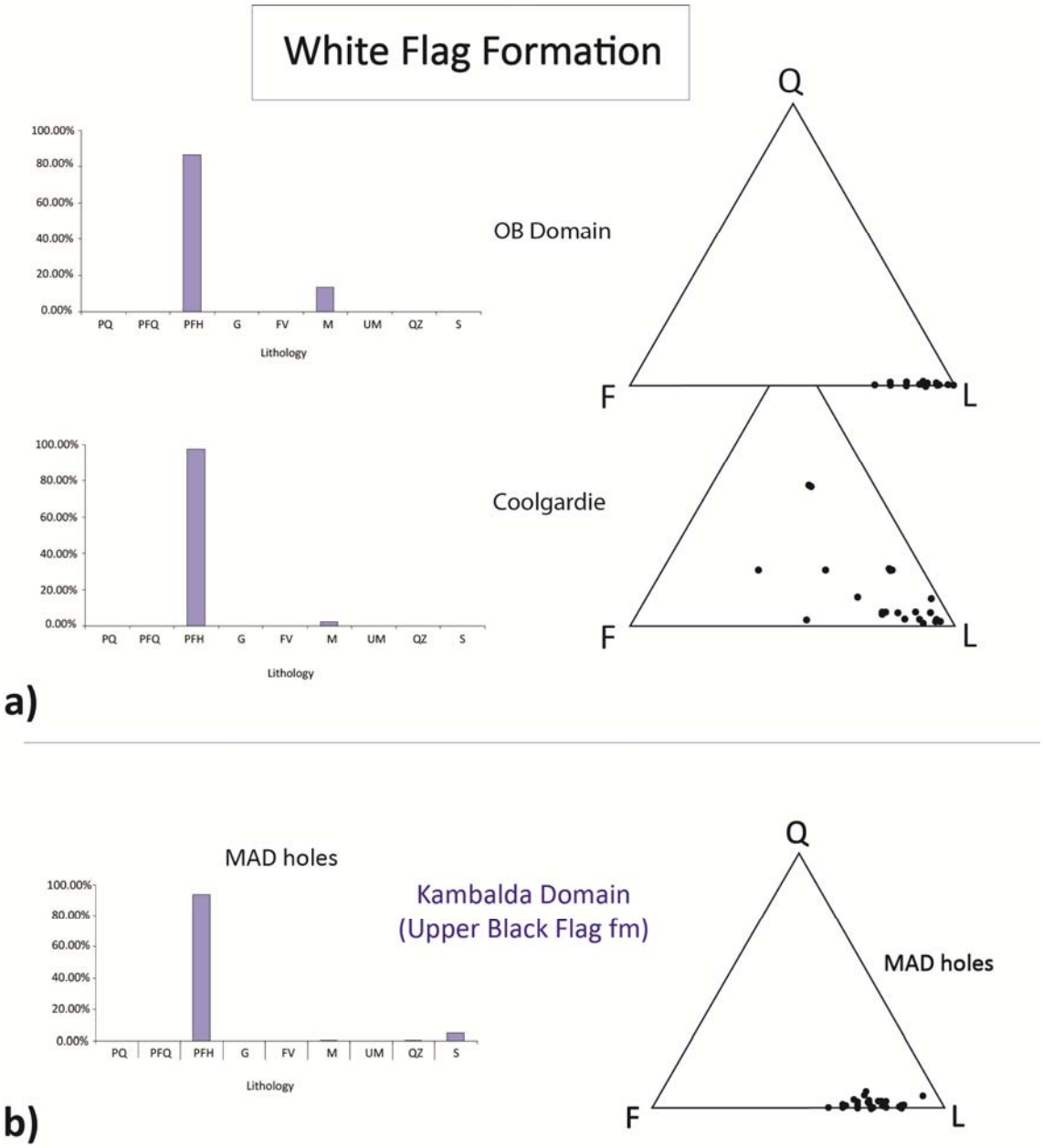

Figure 3.71 – Quantitative mean clast compositions and Q:F:L ratios from interbedded sandstones and conglomerate matrices. a) Comparison of units correlated with White Flag Formation from the Ora Banda and Coolgardie domains showing similar characteristics, b) Data from MAD holes in the Kambalda Domain with superficial similarities to the White Flag Formation, but showing differences in less mafic debris, higher proportion of sedimentary debris in the conglomerates and higher feldspar compositions of the sandstones, despite the dominant hypabyssal hornblende-feldspar porphyry clast components. Clasts types grouped as: PQ – quartz porphyry; PFQ – quartz feldspar porphyry; PFH – hornblende-feldspar porphyry ± quartz; G – granite; FV – felsic volcanic; M – mafic volcanic; UM – ultramafic; QZ – quartz; S – sedimentary. Individual chart labels refer to formations and members as documented in Chapter 3.

of dacitic volcanic rocks overlying Golden Mile Dolerite in the Travis et al. (1971) section is resolved with geochronology in Chapter 4. That sequence, including a section of black shale underlying the Lakewood dacites, is a possible candidate for lower Black Flag formation in the Kambalda Domain.

Krapez and Hand (2008) documented a key intersection in drill hole HLD006 from south of Lakewood in which the Golden Mile Dolerite is apparently unconformably overlain by a sequence of quartzolithic sandstone with fragments of volcanic quartz, andesite and dolerite, overlain by matrix-supported dolerite-basalt-gabbro-andesite boulder conglomerate with upper quartzolithic sandstone and polymictic conglomerate units. The interpretation in that paper ascribed those rocks to a generic 'Black Flag Group', whereas their documented sequence appears to be a possible candidate for correlation with a lower Black Flag formation as determined here.

Detailed information on a thick sequence of conglomeratic rocks overlying the basal ultramafic volcanic succession was taken from several units in the Kanowna district (Fig. 3.45), but correlation of some these rocks with a lower Black Flag formation remains uncertain as discussed in Section 3.5.2. A generally dominant component of hornblende-feldspar hypabyssal porphyry clasts is common to many of the formations in the Kanowna district, but in the case of the Ballarat member, is accompanied by a significant proportion of mafic and ultramafic clasts (Fig. 3.72a). In all units, the conglomerates are polymictic with one or two dominant modes. This characteristic of conglomerate compositions being skewed by the basement rocks, is similar to the descriptions of rocks immediately overlying Golden Mile Dolerite as described by Krapez and Hand (2008).

Sandstone compositions from the Ballarat and Kanowna sequences are lithic dominated with a moderate to significant quartz component (Fig. 3.72b). No quantitative data were collected from the Kundana south rocks in this study, but there are significant proportions of andesite-porphyry dominated conglomerate in the rocks correlated with lower Black Flag formation (see detailed logs in the Appendices). The Kundana south section also contains abundant sandstone / siltstone interbedded units, with quartz-rich components.

Descriptive data on the clast and sandstone compositions of formations: (1) in the Kanowna District, (2) at Lakewood south (Krapez and Hand 2008), and (3) at Kundana south, suggest some marked similarities between the basal parts of these units. In particular, at all three locations there is a dominant clast component that reflects the volcanic substrate upon which the rocks were deposited: mafic-ultramafic in the Kanowna district (Boorara Domain); mafic volcanic and mafic intrusive in the Lakewood south area (Kambalda Domain); and intermediate volcanic in the Kundana south area (Ora Banda Domain). The polymictic nature of the basal conglomeratic sections at Lakewood south suggests the lower Black Flag formation records a significant uplift of the lower mafic-ultramafic substrate. At Kundana south, a predominance of

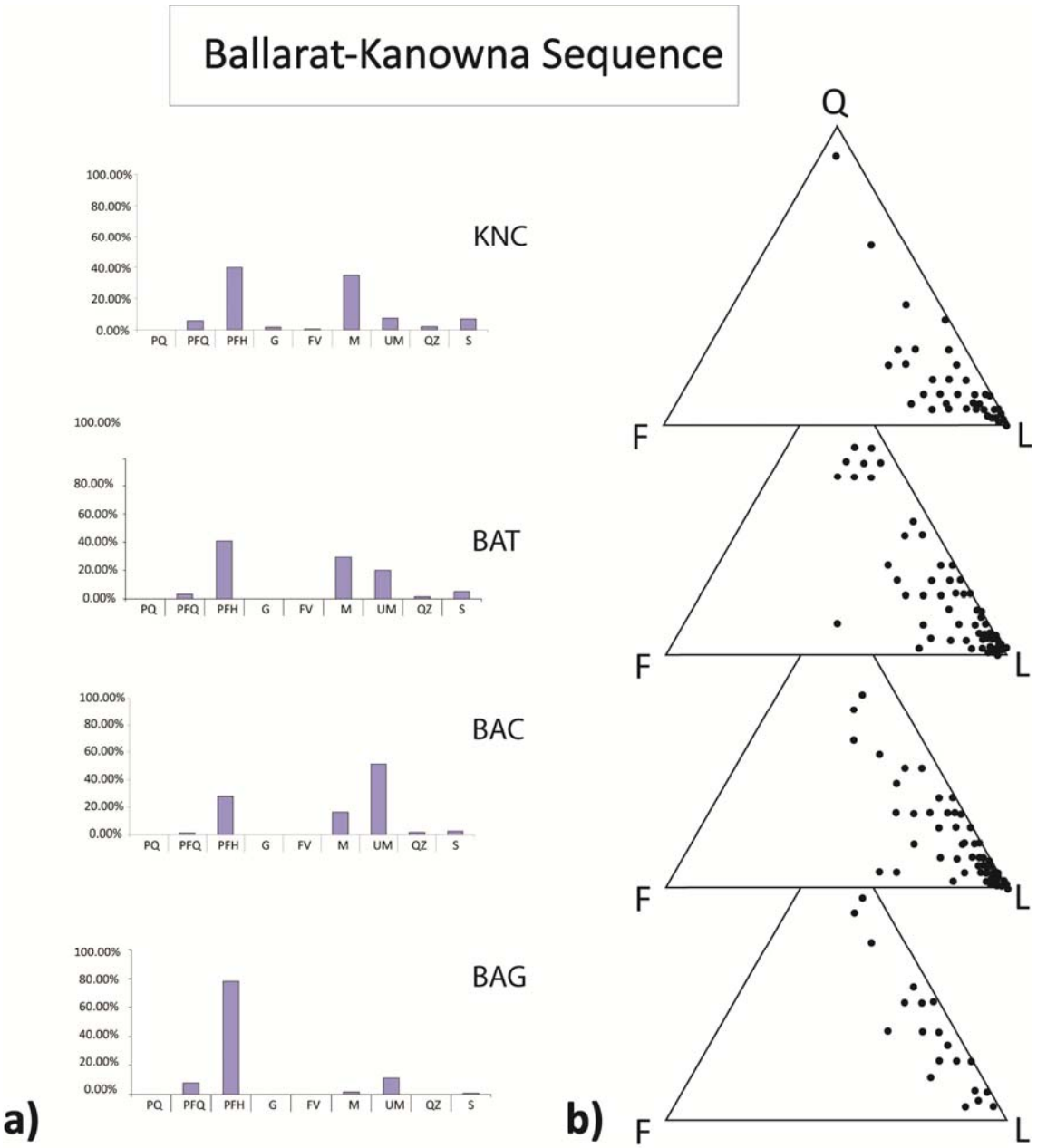

Figure 3.72 – Clast compositions of the Ballarat and Kanowna conglomerate members in the Boorara Domain. Clasts types grouped as: PQ – quartz porphyry; PFQ – quartz feldspar porphyry; PFH – hornblende-feldspar porphyry ± quartz; G – granite; FV – felsic volcanic; M – mafic volcanic; UM – ultramafic; QZ – quartz; S – sedimentary. Individual chart labels refer to formations and members as documented in Chapter 3. (BAG – Ballarat Grit; BAC – Ballarat Conglomerate; BAT – Ballarat Sandstone; KNC – Kanowna Conglomerate).

thick andesitic volcanic successions overlying the Talbot formation sedimentary rocks and Upper Basalt, may account for a dominant intermediate component observed in the basal units of the lower Black Flag formation at that location.

These observations strongly suggest the lower Black Flag formation was deposited in a series of active fault-bounded depositional basins where the substrate of the depositing basin is the same as the source region of nearby uplifted blocks, or reflecting rip-up of that basement. The faults that bound recognised 'domains' of the Kalgoorlie area are worthy candidates for these early growth faults, but in the Kanowna district, faulting may have been more localised. Major clast components of hypabyssal hornblende-feldspar porphyry, in many of the units also suggests a degree of exhumation that exposed moderate-depth to upper-crustal levels, providing a major component of the source material for the coarse clastic units observed.

Upper Black Flag formation

Sequences correlated with upper Black Flag formation include several units from the Kanowna district (Boorara Domain); felsic/andesitic volcanic and conglomeratic rocks from the Gidji area (Kambalda Domain); and the distinctive Binduli porphyry conglomerate and units south of Binduli, interpreted to overlie the Binduli succession continuous to the intersection of the Abattoir and Zuleika Shear Zones (Ora Banda Domain). The basal unconformity of this formation is well documented locally, but remains an interpretation given the generally poor lateral continuity of exposure common in the Binduli area.

In the Ora Banda Domain, the Binduli porphyry conglomerate is dominated by clasts of feldspar porphyry with a minor component of sedimentary clasts (mudstone and quartzite), reflecting the direct substrate of that conglomerate unit, whereas a poorly understood section of deep water deposited shale and felsic volcanic rocks, higher in the sequence, appears to be part of this unit as well. The Gidji rocks (Kambalda Domain) form a complex sequence of: (1) lower felsic volcanics with overlying amygdaloidal basalt, (2) quartz-rich sandstone with polymictic conglomerate layers (Fig. 3.73a) and intercalated rhyodacite volcanic breccia, (3) sandstone / siltstone / shale, and (4) overlying andesitic volcaniclastic rocks with cross-bedded feldspar-lithic sandstones and overlying shale. Boorara Domain units collectively grouped with the upper Black Flag formation include the Golden Valley felsic volcanic rocks, overlying mafic-dominated, polymictic conglomerate and upper units of plane-bedded lithic sandstones (Fig. 3.73b); and the felsic dominated Grave Dam grit with intercalated amygdaloidal basalt flows.

Comparison of the clast compositions of rocks throughout the Kalgoorlie domains correlated with upper Black Flag formation shows generally polymictic provenance, but with dominant modes of hypabyssal hornblende-feldspar porphyry clasts, and in the case of the Golden Valley sandstone and the Gidji conglomerate, clasts of sedimentary rocks (Fig. 3.73b). The strongly unimodal hornblende-feldspar porphyry clast populations observed in the MAD

holes east of Mount Charlotte are interpreted as locally derived, given the presence of coherent andesitic rocks in that same sequence and proximity to the Golden Mile, where alkalic-intermediate intrusions abound. The MAD sequence shares similarities with the Golden Valley felsic rocks in a dominance of hypabyssal porphyry clasts, but clasts in the Golden Valley Felsic unit are typically quartz-feldspar dacite porphyries (Preston 2008).

In the Gidji and Grave Dam sequences, strong similarities of lithotype and depositional setting of these two units are suggested by broadly polymictic clast proportions with quartz-rich sandstone compositions, the presence of intercalated amygdaloidal basalt flows (Fig. 3.73a, c), and rarely preserved accretionary lapilli. The Gidji sequence is organised in plane-graded beds, whereas the Grave Dam sequence is a chaotically arranged succession of very thickly bedded, unsorted breccia and conglomerate units suggested to represent pyroclastic flow deposits (Dr. R. Cas personal communication). Rare examples of accretionary lapilli in both units suggests components of sub-aerial volcanism for those units.

The sandstone compositions of units correlated with upper Black Flag formation show wide spreads of quartz and feldspar components with the exception of the MAD holes and upper units of the Golden Valley member (Fig. 3.74c), reflecting restricted sources during the deposition of those upper units. Clast and sandstone compositions in Figures 3.73 and 3.74, suggest a diverse range of sources from mafic and ultramafic-volcanic to dacitic-volcanic and sedimentary. But with the exception of the Golden Valley conglomerate, the units are dominated by felsic compositions.

Upper Black Flag formation units appear to have an important felsic volcanic (siliciclastic) component in their provenance, but to a greater degree than underlying lower Black Flag formation units. In particular the Boorara Domain units have a strong quartz-rich component and may have sourced the abundant rhyolite-rhyodacite complexes at Four Mile Hill and Perkolilli (Fig. 3.2), which outcrop east of the Kanowna district (tentatively included with lower Black Flag formation). Similar relationships exist for the Binduli porphyry conglomerate which sits unconformably on intercalated felsic volcanics, mudstones and porphyry intrusions, interpreted as a sub-marine lava dome complex.

Kurrawang Formation

Unconformable relationships are demonstrated by the Kurrawang Formation in the Ora Banda Domain and by the Panglo member at Kanowna. The Kurrawang Formation is the youngest Archaean unit in the north Kalgoorlie district from field relationships and SHRIMP geochronology, whereas the inclusion of the Panglo with this formation, although based upon well-constrained field relationships and lithological characters, remains an interpretation that requires corroborating geochronology to be confirmed.

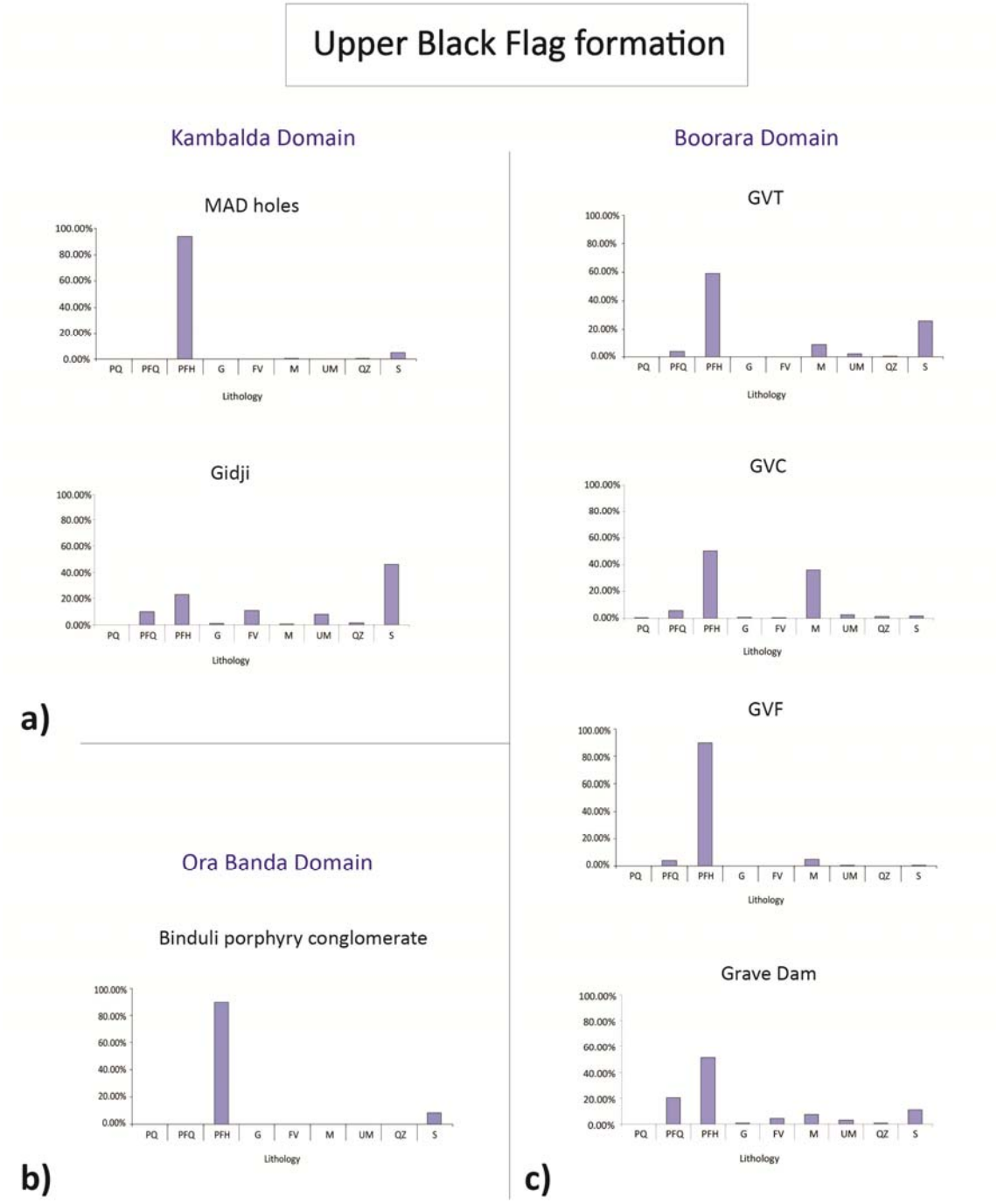

Figure 3.73 – Clast compositions of units correlated with upper Black Flag formation in each of the Ora Banda, Kambalda and Boorara Domains. Clasts types grouped as: PQ – quartz porphyry; PFQ – quartz feldspar porphyry; PFH – hornblende-feldspar porphyry ± quartz; G – granite; FV – felsic volcanic; M – mafic volcanic; UM – ultramafic; QZ – quartz; S – sedimentary. Individual chart labels refer to formations and members as documented in Chapter 3. (GVF – Golden Valley felsic; GVC – Golden Valley conglomerate; GVT – Golden Valley turbidite).

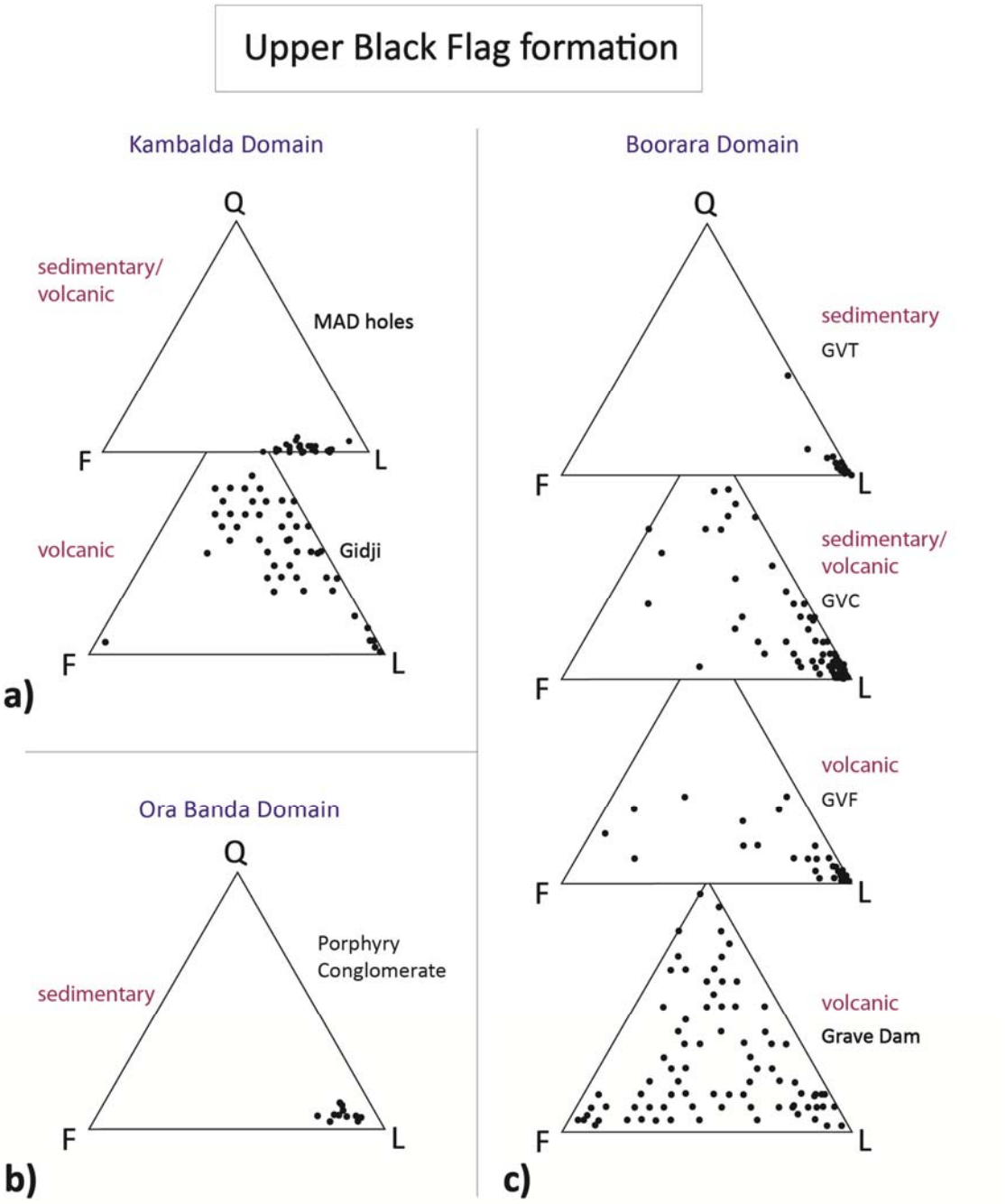

Figure 3.74 – Sandstone compositions of the units correlated with upper Black Flag formation in each of the Ora Banda, Kambalda and Boorara Domains. Individual chart labels refer to formations and members as documented in Chapter 3. (GVF – Golden Valley felsic; GVC – Golden Valley conglomerate; GVT – Golden Valley turbidite).

Two drill holes were used to determine the detailed characteristics of the Kurrawang Conglomerate from Brown Dam and Kundana North, and four drill holes from Kanowna were used to characterise the Panglo member. An important concession here is that the drill holes selected for both units intersected only parts of the basal conglomerate in each. Therefore they are useful to describe the clast compositions of conglomerate beds, and characteristics of interbedded sandstone units, but do not provide any information on the details of upper sandstone layers that make up the bulk of each unit, which were investigated in the field. These latter qualitative data are taken from field exposures that cross the entire unit and detailed petrographic description of field samples (Section 3.2.4).

Clast compositions from the Kurrawang and Panglo units show these rocks to be polymictic with abundant variety in the source rocks, whereas both have a characteristic significant proportion of equigranular granitoid pebbles and Fe-rich banded chert or banded iron formation (grouped under 'QZ' in the clast proportion graphs in Figure 3.75). A key feature of both units is the presence of foliated equigranular granitoid clasts suggesting a source region that contained uplifted and eroded deep basement rocks. In addition, the Kurrawang conglomerate commonly contains metamorphosed mafic clasts and schistose sedimentary clasts.

Sandstone compositions from interbedded sandstone lenses are quartzolithic in composition, but in general, units interbedded with conglomerate are dominantly lithic (Fig. 3.75). This feature is not representative of the bulk of the upper sandstone units of both Kurrawang and Panglo, which are characterised by coarse-grained, cross-bedded quartz sandstone/wacke; documented in Section 3.2.4 for the Kurrawang, and observed in field outcrops of the Panglo sandstones, south of Kanowna Belle. A variation between the units is that the Kurrawang basal conglomerates contain most of the occurrences of banded siliceous chert and banded iron formation pebbles, whereas in the Panglo these pebble types are restricted to layers higher in the sequence (Section 3.5.4). A further difference between the units is a high proportion of siltstone and shale in the upper parts of the Panglo.

Key to the interpretation of these youngest clastic units is the long linear distribution of each, unconformable on their eastern contacts, but constrained on their western contacts bymajor faults sub-parallel to the trend of bedding in the units and also to the trends of lithofacies internal to the unconformable clastic sequences. These relationships strongly suggest a fault control during the deposition of the late clastic sequences since the units appear to be synclinal remnants preserved in the footwall of major faults. The present distribution of the units is unlikely to be representative of original depositional basins. It is significant that the major faults, which localised the youngest Archaean strata, are also important loci of syn-deformation gold deposits and hydrothermal alteration minerals (carbonate and arsenic amongst others; Chapter 7). A full discussion of stratigraphic interpretations and correlations of the mapped

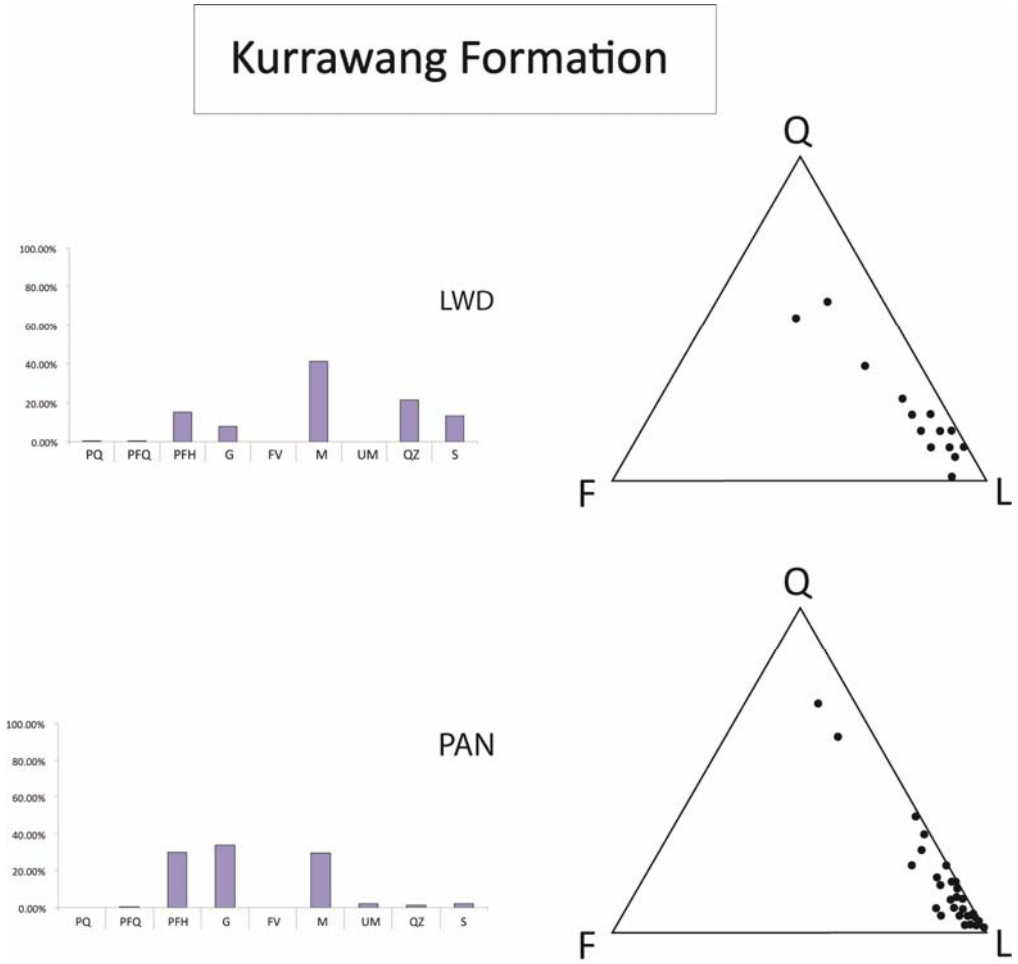

Figure 3.75 – Clast compositions of units correlated with Kurrawang Formation from the LWD drill holes at Brown Dam and the Panglo conglomerate. Clasts types grouped as: PQ – quartz porphyry; PFQ – quartz feldspar porphyry; PFH – hornblende-feldspar porphyry ± quartz; G – granite; FV – felsic volcanic; M – mafic volcanic; UM – ultramafic; QZ – quartz; S – sedimentary. Individual chart labels refer to formations and members as documented in Chapter 3.

sequences from this chapter follows documentation of SHRIMP geochronology from selected units in Chapter 4.

3.8 Summary

Formations previously bracketed as ‘Black Flag Beds’ (Woodall 1965), between the Upper Basalt unit and the unconformable late-clastic Kurrawang Formation, show complex lithofacies associations. Separation of this sequence into upper and lower Black Flag ‘formations’ is justified by the presence of a major, mappable unconformity between those upper and lower units (Fig. 3.76; 3.77). The unconformity between lower and upper Back Flag formation rocks was observed in the Ora Banda, Kambalda and Boorara domains, whereas in the Coolgardie Domain, insufficient work was done here to demonstrate its presence or absence.

In the lower Black Flag formation, felsic volcaniclastic and sedimentary sequences show similarities between domains: Ora Banda Domain (Gibson-Honman rhyodacite volcanics),

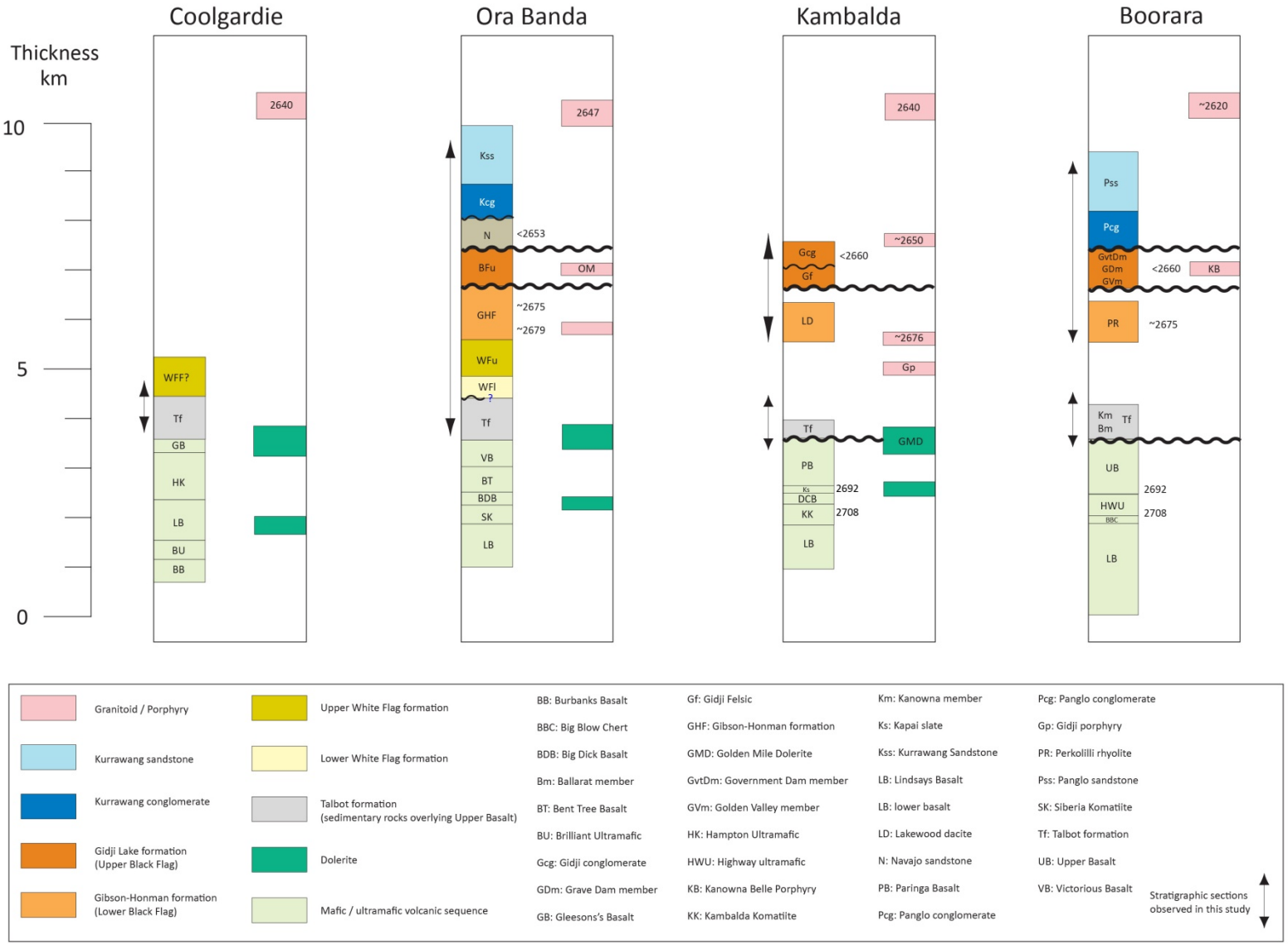

Figure 3.76 – Summary stratigraphic columns for the domains of the Kalgoorlie Terrane based on published information for the lower part of the stratigraphy and new work in this study on the upper parts of the columns. Note: new formation names (Talbot formation, Gibson-Honman formation and Gidji Lake formation) are described in detail in Chapter 4, Section 4.9.3, also Table 3.1-map pocket.

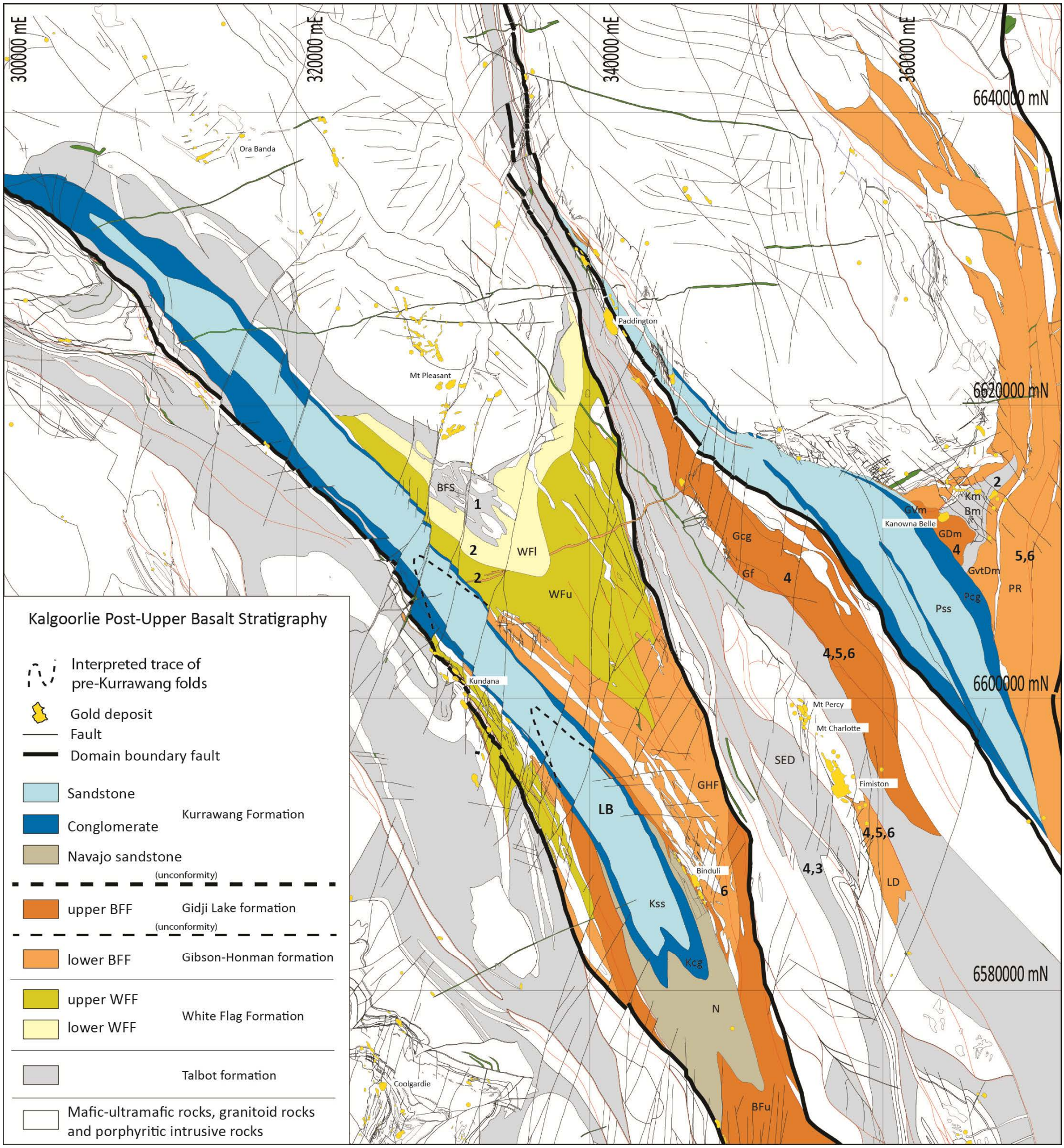

Figure 3.77 – Interpretation map of the distribution of major lithostratigraphic units (post Upper Basalt) in the Kalgoorlie area based on lithology and a consideration of the apparent structural and stratigraphic order. Labels for the units follow the legend in Figure 3.76. Unit numbers reflect the allocated sequences of Barley et al. (2002). Note: new formation names (Talbot formation, Gibson-Honman formation and Gidji Lake formation) are described in detail in Chapter 4, Section 4.9.3; also Table 3.1-map pocket.

Kambalda Domain (Lakewood dacitic volcanics), and Boorara Domain (Perkolilli rhyolite sequence; Taylor 1984). Note that in the Kanowna district, Ballarat and Kanowna coarse clastic sedimentary rocks also may be correlative with lower Black Flag formation.

In the upper Black Flag formation, coarse clastic sedimentary rocks show similarities across domains, in that they are primarily felsic-volcanic derived conglomerate and sandstone with angular unconformity on underlying rocks. The sequences are: Binduli porphyry conglomerate (Ora Banda Domain); Gidji felsic volcanic unit and Gidji Lake conglomerate (Kambalda Domain); Government Dam member, Grave Dam member dacite volcaniclastic rocks, and Golden Valley member polymictic and felsic conglomerates (Boorara Domain).

A new interpretation of the Panglo member in the Kanowna district as a Kurrawang Formation equivalent reinforces the similarity of sequences between domains, but note that this is based on interpreted contact relationships from maps, and descriptive characteristics. Further work including detrital zircon geochronology is required to support this interpretation.

Significant differences between sequences in the domains include the thick succession of White Flag Formation andesite volcanics in the Ora Banda Domain, which is not present in the other domains (but possibly present in the Coolgardie Domain). The nearest units with similar intermediate composition volcanic rocks include andesitic volcanics on the shores of Lake Yindarlgooda, and similar sequences on the northern edge of Lake Lefroy at Kambalda.

Active uplift and early deformation were important controls on the deposition of volcanic and volcaniclastic sedimentary rocks. The diversity of rock assemblages and presence of abundant unconformable volcaniclastic conglomerate sequences reflects those controls. A common characteristic of many of the coarse clastic units is a high proportion of matrix to clast and generally thick massive and disorganised beds up to the scale of several metres. These characters are typical of debris flow deposits in which the transport of clasts and matrix was contemporaneous, and is suggestive of proximal fault controls on rapid exhumation of source regions and deposition of thick coarse clastic packages.

4 Geochronology

4.1 Introduction

Factors contributing to differences between the stratigraphy of fault bounded greenstone domains in Kalgoorlie may be: (1) primary depositional (e.g. fault-controlled structural basins); (2) secondary structural (structural excision/juxtaposition in extension, or strike-slip faulting, or thrust faulting and repetition etc.); (3) non-uniform stratigraphic development across a region; or (4) a combination of these. With major faults separating stratigraphic segments, relative and absolute age determinations are critical components of correlation, and preferably target units that provide relationships via cross-cutting dykes and sills.

Relative age correlation of geologic formations is fundamental to lithostratigraphy supported by information on 'key' contacts (formation boundaries, unconformities etc.); whereas correlation by absolute age determinations requires an appropriate sample medium to provide age data for interpreting a chronostratigraphy. Key field relationships between formations include: lithological character; primary nature of contact relationships; stratigraphic way-up; structural geology; and evidence of cross-cutting and overprinting.

At Kalgoorlie, rocks younger than the mafic volcanic sequence pose particular stratigraphic problems given a localised nature of sedimentary environments with dispersed volcanic centres of variable composition (e.g. Hunter 1993). These problems include: (1) rocks overlying the Upper Basalt that are correlated across domains as Spargoville Formation; (2) definition of major formations within the 'Black Flag Group', in particular the stratigraphic position of White Flag Formation; (3) felsic volcanic rocks and unconformable conglomeratic rocks in the Gidji area, and (4) abundant conglomeratic rocks of localised provenance in the Kanowna district. Intrusions that host or cross-cut gold deposits provide local constraints on the minimum age of stratigraphy and gold deposits. Two intrusions of this type were analysed including Golden Mile Dolerite and Kanowna Belle Porphyry - both important hosts to gold mineralisation. The Owen Monzogranite batholith was analysed to compare with other gold-bearing intrusions in the district.

The objectives of this chapter include documenting new SHRIMP U-Pb zircon ages for the listed formations, cross-cutting mineralised dykes and sills; and assessing the lithostratigraphic correlations of Chapter 3 in light of the new age data. Field constraints and the rationale for analysis of each sample are presented followed by the results and interpretation. Full documentation of analytical data is presented in the Appendix and Sircombe et al. (2007).

4.1.1 Sample site selection

Sixteen samples were selected for analysis from the north Kalgoorlie district following a major geological review by Placer Dome in 2005, and a project documenting the stratigraphy of

coarse clastic rocks by Barrick Gold (Figure 4.1; Tripp et al. 2007a). The geological reviews allowed unprecedented access to broad areas of the Kalgoorlie district including outcrops, mines and exploration drill holes; and provided access to exposures of key formations and contacts. For some samples, Western Mining Corporation 1960's-era diamond drill core was accessed at the GSWA (Geological Survey of Western Australia) drill core library facility in Kalgoorlie, whereas others were collected from drill holes and outcrops generously provided by Kalgoorlie Consolidated Gold Mines and Norton Goldfields Ltd.

Nine samples were collected and documented in the field with Dr. K Cassidy, Dr. J Rogers, K. Joyce and D. Boyd; and analysed by U-Pb SHRIMP analysis of zircons at ANU (Australian National University) and Curtin University by Dr. K. Sircombe (Table 4.1; digital copy of Sircombe et al. 2007 in the appendices). The results and full documentation of age data and analytical procedures are published in a compilation volume by Sircombe et al. (2007). Analytical details for the nine samples are not reproduced here, but details of the age determinations and stratigraphic constraints are documented and discussed. One sample of Government Dam member from Kanowna was analysed by Dr. R. Squire at Curtin University, Perth. The remaining six samples were collected in the field by the author with Dr. K.H. Poulsen and Dr. J. Mortensen; and analysed by the author under the guidance of Dr. J. Wooden and Dr R. Tosdal on the Stanford University SHRIMP-RG in February of 2011 (Table 4.2).

4.1.2 U-Pb SHRIMP analysis of zircon

Six samples for U-Pb SHRIMP analysis (Table 4.2) were processed at the Pacific Centre for Isotopic and Geochemical Research (UBC) using a Rhino jaw crusher, a Bico disk grinder equipped with ceramic grinding plates, and a Wilfley wet shaking table equipped with a machined Plexiglass top, followed by conventional heavy liquids and magnetic separation using a Frantz magnetic separator.

Zircons were handpicked from non-magnetic mineral separates at SUMAC (Stanford University Micro Analytical Centre) using a binocular microscope and mounted on double stick tape on glass slides in 1 x 6 mm rows, with standards, and cast in epoxy, ground and polished to a 1 micron finish on a 25 mm diameter by 4 mm thick disc. All grains were imaged with transmitted/reflected light on a petrographic microscope, and with CL and BSE on a JEOL 5600 SEM to identify internal zircon structure (cores/rims), inclusions and physical defects such as fracturing and metamictisation effects. The mounted grains were washed with a saturated EDTA disodium salt solution or a 1N HCl solution and thoroughly rinsed in distilled water, dried in a vacuum oven, and coated with high purity Au. The mounts sat in a loading chamber at high pressure for several hours before being moved into the source chamber of the SHRIMP-RG.

On the SHRIMP-RG, secondary ions are generated from the target spot with an O_2^- primary ion beam varying from 4-6 nA. The primary ion beam typically produces a spot with a

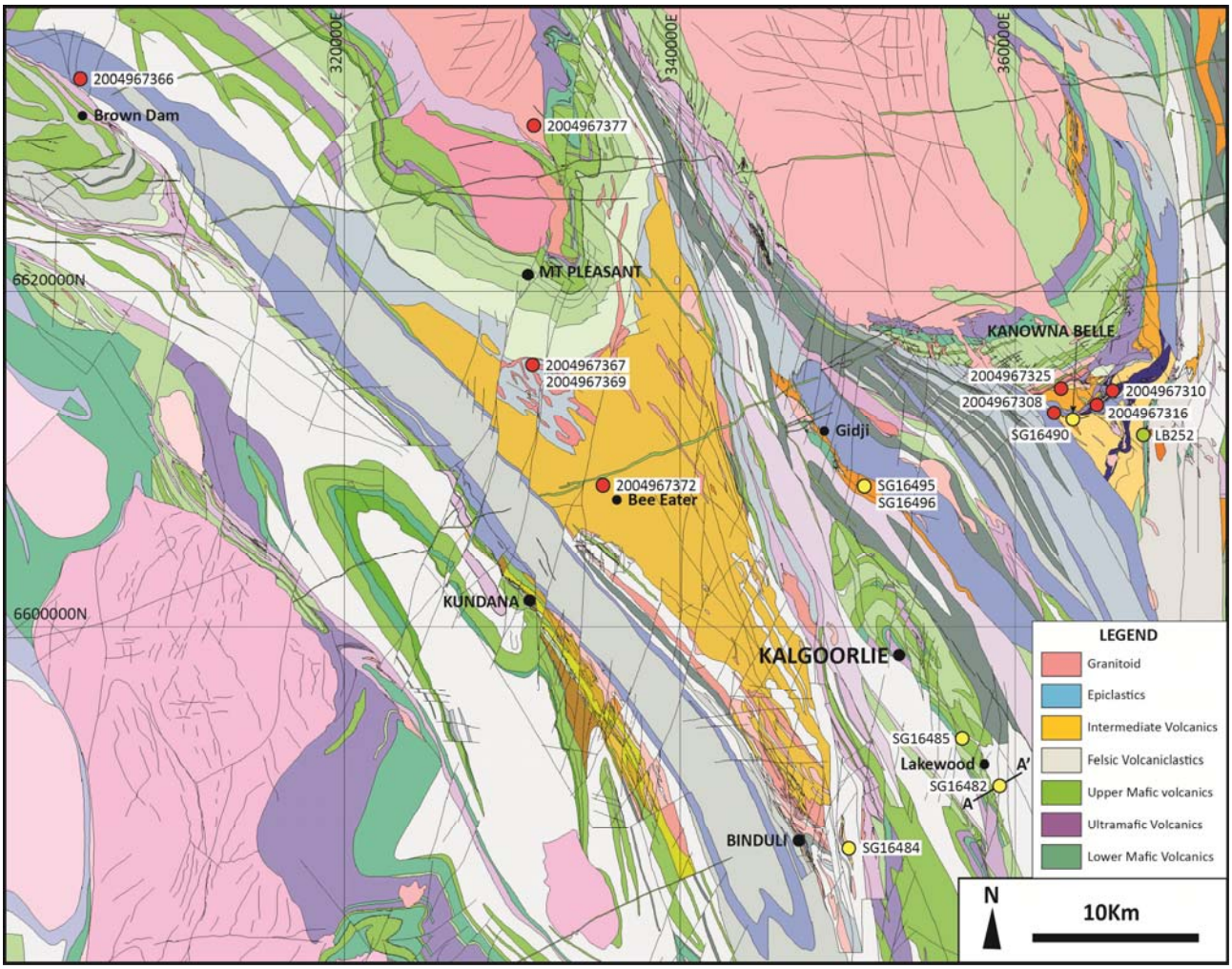

Figure 4.1 – Geological map with location of samples for SHRIMP U-PB geochronology (red marker – Sircombe et al. 2007; yellow marker – recent SUMAC samples; green marker – Curtin sample). See A0 map (Map Pocket) for detailed legend.

Table 4.1 – Details of nine samples analysed by Sircombe et al. (2007).

Sample #	District	Stratigraphy	Lith Description	Age	Error	Hole ID	Depth (m)	Easting	Northing	Purpose
2004967308 (RD35675)	Kanowna	Golden Valley Conglomerate; Kalgoorlie Sequence Stage 4	graded gravel-m.g. sandstone	**2669**	**7**	GVD97	300.85-302.00	362373.22	6612844.34	max dep age
2004967310 (RD35677)	Kanowna	Ballarat Grit ; Kalgoorlie Sequence Stage 4?	v.c.g to gravelly, crystal-rich quartz volcaniclastic	**2693**	**18**	FED02	320.00-321.00	365834.93	6614191.38	max dep age
2004967325 (RD35686)	Kanowna	Interlayered felsic volcanic-ultramafic; Kambalda Sequence	dacite	**2704**	**5**	GVD65	386.75-387.90	362794.68	6614291.82	crystallisation age
2004967316 (RD35712)	Kanowna	Ballarat Grit; Kalgoorlie Sequence Stage 4?	v.c.g to gravelly, crystal-rich quartz volcaniclastic	**2695**	**6**	GVD51	325.15-326.30	364932.48	6613351.72	max dep age
2004967372 (RD35742)	Mount Pleasant	White Flag Formation Kalgoorlie Sequence Stage 2; Bee-Eater	andesitic volcaniclastic	**2690**	**9**	WTD2	115.10-117.20	335399.76	6608534.39	max dep age
2004967366 (RD35743)	Ora Banda	Kurrawang Formation; Late Basin	sandstone	**2657**	**7**	LWD001	91.45-92.16	304171.36	6632852.92	max dep age
2004967367 (RD35752)	Mount Pleasant	Spargoville Formation; Kalgoorlie Sequence Stage 1	turbiditic volcaniclastic sandstone, silt and shale, coarser unit sampled	**2696**	**2**	THD001	123.10-136.95	331206.06	6615757.88	max dep age
2004967369 (RD35754)	Mount Pleasant	Spargoville Formation microdiorite intrusive	Porphyritic andesite sill	**2689**	**2**	THD001	157.62-168.61	331207.33	6615768.69	crystallisation age
2004967377 (RD35757)	Mount Pleasant	Owen Monzogranite Mafic granite	coarse-grained monzogranite	**2655**	**15**	Outcrop	-	331321.00	6630085.00	crystallisation age

Table 4.2 – Details of six samples analysed at SUMAC in February 2011.

Sample #	District	Stratigraphy	Lith Description	Age	Error	Hole ID	Depth (m)	GDA Easting	GDA Northing	Purpose
SG16482	Lakewood	Spargoville Formation	Coherent flow-banded dacite lava rocks	**2672**	**6**	SE3	3854ft - 3875ft	358937	6590357	crystallisation age
SG16484	Gibson-Honman Rock	Black Flag Formation	Strongly weathered feldspar-phyric dacite - single clast	**2677**	**67**	Outcrop	-	349945	6586606	crystallisation age
SG16485	SE end of Golden Mile	Golden Mile Dolerite	sericite-chlorite-carbonate-magnetite altered granophyric quartz-dolerite	**2685**	**4**	JUGD010	264.0 m - 271.5 m	356755	6593116	crystallisation age
SG16490	Kanowna Belle	Kanowna Belle Porphyry	sericite-albite-carbonate altered quartz-hornblende-feldspar porphyry	**2661**	**8**	KBD003	389.9 m - 405.0 m	363339	6612348	crystallisation age
SG16495	Gidji south end	Gidji Felsic volcanic breccia	Quartz-phyric rhyolite clast in felsic volcanic breccia	**2660**	**16**	TPDD001	587 m-587.4 m	350889	6608326	max dep age
SG16496	Gidji south end	Gidji Porphyry	Carbonate altered biotite-hornblende porphyry	**2682**	**6**	TPDD001	646 m-668 m	350889	6608326	crystallisation age

diameter of 20-40 microns and a depth of 1-2 microns for an analysis time of 9-12 minutes. For zircon, the routine procedure included a set of 9 or 10 REE, Y and Hf. The number of scans through the mass sequence and counting times on each peak were varied according to the sample age and the U and Th concentrations to improve counting statistics and age precision.

The SHRIMP-RG is designed to provide higher mass resolution than the standard forward geometry of the SHRIMP I and II (Clement and Compston 1994). This design also provides very clean backgrounds, and combined with the high mass resolution, the EDTA or HCl washing of the mount, and rastering the primary beam for 90-180 seconds over the area to be analysed before data is collected assures that any counts found at mass of $^{204}Pb^{+}$ are from Pb in the zircon and not surface contamination.

For zircon, concentration data for U, Th and all of the measured trace elements were standardized against well-characterised, homogeneous zircon standards MAD-green (4196 ppm U; Barth and Wooden 2010) or CZ3 (550 ppm U; Mazdab and Wooden 2006). Age data for zircon were standardized against VP10 (1200 Ma monzonite, southern California; Sparks et al. 2008), which were analysed throughout the duration of the analytical session after every fourth unknown. In analyses of Archaean rocks, the use of a 1200 Ma standard allows for greater resolution of $^{207}Pb/^{206}Pb$ ratios compared to younger standards such as TEMORA 471 Ma (Black et al. 2003).

Data reduction for geochronology followed the methods described by Williams (1997) and Ireland and Williams (2003), using the Squid and Isoplot MS Excel add-in programs of Ludwig (2001). Data reduction for the trace element concentrations were also done in MS Excel. Average count rates of each element of interest were ratioed to the appropriate high mass normalizing species to account for any primary current drift, and the derived ratios for the unknowns are compared to an average of those for the standards to determine concentrations.

4.2 SHRIMP analysis of rocks overlying Upper Basalt

4.2.1 Rationale for analysis

Spargoville Formation was informally named by Hunter (1993) in reference to felsic volcaniclastic and sedimentary rocks overlying the mafic and ultramafic volcanic successions throughout the Kalgoorlie district. A type locality for Spargoville Formation was not specified, but from field descriptions appears to be near the Spargo's Reward gold mine 70 km south of Kalgoorlie. In this area Hunter (1993) mapped felsic volcaniclastic rocks and interpreted proximal tuff-breccia, with lateral facies changes to distal tuffs interbedded with epiclastic sedimentary rocks. Rocks in this area were later documented as resedimented sandstone and breccia of dacite-provenance with condensed section mudrock (Brown et. al. 2001).

Spargoville Formation rocks are part of the Black Flag Series of Talbot (1934), and the 'Black Flag Beds' of several later authors most notably Woodall (1965). More recently, Krapez et al. (2000) erected a subdivision of the Black Flag Beds with a lower Spargoville Sequence that included 'Spargoville Formation' described as rhyolite and dacite lava interlayered with resedimented volcaniclastic breccia and sandstone, overlain by carbonaceous shale (Table 3.1).

Epiclastic sedimentary rocks, correlated with Spargoville Formation by Hunter (1993), outcrop extensively on the shores of White Flag Lake, 25 km northwest of Kalgoorlie, but appear to lack a significant primary volcanic component in that area, regardless of their dominant feldspathic composition and interpreted volcaniclastic provenance. These differences raise questions of the validity of a long range correlation of this unit with Spargoville Formation at its type locality, and require clarification from absolute age data. Most descriptions of the rocks overlying the Upper Basalt include a lower section of deep-water-deposited sandstone/siltstone and mudstone (e.g. Hunter 1993; Travis et al. 1971), overlain by felsic volcaniclastic and volcanic rocks. Localities at Mount Pleasant and Lakewood were selected for analysis to constrain the ages of rocks overlying the Upper Basalt, and to assess correlation of these rocks with other previously analysed units in the generalised 'Black Flag Group'.

4.2.2 Mount Pleasant - sandstone sample

In the Mount Pleasant district (87 km north of the Spargoville type locality), rocks overlying the Upper Basalt correlated as Spargoville Formation (Hunter 1993) are plane-bedded, deep-water-deposited, turbiditic, graded quartzofeldspathic sandstones with shale and mudstone lacking a felsic volcanic component. Normal depositional contact relationships with Upper Basalt (Section 3.3.1) are unequivocal; hence, a sample of the basal sandstone was selected in an attempt to obtain a maximum depositional age for those rocks.

Sample 2004967367 (Fig. 4.1; Table 4.1) is a composite of sand-sized sections selectively cut from interbedded sandstone-siltstone-mudstone turbidites in diamond drill hole THD001

from 123.1 m-136.95 m at the ‘Three In Hand’ prospect, 6 km south of Mount Pleasant (Fig. 4.2). Drill hole THD001 is 303 m deep and intersected the sandstone / Upper Basalt contact at 218.2 m down hole (Fig. 4.3). The sample is medium- to coarse-grained sandstone comprising altered angular and rare sub-rounded quartz, feldspar and lithic clasts, from at least 166 m above the Upper Basalt contact. Given the deformed and thrust-stacked nature of the sedimentary package, 166 m is not a stratigraphic thickness. Way-up in the THD001 sandstones is up-hole and to the south as for rocks outcropping in the vicinity of the drill hole, which was drilled towards the north into the limb of a southeast plunging syncline (Fig. 4.2). Details of zircon yield and morphology are presented in Sircombe et al. (2007).

Fifty-six analyses of 52 zircon grains produced concordant results with the exception of fourteen analyses that were >5% discordant. Mixture modelling of the concordant distribution yielded three model components at 2696±2 Ma, 2670±4 Ma and 2638±5 Ma (Sircombe et al. 2007). The middle age cluster at 2670±4 Ma is interpreted by Dr. Sircombe as an accidental analytical mixing of the older and younger end member ages.

The youngest 2638±5 Ma age cluster is dispersed and interpreted as affected by ancient Pb-loss, some apparent clustering of the data is interpreted as an artefact of that Pb-loss event. In terms of possible source rocks for the sandstones in THD001, there is no geologically reasonable source at that ~2638 Ma age. The sandstones are at the base of a sequence overlain by andesitic volcanic rocks older than 2638 Ma (Section 4.5), and that andesitic package is unconformably overlain by the Kurrawang Formation (also older than 2638 Ma; Section 4.6). The older end member age of 2696±2 Ma represents the dominant age cluster in the analyses and is interpreted as the maximum depositional age of the sandstones, suggesting deposition after 2694 Ma.

4.2.3 Mount Pleasant - porphyritic microdiorite sample

An intrusive corridor between the Black Flag and Royal Standard faults extends from Bent Tree Basalt up section to the White Flag Formation, with all rocks in this corridor extensively intruded by hornblende-feldspar porphyritic microdiorite sills and dykes (Fig. 4.2). ‘Spargoville Formation’ sedimentary rocks (Hunter 1993) on the northwest edge of White Flag Lake are intruded by these same microdiorite sills and also quartz-feldspar porphyry dykes (Figure 4.2). A sample of porphyritic microdiorite was selected for analysis to provide a minimum age on the deposition of the rocks it cuts.

Sample 2004967369 (Table 4.1), is a 11 m composite taken from 157.62 m-168.61 m in diamond drill hole THD001 (Fig. 4.2; Fig. 4.4). The sample is a weakly-altered hornblende-feldspar porphyritic microdiorite intrusion with sharp contacts that appear sub-parallel to bedding in the sedimentary wallrocks.

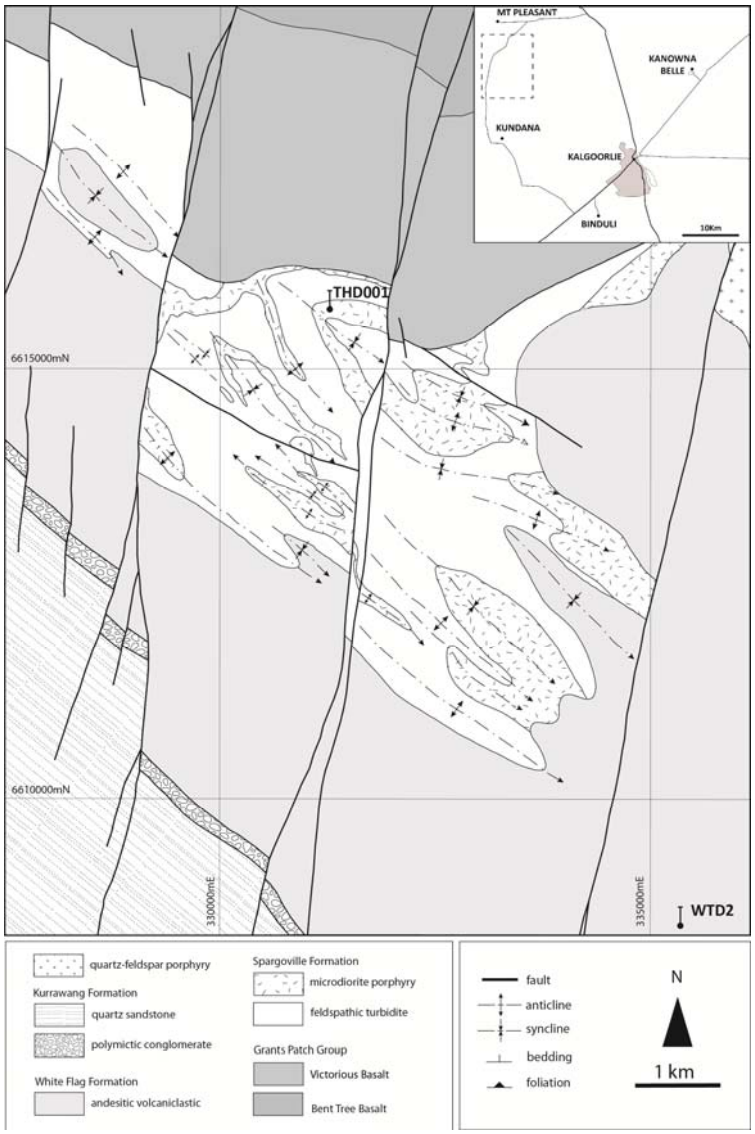

Figure 4.2 – Geology and location of drill holes THD001 sampled in sedimentary rocks overlying Upper Basalt at Mount Pleasant; and drill hole WTD2 sampled for White Flag Formation.

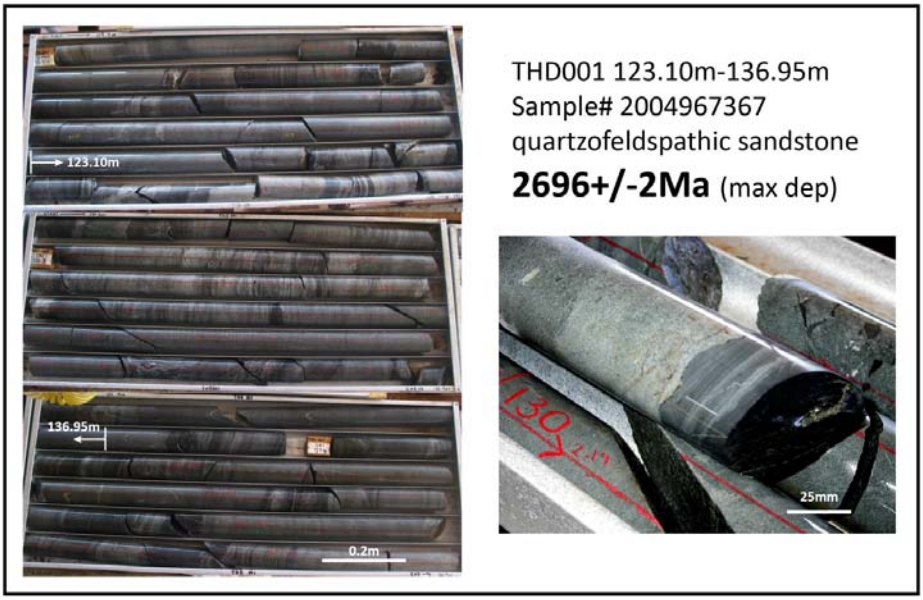

Figure 4.3 – Core photos of sandstone analysed from sample# 2004967367.

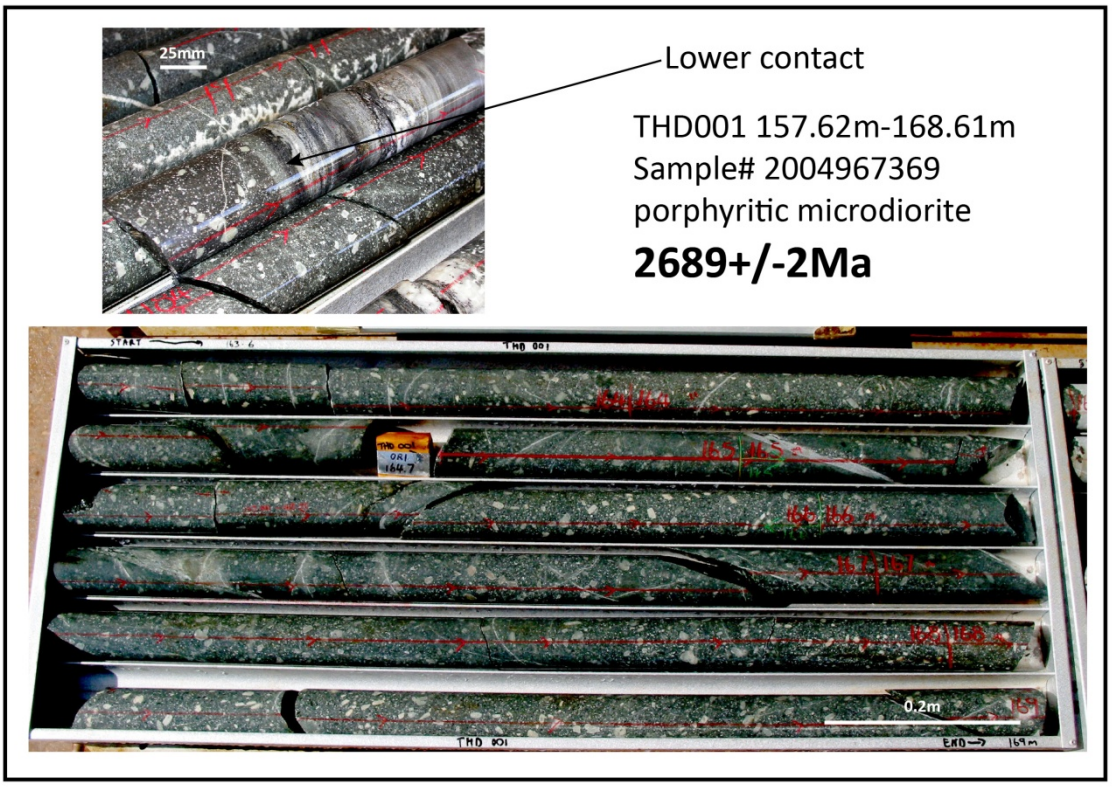

Figure 4.4 – Core photographs of material sampled from microdiorite intruded into sedimentary rocks.

At a map scale the microdiorite is part of a suite of sills that intruded sedimentary bedding prior to regional folding (Fig. 4.2). Details of zircon yield and morphology are presented in Sircombe et al. (2007).

Forty-nine analyses from 44 zircon grains produced concordant results with the exception of 11 analyses that were >5% discordant. A number of zircon grains displayed concentric rims on zoned cores, with analyses of rims and cores from a few grains demonstrating a significant difference in age: Grain #24: core 2689±5 Ma, rim 2652±5 Ma; and Grain #6: core 2687±4 Ma, rim 2668+/-5 Ma. Despite core/rim age differences in some grains, data populations from the bulk of core / rim analyses overlap with no statistical justification for subdividing the calculated ages. High U content in concentric rims caused Pb-loss and may have contributed to the difficulty in subdividing the two populations.

The majority of core/rim analyses shows age correspondence between many core/rim pairs indicating two very close magmatic events. A weighted mean $^{207}Pb/^{206}Pb$ age of 2689±2 Ma (MSWD = 1.16, 95% conf.) is interpreted as a best approximation for the crystallisation age of the intrusion.

4.2.4 Lakewood - flow banded dacite sample

At Lakewood (southern end of the Golden Mile), black mudstones overlie the Golden Mile Dolerite. The mudstones are in turn overlain by dacitic volcanic rocks that were previously

correlated with Spargoville Formation (Hunter 1993; Fig. 4.1; Fig. 4.5). The Travis et al. (1971) Lakewood cross-section is updated from re-logged Western Mining Corporation deep diamond drill holes SE3 and SE4 preserved at the GSWA Core Library in Kalgoorlie (Fig. 4.5). Dacitic volcanic and volcaniclastic rocks overlying black mudstones include volcaniclastic tuff-breccia, flow-banded dacite lava rocks, hyaloclastite, and locally intraformational(?) sedimentary units. Coherent flow-banded dacite in the upper part of SE3 was sampled to provide a volcanic crystallisation age on the dacitic volcanic sequence (Fig. 4.6).

Sample SG16482 (Table 4.2) is a composite sample from 186.6 m-193.2 m (622 ft - 644 ft) down hole in diamond drill hole SE3. The rock is a light grey porphyritic dacite with 3% 5-10 mm sericite-altered feldspar phenocrysts set in a fine-grained groundmass of felted plagioclase and glass. Broad sections through drill hole SE3 show primary volcanic textures with flow-banding, jigsaw breccia and wispy to angular clast shapes indicating that these were proximal volcanic deposits. The porphyritic dacite sampled may be from a syn-volcanic intrusion or primary dacite lava within the volcanic package.

A low zircon yield from this sample (39 zircons) produced 14 acceptable zircons when screened for quality (Fig. 4.7a). Under transmitted light, the zircons are clear, pink coloured, elongate subhedral-prismatic crystals with 250 µm average length; and of good quality with minimal fracturing. The zircons show well-preserved concentric magmatic zoning in CL and BSE images (Fig. 4.7b). Under CL the zircons are generally dark, indicating metamictisation (damage to the crystal structure from the natural decay of U and Th). Rare internal inclusions and cores were noted in a few grains with variable metamictisation effects including radial fracturing on grain margins and generally dark murky images under CL. Spot number 482-13 displays radial fracturing on the margins of a preserved inherited core overgrown by concentric banded magmatic zircon (Fig. 4.7b). Recrystallisation is predominant in many of the zircon grains with wholesale recrystallisation and/or variable preservation of internal growth bands (Fig. 4.7b). Sector recrystallisation is evident in some grains with sharp truncation of pre-existing growth zoning.

Fourteen analyses from 14 grains were completed over a single analytical session. A weighted mean age for all analyses is 2673±5 Ma (MSWD = 1.2). Two analyses with greater than 1% common Pb or >5% discordance are excluded from the age calculations, in grains with excessive cracking and dark zones in BSE images that indicate low-U parts of the crystal. The weighted mean age of the remaining 12 analyses is 2673±5 Ma (MSWD = 1.16). A best fit discordia line for the twelve analyses defining a recent Pb-loss trend, has an upper intercept at 2672±6 Ma (MSWD = 1.3; Fig. 4.7c). The majority of analyses were from variably recrystallised, oscillatory-zoned magmatic zircon; hence, 2672±6 Ma is interpreted as the magmatic crystallisation age of the dacite.

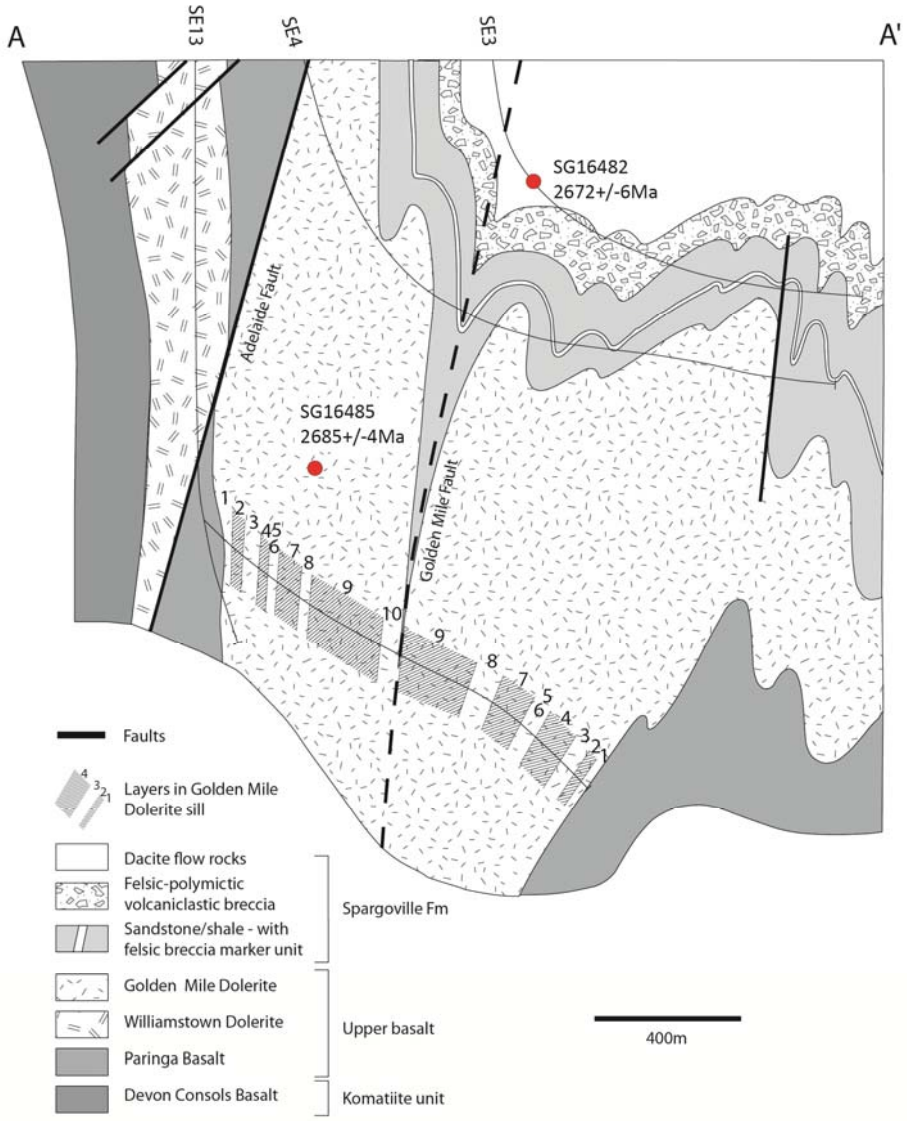

Figure 4.5 – Geological cross-section at Lakewood, south end of the Golden Mile modified from Travis et al. (1971). Line of section is indicated on Figure 4.1, view is to the northwest. Sample SG16485 is projected from 3.5 km off-section to the north (see Fig. 4.1).

Figure 4.6 – Flow-banded dacite sample SG16482 from 186.6 m-193.2 m (622 ft - 644 ft) in Western Mining Corporation drill hole SE3.

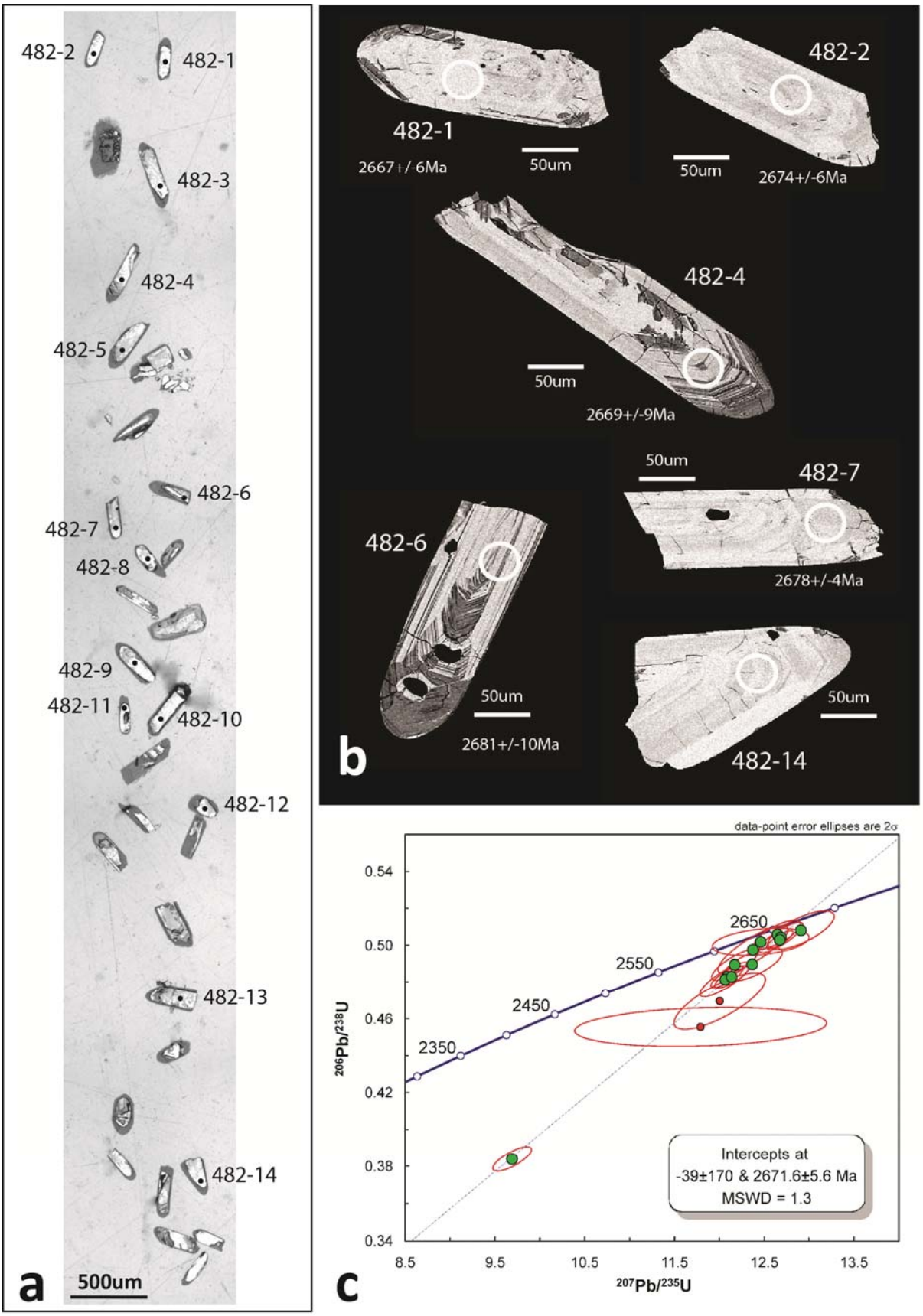

Figure 4.7 – a) Reflected light photograph of sample SG16482 with SHRIMP spot locations; b) BSE images of selected zircons with SHRIMP spot locations and age determinations; c) Concordia plot of all zircon analyses from sample SG16482, rejected analyses in red point markers.

4.3 Black Flag Formation SHRIMP analysis

4.3.1 Rationale for analysis

'Black Flag Formation' (Krapez et al. 2000) is a recent designation given to part of a ‘Kalgoorlie Sequence’, which incorporated lower Black Flag and upper White Flag Formations. The rocks included with Black Flag Formation span wide areas and include thick sections of the units overlying Upper Basalt. Black Flag Formation was described as unconformity-bounded volcaniclastic and epiclastic turbidites with intervening condensed sections of black shale, with minor rhyolite-dacite pyroclastics and lavas (Krapez et al. 2000). A key issue for the stratigraphy in the north Kalgoorlie district is correlation of disconnected sections of felsic volcaniclastic and epiclastic rocks, given very similar descriptions between the Spargoville and Black Flag Formations. Two areas were selected to better define the age of Black Flag Formation rocks at Gidji and Gibson-Honman Rock.

4.3.2 Gidji - rhyolite clast in volcanic breccia sample

A fault-bounded section in the Gidji area ~13 km north of Kalgoorlie (Fig. 4.1; Fig. 4.8), has an east-younging sequence of basal ultramafic volcanic rocks; rhyodacitic volcanic and volcaniclastic rocks; and an unconformable overlying sedimentary succession of quartz-rich sandstone, and pebble conglomerate with rare, thin rhyodacitic volcaniclastic interbeds. The Gidji sequence is part of a tightly thrust-faulted complex of greenstone segments, and its stratigraphic position is enigmatic given a faulted western margin (Gidji Thrust) and an eastern contact against a major domain boundary fault (Bardoc Tectonic Zone).

Detailed descriptions of the stratigraphy and map-scale patterns are outlined in Section 3.5.2 indicating a possible relative age distinction between older felsic volcanic rocks and younger coarse clastic sedimentary/volcanic rocks. An age of 2666±6 Ma (Hand 1998) for a thin rhyodacite volcaniclastic unit in the Gidji conglomerate led Krapez et al. (2000) to correlate the Gidji rocks with Black Flag Formation. The rhyodacite unit analysed by Hand (1998) and reported in Krapez et al. (2000) is mapped as internal to unconformable polymictic conglomerate/sandstone, and is therefore younger than the underlying Gidji felsic volcaniclastic sequence. Determining the age of the felsic volcaniclastic sequence at Gidji is a critical step in correlating these rocks with the surrounding felsic volcanic successions.

Sample SG16495 (Table 4.2) is taken from 587.0 m-587.4 m down hole in diamond drill hole TPDD001. Drill hole TPDD001 intersected a sequence of coarse clastic felsic volcanic and volcaniclastic rocks of rhyolite-dacite composition, with intercalated fine-grained sedimentary turbiditic sandstone-siltstone and porphyritic intrusive rocks (Fig. 4.8). Felsic volcaniclastic breccia/conglomerate from 549 m - 605 m contains clasts of rhyolite with banded/welded textures, porphyritic quartz-eye rhyolite and fine-grained angular clasts of felsic volcanic rock.

A 0.4- m long clast was selected for analysis to provide a source age on the felsic breccia. The rock is coherent, massive quartz-phyric rhyolite with >10% angular to rounded, embayed quartz phenocrysts set in a finely granular groundmass of quartz and feldspar. Moderate sericitic alteration and a weak foliation have affected the rock.

A poor zircon yield from this sample produced 19 grains of which 12 were acceptable for SHRIMP analysis after quality screening. In transmitted light the zircons are light pink, elongate, euhedral prismatic crystals of average 30-50 µm x 150 µm with well preserved magmatic oscillatory zoning in about half of the grains. Patchy to complete recrystallisation is evident in BSE images, whereas in CL the grains are dark grey indicating strong metamictisation with minor magmatic zoning still visible. Moderate to strong fracturing has affected the zircons; hence SHRIMP spots were targeted to avoid fractures and areas of obvious Pb-loss.

Twelve analyses from twelve grains were carried out during an initial session and a further three analyses were attempted on grains 495-2, 495-3 and 495-4 during a second session for a total fifteen analyses, after the mount was reground to accommodate very large zircons in another sample on the same mount. A weighted mean age for all analyses is 2661±15 Ma (MSWD = 6.8). Two analyses had high-U, one analysis had very high common-Pb, and seven analyses were >5% discordant. A weighted mean of eight analyses <5% discordant is 2672±15 Ma (MSWD = 2.7; 95% conf.).

The high MSWD for the total data set calculation suggests more than a single population may be present in the dataset. Two possible groups are visible from the concordia plot. A discordia line of best fit for eight analyses has an upper intercept at 2682±8 Ma (MSWD = 0.2; Fig. 4.9c), with the group defining a recent Pb-loss trend. One concordant analysis (495-4; Fig. 4.9b) returned an age of 2663±9 Ma, with three other analyses in this sub-group forming a separate discordia line of best fit with an upper intercept of 2660±16 Ma (MSWD = 0.49; 95% conf.; Fig. 4.9c).

Poor quality and extensive recrystallisation of the zircons in SG16495, added to the generally low zircon yield, make these results tentative at best. Field relationships suggest that the Gidji felsic volcaniclastic rocks are stratigraphically younger than the ultramafic volcanic rocks to the west; whereas epiclastic sedimentary rocks in the Gidji conglomerate (~2666±6 Ma, Hand 1998) show a well demonstrated map-scale unconformable relationship with the Gidji felsic volcaniclastic and underlying rocks (confirmed by younging reversals across the contact). With these constraints in hand it is likely the 2660±16 Ma upper intercept age represents the crystallisation age of the rhyolite clast, which is in error of the previously analysed rhyodacite volcaniclastic rock in the Gidji conglomerate by Hand (1998). Given strong recrystallisation and metamictisation of the zircons, if 2660±16 Ma represents the crystallisation age of the sampled rhyolite clast, this is a reasonable (but tentative) estimate of the maximum depositional age of

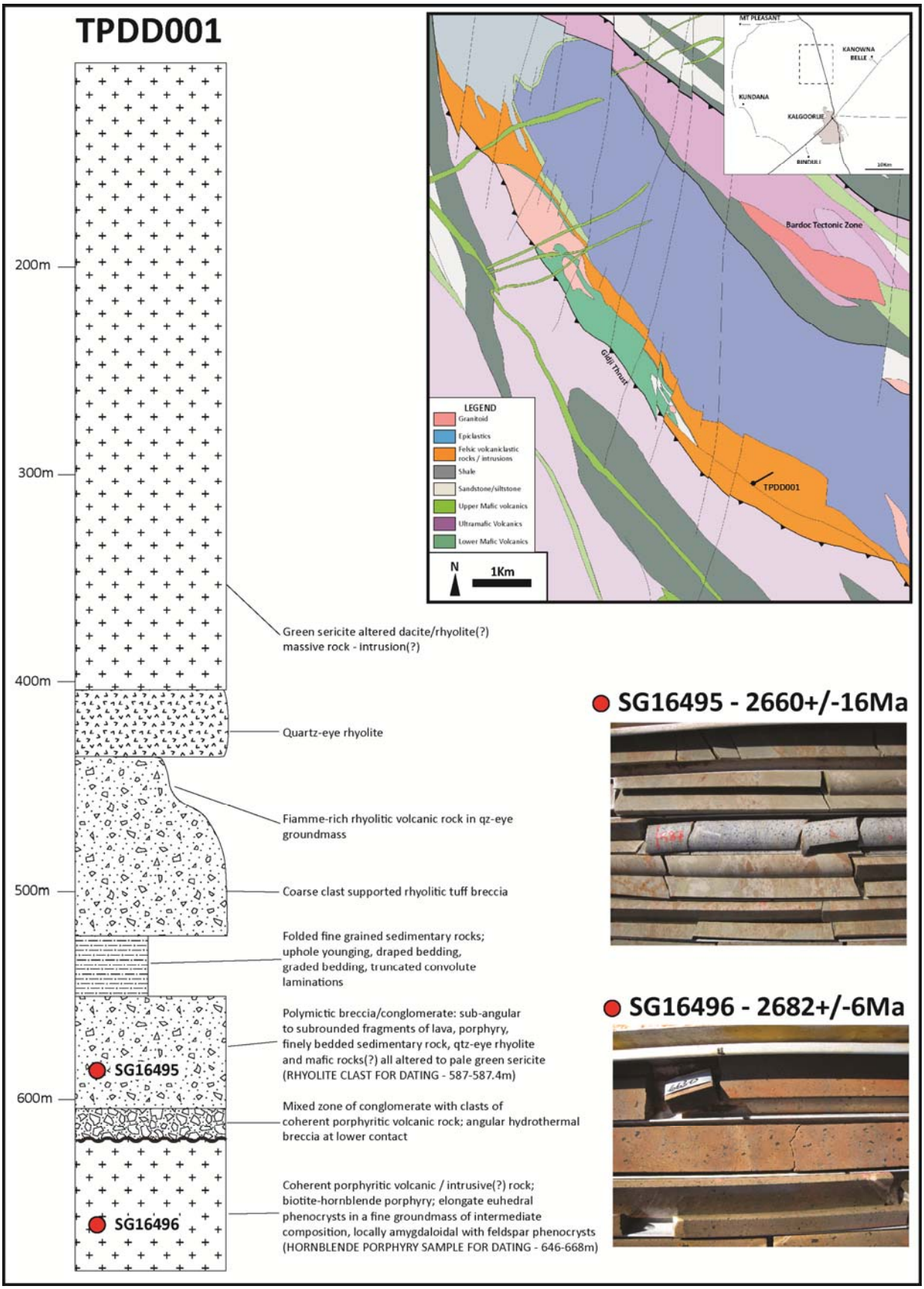

Figure 4.8 – Geology of the Gidji area with location of drill hole TPDD001; graphic log of drill core (starts at 103 m); photographs of rocks sampled for SHRIMP analysis

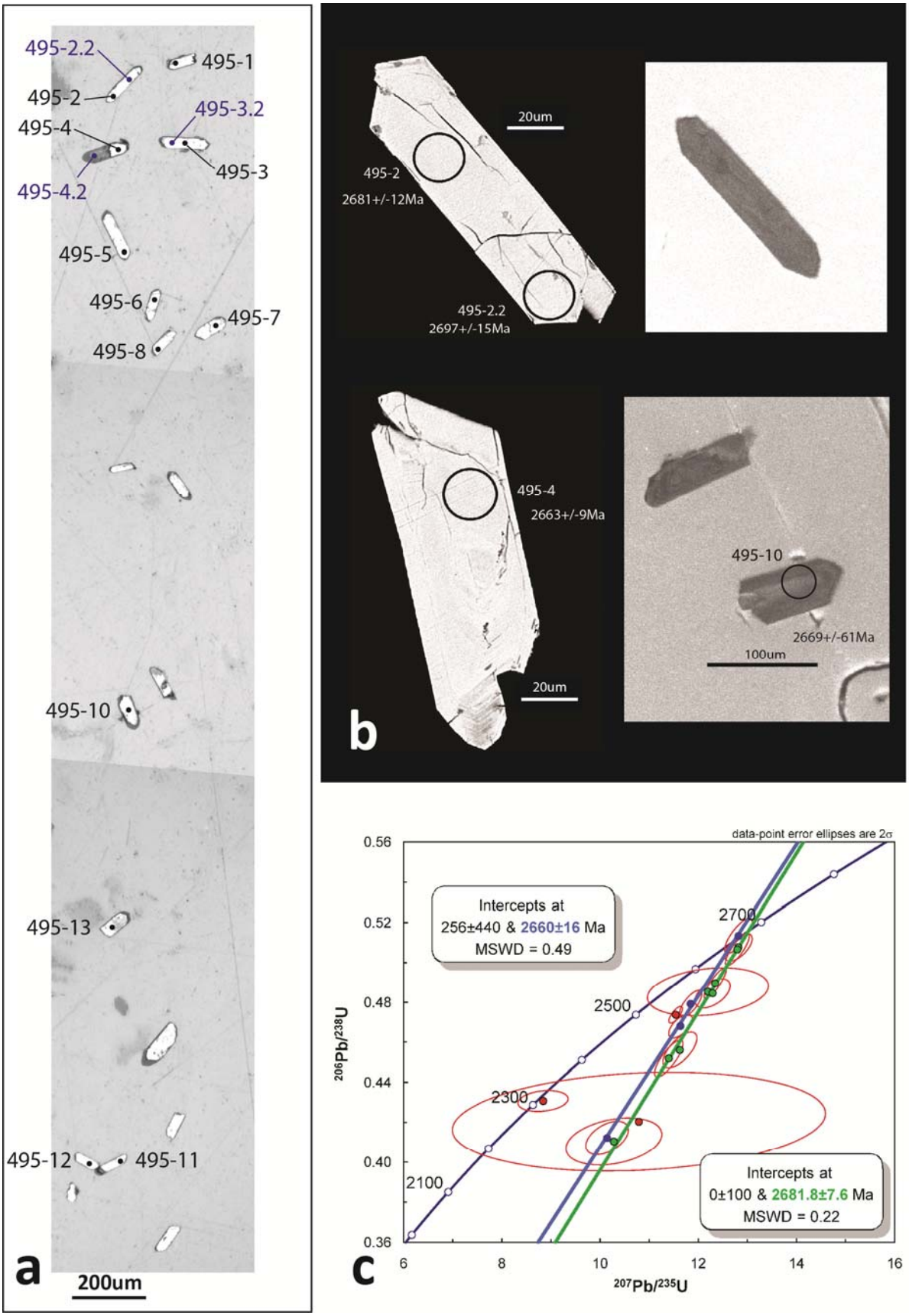

Figure 4.9 – a) Reflected light photograph of sample SG16495 with SHRIMP spot locations; b) BSE and CL images of selected zircons with SHRIMP spot locations and age determinations; c) Concordia plot of all zircon analyses

the volcaniclastic package. The 2682±8 Ma may record inheritance from xenocrystic cores of the zircons, but it is stressed that the quality of the CL/BSE images was too poor to recognise core/rim relationships.

4.3.3 Gidji - hornblende-feldspar porphyry sample

Porphyritic intrusive rocks of andesite to dacite composition make up a considerable portion of the volcaniclastic sequence at Gidji as revealed from widely spaced deep diamond drill holes. The surface geology map compiled from outcrop and bottom-of-hole shallow RAB drill logs (Fig. 4.8) fails to show these intrusions since most of the logs record felsic breccia and only small disconnected occurrences of coherent porphyritic rocks. This discrepancy may be an artefact of poor sample quality in the RAB drill holes leading to incorrect interpretations of the rock type, or alternatively an irregular distribution such that dykes and stocks present at depth may not outcrop extensively in the map area. Nonetheless, drill hole TPDD001 intersected in a thick section of hornblende-feldspar porphyry with polymictic conglomerate at the upper contact, which contains clasts of that coherent hornblende-feldspar porphyry. The contact zone is a 0.9 m-thick angular breccia with quartz-carbonate infill, which may be intrusive in nature; hence, a sample of the porphyry was selected for SHRIMP analysis to determine relative age relationships with the overlying felsic volcaniclastic / conglomerate rocks.

Sample SG16496 (Table 4.2) is taken from 646.0 m-668.0 m down hole in diamond drill hole TPDD001 (Fig. 4.1; Fig. 4.8). A 22 m composite sample of quartered drill core was selected from the least veined and altered parts of the intrusion: of this composite a 50% split was crushed and processed for zircon separation. The rock is a pink-coloured, coherent hornblende-biotite porphyritic andesite-dacite intrusion, with 5-7% dark euhedral flow-aligned phenocrysts of hornblende and minor biotite, set in a fine-grained groundmass. The pink colouration is from strong dolomite-hematite alteration of the groundmass, which is locally vesicular with xenoliths of microcrystalline igneous rock.

A poor zircon yield produced 11 zircons of which eight were selected for analysis after quality screening. In transmitted light the zircons are dark, rounded to broken fragments with rare examples of euhedral crystal faces in 50-200µm diameter equant grains. Images of CL and BSE show some grains with well-preserved oscillatory magmatic zoning and others with extreme metamictisation effects with radial fracturing and extreme damage to the crystal structure with abundant inclusions, and partial to complete recrystallisation (Fig. 4.10a-b). SHRIMP spots were targeted at the best preserved, zoned parts of the crystals.

Eight analyses from eight zircons were completed during a single session. Four analyses were excluded from age calculations due to high U (1621-5715 ppm). The weighted mean age of the remaining four analyses is 2682±6 Ma (MSWD = 1.5; Fig. 4.10c). The four analyses plot close to concordia indicating minimal recent Pb-loss and, considering the very low zircon yield

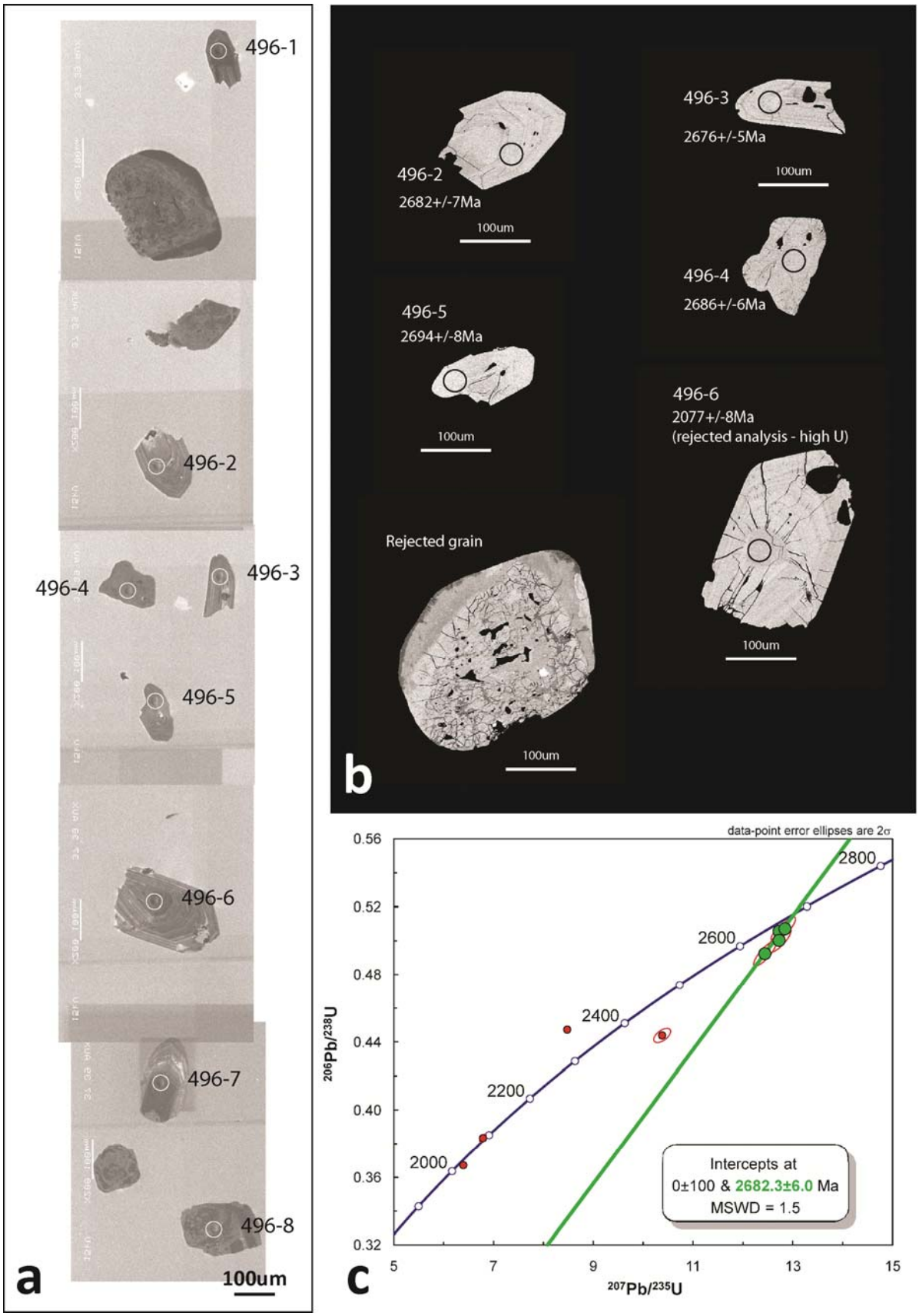

Figure 4.10 – a) CL composite image of sample SG16496 with SHRIMP spot locations; b) BSE images of selected zircons with SHRIMP spot locations and age determinations, including highly metamict grains excluded from age calculations; c) Concordia plot of all zircon analyses

and few analyses, provide a very tentative crystallisation age of the intrusion.

4.3.4 Gibson-Honman Rock - dacite clast in volcanic breccia sample

Gibson-Honman Rock locality (Fig. 4.1; Fig. 4.11) exposes a layered sequence of rhyodacite volcanic and volcaniclastic rocks with intercalated fine mudstone, conglomerate and felspathic sandstone (Section 3.3.3). The presence of these rocks heralds a change from deep water deposited sandstone and mudstone, exposed to the north (down-section) of Gibson-Honman Rock (Fig. 4.11a), to renewed felsic volcanism. Proximal felsic volcanic rocks at this position mark a significant change from the thick sandstone-mudstone deposits that typify rocks above the White Flag Formation, exposed in the Binduli mine area. The stratigraphy in the area from White Flag Lake to Binduli is not well known and is only apparent in exploration drill holes. Relationships at Goldilocks (Kundana South; Section 3.4) suggest a conformable progression between the White Flag Formation and the overlying Binduli sequence. Volcaniclastic dacite conglomerate at Gibson-Honman rock was analysed previously by Krapez et al. (2000) with an interpreted syn-eruptive depositional age of 2676+/-5 Ma. An attempt was made to re-analyse the unit to better understand the age of the Gibson-Honman sequence.

Sample SG16484 (Table 4.2) is taken from a single dacite boulder clast plucked from the outcrop at Gibson-Honman Rock (Fig. 4.1; Fig. 4.11b). On cutting, the boulder showed appreciable weathering in a thick rind on the outer margin of the clast with a relatively fresh interior (Fig. 4.11c). Rock from the centre of the clast was selectively cut from the sample to provide a less weathered sample for zircon separation. The rock is grey brown feldspar-phyric dacite porphyry with fine hornblende needles in a fine-grained groundmass displaying weak brown spotting from carbonate alteration.

A moderate zircon yield produced 52 zircons of which 14 were selected for analysis. In transmitted light the zircons are dark red, large equant euhedral crystals of 100 µm - 250 µm diameter. Under CL the grains show well-preserved oscillatory magmatic zoning, with weak sector recrystallisation and rare examples of xenocrystic cores (Fig. 4.12a, b). The typical appearance of the crystals has alternating light and dark growth banding indicating significant zones of high-U and potential Pb-loss. Initial analyses confirmed the extreme recent Pb-loss which is probably due to poor quality of the weathered sample (see also Clout 1991).

Fourteen analyses of 14 grains were completed during a single session. All analyses suffered from very high levels of common Pb and produced very poor data; however, a coherent group plots roughly along a discordia line of best fit with an intercept point at 2677±67 Ma (MSWD = 0.32; Fig. 4.12c). This intercept age, while being close to the 2676±5 Ma age of Krapez et al. (2000) is unusable due to the large uncertainty, and reflects a poor choice of sample medium. The best estimate of the Gibson-Honman Rock rhyodacite breccia remains that previously reported by Krapez et al. (2000).

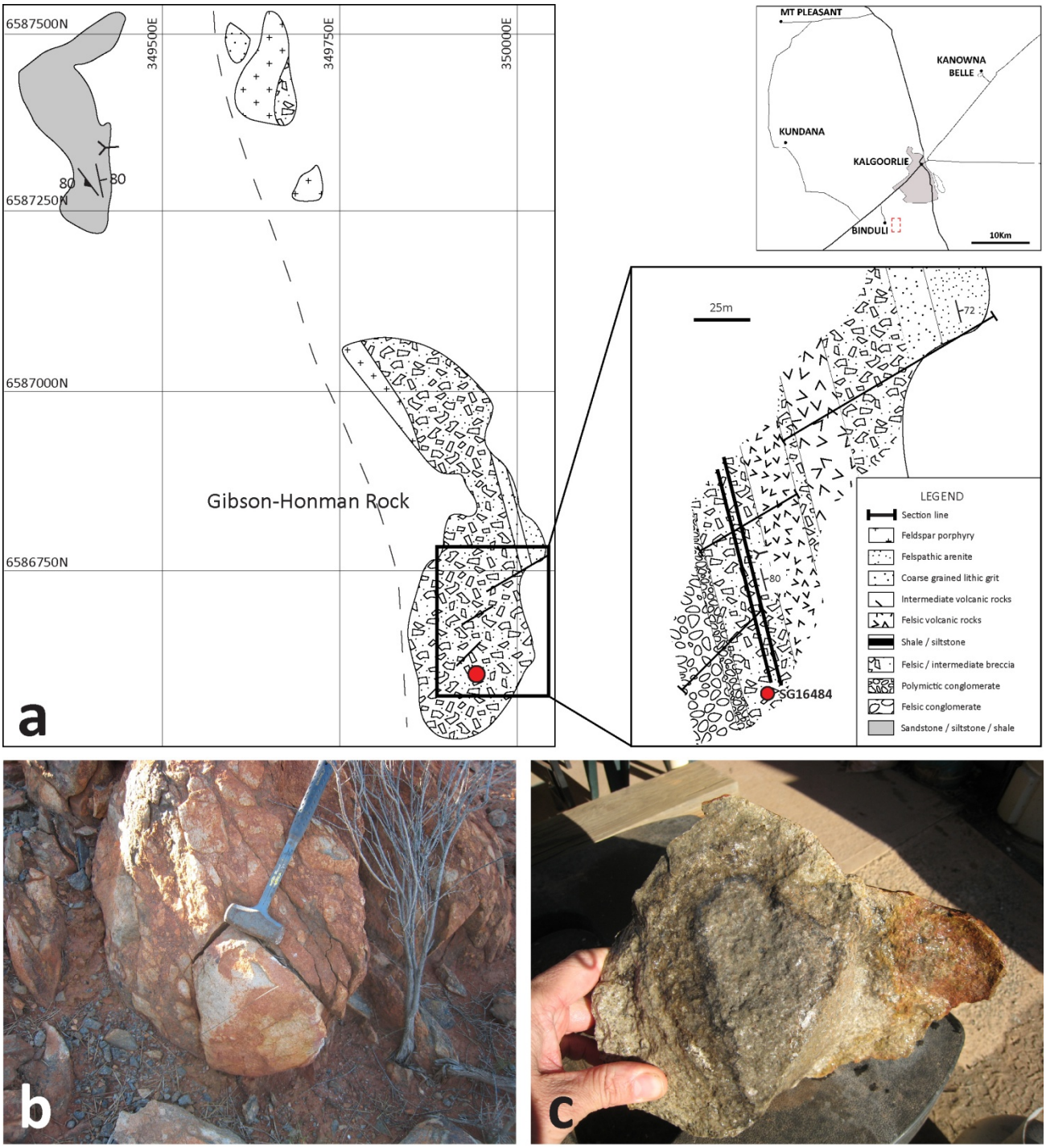

Figure 4.11 – a) Location of SHRIMP sample SG16484 on geology of Gibson-Honman Rock locality; b) outcrop photograph of single dacite boulder removed from the outcrop for analysis; c) broken face of boulder from previous photograph showing strongly weathered rind. Freshest parts of the sample were selectively cut and removed for zircon separation.

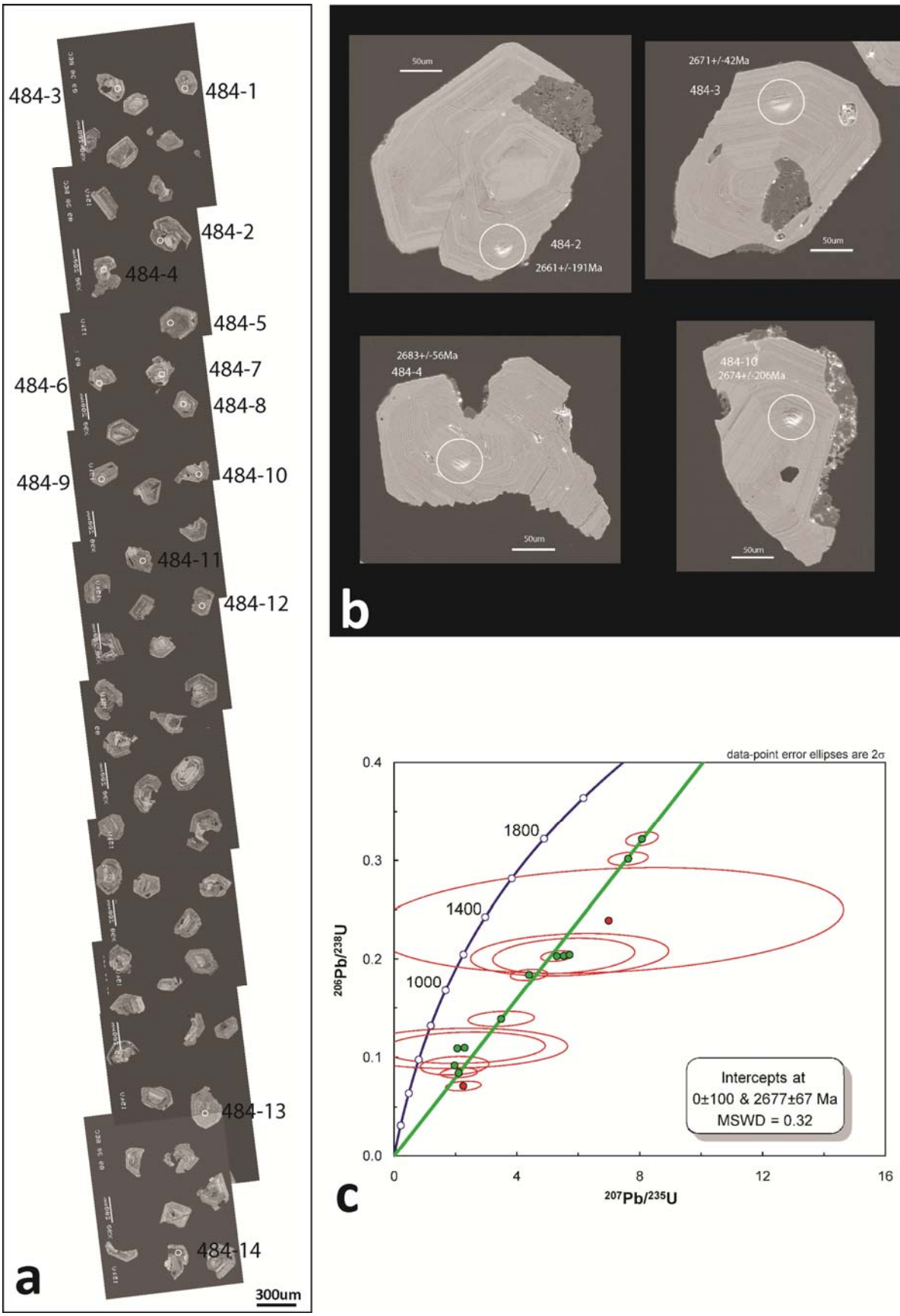

Figure 4.12 – a) BSE composite image of sample SG16484 with SHRIMP spot locations; b) BSE images of selected zircons with SHRIMP spot locations and age determinations; c) Concordia plot of all zircon analyses with extreme recent Pb-loss reflecting poor sample quality.

4.4 White Flag Formation SHRIMP analysis

4.4.1 Rationale for analysis

The revised stratigraphy of the Black Flag Group (Krapez et al. 2000) presented a lower Spargoville Sequence and an upper Kalgoorlie Sequence. The upper Kalgoorlie Sequence was interpreted with two formations: a lower Black Flag Formation overlain by White Flag Formation. Well-preserved outcrops in the field section at White Flag Lake and diamond drill core from Mount Pleasant and Kundana indicate a continuous sequence from sedimentary rocks correlated by Hunter (1993) with 'Spargoville Formation', up section into White Flag Formation andesitic conglomeratic and proximal andesitic volcanic rocks. The lower andesite dominated conglomerate at the base of White Flag Formation may indicate an unconformable lower contact.

South of the White Flag Lake section (up stratigraphy) the sequence includes deep water deposited sandstone/siltstone and shale overlain by the Binduli sequence of felsic-intermediate volcanic rocks (correlated with the Black Flag Formation by Krapez et al. 2000). To the south of Binduli the sequence continues (up section) with deep water deposited sandstone-siltstone and shale, and upper units of felsic volcaniclastic rocks exposed to the west of the New Celebration mining centre (Hunter 1993; Griffin 1990). The proper stratigraphic position of White Flag Formation is therefore controversial, since a significant thickness of sedimentary and volcanic rocks appears to sit stratigraphically above it.

4.4.2 White Flag Lake - andesitic volcanic breccia sample

Andesitic conglomerate was sampled from the base of the White Flag Formation in drill hole WTD2 (Fig. 4.2; Fig 4.13), which is located along strike from the lower andesitic conglomerate. Sample 2004967372 (Table 4.1) is a 2.1 m composite of quartered drill core cut from andesitic volcaniclastic conglomerate in diamond drill hole WTD2 from 115.1 m-117.2 m at the 'Bee Eater' prospect, 14.5 km south of Mount Pleasant (Fig. 4.2, Fig. 4.13). The sample is strongly chlorite-sericite-carbonate altered, clast supported, coarse grained volcaniclastic conglomerate comprising sub-rounded to sub-angular lithic clasts of hornblende-rich andesitic porphyritic rock, dacite and sandstone. Details of zircon yield and morphology are presented in Sircombe et al. (2007).

Ten analyses of 10 zircon grains produced concordant results with the exception of five analyses that were >5% discordant or had high common Pb. The remaining five analyses yielded a concordia age of 2690±9 Ma (MSWD = 5.4). The relatively high MSWD suggests isotopic perturbation of the sample. At best, 2690±9 Ma is a tentative age for the maximum deposition of the syn-volcanic lower conglomerate, given the relatively few analyses. A previous age for this unit was determined as 2813±3 Ma (34 grains), with one grain at 2761±11

Ma (Hand 1998), which was interpreted by Krapez et al. (2000) to be the maximum depositional age of the unit, and yet fails to explain their interpretation that places White Flag Formation at the top of the Black Flag Sequence.

Whereas White Flag Formation has proved notoriously difficult to analyse in the past, this probably reflects the low zircon content of andesitic volcanic rocks generally, and limited access to fresh unaltered exposures in this particular case. The 2813±3 Ma from Hand (1998) was from a tightly concordant group of analyses that presumably represent an old (dominant) source - notably one grain was also analysed at 3480±7 Ma from the same sample. A tentative age from this study at 2690±9 Ma is beset by problems of low zircon yield and a high proportion of discordant grains.

In any case, the field relationships (younging, bedding) at White Flag Lake and in diamond drill core indicate a continuous or unconformable, un-faulted succession from the lower sedimentary 'Spargoville' sequence to the overlying White Flag Formation; hence, the 2690±9 Ma age better fits with mapped field relationships and is interpreted as a tentative estimate for the depositional age of syn-volcanic conglomerates of the White Flag Formation.

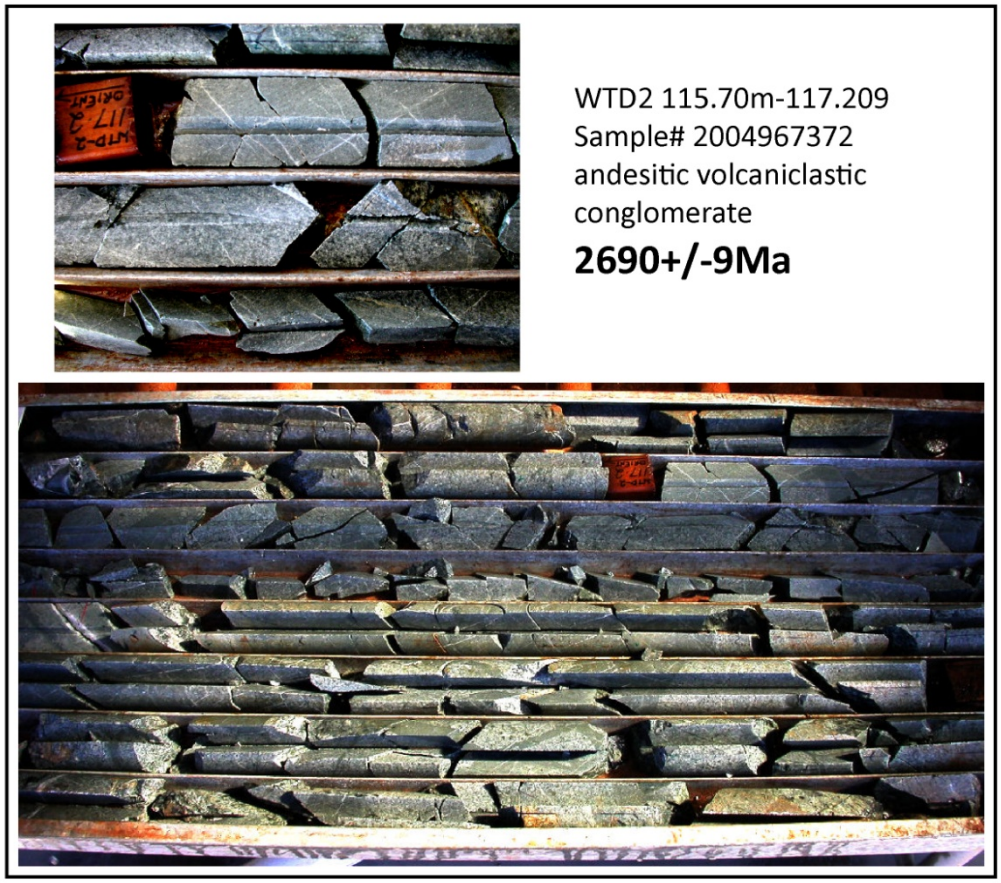

Figure 4.13 – Core photographs of material sampled from White Flag Formation andesitic conglomerate

4.5 Kurrawang Formation SHRIMP analysis

4.5.1 Rationale for analysis

Polymictic conglomerate and cross-bedded sandstone-siltstone-wacke of the Kurrawang Formation are the youngest rocks exposed in the Kalgoorlie district. These rocks have been the subject of intense recent research in several projects looking at similar sequences that span the Eastern Goldfields Province (AMIRA 437A/763, MERIWA 380, pmdCRC). Interest in these rocks is predominantly in their late unconformable nature, and spatial association with gold deposits; both of which tell about geotectonic conditions at the end of the Neoarchaean. Similar sequences documented in Neoarchaean terranes globally show comparable relationships with deformation and gold deposition; hence understanding these rocks has relevance to Archaean greenstone belts generally (Chapter 2).

The Kurrawang Formation is documented as comprising three units: lower Navajo Sandstone, middle Kurrawang polymictic conglomerate, and upper Kurrawang sandstone-siltstone-wacke (Section 3.3.4). Previous work by Krapez (1997) interpreted a map-scale unconformity between Navajo Sandstone and overlying Kurrawang Conglomerate. An outcropping angular unconformity between those units was found and documented in the field in this study (Section 3.4). Drilling information from the Goldilocks area suggests the Navajo Sandstone is much more extensive than portrayed on published maps. U-Pb SHRIMP analysis of zircon from the Navajo Sandstone (Fletcher et al. 2001) returned a maximum depositional age of 2657±4 Ma. Given unconformable contact relationships between Navajo Sandstone and Kurrawang Conglomerate, the latter was selected for analysis to assess the time break between the two units.

4.5.1 Brown Dam - lithic sandstone interbed sample

Lithic sandstone was sampled from a 1.5 m thick zone of interbedded Kurrawang polymictic conglomerate / sandstone from the Brown Dam area (Fig. 4.1; Fig. 4.14). Sample 2004967366 (Table 4.1) is a 0.7 m composite of halved drill core cut from lithic sandstone in diamond drill hole LWD001 from 91.45 m - 92.16 m at the ‘Long Wong’ prospect at Brown Dam, 58 km northwest of Kalgoorlie (Fig. 4.1, Fig. 4.14). The sample is from a grey chlorite-sericite altered fine to medium-grained lens in the upper part of the Kurrawang Conglomerate.

Angular to sub-rounded quartz and feldspar grains, and lithic clasts up to 1 mm size dominate the sandstone, with minor components incuding fine-grained clasts of intergrown quartz-feldspar rocks, chert and mafic volcanic fragments. The composition of the sandstone broadly mirrors that of the clast compositions in the conglomerate. A strongly aligned biotite foliation overprinted the sandstone and conglomerate units. Details of zircon yield and morphology are presented in Sircombe et al. (2007).

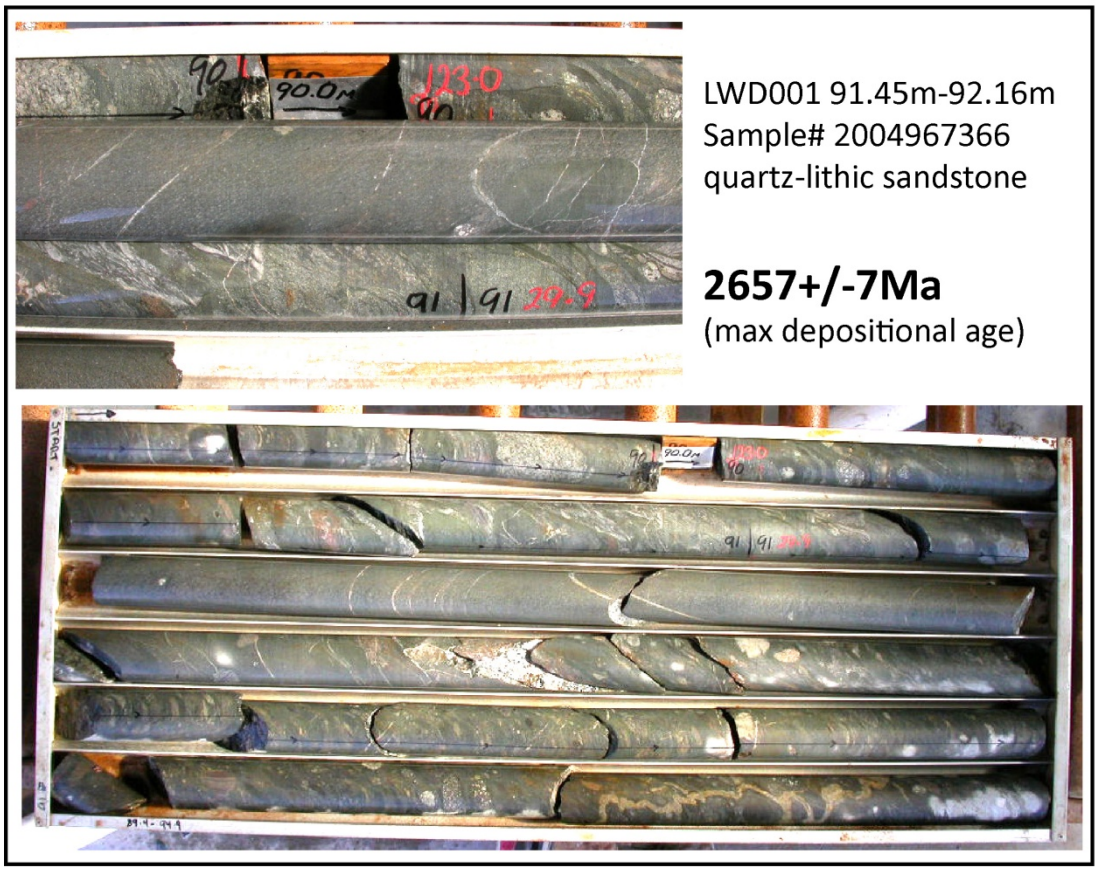

Figure 4.14 – Core photographs of material sampled from Kurrawang Formation lithic sandstone

Eighty analyses of 80 zircon grains produced concordant results with the exception of 21 analyses that were >5% discordant or had high common Pb. The remaining fifty-nine analyses yielded a dispersed cluster between 2750 Ma and 2650 Ma. Four analyses had ages >3200 Ma. Mixture modelling produced model components at 2657±7 Ma; 2680±5 Ma; 2691±8 Ma; 2713±4 Ma; 2720±5 Ma; and 2741±16 Ma. These model components were interpreted by Sircombe et al. (2007) as the original detrital provenance of the sample, with later overprinting events causing Pb-loss. The >3200 Ma analyses were interpreted by Dr. Sircombe as inheritance, however many of the late conglomerate sequences in the Eastern Goldfields Province display a similarly ancient detrital mode, which suggests an extra-basinal source not represented in the Eastern Goldfields Province. The 2657±7 Ma mode is tentatively interpreted as the maximum age of deposition of the sandstone lens in the Kurrawang Conglomerate, suggesting deposition after ~2650 Ma.

4.6 Kanowna district formations SHRIMP analysis

4.6.1 Rationale for analysis

Formations in the Kanowna district (18 km NE of Kalgoorlie) are generally correlated with the Black Flag Formation (Hand 1998), but this is uncertain given the presence of a major

unconformity separating the Boorara and Kambalda Domains (Section 3.6.4), and typically thick sequences of apparently locally-derived conglomerate in the Kanowna district (Fig. 4.15). In terms of the typical definitions of Spargoville Sequence and Kalgoorlie Sequence erected by Krapez et al. (2000) it is not immediately apparent how the Kanowna formations correlate with the Kalgoorlie Terrane based on lithology and depositional environment alone.

Detailed work on the lithostratigraphy of the Kanowna district in Chapter 3 was aimed at deriving a local stratigraphic column. This work was progressing in 2007 at the same time age analysis was completed for three of the major formations at Kanowna: from samples collected with Dr. J. Rogers and K. Joyce (reported in Sircombe et al. 2007). A series of units was selected for analysis to (1) validate the internal lithostratigraphic correlations of the Kanowna district, and (2) to provide correlation with formally defined stratigraphic formations and sequences in the Kalgoorlie Terrane.

Particular problems addressed by the SHRIMP analysis include: (1) apparently intercalated ultramafic and felsic volcanic rocks in the footwall of the Fitzroy fault; (2) age correlation of felsic grit layers in the ultramafic-clast dominant Ballarat sequence - a unique unit in the Kalgoorlie Terrane; (3) age correlation of the mafic-volcanic / granite clast-dominated

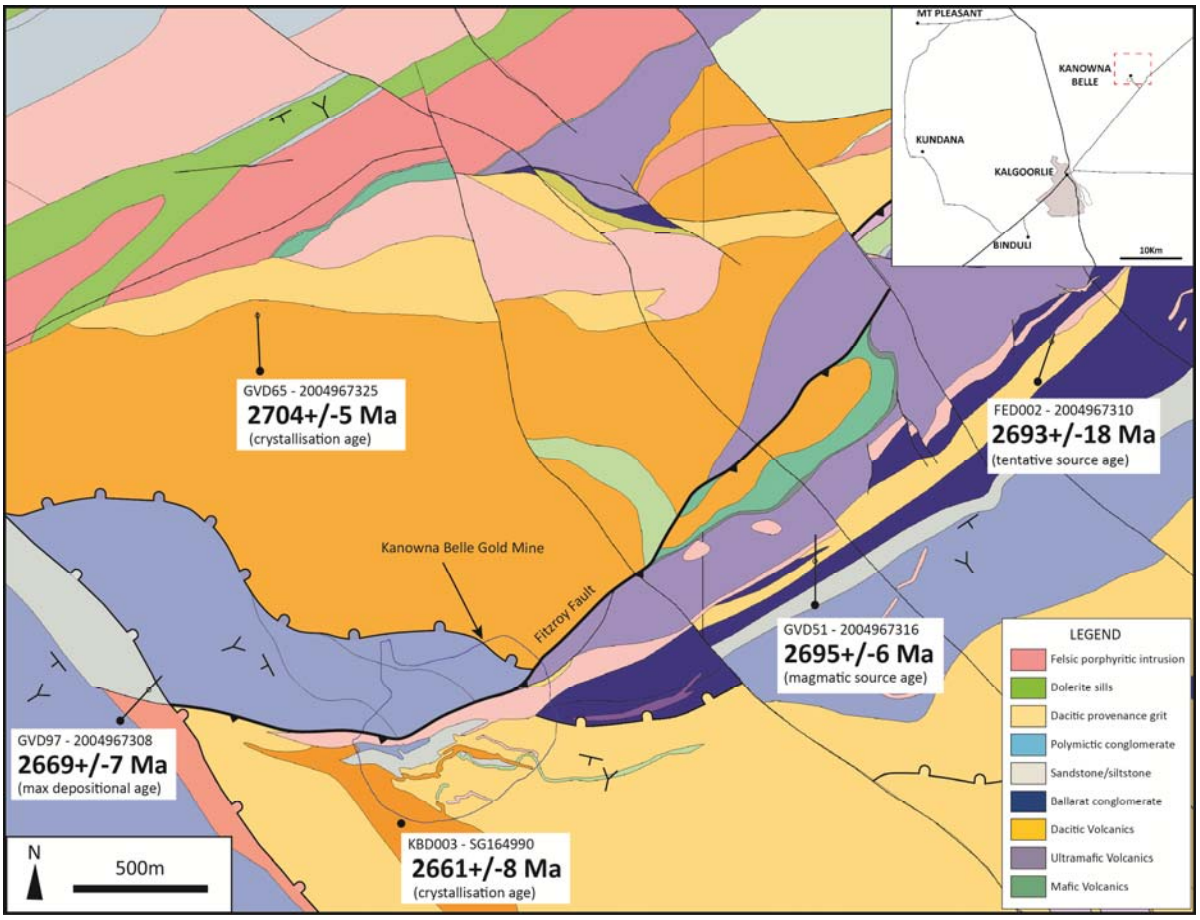

Figure 4.15 – Barrick geological map of the Kanowna district with locations of sampled drill holes and SHRIMP analysis results from Sircombe et al. (2007) and this study.

Golden Valley sequence in the footwall of the Fitzroy Fault; (4) age correlation of the remarkably well-preserved Government Dam deep water deposited sedimentary succession and; (5) age of the Kanowna Belle porphyry given previous difficulties in SHRIMP analyses, its importance as host to a large gold deposit, and its implications for timing major geological and mineralisation events in the district.

4.6.2 Coeval ultramafic/dacite volcanic rocks - dacite lava sample

The Boorara Domain is unique among the domains of the Kalgoorlie Terrane for its coeval komatiite-dacite association. Extensive outcrops in the Kanowna district show intercalated komatiite-dacite volcanic rocks, intrusive komatiite relationships into dacitic apron breccia deposits, and komatiite dykes intruded into bedded sandstones - documented in detail by Trofimovs (2003).

Dacitic volcanic and volcaniclastic rocks intruded by numerous late feldspar porphyritic dykes and sills are present in the footwall and hangingwall of the Fitzroy Fault at Kanowna Belle gold mine. Hangingwall dacitic rocks of the Grave Dam Grit were analysed by Ross et al. (2004) at 2668±10 Ma (maximum depositional age), whereas dacitic rocks in the footwall of the fault are not analysed and appear to show intimate association with komatiite volcanic rocks similar to other areas in the district. Polymictic conglomerate in the footwall (Golden Valley sequence) was also analysed by Ross et al. (2004) at 2668±9 Ma (maximum depositional age), showing no major change in age across the fault at its western extremity in the Kanowna Belle gold mine.

Footwall rocks of the Fitzroy Fault include a section from east to west: ultramafic volcanic rocks / dacitic rocks / polymictic conglomerate with intercalated felsic grit and planed-bedded sandstones. The hangingwall sequence from east to west is: intercalated komatiite dacite with overlying ultramafic conglomerate / unconformable dacitic volcaniclastic rocks (Grave Dam Grit). From east to west the fault juxtaposed sequence is: komatiite thrust over komatiite / komatiite-dacite thrust over Golden Valley sequence / Grave Dam Grit thrust over Golden Valley sequence (Fig. 4.15). Recognition of old-over-young thrusting therefore depends on which segment of the fault is viewed, since the rocks in the footwall and hangingwall dip and young to the southwest.

Constraining the relative ages of the footwall and hangingwall rocks is essential to the interpretation of the local structure and stratigraphy since dacitic rocks in the footwall and hangingwall are superficially similar in lithological character, whereas if these units are markedly different in age, the Fitzroy Fault represents a significant thrust fault placing older rocks over younger rocks. Since the age of the dacitic rocks in the footwall is uncertain, it has not been possible to place an unconformity between the clearly younger Golden Valley

sequence and the komatiite volcanic rocks. A sample of the footwall dacitic rocks was selected to improve this understanding.

Sample 2004967325 (Table 4.1) is a 1.15 m composite of drill core cut from meta-dacite in diamond drill hole GVD65 from 386.75 m - 387.90 m, about 2 km north of Kanowna Belle gold mine, and 18 km northeast of Kalgoorlie (Fig. 4.1, Fig. 4.15). The sample is from fine-grained quartz-feldspar porphyritic, weakly-xenolithic dacite flow rocks with moderate chlorite-sericite alteration. Details of zircon yield and morphology are presented in Sircombe et al. (2007).

Forty-one analyses of 39 zircon grains produced concordant results with the exception of one analysis >5% discordant. The remaining 40 analyses yielded a main cluster at ~2700 Ma with a tail of younger ages extending to ~2665 Ma. Mixture modelling produced model components at 2663±7 Ma; 2681±9 Ma; 2704±5 Ma; and 2727±18 Ma. A dominant cluster at 2704±5 Ma is interpreted by Dr. Sircombe as the original magmatic crystallisation age of the zircons, after which followed a complex series of magmatic events that produced resorption and new zircon growth, ending around 2663±7 Ma.

4.6.3 Ballarat member - intercalated felsic grit samples

Grit of dacitic provenance is intercalated with Ballarat ultramafic clast dominated conglomerate in the Kanowna district (Fig. 4.15). In lithologic character, the Ballarat felsic grit is almost indistinguishable from dacitic grit and conglomerate in the Grave Dam Grit. Map scale relations show the two sequences are separated by several hundred metres thickness of polymictic conglomerate and sandstone (Kanowna Conglomerate), with Grave Dam Grit unconformably overlying and truncating folds in the Ballarat sequence. Two samples of the Ballarat grit were selected for analysis to constrain the maximum depositional age of this unit.

Sample 2004967316 (Table 4.1) is a 1.15 m composite of drill core cut from meta-sandstone in diamond drill hole GVD51 from 325.15 m - 326.3 m, about 1 km east of Kanowna Belle gold mine, and 18 km northeast of Kalgoorlie (Fig. 4.1, Fig. 4.15). The sample is from moderately chlorite-albite-sericite-carbonate altered, medium-grained to very coarse-grained sandstone with crystal fragments and porphyritic dacite-andesite lithic fragments and relict glass shards, indicating a primary volcaniclastic origin. Details of zircon yield and morphology are presented in Sircombe et al. (2007).

Twenty-two analyses of twenty-five zircon grains produced seventeen analyses with >1% common-Pb, also with high U-Th. Remaining analyses were <5% discordant but produced no dominant age cluster. Mixture modelling of Pb^{207}/Pb^{206} ages derived model components at 2652±12 Ma; 2681±11 Ma; and 2695±6 Ma. The data distribution was interpreted by Dr. Sircombe to represent an ancient Pb-loss event. Two analyses at <5% discordance returned ages of 2649±7 Ma and 2659±11 Ma, but these samples lie along discordia related to ancient Pb-Loss

events. A magmatic age of the dominant component was interpreted at 2695±6 Ma, which may represent a tentative maximum depositional age of the unit.

Sample 2004967310 (Table 4.1) is a 1.00 m composite of drill core cut from meta-sandstone in diamond drill hole FED002 from 320.00 m - 321.00 m, about 1 km northeast of Kanowna Belle gold mine, and 18 km northeast of Kalgoorlie (Fig. 4.1, Fig. 4.15). The sample is from the same unit as 2004967316, a medium-grained to very coarse-grained sandstone with crystal fragments and porphyritic dacite-andesite-rhyolite and fuchsitic mafic lithic fragments with relict glass shards, indicating a primary volcaniclastic origin. Details of zircon yield and morphology are presented in Sircombe et al. (2007).

Six analyses of six zircon grains produced generally poor data due to common-Pb and discordant age results, possibly due to a Neoproterozoic Pb-loss event. A discordia line with an upper intercept at 2693±18 Ma is interpreted as a possible age of crystallisation, but as a reconnaissance only.

The tentative age of the previous sample (2004967316) interpreted as a magmatic age of the dominant component at 2695±6 Ma is a better estimate of the syn-volcanic depositional age of the Ballarat grit unit given the dominantly volcanic clastic components, and the preservation of primary glass shards.

4.6.4 Golden Valley member - sandstone sample

Rocks in the immediate footwall of the Fitzroy Fault at Kanowna Belle are part of the Golden Valley member (Section 3.3.2): a complex sequence of interbedded mafic-granite pebble dominated polymictic conglomerate with intercalated dacitic composition grit-conglomerate units, and fine- to medium-grained plane-bedded sandstones in the upper parts of the sequence. The Golden Valley conglomerate was analysed by Ross et al. (2004) with a SHRIMP U-Pb zircon age of 2668±9 Ma from a quartz-feldspar porphyry clast in the conglomerate indicating a maximum depositional age of ~2659 Ma or less. Grave Dam Grit member has an interpreted maximum age of deposition of 2668±9 Ma from detrital zircon analyses (Ross et al. 2004).

Thin dacitic grit interbeds in the Golden Valley member are lithologically indistinguishable from similar rocks in the Grave Dam Grit, and it is possible the two units are lateral time equivalents, with minor intercalation of dacitic-source volcaniclastic debris (Grave Dam Grit) in the mafic volcanic and granite-pebble dominated Golden Valley sequence. A sample of the upper sandstone of the Golden Valley sequence was collected for analysis to assess the previous maximum depositional age determination taken from a single clast.

Sample 2004967308 (Table 4.1) is a 1.15 m composite of drill core cut from meta-sandstone in diamond drill hole GVD97 from 300.85 m-302.00 m, about 1 km west of Kanowna Belle gold mine, and 18 km northeast of Kalgoorlie (Fig. 4.1, Fig. 4.15). The sample is a

medium-grained to coarse–grained lithic sandstone with strong chlorite-sericite alteration. Details of zircon yield and morphology are presented in Sircombe et al. (2007).

Thirty-four analyses of 34 zircon grains produced concordant results with the exception of one analysis with high common-Pb. One grain at 2737±9 Ma was interpreted by Dr. Sircombe as inheritance. A possible inheritance effect was interpreted from dispersion in the age distribution, and a high MSWD from the weighted mean Pb^{207}/Pb^{206} age of 2669±5 Ma (95% conf. MSWD = 3.5). Mixture modelling of the age distribution yielded components at 2657±17 Ma; 2669±7 Ma; and 2691±7 Ma. The younger component was interpreted as representing ancient Pb-loss and the older peak as possible inheritance, or analytical overlap with older zones (Sircombe et al. 2007). A peak of the probability distribution at 2669±7 Ma is interpreted as the maximum depositional age of the sandstone.

4.6.5 Government Dam sandstone sample

Deep water deposited sandstone-siltstone and minor conglomerate at the Government Dam locality form a <1000 m thick section of plane-bedded, graded sedimentary rocks deposited by turbidity currents. The sequence is in probable fault contact with underlying Ballarat conglomerate/grit since 500 m-scale folds in the unit are not present in the basement rocks: suggesting detachment at the contact, and structural thickening of the Government Dam rocks (Section 3.6; Fig. 3.55). Upper and lower contacts of the unit are faulted; hence, the age and stratigraphic position of the Government Dam sequence is unknown, but it is notable that previous company interpretations correlated the Government Dam sedimentary rocks with Grave Dam grit.

A diamond drill hole was reviewed with Dr. Rick Squire (Monash) in 2007 to select a suitable sample for analysis. Dr. Squire was contracted by Barrick Gold to produce a SHRIMP age determination under a commercial agreement: the results of that analysis are presented here.

Sample LB252 (GDA: 367700E-6612210N; Fig. 4.1) is a 3.2 m composite of quartered drill core from 204.2 m - 207.4 m in diamond drill hole KMD12 (Fig. 4.1). The sample is a strongly sericite-altered quartz-rich massive to graded sandstone with minor polymictic volcaniclastic breccia and conglomerate. Detrital zircons were separated at the University of Melbourne using standard techniques of heavy liquid and electromagnetic separation. Analyses were conducted at the John de Laeter Centre of Mass Spectrometry at Curtin University of Technology (Perth). Thirty grains were analysed on 22 April 2006 and 36 grains were analysed on 1 May 2007. Ratios of U-Pb isotopes were calculated using a TEMORA standard (417 Ma).

Six concordant analyses from a total sixty-six produced a mean age of 2661±11 Ma (MSWD = 1.3). A Pb-loss discordia line of best fit for all analyses produced an upper intercept at 2668±8 Ma. The concordant population of 2661±11 Ma was interpreted by Dr. Squire to represent the maximum depositional age of the Government Dam sandstones (Fig. 4.16).

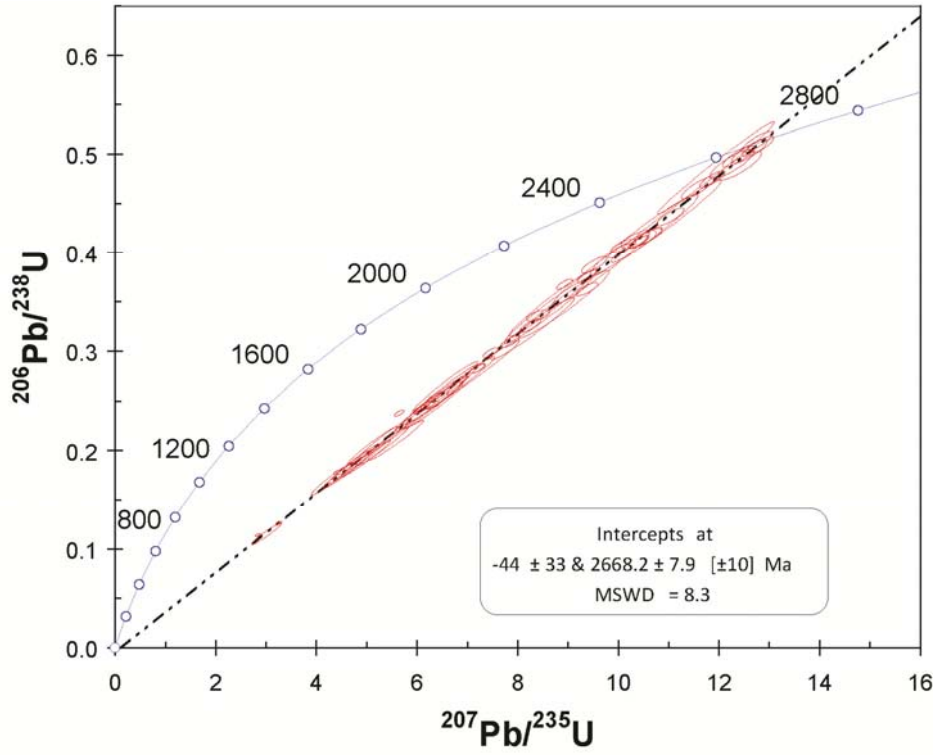

Figure 4.16 – Concordia plot of sixty-six analyses from the Government Dam sandstone.

4.6.6 Kanowna Belle Porphyry sample

Kanowna Belle Porphyry is host to a ~5 million ounce endowment Archaean gold deposit. The intrusion is located on the Fitzroy Fault, a thrust zone that juxtaposes volcanic and sedimentary sequences as discussed previously. In its gross distribution, the Kanowna Belle Porphyry clearly intruded along the 60º southeast-dipping Fitzroy Fault, yet underground exposures reveal strong deformation of the intrusion suggesting post-intrusion shearing.

Since the porphyry intruded a thrust fault, the age of faulting can be bracketed by determining the crystallisation age of the intrusion to provide a minimum age on pre-intrusion thrust movement; in addition, the maximum-age of faulting can be indicated by the age of the youngest rocks in the footwall. This bracketing may be complicated if it can be demonstrated the intrusion was coeval with significant thrust movement on the fault. In that case, the crystallisation age would provide a rough minimum estimate of that thrust movement.

Kanowna Belle Porphyry was analysed previously by Ross et al. (2004) with an interpreted crystallisation age of 2655±6 Ma. The Ross et al. (2004) paper was one of the first to document significant complexity in Archaean zircons from the Kalgoorlie district, and the analysis was hampered by poor quality zircons in a highly-altered sample taken from close to the Fitzroy Fault. A thick section of less-altered Kanowna Belle Porphyry was found in a drill hole further from the fault, and was sampled to attempt to improve on the previous crystallisation age of Ross et al. (2004).

Sample SG16490 (Table 4.2; Fig. 4.1; Fig. 4.17) is a 15.1 m composite of quartered drill core from 389.90 m - 405.00 m in diamond drill hole KBD003. The sample is a light-green moderately sericite-albite-pyrite-carbonate altered porphyritic rock with white euhedral feldspar phenocrysts and rare rounded quartz phenocrysts, and scattered crustiform carbonate veins and minor fuchsite replacement of chlorite-altered hornblende phenocrysts in a fine-grained glassy groundmass (Fig. 4.17).

A moderate zircon yield produced 35 zircons of which 17 were selected for analysis. In transmitted light the zircons are fine light-pink euhedral, elongate crystals with prismatic terminations. Under CL the grains show very well preserved oscillatory magmatic zoning, and abundant examples of xenocrystic cores with oscillatory zoned magmatic overgrowths (Fig. 4.18a). In BSE images the zircons show moderate metamictisation effects with radial fracturing, damage to the crystal structure with fracturing on some magmatic growth planes, and moderate to complete recrystallisation (Fig. 4.18a).

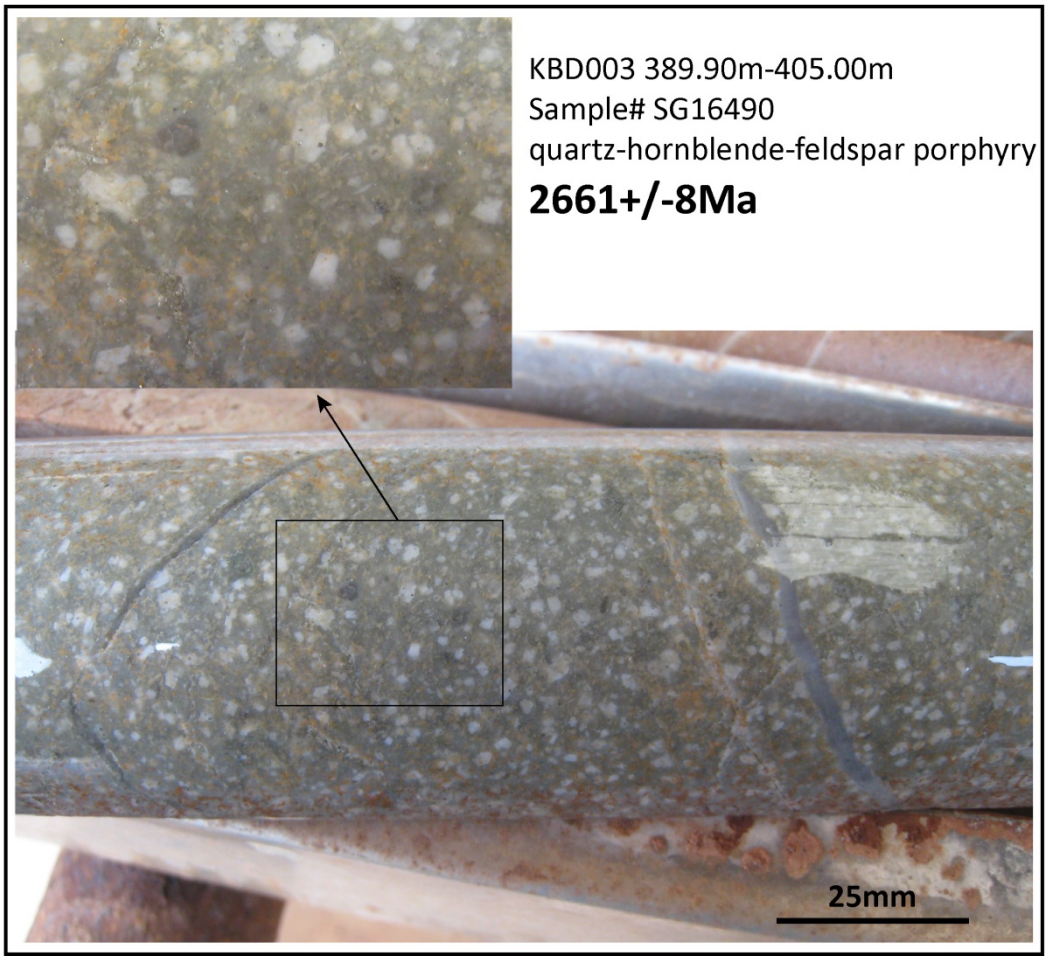

Figure 4.17 – Kanowna Belle Porphyry drill core sampled for analysis: sample SG16490.

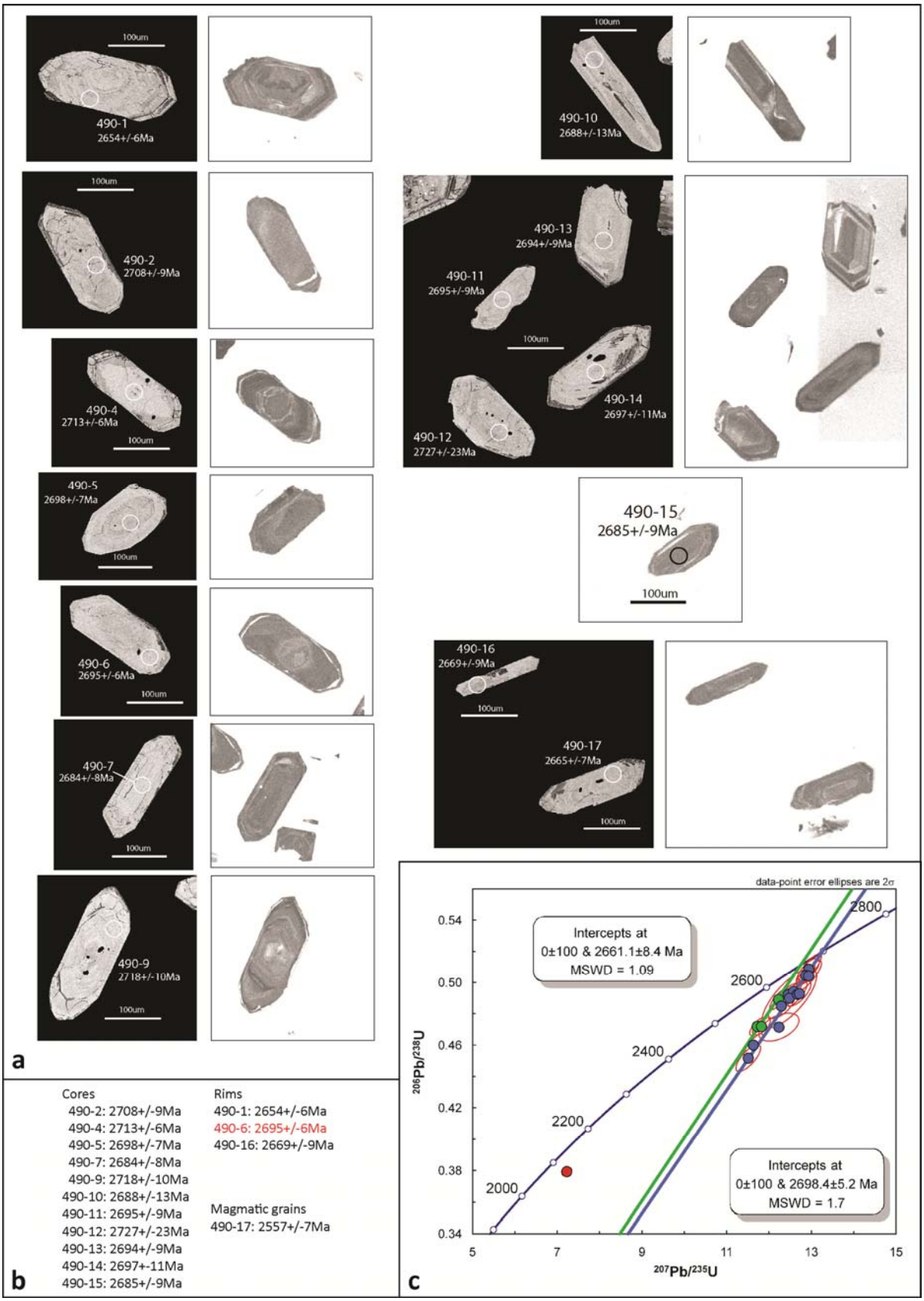

Figure 4.18 – Comparative BSE/CL images of sample SG16490 (Kanowna Belle Porphyry) with SHRIMP spot locations and age determinations; b) tabulation of analyses from cores and rims c) Concordia plot of zircon analyses showing an interpreted older inherited population, and a weakly defined younger population that likely represents the crystallisation age of the intrusion.

Seventeen analyses of 17 grains were completed during a single session. The weighted mean age of all analyses is 2689±10 Ma (MSWD = 5.6, 95% conf.). The very high MSWD suggests more than a single population is represented in the data, which is confirmed by imaged core-rim structure. Six analyses were >5% discordant, including two analyses with high-U. A weighted mean for all eleven concordant analyses is 2700±11 Ma (MSWD = 1.6). The distribution on a concordia plot of all analyses suggests two possible populations, and this is confirmed by the individual ages of core vs. rim analyses (Fig. 4.18a). A discordia line of best fit for the older population has an upper intercept at 2698±5 Ma (MSWD = 1.7); and for the younger population an upper intercept at 2661±8 Ma (MSWD = 1.1; Fig. 4.18c); both populations plot on discordia lines with a zero intercept suggesting recent Pb-loss. One analysis with high-U was rejected (1355 ppm U).

A table of the seventeen analyses separated into cores and rims (Fig. 4.18b), shows consistently older age determinations for the cores, and two rim analyses with younger ages. The analysis for grain 490-6 appears spurious since the images appear to show the zircon rim was analysed, however the central area of the grain is surrounded by a further finely-zoned rim, which may be a further magmatic growth or a later phase of metamorphic overgrowth. One zircon grain in the young population (490-17) appears to be a purely magmatic grain with an age of 2557±7 Ma.

On the basis of textural data and the concordia analysis, the older discordia intercept age of 2698±5 Ma probably represents inheritance, and the younger intercept age of 2661±8 Ma is interpreted to represent the age of crystallisation of the intrusion.

4.7 Owen Monzogranite SHRIMP analysis

4.7.1 Rationale for analysis

Owen Monzogranite batholith is one of two major batholithic intrusions in the north Kalgoorlie district (Fig. 4.1). The intrusion is possibly a composite batholith as indicated by aeromagnetic images that show variable internal structure and magnetic character. Regional geological maps show the batholith contacts are broadly parallel to bedding in the overlying supracrustal rocks, whereas gravity data indicate the subsurface distribution of the Monzogranite transects some contacts at a high angle. The possibility for intrusion controls on timing of structural fabrics and gold deposits in the region is discussed in Chapter 6; hence, understanding the age of the Owen Monzogranite intrusion is important to clarifying that timing. A sample of the monzogranite was collected for SHRIMP analysis.

4.7.1 Owen Monzogranite outcrop sample

Sample 2004967377 (Table 4.1) is a 4kg sample from surface outcrop ~9 km north of Mount Pleasant and 40 km north-northwest of Kalgoorlie (Fig. 4.1). The sample is a light-grey

foliated, medium to coarse-grained, weakly feldspar-porphyritic biotite monzogranite. Details of zircon yield and morphology are presented in Sircombe et al. (2007).

Nine analyses of nine grains were completed during a single session, with five further analyses aborted due to high common-Pb. Four analyses were rejected due to high common-Pb or >5% discordance. The remaining five analyses formed a concordant cluster at 2655±15 Ma (MSWD = 6.7, 95% conf.). Due to the very low number of analyses, and large error this age is tentatively interpreted as the crystallisation age of the intrusion.

4.8 Golden Mile Dolerite SHRIMP analysis

4.8.1 Rationale for analysis

The Golden Mile Dolerite (GMD), host to the ~70 million ounce Golden Mile Archaean greenstone gold deposit, is globally one of the most important Archaean host rocks (Robert et al. 2005). The timing and interpretation of gold deposits in this host rock are highly controversial (e.g. Vielreicher et al. 2010; Gauthier et al. 2004a; Bateman and Hagemann 2004 Phillips 1986; McNaughton et al. 2005).

Since its discovery in 1893, the age of the Golden Mile Dolerite had been determined from relative age relationships, with most authors documenting local-scale intrusive relationships and broad transgressions of the Paringa Basalt / Black Flag Group contact, with local observations of Paringa Basalt above the GMD or slivers of Black Flag Group rocks below the intrusion (Clout et al. 1990). An alternative interpretation of the GMD as a sub-marine flow complex is largely discredited by detailed observations of the slightly transgressive contact relationships and the presence of marginal chilled zones. Differentiation in the Golden Mile Dolerite has produced a parallel-layered sequence of ten texturally and chemically distinct zones including chilled margins against the wallrocks. The most differentiated, Fe-rich layer in the sill is documented as Unit 8 (Travis et al. 1971), which is a granophyric-textured quartz dolerite with abundant magnetite, locally large bladed-skeletal leucoxene altered Ti minerals, and up to >300ppm Zr.

A first attempt at absolute age analysis of the GMD by Woods (1997) derived a concordant age of 2675±2 Ma (95% conf.) determined from four analyses of three zircon grains. Gold-mineralised felsic intrusions abound in the Golden Mile deposit and cross-cutting relationships demand they post-date the crystallisation of the GMD. A recent study (Gauthier et al. 2004a) determined a TIMS-zircon crystallisation age of a feldspar-porphyry dyke in the Golden Mile deposit at 2676±1 Ma. The Woods (1997) dolerite age was based on very few analyses and prompted the attempt to re-analyse the GMD here. More recently the GMD was analysed by Rasmussen et al. (2010), who produced an age of 2680±9 Ma from SHRIMP U-Pb analysis of magmatic zirconolite ($CaZrTi_2O_7$).

Sample SG16485 (Table 4.1; Fig. 4.5; Fig. 4.19a-c) is a 7.5 m composite of quartered drill core from 264.0 m - 271.5 m in diamond drill hole JUGD010 from the Golden Pike area of the Golden Mile. The sample is a light-brown, strongly sericite-chlorite-carbonate-magnetite-leucoxene altered dolerite with abundant magnetite, some of which may be primary (Fig. 4.19c). A moderate to strong foliation is present, as are spaced crustiform carbonate-quartz veinlets with weak pyritic alteration halos.

A low zircon yield produced 19 zircons of which 10 were selected for analysis. The zircons are angular fragments of crystals with equant shapes and ~100µm diameter on average. Under CL, the grains are highly metamict with no visible internal growth banding: any concentric structure is apparently related to metamictisation and zones of high or low-U, associated with strong radial fracturing visible in BSE images (Fig. 4.19a). In BSE images the zircons show strong fracturing and moderate to complete recrystallisation.

Ten analyses of ten grains were completed during a single session. The weighted mean age of all analyses is 2684±4 Ma (MSWD = 1.6). The mean includes one analysis with high-U and two analyses >5% discordant. The weighted mean age of all analyses <5% discordant is 2686±5 Ma (MSWD = 0.53). Two possible trends are present on the concordia plot of all analyses. The main population has a discordia line of best fit with an upper intercept of 2685±4 Ma (MSWD = 0.71; Fig. 4.19b) defining a recent Pb-loss trend, whereas two analyses lie on a discordia line defining an ancient Pb-loss trend at about 1722 Ma.

Data recording the %-discordance show three analyses with weak reverse discordance: two analyses -1% discordant and one analysis -3% discordant. There appears to be no correlation between the weak reverse discordance and U/Th trends, but the analysis with -3% reverse discordance has abnormally high Th; nonetheless those three analyses are less than 5% discordant and included in the calculated intercept age. The best fit discordia line upper intercept age at 2685±4 Ma is interpreted as the crystallisation age of the Golden Mile Dolerite.

4.9 Discussion of new SHRIMP analyses and stratigraphic interpretations

4.9.1 Background to the stratigraphy of rocks post-dating the mafic-ultramafic volcanics

The published stratigraphy of the north Kalgoorlie district is beset with terminology issues that confound attempts to understand the proper stratigraphic order. Table 3.1 (Map Pocket) is a full compilation of all the major published stratigraphic schemes from MacLaren and Thomson (1913) to Krapez and Pickard (2010). Most problems stem from the ‘White Flag’, ‘Black Flag’ and ‘Spargoville’ designations, and the use of these terms variously as descriptors for local formations or major groups; and especially the application of these terms well outside their areas of definition. A point of note is the laterally restricted nature of sedimentary and volcanic sequences in the Eastern Goldfields, which leads to the important question of whether long range correlations are valid or even possible.

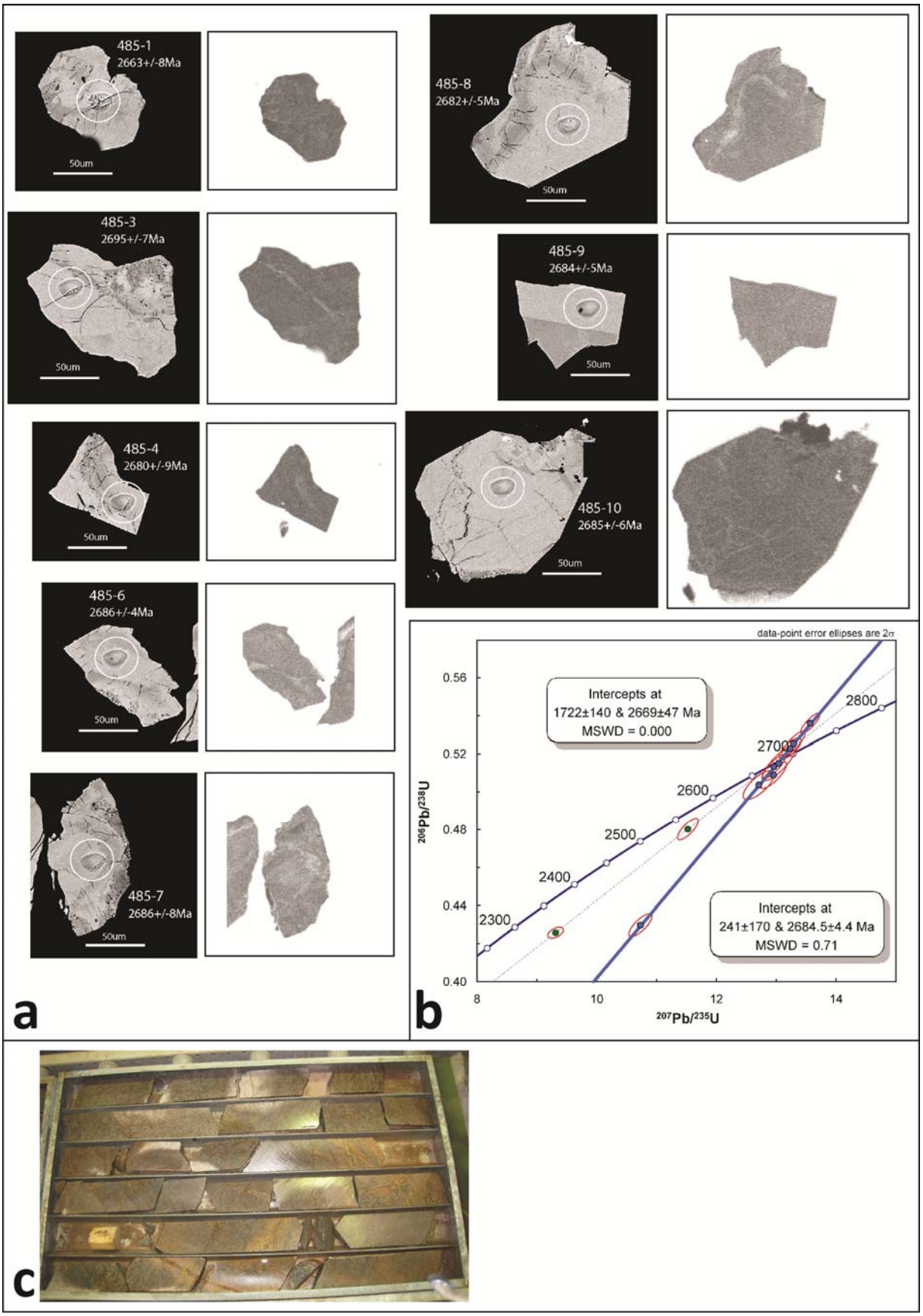

Figure 4.19 – Comparative BSE/CL images of sample SG164850 (Golden Mile Dolerite) with SHRIMP spot locations and age determinations; b) Concordia plot of all zircon analyses showing a well defined older concordant population, and a three analyses with reverse discordance; c) drill core photos of strongly altered dolerite sampled for zircon separation in drill hole JUGD010 (264.0 m-271.5 m).

Prior to the widespread application of modern geochronology, field geologists compiled their observations in tables that presented lithostratigraphic ‘time-series’ comprising members named for their locality and major rock types. For instance prior to 1916, C.S. Honman mapped an area from Kalgoorlie to the southwest of Binduli. His lithostratigraphic time series included a ‘Kalgoorlie Series’ separated into ‘porphyrite volcanic’, ‘sedimentary’ and ‘intrusive’ subdivisions; and an overlying, un-subdivided ‘Kurrawang Series’. Likewise, Talbot (1934) produced a similar time series that built upon the work of C.S. Honman, but included ‘Black Flag Series’, ‘White Flag Series’ and ‘Kundana Series’ in addition to the units previously defined by Honman (1916).

The first regional mapping of the study area was by MacLaren and Thomson (1913), but H.W.B. Talbot produced the first interpretation map of the area between Mount Pleasant and Kalgoorlie (Fig. 4.20). He named superbly preserved sedimentary rocks exposed to the west of Black Flag Lake - ‘Black Flag Series’ and correlated these with similar rocks at Kalgoorlie; and he named the andesitic volcanic rocks on White Flag Lake - ‘White Flag Volcanics’. Later work by Forman (1937, 1953), and Gustafson and Miller (1937), closely followed the designations of Talbot (1934) and Honman (1916). Talbot (1934) also described a separate ‘Kundana Series’, which was later interpreted by Feldtmann (1936) and Forman (1937) as belonging to the Kurrawang Series. Note that ‘Black Flag Series’ as originally intended referred to rocks at Mount Pleasant, above the mafic volcanics and below the White Flag andesites.

A factor complicating later terminology is that much of the well-exposed ‘Black Flag Series’ outcrops on White Flag Lake as well as on the western margin of Black Flag Lake; whereas the southern shore of Black Flag Lake is well within the White Flag Series. The fact these two salt lakes are close together spatially, and the named series are present at both localities is a potential source of confusion.

The next major work that documented a stratigraphy for the Kalgoorlie district was Woodall (1965) in which all units above the Kalgoorlie greenstones, at Kalgoorlie, were grouped into ‘Black Flag Beds’. R. Woodall’s mapping and compilation dealt with rocks in the vicinity of the Golden Mile, and probably was not intended as a belt-wide designation. Woodall’s grouping was followed by subsequent published schemes in the Golden Mile area that also did not attempt to subdivide the group (e.g. Travis et al. 1971). Nevertheless, later authors have applied this ‘Black Flag Beds’ designation to all rocks above the Kalgoorlie greenstones and below the Kurrawang sedimentary rocks, particularly the ‘Felsic Volcanic and Sedimentary Unit' - (Black Flag Group) of Swager et al. (1990), which is the single most referenced stratigraphic scheme. Woodall (1965) and later Swager et al. (1990) appear to be the initial accounts where Talbot’s ‘Black Flag Series’ designation was taken out of its intended local area and applied to rocks far afield from its type locality.

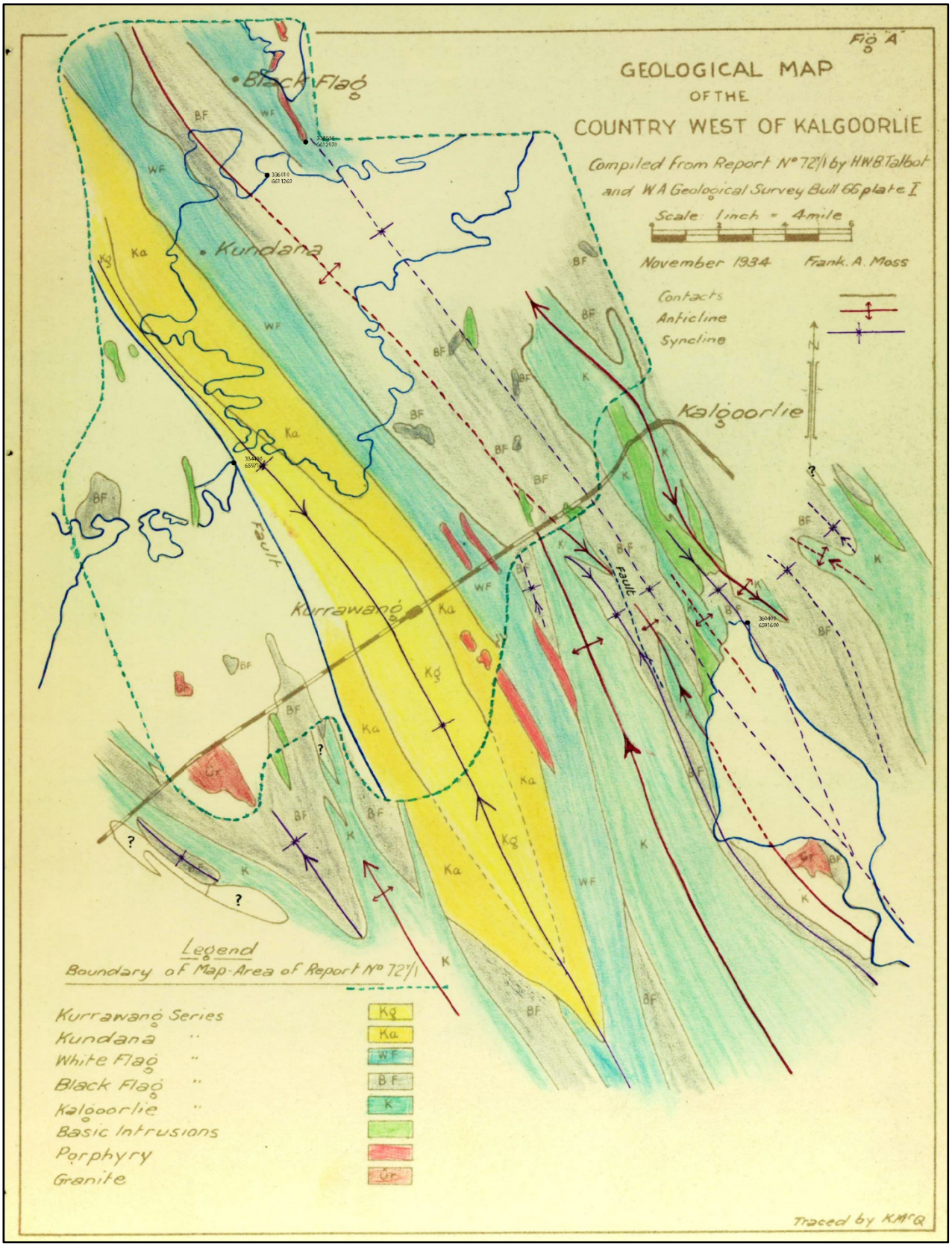

Figure 4.20 – Geological map of the area north and west of Kalgoorlie by H.W.B. Talbot. The map is from an unpublished Western Mining Corporation Limited technical report (Talbot 1934) generously provided to the author by Dr. G. Begg and BHP Minerals.

The mapping of Keats (1987) dealt with rocks from the belt between Gidji and Kalgoorlie, with a lower 'Unit IIIA' - felsic to intermediate volcanic and sub-volcanic rocks; with overlying 'Unit IIIB' - clastic sedimentary rocks. Several authors working in surrounding districts produced local columns: notably Glikson (1971), who produced a stratigraphy for the rocks to the west of the Kurrawang sedimentary rocks, and subdivided the 'Kurrawang Series' with an interpreted unconformity at its base (Table 3.1).

An important departure from the generalised Kalgoorlie - Black Flag - Kurrawang stratigraphy was the work of Gemuts and Theron (1975) that interpreted a multi-cyclic volcanic sequence development and placed ultramafic and related mafic volcanic rocks high in the 'Black Flag' sequence (Table 3.1). This work was later discredited by the structural mapping of Martyn (1987) in the Widgiemooltha district, which showed the apparent cycles were structural repeats from either thrusting or extensional sliding off the margins of intruded granite domes; later work by Swager and Griffin (1992) produced a comparable interpretation.

Separation of the 'Black Flag Group' by Hunter (1993) included a 'Spargoville Formation' (felsic volcaniclastic rocks, flows, intrusions, and meta-sedimentary rocks); grading up into 'White Flag Formation' (intermediate volcaniclastic rocks and minor flows). Importantly he noted a 'thin grey shale horizon' marking the base of the 'Black Flag Group', which may refer to similar units overlying mafic volcanics at Mount Pleasant (i.e. Talbot's original Black Flag Series) and possibly Lakewood. Hunter's report is the first time a 'Spargoville Formation' appears in the literature, and as discussed earlier in this chapter, refers to rocks up to 80 km south of the Kalgoorlie exposures. Rocks at Spargoville were also documented in detail by Fehlberg and Giles (1984), but no stratigraphy was presented in that paper, possibly due to the rapid lateral facies variations of an interpreted felsic lava dome complex.

A major re-interpretation of the Eastern Goldfields Province by multi-disciplinary projects and research consortia (AMIRA projects P437A, P763) led to the publication of a revised stratigraphy (Krapez et al. 2000) that proposed a 'Kalgoorlie Sequence', which included a lower 'Spargoville Formation' and a middle unconformable 'Black Flag Formation', overlain by unconformable 'White Flag Formation'. In detail, four interpreted unconformity-bounded 'tectonic uplift stages' were proposed using a sequence stratigraphic approach, which in the Kalgoorlie district was supported by the rigorous lithostratigraphic mapping of Hand (1998) and is presented in Table 4.3. Some issues with these designations are apparent from field mapped sections in the study area, which will be discussed in the following sub-chapters in the context of recent SHRIMP analyses, and the lithostratigraphic descriptions in Chapter 3.

A stratigraphy for rocks of the Boorara Domain was constructed by Trofimovs (2003) using the generalised stratigraphy of Swager et al. (1990); the previous mapping and interpretations of Archibald (1993); and a complex local stratigraphy of the Kanowna Belle

mine sequence by Beckett et al. (1998). The mapping of Hand (1998) placed the Kanowna sequences within a generalised 'Black Flag Group' (Table 3.1).

A further re-interpretation of the Kalgoorlie stratigraphy by Squire et al. (2010) interpreted two major cycles of deposition. Cycle-One corresponds to a 'Black Flag Group' with 'early BFG' and 'late BFG' subdivisions; Cycle-Two notably introduces a new 'Merougil Group' with early and late subdivisions, with which they correlate the Government Dam and Golden Valley sequences from Kanowna, Merougil Conglomerate from Kambalda, and Navajo Sandstone from Binduli (Table 3.1).

Table 4.3 - Facies, sequence and chronostratigraphic nomenclature for the Kalgoorlie district from Krapez et al. (2000), Barley et al. (2002) including their assignments of rock units at localities described in this thesis.

2658 Ma	Stage 4	Black Flag Formation	Sequence 6	Gibson-Honman; top of hole SE3 (FA-1), Lakewood
			Sequence 5	Government Dam; mid-hole SE3 (FA-3), Lakewood
			Sequence 4	GraveDam/GoldenValley(FA-1); Gidji Lake (FA-1); EMD; SE3 Lakewood
2666 Ma	Stage 3		Sequence 3	Panglo wacke/mudstone (FA-3/4); True Sons (FA-1/4)
2674 Ma	Stage 2		Sequence 2	White Flag Fm; Panglo Conglomerate (FA-1); Ballarat/Kanowna fm (FA-1a)
2682 Ma 2690 Ma	Stage 1	Spargoville Formation	Sequence 1	Spargoville at White Flag Lake

Note that previous workers interpreted the Merougil conglomerate at Kambalda as an early but equivalent sequence of the regionally unconformable Kurrawang Formation (Honman 1916; Cowden and Roberts 1990; Swager et al. 1990; Krapez et al. 2000), whereas Krapez et al. (2000) documented Navajo Sandstone as an unconformable basal unit of the Kurrawang Formation, and a lateral equivalent of the Merougil Conglomerate.

4.9.2 Correlations suggested by new SHRIMP analyses

New SHRIMP U-Pb results from this study are compiled with relevant previous analyses in Table 4.4. One notable aspect of the compiled ages is a general error overlap of almost all analyses in each of the categories: volcanism, sedimentation and intrusion. This aspect indicates a generally poor ability of the SHRIMP analysis method to resolve geological events in the Neoarchaean of Kalgoorlie, and emphasises that documented (and hopefully unambiguous) field relationships and geochronology, provide the most robust method of constraining the major events.

Ultramafic and mafic volcanics

The age of the regional komatiite volcanic unit is generally interpreted from a SHRIMP U-Pb zircon age of 2708±7 Ma from felsic dacitic flow rocks interbedded with the basal

Kalgoorlie District Geochronological Chart

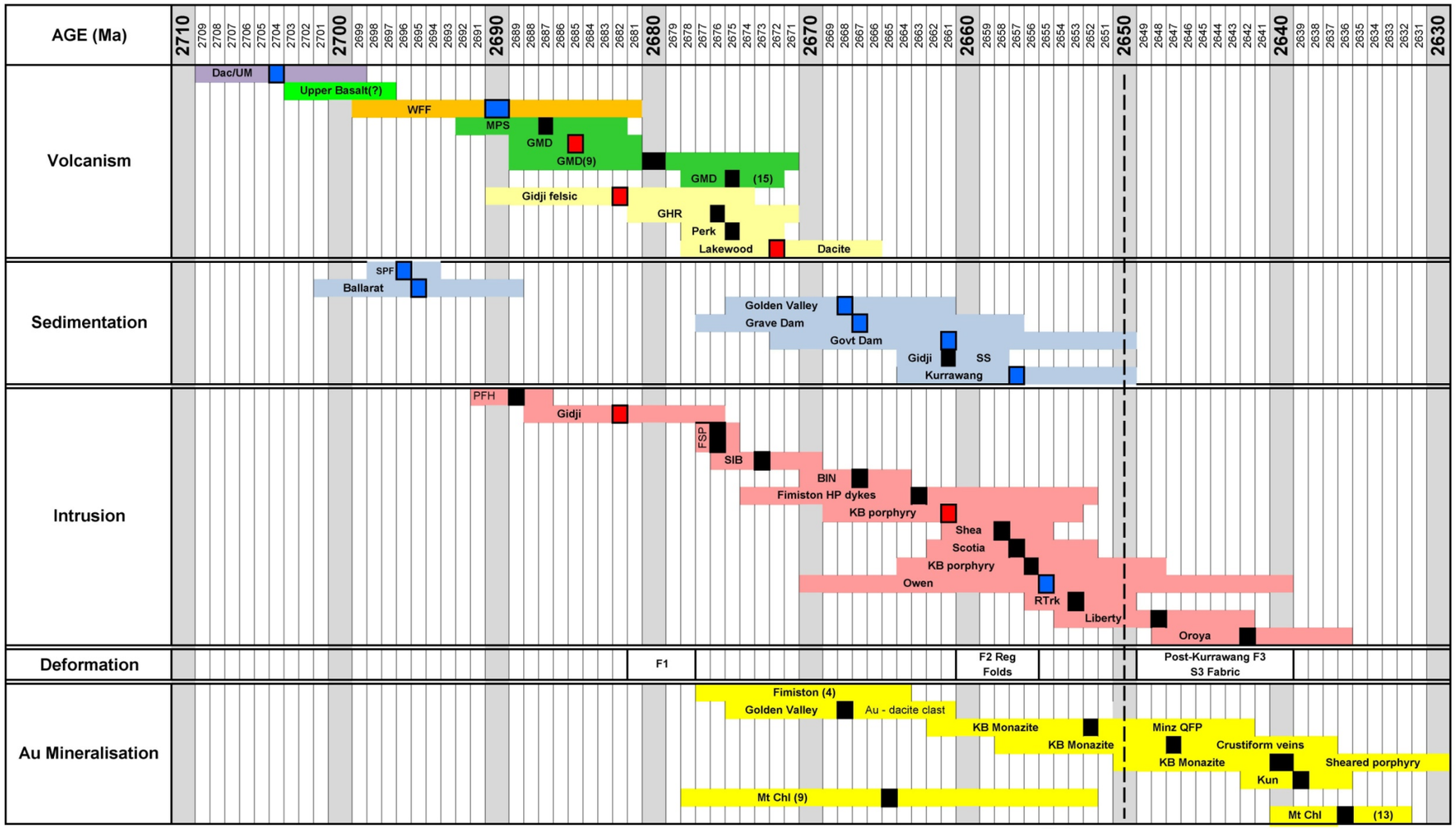

Ballarat Ballarat felsic grit (12)
BIN Centurion feldspar porphyry Binduli (3)
Dac/UM Kanowna/Gordons dacite ultramafic rocks (12)
Fimiston HP Hornblende porphyry dyke (4)
FSP Fimiston Feldspar porphyry dykes (4)
GHR Gibson-Honman Rock porphyritic dacite breccia clast (1)
Gidji Intermediate porphyry clast in conglomerate (3)
Gidji SS Felsic volcanic rock in Gidji Lake Conglomerate
GMD Golden Mile Dolerite sill (9,15)
Golden Valley Golden Valley polymictic conglomerate (12)
Golden Valley Au in dacite clast in Golden Valley Conglomerate (11)
Govt Dam Kanowna Government Dam sandstone (2)
Grave Dam Grave Dam felsic conglomerate/grit (10)
KB Kanowna Belle hydrothermal phosphate (13)
KB porphyry Quartz-feldspar porphyry (14)

Kun Kundana hydrothermal phosphate (13)
Kurrawang Sandstone interbed in Kurrawang Conglomerate (12)
Liberty Liberty biotite granodiorite (6)
MPS Mount Pleasant dolerite sill (5)
Mt Chl Mount Charlotte (9,13)
Oroya Oroya lamprophyre (4)
Owen Owen Batholith biotite monzogranite (12)
Perk Perkolilli rhyolitic volcanic rocks (7)
PFH Microdiorite porphyry - Mt Pleasant (12)
RTrk Racetrack Qz-Fd porphyry (16)
Scotia Scotia batholith hb-bi granodiorite (8)
Shea Mt Shea porphyry (1)
SIB Siberia Battery syenogranite (8)
SPF "Spargoville Formation" sandstone/shale - Mt Pleasant (12)
WFF White Flag Formation intermediate breccia (12)

References

(1) AMIRA P437
(2) Barrick / Squire (2008)
(3) Fletcher et al. (2001)
(4) Gauthier et al. (2004)
(5) Hill et al. (1992)
(6) Kent (1994)
(7) Nelson (1994)
(8) Nelson (1995)
(9) Rasmussen et al. (2008)
(10) Ross (2002)
(11 Ross et al. (2004)
(12) Sircombe et al. (2007)
(13) Vielreicher AMIRA P680
(14) Wang et al.
(15) Woods (1997)
(16) Yeats et al. (2000)

ANU age (this study)
SUMAC age (this study)
Granitoid intrusion
Sedimentary rock
Andesitic volcanic
Felsic volcanic
Mafic/UM sill
Mafic volcanic
Ultramafic volcanic

Table 4.4 – Interpreted rock ages from SHRIMP analyses in this study (coloured points) compiled along with selected ages from previous studies in the north Kalgoorlie district (black points) - see legend for details. The dashed vertical line at 2650 Ma marks the probable maximum depositional age of the Kurrawang Formation.

komatiite unit at Kanowna (Nelson 1997); whereas the Kapai Slate tuffaceous sedimentary rocks at the top of Devon Consols Basalt (upper unit of the komatiite unit) near Kambalda returned an age of 2692±4 Ma (Claoue-Long et al. 1988). These ages bracket komatiitic and associated mafic volcanism between 2715-2688 Ma. Results from this study at Kanowna place the age of komatiitic volcanism no older than ~2709 Ma; and new results from Mount Pleasant indicate the Upper Basalt unit is not younger than at least ~2687 Ma. A SHRIMP U-Pb zircon age of 2687±5 Ma (Hill et al. 1995) determined for the Mount Pleasant Sill, which intruded interflow sedimentary rocks at the base of the Upper Basalt unit, broadly supports the interpreted age bracket for mafic volcanism.

Sedimentary rocks overlying Upper Basalt (Black Flag Series)

The mapped section at White Flag Lake (Section 3.3) in combination with observations from the Kundana area shows a conformable progression up-section from Upper Basalt to the mapped Kurrawang unconformity at the western edge of White Flag Lake. Lowermost sedimentary rocks in normal depositional contact above the mafic volcanics (Victorious Basalt, Section 3.2.1; also presented later in Section 6.6.1.2) indicate no unconformity is present at that contact, which is at odds with the Barley et al. (2002) interpretation. Likewise, the contact between those sedimentary rocks and the overlying White Flag Formation was described as gradational by Hunter (1993) and Hand (1998), and is gradational in the Kundana area (Section 3.4). A prominent very coarse boulder-conglomerate at the base of White Flag Formation exposed on White Flag Lake, suggests at least local unconformable relationships, possibly representing a localised, proximal channel-confined mass-flow deposit.

SHRIMP U-Pb ages for the sedimentary rocks at Mount Pleasant include a 2696±2 Ma detrital zircon age suggesting deposition after ~2694 Ma, whereas a microdiorite sill that intruded those sedimentary rocks is analysed at 2689±2 Ma, providing a minimum age on the deposition of the sandstones. These two ages bracket the depositional age of the sedimentary rocks between 2694 – 2687 Ma. This age bracket is within error of 2698±6 Ma determined for felsic volcaniclastic ‘Spargoville Formation’ rocks at Golden Ridge (16 km SE of Kalgoorlie; Krapez et al. 2000). However, the ‘Spargoville’ designation originated from dacite breccia rocks immediately overlying mafic volcanic sequences at Widgiemooltha (close to the Spargoville type locality) and was published with a youngest population at 2686±3 Ma, and the youngest concordant zircon analysis at 2662±8 Ma, suggesting a significantly younger provenance than for the Mount Pleasant rocks. Near Kalgoorlie, the Golden Ridge and Mount Pleasant sequences were interpreted as ‘Spargoville Formation’ by Krapez et al. (2000), but young detrital zircon components at Widgiemooltha suggest the northern Golden Ridge and Mount Pleasant rocks were formed earlier than the ‘Spargoville’ units at Widgiemooltha. Long range correlation of those northern rocks with the Spargoville Formation at Widgiemooltha may

be invalid. An undeformed sharp contact was observed in drill core between ultramafic rocks and felsic volcanic rocks at Widgiemooltha (Consolidated Minerals drill hole - WDD282; GDA: 356750E; 6526600N), allowing for the possibility of an unconformity at that location.

White Flag Formation

White Flag Formation volcaniclastic breccia, is mapped as conformable to locally unconformable with the underlying sedimentary rocks at Mount Pleasant and interpreted at 2690±9 Ma. This age indicates a general overlap with the minimum age of the underlying sedimentary rocks (>2687 Ma), and supports the mapped field relationships. The previous interpretation of White Flag Formation as unconformably overlying the uppermost Black Flag Formation sequence of Krapez et al. (2000) is at odds with the SHRIMP analyses and field data presented here. White Flag Formation is separated by a thick zone of intercalated andesitic volcanics, deep-water deposited sandstone-shale and dacitic volcanic and volcaniclastic rocks to the south as far as Binduli. Intercalated, east-younging, lower White Flag Formation / upper Binduli sequence rocks are also present in the Goldilocks area south of Kundana (but notably lacking the thick sequences of below-wave-base sedimentary rocks present in the Ora Banda Domain).

At Kanowna, dacitic volcaniclastic sandstone with remnant glassy fragments (Ballarat Grit) is intercalated with the Ballarat conglomerate sequence with gradational contacts. Ballarat conglomerate is interpreted as a series of debris flow deposits from a proximal, actively-uplifted source area of ultramafic rocks with hypabyssal porphyritic intrusions due to the clast proportions and generally angular clast morphology: probably deposited in a restricted marginal basin. A gradational upper contact into the overlying Kanowna Conglomerate suggests this unit is also part of that continuing sedimentary depositional event, albeit with significant gradual changes in provenance up-section.

A 2695±6 Ma age determination for the dacitic sandstone indicates the Ballarat ultramafic-clast dominated conglomerate can be time correlated with either sedimentary rocks at Mount Pleasant (2694 - 2687 Ma) or White Flag Formation rocks at White Flag Lake (2690±9 Ma). Similar results were reported from SHRIMP U-Pb analyses of two samples from the Ballarat and Kanowna members with dominant age populations at ~2682 Ma and ~2687 Ma respectively by Squire et al. (2010). A further corroborating age interpretation of 2682±13 Ma was determined for quartz-rich grits in the Ballarat sequence by Kositcin et al. (2008). Those results combined with the findings of this work support correlation of the Ballarat-Kanowna sequence with rocks older than Lower Black Flag Formation. Interpretation of 2695±6 Ma as a maximum depositional age for the Ballarat conglomerate sequence, suggests deposition after ~2689 Ma. Unconformable relationships between the Ballarat-Kanowna sequence and the overlying Grave Dam member, and given a 2668±9 Ma interpreted maximum depositional age

of the latter (Ross et al. 2004), indicate a significant (>20 Ma) time break represented by the Grave Dam unconformity.

Lower Black Flag Formation

Rhyodacitic volcanic and volcaniclastic rocks at Gibson-Honman Rock indicate a renewal of felsic volcanism post-dating the deep-water sedimentation in the Ora Banda Domain. An attempt to re-analyse those volcanic rocks here was unsuccessful, and the previous age of 2676±5 Ma (Krapez et al. 2000) remains the best estimate of that volcanic event. Reconnaissance mapping and drill hole re-logging to the south (up section) from Gibson-Honman Rock shows deep-water deposited sandstones and mudstones, overlain by a further sequence of felsic volcaniclastic rocks to the west of the New Celebration Mining centre (Hunter 1993; Griffin 1990). The Ora Banda Domain sequence ends where the Zuleika and Abattoir Shear zones intersect in that same area west of New Celebration.

Dacitic volcanic and volcaniclastic rocks from the Lakewood area at the southern end of the Golden Mile overly a thin mudstone sequence with a locally intercalated breccia marker unit of similar composition to the overlying dacite. The age of the overlying dacitic rocks, determined at 2672±6 Ma, suggests they correlate with similar rhyodacitic rocks at Gibson-Honman Rock (2676±5 Ma, Krapez et al. 2000); and a thick sequence of mostly rhyolitic volcanic and volcaniclastic rocks at Perkolilli (2675±3 Ma, Nelson 1995).

The stratigraphy at Lakewood as re-interpreted from the Travis et al. (1971) cross section indicates the mudstone-dacite sequences are in sharp contact with the Golden Mile Dolerite. A 2685±4 Ma age determined for the Golden Mile Dolerite here indicates at least a three million year time gap between the intrusion of the GMD (>2681 Ma) and the Lakewood dacites (<2678 Ma). If the Rasmussen et al. (2010) 2680±9 Ma zirconolite age is correct, the two events overlap in error and no time gap is evident. The GMD age produced here is also within error of a SHRIMP U-Pb zircon age of 2687±5 Ma determined for the Mount Pleasant Sill (Hill et al. 1995) - a comparable strongly-differentiated dolerite sill with a granophyric zone that hosts many lode gold deposits; and the Condenser Dolerite at Kambalda (2680±8 Ma; Carey 1994).

Upper Black Flag Formation

Felsic volcaniclastic rocks at Gidji produced an age of 2660±16 Ma with an inherited component at 2682±8 Ma. These rocks unconformably overly coherent intermediate porphyritic rocks at Gidji analysed here also at 2682±8 Ma. The 2660±16 Ma Gidji volcaniclastic rocks are overlain by polymictic conglomerate-sandstone determined at 2666±6 Ma (Hand 1998). A demonstrable map-scale unconformity marks the base of that conglomerate-sandstone sequence, but the ages of the two units are within error nonetheless. The Gidji volcaniclastic sequence may be a lateral correlative of the Binduli Porphyry Conglomerate (<2664, section 3.3.3), and

the Grave Dam sequence at Kanowna (2668±10 Ma; Ross et al. 2004), all of which are conglomeratic sequences dominated by felsic volcanic debris.

Coherent intermediate rocks at Gidji (2682±8 Ma) are within error of the White Flag Formation (2690±9 Ma) and could be tentatively correlated with that unit. However this correlation cannot account for the andesite dominated southern part of the Gidji conglomerate east of Mount Charlotte (Section 3.5.2), from which a SHRIMP U-Pb zircon age was determined in a single andesite porphyry clast at 2661±3 Ma, and interpreted as the maximum depositional age of that unit (Fletcher et al. 2001).

A new age determination for the Golden Valley sandstone 2669±7 Ma accords well with the previous age of Ross et al. (2004), and considering the age of dacite-ultramafic rocks north of Kanowna Belle (2704±5 Ma), suggests an unconformity can be placed at the base of that unit in the footwall of the Kanowna Belle gold mine. The new age suggests deposition of the upper Golden Valley sandstone took place after ~2662 Ma. Regardless of major differences in lithofacies and bulk composition, Golden Valley conglomerate is time-correlated across the Fitzroy Fault with rocks of the Grave Dam Grit (2668±9 Ma, Ross et al. 2004), with a probable depositional age of the latter at <2659 Ma. These sequences appear to be correlative with the Gidji Conglomerate and Binduli Porphyry Conglomerate.

The crystallisation age of Kanowna Belle Porphyry determined here at 2661±8 Ma (with a dominant inherited component at 2698±5 Ma), is within error of the previously determined 2655±6 Ma age of Ross et al. (2004). These results considered with the age of the footwall rocks roughly bracket the initial thrust movement on the Fitzroy Fault between ~2662 Ma (deposition of the youngest footwall rocks) and ~2649 Ma (minimum error on fault-controlled intrusion). These results have no bearing on the question of whether the Fitzroy Fault represents a reactivated growth fault that controlled deposition of the Ballarat and Kanowna conglomerate sequences; however, the major lithofacies and provenance changes in rocks of comparable age across the fault, are suggestive of fault activity during deposition of the Grave Dam felsic volcaniclastic rocks. This suggested minimum age of fault movement provides a possible maximum age of deposition of the overlying unconformable Panglo conglomerate into which an extension of the Fitzroy Fault could not be found, despite extensive exploration drilling, which suggests truncation of the Fitzroy Fault at the unconformity.

Previous interpretations of the Government Dam sandstone-siltstone sequence (2661±11 Ma) placed these rocks as distal lateral equivalents of the Grave Dam Grit (Placer, Barrick). The quartz-dominated sandstone composition with paucity of feldspar crystal fragments led Dr. Squire to reject correlation of the Government Dam rocks with Grave Dam Grit. However the Grave Dam Grit is a dacitic provenance, quartz-rich sequence (+30% quartz) and this characteristic added to channelised dacite-clast conglomerates in the Government Dam rocks, and a close overlap in ages, could add support to the previously suggested correlation.

Kurrawang Formation

Unconformable clastic sedimentary rocks of the Kurrawang Formation post-date a folded basement that includes all units from the Lower Basalt up-section to felsic volcaniclastic rocks, high in the sequence, to the south of Binduli. The Kurrawang Formation is also folded and overprinted by a strong anastomosing foliation composed of metamorphic biotite. A sandstone interbed near the base of the polymictic Kurrawang conglomerate from Brown Dam with youngest population analysed at 2657±7 Ma suggests deposition of that unit after ~2650 Ma, and provides a maximum age estimate on the folding and foliation that has affected the Kurrawang Formation. An unconformable lower contact of the Kurrawang Formation on underlying Navajo Sandstone was documented in detail in Section 3.4, but a SHRIMP U-Pb zircon analysis of Navajo Sandstone at 2657±4 Ma (Fletcher et al. 2001) shows no major difference in age between the two units, which were considered integral parts of the same sequence by Krapez (1997), albeit with different detrital zircon provenance.

Intrusions

Batholithic granodiorite-granite intrusions form cores to the major regional anticlines in the Ora Banda and Boorara Domains. Previous SHRIMP U-Pb zircon crystallisation ages for the Scotia Batholith were determined at 2657±5 Ma (Nelson 1995), and 2656±3 Ma (AMIRA P482; Cassidy et al. 2002). The age determined for the Owen Batholith in this study (2655±15 Ma) is comparable with ages for the Scotia Batholith and with an age of 2648±6 Ma (Kent 1994) determined for the small Liberty Granodiorite stock in the hinge of the Mount Pleasant Anticline. These intrusions commonly contain a solid-state foliation parallel to the regionally developed pervasive fabric in the greenstones (excepting Liberty Granodiorite; Witt 1990), but given that the Kurrawang Formation and its equivalents are nowhere in contact with the granitic batholiths, a relative timing cannot be established. Whereas the Kurrawang Conglomerate is locally granite-clast rich, there is no substantive evidence that those clasts were sourced from the actual batholithic rocks exposed in the Ora Banda and Boorara Domains; however, the presence of abundant foliated granite clasts in the Kurrawang and Panglo conglomeratic units is suggestive of that possibility.

4.9.3 Stratigraphic interpretation

Most of the formations described in Chapter 3 have been previously interpreted in the context of facies analysis, sequence stratigraphy and chronostratigraphy (Krapez et al. 2000; Barley et al. 2002). The rocks in question are thought (Barley et al. 2002) to belong to two major subdivisions: late-stage sedimentary units interpreted to have been deposited in restricted, syn-collisional, strike-slip basins (‘late-stage basins’) close to terrane and domain boundary faults; and an older more extensive volcaniclastic association belonging to the Black Flag Group

and interpreted to have been deposited in deep-marine, strike-slip, intra-arc basins. The majority of rocks in the Black Flag Group have been interpreted as four facies from proximal (facies FA-1) to distal (facies FA-4) in terms of sedimentation models for submarine fans and gravel-rich slope-apron environments (Table 4.3). The interpreted facies at various localities were also assigned (Barley et al. 2002) to large-scale unconformity bounded genetic units or sequences (Table 4.3). The sequences were grouped into four stages on the basis of the constraints provided by SHRIMP U-Pb zircon geochronology for rocks at selected localities. Each chronostratigraphic stage corresponds to a tectonic cycle beginning with erosion, rapid subsidence and basin filling culminating in uplift accompanied by emplacement of granitoid rocks. This approach places more emphasis on the depositional and tectonic meanings of rock successions than on the classification of formal groups, formations or members (Krapez 1997).

Figure 4.21 is a schematic representation of revised lithostratigraphic columns for each of the domains at Kalgoorlie as interpreted for this study using the stratigraphic nomenclature of AMIRA P437 and P437A projects and new proposed subdivisions. The lower parts of each column are based on previous work (Table 3.1), but the upper parts have been adapted from the results of the current study and the SHRIMP analyses of Krapez et al. (2000) and Barley et al. (2002). The Ora Banda Domain appears to preserve the most complete stratigraphic section exposed in the anticline-syncline pair through Mount Pleasant and the Kurrawang conglomerate respectively. The interpretation of the map distribution of lithostratigraphic units using this nomenclature (Fig. 3.77, and Fig. 4.22 with ages) is based on the documented distinctions among coarse clastic units in terms of composition and texture (Chapter 3) as well as the structural and stratigraphic relationships between adjacent formations inferred from field relationships and supported with new and previous geochronology. The interpretations shown in figures 3.77, 4.21 and 4.22 provide some improvement in understanding of the key units in this area and provide the first (tentative) map of the distribution of the major formations throughout the north Kalgoorlie district.

Historic precedence and the rules of stratigraphic nomenclature demand that the term ‘Black Flag Series’, at its type locality, in the Black Flag mining district should revert to the original definition as outlined in Talbot (1934) and Forman (1937; 1953). To avoid confusion with the units higher in the stratigraphy, the name ‘Talbot formation’ is proposed here as an alternative for Talbot’s ‘Black Flag Series’. Also, application of the term ‘Spargoville Formation’, which has since been applied to all sedimentary and volcanic rocks overlying Upper Basalt (Swager et al. 1990; Hunter 1993) is not supported by the geochronology and chronostratigraphic correlations presented in Section 4.9.2. In the context of these new data, its continued use for units well outside of its type locality is not justified, despite overwhelming acceptance of this term in the literature. Lithofacies and geochronology indicate that the

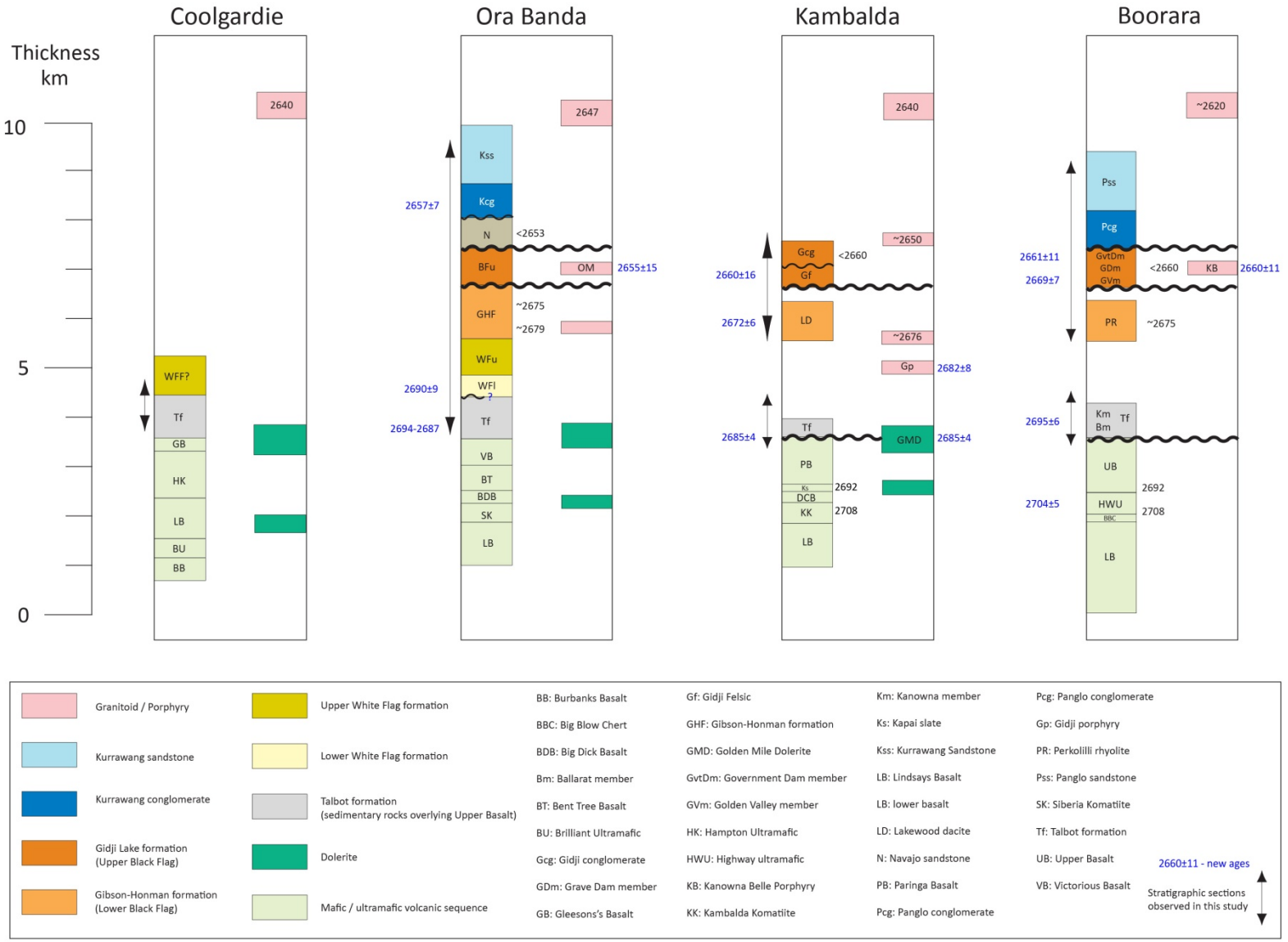

Figure 4.21 - Revised lithostratigraphic columns for each of the four geological domains at Kalgoorlie based on lithostratigraphic data from Chapter 3 and new age results from this study. Where possible the estimated ages of units are constrained by considering all available geochronological data (Table 2.1).

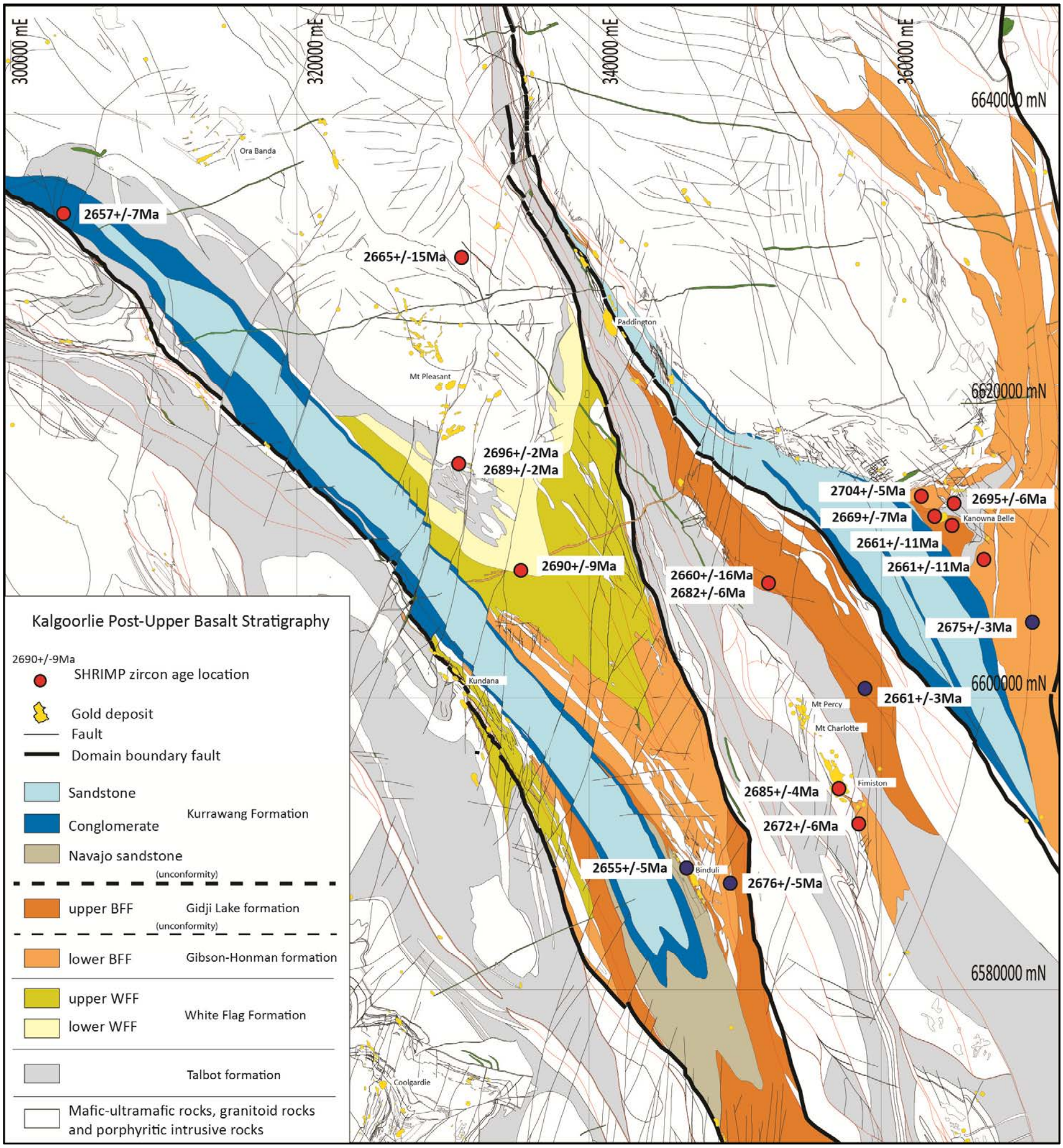

Figure 4.22 – Formation map of the major lithostratigraphic units in the Kalgoorlie area showing the geochronological constraints which guided the interpretation. New ages from this study in red, other ages in blue are from published sources.

sedimentary rocks at Mount Pleasant and Kanowna (Ballarat) are unrelated to the Spargoville felsic volcanic rocks.

White Flag Formation clearly occupies a much lower stratigraphic position than portrayed in reports from AMIRA P437 and P437A projects, and published in Krapez et al. (2000). The exposed section of the White Flag Formation can be divided into (gradational) lower and upper parts. The lower part is composed in large part of conglomerate derived mainly from an andesitic volcanic source and the upper part by juvenile andesitic volcanic rocks. It is essentially a volcanic rock unit and, at a broad scale, the White Flag Formation appears to be conformable with underlying and overlying strata.

The rocks overlying White Flag Formation include significant sections of plane-bedded turbiditic sandstone and mudstone, volcanic rhyodacite breccia at Gibson-Honman Rock and Binduli, and a section of sandstone-mudstone and felsic volcaniclastic rocks that continue up-section to the intersection of the Abattoir and Zuleika shear zones. In lithostratigraphic terms the rocks strongly resemble those at the type section of the Spargoville Formation observed at Widgiemooltha, whereas the Spargoville rocks have a distinctly younger component in their provenance. This leads to two options for nomenclature. One is to continue to use the term 'Spargoville' in the Kalgoorlie area, but modified to acknowledge a 'higher stratigraphic position', particularly in the Ora Banda domain. The second is to introduce a new term 'Gibson-Honman formation' to include the rocks around that geographic locality in the Binduli area, and time correlative sequences at Lakewood and Perkolilli (Figure 4.23).

In Chapter 3, new lithostratigraphic terms were introduced to provide general groupings of the various formations into lower and upper sequences (lower Black Flag formation; upper Black Flag formation). These included rocks interpreted with Stage 4 of Barley et al. (2002), but also sequences south of Gibson-Honman Rock. The Lakewood dacites were left in the ethereal 'Spargoville Formation' since their true stratigraphic position was unknown, but the age presented in Section 4.9.2 suggests the Lakewood dacites correlate with Gibson-Honman Rock, and the Perkolilli rhyolites; and should be allocated to that lower Black Flag formation, or a preferred 'GIbson-Honman formation' subdivision.

The second grouping 'upper Black Flag formation' included rocks south and up - section from Gibson-Honman Rock; unconformable felsic dominated breccia, overlain by unconformable quartz-rich polymictic pebbly sandstone at Gidji; and unconformable Grave Dam and Golden Valley members at Kanowna. New ages from Kanowna and Gidji confirm the correlations suggested in Chapter 3; hence, it may be preferable to include those units in a new stratigraphic unit, here proposed as a ‘Gidji Lake Formation’ for the locality where it is reasonably well exposed. This new formation would include members such as the Gidji felsic unit; Gidji conglomerate and sandstone as well as the volcanic andesite breccias and volcanic-derived conglomeratic rocks in drill holes MAD01 and MAD02 east of Mount Charlotte;

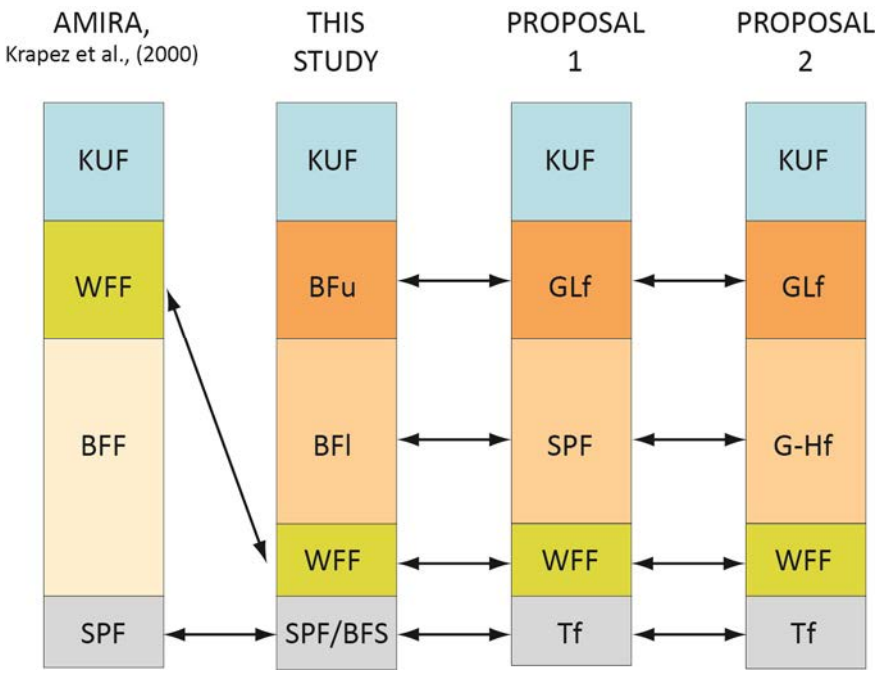

Figure 4.23 – Comparative stratigraphic columns illustrating alternative usage of stratigraphic terms. Arrows link equivalent rock units. SPF – Spargoville Formation; BFS – Black Flag Series; Tf – Talbot formation; WFF – White Flag Formation; BFl/u – Black Flag fm (l-lower, u-upper); G-Hf – Gibson-Honman formation; GLf – Gidji Lake formation; KUF Kurrawang Formation).

Golden Valley and Grave Dam members from Kanowna; and potentially the Kanowna Government Dam sandstones and Binduli porphyry conglomerate.

Given the unconformable cross-cutting relationships of the Panglo conglomerate west of the Kanowna Belle gold mine, and that the unit cuts down section across pre-unconformity folded rocks from Lower Basalt to Perkolilli rhyolites, in similar fashion to the Kurrawang Formation, the Panglo conglomerate is suggested as a correlative of the Kurrawang Formation. This is despite a somewhat different lithostratigraphic column from the type Kurrawang Formation and a lack of corroborating geochronology. Previous authors placed these rocks at a much lower chronostratigraphic position, and placed a major fault along the eastern contact (Section 3.6.4).

Proposal 2 in Figure 4.23 is a preferred way to resolve many of the issues that beset the stratigraphic terminology of the north Kalgoorlie district, and is the recommended stratigraphic designation from this work. This approach particularly deals with the issues of ‘Black Flag’ vs ‘Spargoville’, places the White Flag Formation in its proper location in the sequence, and relates the upper parts of the ‘Felsic Volcanic and Sedimentary Unit’ to major unconformable sequences mappable in outcrop and drilling.

Table 3.1 (Map Pocket) demonstrates the interpreted correlation of these new designations with published stratigraphic columns. In some instances (e.g. Coolgardie, Norseman) these far-

field correlations will not necessarily hold, which is reasonable given the structural controls on stratigraphic development discussed in Chapter 5.

4.9.4 Summary

Sixteen new SHRIMP U-Pb zircon analyses produced fourteen ages on rocks from the major sequences and intrusions from the north Kalgoorlie district. A review of the stratigraphic terminology from 1913 to present demonstrates general consensus in correlations of the mafic and ultramafic volcanic sequences, and the late unconformable clastic sedimentary rocks; but no such consensus exists for the intervening intermediate-felsic volcanic, volcaniclastic and sedimentary rocks. The all-encompassing term 'Black Flag Group' is no longer a useful designation, whereas the term 'Felsic Volcanic and Sedimentary Unit' of Swager et al. (1990) is preferred as a much better description of the major central subdivision of the Kalgoorlie stratigraphy; and would be a useful field term if new exposures are encountered, where the correlations are uncertain.

Since the Ora Banda Domain is widely recognised as containing the least structurally disrupted and best preserved primary geological relationships in the Kalgoorlie district, it follows that the stratigraphy in that domain should form a standard column against which other, partial sequences are compared. Furthermore, since Kalgoorlie has been the main centre of exploration and mining for >100 years, many of the well documented published sections have been derived from that area.

New stratigraphic subdivisions and terms are proposed for the north Kalgoorlie district to better reflect correlations made on the basis of lithostratigraphy and chronostratigraphy, and to provide a series of units that can be translated into a 'formation map'. Such maps that adequately deal with the vast amount of field and exploration drill-hole exposure, extant in the area, provide a much needed simplification of the highly detailed lithological maps produced by industry and government agencies of the past 30-40 years. The lithostratigraphy and chronostratigraphy outlined in Chapters 3 and 4, attempt to document a standard stratigraphic column to that end.

5 Domain boundary faults – Zuleika Shear Zone

5.1 Introduction

A general discussion on shear zones of the study area, and detailed documentation of the Zuleika Shear Zone (ZSZ), is presented here before the deformation history in Chapter 6 since stratigraphic variations indicate some of the shear zones (including the ZSZ) may have been active from the beginning of greenstone formation (DE) to the penultimate shortening event (D3b). Some previous studies recognised early movement on the shear zones, but placed them much later in the deformation history nonetheless, usually as 'D3' with inferred strike-slip kinematics (e.g. Swager et al. 1990; Swager 1997; Krapez et al. 2000). This interpreted late timing reflects that major shear zones separate large, upright anticlines and synclines, generally ascribed to a 'D2' timing. A revised deformation chronology is proposed in this study (see Chapter 6, Table 6.1), which broadly follows that of Swager et al. (1990) and is the scheme referred to in subsequent sections unless otherwise referenced.

A key issue for shear zones is distinguishing strain localisation zones developed during the latest contractional deformation phases, from pre-existing major structures that played a role in the earliest extensional controls on basin formation (i.e. 'terrane' and 'domain' boundary faults). A possible criterion to make that distinction is whether a shear zone has a map pattern control on the distribution of greenstone stratigraphy, as opposed to minor displacements. Major 'terrane boundaries' should logically juxtapose blocks with significant differences in litho-tectonic sequence and geochronology, or metamorphism. 'Domain' boundaries on the other hand would be expected to have wallrocks with similar sequences and ages, albeit with minor local differences.

The Kalgoorlie Terrane subdivision of Swager et al. (1990) was made on the basis of regional stratigraphic variations between interpreted lithostratigraphic domains, and the presence of recognised faults between those domains. However, the domain boundary faults were generally interpreted to occupy a 'D3' structural timing and have been related to interpreted strike-slip events that mostly post-date the greenstone belt construction phase (Swager et al. 1990). In some papers those same faults were interpreted as major accretionary structures or sutures (Krapez and Barley 2008; Barley et al. 2008).

Most domain boundary faults in the Eastern Goldfields Province display steep foliations with variable lineation plunges (Eisenlohr et al. 1989; Passchier 1994; Libby et al. 1990; Vearncombe 1998; Tripp 2002b), which may reflect (1) overprinting of multiple events, or (2) localised controls on the principal axis of stretching along the shear zones, controlled by orientation changes and/or the presence of anisotropy (among other factors). These fabrics are generally considered to relate to the *latest* episodes of movement, except in cases where detailed microstructural work can demonstrate overprinting of events (e.g. Davis et al. 2010).

Hints on the possible role of the faults in *early* greenstone construction phases were addressed by Blewett et al. (2010), and also in work by research consortia of the pmdCRC group (Blewett et al. 2010; Czarnota et al. 2010). These studies attempted to redress the role of the major faults, but with an emphasis on fabric data. Many workers have relied heavily on preserved stretching lineations for the interpretation of early fault movements (Weinberg and Vanderborgh 2008; Blewett et al. 2010a; Williams and Whitaker; Hammond and Nisbet 1992); and particularly, lineations preserved on the south-eastern and north-western margins of granitoid domes (the D2 'strain shadows' of Passchier 1994).

In the study area, the distribution of major shear zones as interpreted from mine exposures, drill hole generated map distributions of stratigraphy, and geophysics is presented on a regional geology plan in Chapter 3 (Fig. 3.1). Domain boundary shear zones are highlighted with thick lines, whereas there are many other intra-domain shear zones observed in outcrops and drill holes, or interpreted from map patterns and geophysics. Some stratigraphic change occurs across the Zuleika and Bardoc shear zones and the Mount Monger Fault (an interpreted terrane boundary; Swager 1997), but other shear zones have a less dramatic control on stratigraphy despite locally strong deformation and wide zones of foliation. Shear zones with major controls on stratigraphic distribution may be extensional faults later reactivated during subsequent thrust and strike-slip events, or may have been original transfer faults that accommodated differential shortening or extension across their boundaries.

The goals of this chapter are (1) to document the character of a 'major' shear zone, (2) to assess the validity of the 'domain boundary' concept, and (3) to assess domain boundary fault controls on the early stratigraphy of the Kalgoorlie greenstones.

5.2 Zuleika Shear Zone (ZSZ)

Of the domain boundary shear zones in the north Kalgoorlie district, the Zuleika Shear Zone was chosen for detailed mapping and structural analysis since it appears to have a long-lived history indicated by (1) variation of the oldest rock units (mafic-ultramafic volcanics) on either side, and (2) linear control on the youngest sedimentary sequences (Kurrawang Formation). Long-lived structures are a likely focus of strain localisation subsequent to their formation, possibly recording later deformation increments; hence, the ZSZ is documented at the beginning of this chapter so that observed fabrics and its role in the context of later deformation events can be better understood.

The ZSZ is poorly exposed at surface with the best exposures restricted to exploration drill holes and mines at the Kundana, Zuleika and Chadwin mining centres (Fig. 5.1). The shear zone is documented as separating generally low-strain, low-middle greenschist facies rocks of the Ora Banda Domain, from high-strain upper greenschist to lower amphibolite facies rocks of the

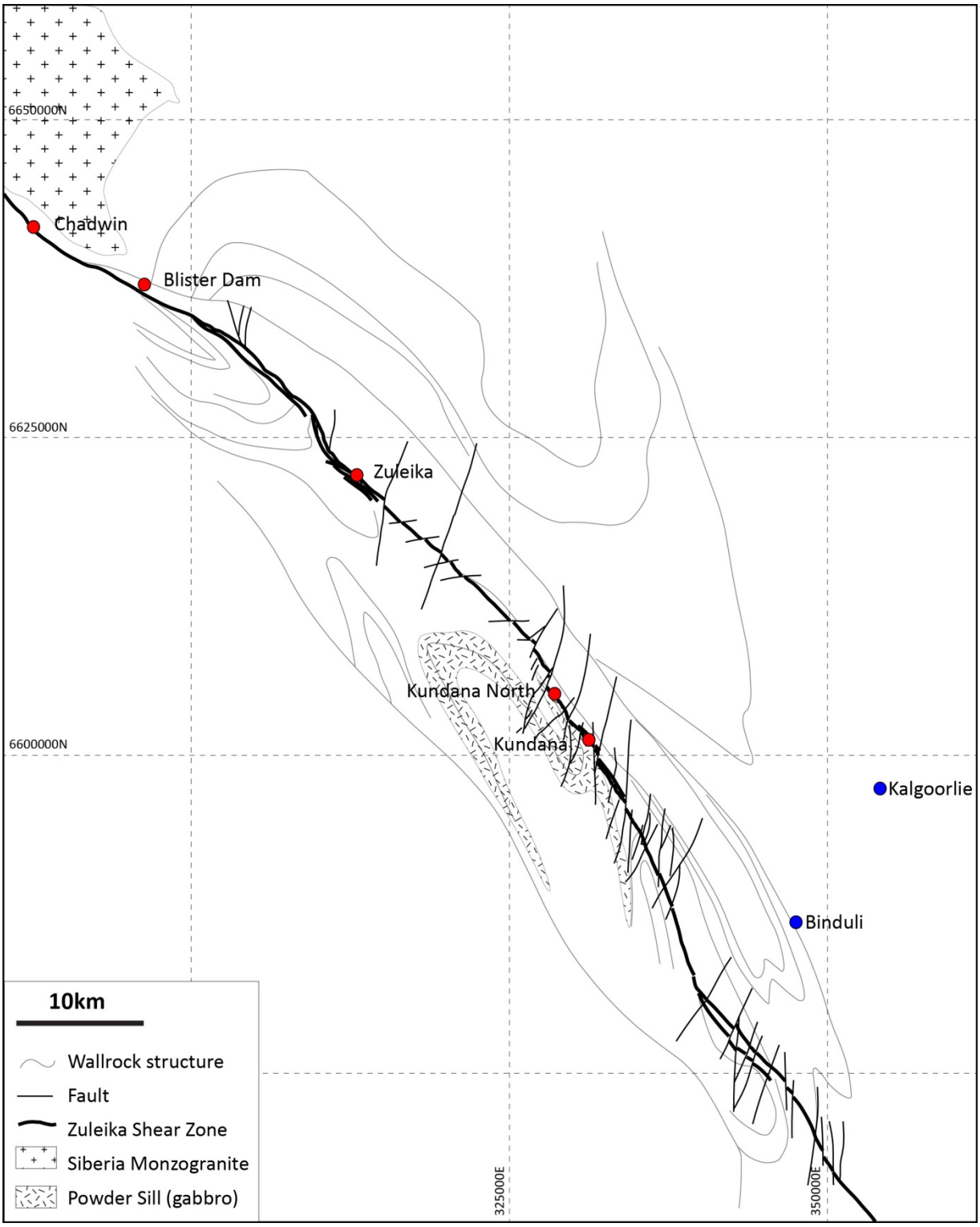

Figure 5.1 – Location of the Zuleika Shear Zone and detailed areas of study marked in red. Thin grey lines are bedding trends in wallrocks of the shear zone; compare with Figure 3.1 for coloured geology.

Coolgardie Domain (Witt 1990; Morris 1993). As discussed in Chapter 2, distributions of metamorphic facies show that the shear zones do not separate diverse crustal blocks.

The following section documents structural relationships and fabric data from four areas along the ZSZ: Kundana/Kundana north, Zuleika, Blister Dam, and Chadwin (Fig. 5.1). These data sets were published in a 2002 field guide by the Australian Institute of Geoscientists (Tripp 2002c), and an extended abstract from the same conference (Tripp 2002b). Note that detailed documentation of the Zuleika Mining Centre was presented in a previous M.Sc study (Tripp 2000) and published in Tripp (2002c). Some new data for that area are presented here, but the orientation data presented later in the summary section (see Figure 5.15 – marked with asterisk *) are from the previous M.Sc study (all other data are from the current study). The previous data are included here for comparison with new observations from a greater number of exposures than were available to the original M.Sc study, which was focussed solely on the Zuleika and Ora Banda districts. The previous and current work will be clearly distinguished in the following sections, which describe exposures of the ZSZ from south to north.

5.2.1 Kundana Mining Centre / Kundana north

Kundana Mining Centre

The location of the ZSZ is well-constrained at Kundana in mines and drill holes (Fig. 5.2), and particularly diamond drill hole CRD97 (Fig. 5.2; Fig. 5.3a-e), which intersects strained sedimentary rocks of the Black Flag Group in the Coolgardie Domain, and a slightly overturned, west-dipping sequence of Upper Basalt unit mafic volcanics, and intrusive and sedimentary rocks of the Ora Banda Domain stratigraphy, including the distinctive Victorious Basalt (Fig. 5.3b, c). These two sequences are separated by a ~12 m-wide zone of mylonite and biotite-quartz-carbonate (ankerite) schist separating sedimentary rocks of the Coolgardie Domain sequence from dolerite at the base of the Ora Banda Domain sequence (Fig. 5.3d). The mylonite is characterised by abundant quartz-ankerite veining with strongly deformed vein textures including boudinage, folding, stretched and dismembered vein segments, and porphyroclastic vein segments wrapped by a quartz-biotite foliation (Fig. 5.3d, e).

Several other zones of high strain intensity are located up to 20 m from the domain boundary fault, and these are likely splay faults of the main ZSZ (Fig. 5.3c). In the Victorious Basalt, those high strain zones display stretching of the plagioclase phenocrysts into elongate, rodlike shapes with axial ratios of up to 7:1 (Fig. 5.3c). This relationship is also confirmed from mapping in the North /Arctic gold mines at Kundana, where the principle stretching axis is represented by steeply northwest-plunging, rodded plagioclase phenocrysts in the Victorious Basalt (Fig. 5.4a, b). The steep lineation is parallel to fold axes of open folds in meta-sedimentary rocks that also plunge at 80º to the northwest (Fig. 5.4c). Shear foliations in the North and Arctic gold mines dip steeply, with reverse kinematics suggested by asymmetric

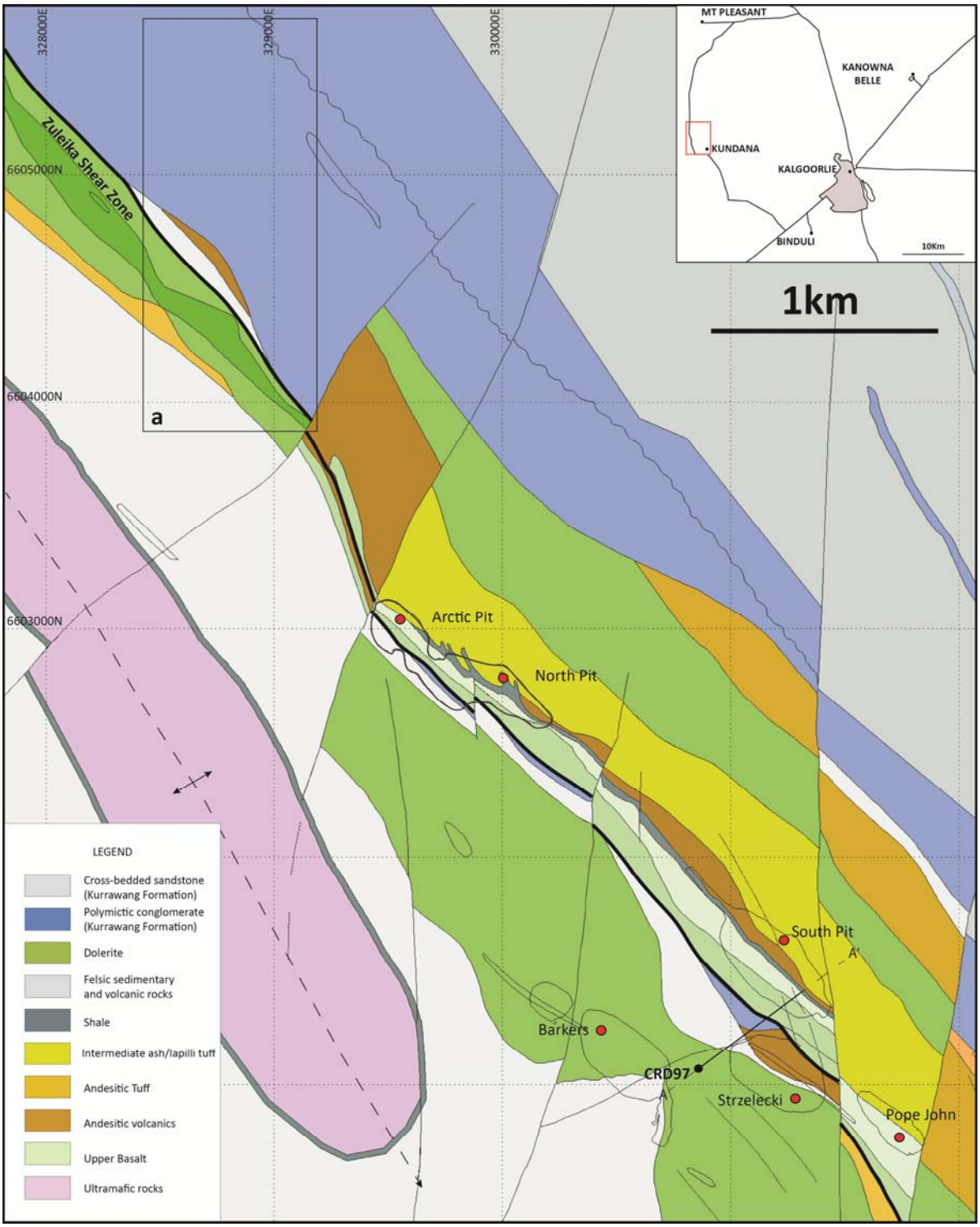

Figure 5.2 – Barrick GIS geology map compiled and re-interpreted from drill holes logged in this study. Note the location of exposures of the Zuleika Shear Zone in the Kundana area, referred to in the text, and the location of drill hole CRD97; the box marked (a) refers to location of Kundana North outcrops (Fig. 5.5).

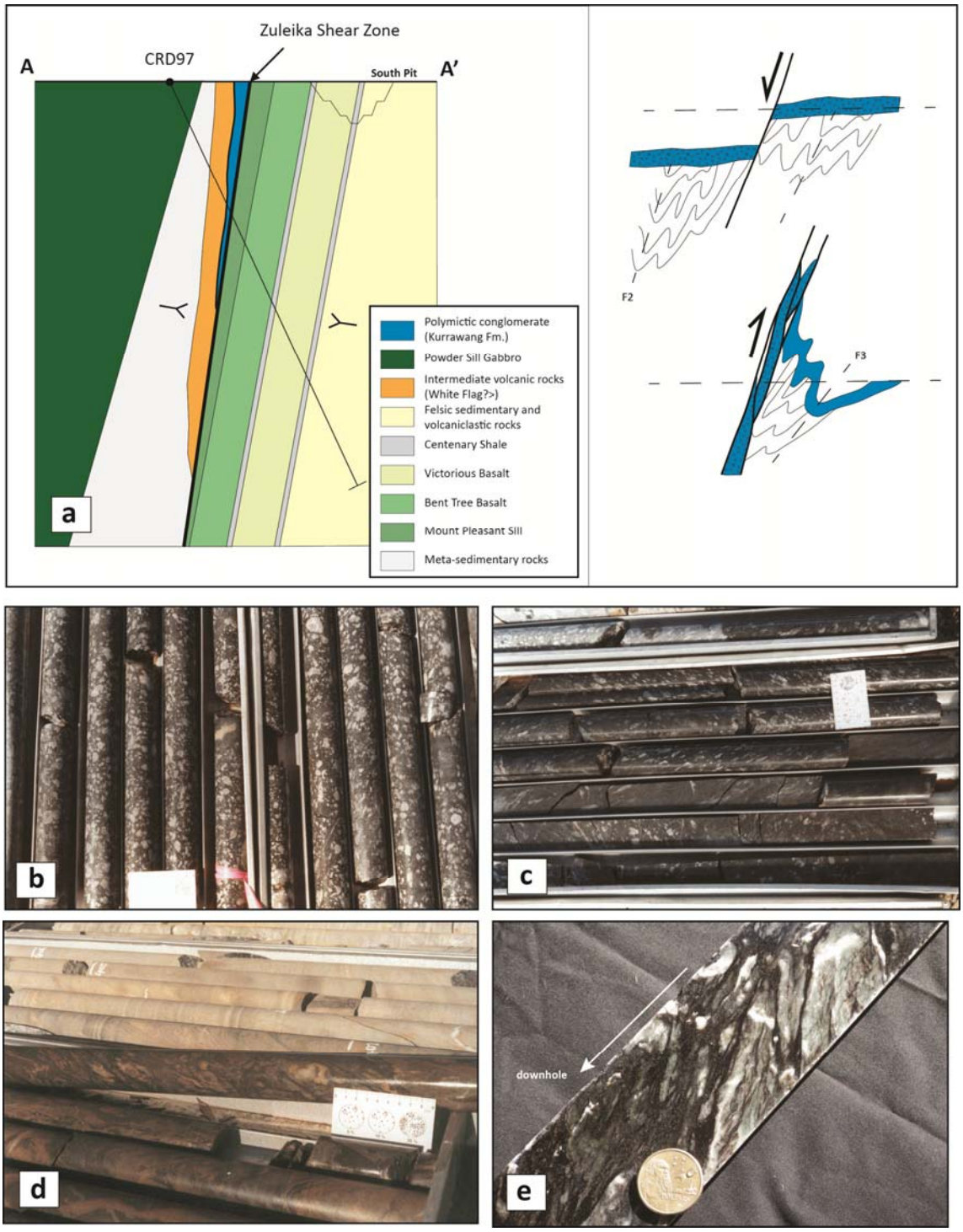

Figure – 5.3 a) Schematic cross-section A-A' located on Figure 5.2 along the trace of drill hole CRD97 - intersecting a sliver of Kurrawang polymictic conglomerate on the western wide of the Zuleika Shear Zone, and a section of east-younging overturned Upper Basalt stratigraphy typical of the Ora Banda Domain. View is to the northwest. Schematic diagrams show a possible explanation for the sliver of Kurrawang Formation entrained within the Zuleika Shear Zone; b) coarse plagioclase-phyric unstrained Victorious Basalt; c) high strain zone in Victorious Basalt with highly stretched plagioclase phenocrysts; d) Zuleika Shear Zone, biotite-altered zone of sheared rocks with abundant carbonate veins, folded and dismembered throughout the shearing; e) Polished slab close-up of strong upright biotite foliation and sheared vein segments in the Zuleika Shear Zone.

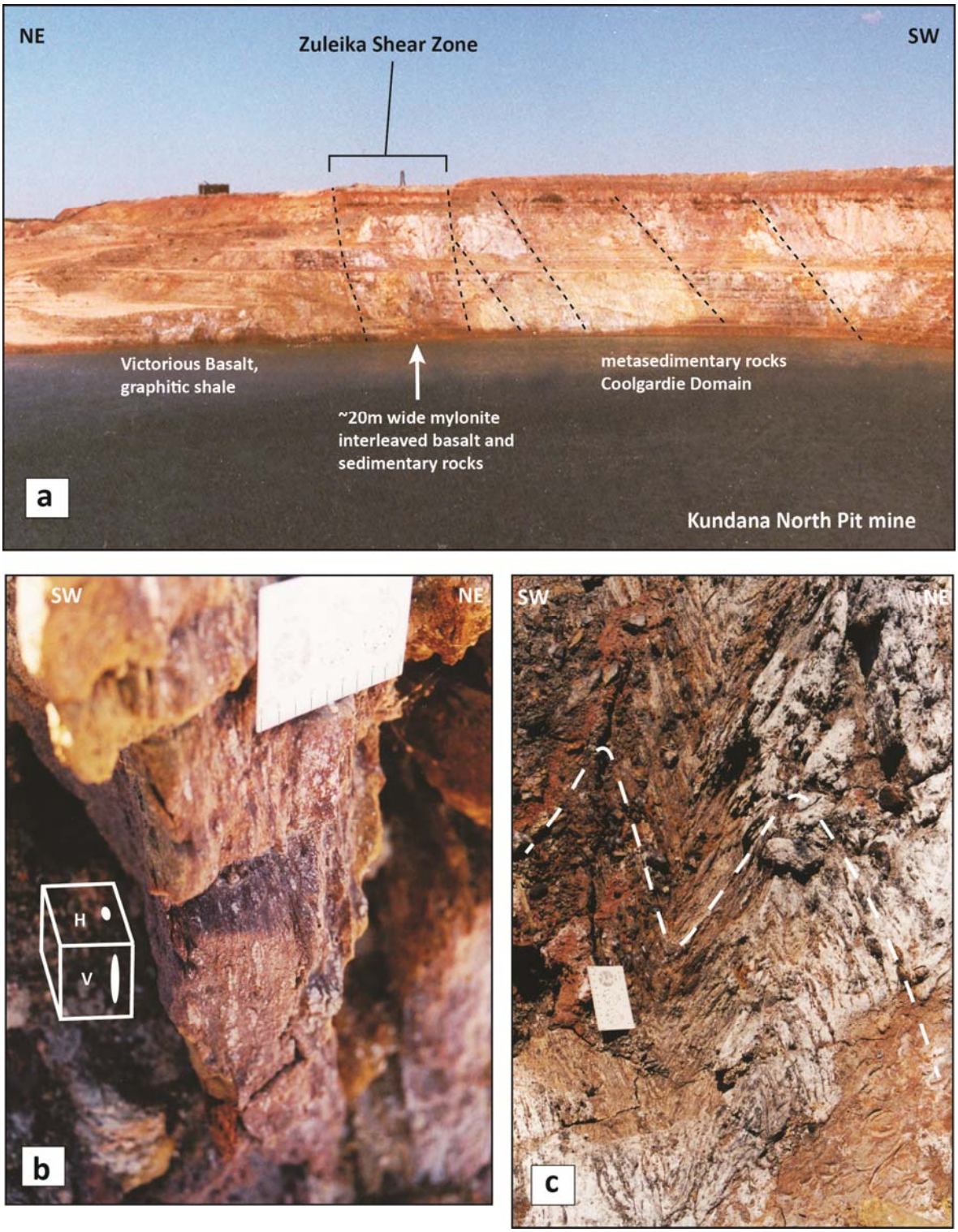

Figure – 5.4 a) View of the North Pit mine at Kundana, looking south. The Zuleika Shear Zone is a sub-vertical zone of intense foliation and shearing separating visibly layered metasedimentary rocks of the Coolgardie Domain from stretched-phenocryst Victorious Basalt to the east; b) 3D mine exposure of steep stretching lineation in highly weathered Victorious Basalt defined by stretched plagioclase phenocrysts H-horizontal plane, V-vertical plane; c) folded metasedimentary rocks in the Arctic Mine with steep 80°N plunging fold axes, parallel to the stretching lineation in (b).

boudinage of quartz veins when viewed in P-section (parallel to stretching lineation / perpendicular to foliation).

In the North pit gold mine, the ZSZ contains small disconnected slivers of polymictic conglomerate composed of clasts of diverse compositions (Fig. 5.2; Fig. 5.3a). The conglomerate slivers are structurally disconnected and appear to be segments of Kurrawang Formation incorporated in the ZSZ. This relationship indicates post-Kurrawang unconformity movement on the ZSZ, and it is likely this movement accompanied S3 foliation development, during D3 deformation (Fig. 5.3a).

Kundana North

Outcrops at Kundana north (Fig. 5.5) expose a mylonitised contact between gabbro and schistose rocks that were originally Kurrawang Formation pebbly sandstones and conglomerates (Fig. 5.6a). Kurrawang Formation sandstones and conglomerates are highly deformed with foliation intensity reaching a maximum at the western contact against the gabbro (Fig. 5.6b, c). The gabbro is part of the Powder Sill unit, which intruded sedimentary rocks of the Coolgardie Domain. Mafic clasts in the conglomerate are stretched into elongate rod-like shapes with axial ratios up to 20:1 in the vicinity of the contact with gabbro (Fig. 5.6d)

A prominent stretching lineation is defined by elongated conglomerate pebbles with a mean plunge of 60°N in a strongly anastomosing mica foliation with steep dips that vary about the vertical (Fig. 5.1; Fig. 5.5; Fig. 5.6e). Outcrops in this area show clast compositions dominated by abundant quartzite and vein-quartz pebbles, but also polymictic clasts including dacite porphyry, equigranular granite, and banded-iron-formation pebbles.

Outcrop-scale kinematic indicators in a horizontal plane show sinistral shear sense (Fig. 5.6f, g). Despite the horizontal plane not being optimal for evaluating the kinematics of a shear zone with a moderate to steep stretching lineation, weak sinistral movement sense is apparent nonetheless (Fig. 5.6f, g).

At a distance of ~750 m east from the ZSZ, thin discontinuous sandstone lenses internal to conglomerate units are folded, as are thin conglomeratic bands in sandstone sequences with folds plunging (~15°) to the south (Fig. 5.6h). The folds plunge sub-parallel to a bedding and cleavage intersection lineation, and are representative of the regional F3 fold axis. Outcrops in the centre of the Kurrawang Formation distant from the ZSZ have pebble elongation lineations that also plunge ~15°S. These relationships suggest a significant rotation of linear fabrics proximal to the ZSZ, and may indicate syn-late D3 movement on the ZSZ.

Quartzite pebbles in the sheared conglomerate have a unique ‘brittle-ductile’ fracturing as a result of dominantly oblique sinistral slip on the ZSZ (Fig. 5.7a-f). In outcrop, the fractures have variable orientations; but in well-located, oriented specimens, have fracture displacement

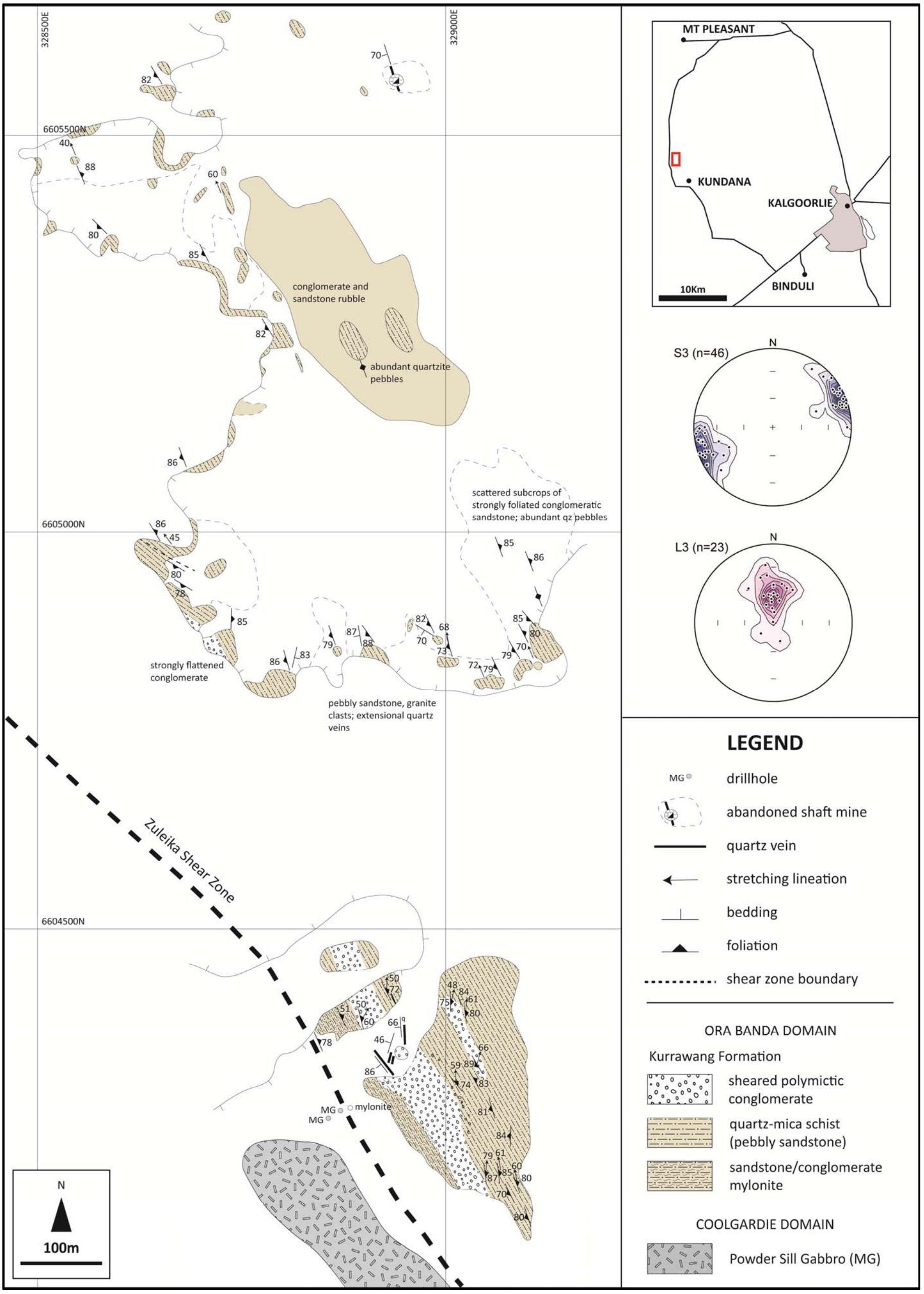

Figure 5.5 – Field map of a rare surface exposure of the Zuleika Shear Zone at Kundana north, location from box “a” on Figure 5.2. Highly sheared sedimentary rocks of the Kurrawang Formation are juxtaposed with relatively undeformed Powder Sill Gabbro. Polymictic conglomerate bands indicate that the strike of bedding is transposed sub-parallel to the shear zone. The principal stretching lineation is determined from mineral alignments in quartz mica schists and aligned clasts in stretched pebble conglomerate with a predominant steep N-plunging stretching axis. This N-plunging stretching lineation contrasts with subvertical (down-dip) stretching lineations at Kundana, and shallow northwest-plunging stretching lineations at Zuleika.

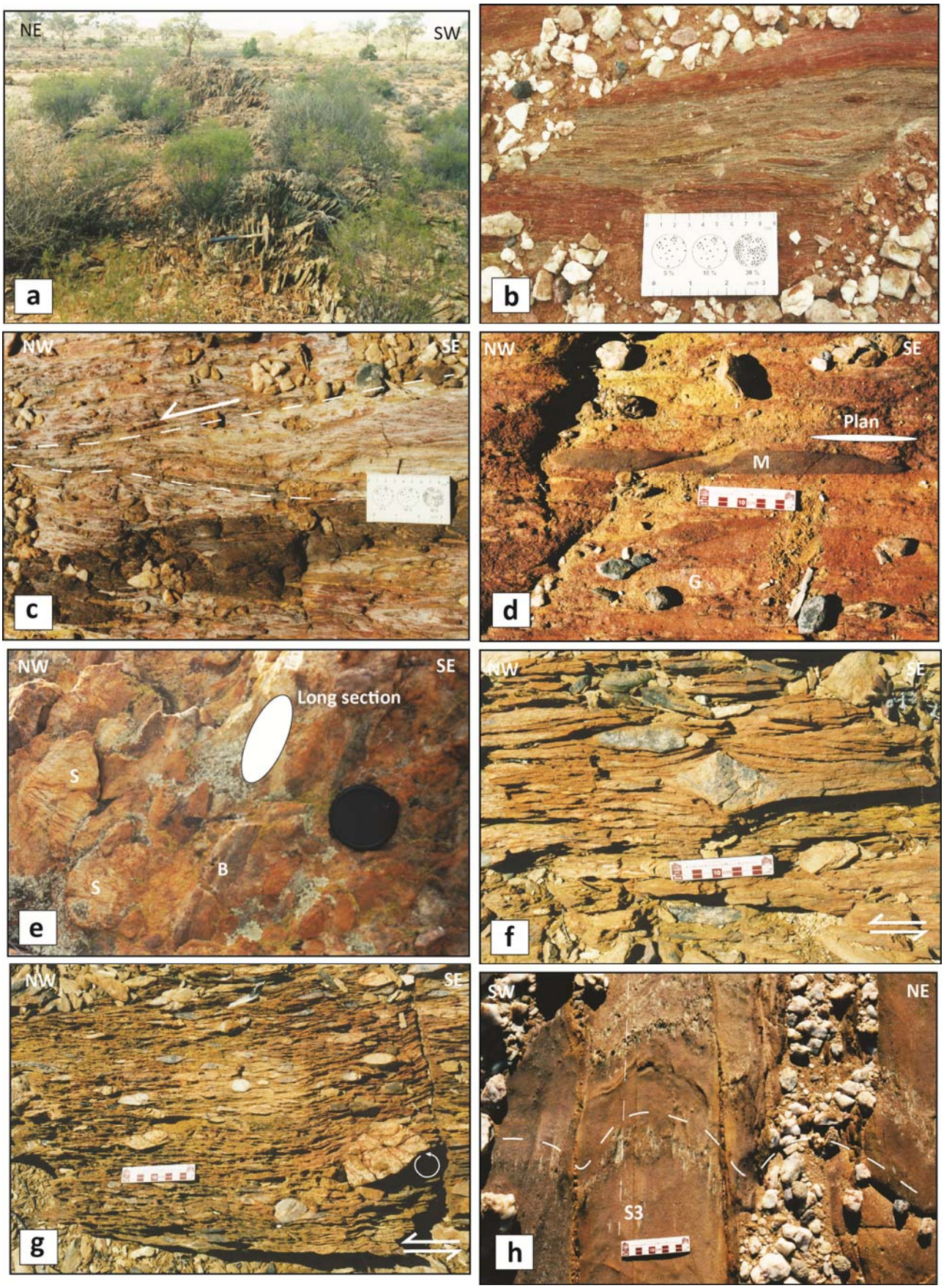
NE
SW
a
b
NW
SE
c
NW
SE
Plan
M
G
d
NW
SE
Long section
S
B
S
e
NW
SE
f
NW
SE
g
SW
NE
S3
h

Figure 5.6

Captions for Figure 5.6 – Zuleika Shear Zone at Kundana north outcrops

a) Outcrop of quartz-mica schist after Kurrawang Formation sandstone/siltstone (GDA: 329100E; 6604124N). The outcrop is located at the western margin of the Kurrawang Formation, with moderately foliated Powder Sill gabbro in adjacent outcrops to the west. The rock is intensely sheared silicified grey slate and forms distinct platy rubble. The dominant foliation is oriented 80º/250º with a poorly defined mineral lineation at 49º/328º. The foliation is parallel and planar in horizontal section, but anastomosing in cross-section, and cut by non-penetrative, but ubiquitous, kink folds with 055° striking axial planes.

b) Intensely sheared conglomeratic sandstone (Zuleika Shear Zone) at the westernmost margin of the Kurrawang Formation (GDA: 328930E; 6604310N). Flattening fabrics are dominant in the outcrop with some suggestion of sinistral strike-slip from pebble asymmetry within a fine grained anastomosing foliated sandstone matrix.

c) Sinistral S-C foliation deflection sense in sheared pebbly sandstone at a contact with Powder Sill Gabbro (GDA: 328953E; 6604355N). The conglomeratic sandstone contains abundant slivers (clasts) of mafic and ultramafic volcanic rocks with an intense shear fabric trending 60º/073º.

d) Outcrop of stretched mafic volcanic clasts in polymictic Kurrawang Conglomerate with ~20:1 axial ratios in the X-Z plane (GDA: 329690E; 6604111N). Highly stretched mafic volcanic pebbles are common in the vicinity of the contact with Powder Sill Gabbro with shallow to moderate northwards plunging long axes. Purple weathered gabbroic rocks are highly strained within 10 m of the contact, but then quite unstrained at >10 m; a sharp strain gradient is accompanied by abundant magnetite alteration (M=mafic; G=granitic).

e) View of longitudinal section in the plane of the shear foliation with steep N-plunging pebble lineation in stretched pebble Kurrawang Conglomerate (GDA: 329054E; 6604268N). The sheared conglomerate contains a range of pebble compositions all with strong moderate to steep N-plunging long axes (S=sedimentary; B=BIF).

f), g) Horizontal pavements showing dominantly sinistral shear sense in deformed cobble conglomerate with abundant quartzite and granite clasts (GDA: 329727E; 6604293N). A granitic pebble in (f) is strongly deformed into a σ-type porphyroclast showing sinistral shear sense with asymmetric stretching of the clast. A rotated granitic clast in (g) likewise shows sinistral sense of shear, amongst several other clasts with asymmetric pressure shadows and clast stretching.

h) Pavements at ~750 m distance from the Zuleika Shear Zone in bedded-sandstone and pebbly conglomeratic Kurrawang Sandstone (GDA: 329782E; 6604001N). Bands of conglomeratic sandstone show open folding. Conglomerate clasts have dominantly mafic composition and are highly flattened with strong alignment parallel to the S3 foliation axial planar to board open folds. Locally the folds are south plunging with S0: 40º/170º and S3: 88º/252º at GDA: 329949E; 6603965N.

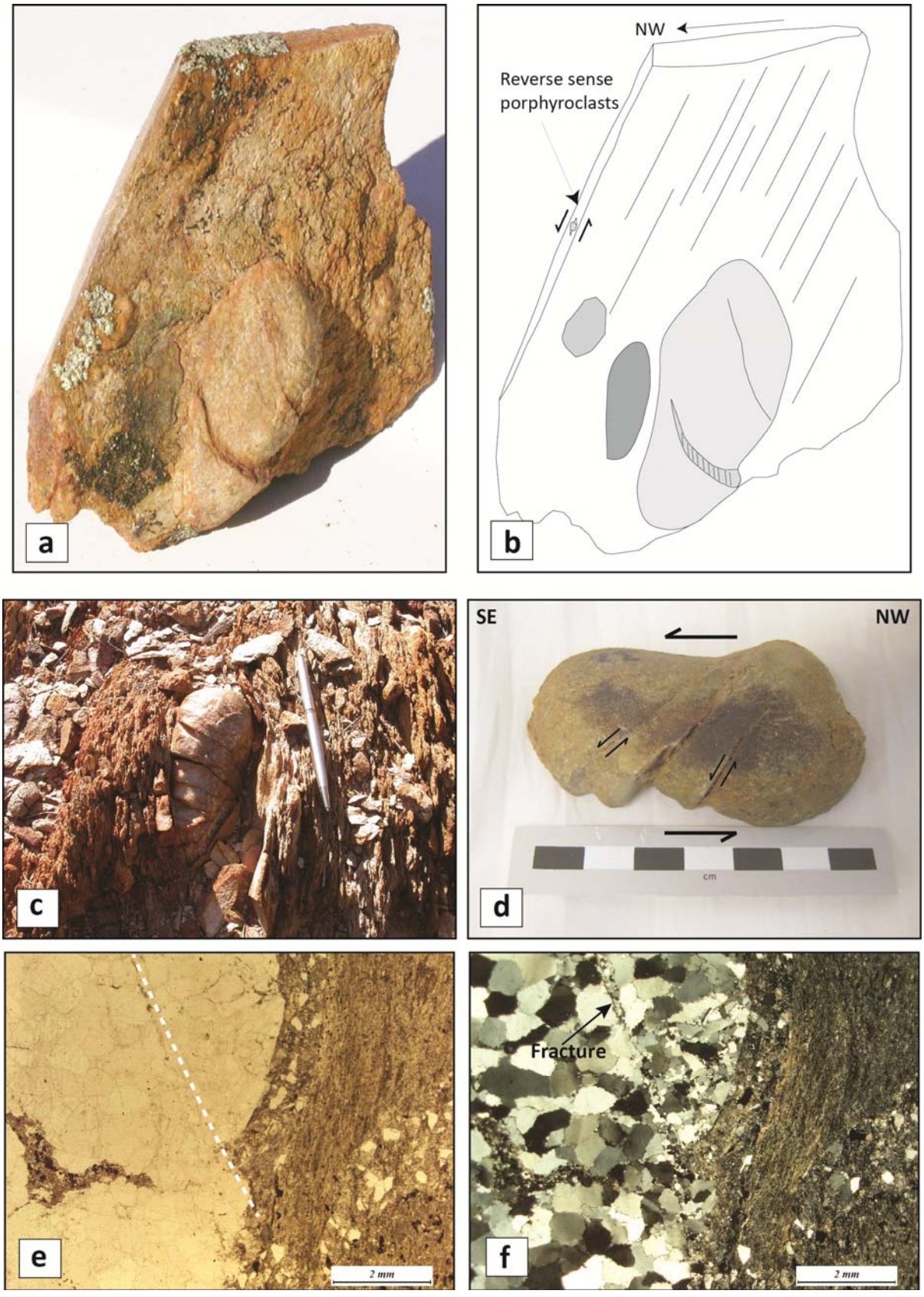
a
NW
Reverse sense
porphyroclasts
b
c
SE
NW
cm
d
e
2 mm
Fracture
f
2 mm

Figure 5.7

Captions for Figure 5.7 – deformed quartzite pebbles in Kurrawang Conglomerate:

a), b) Line drawing and photograph of a quartzite pebble in foliated quartz-sandstone matrix (GDA: 329008E; 6604408N). A prominent stretching lineation is defined by the long axes of pebbles, sand grains and mica folia in the matrix. The sample has two cuts, one horizontal and the other perpendicular to the foliation and parallel to the stretching lineation. Micro-scale porphyroclast kinematic indicators on the latter show sinistral reverse shear sense in the steeply west-dipping shear foliation. Fractures in the large quartzite pebble have a unique brittle-ductile deformation style in which the discontinuous brittle fractures grade into coherent quartzite. On the brittle fracture surface, quartz rods define a slickenside lineation and the fracture offset is compatible with the reverse-sense kinematic indicators in the sheared matrix foliation.

c) Outcrop with fractured pebble wrapped by strongly foliated, schistose quartz sandstone - Kundana North (GDA: 328999E; 6605182N).

d) Fractured quartzite pebble displaying combined brittle and ductile strain (GDA: 329800E; 6604120N). Brittle fracture planes on the lower side of the pebble appear to terminate in coherent recrystallised quartzite. In three dimensions the quartzite pebbles appear to have been twisted with ductile squeezing of the coherent side of the pebble. These unique deformation structures were first described by Maclaren and Thomson (1913).

e) PPL photomicrograph of deformed quartzite pebble from the Kurrawang Conglomerate in drill hole RCDD001 108.2 m (GDA: 327637E; 6608157N). The brittle offset on the margin of the pebble is clear with a strong metamorphic biotite foliation in the matrix wrapping the quartzite clast.

f) XPL photomicrograph of same view in e) showing the microstructure of the fracture plane is composed of fine recrystallised quartz grains with 120 grain boundaries, healing a fracture within dynamically recrystallised quartzite of equant undulose quartz grains with strongly sutured grain boundaries. The termination of the fracture is abrupt where a linear train of fine foam fabric strain-free quartz grains and biotite flakes ends in large sutured quartz grains, suggesting the ductile component of the pebble deformation was accommodated in the undulose quartz.

senses that match with micro-scale kinematic indicators in the surrounding schist (Fig. 5.7a, b, c).

The fractures have an unusual relationship of brittle displacements at the edges of the pebbles that project into ductile shear planes in the centre of the pebbles (Fig. 5.7d). In hand specimen the surfaces of those fractures are covered with quartz rods defining a stretching lineation, whereas in thin section, they are narrow bands of strain-free, very fine-grained recrystallised quartz grains with 120° foam fabrics that terminate in coarse grained recrystallised quartz with strongly sutured grain boundaries (Fig. 5.7e, f).

5.2.2 Zuleika Mining Centre

The ZSZ at the Zuleika mining centre is poorly defined since there are no exposures of the Ora Banda Domain sequence (Fig. 5.8). Ultramafic, mafic volcanic and sedimentary rock units are unconformably overlain by the Kurrawang Formation to the east of the mining centre but those ultramafic rocks are present as kilometre-scale, tectonic slivers with highly deformed margins. Ductile shear zones are located within basalt flow rocks at the Bullant gold mine and at a mafic/ultramafic rock contact in the Wattlebird mine (Tripp 2000, 2002c). Those shear zones are possibly splay faults of the ZSZ, but are unlikely to represent the domain boundary.

Orientation analysis of the shear zones shows a variably dipping foliation with a mean eastward dip of 80º/060º and a shallow northwest 18º plunge of stretching lineations within the shear zone (Fig. 5.8 inset - data from Tripp, 2002c). Detailed microfabric analyses reveal sinistral kinematics from S-C relationships and asymmetric porphyroclasts indicating dominantly sub-horizontal movement sense (Tripp 2002c). Dextral ductile shear zones striking NNW-SSE are conjugate with the dominant NW-SE striking shear zones. Finite strains in the wallrocks display strong flattening of variolitic texture in basalt, and flattened pillow margins that are progressively shortened closer to high strain zones with axial ratios of up to 5:1 (Tripp 2002b,c).

New data from this study

A major shear zone was intersected in drill hole BUGD615 from the Bullant gold mine and drill hole ZULD8 from the Bowerbird prospect (Fig. 5.9a, b, c). The shear zone is localised at a contact between sedimentary rocks and a package of intercalated high-Mg basalt and komatiite, but does not separate demonstrably different stratigraphic sequences (Fig. 5.8). A ~100 m wide deformation zone is characterised by tectonically mixed lithological assemblages comprising sedimentary, felsic volcanic, mafic and ultramafic volcanic rocks, coincident with abundant deformed crustiform, carbonate-quartz veins, and intense carbonate-sericite alteration (Fig. 5.9a, c).

The fabric of the shear zone is dominated by strongly buckled and crenulated veins with sheared-out limbs, within strongly foliated, altered wallrocks (Fig. 5.9b,c). The intense carbonate alteration is typical of most exposures in mines and drill holes and indicates the ZSZ was a

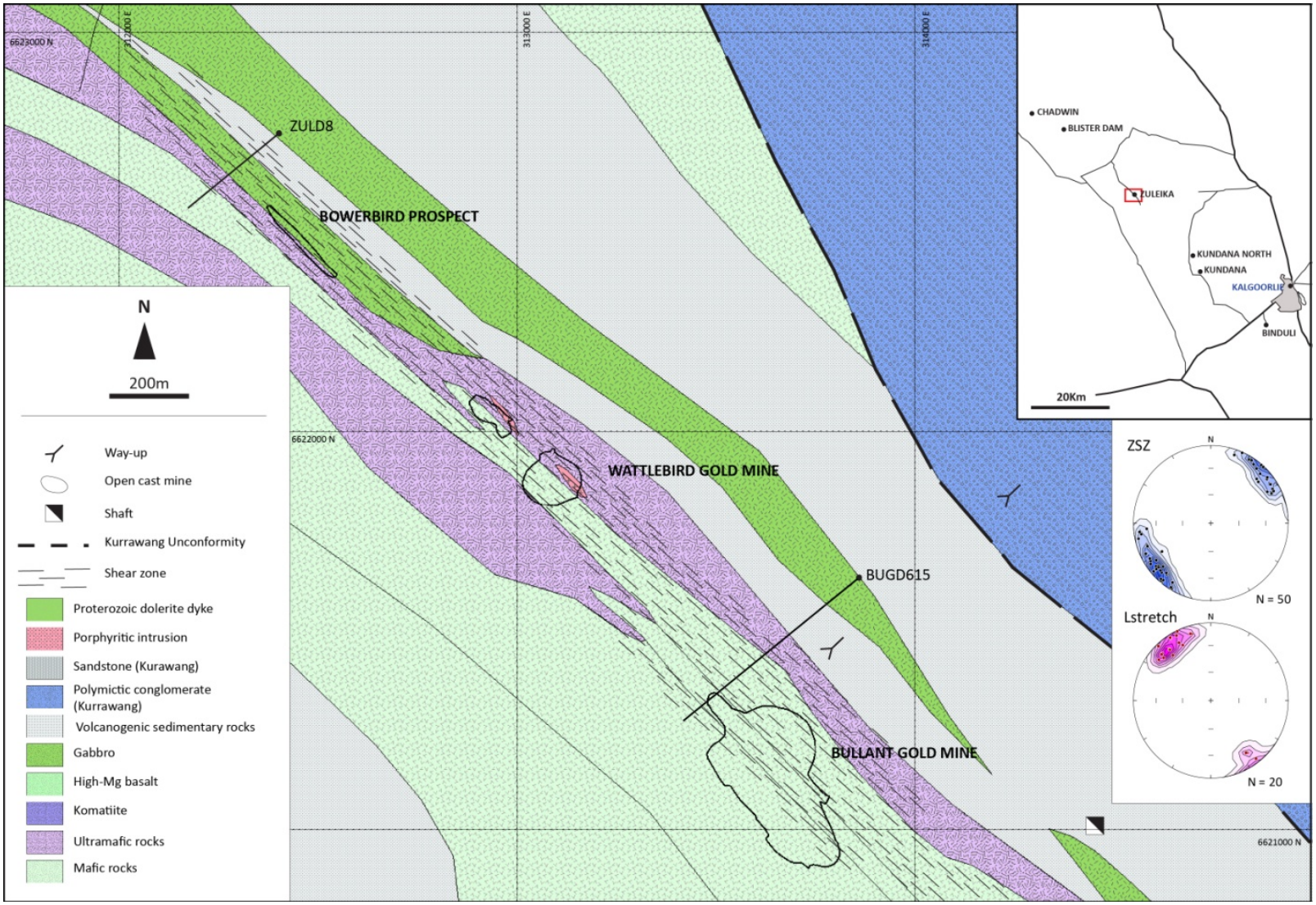

Figure 5.8 – Barrick GIS map of southern Zuleika Mining Centre. Equal area projections show data compiled from the Zuleika Mining Centre (Tripp 2002b). New work here includes mapping in the Bullant - Bowerbird area and re-logging of key drill holes as located on the figure.

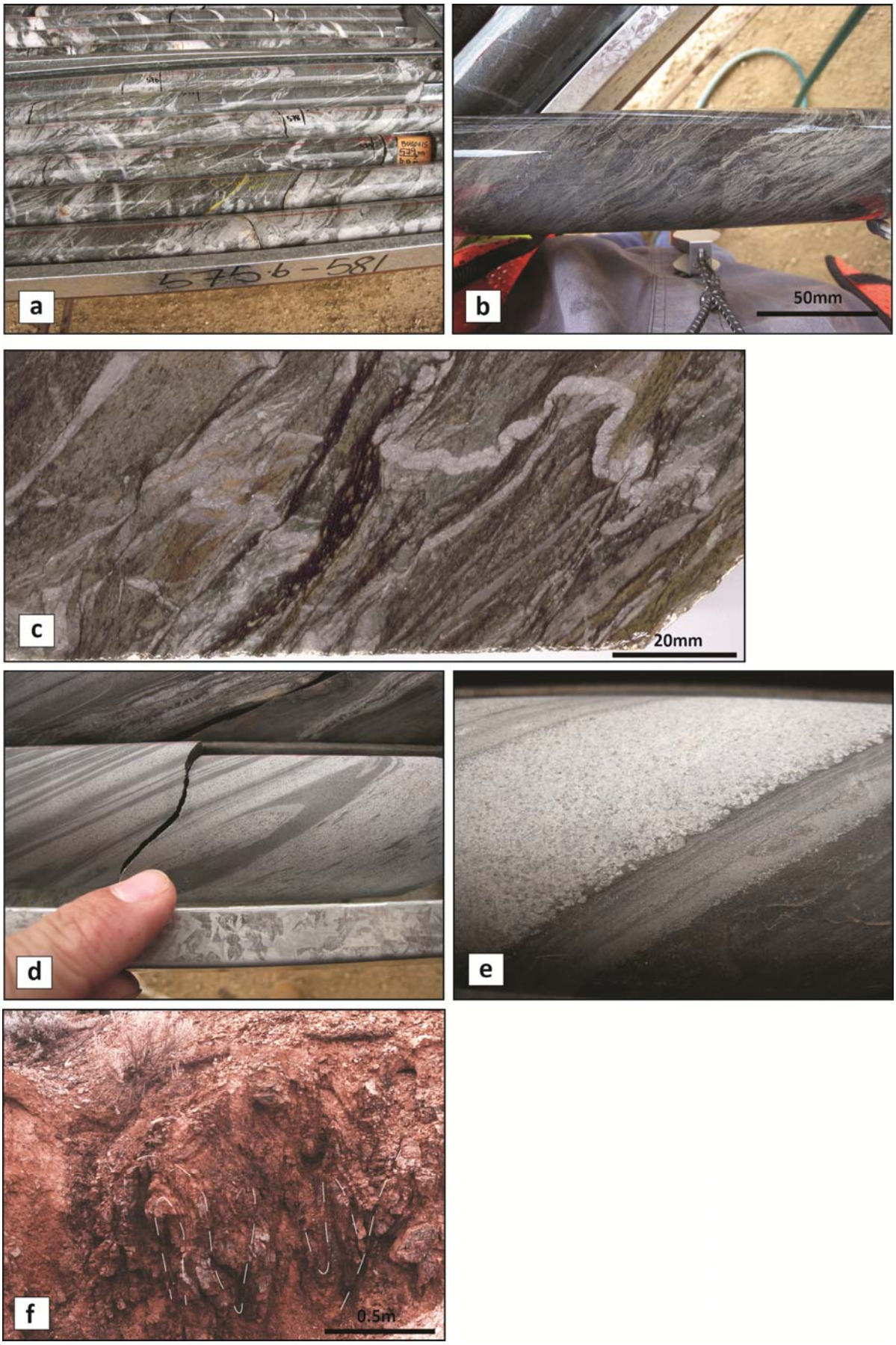

Figure 5.9

Captions for Figure 5.9

a) Drill core intersection of sheared high-Mg basalt at the Bullant gold mine in drill hole BUGD615 573 m to 581 m (GDA: 313858E; 6621632N). Green coloured sections are composed of sericite-carbonate+/-biotite altered, highly sheared, high-Mg massive basalt and variolitic pillowed basalt, interspersed with zones of white, crustiform sulphide-quartz-carbonate veins. The crustiform dolomitic carbonate veins show various levels of deformation from highly buckled and contorted, to massive, mostly unstrained veins that are probably folded at a scale greater than the drill core intersection. White quartz +/-albite? veins overprint the crustiform early veins. High volume hydrothermal veining and alteration in sheared zones is typical of the Zuleika Shear Zone. The shear zone in this drill hole is entirely within mafic volcanic rocks from 517 m to 630 m down hole.

b) Finely banded mylonite from the most intensely sheared parts of BUGD615 517 m to 630 m, composed of white carbonate-sericite-pyrrhotite foliation bands interspersed with deformed vein and rock fragments.

c) Intensely deformed mylonite from the Bowerbird gold mine, drill hole ZULD8 (GDA: 312402E; 6622747N). The shearing is interpreted as the Zuleika Shear Zone, a ~100 m wide interleaved zone of intermediate volcaniclastic rocks, cherty sedimentary rocks, felsic porphyry, mafic volcanic rocks and ultramafic komatiites with an average orientation of 75º/245º. Wallrocks to the east of the shear zone are strongly foliated with flattened leucoxene and biotite. The foliation grades into discrete 1 m wide zones of orthomylonite in intermediate volcaniclastic rocks, characterised by porphyroclasts of plagioclase and coarse-grained crystal-lithic tuff in a fine-grained matrix. Ultramylonite (50 m wide), forms the most intense portion of the shear zone with ribbon quartz and asymmetric porphyroclasts.

d), e) Rare examples of eastward (uphole) younging indicated by sedimentary flame structures in sandstone / shale turbidites in BUGD615 at 446 m; and at 479 m in **(e)** base of photo ~70 mm. At 514.5 m in BUGD615, bedding in strongly deformed graphitic shale with intrafolial folds and sulphide-replaced mudstone layers trends 83º/220º.

f) Mine shaft exposure of highly deformed cherty metasedimentary rocks in the eastern sedimentary succession of the Zuleika district (GDA: 314438E; 6621017N). Tight isoclinal folds plunge at ~10º/010º approximately parallel to stretching lineations measured from shear zones in the Bullant gold mine.

significant zone of hydrothermal fluid flow. Localisation of gold deposits and intimate association of the gold deposits with carbonate alteration suggests synchronous deformation and mineralisation at favourable sites along the shear zone.

At several localities in shafts and trenches, the shearing intensity obscures the original rock types. Fine grained mafic and sedimentary rocks are represented by minor variations of colour in zones of continuous cleavage. The distinguishing characteristics of the Zuleika mining centre exposures are the development of a strong shallow-plunging stretching lineation within an upright foliation (Fig. 5.1; Fig. 5.8). This kinematic style is similar to Blister Dam (next section), but contrasts with other exposures of the ZSZ.

Rare examples of eastward younging are indicated by sedimentary structures in sandstone / shale turbidites of the wallrocks (Fig. 5.9d, e). In drill hole BUGD615 the sedimentary rocks are well preserved with regular graded bedding, whereas shaft exposures of the same sedimentary sequence to the south of the Bullant mine display tight to isoclinal buckle folding (Fig. 5.9f). The overall younging of the sequence appears to be towards the east despite strong upright folding of the sedimentary rocks at a local scale.

5.2.3 Blister Dam

A small exposure of the Kurrawang Formation at Blister Dam is located immediately east of the ZSZ as inferred from aeromagnetic imagery and gross distribution of stratigraphy (Fig. 5.10a). The Kurrawang Formation at this locality comprises polymictic stretched-pebble conglomerate in a strongly foliated matrix. The S3 foliation has an average southwest dip of 80º/220º and pebble long axes that plunge ~30º SE. Stretching lineations are slightly shallower than a bedding-foliation intersection lineation of 55º SE (interpreted regional F3) measured from a small trench at Blister Dam (Fig. 5.10b, c). This exposure is in an area where the strike of the ZSZ turns to a WNW-ESE orientation approaching the Siberia Monzogranite. Stretched pebbles in the conglomerate have axial ratios of up to 8:1 with a mean of 3:1. The rocks at this locality have a higher degree of finite strain than similar rocks at greater distances from the ZSZ. Although the shear zone is not exposed at Blister Dam, the rocks may be influenced by the shearing located 10’s of metres to the west, and identified from mixed interleaved litho-types in exploration drilling.

5.2.4 Chadwin Mining Centre

Magdala gold mine at the Chadwin mining centre exposes the ZSZ where it juxtaposes intensely deformed metasedimentary and metavolcanic rocks of the Coolgardie Domain with amphibolite grade Victorious Basalt (or Lower Basalt?) of the Ora Banda Domain (Fig. 5.1; Fig. 5.11, Fig. 5.12; Figs. 5.13a-h). The mine is located within 1 km of the western contact of the Siberia Monzogranite, and this intrusion has locally metamorphosed the rocks to amphibolites facies, which are of lower metamorphic grade (greenschist) away from the contacts. Mine exposures are

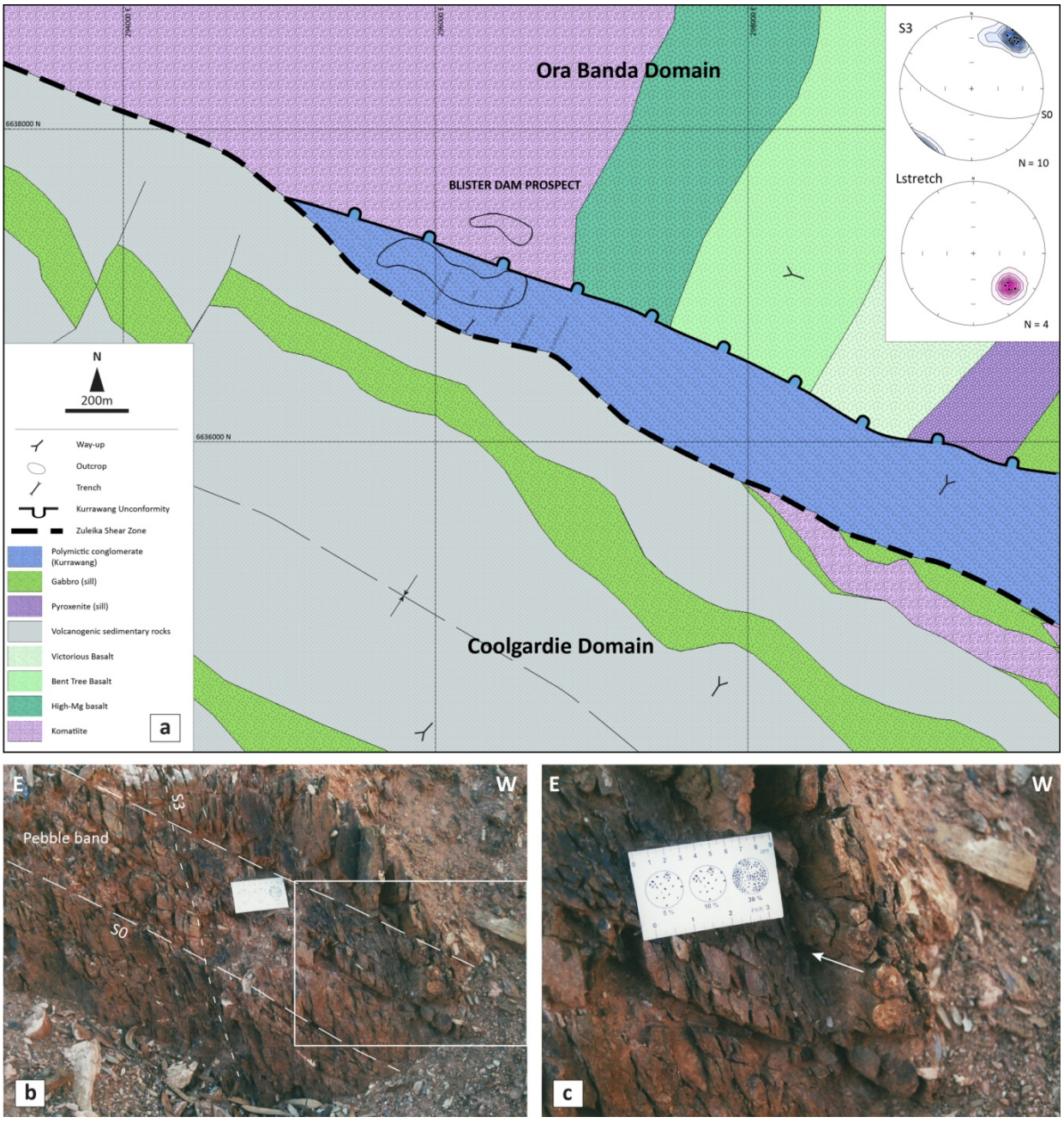

Figure 5.10 – a) Barrick GIS map of Blister Dam prospect area with location of outcrops and major structures, equal area projections (inset) show a shallow plunging pebble stretching lineation within a steep upright penetrative foliation; b) Kurrawang Formation bedding and cleavage relationships from trench located on (a); c) close-up of pebble band from inset in (b) showing moderate southeast plunging pebble long axes (See Figure 5.1 for location of map).

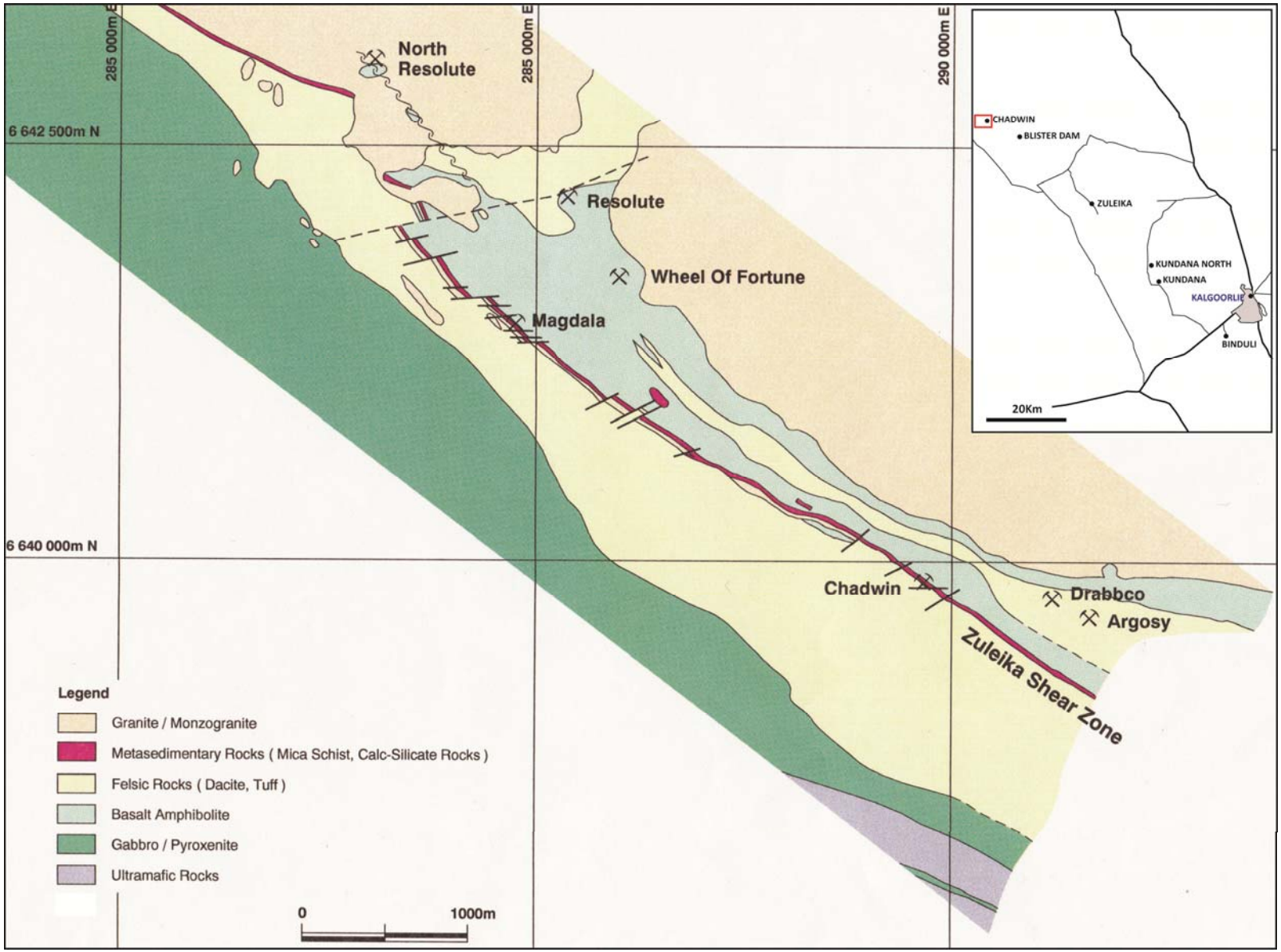

Figure 5.11 – Location and geology of the Chadwin mining district, on the SW margin of the Siberia Batholith. The location of the Zuleika Shear Zone is placed at the western contact of coarsely porphyritic basalt (amphibolite). Similar rocks are present in both Lower Basalt and Upper Basalt units in the Ora Banda Domain.

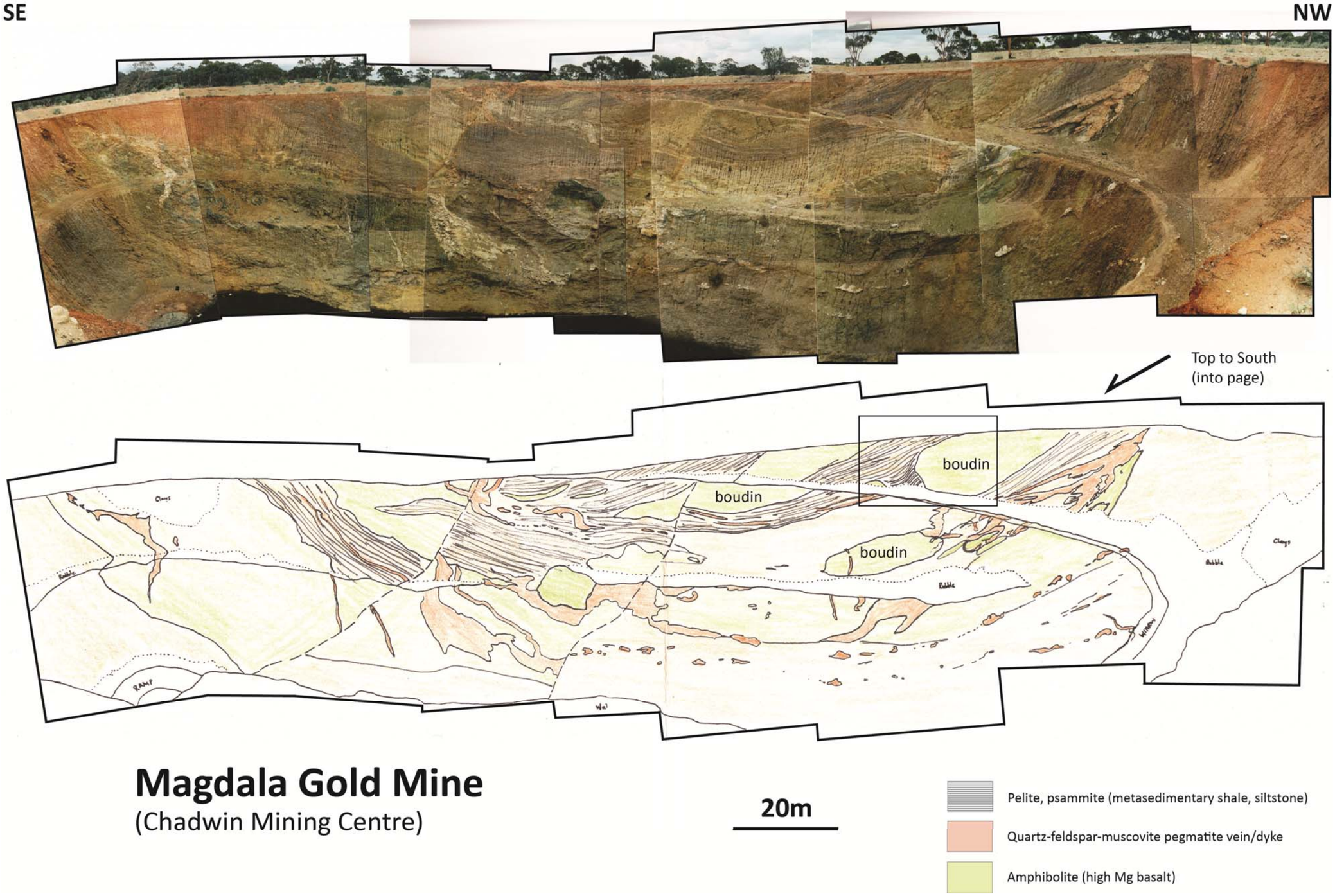

Figure 5.12 – Photomosaic and line drawing of SW wall of the Magdala open pit mine in the Chadwin Mining Centre. The sequence comprises structurally intercalated meta-sedimentary rocks and mega-boudins of amphibolite in psammitic matrix rocks. Pegmatite dykes and sills are deformed with top-to-south extensional kinematics. See previous figure for location.

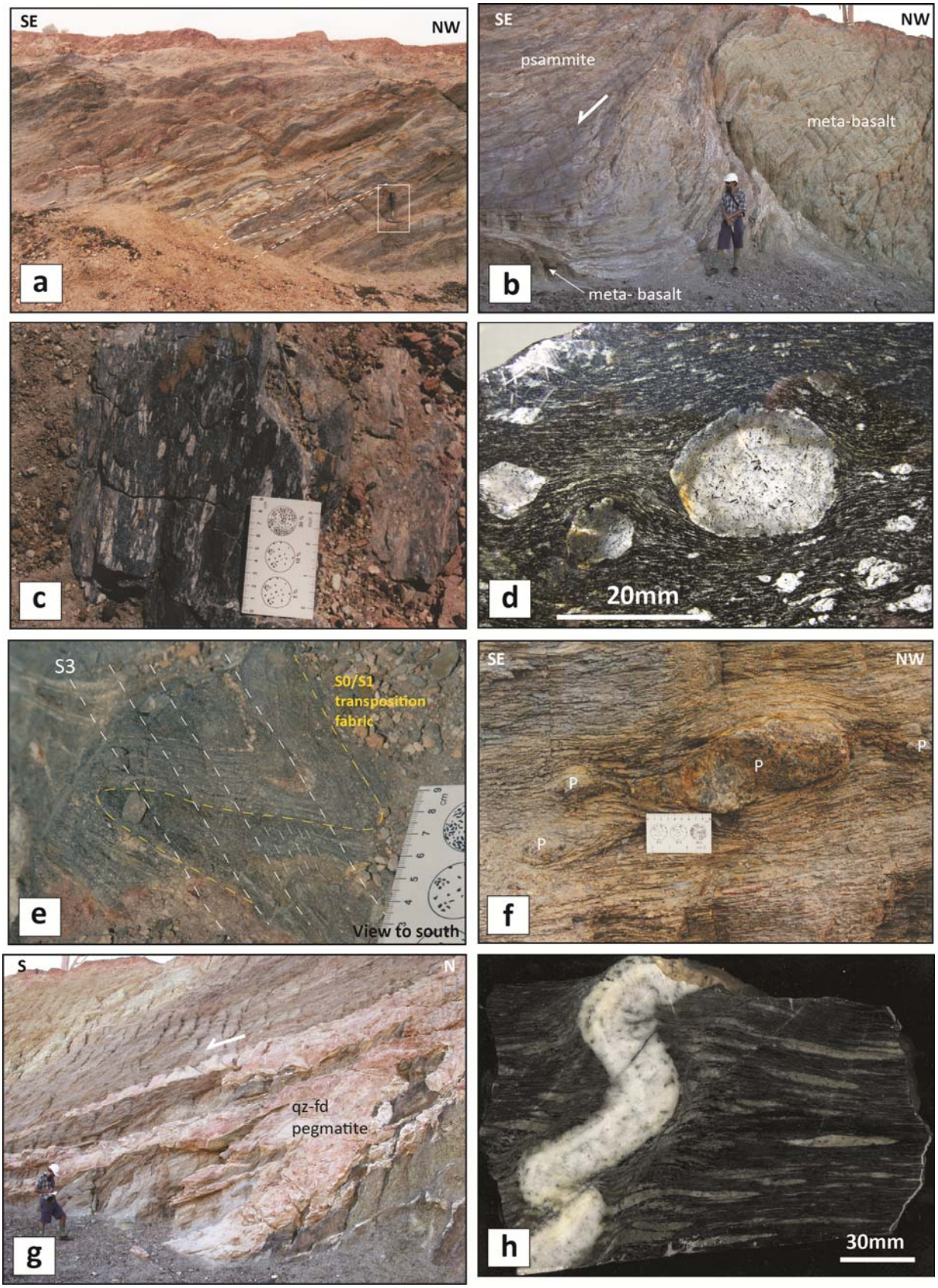

Figure 5.13 - Photographs of fabrics from the Magdala gold mine

Captions for Figure 5.13 – Photographs of fabrics from the Magdala gold mine:

a) Isoclinal folds internal to a transposition foliation in quartz-biotite schist. The folds are developed in fine grained interbedded quartz-rich psammite and pelite. Limbs of the F2 folds are near parallel, but locally are open chevron style folds in coarse grained units. In this instance the folds show a regular folded layering, whereas highly irregular transposed bedding is characteristic particularly in the vicinity of pegmatite dykes and boudins. In meso-scale polished slabs the transposition of light coloured bands within mica rich bands is accompanied by the development of rootless isoclinal intrafolial hook folds and extreme flattening of the rock fabric. A strong biotite lineation is ubiquitous in the plane of the S0/S1 foliation (hammer for scale).

b) Mega-boudins of high-Mg basalt in metasedimentary rocks (hammer for scale; see box on Fig. 5.12 for location). The basalt boudins are located in the lower left and upper right of the photograph with a sequence of metasedimentary rocks strongly flattened between the boudins. Layering in the metasedimentary rocks is a transposed S0/S1fabric with a wrapping relationship to the basalt, and includes chaotically folded quartz-feldspar pegmatite dykes/sills that appear locally parallel to the transposition fabric. The transposition and boudinage were likely synchronous expressions of the same shortening with variable rheology between lithotypes in an originally an intercalated basalt / sedimentary rock package. Structural interfingering of metasedimentary rocks with the basalt is suggested by a sliver of the metasedimentary rocks extending into the basalt boudin above the figure in the photograph.

c) Stretched-phenocryst plagioclase-phyric basalt amphibolite. The photograph shows an exposed foliation surface that displays elongate ellipsoids produced by deformed phenocrysts plunging southeast in the plane of the foliation. On sections normal to the foliation and parallel to the lineation, the shapes of the phenocrysts are strongly flattened.

d) Recrystallised porphyritic basalt amphibolite with fine to coarse grained actinolite/hornblende foliation wrapping recrystallised plagioclase megacrysts. Wrapping foliations show no evidence of asymmetry suggesting a dominant component of pure shear in the deformation. The rock is a less strained version of the basalt amphibolite in (c). Remnant phenocrysts display equant shapes in large crystals that are typical of the Victorious Basalt in the Ora Banda Domain. Plagioclase contains acicular inclusions of randomly oriented hornblende, visible in the large central phenocryst.

e) F2 folded S0/S1 transposition foliation cut by spaced S3 foliation. Wispy felsic segregations (pegmatites) are contained within a penetrative early S0/S1 transposition fabric in medium-coarse grained sandstones. The early fabric is folded into open to locally isoclinal F2 folds that were later overprinted by a transecting S3 foliation.

f) Extended and boudinaged dyke fragments entrained within a penetrative shallow south plunging quartz-biotite schist. Quartz-feldspar-muscovite pegmatite dykes are boudinaged within the low angle foliation with fragment offsets and porphyroclast asymmetry that indicate extensional deformation during top-block-west and down (off-dome) sense of shear. The occurrence of pegmatites dykes at all stages of the shearing indicates that pegmatite emplacement (Siberia Batholith) was synchronous with, and possibly a cause of deformation in the wallrocks.

g) Folded and extended quartz-feldspar-muscovite pegmatite dykes intruded into deformed metasedimentary rocks. The penetrative wallrock foliation locally is truncated against the margins of the dykes, but parallel to extended apophyses of pegmatite within the schist.

h) Buckled and faulted pegmatite vein intruded into strongly flattened porphyritic basalt amphibolite. Minor buckling of the pegmatite vein contrasts with strong flattening of original phenocrysts in the basalt amphibolite suggesting the pegmatite vein intrusion was relatively late in the flattening history of the sample.

characterised by strong deformation in the wallrocks of a series of sheared quartz-sulphide veins that mark the location of the Zuleika Shear Zone.

Metasedimentary rocks in the western wall of the mine are typical of the interpreted Coolgardie Domain sequences exposed in the Zuleika and Kundana areas with quartzofeldspathic sandstone, siltstone, mudstone and intercalated high-Mg basaltic volcanic rocks. The eastern domain is dominated by a coarsely plagioclase-phyric, amphibolite-grade metabasalt sequence that is interpreted as a possible equivalent of Victorious Basalt on the grounds of its location and the textural characteristics of the rock. Note that fine grained plagioclase phyric metabasalt is also present in the Lower Basalt sequence at the Black Rabbit area southeast of the Siberia Batholith; hence, Lower Basalt could be an alternative interpretation of the stratigraphic position of the metabasalt. The eastern porphyritic metabasalt unit is interpreted as Ora Banda Domain stratigraphy nonetheless.

Structural geology

Coolgardie Domain metasedimentary rocks display an intense transposition foliation (local S1) parallel to bedding that is folded into tight local F2 folds and wraps boudins of mafic/ultramafic rocks that measure up to 50 m in long axis (Fig. 5.12; Fig. 5.13a, b). Detached boudins composed of mafic/ultramafic rocks also contain a folded foliation with axes that plunge sub-parallel to the folds in meta-sedimentary rocks.

Folds (F2) in the meta-sedimentary rocks are tight isoclines and locally open folds with a mean plunge of 29º/166º, trending broadly sub-parallel to a well-defined biotite mineral stretching lineation (35º/184º) on the plane of foliation in the metasedimentary rocks (Fig. 5.13a; Fig. 5.14a, b). The folds are interpreted as F2 since they fold bedding and an earlier transposition fabric, but there is no evidence of interference folding in the mine exposures. The parallelism of F2 isoclinal folds and the biotite stretching lineation suggests they are related fabrics, and may reflect a high degree of ductile strain during shearing, or alternatively rotation of fold axes into parallelism with the dominant stretching axis. In any case the fabrics are likely part of the same deformation and the lineation is ascribed as L2.

The Victorious Basalt in the eastern wall contains a prominent stretching lineation defined by the long axes of rodded plagioclase phenocrysts, which display round shapes in N-section and highly stretched ellipsoids in P-section (Fig. 5.13c). Those lineations plunge 21º/146º on average and are contained within a medium-grained amphibolite grade meta-basalt (Fig. 5.13d; Fig. 5.14c).

Foliations measured from the separate domains (S0/S1 in western metasedimentary rocks / S1 in eastern porphyritic basalt) have broadly similar orientations, with a 10º variance in strike (Fig. 5.14 a, c). Stretching lineations L2 however, have a ~35º variance in plunge orientations. The two clusters of lineations are unlikely to represent separate deformation stages since they

are both developed in medium-high metamorphic grade rocks, within foliations that are adjacent and broadly parallel in orientation.

A late S3 cleavage overprints and transects S0/S1 and F2 folds (Fig. 5.13e). The S3 cleavage forms a tight cluster of steep-dipping foliations with a mean 73º/130º orientation, parallel to the regional S3 penetrative fabric (Fig. 5.13d). Late brittle cross faults (Fig. 5.11; Fig. 5.12) offset the early ductile fabrics and are parallel to a spaced planar fracture cleavage that contains retrogressive chlorite.

The contact between metasedimentary rocks and porphyritic basalt was a significant locus

of pegmatite dyke and vein intrusion with several generations of dykes that are timed by their

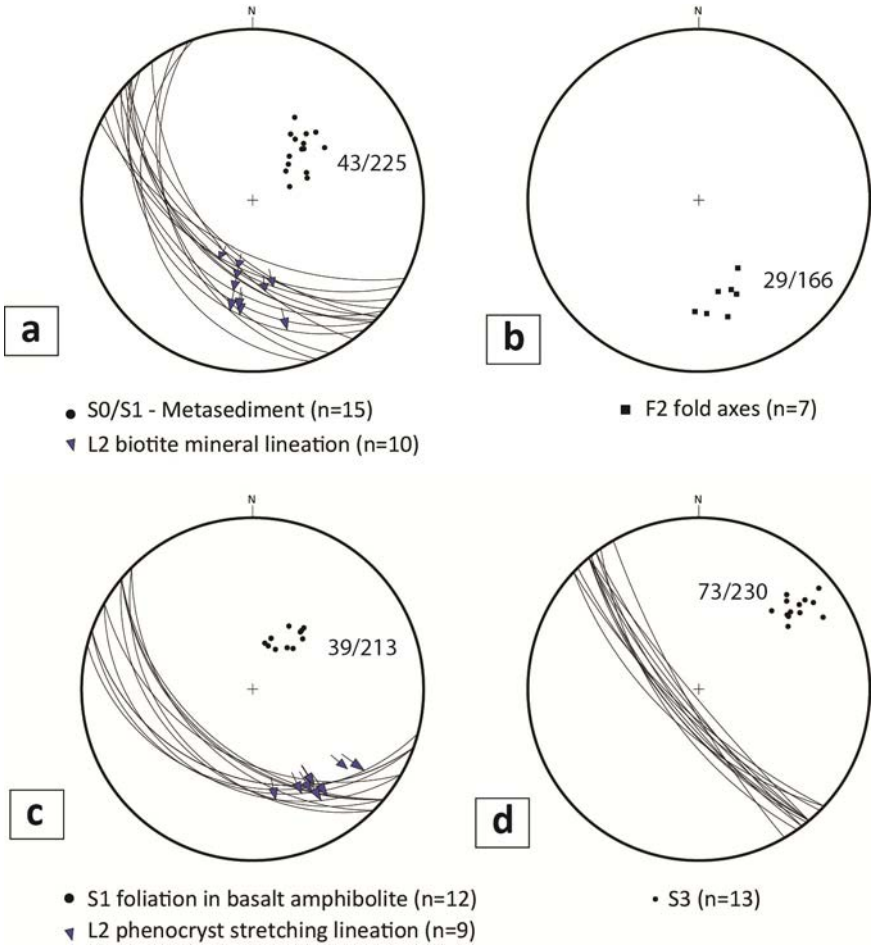

Figure 5.14 – Fabric data for the Magdala gold mine. A penetrative shallow SW-dipping foliation is present in wallrocks of the Zuleika Shear Zone **(a)**, but with variable plunge orientations of the dominant stretching lineations: 35º/184º for biotite mineral lineations in metasedimentary rocks **(a)**; 21º/146º for stretched phenocrysts in basalt amphibolite **(c),** a difference of ~36° in plunge orientation. This difference may be attributed to a rotational component on the Zuleika Shear Zone or possibly rotation of early linear fabrics related to granite emplacement as younger phases of the Siberia Batholith were emplaced. A late rotation is consistent with variation of the dip of the ZSZ to moderate SW-dipping in the vicinity of the Siberia Batholith; **b)** Folds (F2) in the transposition fabric (S0/S1) plunge shallow south, whereas all early fabrics are cut by an upright to steep-SW-dipping S3 spaced cleavage **(d)**.

relationships with the fabrics and variable deformation within the dykes. Cross-cutting relationships for the pegmatites include: pegmatite dykes intruding S1 and boudinaged within it (Fig. 5.13f); pegmatite dykes cross-cutting S1 and folded into F2 folds (Fig. 5.13g, h), and pegmatite dykes cross-cutting S1 and F2, but later sheared by the ZSZ (Fig. 5.12; Fig. 5.13f).

Interpretation

Ductile deformation fabrics at Magdala gold mine are defined by metamorphic minerals that indicate elevated metamorphic grades compared with other exposures of the Zuleika Shear Zone to the south. The proximity of the Siberia Batholith and presence of abundant deformed pegmatite dykes and sills, with pre-, syn- and post-shear timing relationships indicate probable deformation during granitoid emplacement with contact metamorphism of the deforming greenstone sequences. Extensional fabrics are expressed by a southwest dipping penetrative early foliation and strong penetrative shallow S-SE plunging stretching lineations that were produced with 'granite-up / greenstone-down' kinematics. The normal displacement sense of extended and boudinaged pegmatite lenses and veins suggests the deformation was primarily an extension related to doming during emplacement of the Siberia Batholith, since most fabric elements are defined by medium-grade metamorphic minerals.

At Chadwin, the Zuleika Shear Zone lacks a widespread interleaving of rocks types or abundant carbonate vein emplacement typical of southern exposures. The break is interpreted between Coolgardie Domain metasedimentary rocks and rocks interpreted as belonging to the Ora Banda Domain stratigraphy, with no significant change of metamorphic grade across the shear zone.

Variation in the orientation of the dominant ductile fabrics across the shear zone at Magdala gold mine may indicate multiple events in the history of the shear zone, or may relate to more local factors. Possible explanations for the variance include a rotational component of movement on the Zuleika Shear Zone, or alternatively deformation of early linear fabrics related to initial granite emplacement that were rotated as younger phases of the Siberia Batholith were emplaced. This issue highlights a problem in distinguishing how much of the wallrock fabric at Chadwin is related to ZSZ movements versus granite emplacement. Intimate association of pegmatite intrusions with the deformed rocks suggests a significant proportion of the metamorphic fabric is related to the latter.

5.2.5 Summary

Kinematic interpretation

Shear zone kinematics are variable along the ZSZ with sinistral-oblique sense at Kundana; sinistral strike-slip sense at Zuleika; sinistral-extension at Chadwin and also Blister Dam. Overall sinistral movement sense is typical of major uniform NW-striking shear zones

throughout the goldfields and is apparent on small scale aeromagnetic images in several locations (e.g. Agnew; South Laverton Tectonic Zone; Keith Kilkenny Fault). Note that changes in orientation of the shear zones around major granitoid batholiths can affect the kinematic sense, where N-S striking segments in general have dextral kinematics. These kinematic changes have been explained as a result of bulk co-axial shortening with an ENE-WSW resolved contraction direction (Tripp 2002b).

Stretching lineation plunges in the ZSZ vary: steeply-north plunging at Kundana; sub-horizontal plunging at Zuleika; shallow southeast plunging at Blister Dam; and moderately south-southeast plunging at Chadwin (Fig. 5.15). This apparent conflict between separate measurements of kinematics within the same shear zone is well documented in the EGP (Eisenlohr et al. 1989, Passchier, 1994, Libby et al. 1990, Vearncombe, 1998). Discrepancies can be explained by (1) overprinting of separate deformation stages, or (2) localised rotation of the finite strain ellipsoid in the presence of syn-tectonic intrusions such as the Siberia Monzogranite and at changes in orientation of the shear zone. The difference observed between the steep lineations at Kundana and shallow lineations at Zuleika may result from the presence of anisotropy caused by influence of the rigid Powder Sill, which is folded into and truncated by the ZSZ at Kundana, yet shows little evidence of internal strain.

Shear fabrics described from the best exposures of the ZSZ record the latest (D2 and later) fabric-forming deformation events. Interpretation of earlier (DE) fabrics is equivocal especially when near the limbs of regional folds and the contacts of syn-tectonic granites. Earlier fabrics co-planar with F2 axial planes discussed for the Magdala mine may be a result of the influence of the Siberia Monzogranite in this area, which has not been experienced elsewhere (e.g. Zuleika and Kundana).

A common factor at all the locations presented is the similar orientation, and in some cases parallelism, of fold axes in the wallrocks with the principal stretching lineation of the shear zone (Fig. 5.1). A possible explanation for the parallelism of fold axes and dominant stretching lineations involves rotation of the folds in the vicinity of high strain zones, or a high ratio of pure shear to simple shear. Fold axis orientations with regular (regional F2/F3) sub-parallel orientations at distance from the high strain zone suggest localised strain partitioning.

Stratigraphic controls

The Zuleika Shear Zone does not juxtapose domains of Archaean crust with marked differences in deformation or metamorphic grades, but it does mark a break between domains with minor differences in a regional stratigraphy. In particular is the absence of Upper Basalt and other typical Ora Banda Domain stratigraphic formations in the Coolgardie Domain. Similar metamorphic grades across the ZSZ at Chadwin confirm the observations of Mikucki and Roberts (2003) and Goscombe et al. (2010) that metamorphic isograds are systematically

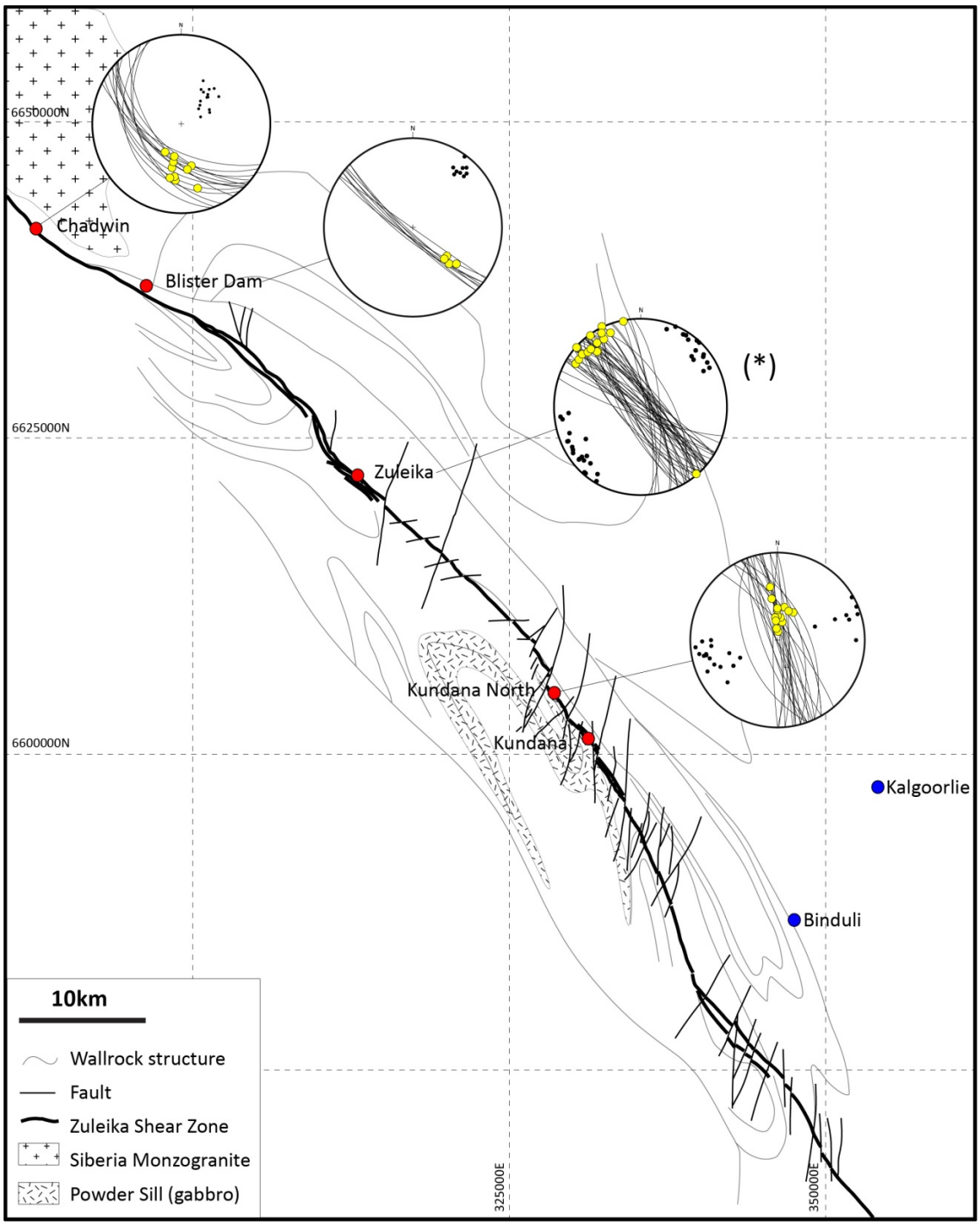

Figure 5.15 – Summary map of the Zuleika Shear Zone and cross-cutting late faults in the study area, with equal area projections of fabric data and principal stretching lineations (explained in the previous sections). A broadly anastomosing geometry with divergent splay shear zones is typical of the ZSZ. Dominant foliations in the shear zone are steep, and vary about the vertical except in the vicinity of the Siberia Batholith, which possibly indicates post-movement rotation of the shear zone from an originally steep orientation in that area. Principal stretching lineations and kinematics are variable along the length of the shear zone, possibly influenced by the presence of anisotropy including the Siberia Batholith and the rigid Power Sill at Kundana. The data marked with an asterisk (*) are from an MSc study of the Zuleika mining centre (Tripp 2000), all other data are newly collected from this study.

disposed about granitoid intrusions rather than controlled by major faults. Metamorphic isograds crossing shear zones indicate the ZSZ had a history of movement earlier than that recorded by the latest fabrics, and that the shear zone had a significant control on the distribution of the mafic volcanic stratigraphy.

An important question is how to explain a lack of widespread stratigraphic repetition via thrusting in the Ora Banda Domain, compared with other domains. One possible explanation is that the Coolgardie Domain represents a slice of crust that has been uplifted relative to the Ora Banda Domain or laterally sheared in by wrench faulting from a widely different geographic location, juxtaposing rocks with contrasting histories. Such juxtaposition would require a major extensional event prior to the onset of D2 with preferential exhumation of the Coolgardie Domain relative to the Ora Banda Domain during D2, or a major terrane accretion-type event accomplished by horizontal shearing.

These scenarios could explain local differences of metamorphic grade and some of the strain, however none explain the lack of repetition of stratigraphy in the Ora Banda Domain since D1 was (apparently) an early N-S directed event. A preferred interpretation of the ZSZ is that of an early extensional fault that controlled the deposition of the mafic volcanic sequences, but was later reactivated as a sub-vertical transfer zone during D1. This would allow for the accommodation of differential shortening or extension across its boundaries.

Summary

The Zuleika Shear Zone is an Archaean ductile shear zone that may have originated as an early extensional fault controlling the stratigraphic development of adjacent sub-basins. Later deformation steepened the shear zone with dominantly D1 transfer movement, accommodating differential shortening or extension between the Ora Banda and Coolgardie Domains. Later D2 ENE-WSW shortening produced F2 folds in the wallrocks and reactivated the transfer zone with local kinematic histories determined by the presence of anisotropy and local granitoid intrusions that enhanced the partitioning of strain.

The shear zone acted as a gold-fluid conduit during metamorphic dewatering in peak and retrograde metamorphic cycles, with major gold deposition in the ductile shear zone, sub-parallel wallrock splays, and rock contacts. A further gold mineralisation event post-dated movement on the shear zone during brittle-ductile faulting (Chapter 7).

5.3 Justification for ‘domain’ and ‘terrane’ boundary classifications

5.3.1 Stratigraphic thickness variations between Kalgoorlie ‘domains’

Pre-requisite to interpreting fault controls on stratigraphy is the presence of suitable marker units with well understood sequence and thickness. Mafic and ultramafic volcanic sequences are present in all fault-bounded domains of the Kalgoorlie Terrane and are

characterised by strike-continuous lithologic units. This continuity may reflect depositional conditions in submarine environments dominated by fissure volcanism, and low viscosity, high-temperature mafic and ultramafic magmatism.

Sub-regional strike continuity in the mafic sequences is contrasted with the overlying Felsic Volcanic and Sedimentary Unit; the latter is typified by localised felsic and intermediate volcanic centres and volcaniclastic sequences of restricted provenance. This contrast appears to favour the mafic volcanic sequences as potential indicators of early structural controls on greenstone development. Of the various component units of the mafic and ultramafic volcanic sequences, the stratigraphy of the Upper Basalt unit is best understood throughout the Kalgoorlie Terrane due it hosting many of the gold deposits, whereas greater variation and complexity is typical of the Lower Basalt and Komatiite units.

Upper Basalt unit

Type sections of the Upper Basalt unit are present in the Ora Banda and Kambalda Domains (Harrison et al. 1990; Morris 1993; Witt 1990; Table 5.1). Upper Basalt units in the Ora Banda Domain include the Victorious and Bent Tree Basalts (Grants Patch Group of Witt 1990), which form parallel layers with sub-regional strike-continuity, composed of intercalated basalt flow units with thin, interflow carbonaceous shale beds. The Victorious and Bent Tree basalts are well documented at Ora Banda and Mount Pleasant with a combined stratigraphic thickness of ~3000 m (Harrison et al. 1990; Morris 1993; Witt 1990; Table 5.1). In the Kambalda Domain the Upper Basalt Unit is represented by the Paringa Basalt, which has some variability in thickness throughout the domain: <900 m at Kalgoorlie (Woodall 1965); ~1500 m at Feysville (Keats 1987); <1500 m at Kambalda (Gresham and Loftus-Hills 1981. At Kambalda, Connors et al. (2003) recognised Paringa Basalt as comprising 1000-1500 m of quartz tholeiites and siliceous high-Mg basalts including dolerite sills. A ~2100 m thick sequence of pillow basalts with intrusive, bedding-parallel differentiated mafic sills is correlated with the Upper Basalt in the Boorara Domain (Placer / Barrick). The unit sits stratigraphically above high-Mg basalt flows at the top of the Harper Lagoon ultramafic unit, with dips and way-up to the south.

From new mapping of the Coolgardie district, Standing and Castleden (2002) concluded that sequences at Coolgardie cannot be correlated with the generalised stratigraphy of the Kalgoorlie Terrane of Swager et al. (1990); whereas most previous workers in that domain made correlations with Swager et al. (1990) to deal with large areas of basaltic rocks in the Coolgardie area and Bullabulling Domain (e.g. Hunter 1993). The Coolgardie Domain stratigraphy outlined by Standing and Castleden (2002) interpreted two levels of komatiite with intercalated high-Mg and tholeiitic basalt flow rocks, which is unique for the Kalgoorlie

Table 5.1 – Stratigraphic thickness of mafic/ultramafic volcanic units, highlighting the Upper Basalt Unit

Regional Unit	Coolgardie Domain		Ora Banda Domain		Kambalda Domain				Boorara Domain	
	Coolgardie	Thickness	Ora Banda	Thickness	Kalgoorlie	Thickness	Kambalda	Thickness	Kanowna north	Thickness
Upper Basalt	Not Recognised	-	Victorious Basalt	1000 m	Paringa Basalt	300-900 m	Paringa Basalt	50-1500 m	Six Mile mafic volcanics and sills	~2100 m
			Bent Tree Basalt	2000 m						
Komatiite Unit	Significant differences in lithostratigrapy and geochemistry from the recognised Kalgoorlie Terrane units	-	Big Dick Basalt	500 m	Devon Consols Basalt	60-100 m	Devon Consols Basalt		High Mg Basalt	~500 m
		-	Siberia Komatiite	2800 m	Hannans Lake Serpentinite	300-900 m	Kambalda Komatiite	>1000 m	Harper Lagoon Ultramafics	~850 m
Lower Basalt		-	Missouri/Wongi Basalt	>3000 m	Lunnon Basalt	?	Lunnon Basalt	>2000 m	Lower Basalt	>3000 m
	Standing and Castleden (2002)		Witt 1990		Travis et al (1971)		Gresham and Loftus-Hills (1981); Connors et al. (2003)		Barrick unpublished data (2011)	

Terrane, and may support a suggestion that the Kunanalling Shear Zone represents a more fundamental break than previously recognised.

Figure 5.16 shows a schematic map of the distribution of Upper Basalt sequences removed from the Barrick regional GIS layer. This analysis shows areas of thickness variation in the development of the Upper Basalt Unit, but the map scale distribution does not necessarily reflect the true thickness of those units. Given that most of the units are folded and dipping into the page, the apparent thickness of the units on the map is an overestimate. Several other issues include the possibility of primary thickness variation due to ballooning of sub-horizontal volcanic flows, deposition onto a varied topography, or tectonic thickening or excision. For these reasons the image in Figure 5.16 is a schematic view intended only to identify areas of thick development of the Upper Basalt at a regional-scale. This analysis may allow for the interpretation of areas that were possibly deep basins or adjacent exhumed blocks at the time of Upper Basalt volcanism.

The types of faults that separated the Upper Basalt distributions are portrayed on Figure 5.16 as long linear breaks parallel to the prominent NNW-SSE trending fabric of the belt. Given the significant stratigraphic differences outlined by Standing and Castleden (2002) for the Coolgardie domain, the break at the edge of the western block may have separated an exhumed margin to the west of the central Kalgoorlie area, or may have been a major strike slip fault. No role is indicated for the Abattoir Shear Zone, which does not appear to control the distribution of the Upper Basalt Unit, but reference to the regional gravity image in Chapter 6 shows a major truncation of a large high-density block on the eastern contact of the Abattoir Shear Zone.

A thick trough of Upper Basalt extends through the Ora Banda and Kambalda Domains, and is present in the Boorara Domain; whereas the grey zone labelled ‘BTZ’ contains only small sporadic occurrences of mafic volcanic rocks that have uncertain affiliation with the Upper

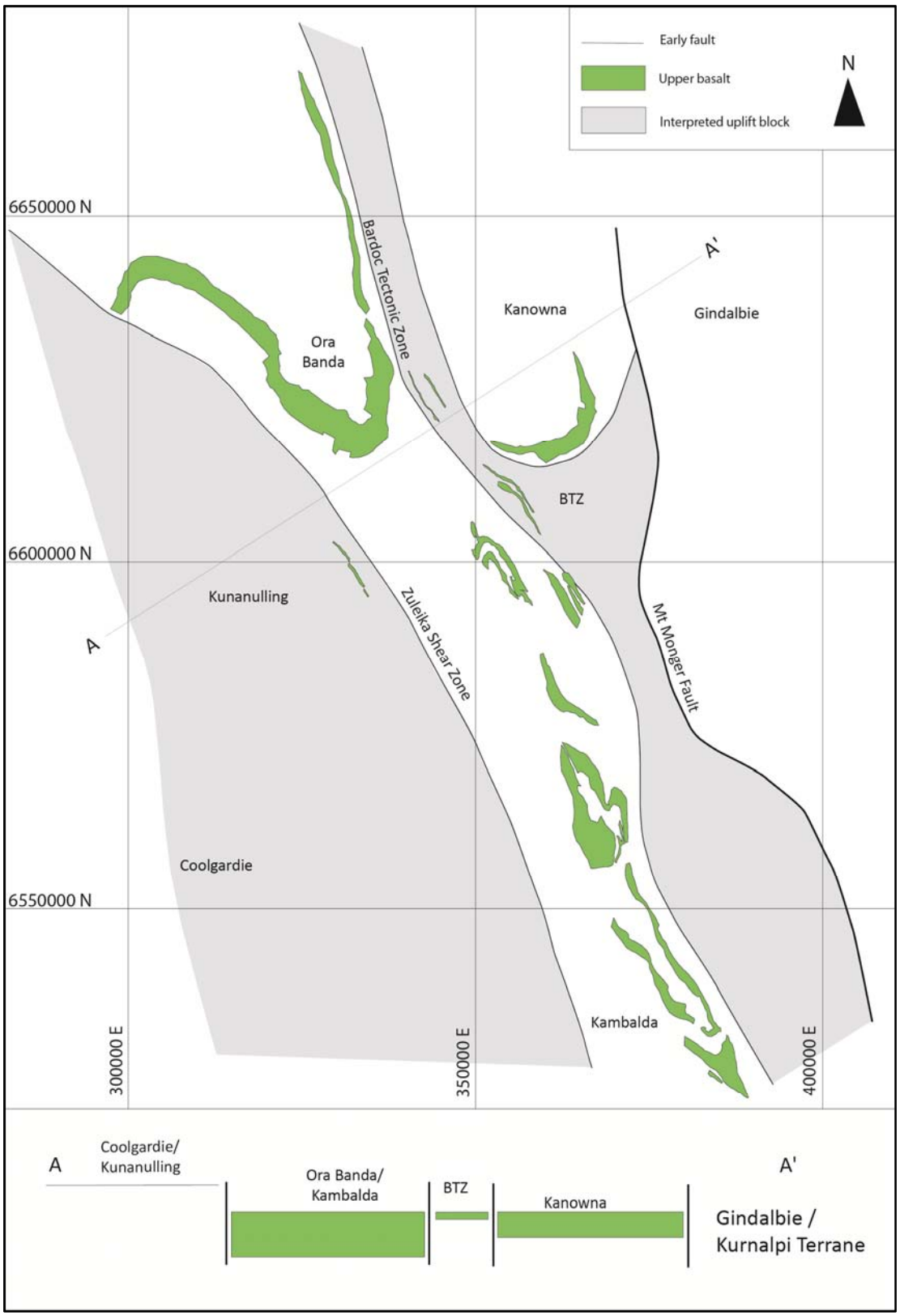

Figure 5.16 – Map of the distribution of Upper Basalt polygons removed from the Barrick regional GIS and presented against a schematic image of major boundaries. The image attempts to interpret separate crustal blocks that have variations in the thickness of a regionally continuous marker unit. These areas presumably would have occupied deeper sections of a connected series of sub-basins prior to the latest shortening, which dominates the present day fabric and distribution of the greenstones.

Basalt Unit. Furthermore, the linear central belt of thick Upper Basalt sequences is separated from the grey-coloured western area in which there are no known occurrences of rocks correlated with Upper Basalt Unit. The boundaries of the central trough of Upper Basalt are marked by the Zuleika Shear Zone and Bardoc Tectonic Zone, and at the least, it appears these faults have some control on the distribution of the Upper Basalt unit.

The Kalgoorlie domains appear not to be remnants of a stratigraphic package simply dissected by faults during late deformation, and lithostratigraphic differences between contemporaneous sequences, suggest a role for early faults in the developing basins. Late deformation was primarily a control on reorganisation of the greenstones, including later folding and structural juxtaposition. Given a broadly consistent stratigraphy between the fault bounded domains (Chapters 3 and 4) it is unlikely they represent amalgamated diverse blocks, but are probably a series of shortened, originally adjacent, fault-separated depositional basins. If this is the case, the changes in Upper Basalt thickness across some of the faults could be argued as controlled by relative fault movements resulting in differential uplift between a series of extensional basins; hence, some of the major faults were arguably active since the time of the earliest extension and should occupy a place in the deformation history older than the common 'D3' timing of most previous authors.

Other faults with evidence of early extensional deformation

Local examples of early fault movements on superficially 'late' faults can be shown by their controls on stratigraphic distribution. The Shamrock Fault in the Kanowna district (Fig. 3.45, 3.55) shows a juxtaposition of ~2705 ma layered komatiite flows in the hangingwall of the fault, against 2661±11 Ma quartz-rich sedimentary rocks in the footwall (Chapter 4). Since the Shamrock fault is dominated by thrust kinematics, the youngest rocks in the footwall provide a maximum age on the last fault movement (<2661±11 Ma). There are significant changes in the thickness of fault-bounded komatiite units in the Kanowna district, and there are areas where members of the stratigraphy are not developed; hence correlation of adjacent ultramafic units is necessarily tenuous.

Ultramafic rocks and high-Mg basalt (~300 m-thick) in the hangingwall of the Shamrock fault are overlain by deep-water shales and siltstones, and form a sequence that is unconformably overlain by felsic volcaniclastic rocks of the Perkolilli sequence (2675±3 Ma; Nelson 1994). Deep water shales and siltstones of the lower sequence are strike continuous to an area where those bedded sedimentary rocks were intruded by ultramafic lava flows; hence the sedimentary rocks are older or broadly co-eval with the ultramafic rocks (~2705 Ma). The age difference between ~2705 Ma komatiite and ~2678 Ma rhyolite appears to indicate a ~27 million years period of non-deposition, since there is no evidence of folding or excision of the strike continuous Shamrock ultramafic sequence. This sequence contrasts with areas on the

western side of the Shamrock Fault, where no ultramafic rocks are developed until the ~1000 m thick Robinson's Komatiite unit, which is in faulted contact and locally unconformably overlain by ~650 m of conglomerate and sandstone (Ballarat and Kanowna members, ~2696±5 Ma).

The Shamrock Fault appears to have had movements older than the minimum age constraints interpreted from the age of the youngest footwall units. In this respect the Shamrock Fault may represent an early extensional fault that potentially separated a hangingwall slice of ultramafic rocks (eastern side) from a thick ultramafic succession to the west. The current eastwards dip of the Shamrock thrust fault may not be the original orientation of the fault, but may have been steepened during later deformation, potentially influenced by doming of the Scotia granitoid batholith. In support of this last contention is the wrapping geometry of the fault around the Scotia Dome, along strike towards the north (Fig. 3.2).

Summary

The Zuleika Shear Zone, Shamrock Fault, and Kunanalling / Abattoir / Bardoc faults are intra-terrane faults that separate sections of stratigraphy (domains) with minor differences of sequence, lithotype and age. Variations of sequence and age across those faults are key criteria for allocating their importance to stratigraphic development and tectonic history. In that respect the faults / shear zones in the Kalgoorlie district are of local significance only and accommodated rearrangements and small-scale dislocations of the stratigraphy. Most of those faults now display oblique-slip kinematics, but juxtaposition of different aged sequences demands that there was previous extensional or thrust movement at a very early stage in the development of the post ~2700 Ma Neoarchaean greenstone sequences.

5.3.2 Kalgoorlie / Gindalbie-Kurnalpi terrane boundary

Published interpretations of the boundaries to the 'Kalgoorlie Terrane' have identified the Ida Fault and Mount Monger faults as the western and eastern terrane boundaries respectively (Fig. 5.16; Swager et al. 1990; Swager 1997; Cassidy et al. 2006). The Ida Fault juxtaposes the Kalgoorlie greenstone sequences with granitoid / gneiss terranes to the west, and forms a major break in the geology of the Yilgarn Craton as indicated by rock types, geochronology and isotopic data (Cassidy et al. 2006).

The term 'terrane' has been used very specifically in the literature of the Eastern Goldfields Province, particularly from an interpretive basis to support subduction / arc-accretion tectonic models for the Neoarchaean (e.g. Barley et al. 1989; Swager et al. 1990 who suggested subduction as a working model; Krapez et al. 2000; Barley et al. 2008; Kositcin et al. 2008; Krapez et al. 2008; Czarnota et al. 2010). A later paper by Swager (1997) settled on an ensialic rift as the preferred tectonic setting of the Kalgoorlie greenstones, and stated "...there is little convincing evidence for a distinction within the greenstone terranes between a western

back arc and an eastern magmatic or volcanic arc environment" (cf. Barley et al. 1989; Witt 1990; Morris and Witt 1997). Nevertheless, much of the 'terrane' definition and terminology comes from many reports and papers by C. Swager, and references to that author.

Major lithostratigraphic associations were assigned to three major 'terranes' by Cassidy et al. (2006), whereas seven major terranes were interpreted for the same area by Barley et al. (2008). In each of those studies the eastern boundary of the Kalgoorlie Terrane was placed on an interpreted 'Mt Monger Fault' separating a 'Kalgoorlie Terrane' from rocks in an eastern 'Gindalbie Terrane' (Barley et al. 2008); or the generalised 'Kurnalpi Terrane' of Cassidy et al. (2006). The Mount Monger Fault was originally identified by Maclaren and Thomson (1913) as "the great Mt. Monger thrust plane", which was considered an eastern boundary past which "Kurrawang Series" rocks were not found. The separation of a Gindalbie Terrane as distinct from a Kalgoorlie Terrane was developed in detail by Swager (1995).

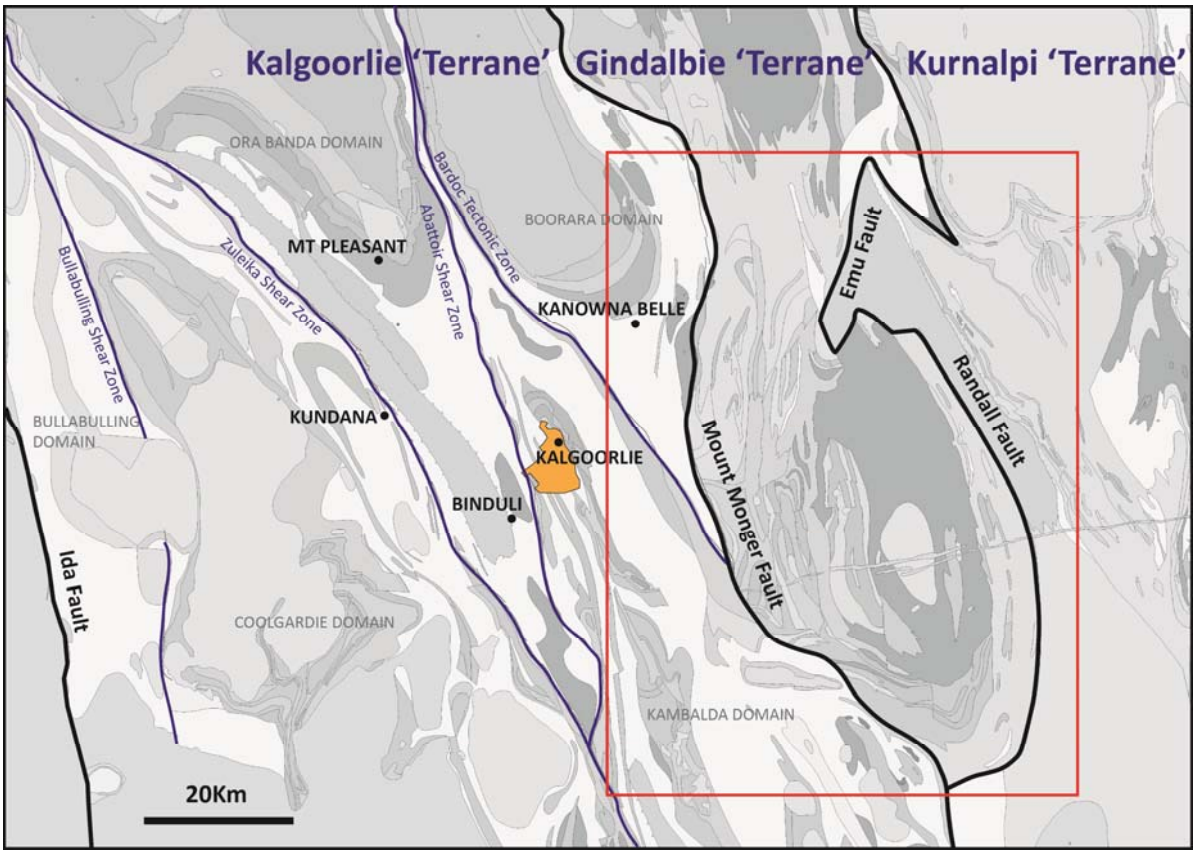

Figure 5.16 – Map of the GSWA geology, grey scaled to highlight the location of major faults. Ida Fault and Mount Monger Fault (thick black lines) are interpreted boundaries of the Kalgoorlie Terrane of Swager et al. (1990). Thin blue lines are the boundary shear zones of domains in the Kalgoorlie Terrane. The Gindalbie/Kurnalpi 'Terrane' boundary is a complicated series of faults originally mapped as separate entities including the Randall and Emu Faults, and compiled into a 'terrane boundary' on the premise of a Gindalbie 'Terrane' comprising bimodal volcanic rocks, and calc-alkaline volcanics interpreted as 'arc rocks' (Swager 1994; Barley et al. 2008). Labels mark the location of mining centres as documented in this study; the orange polygon is the city of Kalgoorlie-Boulder; the red box marks the location of Figure 5.17.

Field and published data from Yindarlgooda northeast

A review of the existing stratigraphy and geochronology for the eastern margin of the Kalgoorlie 'Terrane' is presented in Figure 5.17. The Yindarlgooda Dome is a major structural feature of the greenstones located east of the Kalgoorlie district. Fieldwork conducted in that area shows the stratigraphic sequences are generally shallow-dipping in an 'off-dome' fashion as recorded by sedimentary bedding dips, way-up and foliations. In particular, clastic sedimentary rocks were targeted in the north-eastern margin of the Yindarlgooda Dome since there is an historic Ministerial Reserve in that area previously placed by the Government of Western Australia on the assumption of potential base-metal mineral deposits of strategic value to the state. The reserve covers an area of syn-volcanic stratiform pyrite mineralisation and sericite alteration that was drilled and returned assays with anomalous base metals, indicating the presence of palaeo- seafloor hydrothermal alteration (Sofoulis et al. 1968, 1969).

Unconformably overlying those rocks is a combined sequence of clastic sedimentary rocks collectively referred to previously as 'Penny Dam Conglomerate' (Swager 1994; Krapez et al. 2000; Krapez and Pickard 2010). The sequence comprises two distinctly different clastic sedimentary units: (1) a lower mafic-volcanic-clast dominated conglomerate, with a minor (5%) component of hypabyssal hornblende-feldspar porphyry clasts, which unconformably overlies older felsic volcanic sequences and stratiform pyrite mineralisation, and (2) an upper, downwards-facing, quartz-rich, trough-cross-bedded sandstone and polymictic granite-clast conglomerate unit, which sits unconformably on all lower units (Fig. 5.17). The lower mafic-clast conglomerate has a zircon SHRIMP U-Pb age determination at 2672±3 Ma (Fig. 5.17; Krapez et al 2000); whereas the upper Kurrawang-type, polymictic clastic unit has an age determination at 2669±4 Ma (Fig. 5.17; Krapez and Pickard 2010).

The clastic sedimentary units are in unconformable contact with a sequence of rocks that includes: (1) lower high-Mg pillowed, variolitic mafic volcanic rocks akin to the Lower Basalt; (2) middle units of contemporaneous ultramafic and felsic volcanic rocks with age determinations and relationships identical to the Kanowna sequences (Fig. 5.17); (3) upper tholeiitic mafic volcanic flow rocks with intrusive differentiated dolerite sills interpreted by current workers as Upper Basalt (C. Young personal communication 2011); and (4) overlying sequences of intermediate andesite-dacite volcanic rocks suggested as correlative of the White Flag Formation (Forman 1953) or possibly with the Binduli sequence.

This package of rocks with sequence, and age groups identical to those of the Kalgoorlie Terrane, including the typical late clastic sedimentary rocks (Fig. 5.17), casts significant doubt on the interpretation of a major terrane boundary at the western margin of the Yindarlgooda Dome, and allows for the possibility that the Yindarlgooda rocks are simply an eastwards continuation of the sequences in the Kalgoorlie district. It is notable that Drummond et al. (1991) could not identify the interpreted Mount Monger Fault in deep seismic data.

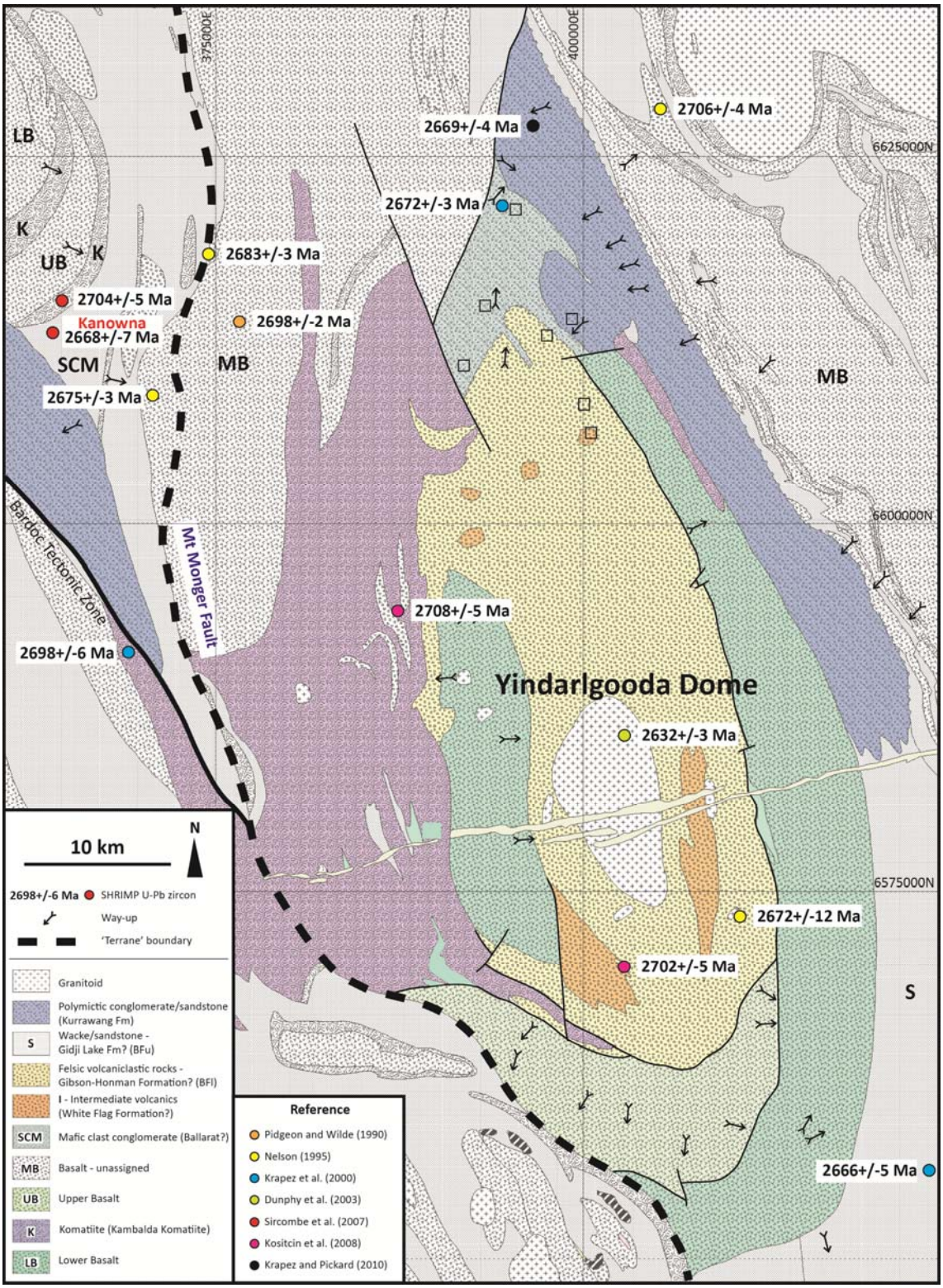

Figure 5.17 – Geology, structure and geochronology of the Yindarlgooda Dome in the Gindalbie Terrane of Swager (1995). Stratigraphic sequences and geochronological age ranges are compatible with those of the Kalgoorlie Terrane (highlighted with colours) despite the persistent interpretation of a major terrane boundary separating an interpreted 'back-arc basin' Kalgoorlie Terrane from a Gindalbie-Kurnalpi 'Ca-Alk arc terrane' (e.g. Barley et al 2008). Note the Penny Dam Conglomerate is separated, based on new observations in this study and previous geochronology, into a mafic-clast dominated conglomerate (Ballarat equivalent? - marked 'SCM' in the legend), and a downward facing, typical Kurrawang-type late clastic sequence (marked 'Kurrawang Fm.' in the legend). The geology is significantly simplified from a compilation map of Swager et al. (1990), using field mapping data from GSWA 1:100K map sheets and limited reconnaissance observations from field traverses in this study targeted at the late clastic sequences (marked by square symbols).

An interpretation of the Yindarlgooda Dome by Swager (1997) shows a thrust faulted contact between a "ultramafic-mafic volcanic assemblage" and a "Calc-alkaline assemblage", which if true would allow for the possibility that Kalgoorlie Terrane rocks were thrust over the Gindalbie Terrane. However, reference to the original mapping of Ahmat (1995), shows the contacts between the units in question as primary (no faults) with interleaving of the felsic volcanic units and ultramafic volcanics in detail (typical in the Kanowna and Gordon-Sirdar areas in the adjacent Kalgoorlie Terrane). There are also zircon age analyses from the internal felsic volcanic units on the southern flank of the Yindarlgooda Dome that are +2700 Ma suggesting that the map pattern showing continuous internal felsic successions may be erroneous. This 'felsic' unit also includes the Lake Yindarlgooda andesites, which Forman (1953) identified as identical to the White Flag Formation of the Kalgoorlie Terrane.

Differences in the chemistry of the felsic volcanic rocks between 'terranes' include interleaved high-SiO_2 rhyolite and basaltic andesite in the 'Gindalbie Terrane' compared to dominantly dacitic felsic volcanics in the Kalgoorlie Terrane (Morris and Witt 1997). But note that the 'dacitic felsic volcanics' also include occurrences of andesite; and the Perkolilli high-SiO_2 rhyolites in the Kalgoorlie Terrane have similar flat REE patterns, high Y and low Zr/Y, and low Th/Yb as for the Melita and Jeedamya complexes in the 'Gindalbie Terrane' (Witt et al. 1996). Witt (1995) identified differences in the bulk chemistry of mafic-ultramafic sills between the 'terranes'. That work compared sills at Melita in the Leonora district with sills from the central Kalgoorlie district.

The presence of the same stratigraphic units and, in the case of rhyolitic complexes, chemistry across a 'terrane boundary' including: (1) the unique ~2705 Ma co-magmatic ultramafic/dacite association, (2) 'Penny Dam Conglomerate' which includes units very similar to the Kanowna Ballarat member and Kurrawang Formation, (3) other units which the current workers in the district correlate with the Lower and Upper Basalts of the Kalgoorlie Terrane, and (4) the presence of Forman's 'White Flag' rocks casts doubt about the nature of the western boundary, and suggests that the Mount Monger Fault 'terrane boundary' is suspect.

Published arguments against accreted terranes

Gindalbie Terrane rocks have been interpreted as a bi-modal, tholeiitic basalt / rhyolite-dacite association, and considered a unique association in the southern goldfields (Swager 1995). Barley et al. (2008) considered the Yindarlgooda Dome as typical of isolated felsic volcanic centres with arc-affinities, which formed part of an arc-terrane distinct from a back-arc Kalgoorlie Terrane.

Recent publications dealing with this particular sequence of rocks have disputed the previous interpretations of remnant arcs (Wyche et al. 2012; Barnes et al. 2012). As presented in the Literature Review of Chapter 2, Wyche et al. (2012) concluded that due to their degrees of

isotopic similarity, adjacent ‘terranes’ in the Eastern Goldfields Province may never have been significantly separate entities, and were not necessarily the products of arc accretion of exotic fragments. Their preferred interpretation is that a widely recognised ~2800 Ma magmatic event may have initiated rifting of early formed components of the Eastern Goldfields Province. The contention of a ~2800 Ma rifting event is supported by the presence of rare, old (<2800 - 2900 Ma) greenstone fragments that flank the bulk of the Eastern Goldfields granite-greenstone sequences (Chapter 8).

Barnes et al. (2012) were particularly critical of the arc-accretion hypothesis advanced for the Eastern Goldfields Province and wider Yilgarn Craton by Barley et al. (2008). Their arguments centred on geochemistry and the issue of scale in the subduction / arc-accretion models advanced by Barley et al. (2008) and Czarnota et al. (2010).

For the lithotectonic assemblages previously described, Barnes et al. (2010) concluded there is no evidence anywhere in the Eastern Goldfields Province for basaltic rocks with characteristic island arc basalt signatures (Nb-depleted, low-Ni, low-Cr). Furthermore they state that andesites in the Kurnalpi (including Gindalbie) Terrane are not necessarily products of subduction, nor in fact are they exclusive to arc settings generally; and that low-Th basalt populations from the adjacent Kalgoorlie ‘terrane’ (interpreted back-arc), and Kurnalpi ‘terrane’ (interpreted arc), are essentially indistinguishable from one another.

5.4 Summary

The Zuleika Shear Zone is an intra-terrane shear zone that separates tectonostratigraphic terranes with minor variations in stratigraphy in the adjacent Ora Banda and Coolgardie domains. In most exposures the width of the high strain zone is not significant (<30 m), but in locations at the Zuleika mining centre the ZSZ can attain thicknesses of >100 m. Aeromagnetic images suggest that kilometre-scale, lensoid tectonic slivers of ultramafic rocks define portions of the ZSZ, and this is also typical of other shear zones in the EGP.

In terms of the stratigraphy of domains separated by the ZSZ, the main differences appear to be in the development of early mafic and ultramafic volcanic sequences suggesting the ZSZ had a history of movement that includes the earliest extension that accommodated accumulation of thick sequences of sub-marine mafic and ultramafic volcanic rocks. This early history is clear despite the dominantly contractional and transpressional fabrics now visible in outcrops and drill holes.

The Kalgoorlie ‘Terrane’ has previously been identified as a distinct group of rocks with a regular mappable stratigraphy that was considered as formed in a back-arc basin to an inferred marginal calc-alkaline volcanic arc postulated to the east. Mapped geology and SHRIMP U-Pb analyses suggest the Gindalbie ‘Terrane’ contains rock groups of similar age-range and composition as present in the Kalgoorlie Terrane, particularly the contemporaneous komatiite-

dacite volcanic association in the adjacent Boorara Domain. This factor alone casts significant doubt on the validity of placing a major terrane boundary at the location of the Mount Monger Fault, and is supported by geochemical arguments that indicate mafic volcanic rocks in both ‘terranes’ are indistinguishable. The presence of proximal andesitic volcanic rocks at Lake Yindarlgooda that are near identical to the White Flag andesites, and Morgans Island andesites on Lake Lefroy at Kambalda (Forman 1953; Hand 1998), is further evidence that intermediate volcanic centres are not unique to the interpreted ‘arc-terranes’ of the Gindalbie and Kurnalpi Terranes.

Major faults and shear zones in the Kalgoorlie district have a control on the distribution of early stratigraphy and have a spatial association with Neoarchaean gold deposits, but their role as sutures or accretionary structures separating ‘terranes’ is far from certain. Given this uncertainty, considerable doubt surrounds the application of subduction / arc-accretion plate tectonic mechanisms to explain the major faults and structural geology of the Kalgoorlie greenstones.

6 Structural geology of the north Kalgoorlie district

6.1 Introduction

Archaean greenstone belts are generally considered to be highly deformed, and whereas this is the case for many areas in the Eastern Goldfields Province of Western Australia, the north Kalgoorlie district contains locally well-preserved stratigraphic sections with primary depositional structures and rock textures (Chapter 3). This preservation was a result of typical low-to-moderate metamorphic grades and heterogeneous strain distribution, which allows for confident assessment of (1) district-scale stratigraphic variations (2) kinematic / strain characteristics of the controlling tectonic events, and (3) high strain zones and whether observed complex movement histories have regional significance.

Stratigraphic growth sequences, excision and juxtaposition can be integral to a primary basin development phase, or can be produced during later tectonic accretion phases. In the cases of excision and juxtaposition of sequence, these may reflect purely post-basin deformation, but if large crustal blocks are involved, some degree of uplift and unconformity might be expected. These scenarios pose some key questions:

1. Were any of the major faults active during post-Upper-Basalt sedimentation?
2. Did any penetrative fabrics develop with the early re-arrangement of crustal blocks?
3. Do all solid-state fabrics post-date greenstone belt construction and assembly; or are some synchronous with it?
4. Are the fabrics we see related to events that significantly post-dated late basins, or are some related to tectonics that controlled early syn-orogenic sedimentation, uplift and unconformity?
5. Are the granite-greenstone contact fabrics related to externally-imposed regional deformation events or do they simply record solid state deformation related to localised granite emplacement?
6. What is the timing of fabrics with respect to mappable unconformities? Do folds and foliations cross-cut unconformities, or do conglomerates contain foliated clasts?

Constructing a deformation history requires a knowledge of the role of domain bounding faults in greenstone assembly - i.e. do the faults represent breaks between allochthonous crustal blocks; or do they simply identify high-strain compartments in a continuous (but deformed) stratigraphic succession? Additional information about the fabric histories in adjacent domains is required to assess the timing relationships between folding/foliation events and shear zone timing, and their regional or local significance.

In the north Kalgoorlie district, strain data taken from small, isolated outcrops and diamond drill holes can have wide variations in local orientation, kinematics, intensity and style of deformation. A consideration of rock types and local structural settings shows that these variations result from diverse factors including: (1) strain localisation and intensity [reflecting rock strength and anisotropy; and strain accumulation with time], (2) strain partitioning where simple-shear and pure-shear components may reflect local rheological controls on the orientation of stretching axes, (3) kinematic modes [left/right lateral] controlled by rigid bodies and shear zone orientation with respect to the regional axes of bulk shortening, and (4) structural styles that reflect variable strain-rates [brittle and ductile strains] and locally elevated palaeo- fluid-pressure gradients. Deformation fabrics can record regional tectonic episodes, whereas in areas of high palaeo- fluid flow, finite strain development may be overwhelmed by local influences.

This last point has particular currency given that much available outcrop of acceptable quality for detailed structural work comes from mines and diamond drill holes in areas of high intensity alteration and mineralisation that were loci of high palaeo-fluid flow, commonly located in the vicinity of major intrusions. In those settings, correlating kinematic styles or orientations across broad areas can be problematic considering the variable strain response of different lithotypes, and the possible influence of fluid pressure in deformation.

An illustration of this problem comes from the Paddington gold mine (Fig. 6.1a), in which multiple crenulation cleavages are developed in highly deformed shales produced by the intersection of successive foliations that are progressively imposed at small angles (or sub-parallel) to earlier foliations, whereas surrounding rock sequences show no fabric evidence of multiple overprinting deformation events.

The rocks at Paddington mine include shales, dolerite sills and ultramafic volcanic rocks localised between two major granitoid domes (Owen / Scotia Batholiths; Fig. 6.1a). In the Paddington shales an early bedding-parallel foliation (nominal ‘S1’) was deformed by a later event at a low-angle, which produced a differentiated crenulation cleavage (nominal ‘S2’; Fig. 6.1 c, d). That ‘S2’ crenulation cleavage and earlier fabrics were folded by a later deformation (nominal ‘S3’; Fig. 6.1b, e, f).

Clearly a complex strain history is recorded by the Paddington shales, whereas no evidence of this *particular* sequence of polyphase deformations is evident at a mine or regional scale - particularly in medium to coarse-grained sedimentary, intrusive and volcanic rocks. From a local perspective the Paddington shales have acted as a zone of strain localisation, and being the weakest rocks between two major intrusions have accommodated various strain increments, which appear to have had broadly similar axes of bulk shortening (interpreted from low dip angles between the various foliations).

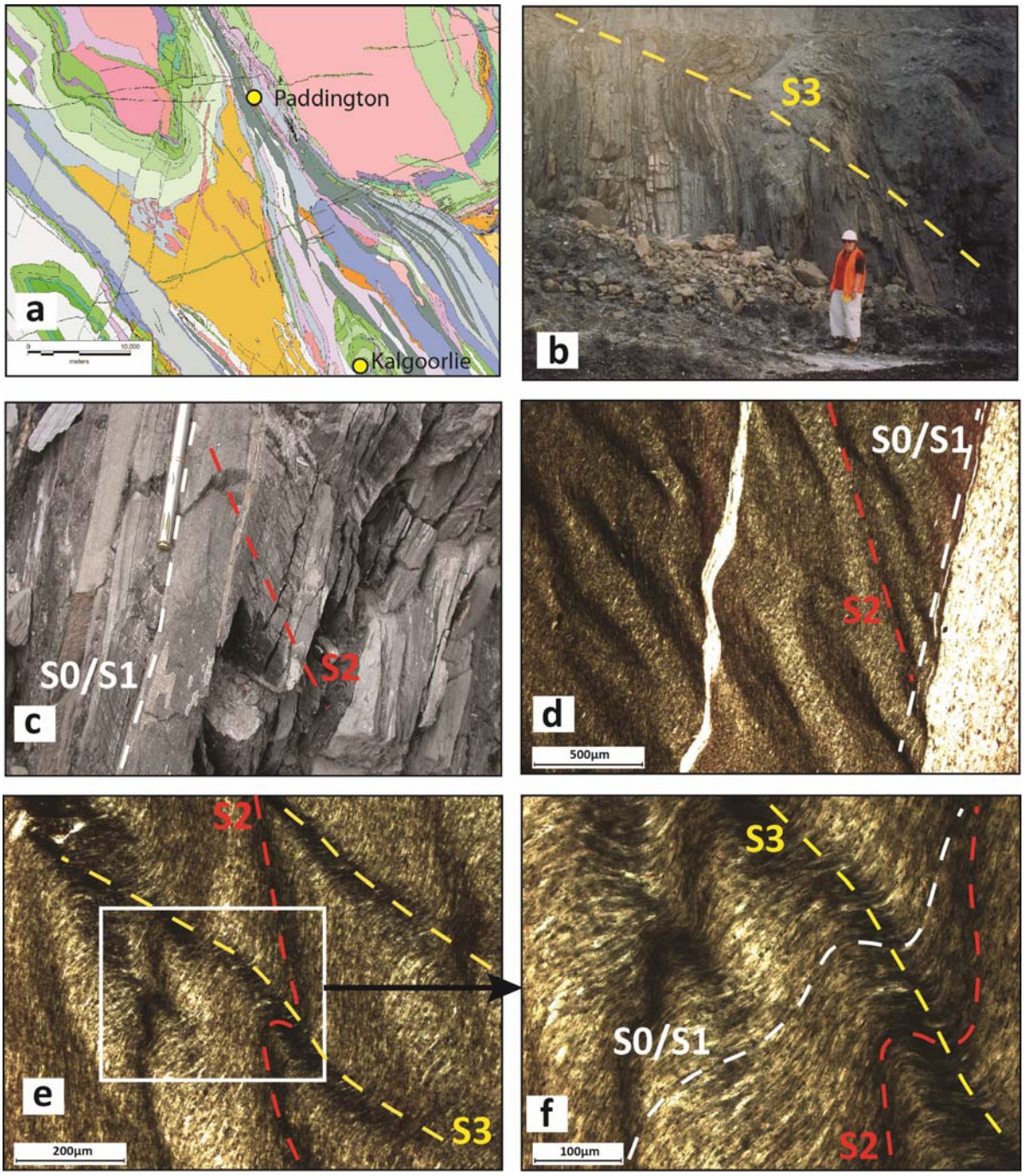

Figure 6.1 – a) Location of Paddington gold mine in greenstones between Liberty Granodiorite and Scotia Batholith, see A0 map in pocket for detailed lithological coding; b) Paddington gold mine central bench between northern and southern mining areas, carbonaceous shale-sandstone-siltstone beds with vertical bedding (S0) and bedding-parallel foliation (S1), overprinted by late folds (F3?) with shallow east-dipping axial planes suggestive of a sub-vertical shortening (view to north west); c) close-up of bedding (S0) and sub-parallel fabric (S1) cut by steeply east-dipping crenulation cleavage (S2); d) PPL photomicrograph of bedding (S0) and bedding-parallel fabric (S1) – quartz-rich layer (right) and phyllosilicate-rich layer (left), with steeply east-dipping S2 crenulation cleavage; e) PPL photomicrograph of crenulation cleavage (S2) crenulated by a shallow to moderate east-dipping S3 spaced crenulation cleavage; f) PPL close-up photomicrograph of (e) showing S0/S1–S2–S3 fabric relationships. In all photos S1 is penetrative parallel to bedding, S2 is a differentiated crenulation cleavage and S3 is a spaced crenulation cleavage that folds the earlier S2 crenulation cleavage. The orientation of S3 is suggestive of a steep axis of shortening (views to the north west). Compare S1/S2/S3 at Paddington mine with the deformation scheme presented in Table 6.1.

This point raises the important question of how representative local fabric histories are, given variable rock type and rheology, and the capacity of strong vs. weak rocks to record strain (e.g. dolerite vs. shale) under similar P,T, and strain-rate conditions. For these reasons a comprehensive approach is used here including the use of stratigraphy and greenstone distribution to attempt a structural analysis of the study area.

For the Kalgoorlie greenstones a structural analysis approach focussed *only* on solid-state fabrics (correlating fabric style and orientation across the district) is likely to produce overly-complex structural histories, given a heterogeneous and strongly localised distribution and accumulation of strain. This chapter attempts to construct a structural history using regional geophysical data sets, stratigraphic distributions in map patterns, and fabric data from broad disconnected exposures, combined with observations of cross-cutting relationships at key localities.

6.2 Upper crustal structure (geophysical data and map patterns)

The prodigious gold endowment of the north Kalgoorlie district has resulted in significant investments by industry, government and research groups in major sub-regional geophysical surveys including (for the study area): >290 line kilometres of reflection seismic surveys; >8000 km^2 aeromagnetic surveys, dominantly 200 m line-spaced; and a recent (2002) ~3600 km^2 ground gravity survey with ~200 m-spaced gravity stations.

A sub-regional scale inversion model of gravity data was constructed for the study area by Placer and Barrick geophysicists using a UBC (University of British Columbia) inversion code. Critical to gravity inversion models is applying geological constraints to guide interpretations of the subsurface distribution of rock density. In the case of the north Kalgoorlie district, gravity and aeromagnetic modelling were guided by a sub-regional 3D geological model of the district created with a revised geological map and crustal cross-sections constructed from the 2D surface map by a team of Placer Dome geologists in 2003. This model was used interactively with new geophysical data sets to validate geological interpretations and guide geophysical inversion modelling, geological interpretation and cross-section construction. This work was team-based and the author was involved throughout the process for geological input and forward modelling of the 3D gravity.

Regional seismic surveys undertaken by GA (Geoscience Australia, previously AGSO - Australian Geological Survey Organisation) have been fully documented in several papers (Drummond et al. 1993; Goleby et al. 2000, Archibald et al. 1998; Goleby et. al. 2004), whereas sub-regional aeromagnetic surveys and in-house industry gravity data have not been widely documented, and in the latter case are unavailable to public access.

A benefit of regional scale aeromagnetic and gravity surveys is an ability to assess the broad geometry of greenstone and granitoid lithological magnetic and density responses from a

single data-set. The Barrick geological map of Kalgoorlie is also useful in this respect, but is by nature a compilation of the observations of many geologists of varying experience over three decades; hence, a single geophysical data-set has advantages that complement observational data. Deformation kinematics have been interpreted from the orientation and distribution of units in 2D aeromagnetic images of the Eastern Goldfields (e.g. Blewett et al. 2010a; See Chapter 8). These observations are corroborated by outcrop kinematic data which show that regional geometric patterns in aeromagnetic imagery have substance at an outcrop scale.

This section presents new interpretations of the listed data sets that reveal information about the upper crustal structure of the study area. Previous interpretations of the seismic data are discussed, and some new interpretations of those data are presented later in this chapter.

6.2.1 Regional gravity data

A comparison of the study area geology against available gravity data shows there is not a 1:1 correlation between the surface distribution of mafic and ultramafic volcanic rocks and areas of high density in the gravity images (Fig. 6.2). The image in Figure 6.2b is a composite of aeromagnetics (texture) and Bouguer gravity (colours). The white box in Figure 6.2b covers the Ora Banda area, where outcrops, mine exposures and aeromagnetic data (texture) indicate a continuous sequence of mafic volcanic rocks of the Upper Basalt unit, whereas the same area has a coincident gravity low signature that appears to extend from the major Owen Monzogranite complex to the east. Numerous minor quartz-feldspar porphyry dykes and sills outcropping in the Ora Banda district are probably a surface indication of a significant body of low density rock at depth (Tripp 2002a), as also indicated by a UBC gravity inversion model (Fig. 6.3a). Comparatively sharp margins of low density areas against high density mafic and ultramafic volcanic rocks are reflected in the depth distribution of the Scotia Batholith where the gravity inversion model shows the margins are steep (Fig. 6.3b).

A broader-scale comparison of rock density with surface distribution of high-density mafic and ultramafic rocks is shown in Figure 6.2c and d. The green polygons in Figure 6.2d contain all occurrences of mafic and ultramafic volcanic and intrusive rocks selected from the regional GIS, whereas the grey and red polygons are outlines of the low gravity and high gravity areas respectively, digitised from the image in Figure 6.2c. Intermediate gravity response areas are left blank, and whereas these are represented by high density rocks at surface, the blank areas appear to coincide with gradient zones between extreme high and low gravity areas or areas of abundant felsic volcanic and sedimentary strata.

Red dashed circles in Figure 6.2d surround high gravity response zones, but these lie over areas that are dominated by low density felsic volcanic and sedimentary rocks at the surface. These areas are true geophysical anomalies: the rocks and structure predicted from the geophysics are not the same as observed in the field. The north-western anomaly (labelled ‘H1’)

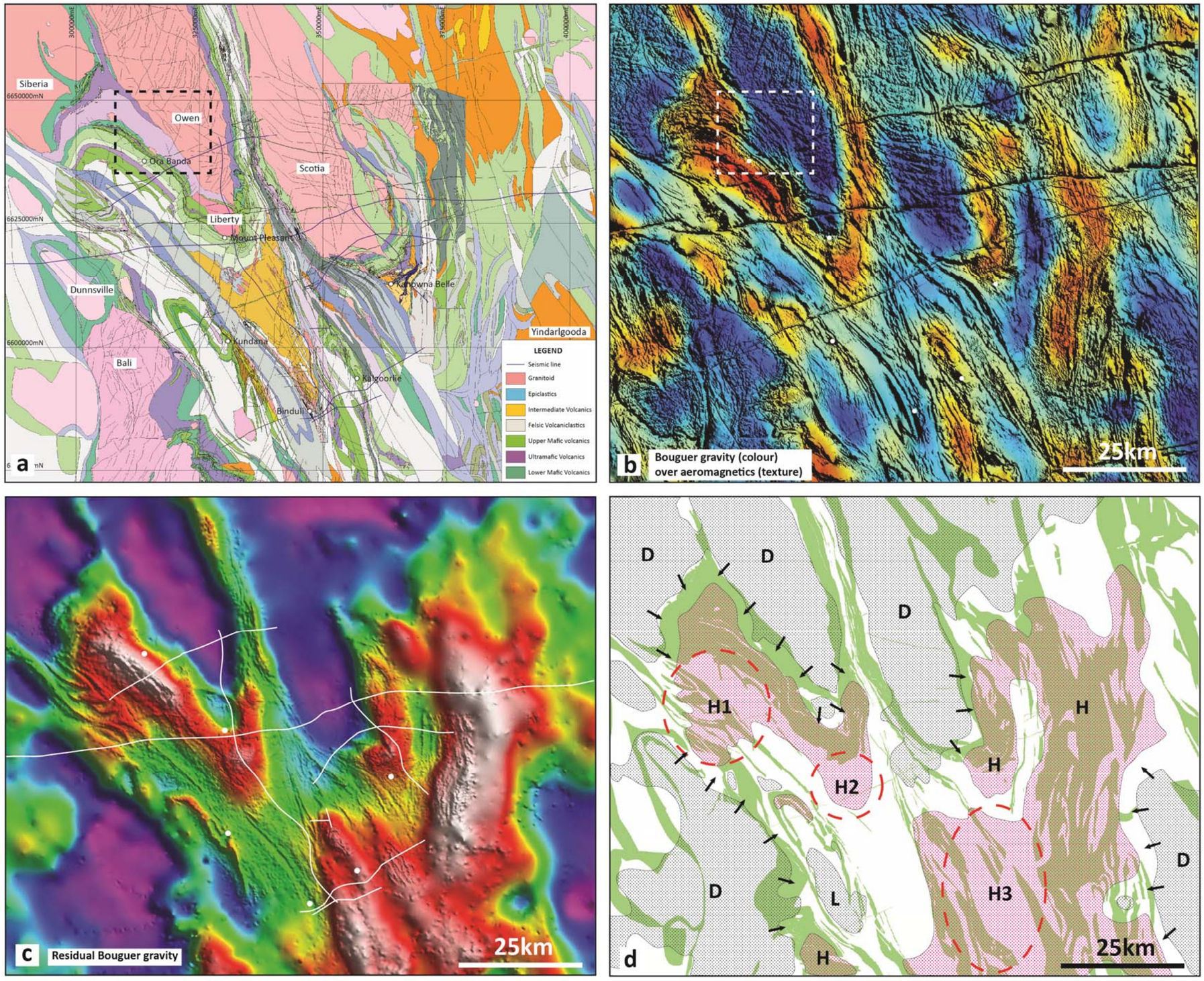

Figure 6.2 – a) Geology of the north Kalgoorlie district with locations of seismic lines, and major batholithic domes labelled - see detailed version in Map Pocket for detailed legend; b) Image of Bouguer gravity (colour) over image of the 1st vertical derivative of the aeromagnetic data (texture), white dashed box matches same area in (a); c) Image of residual Bouguer gravity (hot colours=high gravity response; cool colours=low gravity response); d) Interpretation of the image in (c) with high and low gravity areas superimposed on all high-density-rock outlines (mafic/ultramafic volcanic and intrusive rocks). “D” = granitoid dome, arrows indicate a general direction at 90 degrees to the foliation in the wallrocks. Red dashed circles indicate anomalous areas where gravity is high, but amount of exposed mafic/UM rocks is thin.

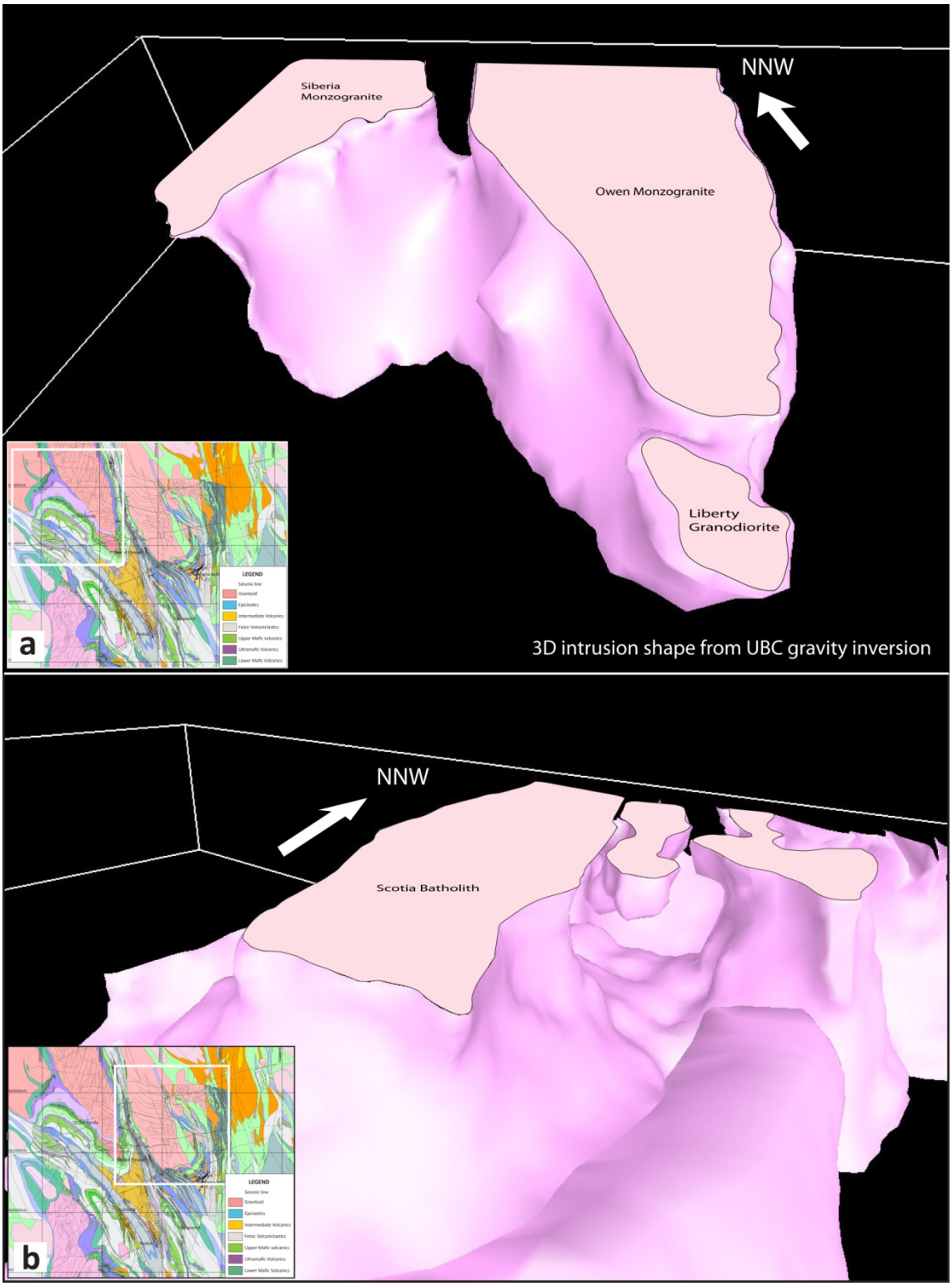

Figure 6.3 – Rotated 3D model view of predicted sub-surface shapes of the two major granitoid batholiths in the north Kalgoorlie district - a) Owen Monzogranite, and b) Scotia Batholith. Pink shapes are models of the ~2.7g/cm3 density distribution predicted from gravity inversions, using the UBC code (performed by Barrick/Placer geophysicists as part of a regional 3D geological modelling project). Flat surface plane of batholiths is indicated by the dull pink, labelled polygons. Of particular note is the irregular shape of the sub-surface intrusion on the western margin of the Owen complex under Ora Banda, which corresponds with abundant quartz-feldspar porphyry dykes and sills in outcrop; and the sub-vertical eastern contact of the Scotia Batholith (confirmed as a mylonitic shear zone in drill holes at the contact).

is coincident with a zone of folded, thin gabbroic sills in sedimentary rocks to the west of the Zuleika Shear Zone. It is unlikely that these thin sills are responsible for the gravity-high anomaly, but more likely that the gravity signature reflects the Ora Banda Domain mafic stratigraphy dipping beneath the rocks in that area. However, the Ora Banda mafic stratigraphy has a linear NW-SE trend on the western side of the Owen Batholith, whereas the gravity anomaly in question is an irregular E-W protrusion from that trend. It is possible the excess density is related to abnormally thickened mafic sequences at depth beneath the Kurrawang Formation in that northern area.

A similar protrusion from an otherwise consistent trend of the Ora Banda mafic stratigraphy occurs at the apex of the Mount Pleasant Anticline (labelled 'H2'), where a high density zone projects to the south under the Kurrawang Formation and into the Kundana South area. Detailed mapping (Chapter 3) indicates there is indeed a sliver of the distinctive Ora Banda Upper Basalt unit in the Kundana-Kundana South area, explaining the elevated gravity signature.

Discussions in Chapter 3 settled on an interpretation of the Upper Basalt being folded under the Kurrawang, yet previous authors have suggested alternative possibilities for this occurrence of the Ora Banda Upper Basalt at Kundana, including strike-slip displacement across the Zuleika Shear Zone (Witt 1990). The continuity of the gravity signature from Mount Pleasant to Kundana favours the interpretation of folding, and the location of the Zuleika Shear Zone to the west of those exposures supports that contention.

A further high gravity zone sits under the Golden Mile stratigraphy at Kalgoorlie, and to the east of that area (labelled 'H3'). The red circle in Figure 6.2d covers a large area of high gravity response, but that area is dominated at surface by thin, linear mafic and ultramafic units surrounded by thick sequences of felsic volcanic and sedimentary rocks. This high-density zone is continuous with a large high-gravity zone extending from the western edge of the Yindarlgooda Dome. The rocks in that vicinity are thick, structurally stacked and contorted sequences of mostly ultramafic volcanic rocks with high-Mg basalts (Williams 1970).

Empirically, the highlighted anomalous areas have a high-density response, and are probably underlain by significant thicknesses of strata likely composed of mafic or ultramafic volcanic and intrusive rocks. Whether those thicknesses are primary or structural is unknown, but the unusually stacked section of rocks west of the Yindarlgooda Dome is suggestive of the latter. Conversely, the location of this unusual stacking restricted to the western side of the Yindarlgooda Dome could suggest a greater primary thickness of the ultramafic volcanic sequence in this area.

Granitoid dome emplacement is a possible mechanism to explain the unusual thickness of those mafic-ultramafic rocks, given the restriction of the thickening to the western margin of the dome. Alternatively, thrust stacking may also explain the enhanced gravity signature between

Yindarlgooda Dome and the Golden Mile. These explanations could equally apply to the unusually high gravity west of the Owen complex ('H1' on Fig. 6.2b). Figure 6.2d shows a series of arrows trending off dome in several areas. Note that these arrows are not measured stretching lineations as presented; but in the case of the Siberia; Dunnsville; Bali and Scotia domes, the arrows are about parallel to the few documented stretching lineations in those areas (Section 6.2.2).

An exception to the previous relationships occurs on the eastern margin of the Bali Monzogranite dome, where a sharp granite contact with dissected ultramafic rocks across the Kunanalling Shear Zone has no significant gravity signature. This may be a result of: (1) structural excision of the stratigraphy, (2) that a significant thickness of mafic and ultramafic rocks was never present, (3) hydrothermal alteration, or (4) that the Kunanalling Shear Zone marks a major regional break possibly related to (1).

A close inspection of Figure 6.2c shows that several of the known major structures in the north Kalgoorlie district are visible on the gravity image including: the Zuleika Shear Zone; the Kurrawang unconformity; Bardoc Tectonic Zone; Panglo unconformity; and the N-S trending Mount Monger Fault on the edge of the gravity-high at the east of the image. A particular point of note is the western edge of the previously discussed gravity anomaly at the Golden Mile, which is a sharp boundary marked by the Abattoir Shear Zone. This break appears to indicate that the Abattoir Shear Zone marks a more fundamental structural contact, than suggested by surface exposures alone.

6.2.2 Aeromagnetic images of greenstone distribution and structure

Images of aeromagnetic data from the north Kalgoorlie district, processed from regional airborne surveys at 200 line-spacing and 40 m sensor height, are a critical tool in regional mapping and exploration by government geological surveys and industry. Much of the data in Figure 6.4 was collected as multi-client regional surveys by World Geoscience Corporation, supplemented with local 25 m spaced helicopter-surveys by industry, and reprocessed to a single image by Placer and Barrick geophysicists.

Aeromagnetic images show the distribution of primary magnetic minerals in rocks (magnetite, titanomagnetite and ilmenite). Primary signatures are further modified by magnetite destructive alteration, which is common in Archaean lode gold systems, including chlorite, silica, white mica and carbonate alteration, but may also include hydrothermal magnetite and magnetic pyrrhotite that enhance the magnetic response. Alteration effects can swamp aeromagnetic signals at a deposit scale, but the localised nature of the proximal alteration assemblages in those systems, allows primary magnetic signatures of strike-persistent mafic and ultramafic rocks to be mapped at a sub-regional scale.

Greenstone distribution and kinematics from aeromagnetic images

Images of aeromagnetic data for the north Kalgoorlie district (Fig. 6.4) show a clear NNW-SSE striking structural grain, also identified by many previous authors (e.g. Isles et al. 1989; Swager et al. 1990; Witt 1990; Whitaker 2001, 2004). A significant aspect that was not emphasised previously is a strongly orthorhombic symmetry displayed in aeromagnetic images of the north Kalgoorlie district (Vearncombe 1998), compared to published examples from elsewhere in the Eastern Goldfields Province that appear to show a strong monoclinic symmetry (e.g. Swager and Nelson 1997). Several major truncations of stratigraphy are visible in Figure. 6.4, but there appears to be few examples of asymmetry that could be interpreted as strike slip shear zones at a regional scale in the selected study area. An exception is the Telegraph Syncline, north of Kunanalling, which shows an apparent ~13 km offset of ultramafic rocks of the Hampton Ultramafic Unit in the Coolgardie Domain (Swager 1994; Fig. 6.4; See also Weinberg et al. 2004). Prominent examples of major asymmetric zones with interpreted strike-slip elsewhere in the Eastern Goldfields Province are located on the Keith Kilkenny Lineament (Fig. 6.6a) and the South Laverton Tectonic Zone (Fig. 6.6b) among others.

In the north Kalgoorlie district, the kinematic nature of the major faults (Fig. 6.5) is not indicated by geometries displayed on aeromagnetic images, other than to show major truncations of continuous stratigraphy. If these faults were major strike slip zones, a monoclinic asymmetry of surrounding rocks units might be expected, with surrounding wallrock units bending into the major shear zones, but this appears not to be the case. An alternative is that the prevalent stretching direction of those major faults is into the page, and typical shear-sense asymmetry is neither observed nor expected. Kinematic data from outcrops commonly show sub-horizontal lineations in steeply dipping faults, but this may reflect the latest movements on those structures (Vearncombe et al. 1989; Weinberg et al. 2004, 2005).

Figure 6.5 is a structural sketch map of approximately the same area as covered in the aeromagnetic image of Fig. 6.4, with a foliation trajectory layer interpreted from ~850 compiled outcrop measurements of foliation and cleavage from various sources including GSWA 1:100,000 scale mapping (Witt 1990; Ahmat 1995; Swager 1995; Wyche and Witt 1990; Hunter 1993); Crossing (2003); Archibald (1993) and summarised observations from detailed mapping areas in this study, processed using Spheristat 3.1 software.

Several of the granitoid domes (Siberia, Dunnsville, Bali) have concentric foliations that appear related to emplacement of the domes, whereas others (Scotia) have no apparent relationship to the trajectories of pervasive foliations. Concentric foliations also appear to surround the small Liberty Granodiorite stock at the southern margin of the Owen complex. At the southern margin of the Scotia Dome, a consistently oriented NNW-SSE striking foliation tracks across the regional-scale long wavelength folds, and across the Panglo unconformity; which itself cuts those regional-scale folds. The pervasive foliation transects the limbs of NE-

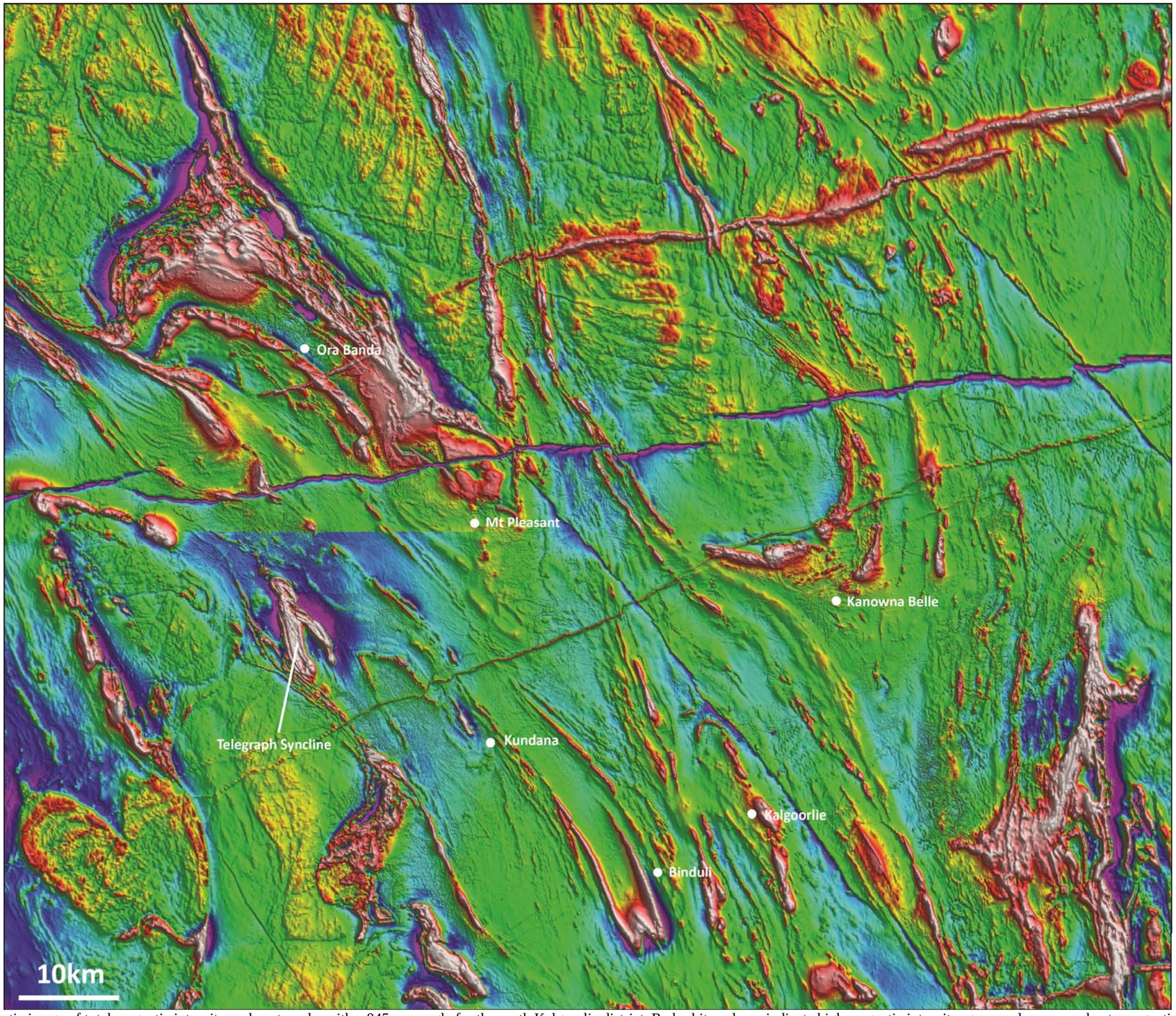

Figure 6.4 – Composite aeromagnetic image of total magnetic intensity, reduce to pole, with a 045 sun-angle for the north Kalgoorlie district. Red-white colours indicate high magnetic intensity; green colours – moderate magnetic intensity. Purple-blue colours generally indicate low magnetic intensity, but in linear zones may represent a dipole effect of the imaging technique, which is an artefact produced by the close juxtaposition of areas of very-high and low magnetic intensity. The sharp E-W line under 'Mt Pleasant' is a sheet edge effect.

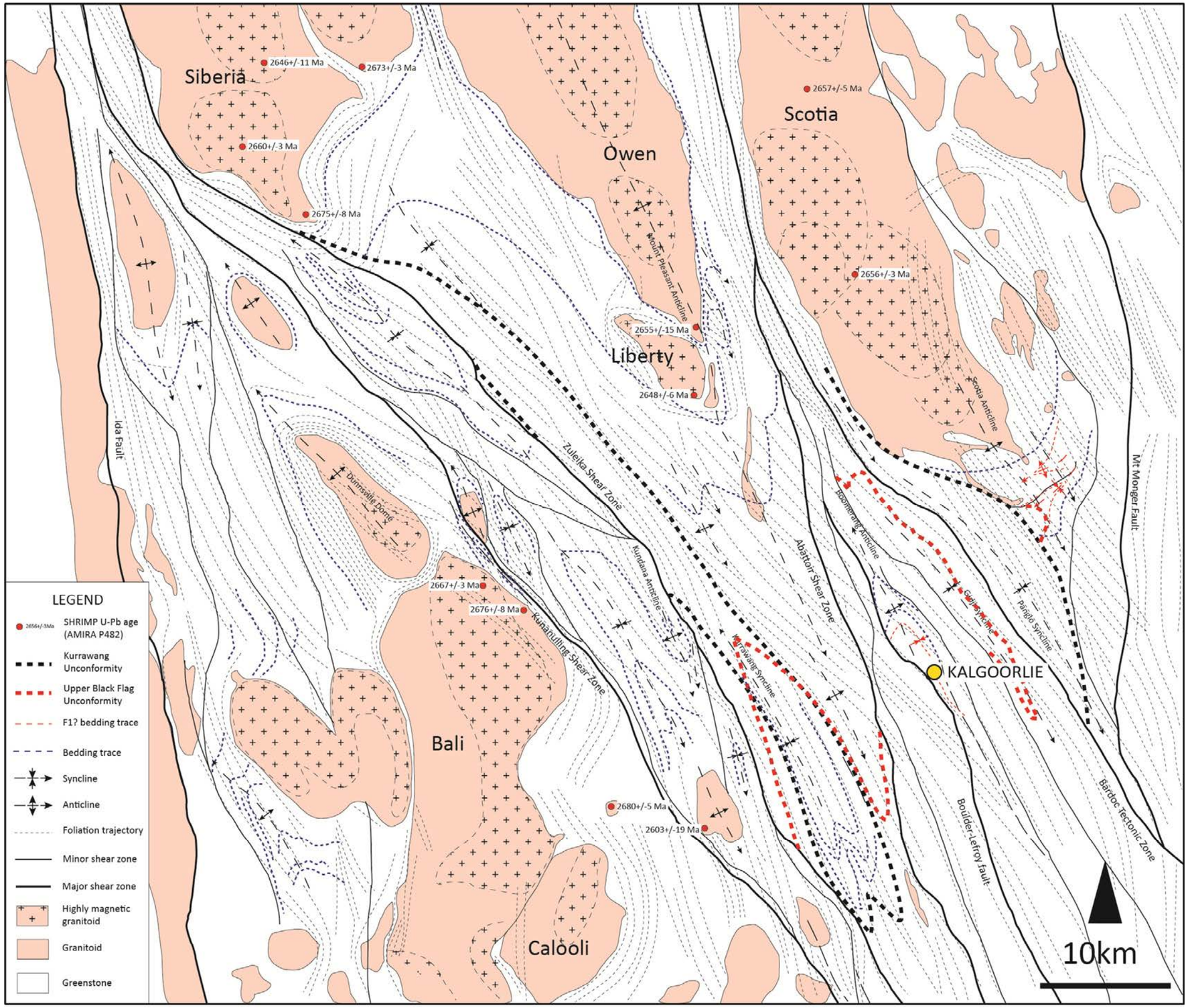

Figure 6.5 – Sketch map of the Archaean structure in the north Kalgoorlie district from aeromagnetic interpretation (Proterozoic dykes not included). Foliation trajectories from regional compilation of fabric data.

Figure 6.6 – a) Aeromagnetic RTP image of Keith Kilkenny Tectonic Zone (KKTZ) in the Agnew district showing zones of sinistral and dextral asymmetries from fabric deflection into major shear zones. The shear zones appear to have cross cutting relationships, but the sense of offset is ambiguous if dextral NNE-SSW shear zones were overprinted by NW-SE striking sinistral shear zones. Sinistral and dextral shear zones may have developed synchronously during a bulk shortening; b) South Laverton Tectonic Zone (SLTZ) showing dextral asymmetry from fabric deflection and a tear-drop shaped intrusion.

SW striking folds that are apparently folded around the Scotia anticline, but is broadly axial planar to the folded Panglo member.

Aeromagnetic responses in Figure 6.4 appear to show internal complexity in the major domes, with semi-circular zones of high magnetic susceptibility, and variable aeromagnetic texture internal to the major batholiths. Similar observations were made by Witt and Davy (1997), but the aeromagnetic data in Figure 6.4 are a significant improvement on previously available images. That particular study attempted to sub-divide the granitoid intrusions into pre-regional folding (foliated) and post-regional folding (unfoliated), but given heterogeneous strain, their subdivision was also made on the basis of relationships of granitoids with major folds, shear zones, and internal complexity. Some of the domes have SHRIMP U-Pb analyses of zircons that show they are composed of multiple intrusive phases (Fig. 6.5). It should be noted the granitoid rocks in the north Kalgoorlie district are some of the least exposed, and usually strongly weathered with a thick mantle of sandy soil, and the available material for sampling is minimal.

The relationships displayed in Figure 6.5 suggest several problems with a simple ‘S2’ axial planar cleavage interpretation for the pervasive upright foliations widely observed in the study area. A key question regards the timing of foliations developed internal to domes, versus those developed external to the granitoid domes. In the case of the Siberia and Dunnsville domes, the highly concentric nature of the external foliation trajectories suggests those fabrics were formed as a by-product of intrusion. In the case of the Bali dome there appears to be a significant overprinting of dome-intrusion fabrics modified by later strike slip. The Scotia Dome appears to have intruded prior to the imposition of a later pervasive foliation, but exposure in that dome is not ideal, and conclusive relationships remain unclear. Internal composite intrusions suggested by the aeromagnetic data and confirmed by geochronology may indicate that the construction of the batholiths took place over an extended time period; hence the concentric fabrics may be a product of the latest phases that ballooned into the centre of the granitoid batholiths, and produced solid state fabrics at the periphery.

Witt and Davy (1997) considered batholiths with a strong concentric fabric on the margin, and contacts sub-parallel to surrounding greenstones to constitute ‘pre-regional folding’ intrusions with a characteristic strong continuous to spaced NNW-SSE internal foliation, and widespread ‘granite-up, greenstone-down’ contact kinematics (unfortunately these internal observations are not available with the published fabric data). Their description of the contact relationships of their ‘post-regional folding’ intrusions were remarkably similar to those of the ‘pre-regional folding’ intrusions, hence the distinction between pre- and post-folding may have been a superficial one.

The spread of ages in the intrusions on Figure 6.5, and the variable contact relationships and internal compositions, would support an interpretation that doming was important in the

deformation of the greenstones in the north Kalgoorlie district, perhaps beginning as early as 2676±8 Ma in the larger composite batholiths. The 1.5 km x 1.5 km Bonnivale Tonalite stock has a U-Pb SHRIMP age of 2680±5 Ma (Hill et al. 1992) and is the oldest age for a felsic intrusive rock in the study area (Fig. 6.5).

Geochronological data from Chapter 4 indicate the end of mafic volcanism at around 2685±4 Ma with the intrusion of the Golden Mile Dolerite into the contact of the Paringa Basalt with overlying shales; hence, granitoid doming may not have been a significant extensional process contributing to the extension that permitted deposition of the mafic and ultramafic volcanic sequences.

The following sections outline a proposed deformation history of the study area separated into 'events' (D1, D2.....etc.). Since this deformation history is compiled from observations across a broad district, continuous reference will be made back to Table 6.1 which is an interpretation of structural events for the study area based on stratigraphic sequences, intrusion ages, key timing criteria, and manifestations of structural events in each of the four domains; with an estimate of the duration of each deformation phase. This may assist the reader in assessing the veracity of correlations and interpretations of the structure.

6.3 Extensional deformation (DE)

The earliest deformation in the Eastern Goldfields Province is generally documented as an extension responsible for the deposition of much of the Archaean greenstone successions (Williams and Whitaker 1993; Martyn 1987; Hammond and Nisbet 1992; Table 6.1). The oldest greenstones are mafic volcanic rocks of the lower Penneshaw Formation in the Norseman Terrane (Swager et al. 1990; Table 4.3), but no exposures of an older sialic basement to the greenstones have been recognised (Archibald et al. 1987; Swager et al. 1990). Geochemical arguments including crustal contamination of mafic volcanic rocks and the presence of >3100 Ma xenocrystic zircons widely reported for mafic, felsic and sedimentary units (e.g. Barley et al. 1989; Turek and Compston 1971; Swager 1997; Compston et al. 1986; Claoue-Long et al. 1988; Smithies et al. 2003; Czarnota et al .2010) are used to argue for an ancient continental mass that was extended prior to greenstone deposition. Extensive discussion in the literature of this problem of identifying the basement to the greenstones has moved from interpretations of marginal high-grade TTG (tonalite-trondjhemite-gneiss) rocks as possible candidates (Archibald and Bettenay 1977), to later concessions based on the geochronology of gneissic rocks that no basement to the Eastern Goldfields can be unequivocally demonstrated (Turek and Compston 1971; Swager 1997; Compston et al. 1986; Claoue-Long et al. 1988).

Critical to the discussion of early extension is an understanding of what factors influenced the stretching of the crust, and how this stretching was accommodated. Two main lines of argument include (1) extension by density-driven doming of the intruding granite batholiths,

Table 6.1 – Deformation event sequence with styles, ages, key timing criteria and manifestations of events in each of the fault bounded domains of the north Kalgoorlie district. Estimates of the age range of each event are based on timing criteria; mineralisation events are listed on the basis of structural cross-cutting.

Event	Style/Kinematics	Estimated age range	Mineralisation	Granitoid intrusions	Key timing criteria	Manifestations			
						Coolgardie Domain	Ora Banda Domain	Kambalda Domain	Boorara Domain
E	Extensional faulting of unknown vector; possible origin of major faults - potential control on thickness changes in the mafic and ultramafic stratigraphy Likely continued extensional fault activity during deposition of 'Upper Felsic Volcanic and Sedimentary Unit'	2715 - 2688 Ma (Komatiite Unit) >2694 Ma (Upper Basalt)	Magmatic Ni-Cu-PGE		- 2708±7 Ma: intercalated dacite / komatiite at Kanowna (Nelson (1997) - 2692±4 Ma: Kapai Slate, top Devon Consols Basalt (Claoue-Long et al. 1988) - 2687±5 Ma: Mt Pleasant Sill intruded interflow sedimentary rocks at base of Upper basalt (Hill et al. 1995) - 2694-2687Ma: Sedimentary rocks overlying Upper Basalt	MAFIC STRATIGRAPHY: **(1)** significant thickness of basalt / Komatiite units with abundant intercalated mafic sills (two levels of komatiite; Standing, 2007) **(2)** Upper Basalt not recognised	MAFIC STRATIGRAPHY: **(1)** greatest thickness of Komatiite Unit in the district **(2)** ~3.1km Upper Basalt (Mt Pleasant Anticline; abundant mafic-UM sills	MAFIC STRATIGRAPHY: **(1)** significant thickness of Komatiite Unit with abundant Ni deposits **(2)** significant thicknesses of Paringa basalt at New Celebration / Kambalda; abundant mafic sills	MAFIC STRATIGRAPHY: **(1)** significant thickness of Lower Basalt and Komatiite Unit **(2)** significant thickness of Upper Basalt(?) with abundant mafic sills
	Abundance of coarse clastic rocks in the north Kalgoorlie district suggests localised high-relief between intra-basinal sources / depocentres - possibly controlled by extensional faulting					FELSIC VOLCANIC AND SEDIMENTARY STRATIGRAPHY:	FELSIC VOLCANIC AND SEDIMENTARY STRATIGRAPHY:	FELSIC VOLCANIC AND SEDIMENTARY STRATIGRAPHY:	FELSIC VOLCANIC AND SEDIMENTARY STRATIGRAPHY:
		2694-2687Ma (Sedimentary rocks overlying Upper Basalt)			2694-2687Ma bracket of deposition for sedimentary rocks at White Flag Lake	**(1)** broad areas of turbiditic sedimentary rocks with mafic sills	(1) Talbot formation turbiditic sedimentary rocks	**(1)** Sedimentary rocks overlying Upper Basalt (conglomerate / shale) at Lakewood south (Krapez and Hand, 2008)	**(1)** Fine grained graded turbiditic sedimentary rocks overlying Upper basalt **(2)** Ballarat coarse clastic ultramafic clast conglomerates / polymictic conglomerate and sandstone
		~2687 - 2681Ma			- 2690±9 Ma: White Flag Formation - 2695±6 Ma: maximum depositional age of Ballarat conglomerate	**(2)** White Flag Formation(?) andesitic volcaniclastic rocks (Powder Sill?)	**(2)** White Flag Formation andesitic volcanics Mt Pleasant Sill 2687±5 Ma Ora Banda Sill?	**(2)** not recognised Gidji Porphyry? (2682 ±8 Ma) - Sub-volcanic mafic sills: Golden Mile Dolerite 2685±4 Ma Condenser Dolerite 2680±8 Ma	Ballarat and Kanowna units may overlap with this sequence
	Batholithic granitoids possible sub-volcanic sources to Lower Black Flag Formation volcanic rocks	~2678-2666Ma	Au-rich sulphide replacement styles: Binduli ECM?; Lake Yindarlgooda Cu-Zn stratiform, massive pyrite deposits; Spargoville stratiform sulphide replacement deposits?	- 2675±8Ma - Siberia Monzogranite - 2676±8Ma - Bali Monzogranite (older phases of composite batholiths)	- 2676±5 Ma Gibson-Honman Rock - 2675±3 Ma Perkolilli rhyolites - 2672±6 Ma Lakewood dacites		**(3)** Intercalated andesitic / dacitic volcanic rocks correlated with Lower Black Flag Formation Gibson-Honman Rock (GIBSON-HONMAN FORMATION)	**(3)** Lakewood dacitic volcanics and intercalated sedimentary rocks correlated with Lower Black Flag Formation	**(3)** Perkolilli rhyolitic volcanics correlated with Lower Black Flag Formation
1a	No evidence for N-S shortening (e.g. Kambalda style in study area); '1a' may reflect off-dome gravitational sliding; may be a continuation of DE; Alternatively an early recumbent folding phase preceding prominent, long-lived ENE-WSW shortening event)	~2677-2663Ma	Au-rich porphyry clasts, epithermal vein clasts and massive sulphide clasts (source to Golden Valley Conglomerate)		- Lakewood dacites folded with GMD - Early NE-SW folds in the Ballarat cut by upper Black Flag unconformity		Extensional slides and faults with early recumbent F1 folds (?)	F1: Isoclinal folding of the Golden Mile stratigraphy in cluding Lakewood Dacites; Kalgoorlie Syncline	F1: early folds in the Ballarat-Kanowna sequences, and underlying ultramafic rocks
				Upper Black Flag Formation Unconformity					
1b	Uplift and erosion Continued volcanism, due to high level granitoid emplacement (no isoclinal recumbent folding of Upper Black Flag Formation units recognised) Kinematics as extensional or contractional unknown; possibly the beginning of regional contraction	~2668-2661Ma	Early stage high-level Au-Te Fimiston veins (Gauthier etal. 2004) Kanowna Belle high-level Au-telluride and later py-vein stock work disseminated style?	- 2667±3Ma - Bali Monzogranite (younger phases of composite batholith) - 2661±8 Ma Kanowna Belle Porphyry intruded along Fitzroy Fault - 2662-2649Ma bracket on initial Fitzroy Fault movement at Kanowna Belle - 2655±15Ma - Owen Complex - 2660±3Ma - Siberia Monzogranite (younger phases of composite batholith)	- Basal unconformities: (Binduli porphyry conglomerate <2664Ma / Gidji conglomerates / Grave Dam volcaniclastics and conglomerate - Clasts of Au-rich dacite porphyry, crustiform banded qz-carbonate veins, and massive sulphide in GVC	Chadwin granite-up / greenstone-down extensional foliation related to Siberia granite emplacement (S1)	**(4)** Upper Black Flag Formation dacitic volcanics and sedimentary rocks	**(4)** Upper Black Flag Formation Gidji Felsic volcanics / conglomerate and MAD andesitic volcanics and sedimentary rocks (GIDJI LAKE FORMATION)	**(4)** Unconformable dacitic volcaniclastics (Grave Dam), polymictic conglomerate (Golden Valley), and volcaniclastic turbidites - Fitzroy Fault (initial movement <2662Ma - minimum age of youngest footwall unit)
				Cessation of extrusive volcanism					
2	Contractional deformation - broad wavelength upright folds; ramp-anticlines, fault-bend folding in sedimentary rocks; disharmonic folding at sub-regional scale; possible involvement of granite batholiths in deformation Not a major meso-scale foliation forming event in greenstones (thin skinned stacking?)	2660 - 2650Ma		- 2655±15Ma - Owen Complex (contacts sub-parallel to stratigraphy)	- Folding at sub-regional scale of all formations - F1 folds at Kanowna rotated; and F1 at Golden Mile re-folded by F2 - 2661±11 Ma footwall rocks to the Shamrock thrust fault	- F2: Telegraph Anticline; Kundana Anticline; Powder Sill Syncline; Carbine-Brown Dam Syncline	- F2: Mount Pleasant Anticline-syncline couplet - Mt Pleasant detachment fault post-dates folds in Upper Basalt - Grants Patch Fault? (Km-scale fault displacements in older greenstones, cut by Kurrawang unconformity)	- F2: Boomerang Anticline; Gidji Syncline - Gidji Fault	- F2: Scotia anticline - rotation of F1 folds(?) to NE-SW orientation? - Shamrock Fault E over W thrust
				Kurrawang Unconformity					
3a	Uplift and erosion: deposition of syn-orogenic long-linear polymictic siliciclastic sedimentary rocks in fluvial to marginal marine settings; controlled by major faults (strike slip?) Contraction or extension? Interpreted as major extensional episode by pmcCRC	<2650Ma		- 2657±5Ma - Scotia Batholith (contacts appear to cut folded Lower Basalt/UM/Upper Basalt stratigraphy; marginal granite dykes are cut by unconformable Panglo)	- 2655±5Ma (Navajo Sandstone) - 2657±7Ma (Kurrawang conglomerate - Truncation of major F2 folds at basal unconformity of Kurrawang and Panglo sequences - Scotia Batholith appears to cut F2 Scotia Anticline, with major faulted eastern margin	Late clastics not recognised	Kurrawang Formation	Merougil Formation at Kambalda (but not recognised in the study area)	Panglo conglomerate (truncates marginal porphyritic phases of Scotia Batholith)
3b	Burial to significant(?) depths; contractional deformation with imposed pervasive NNW-striking metamorphic fabric 'S3'	~2650-2636Ma	Syn-post foliation mesothermal lode-gold, quartz carbonate vein deposits (Kundana, White Feather, Shamrock, early quartz-molybdenite veins at Ora Banda; Kanowna Belle Troy Lodes?)		- F1 folds at Kanowna and Golden Mile transected by S3 foliation and cleavage - Binduli porphyry conglomerate unconformity folded and cut by S3 foliation and cleavage - Ramp-anticline detachment faults (Mt Pleasant) overprinted by S3 foliation - Chadwin granite-up / greenstone-down extensional foliation and sheath folds overprinted by second foliation (S3?) - Conglomerates contain foliated plutonic clasts - 2639±3 Ma age of hydrothermal xenotime from Rubicon veins that cut pervasive foliation	S3 - pervasive metamorphic biotite foliation	F3 - Kurrawang syncline S3 - pervasive metamorphic biotite foliation; disjunctive cleavage	S3 - pervasive metamorphic biotite foliation	F3 - Panglo Syncline S3 - pervasive metamorphic foliation (overprinted by hydrothermal sericite-chlorite) Reactivation of Fitzroy Fault
4	Low-displacement, late brittle / brittle-ductile faulting; conjugate fault networks with ENE-WSW principal shortening axis	<2636Ma	Post foliation mesothermal lode-gold, quartz carbonate vein deposits (Mt Pleasant, Ora Banda, Mount Charlotte, Red Hill, Binduli WCM veins)	- 2648±6Ma - Liberty Granodiorite - Post faulting/gold, Lone Hand Monzogranite at Ora Banda	- Basal fault of Talbot formation at Mt Pleasant cuts foliated wallrocks, but is overprinted by late extensional fabric (related to Liberty intrusion?) - Black Flag Fault and others cut Zuleika Shear Zone and folds / foliations in Kurrawang Formation - Mesothermal veins at Kundana cut by late fault movements		Abundant late faults (Ora Banda faults; Grants Patch Fault; Black Flag Fault; Royal Standard Fault; Mary Fault)	Adelaide, Mystery, Golden Pike Faults at the Golden Mile (Possible control on stockwork vein development at Mt Charlotte)	Late movement on Shamrock Fault polylithic breccias

with a dome and keel style, granite-up / greenstone-down mechanism, and (2) extension driven by a horizontal stretching of the crust with most of the early structure produced by planar extensional faults.

A key objective of Chapter 5 was to understand if the mapped domain boundary faults had a control on the early structure of the granite-greenstone terrane, prior to the later thrusting and shortening events. Scenario (1) above would appear to have a problem in that density driven doming requires a thick mafic greenstone cover, over low density felsic rocks, to provide a density differential to initiate the doming; whereas the early extensional models of the various authors listed above, deal with an extensional event that led to greenstone volcanism. Given these constraints, scenario (2) is a possible alternative, but it is likely that density-driven doming proceeded after the initial deposition of mafic and ultramafic volcanic rocks (post-DE).

6.4 First folds (D1a) - open to isoclinal

The most obvious and dominant folding phases in the study area (F2/F3) produced broad upright regional-scale folds with NNW-SSE plunging axes and steep axial planes (Fig. 6.5). However, two major areas of *early* folding (F1) that pre-date the dominant folding events are located at Kanowna and at the Golden Mile, Kalgoorlie. Mesoscopic examples of F1 folds are also found in sedimentary rocks at Mount Pleasant and Gidji.

6.4.1 Kanowna early folds (D1a)

At Kanowna, early folds are developed at a local scale (1:10,000) and are evident from map patterns only. Folds (F1) at Kanowna oriented at a high angle to the regional NNW-SSE grain of the Kalgoorlie greenstones, are significantly disrupted by faults that are parallel to the F1 fold limbs and fold axial traces (Fitzroy Fault), which may be of the same age (D1a) or slightly younger than the F1 folds they cut (Fig. 6.7). Early F1 folds shown by the map pattern distribution, and measured bedding trends of the Ballarat and Kanowna conglomerate sequences and underlying ultramafic rocks, are open, upright folds. Sequences younger than the Kanowna member appear unaffected by the early phase of folding, which is unconformably cross-cut by the Grave Dam member and younger units (Section 3.53).

A prominent cross-cutting relationship with a later pervasive foliation is demonstrated by a foliation trajectory map of the Kanowna district in Figure 6.7. Pervasive fabrics throughout the map area trend NNW-SSE and transect both limbs of the early folds, but are axial planar to SSE-plunging folds in the Government Dam sequence. Interference folds of a later generation are not obvious at Kanowna, whereas sequences younger than the Kanowna conglomerate member are folded into upright SE-plunging folds and are also affected by the later S3 foliation. A lack of interference folding may reflect a widely accepted ‘strain shadow’ concept (e.g. Passchier 1994; Blewett et al. 2010a), whereby rocks located in the hinge of major batholith domes are considered

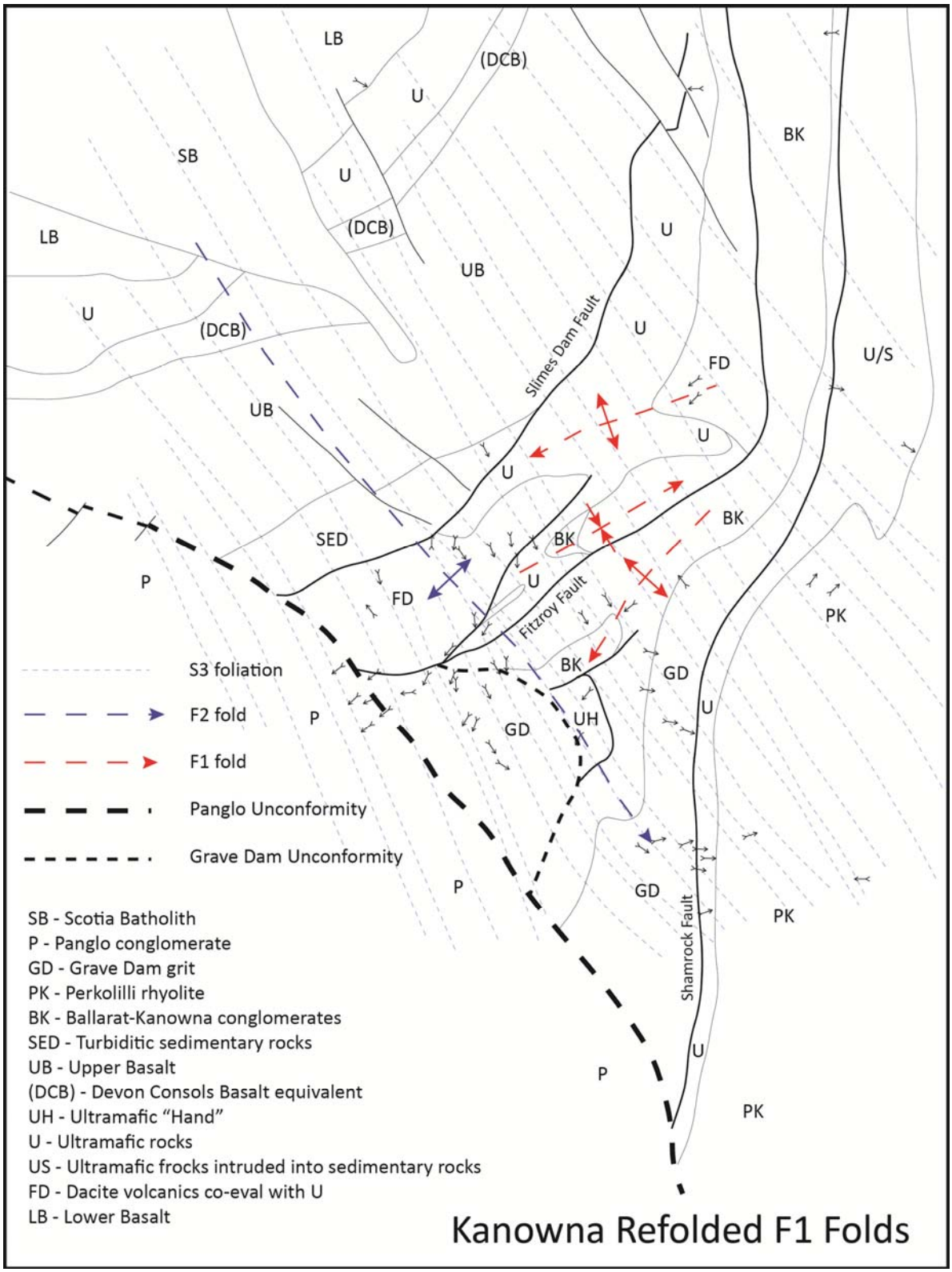

Figure 6.7 – Map of the distribution of units in the Kanowna district showing structure and younging. Early F1 north east trending folds were truncated by the Grave Dam Unconformity and the sequence including early faults (Fitzroy, Shamrock) was folded by F2 folds. Later exhumation allowed truncation of the entire F1/F2 folded sequence by the Panglo angular unconformity prior to F3 folding and S3 foliation. Younging data from outcrop and drill core observations.

to be shielded from much of the effects of late ENE-WSW shortening. This concept appears to have validity at Kanowna and, at the least, may afford preferential preservation of early deformation fabrics. Mesoscopic-scale folds of F1 generation were not observed in this study at Kanowna, which could reflect poor exposure, or that massive-bedded coarse clastic rocks that make up the sequences in the Kanowna district were not mesoscopically folded (Section 3.5). Crenulation cleavages are also not widely observed - possibly a consequence of exposure, the coarse clastic rock types, or alternatively the early folding was perhaps not accompanied by development of a pervasive axial planar foliation. Early D1a deformation may explain a curious occurrence of ultramafic rocks in the centre of the Kanowna map area (Fig. 6.7; the 'Ultramafic Hand'), which is apparently surrounded by felsic volcaniclastic rocks of superficially similar lithotype to the Grave Dam member. Recent diamond drilling of the contacts of this unit (planned and logged by the author) intersected primary relationships between those ultramafic rocks and the surrounding dacite-rhyolite felsic volcaniclastic rocks. The eastern contact of the ultramafic unit has intercalated dacitic volcaniclastic rocks with sharp undeformed contacts against spinifex textured komatiite, and pebbles of ultramafic rock immediately above the contact; whereas the western contact has sharp, undeformed apparently primary (depositional or intrusive) dacite-breccia / ultramafic-volcanic contacts.

This relationship of contemporaneous ultramafic and dacitic volcanism is well known throughout the Kanowna district as documented by Trofimovs et al. (2003). Given close association with ultramafic rocks, the age of those dacitic volcaniclastic rocks is assumed to be similar to the age of ultramafic-dacite sequences elsewhere in the district ~2705 Ma (Nelson 1997). Early folding/faulting at a high-angle to the regional trends could adequately explain juxtaposition of the oldest and youngest (pre-Panglo / Kurrawang) rocks in the district.

The NE-SW orientation of early folds at Kanowna is a significant variance that is unique for the study area and the Kalgoorlie district generally, with near orthogonal angular relationships of axial traces between F1 and F2/F3 folds; and is a prominent feature of the structural grain at Kanowna in aeromagnetic images (Fig. 6.7). Possible explanations for the NE-SW orientation of early folds include (1) early thrusting or extension in a N-S orientation, or (2) influence of the Scotia Batholith intrusion. The current orientation is unlikely to represent the original orientation of the folds since early folds have NNW-SSE striking axial planes elsewhere in the study area, and there is a general lack of evidence for early N-S thrusting.

6.4.2 Golden Mile isoclinal folding and faulting (D1a)

A major refolded F1 fold has been widely documented for the Golden Mile ultramafic-mafic volcanic sequence at Kalgoorlie (Western Mining Corporation 1966; Swager 1989; Bateman 2001; Fig. 6.8). The sequence includes from oldest to youngest: ultramafic volcanic rocks, mafic volcanic rocks with interflow sedimentary rocks, and mafic intrusive dolerite sills.

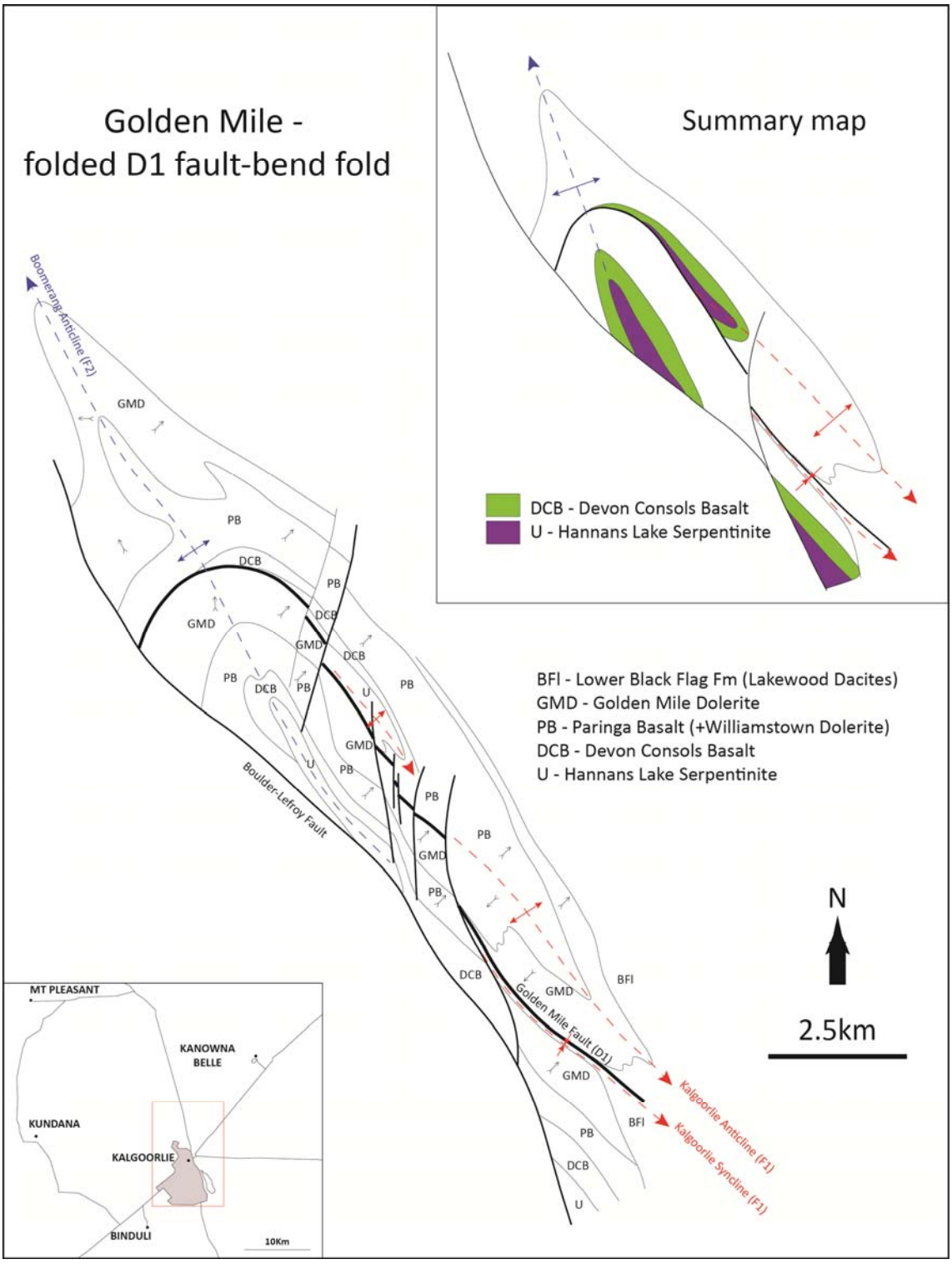

Figure 6.8 – Map of the distribution of units in the Golden Mile sequence showing structure and facing data re-interpreted from a basement interpretation of Keats (1987). A summary of the key units demonstrates an F1 isoclinal fault-bend-fold and a D1 thrust ramp that have been refolded by F2 folds. A D3 strike slip fault (Boulder-Lefroy Fault) cuts off the western segment of the sequence, and later NNE-SSW brittle faults (D4) have dissected the early folds. The Golden Mile gold deposit is located in one of only two areas with demonstrable map scale D1 deformation, the other is at Kanowna.

The Golden Mile gold deposit is situated on the limbs of an upright syncline-anticline pair that was later folded into the sub-regional scale, north-west plunging Boomerang Anticline.

Axial planes of the early F1 folds are folded around the F2 Boomerang Anticline, but the interference of two separate folding events is not obvious from map patterns, as the hinges of F1 folds are cut-off to the west by the Boulder-Lefroy Fault. The major F1 fold axis at the Golden Mile is faulted and is identified by a narrow zone of black shale at the upper contact of the Golden Mile Dolerite. Layered differentiation zones in the dolerite are folded into a major syncline which is the locus of the giant Golden Mile lode-gold deposit (Stillwell 1929; Gustafson and Miller 1937; Clout et al. 1990; Gauthier et al. 2004a).

The mafic-ultramafic rocks of the Boomerang Anticline form a disconnected window of the mafic volcanic stratigraphy surrounded by faulted or primary depositional contacts with rocks of the Upper Felsic Volcanic and Sedimentary Unit. Other major sequences of the mafic-ultramafic stratigraphy are preserved in the Ora Banda and Boorara domains, but in those two domains the mafic/ultramafic sequences lack any evidence of early folding or stratigraphic repetition.

6.4.3 Refolded folds in Talbot formation sedimentary rocks (D1a)

Mesocopic–scale refolded F1 folds are developed in sedimentary rocks of the Talbot formation at White Flag Lake south of Mount Pleasant (Fig. 6.9; Fig. 6.10; Fig. 6.11; Fig. 6.12 a, b); in deep-water deposited shales and sandstone/siltstone in the Gidji area (Fig. 6.12c); and in exposures of sedimentary rocks at Mount Hunt south of Kalgoorlie. The F1 folds at White Flag Lake and Gidji show spectacular refold patterns (Fig. 6.12b, c), and are also identified by downward facing mesoscopic folds.

On the northern shores of White Flag Lake, several areas of well exposed sedimentary rocks of the Talbot formation show strong zones of deformation up to 10 m-wide, which include refolded folds separating broad regions of open upright F2/F3 folding (Fig. 6.10). The zones have generally complex deformation, but the F1 fold axes have systematic orientations across broad areas with shallow plunges to the north-west and rarely, steep plunges to the south-east (equal area projection insets in Fig. 6.9 and Fig. 6.10). Domino-style extensional faults are common in finely-bedded sedimentary sequences of the rocks surrounding D1a deformation zones (Fig. 6.12d, e); and extensional glide structures characterised by asymmetric boudinage are developed on bedding parallel shear planes within the sedimentary sequences (Fig. 6.12f, g). Rare exposures show post-extension folding and foliation (S3) of extensional fault blocks (Fig. 6.12h). Extensional faults are developed in Talbot formation rocks at the Natal gold mine at Mount Pleasant (Fig. 6.9) showing top-block-south-and-down movement sense on shallow south-dipping normal faults. Small creek exposures show refolding at a metres-scale and clearly demonstrate the early nature of this folding event with both limbs of isoclinal F1 folds transected by a regionally pervasive foliation (interpreted S3; Fig. 6.11).

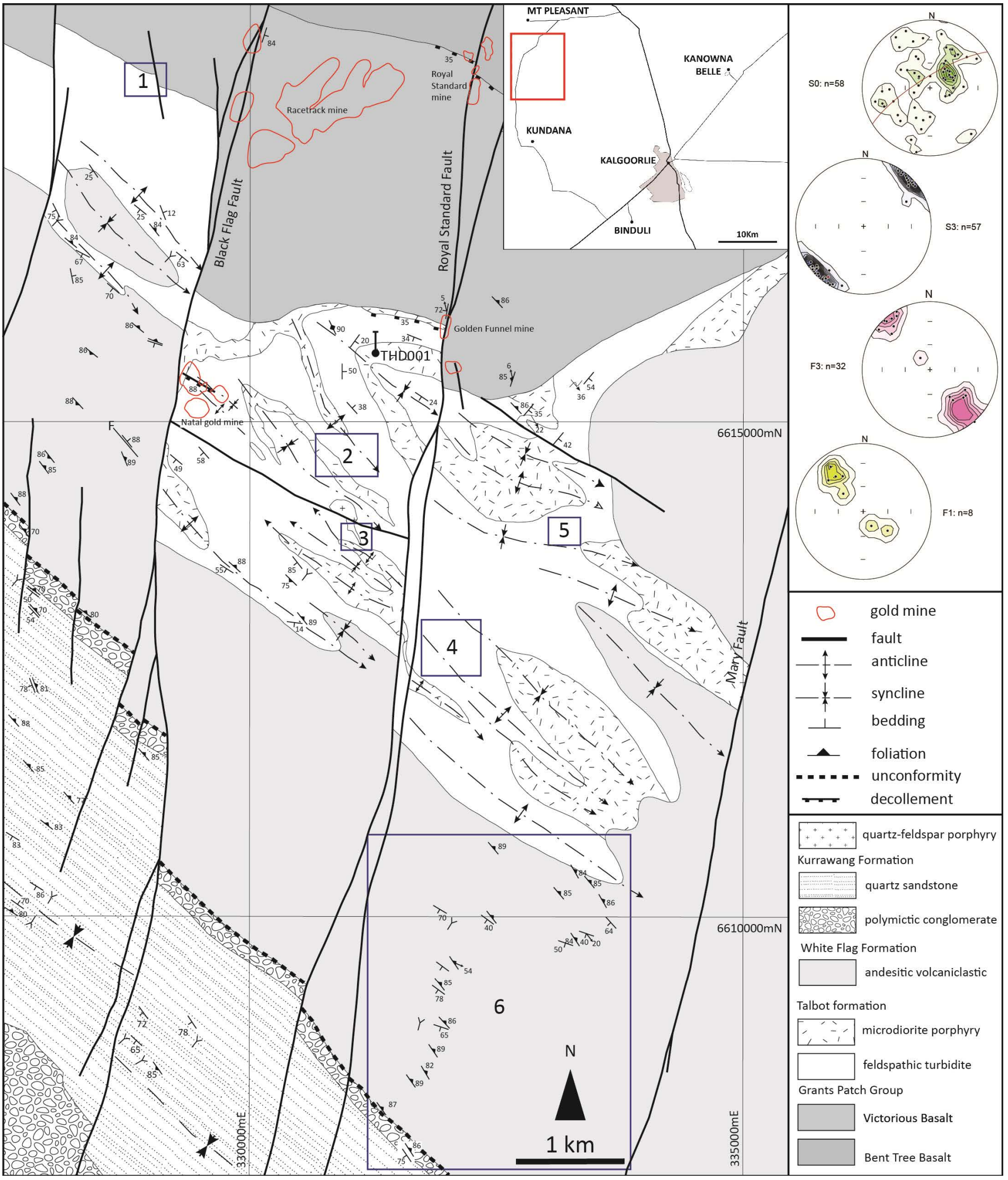

Figure 6.9 – Geological map of an area SW of Mount Pleasant with numbered boxes showing areas of detailed mapping: 1 – Upper basalt contact shown in Fig. 6.18; 2 – pavements on White Flag Lake; 3 – detachment fault on White Flag Lake; 4 – spectacularly preserved exposures of turbidites with early folding; 5 – creek exposures of refolded folds; and 6 – White Flag Formation section from Fig. 3.7. Note drill hole THD001 that intersects the shallow dipping Upper Basalt contact; mine exposures mapped in this study are indicated in red polygons. The map area covers the SW part of the hinge zone of the Mount Pleasant Anticline.

Equal area projections (inset) show the distribution of major fabric elements from the data on the map. A strong cluster of bedding S0 demonstrates the location of these exposures on the western limb of the Mount Pleasant Anticline; F2 folds have dominant plunges to the SSE and subordinate plunges to the NNW, and are overprinted by pervasive foliation S3; F1 folds have a dominant shallow NW plunge in the plane of S3 suggesting rotation into parallelism with later fabrics.

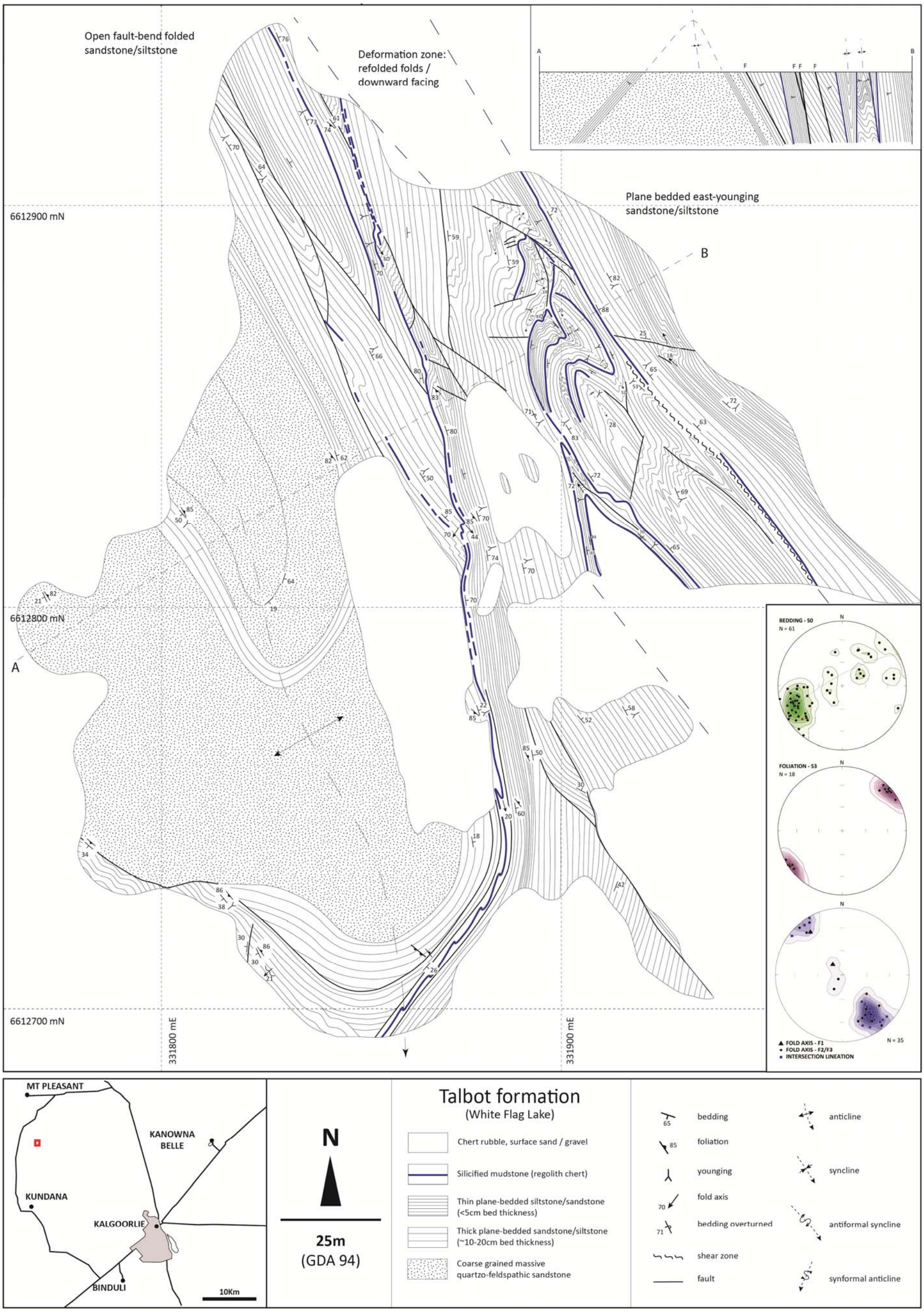

Figure 6.10 – Detailed geological map #4 from Fig. 6.9 of sandstone/siltstone turbidites in a pavement exposure on the western shores of White Flake Lake. A narrow zone of strong deformation with downward facing folds and spectacular refolded folds, separates broad areas of upright facing, south plunging folded rocks. Silicified black shale horizons are preserved as silicified 'regolith' cherts, and locally form extensional slip planes. The refolded fold zone is a possible D1 extensional glide plane with early folds that were later refolded by F2 folding. The map area is a complexly deformed zone that includes both extensional and contractional structures.

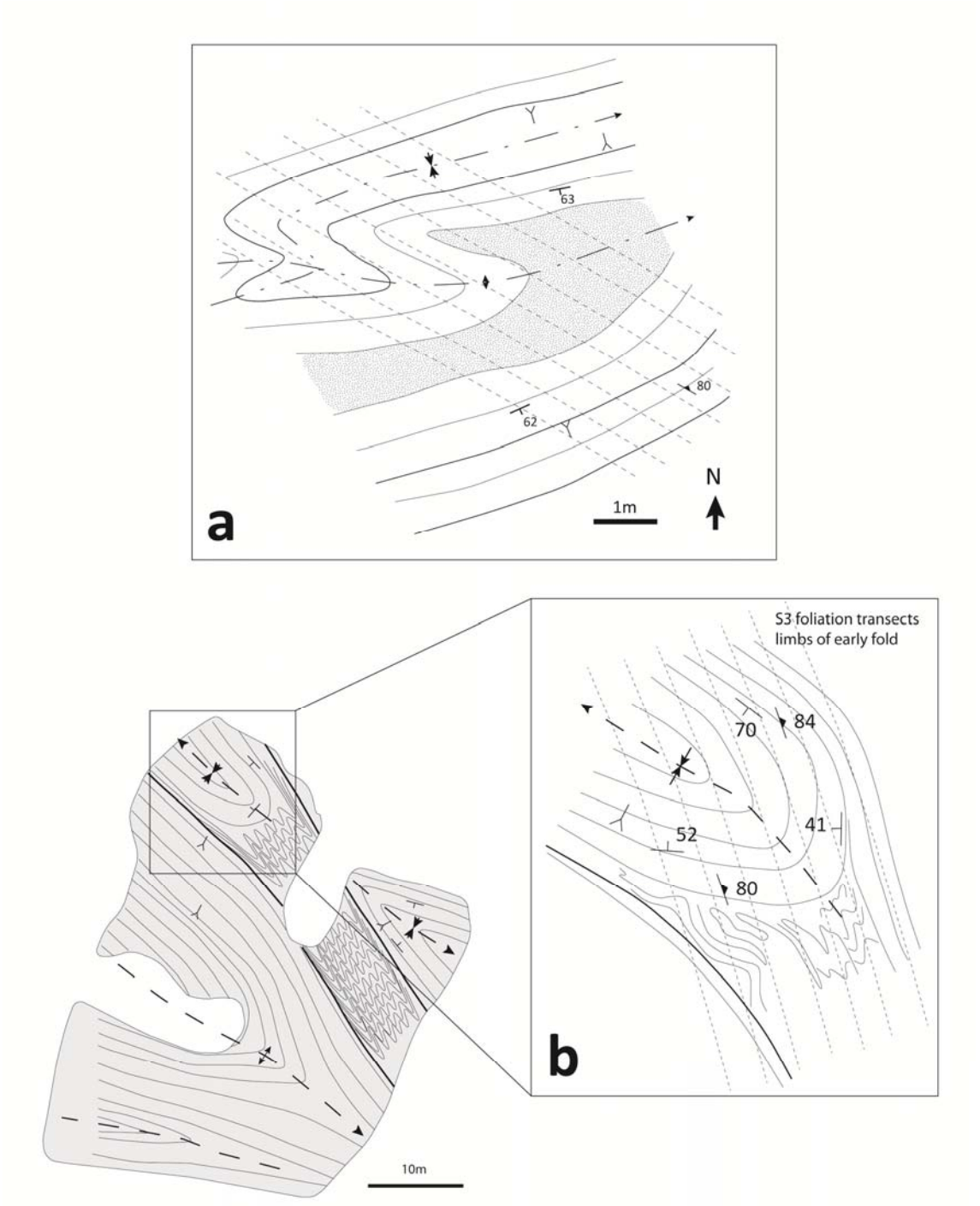

Figure 6.11 – Detailed map #5 from Figure 6.9. Creek pavement exposures of a) refolded folds with fold axial trace orientations markedly different to the sub-regional SSE plunge of F2 folds, and b) early F1 folds transected by S3 cleavage. The folds in b) are also considered to be early F1 folds since they are at variance with the average trend of F2 folds in the map area of Fig. 6.9. The cleavage is interpreted as S3 since this foliation is parallel to fold axes and foliation in the Kurrawang Formation, which unconformably overlies all underlying rocks.

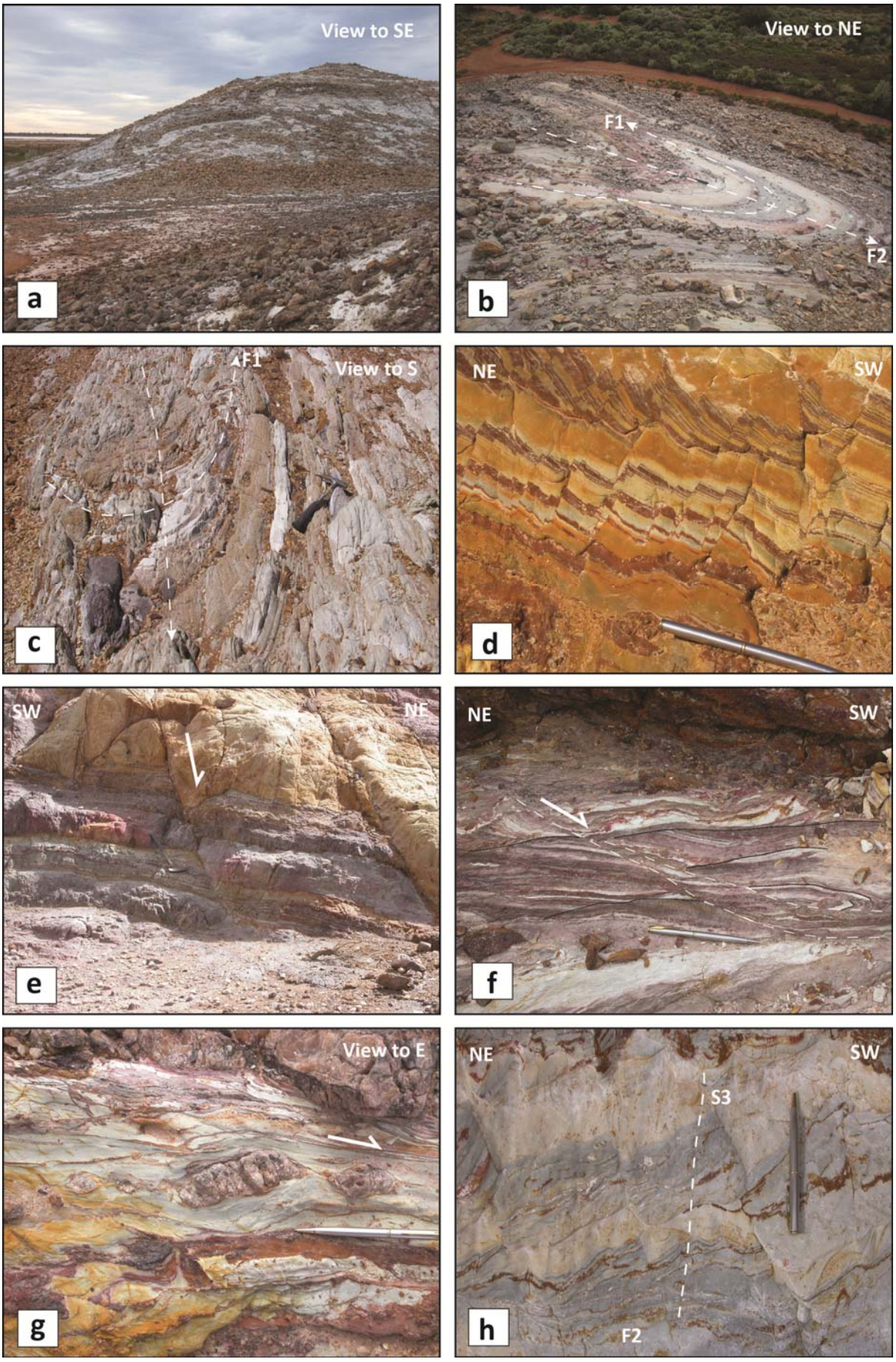
View to SE
a
View to NE
F1
F2
b
F1
View to S
c
NE
SW
d
SW
NE
e
NE
SW
f
View to E
g
NE
SW
S3
F2
h
Figure 6.12

Figure 6.12 – Photographs of D1 fabrics:

a) Outcrop photo of a large pavement area presented as a map in Figure 6.10 from the shores of White Flag Lake. The pavement and a series of nearby hills expose a thick sequence of deformed Talbot formation sandstone – siltstone – mudstone turbidites. Light coloured rock in the photo is weathered sandstone and siltstone, whereas the dark coloured material is scree boulders of silicified mudstone. Silicified mudstone beds are resistant ridges in the outcrop that form convenient marker layers and allow the structure of the sequence to be mapped. Although the sequence is deformed at outcrop scale, the level of mesoscopic finite strain is minimal, and much of the sedimentary structure and primary younging relationships are preserved in the rocks. The photograph is centred on a central zone of refolding and deformation that is flanked by upright, open folded sedimentary rocks as indicated on Figure 6.10. Hammer for scale along the F1 fold axial plane.

b) Refolded F1 folds in Talbot formation sandstone-siltstone turbidites at White Flag Lake - a locally spectacular example of refolded folds within the central deformation zone in the outcrop (GDA: 331904E; 6612866N). The F1 fold axis plunges 20º/324º with a folded axial plane. The F2 fold axis plunges 52º/128º with a steeply with a steeply dipping axial plane. Younging determined from sedimentary structures including soft sediment convolute lamination, and dewatering flame structures in sandstone-siltstone beds, shows that the structure is an antiformal syncline and probably represents an F2 folded, overturned lower limb of an F1 isoclinal fold. Several other refolded folds are present in this outcrop.

c) Refolded F1 folds at Gidji (GDA: 345043E; 6616107N). Refolding at this outcrop is present in quartzofeldspathic sandstone-siltstone turbidites above a low angle fault in a zone of strong deformation, in which the low angle faults are also buckled. This is a spectacular, but rare example for the Gidji trend, which is characterised by widespread downward facing in Talbot formation sandstone-siltstones, where only partial folds are preserved in the highly weathered outcrops that hint at downward facing structure.

d) Tiled extensional faults in the Talbot formation rocks at White Flag Lake (GDA: 330944E; 6614596N). The faults are a mesoscopic expression of larger scale extensional faults throughout the pavements on the shores of White Flag Lake. Key to the interpretation of the faults is their NE and SW dipping orientations and overprinting by the regional S3 foliation which trends 88º/046º.

e) Horst-and-graben type extensional faults in coarse sandstone / shale interbeds (GDA: 331124E; 6614687N). The east dipping faults are oriented 75º/040º on the eastern side of an extended sequence of coarse grained sandstones, with west dipping extensional faults further to the west (out of shot). Siltstone and shale above the sandstone is draped on top of the extended blocks.

f) Low-angle extensional slides affecting bedded sandstone-siltstone turbidites, White Flag Lake (GDA: 331868E; 6612730N). The extensional glide planes are located in a strongly deformed sequence of fine siltstones in contact with a layer of highly contorted cherty silicified mudstone beds at the southern apex of the large south plunging anticline on Figure 6.10. Early folding related to extensional slides is bedding parallel and overprinted by the regional S3 foliation at 84º/052º. Some folding appears disharmonic as accommodation folds around rigid chert blocks.

g) Extended quartz vein fragments with aymmetric boudinage in a shallow south-dipping sheared sedimentary sequence, White Flag Lake (GDA: 331294E; 6614720N). The extensional glide plane is confined to a narrow 1 m-wide zone that truncates folded sedimentary rocks at a high angle, but is also folded. As for other extensional structures in the district, the extensional glide is surrounded by open folded, upright and gently dipping stratigraphy.

h) Tiled extensional faults in Talbot formation turbidites folded and foliated by S3, White Flag Lake (GDA: 331842E; 6612716N). Extensional faults trending 82º/200º are developed in a siltstone/mudstone sequence that was later shortened with minor crenulation folds of the bedding and overprinted by the steeply east-dipping regional S3 foliation.

At Gidji (Fig. 6.12c), locally well-preserved re-folded folds are present with mesoscopic downward facing folds in adjacent sedimentary sequences. The refolded F1 folds at this locality are truncated against a shallow dipping planar fault that separates the refolded rocks from sandstone and siltstone with vertical bedding. Refolded folds at Gidji are developed in strongly deformed sedimentary rocks that are structurally juxtaposed with adjacent rocks of the mafic-ultramafic stratigraphy and the overlying Gidji felsic volcanic and conglomerate units. The strong deformation zone appears to have a linear distribution along a NNW-SSE strike that trends sub-parallel to the Gidji fault.

6.4.4 Timing constraints on F1 folding

At Kanowna, the Grave Dam member volcaniclastic rocks (2668±10 Ma) unconformably cut F1 folds in underlying units, which provides a minimum time constraint on the F1 folding probably at <2658 Ma. The Scotia Batholith returned crystallisation age estimates from SHRIMP U-Pb zircon analyses at 2656±3 Ma for phases in the southern half of the batholith (Ross et al. 2004). Since the Scotia Batholith is significantly younger than the units that cut F1 folds, it is unlikely that forceful intrusion of the Scotia Batholith is responsible for F1 folding in the Kanowna district, whereas granitoid and porphyry dykes truncated at the Panglo Unconformity indicate the intrusions at least pre-date that depositional event and may provide a maximum estimate on the timing of the Panglo Unconformity at ~2653-2659 Ma. This is further supported by a penetrative fabric that affects the Scotia Batholith. Batholith uplift and intrusion during later ENE-WSW shortening, while not a likely cause of the F1 folding, may be responsible for rotation of those folds from an earlier orientation.

New SHRIMP U-Pb analyses of zircons from the Lakewood dacites from this study produced an age of 2672±6 Ma, which provides a maximum age on F1 folding at the Golden Mile since these are the youngest known rocks deformed by the Kalgoorlie Syncline (Figure 3.35). The age of F1 folding is therefore bracketed between 2672±6 Ma and 2668±10 Ma.

At White Flag Lake and Gidji, folds (F1) are developed entirely within sedimentary rocks that overlie the Upper Basalt unit. The timing of these folds is uncertain, except to note that the regionally pervasive foliation transects both limbs of the folds, which places those folds as earlier than regional F2/F3 folding.

6.4.5 Kinematics of F1 folding

Major ultramafic-mafic volcanic sequences are not refolded in the Ora Banda Domain or the Boorara Domain, and in those domains the early deformation appears restricted to overlying sedimentary rocks. In those sedimentary rocks, the restricted presence of refolded folds in planar zones of intense deformation, but general upright facing over broad areas, suggests the F1 folding event was tightly structurally bounded by either thrust planes or extensional slides.

Unequivocal kinematics is not obtainable from the current surface exposures of these early fold structures and faults, as later deformation has rotated the early fold axes into parallelism with F2/F3 fold axes, or the kinematics of both events was co-axial.

In the Kambalda Domain, mafic and ultramafic volcanic rocks were probably folded with nappe-style transport; however, when effects of major F2 folds are removed at the Golden Mile, structural analysis of F1 fold hinges and D1 faults suggests fault-bend folding with a possible E-W transport direction given the shallow S-plunge of the Kalgoorlie Anticline (Fig. 6.8). Several authors have argued for N-S tectonic transport for early deformation in the Kambalda area (Swager and Griffin 1990; Archibald 1979), and in the Kanowna area (Davis et al. 2000); whereas Swager and Griffin (1990) conceded that an interpreted N-S roof-and-floor thrust geometry interpreted for the Kambalda area could be equally interpreted as a lateral ramp system in an east or west verging thrust duplex (Chapter 2). Swager (1989, 1997) argued for E-W tectonic transport to explain early folding at the Golden Mile; whereas Martyn (1987) proposed a model for folding and thrust stacking of the greenstones as a result of off-dome extensional sliding related to granitoid emplacement.

Mesoscopic-scale data from Talbot formation rocks in this study do not provide diagnostic kinematics for the early folding event, but the close association of refolded folds and extensional faults that are foliated by S3, is suggestive of an extensional mode for the early fabrics, or that early thrusts were reactivated during later extensional deformation. A minor wrapping (rotation) of F1 fold axes from west to east around the Mount Pleasant dome indicates a possible role for granitoid intrusion in the deformation of F1 folds, but the exposure is not of sufficient breadth to provide unequivocal relationships. The minimum age of D1 at 2668±10 Ma from Kanowna is within error of the ages determined for major batholiths (Scotia - 2657±5 Ma; Owen 2655±15 Ma). Likewise, refolded folds and downward-facing folds at Gidji have near parallelism with later F2/F3 fold axes, which may reflect original orientations, or later rotation of early fold axes in high strain rocks in that area.

Older intrusive phases within the composite batholiths (Siberia Monzogranite - 2675±8 Ma; Bali Monzogranite - 2676±8 Ma) are also within error of the D1a time bracket determined above (2672±6 Ma - 2668±10 Ma); hence, a role for granitoid intrusion and off-dome extensional sliding in D1a deformation cannot be ruled out and may, at the least, include early fabrics at the Magdala gold mine.

6.5 Uplift (D1b) - deposition of coarse clastic and volcaniclastic rocks

Volcaniclastic and sedimentary rocks (upper Black Flag formation; Fig. 6.13) unconformably overlie F1 folded sequences at Kanowna, whereas F1 folds at the Golden Mile have no exposed primary depositional contacts with younger sequences. F1 folds in the Ora Banda and Kambalda domains are restricted to the oldest sedimentary rocks overlying the

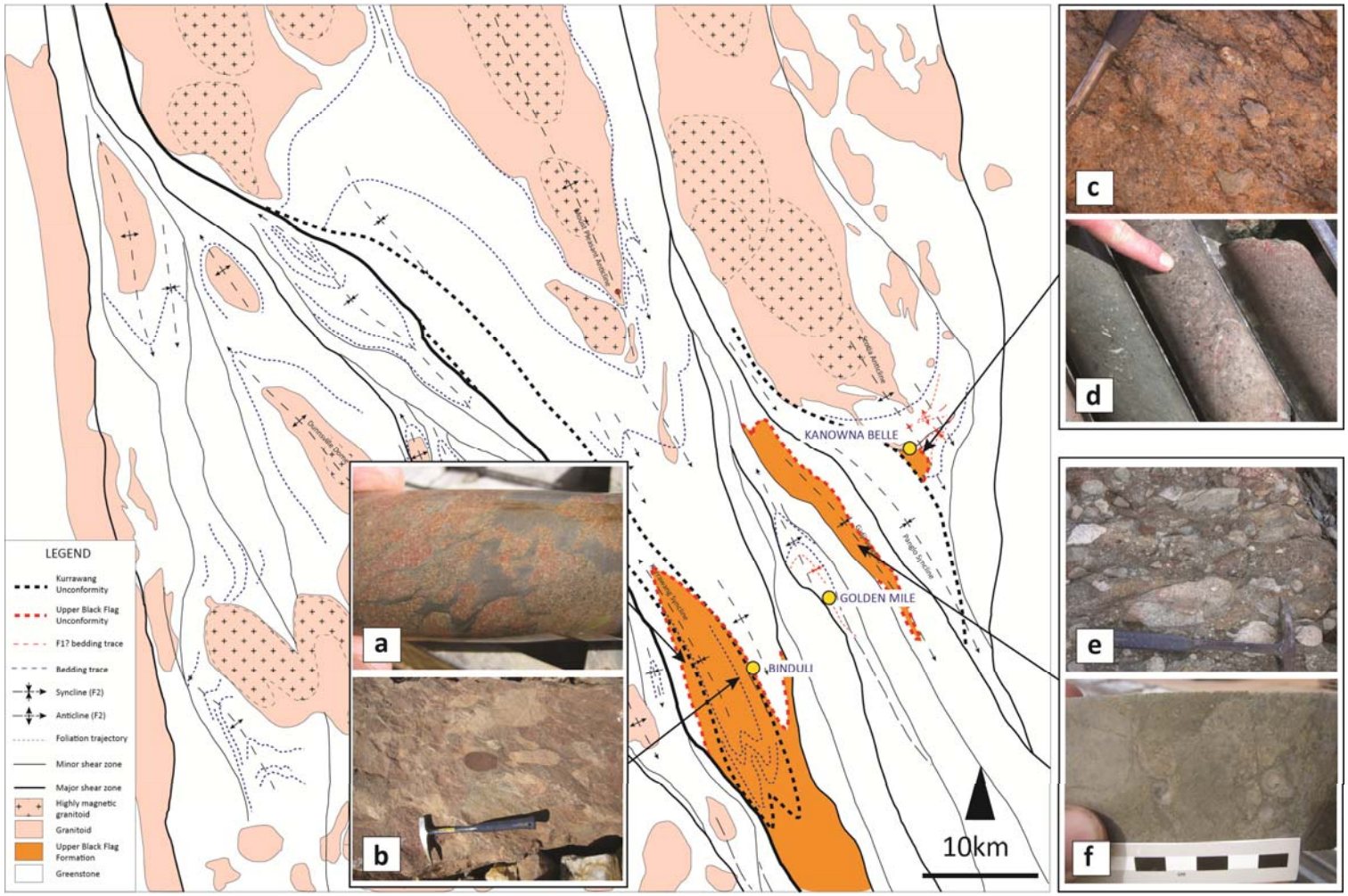

Figure 6.13 – Map of the distribution of Upper Black Flag formation rocks and major gold deposits at Binduli, Golden Mile and Kanowna Belle. Note the interpreted distribution at Binduli reflects pre-Kurrawang folding and portrays the unit as if the Kurrawang Formation was removed. Note also the association of the two largest gold deposits in the district with map scale F1 folds at the Golden Mile and Kanowna Belle. a) Goldilocks rhyodacite peperite suggesting a sub-marine component to the volcanic environment (GOLD07-907 199.5-219.6 m) b) Binduli Porphyry Conglomerate from Centurion gold mine (GDA: 347220E; 6587340N); c) Grave Dam member dacite volcaniclastic conglomerate (GDA: 365664E; 6612157N); d) accretionary lapilli in volcanic units of the Grave Dam member suggesting a sub-aerial component to the volcanic environment (GDD540 950.15 m); e) Gidji polymictic conglomerate (Gidji Lake GDA: 347650E-6613456N); f) possible accretionary lapilli in rhyolite volcaniclastic rocks of the Gidji felsic unit (EMD021 438.2-444 m).

Upper Basalt unit, but were not observed in the overlying volcaniclastic and sedimentary rocks. In this respect the younger unconformities provide a minimum age on F1 folding (Gidji Conglomerate; Grave Dam).

Deposition of the sequences correlated with upper Black Flag formation (Grave Dam member; Gidji felsic volcanics; Binduli porphyry conglomerate; Fig. 6.13a-f) were probably deposited in restricted marginal basins synchronous with rapid exhumation, and coincident with voluminous dacitic to rhyolitic volcanism. Volcanic rocks co-eval with the coarse clastic sedimentation are primarily submarine deposited extrusive sequences (Fig. 6.13a), but the units contain a significant proportion of conglomerate (Fig. 6.13b, c, e). In the case of the Grave Dam member at Kanowna, and the Gidji Felsic volcanics, these units may have included a sub-aerial pyroclastic input indicated by the presence of accretionary lapilli in those units (Fig. 6.13 d, f).

The cause of uplift with local source regions and formation of adjacent depositional basins may be related to syn-orogenic extension from D1a, but may have included a contractional or strike-slip component (e.g. Krapez et al. 2000). In the Ora Banda Domain there is no structural evidence of localised strike-slip basins in the upper Black Flag formation, whereas the Gidji felsic volcanics and conglomerates form a long linear sequence parallel to, and bounded by, the NNW-SSE striking Gidji Fault.

Irrespective of the tectonic mode of formation, this depositional event produced a major portion of the coarse clastic sequences that dominate the post - Upper Basalt stratigraphy of the Kalgoorlie Terrane. Significant localised extension would have been required to provide deep-water depocentres as indicated by the presence of abundant intercalated shales and turbidites in the Upper Black Flag formation.

D1b is proposed as a separate phase of D1 since the sequences deposited by the tectonic exhumation events (D1b) unconformably overlie F1 (D1a) folded rocks. Gidji conglomerates are not observed in unconformable contact with the Golden Mile sequence in the Kambalda Domain, but given a close spatial association of those sequences with the presence of alkalic hornblende-feldspar bearing porphyry dykes in the Golden Mile and clasts of similar rocks in the MAD sequences (Fig. 3.43), the possibility remains that an unconformity was removed by erosion.

6.6 Second folds (D2) - Pre-Kurrawang contractional deformation

Major post-volcanic contractional, fabric-forming deformation phases in the study area are separated here into Pre-Kurrawang and Post-Kurrawang events. The Kurrawang unconformity is recognised as a reliable deformation time marker in the geological history of the Kalgoorlie Terrane, primarily because it cuts folded rocks, but was itself later folded, foliated and metamorphosed.

6.6.1 Regional fault-bend folding (F2 folds; D2 detachment faults)

Pre-Kurrawang deformation is manifest as regional-scale anticlines and synclines in the mafic-ultramafic volcanic sequences and as ramp anticlines with associated detachment faults in plane bedded turbiditic sedimentary sequences at Mount Pleasant and Gidji (Fig. 6.9; Fig. 6.10). Major anticlines in the study area cored by granitoid batholiths plunge to the SSE (Mount Pleasant and Scotia anticlines). The Boomerang Anticline at Kalgoorlie plunges NNW; but whereas it has no large associated granitoid intrusions, hornblende-porphyry and quartz-feldspar porphyry dykes abound in the Golden Mile deposit (Gauthier et al. 2004a).

6.6.1.1 Mount Pleasant Anticline

Major anticlines in the study area have variable morphology and are generally open folds. Mount Pleasant Anticline has a markedly angular hinge zone with a 45º dipping western limb and a 75º dipping eastern limb. Granite-greenstone contacts are mostly sub-parallel to bedding in the greenstones, but gravity data at Ora Banda indicate the western contact is irregular and some stoping of the greenstones may have occurred in that area (Fig. 6.2b). A late tectonic granitoid stock (Liberty Granodiorite) has intruded the nose of the Mount Pleasant Anticline, significantly disrupting the orientation of bedding.

In the Mount Pleasant Anticline, the amount of shortening in the Talbot formation sedimentary rocks is significantly greater than in thick-layered mafic volcanic rocks lower in the sequence; suggesting that (at a regional scale) F2 folding was disharmonic, and that the sedimentary sequences may have accommodated slip between sub- regional-scale rigid layers. The White Flag Formation overlying the Talbot formation is a thick sequence of layered andesitic volcanic and sedimentary rocks, and does not display evidence of structural thickening by thrust stacking or mesoscopic-scale folding. Strain in the White Flag Formation is dominated by a spaced, disjunctive cleavage that wraps clasts in volcanic breccia, and a continuous cleavage that is localised in fine-grained sedimentary units within the volcanic package: these are considered S3 fabrics.

Deformation (D2) in fine-grained Talbot formation sedimentary rocks comprises upright open folds separated by detachment faults, with widespread examples of ramp anticlines developed at a scale of 10’s of metres (Fig. 6.14; Fig. 6.15a-f; also Fig. 6.9; Fig. 6.10). The detachment surfaces are bedding planes at the base of over-thrust ramp-anticlines, but in most exposures, the lower plate sequences are also folded as exhibited in Figure 6.15a, b. Critically the detachment surfaces and folds are overprinted by a later pervasive foliation (S3) indicating that the D2 shortening event was probably a high-level thin-skinned stacking in the Talbot

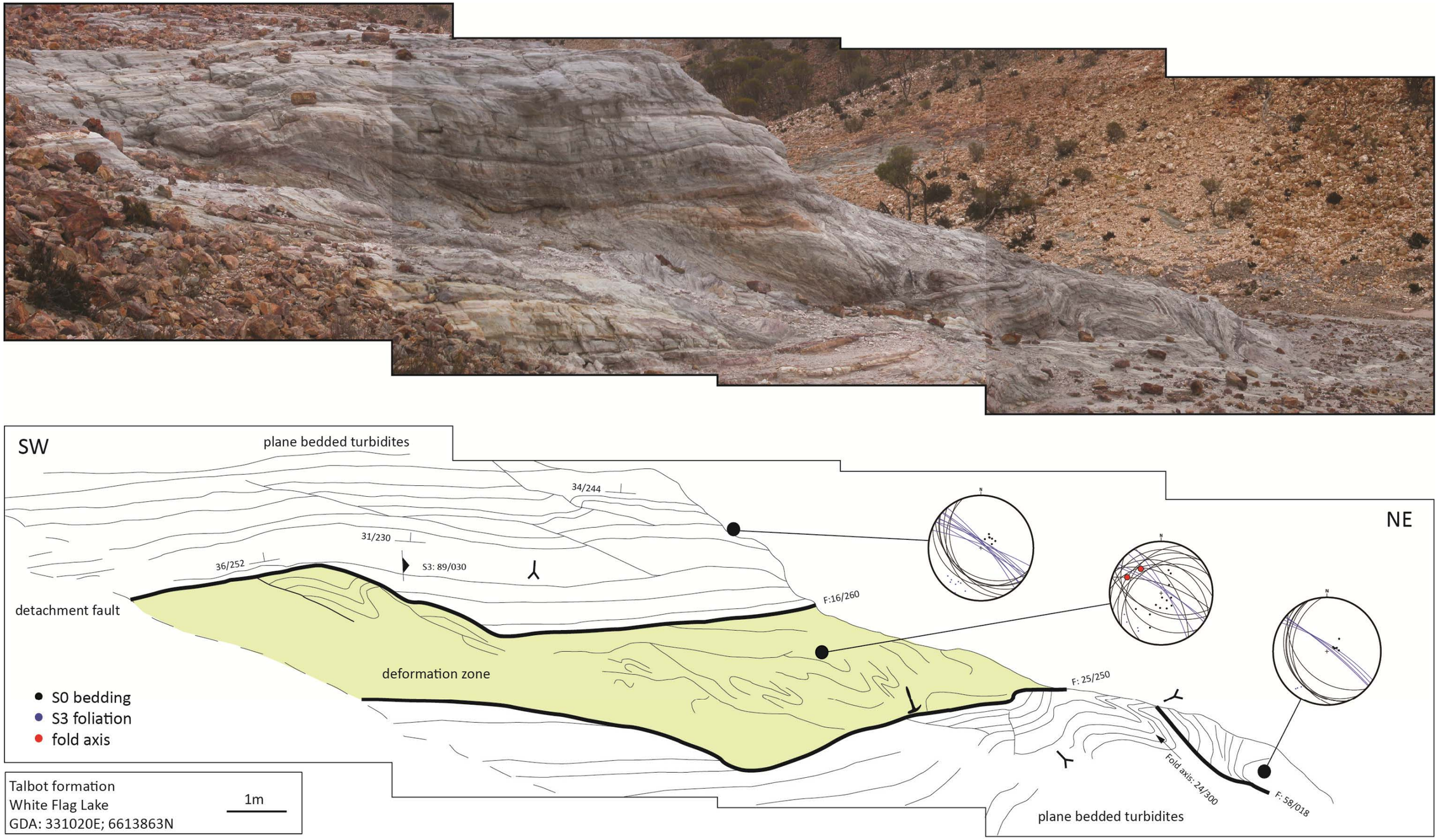

Figure 6.14 – Outcrop of a detachment fault at White Flag Lake from Box #3 on Figure 6.9, and located on Fig. 6.17. The green highlight marks a fault-bounded zone of chaotic folding and deformation, separating mostly upward younging, gently dipping, plane-bedded sedimentary rocks. Consistent foliation orientations across the zone indicate this is a pre pre-S3 structure. The timing of the structure as D1 (extensional) or D2 (contractional) is not evident in the outcrop as no consistent kinematic indicators are available. However, thick areas of contorted folding in the Talbot formation rocks with re-folded folds are typical of the earliest extensional deformation in the district, and fold axes in the deformation zone are parallel to F1/F2 fold axes as documented in Figure 6.10.

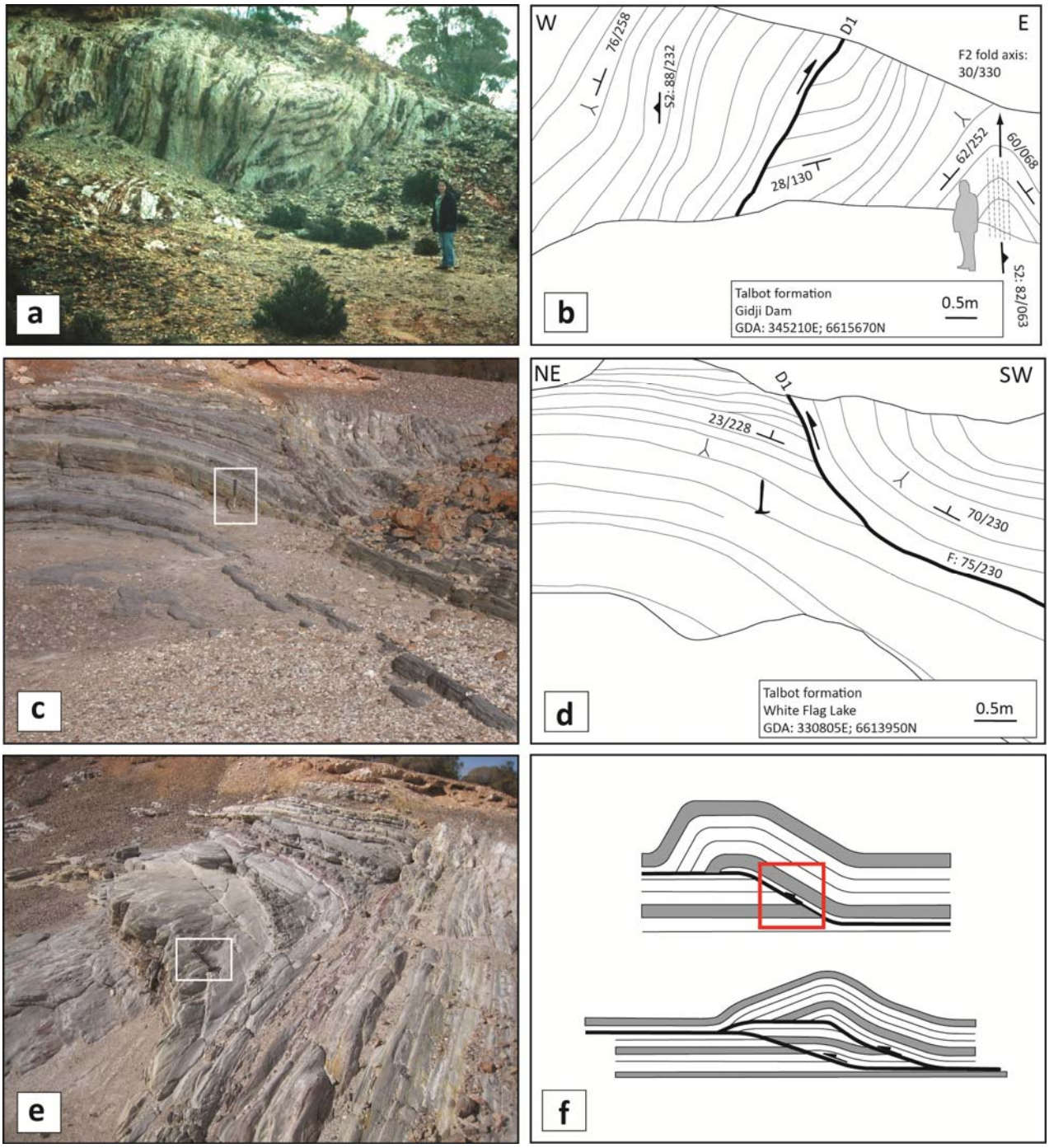

Figure 6.15 – Fault-bend folds in highly weathered sedimentary rocks at Gidji. a, b) Photo and line drawing of east-verging detachment fault with footwall rocks folded into upright anticlines, facing data indicate rocks on both sides of the fault are right way up; c, d) Photo and line drawing of similar east-verging detachment fault at White Flag Lake; e) oblique view of same outcrop in c); f) fault-bend folding model of Suppe (1983), with suggested area of the fault bend folds preserved in the outcrops at White Flag Lake and Gidji. Location of outcrops c)-e) on Figure 6.17.

formation rocks, lacking penetrative foliation (Fig. 6.14; Fig. 6.15a, b). The observation of a pervasive foliation overprinting D2 detachment faults that are synchronous with F2 ramp-anticlines provides a key timing criterion that allows the pervasive foliation to be correlated with S3.

In the Mount Pleasant area, F2 fold axes plunge with a dominant orientation of 20º/135º and a minor orientation plunging at 5°/315° (Fig. 6.16a). This variable plunge of mesoscopic folds is reflected at a regional scale with major anticlines throughout the Eastern Goldfields Province plunging NNW or SSE. A possible post-D2 belt-parallel shortening event was proposed by Glikson (1971a) to explain the variable fold plunges at a regional scale: this is confirmed from field exposures in the Paddington Mine, which show folding of vertical bedding with steep fold plunges and E-W trending fold axes.

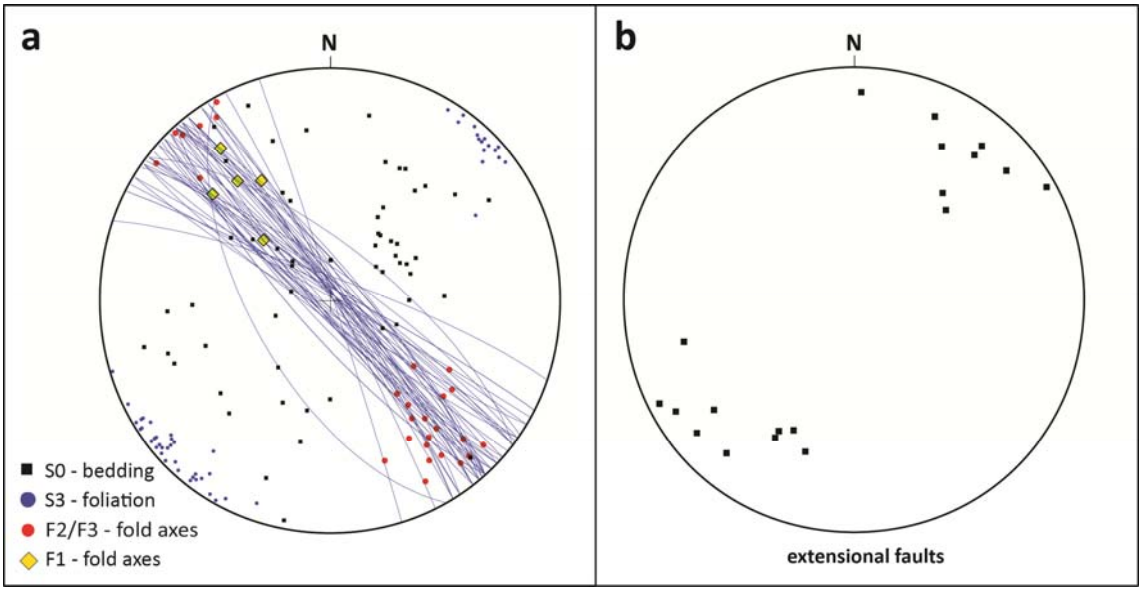

Figure 6.16 – a) Summary equal area projection of fabric elements in the area south of Mount Pleasant; b) equal area projection of extensional faults exposed on the shores of White Flag Lake. Horst-and-graben type extensional faults dip in opposite directions, but strike sub-parallel to the regional fabric trends of S3 suggesting a reversal of kinematics from early extension to later contraction.

Mesoscopic-scale horst-and-graben style D1 extensional faults on the shores of White Flag Lake were reactivated and folded by later D2 and D3 deformation (Fig. 6.17). The early faults separate blocks of sedimentary rock that are folded into upright anticlines and synclines, with ~10º southeast-plunging fold axes. Early faults cluster into two main orientations with equivalent strike, but with opposing dip directions (Fig. 6.16b). The D1 fault orientations suggest that the extension vector was to the NE-SW, and later upright F2 folds suggest that the late contraction vector was co-linear with the early extensional vector. An alternative possible interpretation of the NE and SW dips of mesoscopic extensional faults is D1 off-dome sliding during granitoid intrusion.

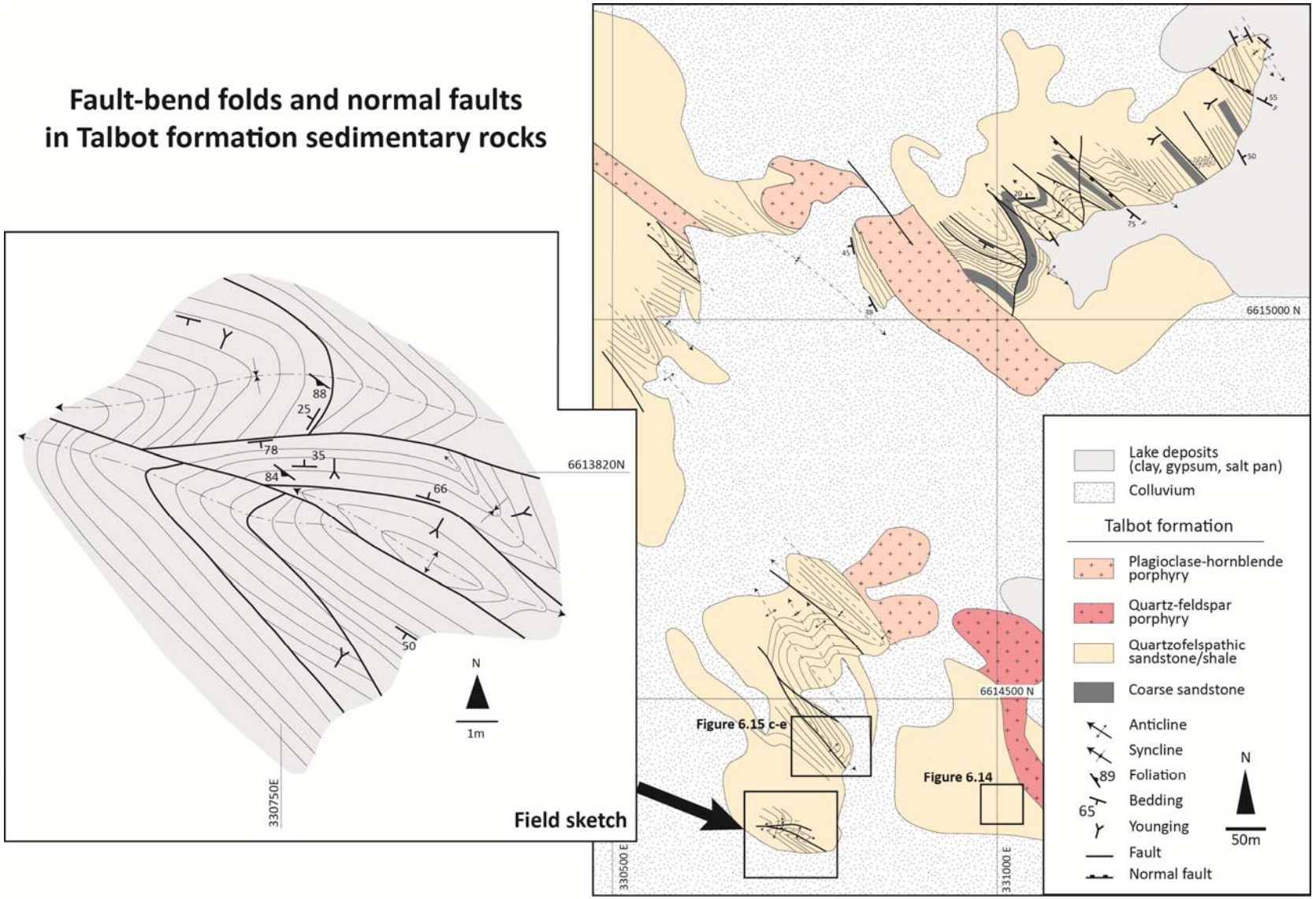

Figure 6.17 – Exposures of Talbot formation sedimentary rocks on the shores of White Flag Lake with widespread ramp anticlines at 10's of metres scale, and local evidence of early extensional faults overprinted by F2 folding. Map area is from Box#2 on Figure 6.9.

6.6.1.2 Detachment fault (D2) separating Upper Basalt from Talbot formation

A low-angle south-dipping detachment fault separates Victorious Basalt from overlying sedimentary rocks of Talbot formation at Mount Pleasant (Fig. 6.18a-d). The fault is variably developed at a major lithological contact and appears to truncate a gently warped primary depositional contact, with windows of the primary contact relationships preserved in shallow pre-faulting synclines (Fig. 6.18a). Exploration drilling to the south of the outcrop demonstrates the detachment fault sits above a preserved primary sedimentary rock / basalt contact (where drilled into mapped mesoscopic synclines); whereas the contact is faulted in drillholes that intersected mapped mesoscopic anticlines. These relationships suggest that initial fault movement may have been synchronous with F2 folding, and produced detachment at the contact to accommodate differential shortening of rocks across its boundaries.

Sedimentary rocks above and below the detachment fault contain a steep-dipping penetrative S3 foliation (Fig. 6.18a), and the rocks above the contact display tight folding; whereas the sedimentary rocks below the contact are foliated, but not folded at a mesoscopic scale. The detachment fault probably accommodated dis-harmonic, short wavelength D2 folding and thrust stacking of the Talbot formation sedimentary rocks; compared to km-scale wavelength folds in the underlying mafic volcanic rocks, which lack evidence of thrust repetition. The detachment fault is not visibly affected by the regional penetrative upright foliation (S3), which suggests late movement on the fault post-dated F3 folding and foliation. With these constraints, this phase of extensional movement cannot be equated with D1, but may be significantly younger (D4?).

Foliation deflection sense and folded quartz veins in the outcrop and drill hole THD001 (Fig. 6.9) indicate reverse thrust movement overprinted by late extensional deformation (Fig. 6.18c; Fig. 6.19 a-h). Kinematic indicators in the detachment fault at the outcrop include a strong south-plunging stretching lineation, and rodding in shear-zone-hosted quartz veins that suggest mostly dip-slip movement on the fault (Fig. 6.18d). Micro-scale kinematic indicators from the fault in drillhole THD001 have early thrust kinematics (D2) defined by reverse-sense S-C fabrics and rotated delta-type porphyroclasts (Fig. 6.19 d-f); but these are overprinted by extensional deformation (D4?) defined by stretched and deformed quartz veins (Fig. 6.19 e, f), spaced shear bands with normal foliation deflection sense (Fig. 6.19g), and a shallow north-dipping spaced crenulation cleavage that crenulated the main shear fabric (Fig. 6.19h).

Other shallow south-dipping unit contacts in the Mount Pleasant district also show dominantly normal movement as indicated by foliation deflection sense. The Royal Standard north pit (Fig. 6.9) exposes quartz-feldspar porphyry intruded into black shale at a south-dipping sheared contact between Bent Tree Basalt and Victorious Basalt, with normal top-block-down-and-south movement sense. A south-dipping sheared contact in the Golden Funnel mine has

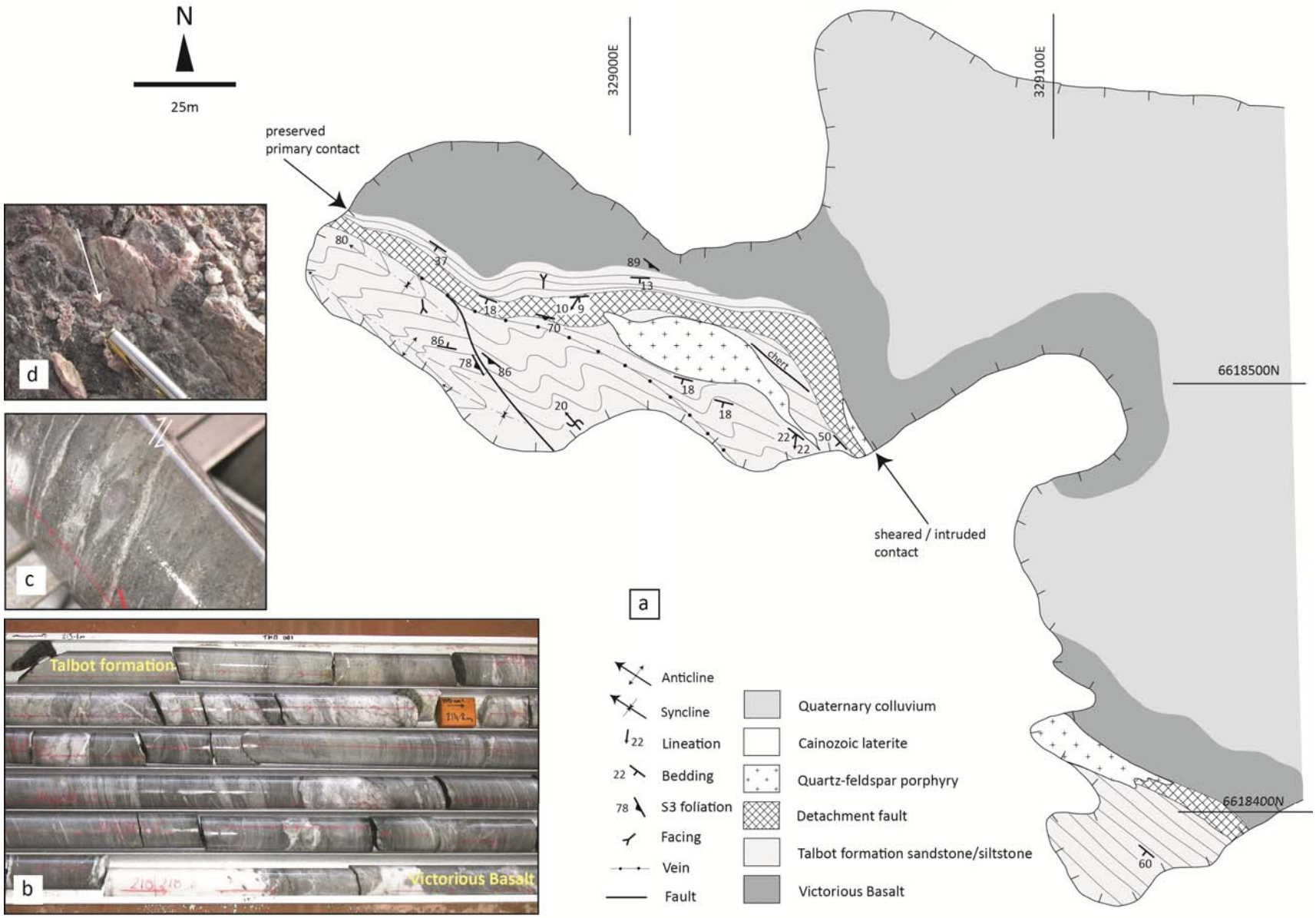

Figure 6.18 – a) Geological map of the lower SUB / Upper Basalt contact at Mount Pleasant (from box #1 on Figure 6.9); b) drill hole intersection of the basalt detachment fault showing high intensity foliation; c) reverse-sense sigma-type vein-quartz porphyroclasts with asymmetric tails; d) down-dip slickenside lineation defined by rodded segments on quartz veins and parallel grooves.

foliation deflection sense that indicates normal displacement (Fig. 6.9); whereas interflow contacts in Victorious Basalt observed in the Woolshed gold mine show reverse-sense foliation deflection, but this may be influenced by strike slip movement on the adjacent Black Flag Fault, or alternatively may indicate the contacts were simply not reactivated by the late extensional deformation (Section 6.9.1).

Interpretation

Contractional deformation of the Upper Basalt Unit (D2) produced open, gentle folds of ~20 km wavelength, probably related to early stages of ENE-WSW contraction. Contemporaneous movement on the Upper Basalt - Talbot formation detachment fault accommodated thrust stacking and tight folding of sedimentary sequences overlying the fault, but only a gentle warping of the Upper Basalt - Talbot formation contact, underlying the fault.

Thrust stacking of the Talbot formation rocks must have commenced prior to the imposition of the regional pervasive fabric (S3), since tightly folded rocks in the hangingwall of the detachment fault, and plane-bedded gently warped rocks of the same unit in the footwall of the fault, are both overprinted by the same pervasive fabric (S3). These relationships suggest the detachment fault and tight F2 folds developed during D2, but were later overprinted by the pervasive foliation, which is therefore not an axial planar fabric synchronous with F2 folds. This outcrop may provide key mesoscopic evidence of the F2 (pre-Kurrawang unconformity / pre-S3 foliation) folding event suggested by regional map patterns.

Since the detachment fault does not interact with either the lower Black Flag formation unconformity or the Kurrawang unconformity, the timing of final extensional movements on the detachment fault at Mount Pleasant is equivocal. The age of the final movement however must be younger than 2657+/-7 Ma (<2650 Ma), which is the interpreted maximum depositional age of the Kurrawang Formation (since the regional pervasive S3 foliation is axial planar to F3 folds in the Kurrawang rocks, and the last movement on the detachment fault has destroyed that fabric). Late, normal movement sense on the Upper Basalt - Talbot formation detachment fault and other low-angle structures dipping away from the Mount Pleasant Anticline may have been produced by a late-stage, forceful granitoid emplacement into the core of the Mount Pleasant Anticline by the Liberty Granodiorite (2648+/-6 Ma; Kent 1994). The extensional mechanism is likely to be a granite-up greenstone-down relationship whereby much of the movement is accommodated by weak interflow units, and contacts with a rheological contrast.

A further possibility for normal movement on low-angle sheared contacts and faults is a late orogenic collapse as suggested for other areas in the Eastern Goldfields by Davis and Maidens (2003). Localised extension related to granitoid emplacement is a preferred explanation for the late, low-angle fabrics at Mount Pleasant since bedding dips are steepened in

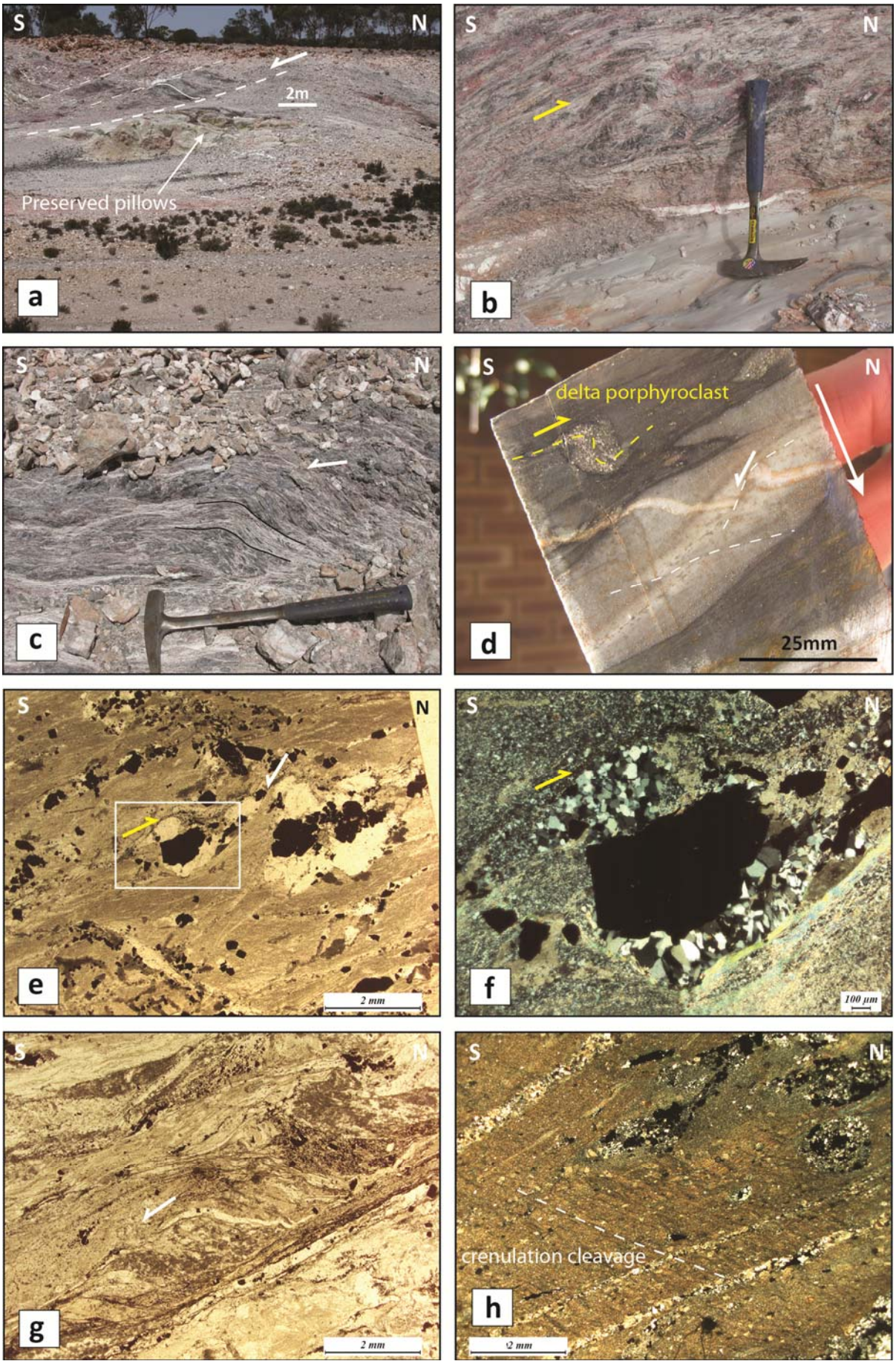
S
N
2m
Preserved pillows
a
b
c
delta porphyroclast
d
25mm
e
2 mm
f
100 µm
g
2 mm
crenulation cleavage
h
2 mm

Figure 6.19

Captions for Figure 6.19 – Mount Pleasant detachment fault (all viewed to the west)

a) Macroscopic fabric in the detachment fault with extensional foliation deflection sense above a contact with weakly deformed pillow basalt from the map in Figure 6.18 (GDA: 329000E; 6618500N). The outcrop is an erosional breakaway at the edge of a laterite pan that exposes a spectacularly preserved Archaean seafloor contact between lower porphyritic pillow basalt and conformably overlying sedimentary rocks, including fine grained sandstone/siltstone and silicified mudstone in the interpillow voids (See also Fig. 3.4). The preservation is due to pre-shear warping of the contact, which allowed preservation of primary contact zones in synclinal depressions. The thick dashed white line marks the position of a detachment fault with an apparent low-angle extensional foliation deflection sense. Large 1-2 m basalt pillows are visible below the fault.

b) Stage 1 reverse-sense shear fold in a silicified shale layer within the detachment fault. The white layer marks the lower boundary of the detachment fault against weakly deformed plane-bedded turbiditic sandstone-siltstone, from the breakaway in (a). Fine grained sandstones below the detachment fault contain an upright mica foliation and cleavage, whereas the overlying detachment fault contains only shallow south dipping fabrics. The reverse shear sense was later overprinted by extensional reactivation.

c) Low angle shear zone with extensional foliation deflection sense – approximately 2 m to the right hand side of (b).

d) Oriented drill core showing reverse sense delta porphyroclast in a pyritic quartz vein, with late low-angle extensional faulting of a silicified band, drill hole THD001 216.2 – 216.25 m (GDA: 331202E; 6615692N). View is to the west, down hole is to the north.

e), f) PPL and XPL photomicrographs of reverse shear folded pyritic veins with late low angle extensional faults. The pyritic veins are composed of recrystallised vein quartz in segments around pyrite crystals. Early reverse shearing has buckled the veins and rotated the pyritic crystals and adjacent quartz segments. Later extensional deformation has offset the left hand vein segment and extended the lower limb of the microfold (white arrow); NATDD004 203.2 m (GDA: 330926E; 6614077N).

g) PPL photomicrograph of late extensional fabric defined by deformed quartz-carbonate veins and through- going low-angle extensional faults. Foliation deflection suggests top block down to the left, extensional sense of shear. NATDD004 203.2 m (GDA: 330926E; 6614077N).

h) XPL photomicrograph of gently north-dipping crenulation cleavage overprinting earlier detachment-parallel penetrative foliation; THD001 217.02 m.

the vicinity of the Liberty Granodiorite, suggesting that bedding and fold orientations were strongly influenced by that intrusion event.

6.6.1.3 Seismic evidence of intrusion control on fold architecture (Mt Pleasant Anticline)

Sub-surface geometry of the Mount Pleasant Anticline is revealed in a seismic section shot along the trend of the anticline fold axis, augmented with surface mapped contacts and subsurface drill holes. The seismic section in Figure 6.20 is a reprocessed subset of a much longer NNW-SSE trending seismic line (99Y4 - Goleby et al. 2000) covering the southern part of the Owen Batholith and the Mount Pleasant Anticline.

The seismic image (Fig. 6.20a) shows several groups of features: (1) strong, moderately south dipping reflectors; (2) strong, shallow south-dipping reflectors; (3) weak reflectors in various orientations; (4) zones of non-reflectivity at the northern and southern edges of the image; (5) a deep zone of strong sub-horizontal reflectors; and (6) narrow subvertical breaks in the reflectors. An interpretation in Figure 6.20b marks strong and weak reflectors, and then attempts to marry these with known fault and unit contacts at surface, with a solid rock interpretation in Figure 6.20c.

Moderate south-dipping reflectors are well accounted for by correlating these with known contacts of major units in the Mount Pleasant district. A northern zone of non-reflectivity correlates with Liberty Granodiorite, and is coincident with a zone of anomalous low gravity response in that same area. Suppressed acoustic impedance combined with a low-density gravity signature is typical of Archaean granitoid batholiths in the Eastern Goldfields Province (Goleby et al. 2000).

The southern area of low reflectivity is interpreted as subsurface intermediate porphyritic intrusive rocks that are commonly seen as feeders and intrusions in the White Flag Formation andesitic volcanic complex, and as dyke swarms in the upper Victorious Basalt at Mount Pleasant. A patch of strong reflectors in the upper southern end of the image is interpreted as White Flag Formation andesite, where a transition from seismically quiet Talbot formation sandstone-shale to White Flag Formation andesite is located. The narrow sub-vertical non-reflective breaks in the strong reflectors correlate with mapped faults at surface, and are interpreted as faults on this basis.

A predominant geometric feature is a gradual steepening of the dips of major contacts towards the Liberty Granodiorite (box ‘c’ on Figure 6.20c). Field measurements of contacts in the Golden Funnel, and Royal Standard mines show 40°S dips, which contrast with <10°S dips in Talbot formation outcrops (validated by drill hole intersections of the White Flag Formation / Talbot formation contact at ~100 m depth, almost 1 km south of the same outcropping contact). Bedding measured in outcrops of the Coppermine Shale interflow unit at 326532E; 6624678N is

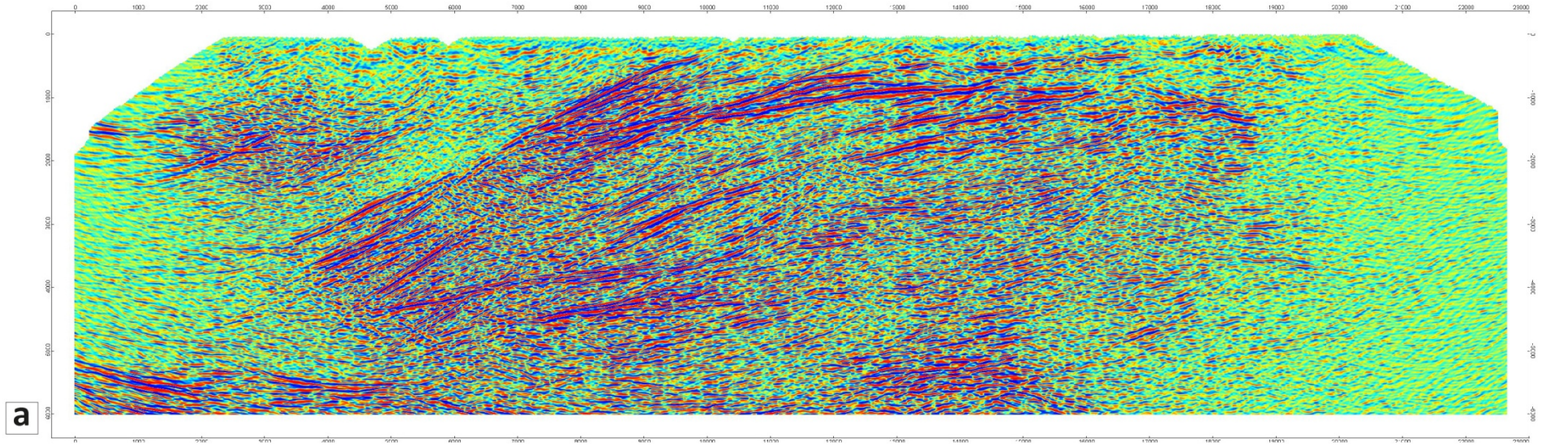

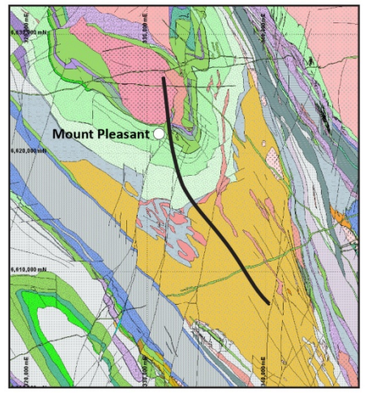

Seismic Line - 99Y4
(Geoscience Australia)
Residual stack, depth migrated; reprocessed by Curtin University, Perth WA

(line segment: 331360E; 6607266N - 340290E; 6626403N)

3km

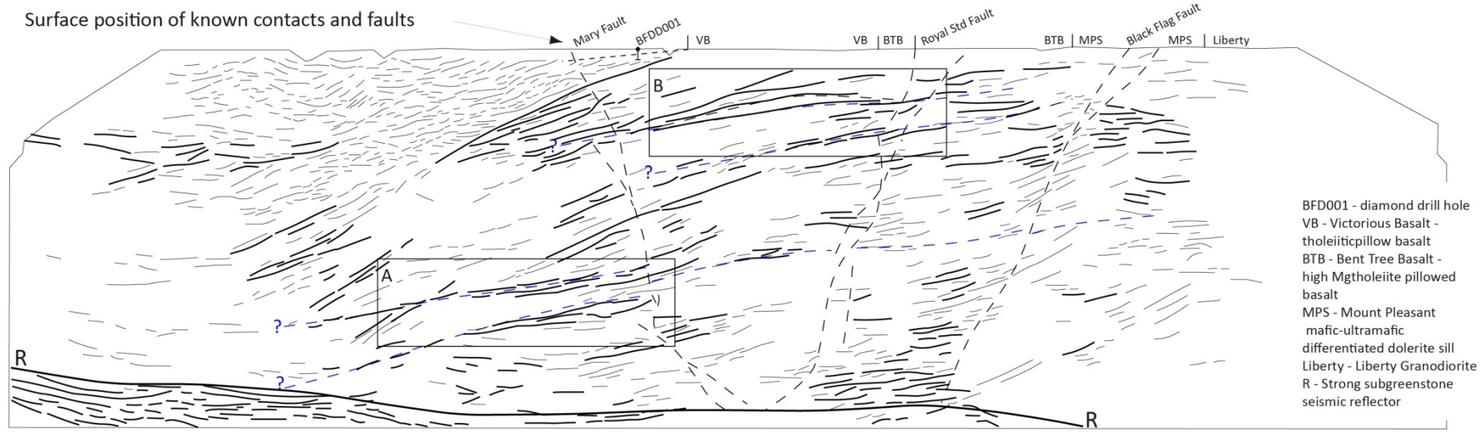

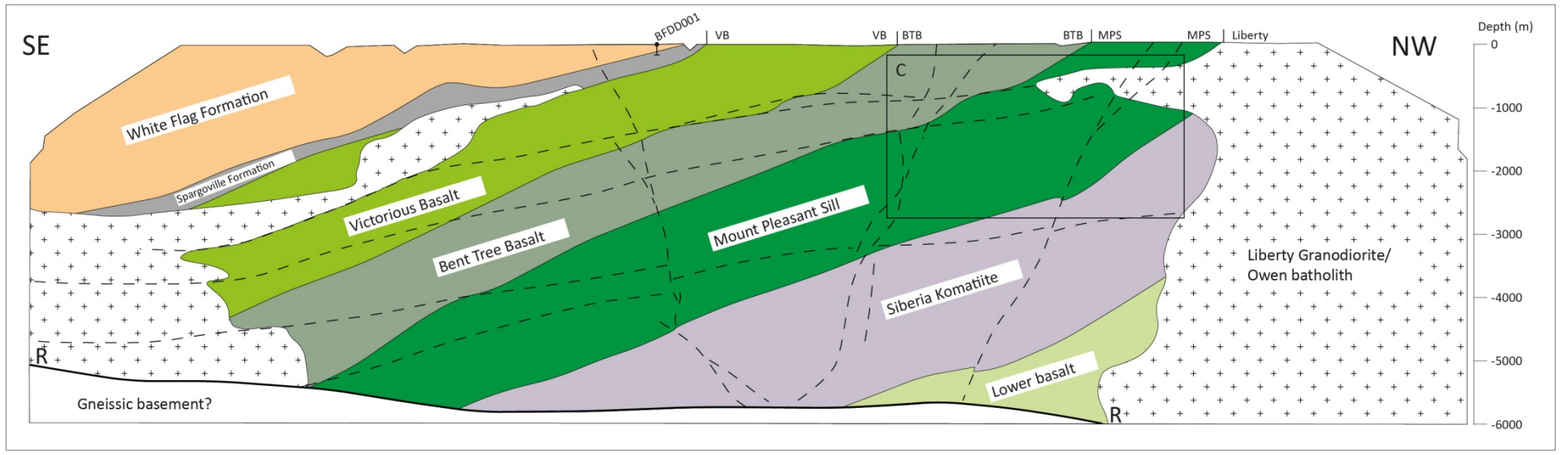

Figure 6.20 – a) Segment of Geoscience Australia seismic reflection line 99Y4 along the trace of the Mount Pleasant Anticline reprocessed at Curtin University of Technology Perth by Dr. Milovan Urosevic; b) line tracing of strong and weak reflectors in a); c) geological section along the seismic line tying seismic reflections to known features form outcrop and exploration drilling.

oriented at 51º/240º. This steepening relationship is also well demonstrated on serial cross-sections generated across and along the Mount Pleasant Anticline.

Given that major features of the seismic section are easily explained by known surface and drill hole geology, a question remains: “what has produced the shallow south dipping strong reflectors?” (indicated in boxes ‘a’ and ‘b’ on Figure 6.20 a and b). A geometric structural approach could easily interpret a top-to-the-north thrust system from apparent asymmetry between the shallow south-dipping and moderately south-dipping reflectors, yet map-scale geology precludes this possibility since there is no evidence of major thrust dislocation of mafic volcanic units or broad stratigraphic repetition. Two possibilities to explain the shallow south-dipping reflectors include (1) top-to-south slides produced by up-doming of the Liberty Granodiorite, or (2) out-of plane reflections from the Black Flag quartz-feldspar, rhyolite porphyry dyke (Location map on Fig. 6.20).

Serial cross-sections and three-dimensional modelling show that steepening of contact dips with proximity to the Liberty Granodiorite is developed on all sides of the intrusion. This relationship and several pieces of local evidence (Upper Basalt detachment fault; extensional slide faults in the Natal mine, top-to-south fabrics of the Victorious Basalt / Bent Tree Basalt contact in Royal Standard north mine; Fig. 6.9) argue strongly for up-doming of the stratigraphy by a forcefully emplaced Liberty Granodiorite. Stretching lineations and shearing fabrics in the Upper Basalt contact fault indicate a movement vector towards 190° in wallrocks on the SW margin of the Liberty Granodiorite. Shallow south-dipping reflectors in the seismic section may be imaging low-angle, top-to-south faults that accommodated up-doming of the stratigraphic sequence, but failed to cut through to the surface.

An alternative option to explain the shallow south-dipping reflections is out-of-section reflectors. Reflections from planar bodies and scattering effects from out-of-section point sources can plot as moderately dipping reflections (Goleby et al. 2004; Hobbs et al. 2006; Hamilton 2010). In the area of the 99Y4 section, a N-S to NW-SE trending intrusion (Black Flag felsic porphyry dyke) varies from 3.8 km to 1.3 km east of, and trending sub-parallel to, the 99Y4 seismic section (Fig. 6.20). Exploration drill holes indicate the western contact of the dyke is dipping to the west. The possibility shallow south-dipping reflectors resulted from proximity of the seismic section to the Black Flag dyke cannot be discounted.

Shallow dips of the Mount Pleasant stratigraphy and a shallow plunge of the Mount Pleasant Anticline away from the influence of sizeable plutons and batholiths suggest that late intrusion may be a significant process disrupting the broad open anticlinal fold patterns present on maps of the Mount Pleasant district. Liberty Granodiorite, if interpreted correctly at depth, cross-cuts the Archaean volcanic stratigraphy at a high angle and this relationship agrees with the map pattern distribution of the intrusion. The aerially extensive Owen Complex has contacts that are broadly parallel to lower ultramafic volcanic rocks suggesting a possible doming control

on the regional folds. An exception to this generalisation is at Ora Banda, where gravity images clearly show sharp cross-cutting of low density intrusive rock, and may indicate similar late intrusions (akin to Liberty Granodiorite) are responsible for major disruption to the stratigraphy and regional foliation, which has been disrupted in the Ora Banda district to a dominant orientation of 54º/267º (cf. general steeply dipping, NW-striking S3 regional foliation).

6.6.1.4 F2 Scotia Anticline

The Scotia Anticline has a rounded fold hinge and isoclinal fold limbs, with sub-vertical dips on the western limb and about 60º dip of the eastern limb (Fig. 6.5). Drill hole exposures of the eastern edge of the Scotia Batholith, show strongly mylonitised granitoid rocks in drill chips, whereas the western contact has a prominent down-dip mineral elongation lineation in recrystallised equigranular granodiorite (oriented sample provided by Dr. B. Davis).

Granitoid intrusion is generally considered a significant influence on the formation of major fold domes in the Eastern Goldfields Province, with magmatic ballooning in the centre of composite plutons and batholiths as a suggested emplacement mechanism (Witt and Davy 1997). The Scotia Batholith on the other hand, appears to have intruded post-folding of the Scotia Anticline with granite porphyry dykes cutting across folded bedding in the axial plane of the fold (Fig. 6.5) and a sharp sub-vertical eastern faulted contact as indicated by drill hole intersections and regional gravity data.

6.6.1.5 Goldilocks / Binduli

Pre-Kurrawang F2 folding is interpreted to explain the presence of the Upper Basalt Unit, White Flag Formation and Binduli felsic volcano-sedimentary sequences - located at Goldilocks, south of Kundana (Section 3.23). The rocks in that area contain sections of several units that are unique to the Ora Banda Domain, but located on the western side of the Kurrawang Formation with clear unconformable relationships as interpreted from bedding trends, and exposed in drill holes (Section 3.23; Fig. 3.15).

A revised stratigraphic interpretation for the Goldilocks area at Kundana south, presented in Section 3.23, demonstrates a thick sequence of intermediate to felsic volcanic and sedimentary rocks with strong similarities to the Binduli sequence. Aeromagnetic images show the rocks at Goldilocks have similar magnetic character to the Binduli rocks, supporting an interpretation of the Binduli sequence as folded pre-Kurrawang, yet cut unconformably by that unit. The presence of the Ora Banda Domain Upper Basalt mafic volcanics is further strong evidence that supports this contention. Steep easterly dips in the east-younging Binduli sequence rocks at Goldilocks (Fig. 3.15), and moderate westerly dips of the west-younging sequence in the Binduli mining centre indicate the presence of a large, tight, south-plunging

syncline, with an inferred closure at about the centre of the Kurrawang Formation, to the east of the Kundana Mining Centre (Fig. 3.20).

Significantly thinned sequences of Upper Basalt unit, White Flag Formation rocks and lower Black Flag formation rocks between the Kundana exposures and the Ora Banda Domain exposures (on the eastern side of the Kurrawang Formation) suggest: (1) the possible presence of a growth sequence across a pre-Kurrawang fault, (2) structural thinning in the vicinity of the Zuleika Shear Zone at Kundana, or (3) that the Kundana units are at the margins of an original depositional basin that deepened towards the northeast. Deformation in the Goldilocks and Kundana rocks is strongly localised into <10 m wide shear bands; hence, tectonic thinning appears inadequate to explain the much reduced section exposed west of the Kurrawang unconformity.

6.7 Uplift (D3a) - deposition of coarse clastic sedimentary rocks

Unconformable late clastic sequences of the Kurrawang Formation and Panglo member are distributed in long, linear synclinal belts, largely constrained on their western margins by major domain boundary faults, with preserved unconformities on their eastern margins. The interpretation of the Panglo member as part of the Kurrawang Formation is a new and key understanding for the district and offers new possibilities for the interpretation of late clastic sequences. This depositional event is listed in the deformation scheme as D3a since the Kurrawang Formation and Panglo member, by way of clast compositions and lithofacies, indicate rapid exhumation of a diverse hinterland with exposures of deformed batholithic plutonic granitoid rocks and hypabyssal porphyries. The nature of that exhumation (extensional or contractional) is debated in the literature (e.g. Krapez and Barley 2008; Blewett et al. 2010a), linear fault controls on the distribution of those rocks suggest that deposition was syn-orogenic.

Recent detailed studies on the sedimentology and zircon provenance of at least six documented ‘late basins’ in the Eastern Goldfields (Krapez 1996; Howe 1999l; Krapez et al. 2000; Godfrey 2004; Barley et al, 2002; Squire et al. 2010; Blewett et al 2008; Krapez and Pickard 2010) have produced various interpretations for those units, ranging from strike-slip basins; fault-bounded marginal to deep-marine basins; and basins produced by an interpreted Eastern Goldfields-wide extensional deformation event related to thermal relaxation, and influenced by post tectonic Low-Ca series granite intrusions (Davis and Maidens 2003). This discussion will focus on the Kurrawang and Panglo units in the study area.

A key feature of the late clastic sequences is that they are predominantly polymictic, siliciclastic sedimentary rocks lacking co-eval volcanics (e.g. Krapez et al. 2000). Cessation of volcanism coincided with exhumation and deposition of thick fluvial to marine sequences above unconformities. Deposition of the late clastic sequences was followed quickly by burial to significant depths that produced a strong metamorphic fabric that is axial planar to folds in the

unconformable sequences; hence, it is likely the appearance of these units predates the onset of penetrative deformation in the granite-greenstone terranes (e.g. Robert et al. 2005). The rapid timing is indicated by a maximum depositional age of the Kurrawang Formation (<2650) and an age determination for syn-post deformational mineralisation at Kundana by Vielreicher et al. (2006) of 2639±3 Ma (Chapter 7), suggesting an interval of ~11 Myr for deposition, burial, folding and metamorphism of the Kurrawang Formation.

An important observation is that the Kurrawang and Panglo units are not 'basins' as such, since no basin margins are evident from the lithofacies exposed; but rather are synclinal basin remnants preserved in the footwalls of major faults: Zuleika Shear Zone (Kurrawang); Bardoc Tectonic Zone (Panglo). This raises an important question about whether faults controlled the deposition of the units as syn-orogenic conglomerate basins, or whether the faults were solely responsible for the preservation of slivers of an originally widely distributed single formation.

The extensional deformation event of Czarnota et al. (2010) explained the restricted linear distributions of these units in terms of extensional core-complex type deformation, producing spatially separated linear depocentres, during a hiatus in subduction. They also used this mechanism to explain the presence of broad, late clastic sedimentary units that wrap major granite-cored domes at Yindarlgooda (Penny Dam formation) and Mt Margaret (Wallaby Conglomerate). Barley et al. (2002) preferred an oblique subduction model that produced intra-orogen, strike-slip basins controlled by major faults interpreted to be syn-accretionary structures, whereas Swager (1997) interpreted the units as a result of a separate, and distinctive extensional deformation event that produced roll-over anticlines in the hangingwalls of major extensional faults. Folding of the underlying volcanic sequences such that they appear on both sides of the Kurrawang Formation would be an unlikely consequence of the inversion of extensional faults and appears to discount the model of Swager (1997).

Modern fluvial/alluvial systems in actively deforming transpressional settings (Markham Valley, Australia-New Guinea Margin - Tingey and Grainger 1976; Cordillera Domeyko in northern Chile - Cornejo et al. 1997; and the Phillipine Fault - Corbett and Leach 1998) can produce fault-controlled, linear polymictic basins with similar structural settings to the Kurrawang and Merougil sequences at Kalgoorlie. The Panglo member appears different to the Kurrawang Formation in that much of the Panglo sequence is composed of shales and siltstones probably deposited in quiescent conditions. This contrasts with the Kurrawang, which contains lower fluvial polymictic conglomerate and predominantly coarse-grained, trough-cross-bedded quartz sandstone and wacke with minor siltstones at the top of the sequence. In this respect the Panglo may represent a more distal depositional environment, or may have undergone rapid deepening of the depocentre in a scenario as envisaged by Krapez et al. (2000) for the Mt Belches greywacke sequence.

Rapid and extensive exhumation is required to expose deep batholithic cores as indicated by abundant equigranular granitic detritus (including foliated granitoid clasts), hypabyssal porphyries in the conglomerates (Section 3.2.4) and their predominantly quartz-rich matrix sandstones with widely variable zircon provenance. Whereas this kind of exhumation can be achieved by strike-slip deformation (e.g. Death Valley, California) or crustal extension (e.g. East African Rift Valley), the typical lithofacies of the late clastic sequences in Kalgoorlie, and lack of co-eval volcanics, would be unusual in those settings. Major extension is a response to crustal thinning during thermal upwelling in the Basin and Range of western North America, and asthenospheric intrusion in the upper mantle underlying the East African Rift (Chorowicz 2005). In both of those settings volcanism and intrusion are important upper crustal expressions of the underlying mechanisms of extension, and if major extension was the mechanism for deposition of Archaean late clastic sequences, syn-basin volcanic sequences would be expected as is observed for the Timiskaming of the Abitibi belt in Canada (e.g. Hewitt 1963; Hyde 1980).

The deformation responsible for D3a exhumation and unconformable deposition of clastic sedimentary rocks is not easily resolved as being either extensional or contractional, but the evidence of modern systems developing as linear syn-orogenic, fault-controlled basins in mountain belts in South America and Papua New Guinea provides a possible alternative to wholesale tectonic mode switching, and may explain: (1) their geometry and rapid burial, (2) post-deposition deformation, and (3) lack of co-eval volcanic rocks. These features may be better explained in an environment of contractional deformation with fault-controlled linear depocentres.

6.8 Third folds (D3b) - Post-Kurrawang deformation

Major Post-Kurrawang contractional deformation produced folds (F3) and a regionally pervasive axial planar foliation S3. All major formations in the study area show evidence of D3b deformation (penetrative foliation), but the timing of that event is determined by folding of the two youngest unconformable units in the study area (Kurrawang Formation and Panglo member at Kanowna).

6.8.1 Folds (F3)

The Kurrawang Formation is a linear syncline bounded on its western margin by the Zuleika Shear Zone with a preserved unconformity on its eastern contact that cuts F2 folded rocks (Section 3.2.4). The Kurrawang Syncline is characterised by beds dipping towards the centre of the formation and younging indicators that show the sequence is right way up (trough cross-bedding, scour and fill structures). Gross folding of the unit is indicated by the presence of a strongly magnetic internal marker unit, which in outcrop corresponds with a 10-15 m layer of clast-supported, magnetite-rich polymictic conglomerate including magnetite-replaced, banded-

iron-formation clasts (Section 3.2.4). The western limb is slightly overturned locally (Goldilocks), with steeply west-dipping, east-younging beds. Minor fold axes have generally shallow plunges to the NNW and SSE, and the southern termination of the sequence is a north-plunging double-fold closure as revealed in aeromagnetic images (Fig. 6.4; Fig. 6.5). The northern termination of the formation is a shallow south-plunging syncline interpreted from aeromagnetic imagery and rare bedding exposures; hence, the fold axis is gently undulating along its trend. Assessment of the axial plane orientation is difficult from poor exposure, but can be attempted based on projected bedding dips and assumed constant bed thickness with an average orientation of 84º/225º (note the along strike variation of the strike of the axial plane).

Folding in the Panglo member at Kanowna is indicated by bedding orientations and a repeated sequence of distinct chert-clast conglomerate with Fe-rich banding similar to the Kurrawang Formation, yet lacking the distinctive red jasperitic chert clasts of the Kurrawang. Younging in the lower parts of the sequence, from drill core and rare outcropping cross-bedded quartz sandstones, indicates the sequence is right way up. The Panglo member has similar cross-cutting characteristics to the Kurrawang Formation with a faulted western margin and an unconformable eastern contact that also cuts F2 folded rocks.

Separating the timing of F3 folds from the major F2 folding event is determined from F3 folds and foliations cross-cutting axial planes of F2 folds. The best example is at the northern end of the Kurrawang Formation where the F3 Kurrawang Syncline cuts a major F2 syncline in the Ora Banda Domain (Fig. 6.5; see also Witt 1990; Tripp 2000). A supporting observation is that the Kurrawang rocks are not folded around the Major Mount Pleasant Anticline.

6.8.2 Axial plane foliation S3

All rocks in the study area are affected to some degree by an upright pervasive foliation that varies in orientation about a NNW-SSE average strike, with steep to sub-vertical dips (Fig. 6.5). The distribution and intensity of foliation are controlled by rock type and rheology, but there are also localised zones of elevated strain (within sequences) that are not logically related to contacts, rheological contrasts or major thrusts: strain localisation is a key consideration when interpreting the major structure. For example, foliation zones several tens of metres thick are localised within mafic volcanic sequences at Harper Lagoon (Kanowna) that show no evidence of contact offset or redistribution of stratigraphy (see Fripp and Jones 1997). These types of deformation zones are ‘shear zones’ by definition, but are not considered ‘major’ in the sense of domain boundary faults or other shear zones and faults that dislocate stratigraphy.

Pervasive S3 foliations are rarely penetrative across scales, whereas localised strain is typical. In fine-grained to coarse-grained sandstones of the Talbot formation, the foliations are generally evenly spaced at an outcrop scale (Fig. 6.21a, b), but are disjunctive at a micro-scale with mica folia defined by metamorphic biotite and muscovite wrapping individual sand grains

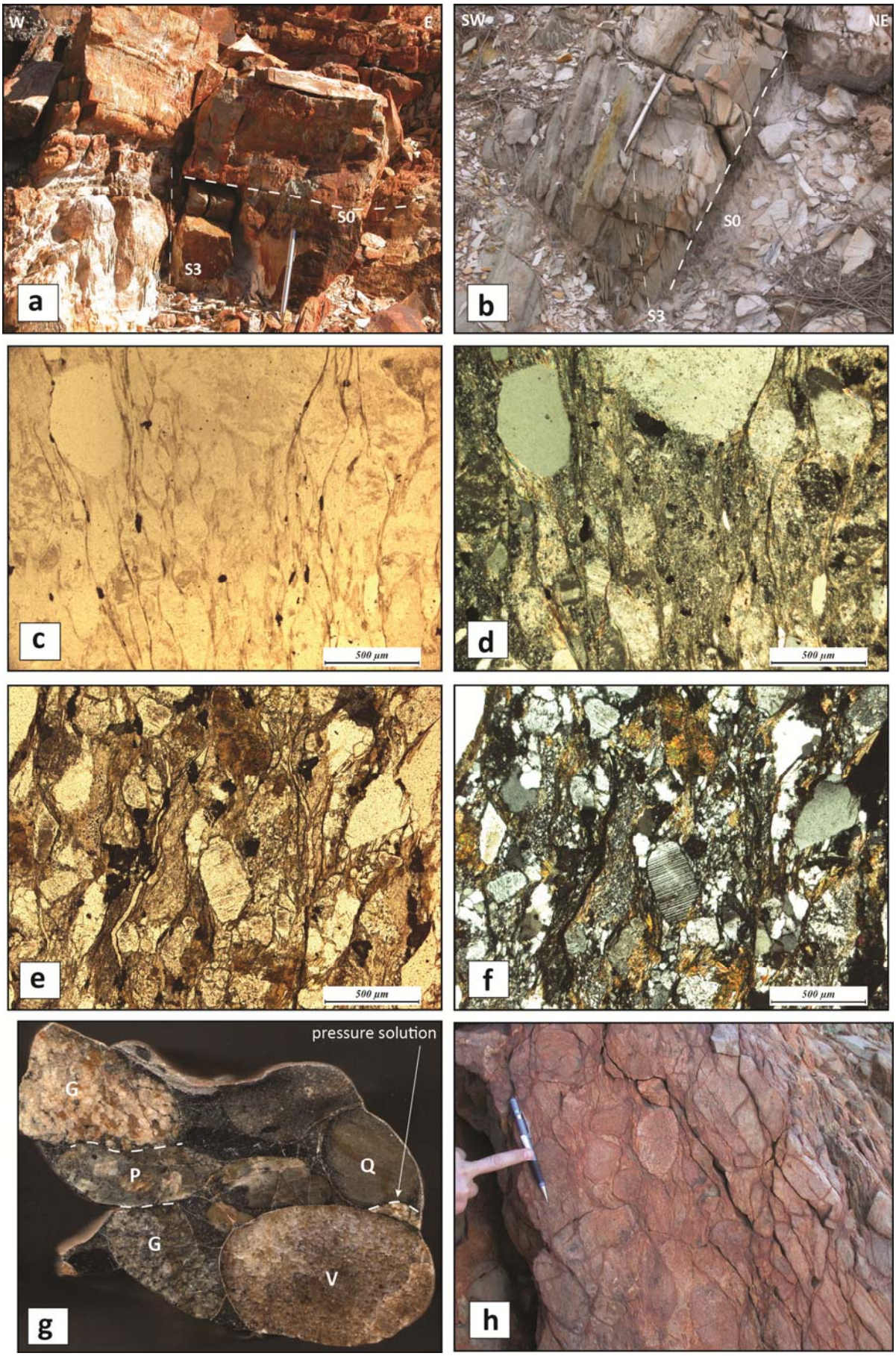
W
E
S0
S3
a
SW
NE
S0
S3
b
c
500 µm
d
500 µm
e
500 µm
f
500 µm
pressure solution
G
P
Q
G
V
g
h

Figure 6.21

Captions for Figure 6.21 - S3 foliations

a) Bedding / foliation relationships in Talbot formation sandstone/siltstone turbidites on the northern shore of White Flag Lake at the Three-In-Hand prospect (GDA: 330819E-6614558N). S0 dips shallowly on the western limb of a parasitic syncline at 3º/020º; S3 foliation is oriented at 82º/229º. The structure is upward facing with flame structures and graded bedding indicating upward younging.

b) Outcrop in an area of predominantly fine-grained cherty/siliceous shales near the top of the Talbot formation sequence, possibly close to the WFF basal contact. Bedding dips 28º/242º, overprinted by a strong sub-vertical S3 cleavage at 88º/042º (GDA: 330199E; 6613574N).

c), d) PPL and XPL photomicrographs of S3 foliation in metasedimentary rocks of the Talbot formation, in oriented drill hole NVDD001 156.5 m (GDA: 333725E; 6610479N). The rock is a moderately sericite altered coarse grained sandstone with sub-angular to angular (and locally sub-rounded) grains of strain free quartz; feldspar grains that show patchy sericite alteration and some examples of multiple twinning; lithic fragments are set in a very fine grained sericite altered quartzofeldspathic matrix. The S3 foliation is a spaced disjunctive cleavage at the scale of the thin section showing sharply defined foliation seams defined by biotite and locally overprinted by sericite micas that wrap the clastic sand grains. The thin section is a plan view of the foliation with the top of section pointing to the northwest. No consistent shear of sense is visible other than flattening of the rock with the S3 foliation wrapping the clasts. Thin sections that were cut parallel to the foliation showed no preferred orientation of sand grains suggesting that simple shear displacement was not an important process. The presence of angular strain free grains of volcanic quartz and feldspar suggests a relatively immature sedimentary product of a rapidly exhumed volcanic source terrane.

e), f) PPL and XPL photomicrographs of S3 foliation in fine grained quartzofeldspathic sandstone of Kurrawang Formation (Sample PHD14 – GDA: 327372E; 6611578N). The rock is a fine to medium grained sandstone composed of sub-angular to angular (and locally sub-rounded) grains of strained volcanic quartz and locally recrystallised plutonic quartz; and twinned plagioclase in a fine grained quartzofeldspathic matrix. Other samples throughout the Kurrawang have abundant angular to euhedral volcanic quartz grains, or locally well-rounded strain free quartz. The dominance of quartz is a type characteristic of sandstones in the Kurrawang Formation (with the exception of rare lensoid interbeds in the Kurrawang Conglomerate, which are lithic dominated). The S3 foliation at thin section scale manifests as a disjunctive cleavage wrapping individual grains, but in this case also shows a significant deformation of the matrix siltstone. Planar biotite folia and clusters of randomly oriented metamorphic biotite define the S3 cleavage, which is generally wrapping the sand grains. The biotite also forms pressure shadow beards on sand grains. No consistent kinematic sense is displayed by the S3 fabric.

g) Polished hand sample of Kurrawang Conglomerate from a prominent road-cut at GDA: 344900E; 6589220N. The sample is composed of polymictic well-rounded clasts of granite, quartzite, recrystallised vein quartz and small flattened mafic volcanic rocks in a fine grained micaceous sandy matrix. The sample highlights the anastomosing S3 foliation wrapping the clasts, and pressure solution seams on touching clast faces. The S3 cleavage trends 74º/082º and contains the long axes of pebbles that plunge 11º/165º. Bedding in this outcrop is defined by thin 20cm laminated sandstone interbeds oriented at 75º/260º. The relationship between the pebble stretching lineation and the S0/S1 intersection lineation remains unclear.

h) Outcrop of coarse-grained volcaniclastic andesitic rocks of the White Flag Formation at GDA: 333465E; 6610000N. The rock is an oligomictic volcaniclastic conglomerate at the base of the White Flag Formation dominated by andesitic debris with rare dark amphibolite fragments. Clasts are set in a sandy matrix of feldspar and hornblende sandstone, and are separated by a spaced disjunctive cleavage that is not well defined mineralogically in these rocks. In plan view the clasts are lensoid, but round shaped in section suggesting a sub-horizontal component of elongation.

and localised foliation bands within siltstone and mudstone beds (Fig. 6.21 c, d). Similar relationships are exhibited by fine grained sandstones of the Kurrawang Formation (Fig. 6.21e, f), with long axes of quartz, plagioclase and lithic sand grains also defining the S3 fabric.

In contrast, *coarse* clastic rocks in the Kurrawang Conglomerate display spaced cleavages that wrap clast boundaries, form pressure shadow beards in low strain sites, and are partially defined by pressure solution seams located where adjacent clast faces touch (Fig. 6.21g; see also figures in Section 3.2.4). Coarse volcaniclastic rocks in the White Flag Formation accommodated strain in a similar fashion to other coarse clastic rocks in the district with a disjunctive cleavage that wraps the clasts. Elongation of clasts and rotation of clast long axes parallel to the S3 foliation is typical in coarse clastic rocks of the Kalgoorlie district (Fig. 6.21h).

6.8.3 Timing Criteria

Timing of the S3 foliation is determined by relative cross-cutting as there are no robust ages for the fabric formation. Attempts to assess the age of fabric development using Ar-Ar on mica inclusions in pyrite (e.g. Phillips and Miller 2004), produced unrealistically young ages that are considered to reflect re-setting related to Proterozoic thermal events. The key timing indicator for S3 foliation is its development as an axial plane foliation to F3 folds in late clastic sedimentary rocks that unconformably overlie all older sequences. Previously the regional pervasive fabric was recognised as ‘S2’related to F2 folding (e.g. Witt 1990, 1993; Swager et al. 1990), but the identification of folded unconformities that cross-cut F2 folded rocks is a critical piece of evidence (Tripp 2000; also later recognised by Blewett et al. 2004).

A comparison of foliations measured within and external to the Kurrawang Formation was made to determine if those foliations are the same generation of fabrics, or if they are resolvable into separate deformation events. Field data from Mount Pleasant to Kundana (Fig. 6.22a-c) were separated on the basis of foliations measured from the Kurrawang Formation versus foliations measured from the underlying rocks. In all cases an upright, steeply-dipping foliation is the pervasive fabric in the outcrops without other prominent foliations or crenulation cleavages; crenulation cleavages are generally well developed in shale/mudstone units throughout the study area (Fig. 6.1). From the equal area projections in Figure 6.22a-c:

1. There is no significant difference between foliation in the Talbot formation and overlying White Flag Formation: hence these are considered the same generation of fabrics (Fig. 6.22 b,c).
2. Slight discordance of the S3 foliation and F2 fold axial planes is suggested by the bedding and foliation data for the Talbot formation (Fig. 6.22b; also Fig. 6.5).
3. The Kurrawang foliation data, while having a slightly wider spread, seem to have no resolvable clusters (Fig. 6.22a). The data were collected over the extent of the unit and

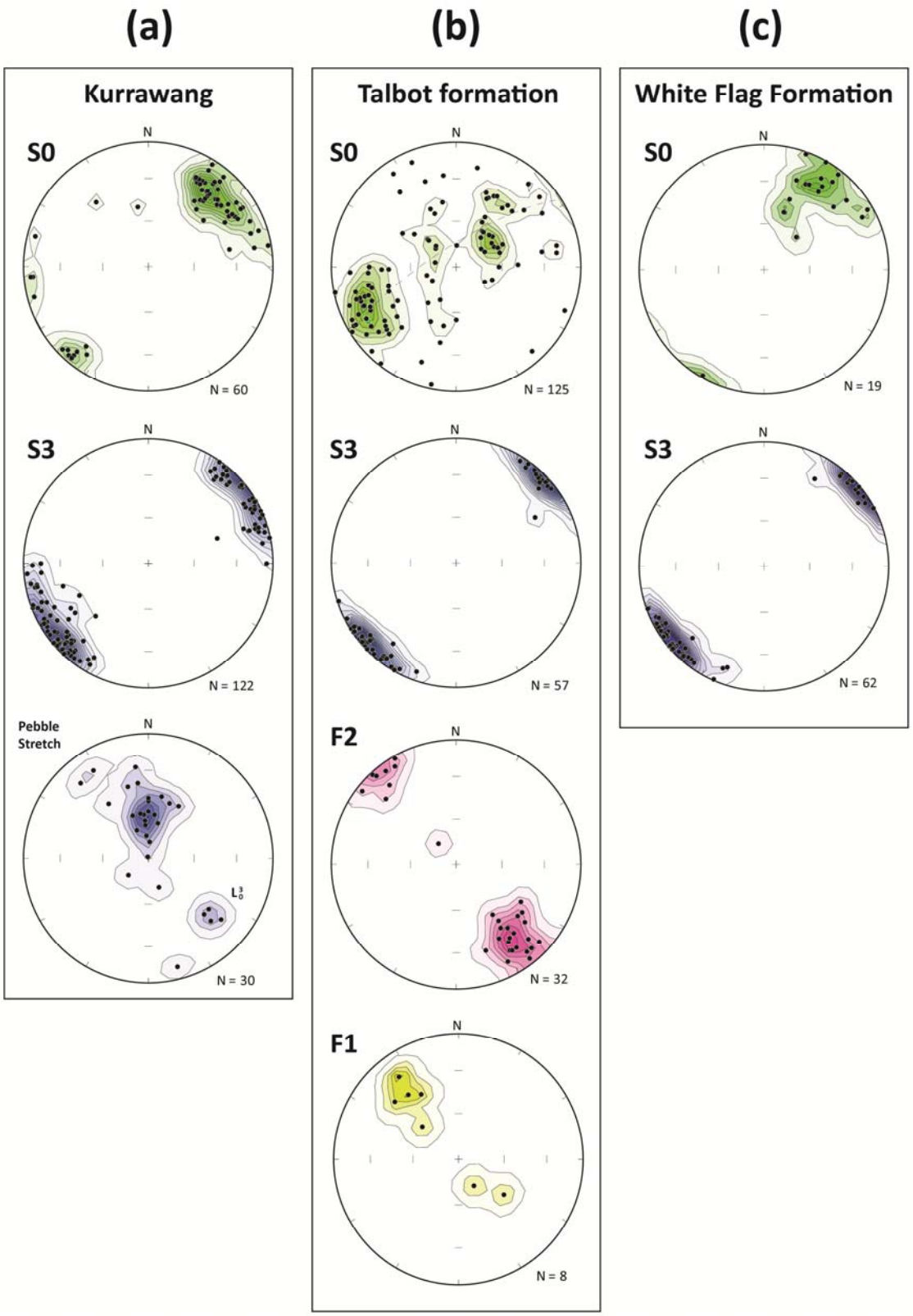

Figure 6.22 – a) Fabric data from outcrops of the Kurrawang Formation collected from the entirety of the unit, compared with similar data from Talbot formation and White Flag formation. Few bedding readings in the NE-dipping cluster of the Kurrawang reflect that most available exposures are located on the eastern limb of the Kurrawang Syncline; b) Bedding, foliation and fold data from the Talbot formation rocks south of Mount Pleasant; c) Bedding and foliation data from the spectacular section of White Flag Formation exposed on the edge of White Flag Lake. The foliation data from rocks above and below the Kurrawang unconformity are essentially the same. Note the similar orientations of F1 fold axes (Mt Pleasant) and L1 pebble stretching lineations from the western margin of the Kurrawang Formation.

the wider spread may reflect a slight change to a more NNW-strike in the Binduli area; or general anastomosing produced by a later belt-parallel shortening event.

4. Penetrative axial planar foliations in the Kurrawang, and foliations from underlying formations have essentially the same orientation, microstructural, and mineralogical characteristics, and are considered to be produced by the same event

This last point is crucial to the interpretation of the regionally pervasive NNW-SSE trending foliation since in pre-Kurrawang unconformity F2-folded rocks, the S3 pervasive fabric may strike parallel to F2 fold axial planes, whereas the Kurrawang and its folding clearly post-date F2. To ascribe the pervasive regional foliation to S3 and not S2 is a critical understanding for the district, but would likely sit uncomfortably with a geologist mapping an area that doesn't contain a Kurrawang-aged unconformity. Nonetheless, the timing presented here is supported by: (1) Kurrawang Formation unconformably overlying earlier F2 folded rocks, (2) F3 folding of the Kurrawang Formation with an axial planar S3 cleavage, and (3) a general absence of crenulated early fabrics. Tightening of F2 folds was a suggested consequence of D3 shortening by Swager (1997).

Fold axis orientation data show no systematic re-distribution of earlier F1 folds (e.g Ramsay 1963), but this may reflect that available exposures are restricted to the western limb of the broadly folded Mt Pleasant Anticline (Fig. 6.22b). Refolded F1 folds are generally localized in strong deformation zones, suggesting those folds may have been associated with early detachment faults. F2 fold axes were affected by later shortening events resulting in plunge variations to the northwest and southeast. This plunge variation was thought to represent a late orogen-parallel contractional event (e.g. Glikson 1971) with WNW-ESE oriented axial planes; and is evident at mesoscopic scales by a gentle warping of the upright fabric that produced open folds with E-W trending axial planes in the Paddington gold mine. On the regional foliation compilation map (Fig. 6.5) there is an E-W foliation subset, possibly part of this later group.

Key criteria for F3 fold timing include: (1) the rare occurrence of folded unconformities at the base of late clastic conglomeratic sedimentary sequences, (2) folding and foliation within those sequences, or critically, (3) that S3 foliations transect the axial planes of F2 folds. Folds of demonstrable F3 generation are present in the Kurrawang Formation and the Panglo member at Kanowna. Other folds in the district may be of this generation, yet their timing is difficult to substantiate at distance from D3a unconformities.

Further evidence of 'S3' timing for the regional pervasive foliation comes from the relationships of the foliation to earlier fold axial planes. The gross geometry of F2 and F3 folds is broadly similar, whereas foliation trajectory maps (Fig. 6.5) and fabric data (Fig. 6.22b) indicate the pervasive foliation transects the axial planes of F2 folds. The S3 foliation is oriented across F2 fold limbs and overprints earlier domain boundary faults (Fig. 6.5).

In addition, early F1 folds at Kanowna and the Golden Mile are transected by the S3 foliation and cleavage, as is the Binduli Porphyry Conglomerate unconformity. Other D2 structures are overprinted by the S3 foliation including ramp–anticline decollement faults at Mount Pleasant; granite-up / greenstone-down extensional foliations; and later folds at Chadwin Mining Centre that are locally overprinted by a second foliation (interpreted S3; Chapter 5).

A minimum age estimate on the S3 foliation is given by a SHRIMP U-Pb analysis of hydrothermal xenotime from quartz-carbonate-gold veins in the Rubicon mine at Kundana that cut the pervasive foliation. Veins analysed by the AMIRA P680 project returned an age estimate of 2639±3 Ma (Section 7.3.8; Vielreicher et al. 2006). This age provides a minimum estimate of the S3 foliation age, and accords well with the interpreted maximum depositional age of the Kurrawang Formation at <2650 Ma. These constraints suggest deposition, burial, F3 folding and metamorphism took place within ~11 Ma.

6.9 Post-Kurrawang deformation (D4) - late stage faults

Late stage faulting is ubiquitous in the study area and is widely recognised as controlling abundant lode-gold vein deposits particularly in small-scale, low-displacement faults (Vearncombe et al 1989; Vearncombe 1998; Tripp and Vearncombe 2004). The characteristics of the D4 faults are documented in the Ora Banda Domain (Tripp 2000; Tripp and Vearncombe 2004) and display common features including: (1) combined brittle and ductile fabrics (vein, and foliation) with tensional shear vein arrays and multi-stage hydrothermal breccia, (2) conjugate fault networks composed of distinct principal orientations (NE-SW; NNE-SSW and N-S), and (3) regular kinematic displacement sense in each of the three principal orientations (NE-SW dextral; E-W sinistral; and N-S dextral). Local kinematic analyses demonstrate an ENE-WSW directed principal shortening axis for the late faults (Tripp and Vearncombe 2004).

Notwithstanding generally low displacements on the majority of D4 faults, several major D4 faults are visible in maps and geophysical images with significant displacements of up to 1000 m, which offset major lithological contacts, unconformities and domain boundary shear zones (e.g. Black Flag Fault - section 6.9.1). Three major faults were studied in detail to assess the deformation character of the late D4 faulting event. The results demonstrate marked similarities across wide areas and, in one case, provide information on reactivation of pre-existing early faults during late ENE-WSW contraction.

6.9.1 Black Flag Fault

On aeromagnetic images the Black Flag Fault (BFF) stands out with a distinct, apparent-dextral offset of the Kurrawang unconformity and the Zuleika Shear Zone at Kundana, but with diminishing displacement along its length to the north, ending at the Mount Pleasant mining district with zero displacement (Fig. 6.23a; Micklethwaite and Cox 2004). The northern end of

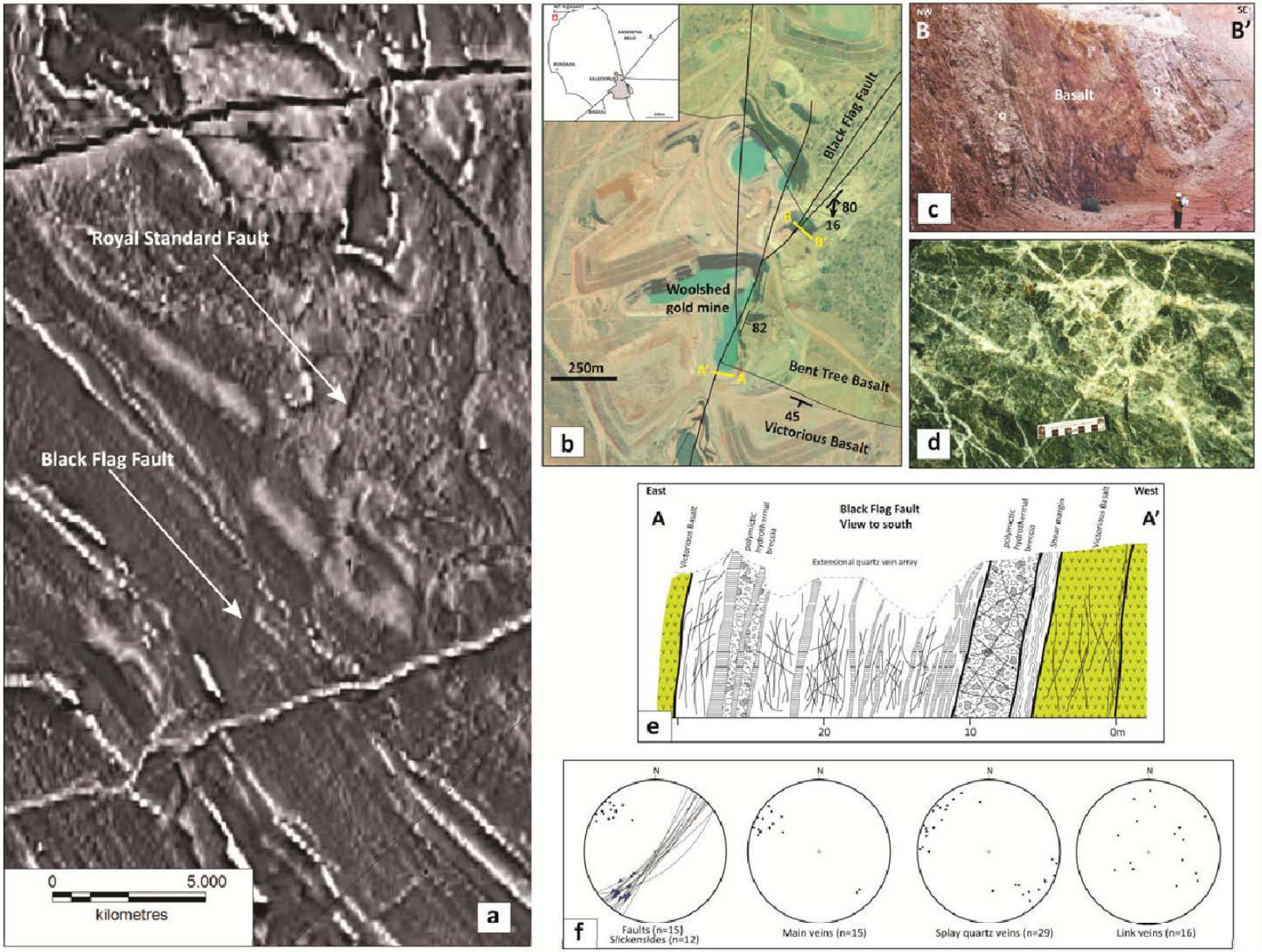
Royal Standard Fault
Black Flag Fault
0
5.000
kilometres
a
Black Flag Fault
80
16
B
B'
Woolshed
gold mine
82
250m
A'
A
Bent Tree Basalt
45
Victorious Basalt
b
NW
SE
B
B'
Basalt
q
q
c
d
East
West
A
A'
Victorious Basalt
polymictic hydrothermal breccia
Black Flag Fault
View to south
Extensional quartz vein array
polymictic hydrothermal breccia
Shear margin
Victorious Basalt
20
10
0m
e
N
N
N
N
Faults (n=15)
Slickensides (n=12)
Main veins (n=15)
Splay quartz veins (n=29)
Link veins (n=16)
f

Figure 6.23

Captions for Figure 6.23 – a) Aeromagnetic image (RTP_1VD) of the Mount Pleasant district showing clear breaks and offsets of layering across linear magnetic low zones that correspond with late faults; b) Aerial photograph of the Henning area including Woolshed and Black Flag gold mines at Mount Pleasant, with draped geology showing contact of Victorious and Bent Tree Basalts with ~700 m apparent dextral strike-slip displacement; c) thick multi-stage quartz-vein breccia zones cutting volcanic rocks - NE wall of Black Flag gold mine; d) complex quartz vein stockwork / breccia (Woolshed gold mine); e) Mine wall map for the southern wall of the Woolshed gold mine – a ductile shear zone is located at the margin of ~15 m wide zone of vein stockworks with polymictic hydrothermal breccia zones [assays average 0.06 ppm Au from quartz stockworks, 1.42 ppm Au from the footwall shear zone]; f) equal area projections of faults planes and veins from the Black Flag Fault – steep SE-dipping fault planes contain average 16S-plunging slickenside lineations.

the Black Flag Fault was interpreted as the rupture termination of a possible M6 Archaean earthquake event (Micklethwaite and Cox 2004; Micklethwaite 2007), and the rupture terminations were interpreted as resulting in damage zones that facilitated high fluid flux during Neoarchaean gold mineralisation events (Micklethwaite and Cox 2004).

Several open pit mine exposures of the BFF demonstrate a close association of gold mineralisation and hydrothermal fluid-flow with late faulting. Ductile shearing of adjacent wallrocks is contrasted with thick zones of multistage hydrothermal breccia particularly at right-stepping bends in the orientation of the fault. At the Black Flag gold mine a major right-handed bend in the fault has produced a >30 m-wide zone of extensional vein arrays and complex quartz-carbonate vein networks (Fig. 6.23b, c, d).

In the vicinity of those mines (Henning area at Mount Pleasant) the BFF turns from a mostly 020º strike to a 045º strike: a change that is accompanied by a major zone of dilation and vein emplacement. The volume of quartz veins and numerous extensional vein emplacement generations indicate the fault has been repeatedly reactivated with successive failure events. Recently the area was the focus of research into the role of stress-transfer during aftershock activity, in controlling fracture generation, fault growth/linkage and fluid flow (Micklethwaite and Cox 2004). Henning area is where the displacement across the BFF decreases at the location of a major dilational jog.

In the Woolshed gold mine (Fig. 6.23b) the BFF dips steeply east and has a 2 m thick ductile shear zone with normal-sense S-C fabrics on the footwall against a 4 m-thick, multi-stage hydrothermal breccia zone (Fig. 6.23e). Against the breccia zone is a 2 m-wide zone of parallel quartz veins, which precedes a 14 m-thick extensional vein array in the hangingwall. The extensional vein array is composed of master veins (>100 mm thick) that are sub-parallel to the fault and swarms of interlinked splay veins and linking cross veins. Detailed niche sampling of the various veins returned gold mineralisation with assays of 1.42 ppm Au from the main footwall shear.

The BFF has ~700 m of apparent dextral displacement, which is well constrained by an offset of the contact between Bent Tree Basalt and Victorious Basalt (Fig. 6.23b). The contact is located at the southern end of the Woolshed gold mine on the eastern side of the fault and the

corresponding contact on the western side of the fault outcrops in the Homestead mine to the north. Shallow plunging slickenside lineations indicate the latest movement was dextral strike slip, which is confirmed by offset of stratigraphy and the geometry of 060º striking shear vein arrays in the wallrocks of the fault (Fig. 6.23f).

The surface expression of the BFF is a large prominent quartz vein on the footwall contact. The quartz is not a single vein, but a multi-stage siliceous breccia with late fibrous cross-cutting veins. Exposed faces show sub-horizontal slickenside grooves with a mean plunge of 12º/217º (Fig. 6.23f). Measurements of the fault away from the strike change show a moderate north-plunging slip vector, which may indicate that the 'jog' event on the fault has different kinematics that overprint earlier ductile movements on the structure.

6.9.2 Mary Fault

Several major late D4 faults dissect the stratigraphy at Kundana including the Black Flag Fault and other named faults with similar structural characters to the Black Flag Fault at Mount Pleasant. A type example is the Mary Fault, which is intersected by diamond drill holes and provides an opportunity to view the complex multi-stage hydrothermal brecciation associated with late fault movements (Fig. 6.24). The fault displays strike-slip kinematics with a steep orientation 86º/277º and 3º-15ºN plunging stretching lineations. In drill hole HOPD026 drilled at the Hornet prospect, Kundana, the Mary Fault has typical ductile shearing of volcano-sedimentary wallrock formations, locally with thick zones of quartz breccia, developed at changes in fault orientation and at intersections with major stratigraphic contacts. A gold-rich, laminated quartz-calcite-pyrite-galena-Au lode vein is present at the upper (western) contact of the fault, with a 3.2 m wide intersection of 56.2 ppm Au (vein plus breccia).

Five breccia types are recognised within the fault including: Type 1 - grey siliceous quartz breccia; Type 2 - multistage hydrothermal breccia with lithic clasts; Type 3 - polylithic breccia with tabular shaped clasts; Type 4 - crowded lithic breccia with grey siliceous matrix; Type 5 - multistage hydrothermal breccia with lithic clasts. The breccia types are distinguished by clast composition, clast shape, mineralogy and descriptive characteristics. Multiple stages of breccia and re-brecciation of earlier stages are evident from xenoliths of earlier breccia types contained as clasts within later breccia types. A key point is that despite a complex hydrothermal history at Kundana, the multi-stage fault movements are not related to gold mineralisation with only a minor laminated vein at the contact of the fault, whereas the same faults are mineralised where they intersect mafic volcanic rocks at Mount Pleasant.

6.9.3 Shamrock Fault

The Shamrock Fault at Kanowna, as discussed in Section 5.3.1, displays evidence of an early history, whereas late reactivation of the fault is suggested by the presence of multi-stage

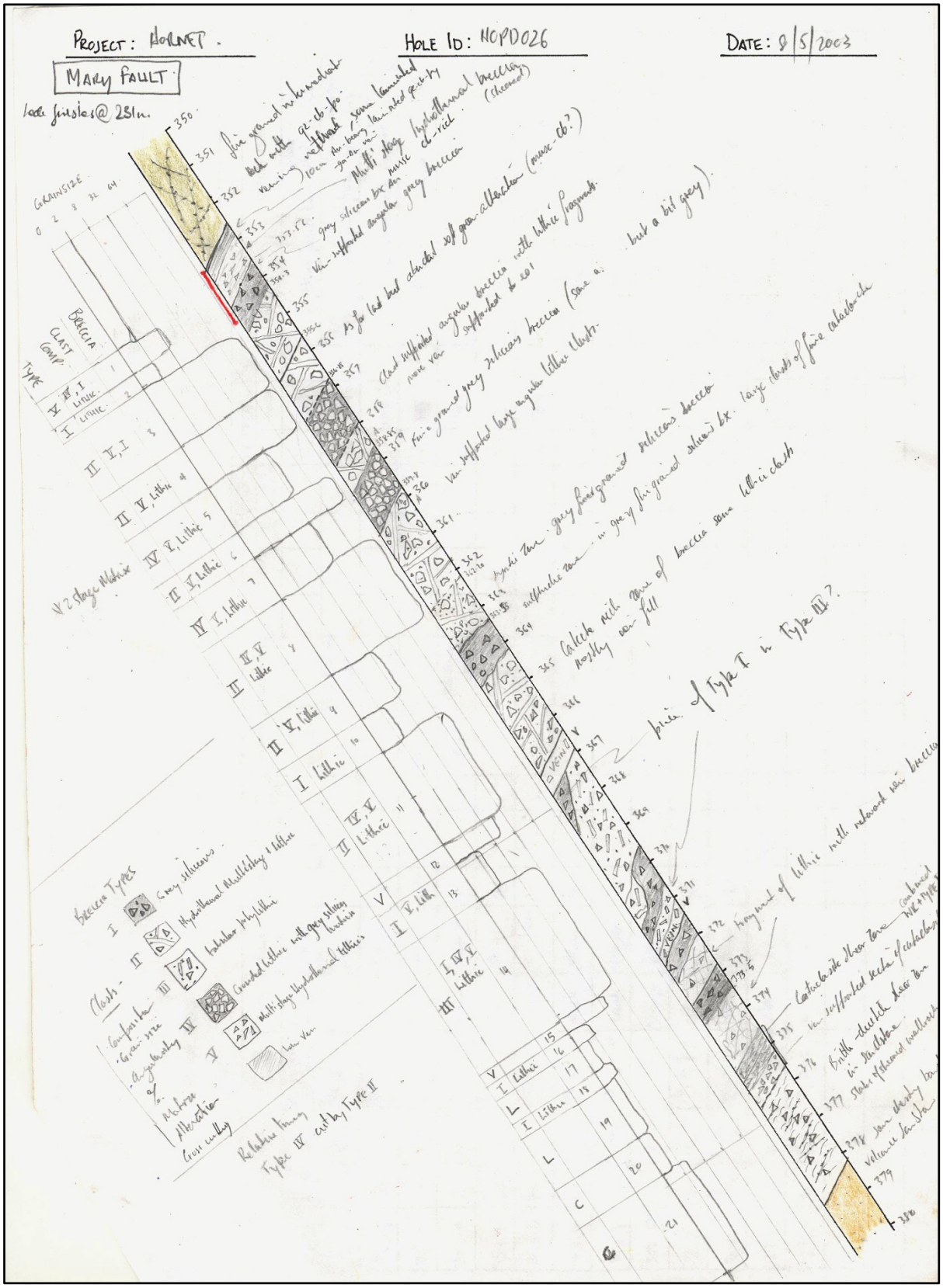

Figure 6.24 – Graphic drill log of multi-stage hydrothermal breccia internal to narrow ductile shear zones in the wallrocks of the Mary Fault. Drill hole HOPD026 from the Hornet prospect at Kundana mining centre.

net-veined siliceous breccia within strongly ductile-deformed wallrocks. Quartz rubble with characteristic breccia textures is present at most localities where the Shamrock Fault outcrops, but a significant thickness of quartz breccia is located at a major right-handed bend in the fault with identical relationships to the Black Flag and Mary Faults.

6.10 Summary - structural history and timing

This chapter documents a 7-stage deformation history grouped into five major events (Table 6.1; Fig. 6.25; Fig. 6.26). The sequence is essentially a change from bulk extension, which accommodated volcanism and sedimentation, to bulk contraction that initially shortened the greenstones, but also accommodated late, syn-orogenic sedimentation in long linear fault controlled basins.

Geochronological data from Chapter 4 indicate that the end of mafic volcanism occurred at around 2685±4 Ma with the intrusion of the Golden Mile Dolerite into the contact of the Paringa Basalt with overlying shales. Granitic batholith ages in the study area younger than the Golden Mile Dolerite indicate granitoid doming may not have been a significant process controlling the structure of depositional basins for the earliest mafic and ultramafic volcanic sequences.

Tectonic control on stratigraphic development of the greenstone sequences is clear at several stages in the deformation history. The earliest extensional events are largely obscured in terms of fabrics, but are evident from the areal distribution of stratigraphy. Stratigraphic thickness variations are interpreted as a probable result of extensional faulting and sub-basin development. The boundary faults that demarcate zones of major stratigraphic change are the same faults that were possibly active throughout the contractional deformation history of the greenstones since they controlled the youngest stratigraphic sequences, and were then finally overprinted by D4 faults.

6.10.1 Deformation DE

The earliest extensional event accounts for a bulk of the stratigraphy including mafic / ultramafic volcanic rocks of the Lower Basalt, Komatiite Unit and Upper Basalt; and turbiditic sedimentary rocks of the Talbot formation from ~2715–2690 Ma (Fig. 6.26). Continued extension from ~2690–2670 Ma produced andesitic, dacitic and rhyolitic volcanic centres across wide areas (White Flag Formation; Lower Black Flag formation at Gibson-Honman Rock and Perkolilli volcanics; Fig. 6.26); and locally-sourced conglomeratic and volcaniclastic sequences (Ballarat member at Kanowna). Granitoid intrusion co-eval with these early stages of volcanism is manifest in scant age data from older phases of the major batholiths that coincide with ages of major felsic volcanic formations (Siberia Batholith - 2675±8 Ma; Bali Monzogranite - 2676±8 Ma; Table 6.1; Fig. 6.5). Felsic batholiths and high level porphyritic intrusions were possible

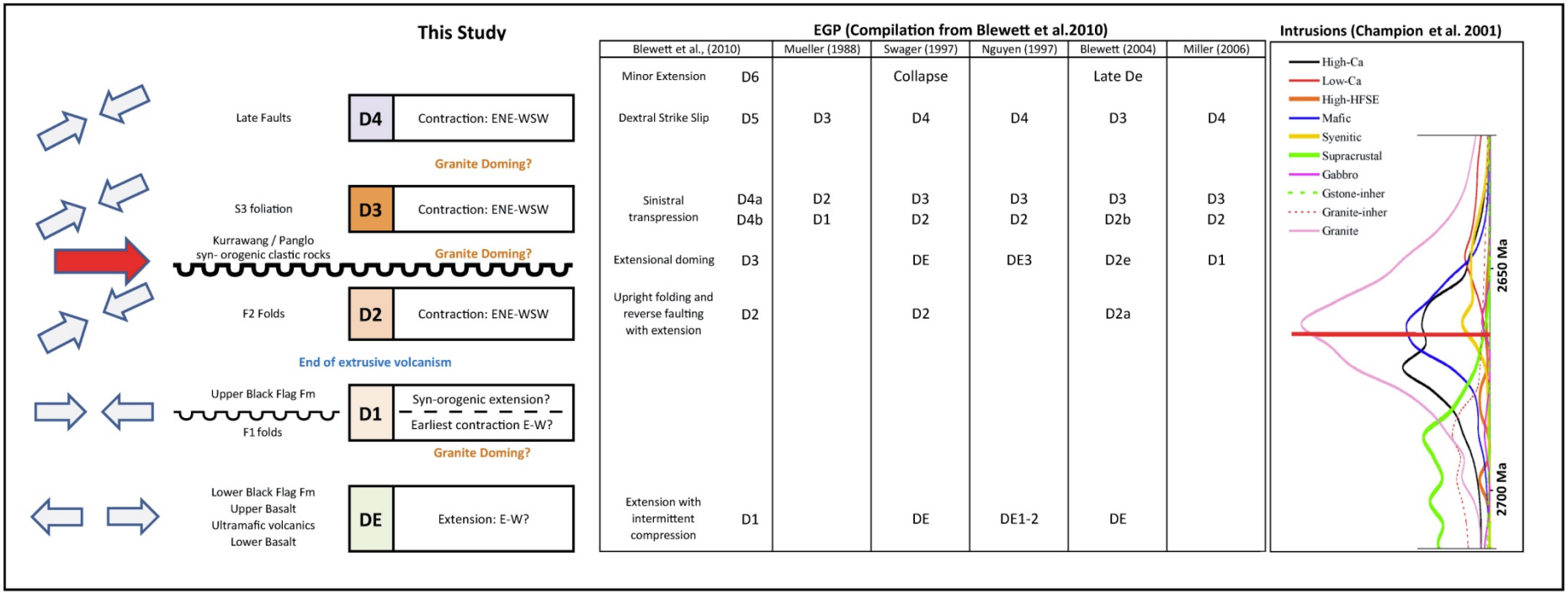

Figure 6.25 – Summary schematic of the deformation history listed in Table 6.1 compared with published schemes for the Eastern Goldfield Province. Most published regional schemes are compatible with the study area since the Kalgoorlie-Kambalda region is the best studied of all areas in the EGP. In this study, major events are constrained by stratigraphy as well as fabric data and show that the stratigraphy was developed as an active response to tectonic events in the Neoarchaean. Broadly, bulk extension changed to bulk contraction after the end of extrusive volcanism, but the early F1 folds may be the first evidence of contraction. Doming-related extension is another possible explanation for these early folds and detachments, but critical evidence in support of that hypothesis is lacking. Note the Kurrawang unconformity event is considered syn-orogenic, and need not have been the result of major changes from contraction to extension, as for the earlier upper Black Flag formation. Granitoid doming is considered to be a possible contributing process throughout the deformation history of the Kalgoorlie greenstones.

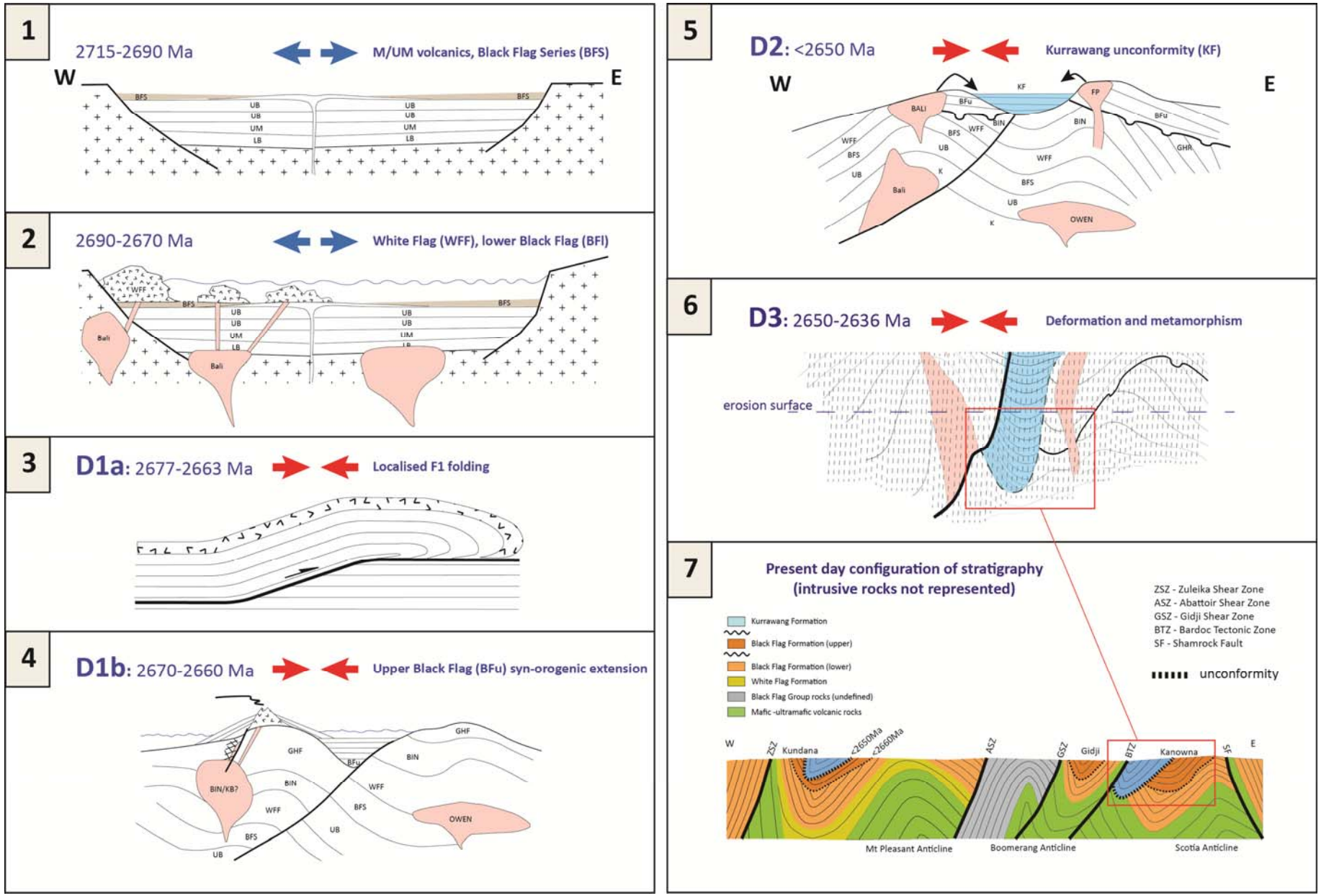

Figure 6.26 – Regional deformation sequence illustrated on a schematic cross-section throughout the various phases of extension and shortening

sub-volcanic sources of the intermediate to felsic volcanics of the lower Black Flag formation. The depositional environments of most of those sequences were submarine, characterised by felsic lava dome complexes extruded contemporaneously with deep water deposited turbiditic sedimentary rocks.

6.10.2 Deformation D1a

The first folding event occurred in a period between the deposition of the lower Black Flag formation at ~2677 Ma, and the unconformable upper Black Flag formation felsic volcanic and volcaniclastic rocks at <2663 Ma. Two unequivocal areas of D1a folding are located at Kanowna and Kalgoorlie - other early folds and extensional slides are arguably of that generation. The mode of folding is uncertain as contractional or extensional, but if the latter, was possibly related to granitoid doming supported by a close correspondence of batholith ages with the folding event, and a by a spatially restricted distribution of F1 folds.

A preferred interpretation for D1a is that it was the initial stage of E-W contraction that culminated in the penetrative ENE-WSW D3 contraction. Early nappe-style transport produced fault-bend folds accommodated on bedding-parallel detachment faults, and produced localised areas of possibly recumbent folding and downwards facing. Later influence from granitoid intrusions may have rotated some of these folds that are now at high angles to the penetrative fabric of the belt (e.g. Kanowna). Note that distinguishing between extensional structures and later D2 localised deformation zones in the sedimentary rocks at White Flag Lake south of Mount Pleasant is difficult and not fully resolved by this work. Reactivation and overprinting may obscure early fabrics.

6.10.3 Deformation D1b

Syn-orogenic uplift and erosion with continued (locally sub-aerial) felsic volcanism, possibly fed by Mafic-suite high-level granitoid intrusions, led to the deposition of upper Black Flag formation rocks above unconformities at Kanowna Belle, Binduli and Gidji. Younger phases of the major batholiths have ages comparable with the upper Black Flag formation rocks (Siberia Batholith - 2660±3 Ma; Bali Monzogranite - 2667±3 Ma), and Mafic-suite hypabyssal porphyry intrusions that were intruded into faults active at the time of volcanism and deposition (Kanowna Belle - 2661±8 Ma; Centurion Porphyry 2667±3 Ma).

6.10.4 Deformation D2

The onset of Pre-Kurrawang contractional deformation marks the cessation of extrusive volcanism, and produced broad wavelength upright folds, ramp anticlines, and fault-bend folding typical of thin-skinned upper crustal deformation in the time range ~2660-2650 Ma. Major batholiths (Owen Complex) were intruded with their contacts parallel to bedding in the

greenstones around this time. Refolding of early F1 folds at Kanowna and the Golden Mile has a poorly constrained timing of 2661±11 Ma (youngest rocks in the footwall of the Shamrock thrust fault).

6.10.5 Deformation D3a

Deposition of the Kurrawang Formation and Panglo member above unconformities marks an important time break between initial contraction of the thick greenstone sequences and the onset of major orogenesis and metamorphism. D3a is an exhumation event that exposed the deepest granitoid rocks in the EGP and sourced old (>3.0 Ga) terrains that are not represented in the EGP rock record. Deposition was in long linear, fault-controlled syn-orogenic basins suggesting active exhumation and deposition during the orogeny. This is in contrast to other models that interpret the deposition of the youngest sequences as a major EGP-wide core-complex style extensional event. The deposition occurred in a relatively short time period after ~2650 Ma, but prior to later folding, foliation and metamorphism, which was no younger than 2639±3 Ma (Section 6.3.6).

6.10.6 Deformation D3b

The major fabric-forming deformation and metamorphic event in the Goldfields produced F3 folds in the Kurrawang and Panglo synclines and a biotite metamorphic foliation and cleavage, pervasive across the district. The S3 foliation transects F1 and F2 fold axial planes, early extensional fabrics on the margins of the Siberia Batholith, and overprints early extensional faults and fabrics in the Mount Pleasant district. Mineralisation, broadly synchronous with and overprinting the foliation, is timed by hydrothermal xenotime ages at Kundana (2639±3 Ma).

6.10.7 Deformation D4

Late faults cut and offset the Zuleika Shear Zone, folded/foliated Kurrawang Formation, and mesothermal quartz-Au veins at Kundana. A fault at the base of the Talbot formation cuts foliated and folded rocks, has an extensional overprinting crenulation cleavage possibly related to the Liberty Granodiorite intrusion (2648±6 Ma), and was later cut by the Black Flag and Royal Standard Faults. Those faults cross-cut the regional pervasive fabric constrained at 2639±3 Ma, indicating that D4 faulting probably took place after 2636 Ma.

6.10.8 Comparison with published schemes

The structural history of the north Kalgoorlie district demonstrates close links between Neoarchaean tectonism and stratigraphic development - as is typical for modern orogens globally. This work has some significant differences to published deformation schemes, particularly: that deformation events are clearly separated into Pre-Kurrawang and Post-

Kurrawang phases to reflect a major time marker in the geological history of Kalgoorlie, and the timing of major events is constrained by stratigraphic and intrusion ages.

Post-extension basin inversion and subsequent contractions produced thrusting, folding and shearing, which redistributed rock units and masked the original geometric relationships. Inferring the positions and kinematics of original graben and extensional faults etc. would rely on interpreting thickness changes in marker layers, and reconstructing the original geometry from gravity modelling and balanced cross-sections. Many of the major faults and examples of stratigraphic repetition in the current structure of the greenstones may be remnants of an early extensional architecture, but the kinematics recorded in those structures is generally a product of later contractional deformations.

Published deformation schemes for the EGP (Fig. 6.25) broadly match the major events as listed here, but many have not recognised a spatially restricted F1 folding event or the Upper Black Flag formation unconformity. Some studies allocated a major extensional event to the Kurrawang deposition and applied specific kinematics to late contractional deformations (Blewett et al. 2004; Czarnota et al.2010). Evidence from outcrop and aeromagnetic imagery shows that kinematics can be affected by local influences. Major orientation changes around rigid bodies can influence the dextral/sinistral kinematic sense, or locally can produce dip-slip kinematics in major shear zones, that are strike slip elsewhere (e.g. Zuleika Shear Zone at Kundana). A preliminary compilation of shear zone kinematics from the district shows that shear zone stretching lineations can be highly variable along strike (Fig. 6.27).

Interpretations from the district-scale foliation trajectory map and structural interpretation in Figure 6.5 are fundamentally based on regional-scale data sets of geophysics and published field data, and reveal some key structural relationships. For instance, the most critical observation in the district is that folded, thick greenstone sequences are truncated against the Kurrawang unconformity, and that a NNW-SSE pervasive foliation is axial planar to F3 folds in the Kurrawang Formation and cross-cuts the unconformity into underlying rocks.

Recent workers have suggested that there are observable differences in the kinematics of foliation-producing fabric events that number up to ‘D14’ across the Eastern Goldfields Province (Blewett 2005), and warned against the use of a consistently oriented foliation as a deformation event marker (Blewett et al. 2010a; Czarnota and Blewett 2007). In the mapping presented in the previous sections, this issue was considered, but outcrops with more than one pervasive foliation are rare, with no consistent sense of overprinting and no mineralogical basis with which to justify a separation of the fabrics (compare the Paddington shale example at the beginning of the chapter; Fig. 6.1). Another factor is the anastomosing nature of foliations produced during bulk inhomogeneous shortening generally (Bell 1981). Minor variations in orientation and kinematics, controlled by the presence of anisotropy or even passively

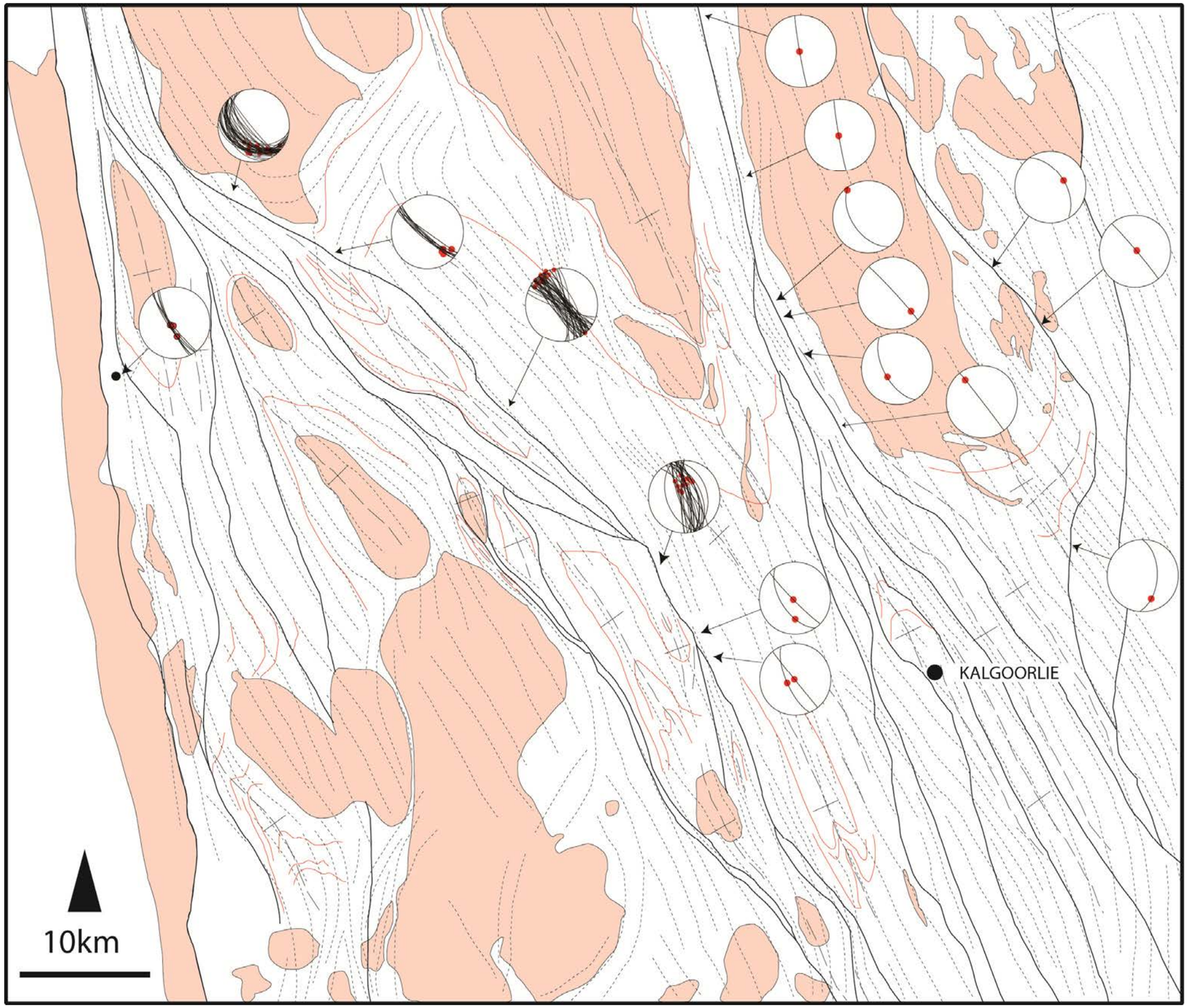

Figure 6.27 – Compilation of detailed fabric data from the Zuleika Shear Zone, and preliminary reconnaissance observations of fabric orientation and stretching lineations from the other major shear zones in the study area. Consistent kinematic sense is lacking from all major shear zones, which display local changes based on shear zone oientation, presence of anisotropy in the wall rock sequences and relative components of pure and simple shear in the deformation.

controlled by the anastomosing nature of shear zone segments, may have no justification for separation into successive events.

With knowledge of the relationships of NNW-SSE fabrics to F3 folds in the Kurrawang Formation it is possible to ascribe that fabric to a regional S3. This presents a new problem of distinguishing F2 mesoscopic folds from F3 generation folds since pervasive foliations strike approximately parallel to the fold axial traces of both fold generations, whereas the Kurrawang unconformity is a sub-regional-scale truncating feature. Where possible, transected cleavages were noted cutting the limbs of F1 and F2 folds, but elsewhere the angularity between F2 folds and the S3 cleavage is minimal. This presents a problem for field geologists working away from the Kurrawang unconformity, since the key relationships of that unconformity will not be obvious at a local scale. Axial traces of F2 folds in the Ora Banda Domain are transected by the S3 cleavage (Fig. 6.5). This regional-scale relationship and the observation of a folded and foliated Kurrawang unconformity are solid pieces of evidence that support the presented interpretation.

7 Key controls and timing constraints on diverse gold deposit styles

7.1 Introduction

Neoarchaean gold deposits in the north Kalgoorlie district are rarely simple in terms of their field geology or their relationships to volcanism and deformation, but taken as a whole, there is a spectrum of deposits ranging from early disseminated sulphide-replacement styles hosted in sedimentary rocks (possibly syn-genetic), porphyry 'associated' stockwork and disseminated sulphide styles, and quartz-carbonate-base metal vein deposits (Poulsen et al. 1992; Robert and Poulsen 1997; Robert 2001; Robert et al. 2005; Dube and Gosselin 2007; Robert et al. 2007). These styles are based upon the relationships of ore lodes to host rocks and deformation events, and the physical (vein texture) and chemical characteristics (P-T-X determined from fluid inclusions) of ore components that allow inferences to be made about the crustal setting of major Archaean gold deposits. The range of mineral deposit styles observed in a terrane may influence the interpretation of possible tectonic settings for the Neoarchaean (Hutchinson et al. 1971; Hutchinson 1981; Groves and Batt 1984; Poulsen et al. 1992).

Difficulty in assessing the structural timing of gold mineralisation with respect to major volcanic and sedimentary events is a particular problem acknowledged by many authors, since the key criteria of cross-cutting relationships and timing are not always conveniently available at the location of individual mineral deposits. This point is relevant in that late clastic sedimentary formations, which provide unambiguous timing criteria, have a restricted preservation and aerial distribution, and may not be exposed in all locations with major gold deposits. Complex structural geology - particularly seismic-induced, cyclical fluid flow events (e.g. Sibson 1987) - can produce ambiguous relationships between deformation fabrics and ore components at a local scale. A recent paper aimed at resolving these issues advocated paragenetic studies using vein *formation* and vein *deformation* criteria to identify discrete mineralisation and alteration events (Robert and Poulsen 2001).

Many publications on Neoarchaean gold deposits document a 'late epigenetic' timing for Neoarchaean gold mineralisation, and include most of the gold deposits with an 'Orogenic' classification (e.g. Boulter et al. 1987; Groves 2000; Vielreicher et al. 2010). In the north Kalgoorlie district a few notable exceptions include Bateman and Hagemann (2004); Gauthier et al. (2004a); and Robert et al. (2005) who have emphasised a diversity of timing and mineralisation styles. A key aim of this chapter is to determine the relative timing of mineralisation using field observations in context with the structural history outlined in Chapter 6, and to assess whether the classification of all the gold deposits as 'Orogenic' is justified. Two gold deposits in the study area were selected for detailed analysis particularly because they show examples of gold deposit timing with clear cross-cutting relationships: (1) Kundana gold deposits - Quartz-carbonate-vein lode and vein-stockwork gold deposits, with syn- to post-

regional foliation timing, and (2) Centurion gold deposit at Binduli - which contains two discrete mineralisation styles separated by a major unconformity, regional folding and foliation.

A critical assumption for the timing constraints presented is that a regional, consistently oriented, upright metamorphic foliation throughout the study area represents a single deformation stage, except in areas of the most intense strain localisation and reactivation along shear zones and major contacts. It is notable that in correlating deformation across the entire Eastern Goldfields Province, Czarnota and Blewett (2008) determined diachronous timing of structural events and discounted the use of marker fabrics for cross-cutting relationships and timing. The present study covers a contiguous terrane that is small compared to the area studied by Czarnota and Blewett (2008). The regional NNW-SSE trending pervasive foliation is treated here as a distinct stage of deformation since it is constrained in the study area by clear and unambiguous unconformities that it overprints, it has regular orientation and styles of fabrics, and consistent D3/S3 relationships with respect to earlier structures in the Kalgoorlie district.

7.2 Geographic distribution of gold deposits, mineralisation and alteration

As for stratigraphy and structural geology, the available exposure of mineralisation in the Eastern Goldfields is minimal, thus widely-spaced vertical drilling to fresh or weakly weathered bedrock is used to assess the distribution of alteration elements and minerals associated with clusters of gold deposits. Mineral deposits are generally accepted as unique occurrences where many favourable factors for ore concentration came together in one place, but the tendency of mineral deposits to cluster in camps is a general character of mineral systems, particularly those related to magmatism (e.g. oxidised intrusion related - porphyry) and high-level fault-hosted vein systems (e.g. high sulphidation epithermal; Seedorf et al. 2005; Hedenquist et al. 2000). This tendency to cluster also applies to the greenstone-hosted gold deposits of the Eastern Goldfields Province of Western Australia. Gold deposits in the EGP cluster in camps generally spaced at 30-50 km (Hall 1998, Groves 1993, Weinberg et al. 2004).

In the study area, plots of maximum drill hole intercepts of Au and As in exploration drill holes (Fig. 7.1; Fig 7.2) show two types of spatial Au trends - linear and clustered. The linear trends correlate with certain segments of major shear zones, or with linear belts of favourable host stratigraphy that are apparently unrelated to major domain bounding shear zones. Some of these correlate with intra-domain shear zones (i.e. the Centurion Fault at Binduli; and the Gidji Shear Zone to the north of Kalgoorlie), but those shear zones have no major control on greenstone distribution and are considered to be strain localisation zones related to the regional D3 ENE-WSW contraction. That large segments of the major shear zones have no significant gold mineralisation along them raises questions of their role as regional scale fluid pathways. A non-systematic relationship is also observed on plots of maximum arsenic, which is a pathfinder element in exploration for Archaean lode-gold deposits (Fig. 7.2). Arsenic distribution has a

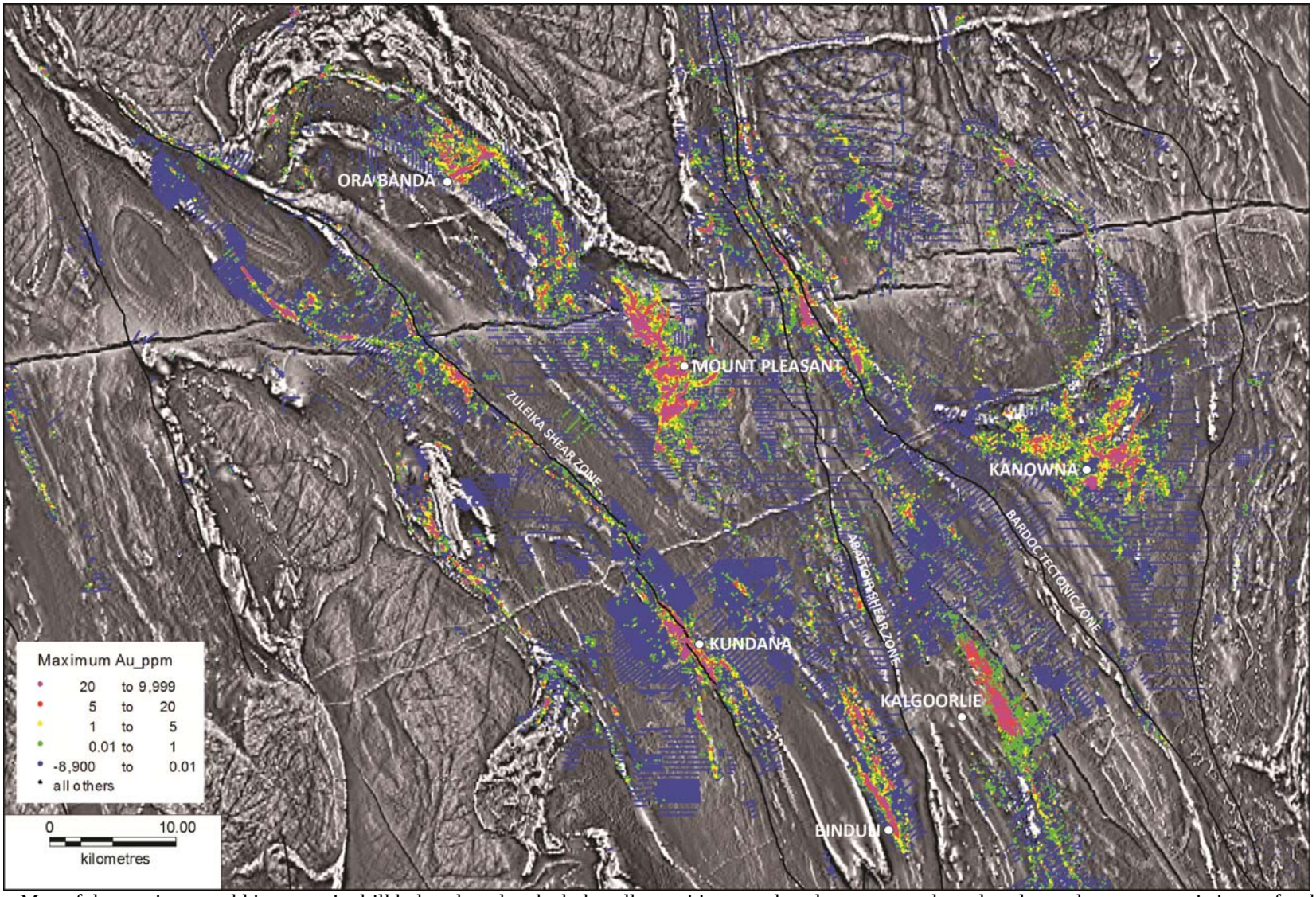

Figure 7.1 – Map of the maximum gold intercept in drill holes plotted at the hole collar position, overlayed on a greyscale, reduced-to-pole aeromagnetic image for the north Kalgoorlie district. Strong linear trends indicate fertility along the Zuleika Shear Zone and other NNW-trending layers in areas distant from major shear zones Note two parallel mineralised trends at Binduli. Drill hole data for the immediate Kalgoorlie area were made available by KCGM.

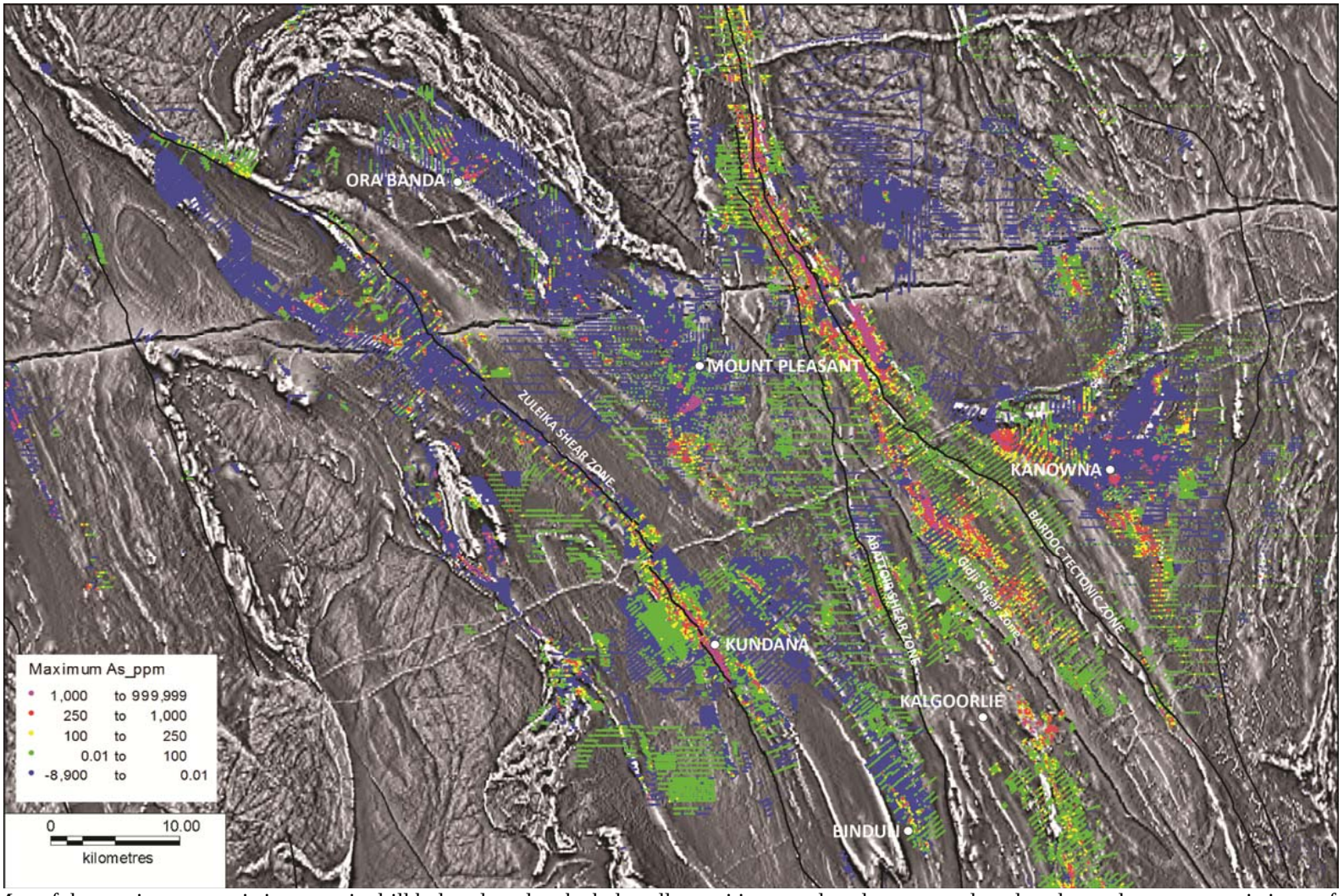

Figure 7.2 – Map of the maximum arsenic intercept in drill holes plotted at the hole collar position, overlayed on greyscale reduced-to-pole aeromagnetic image for the north Kalgoorlie district. Linear trends identify parts of the major shear zones; as well as the Gidji area between the Abattoir and Bardoc shear zones. Significant As is present along the Panglo unconformity to the west of Kanowna. Strong As at Kundana and Paddington (east of Mount Pleasant) is coincident with the presence of black carbonaceous shales in some of those deposits. The Gimlet South deposit at Ora Banda and the Racetrack deposit at Mount Pleasant stand out as localised clusters of >1000 ppm maximum As in drill holes at significant distances from major shear zones.

greater dispersion from ore bearing conduits than gold, and is a useful proxy for mapping the extent of alteration halos to gold deposits. Some intra-domain shear zones such as the Gidji Shear Zone (Fig. 7.2) appear to be much more fundamental channel ways for hydrothermal alteration and mineralisation than for example the domain-bounding Abattoir Shear Zone, and southern segments of the Bardoc Tectonic Zone (Fig. 7.1; Fig. 7.2).

The gold trends on Figure 7.1 show clusters with about 10 km x 10 km dimensions. At Ora Banda and Mount Pleasant those corridors of mineralisation are typified by quartz-carbonate-sulphide vein and breccia lode-gold deposits (Tripp and Vearncombe 2004), whereas there are also significant quartz-sand/pebble palaeochannel gold deposits to the north of Mount Pleasant, and also at Kanowna. Similar 'lode gold' ore styles are present at Kanowna except for the Kanowna Belle gold deposit, which is typified by porphyry-hosted stockwork veins and wallrock disseminated sulphide mineralisation. A strong linear halo of Au and As at the Kundana mines is produced by lithological contact-hosted quartz-carbonate-sulphide laminated shear veins, in deposits that are considered as a typical 'lode gold' style. Two strong linear trends of gold are present at the Binduli mining centre, which are localised along stratigraphic contacts that were voluminously intruded by quartz-feldspar porphyritic intrusions (Fig. 7.1). The As signature of the Binduli deposits is subdued in a similar fashion to the Kanowna region.

A key observation from the empirical data is that some gold deposit clusters are located at significant distances from major shear zones, requiring alternative explanations for mineralisation besides location along transcrustal faults or lower order splay faults (e.g. Ora Banda - Tripp and Vearncombe 2004; the Mount Pleasant deposits; and the Golden Cities group of deposits in the centre of the Scotia Batholith ~30 km north west of Kanowna - Phillips and Zhou 1999). In each of the cited cases, the ore hosting faults post date the major shear zones.

Of those major shear zones, the Zuleika Shear Zone seems to show the most continuous linear distribution of gold mineralisation along it, which is well documented as a zone of major carbonate alteration with localised zones of abundant dykes and stocks of granodiorite and albitite porphyry (Witt and Swager 1989; Tripp 2000). Extensive linear trends of As (also with Zn, Sb) along the Gidji Shear Zone and Panglo unconformity may reflect lithology, in areas with a greater abundance of carbonaceous sedimentary rocks.

7.3 Kundana syn- post-S3 foliation, quartz-carbonate-vein lode and stockwork gold deposits

7.3.1 Introduction

Gold deposits in the Kundana mining centre are shear-laminated, quartz-carbonate-Au-base metal veins, located at lithological contacts in the wallrocks of the Zuleika Shear Zone (Fig. 7.3). Two main ore horizons host gold deposits: a western 'Strzelecki' line and an eastern 'K2' line. The Strzelecki line is dominated by deposits located at dolerite sill / volcaniclastic

rock contacts, whereas the K2 line is dominated by deposits hosted in carbonaceous shale at a mafic-volcanic / sedimentary-rock contact. Kundana gold deposits were first described as a coherent group by Lea (1998). The deposits account for a total 4,935,351 oz gold endowment from over fourteen individual deposits (Table 7.1).

Table 7.1 - Deposit statistics for the Kundana mining centre; data for the Frogs Leg deposit (*) from public resource statements of Cogema Energy.

Deposit	Tonnes	Grade	Endowment (oz)
Raleigh	1,498,000	17.2	828,383
Barkers/21-Mile	4,045,000	6.92	899,944
Strzelecki	1,234,000	13.14	521,316
Arctic	212,000	2.2	14,995
North Pit	3,450,000	2.1	232,932
South Pit	1,225,000	3.7	145,723
Centenary U/G	1,955,000	5.5	345,701
Pope John	955,000	3	92,112
Moonbeam	500,000	4.6	73,947
Drake	100,000	2	6,430
Pegasus	1,291,000	5.2	215,834
Rubicon	1,345,000	7.4	319,996
Hornet	1,623,000	5.4	281,776
Frogs Leg*	4,900,000	6.07	956,260
Total	**24,333,000**	**6.31**	**4,935,351**

Detailed assessments in this study include mine-scale mapping, structural analysis of the Rubicon deposit, and a vein paragenesis study of the collective major deposits (published in a GSWA Record - Tripp 2004); and character sampling, geochemical and structural analysis of high-grade veins from the Raleigh, Barkers/21-Mile and Strzelecki deposits. Samples collected and described in this study from the Rubicon, Barkers and Raleigh deposits were provided to Dr. S. Hagemann for fluid inclusion analysis under contract to Placer Dome/Barrick Gold. Samples from the Rubicon deposit were provided to Dr. N. Vielreicher for SHRIMP U-Pb analysis of hydrothermal phosphates in an attempt to determine an absolute age of mineralisation with AMIRA project P680.

Descriptions for the two main lines of lode at Kundana will focus on the Raleigh gold deposit for the Strzelecki Line and the Rubicon deposit for the K2 Line. Broad structural controls were determined from Placer/Barrick underground face maps at the Strzelecki and Barkers mines.

7.3.2 Lithological and Structural Setting

The stratigraphy at Kundana is deformed into a series of anticlines and synclines that have variously sheared out limbs and fold hinges, whereas abundant way-up information provides control on the gross structure (Fig. 7.3). Much of the deformation is part of the regional F3 folding event that produced a pervasive axial plane cleavage across the district, and later reactivation of contacts and shear zones; however, the location of Kundana close to the long-

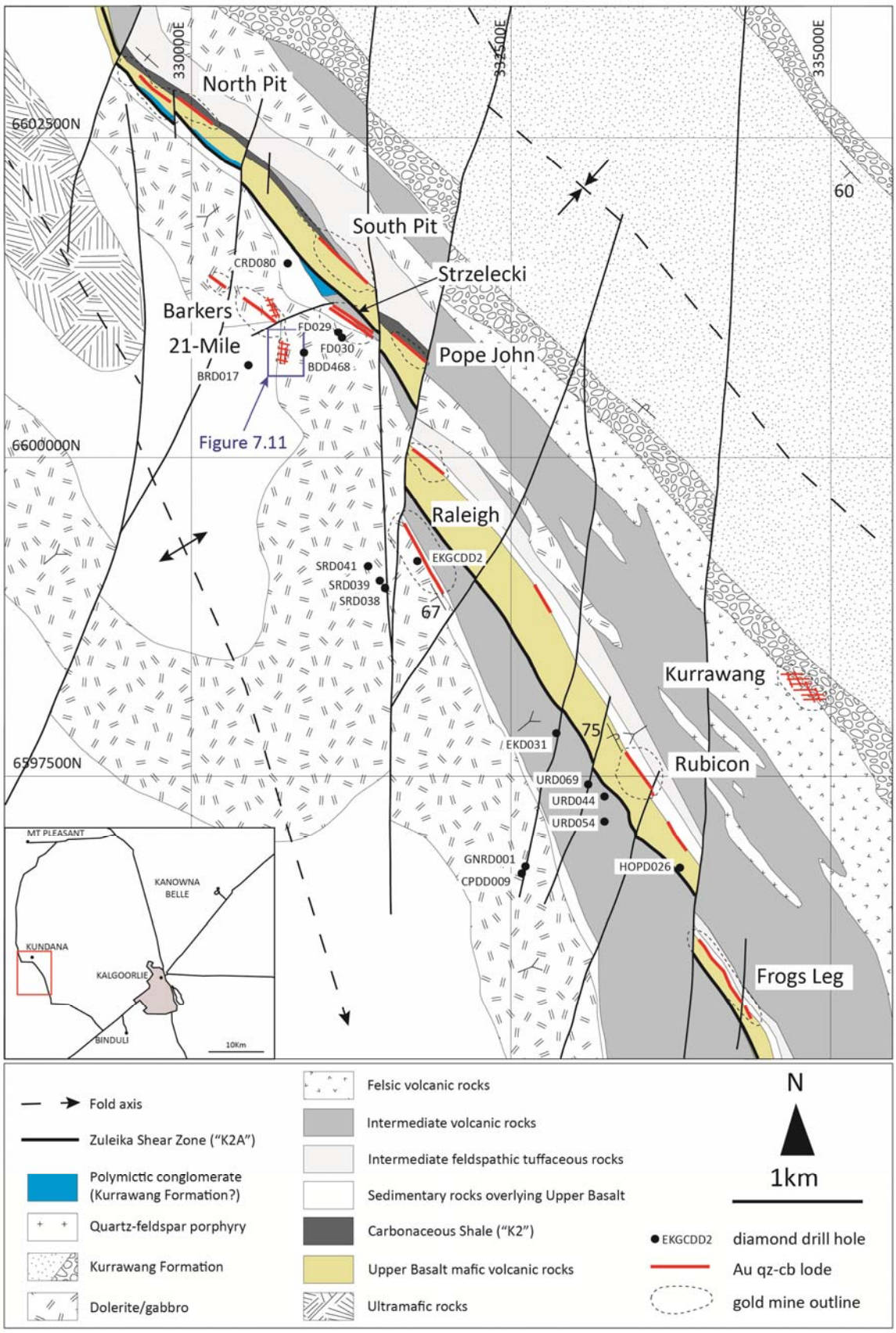

Figure 7.3 – Geology and gold deposits of the Kundana mining district showing location of diamond drill holes logged in this study.

lived Zuleika Shear Zone makes it likely that early deformation of the host sequences was overprinted by later events. The two lines of deposits are separated by the Zuleika Shear Zone and are disrupted by N-S trending faults that cut and offset mineralised lodes. Those faults include the Black Flag and Mary faults documented in Chapter 6.

The Rubicon open pit mine and other deposits on the eastern K2-Line, expose Upper Basalt mafic volcanic rocks and Black Flag / White Flag Formation sedimentary and intermediate volcanic rocks of the Ora Banda Domain (Fig. 7.4); whereas deposits on the western Strzelecki Line are located at the contact of the Powder Sill with meta-sedimentary rocks of the Coolgardie Domain (Fig. 7.3). On the K2-Line, sedimentary rocks in the footwall of the ore bodies, are folded with west-dipping penetrative axial plane foliations (Fig. 7.5a, b) and way-up is to the east indicating a slightly overturned sequence.

Upper Basalt mafic volcanic rocks, in the hanging walls of the ore bodies, are intensely sheared with localised high-strain zones that trend at an angle to the main ore vein, are steeply dipping, and have steep north-plunging mineral stretching lineations defined by oblate plagioclase phenocrysts (Fig. 7.5c, d, e). Cross faults disrupt the main ore veins with up to 11 m of displacement in the Rubicon mine (White Foil Fault; Fig. 7.4), whereas other N-S striking faults offset the stratigraphy with up to 800 m apparent displacement in map view (Fig. 7.3). The White Foil Fault in the Rubicon mine has moderate northeast-plunging stretching lineations in deformed porphyritic Victorious Basalt indicating oblique slip kinematics; hence map-scale offsets do not reflect true displacements.

Mineralization is hosted in 0.3-0.8 m-thick laminated quartz veins along mafic volcanic-sedimentary rock contacts in the mines (Fig. 7.5f, g). ‘Main’ veins in the Rubicon and Barkers deposits have several other associated veins arrays including flats; footwall stockworks; and splay veins that materially affect the grade and location of high-grade ore shoots (Fig. 7.5h). Main veins are best mineralized in areas where disrupted by other vein intersections and micro-faulting of the vein fabrics. Shear zones that meet the Rubicon main ore vein at an angle produce steep south-plunging intersection lineations that may control the geometry and distribution of high-grade ore shoots in that mine.

7.3.3 Mineralisation Styles

7.3.3.1 Quartz Carbonate veins

The main vein at Rubicon (Fig. 7.3) is a laminated shear vein up to 1.2 m thick, but generally on the order of 0.3-0.8 m thick (Fig. 7.5f, g). The vein dips steeply west and in some placed is dipping to the east, but maintains a steep dip of 75-85°. In most exposures, wallrock foliations are truncated against the vein, whereas in some instances the foliation bends into the vein with reverse deflection sense.

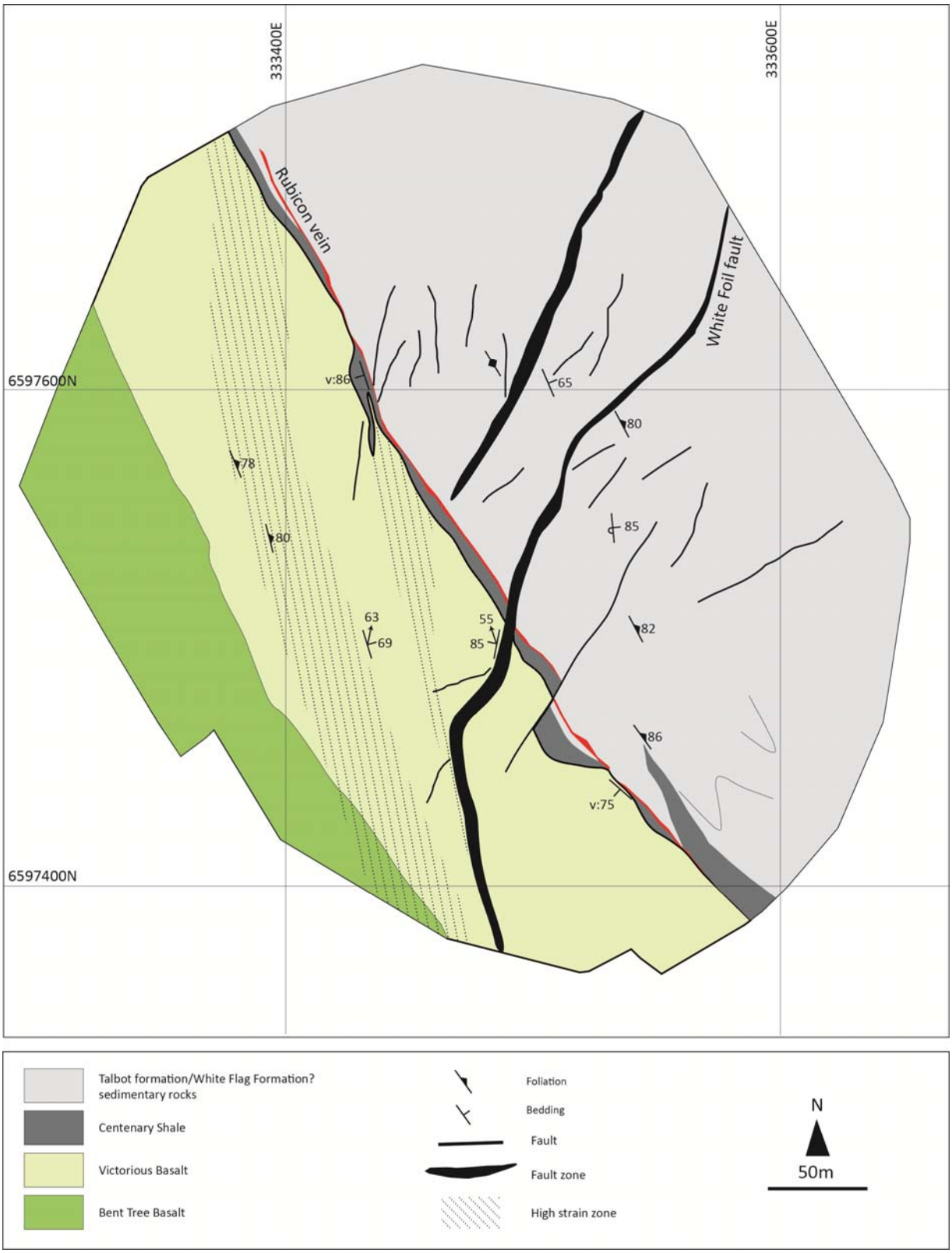

Figure 7.4 – Summary geological map of the Rubicon mine showing the coincidence of the ore vein with the hangingwall contact of the Centurion Shale, and late fault offsets of the ore. Way-up is to the north east.

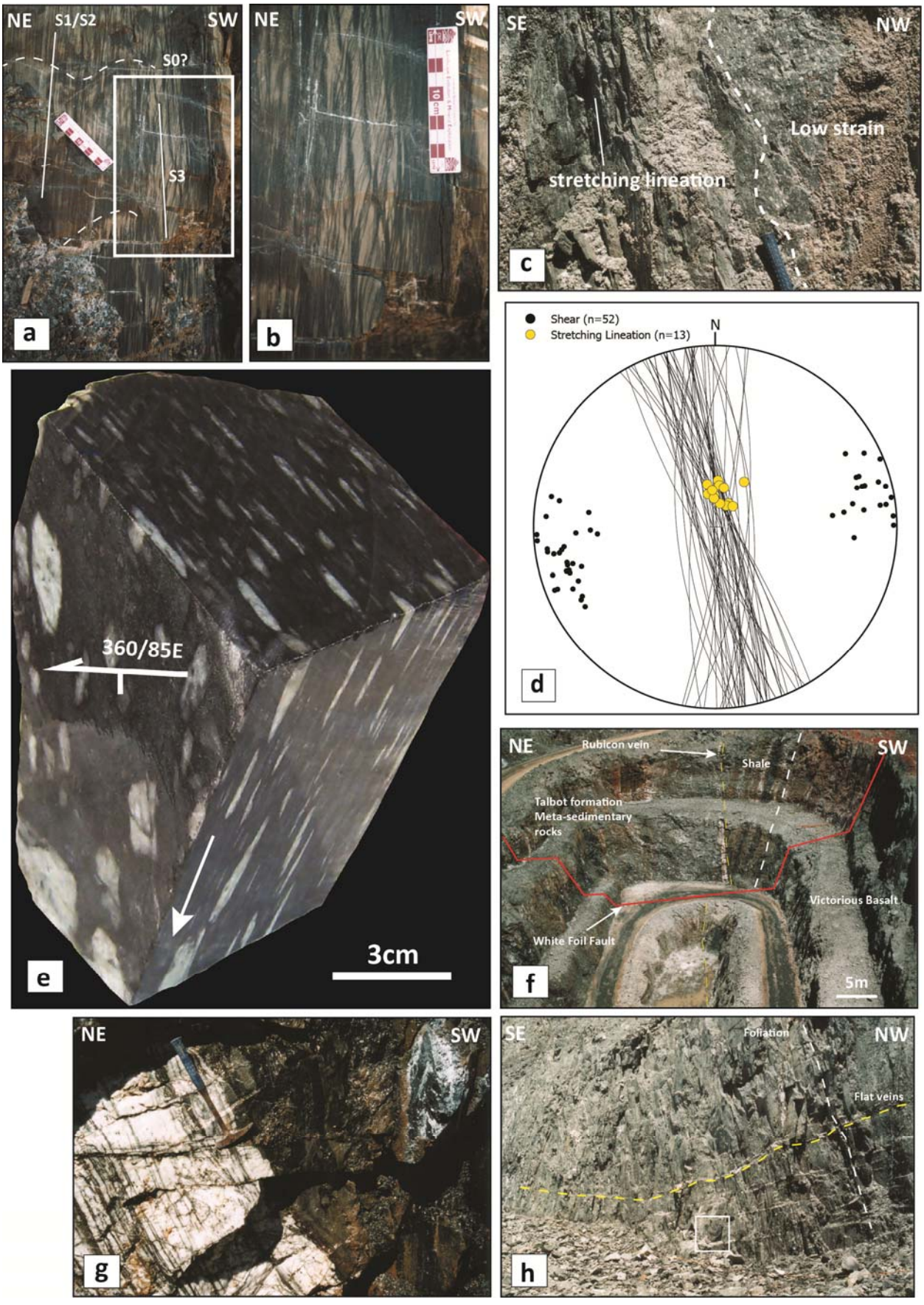
NE
S1/S2
SW
S0?
S3
a
NE
SW
b
SE
NW
Low strain
stretching lineation
c
Shear (n=52)
Stretching Lineation (n=13)
N
d
360/85E
3cm
e
NE
Rubicon vein
Shale
SW
Talbot formation
Meta-sedimentary
rocks
Victorious Basalt
White Foil Fault
5m
f
NE
SW
g
SE
Foliation
NW
Flat veins
h

Figure 7.5

Captions for Figure 7.5

a) Open pit photograph of highly strained metasedimentary rocks. Fine grained sandstone and siltstone of the Talbot Formation directly overlie the Centenary Shale in the Rubicon gold mine. of quartz-rich and mica rich bedding. The metasedimentary rocks contain two well developed foliations (1) an early penetrative mineral alignment and (2) a later spaced foliation defined by dark chloritic bands. The two foliations are very close in orientation and are possibly synchronous with shearing of the rock defining a weak crenulation cleavage and possibly S-C fabric. Bedding in the photo is defined by alternate dark and light bands possibly reflecting original mica content of the rock and is folded into upright folds with S1/S2? axial planar cleavage and a later overprinting S3discrete shear fabric. View to the SE.

b) Close up of section in (a). Viewed with a hand-lens the S1and S2fabrics display very little angular discordance, but are cross-cut and re-oriented by the S3shear bands, which also displace the fold limbs in S0.

c) Intense ductile shear zone in Victorious Basalt. The hammer handle is located at the margin of the shear zone with undeformed porphyritic basalt, which demonstrates a highly localized nature of the strain. A strong steep north-pitching stretching lineation is visible on the shear surface defined by stretched plagioclase phenocrysts.

d) Equal area, lower hemisphere equal area projection of orientations from high strain zones in the Rubicon gold mine showing dominantly sub-vertical NNW-SSE striking shear planes with prominent steep north plunging stretching lineations.

e) Three dimensional oriented block from a high strain zone in the plagioclase-porphyritic Victorious Basalt, Rubicon gold mine. The sample is cut with faces aligned parallel to the X, Y and Z principal axes of shortening. Unstrained samples of the Victorious Basalt show that the plagioclase phenocrysts are equant shapes rather than tabular laths, and display euhedral equi-dimensional crystal habits on all randomly exposed faces. In this respect, the plagioclase phenocrysts are approximately cubic shapes and are an adequate strain marker. The stretching lineation in the rock is steeply north plunging and indicates a high degree of oblate strain during shearing. High strain zones in the western wall of the Rubicon gold mine are localized flattening zones with sharp strain gradients against relatively undeformed rock.

f) Photograph of the southern wall of the Rubicon gold mine showing the 0.8-1.5 m wide Rubicon ‘main’ vein at the contact of Centenary Shale with overlying Talbot Formation metasedimentary rocks to the east. The vein is cut by a late fault with apparent dextral strike slip offset in plan view.

g) Rubicon laminated shear vein in contact with Centenary Shale. The vein contains abundant dark bands that are sheared remnants of wallrock slices (laminations) included into the vein with progressive fracturing and vein precipitation events. Strong chlorite and carbonate alteration overprints the carbonaceous shale in the vicinity of the ore veins. Hammer for scale.

h) Strongly foliated Victorious Basalt in western wall of the Rubicon gold mine overprinted by arrays of shallow dipping quartz-carbonate veins. The flat veins are systematically arranged as a consistently south dipping cluster produced during reverse shearing related to emplacement of the main vein. The intersection lineation of the flats with the main vein plunges shallow south and parallel to the intersection of mineralised wallrock stock work veins, which are arranged in three mutually cross-cutting sets that intersect with a shallow south plunge. Hammer for scale marked by box.

The Rubicon main vein has laminated margins with shear laminations on the footwall side being wider and more intense than shear laminations on the hangingwall side of the vein (Fig. 7.5g). Mineralized footwall flats, stockwork veins and breccia zones in the wallrocks of the main vein contribute to a total ore zone width up to 5 m wide (Fig. 7.5h). Carbonaceous shale in contact with the main ore vein is intensely altered to green chlorite with abundant disseminated, fine-grained pyrite, and coarse-grained arsenopyrite (Fig. 7.5g). The quartz-carbonate vein contains coarse-grained, disseminated galena, sphalerite, scheelite, and tourmaline, locally with bonanza gold grades (Fig 7.6).

Arsenopyrite in the vein is usually contained within wallrock shale slices that were included in the vein during shearing. Arsenopyrite is common in the eastern K2 line, but is uncommon in mines of the western Strzelecki line, which is dominated by base metal sulphides. The difference in sulphide species may reflect variable sulphidation state conditions between the two mineralised horizons given the presence of carbonaceous host units in the K2 line. Abundant arsenopyrite probably reflects a highly reducing nature of the carbonaceous shale rather than the presence of a distinct ore fluid, since trace element analyses indicate elevated As in veins niche-sampled from the Raleigh deposit. Chlorite is the dominant proximal alteration mineral in both K2 and Strzelecki lines of lode.

Raleigh gold mine (Fig. 7.3) exposes a laminated shear vein at the contact of the Powder Sill with sedimentary and andesitic volcanic rocks (Fig. 7.7a, b). This setting is similar to the setting of the Barkers and Strzelecki mines, whereas the Barkers mine is developed primarily at a contact infolded within the western margin of the Powder Sill (Fig. 7.3). Shearing along the lithological contact at the Raleigh mine produced a ~1 m thick ribbon vein, with locally stacked sections over-thickening the vein as seen in underground drives and exploration drill holes (Fig 7.7a). The laminated veins are probable remnants of sigmoidal shear vein arrays preserved at an advanced stage of the shearing. Evidence of this includes large screens of relatively undeformed veined wallrock, preserved as inclusions within the sheared quartz (Fig. 7.7b). Strong localisation of strain may have allowed the original wallrock fragments to be preserved.

The Raleigh vein contains quartz-calcite-Au-pyrite-galena-scheelite and minor pyrrhotite localised along fine laminations and late fractures that overprint the laminations (Fig. 7.8). Late brittle structures that deform the Raleigh laminated veins also control the location of Au and base metal sulphides, which implies a continuing mineralisation event that overlapped laminated vein emplacement and late deformation of the veins (Fig. 7.8).

The white quartz emplacement event in Figure 7.8 contains sphalerite, scheelite and galena, but other polished rocks from the Raleigh mine, and also samples taken from the Strzelecki and Barkers underground mines, show abundant coarse native gold and base metal sulphides contained with within the quartz and localised along stylolitised laminations. Similar

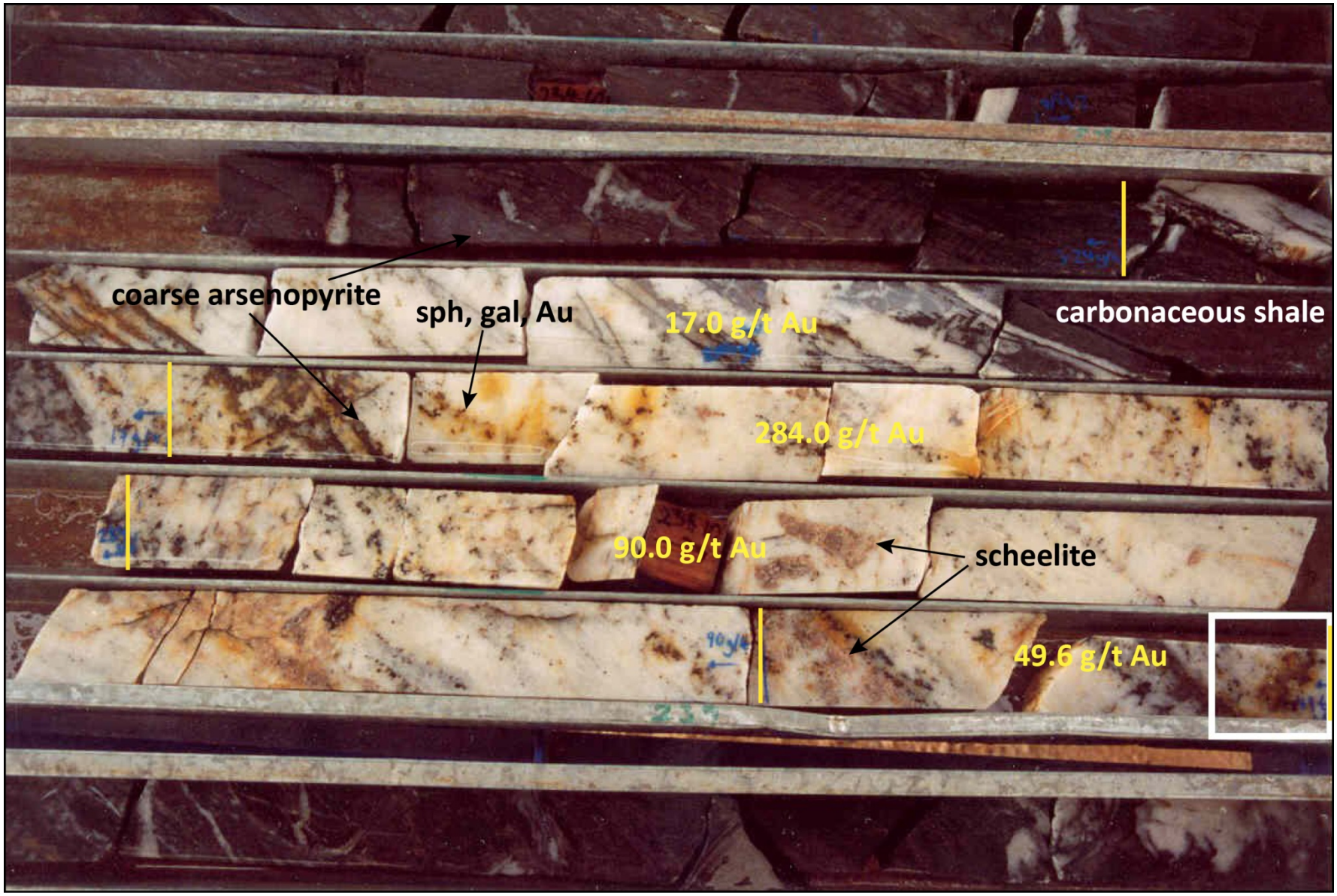

Figure 7.6 – Rubicon high-grade laminated shear vein (4 m @ 85.2 ppm Au) with coarse scheelite, gold and base metal sulphides (URD044 239.5 m).

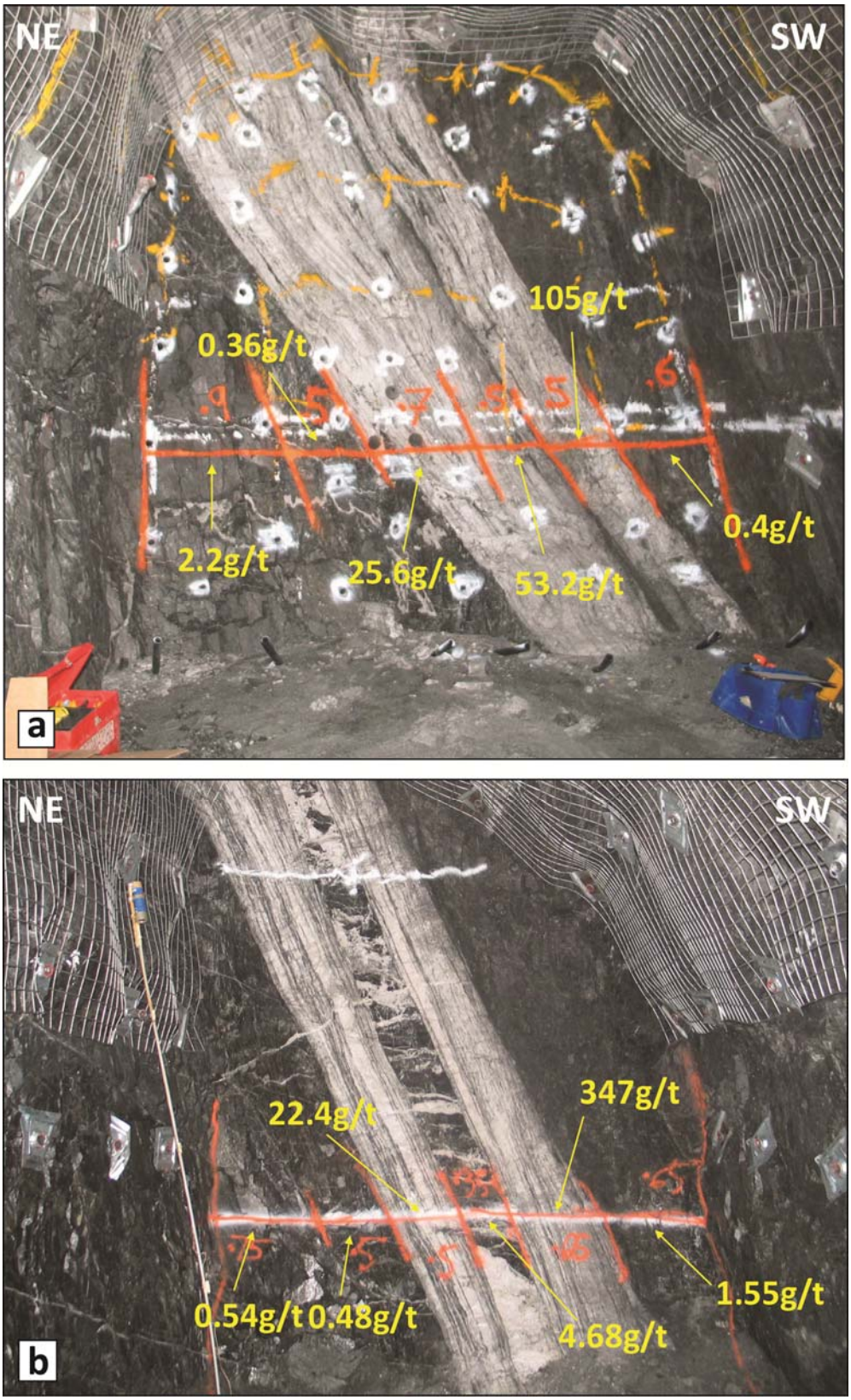

Figure 7.7 – Underground face photographs of the Raleigh vein with face sample intervals for scale (red numbers in metres) and assayed gold grades (yellow: grams per tonne, or ppm Au); a) the ore is contained in a 1-2 m thick laminated quartz-carbonate vein emplaced within a thin metasedimentary unit at a contact between andesite and gabbro; b) bonanza grade, strongly laminated quartz carbonate vein with a large inclusion of rock and extensional veins that may be a preserved remnant of the original extensional shear vein array, progressively sheared to form the finely banded quartz/wallrock ribbon vein. Photos from Placer Dome underground mine face documents (R. Hutchison written communication 2006).

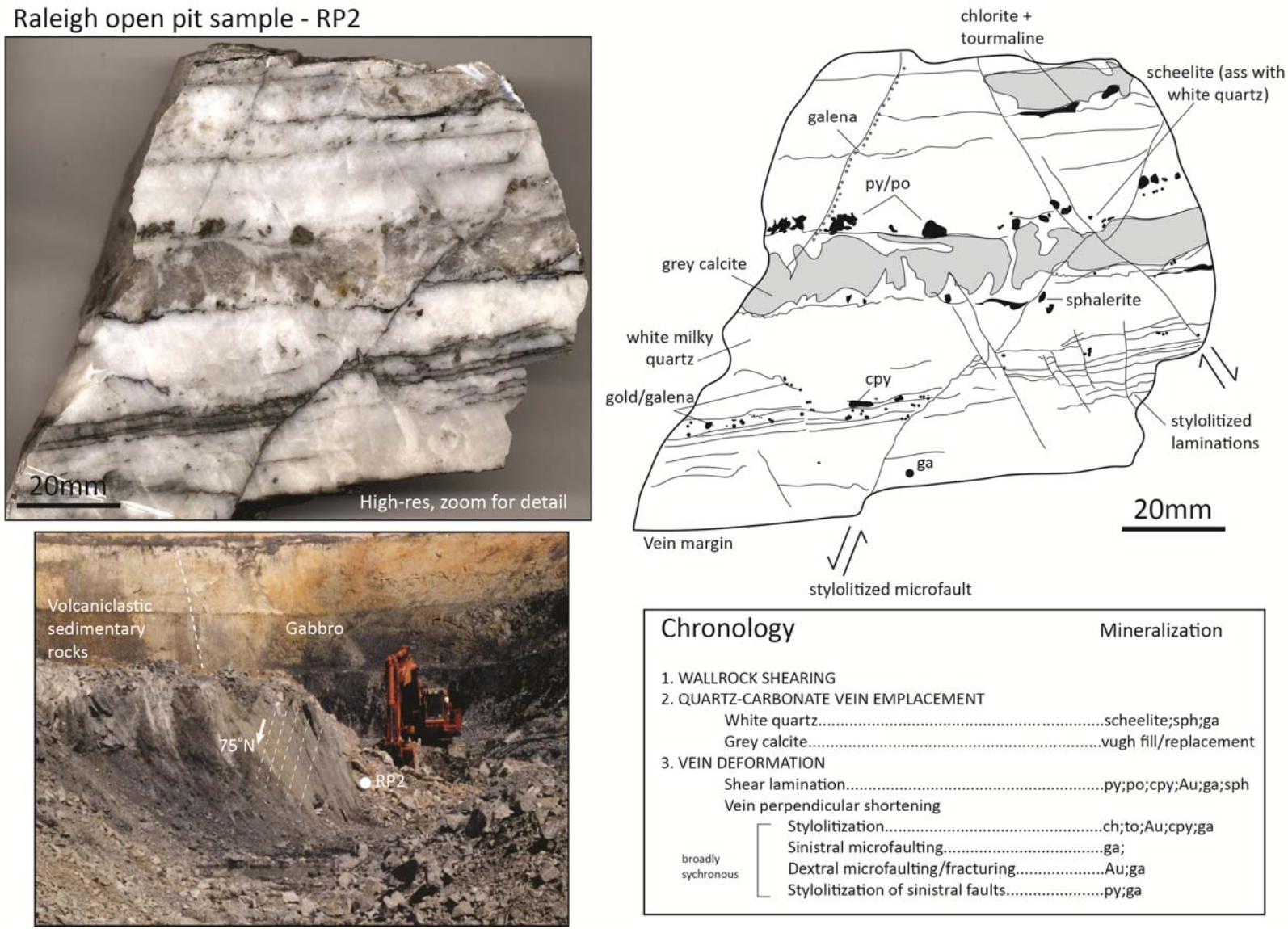

Figure 7.8 - Hand sample from the Raleigh mine with gold and base metals in syn-post vein-emplacement deformation structures. The mine photo shows slickenside lineations on the vein surface pitching ~75°N (View to the south east).

textures are present in the Rubicon vein with coarse gold, scheelite and base metals in laminated and deformed quartz veins (Fig. 7.6).

Reflected light photomicrographs of high-grade ore samples from Rubicon, Raleigh and Barkers mines show a close association of coarse native gold with base metal sulphides and other Fe-sulphides (Fig. 7.9a-h). Native gold is sited in late infill sites with typical triangular infill textures (Taylor 2009; Fig. 7.9 e,f,g,h), as fracture fills peripheral to coarse euhedral arsenopyrite and pyrrhotite crystals (Fig. 7.9a, e), and as indistinct fracture fills in quartz gangue (Fig. 7.9b). Native gold is also present with sphalerite as inclusions within coarse galena filling voids in the vein gangue (Fig 7.9d).

In general the ore stage sulphides and native gold are located in sites that indicate late-stage precipitation in the vein gangue and within late-stage microstructures that deformed the veins. Mineralogy between main stage veins and wallrock flats and stockwork veins is identical providing further evidence for synchronous timing between high-angle, reverse-fault hosted shear veins (Fig. 7.10a) and wallrock flat veins (Fig. 7.10b, Fig. 7.10c; e.g. Sibson et al. 1988).

Drill hole intersections of the ore vein in the Raleigh gold mine display a trend towards higher gold grades where the vein has a NW-SE orientation (Fig. 7.10d). This is confirmed from open pit mine grade control, where a change in orientation of the vein from NNW-SSE to NW-SE is accompanied by increased vein thickness and elevated gold grades.

7.3.3.2 Stockwork veins

In the Rubicon mine, footwall stockwork veins, shear vein arrays, splay veins, and wallrock veins are common. Stockwork veins are generally developed in the footwall of the main vein with several well-defined average orientations (Fig. 7.10c). The veins are simple fracture-fill quartz-carbonate veins (with little or no internal structure), or laminated shear veins. Footwall stockwork veins in drill hole URD044 are distributed over 25 m in three main clusters of gold bearing veins, with a common intersection point of about 15°/145° (Fig. 7.10c). Each of the three clusters is representative of average orientations for the three main ore-stage orientations (V3a/V3b/V4); however, some of the recorded veins have mineralogy typical of the post-ore stage veins (quartz-tourmaline/actinolite). Throughout this stockwork, the highest gold grades are associated with quartz-tourmaline veins; hence, there may be more than one phase of tourmaline vein emplacement; i.e. (1) an early stage synchronous with gold, and (2) a later stage post-dating high-grade gold veins. The intersection point of these three vein sets plunges at about 90° to the average stretching lineation of ductile shear zones in the mine, and is coincident with the intersection direction of wallrock flat veins with the Rubicon main veins. This relationship may indicate that mineralization was synchronous with the shearing that disrupted the main Rubicon ore vein, and generated mineralized footwall stockworks. The Rubicon main vein is best mineralised where it is disrupted at both macro and micro scales.

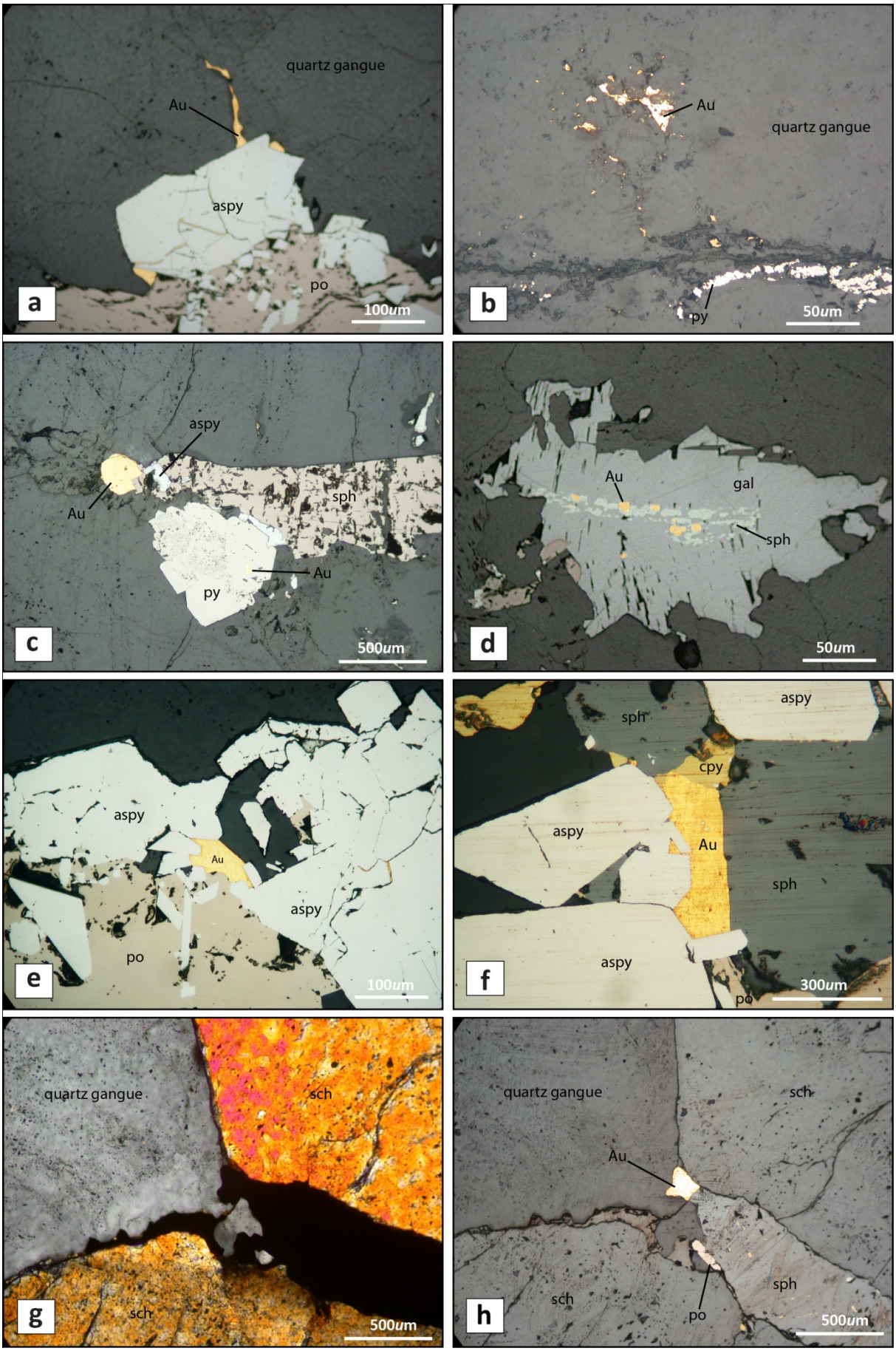
quartz gangue
Au
aspy
po
a
100um
Au
quartz gangue
py
b
50um
aspy
Au
sph
Au
py
c
500um
Au
gal
sph
d
50um
aspy
Au
aspy
po
e
100um
sph
aspy
cpy
aspy
Au
sph
aspy
po
f
300um
quartz gangue
sch
sch
g
500um
quartz gangue
sch
Au
sch
po
sph
h
500um

Figure 7.9

Captions for Figure 7.9 – Reflected light photomicrographs of ores from the Kundana gold mines

a) Reflected light photomicrograph showing native gold infilling fractures in vein quartz and arsenopyrite crystals. Arsenopyrite and pyrrhotite are intergrown within a vein lamination internal to the quartz vein, but gold is sited in late fractures that cut the veins and the contain sulphides. See Figure 7.6 for location of the polished thin section (Rubicon gold mine URD044-237.10 m; GDA:

b) Reflected light photomicrograph of a quartz veins with native gold in fractures and voids within quartz gangue. The lower part of the photomicrograph shows a vein lamination with ragged pyrite and native gold grains, with the majority of the gold showing clear infill textures in voids within the quartz. The vein interval assay returned 62ppm Au over 0.43 m (Raleigh gold mine, SRD041-251.6; GDA: 331528E; 6599283N).

c) Reflected light photomicrograph showing native gold, arsenopyrite, sphalerite and pyrite in within a V4 flat vein. The V4 veins are typically thin fracture fill quartz-carbonate-sulphide veins, with localised sites infilled with native gold and base metal sulphides. Native gold is intergrown with sphalerite and is also present as inclusions in multi-stage pyrite that has inclusion-rich cores and inclusion free rims Barkers Mine (BKD017-160.4 m; GDA: 330588E; 6600880N).

d) Reflected light photomicrograph showing native gold and sphalerite trails within a coarse galena crystal infilling voids in a main ore-stage quartz vein with typical ‘triangular’ infill textures. The galena shows typical cleavage pits parallel to the short axis of the image with native gold and sphalerite oriented across the fabric trend (Raleigh mine, SRD041-251.6a).

e) Reflected light photomicrograph showing native gold void infill within coarse euhedral arsenopyrite and pyrrhotite (Rubicon mine URD044-237.10 m; GDA: 333382E; 6597472N).

f) Reflected light photomicrograph showing native gold void infill with coarse euhedral sphalerite, arsenopyrite, chalcopyrite (Rubicon mine URD044-237.10 m).

g) XPL transmitted light photomicrograph of coarse scheelite (orange crystals) in quartz vein with opaques (Rubicon mine, URD044-238.3 m).

h) Reflected light photomicrograph of same view in (g) showing sphalerite, coarse gold and pyrrhotite infill between coarse scheelite. The native gold occurs as fine grains intergrown with the sphalerite and one small grain in the scheelite gangue (Rubicon mine, URD044-238.3 m).

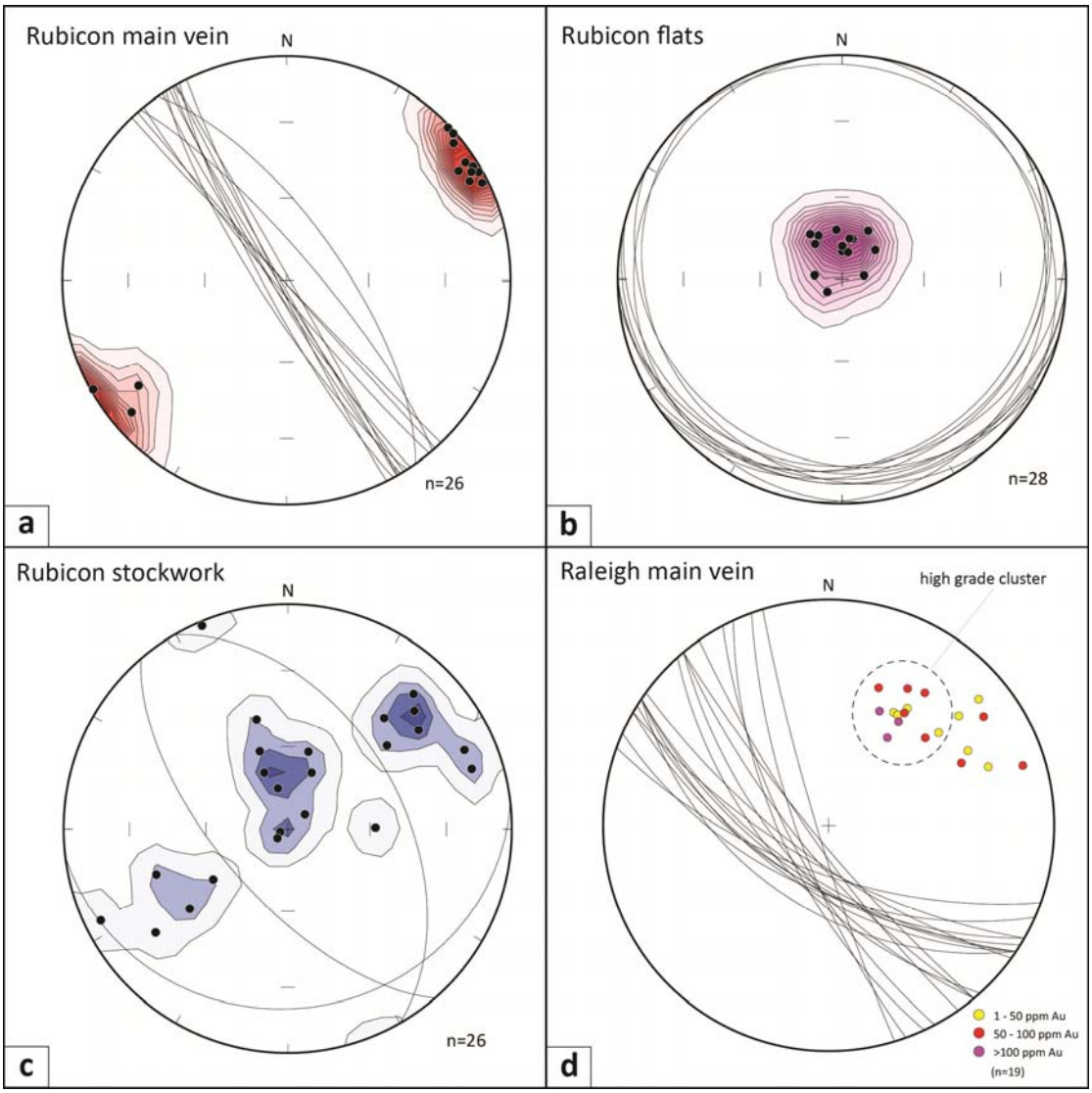

Figure 7.10 – Equal area projections of vein data for the Kundana gold mines; a) main vein measurements for the Rubicon gold mine display an overall very steep south-westerly dip, which cuts across steeply NE-dipping bedding in the mine; b) wallrock flat veins with a dominantly southwards shallow dip in quartz-carbonate veins that are spaced up to 0.5 m in the wallrocks of the main Rubicon vein, the intersection of those veins with the Rubicon main vein is a shallow SE-plunging intersection lineation; c) footwall stockwork veins from Rubicon measured in drill hole URD044 with a common intersection point at about 15º/145º co-linear with the intersection lineation of the flats and main vein; d) Raleigh main vein measurements with poles coloured according to the assay grade of each vein measured; high Au grades are coincident with a cluster of NW-SE trending vein orientations.

At the Barkers mine (Fig. 7.3), the 21-Mile section of the pit exposes a N-S trending contact between Powder Sill gabbro and deformed sedimentary rocks (Fig. 7.3; Fig. 7.11). The contact is a primary intrusive contact, with exposures in the ramp showing injection dykes of gabbro into the sedimentary rocks, and an irregular geometry trending broadly NNE-SSW. Bedding in the sedimentary rocks dips 58º/126º, sub-parallel to the intrusive contact.

Veins occur in three principal orientations: (80º/195º; 29º/098º; 59º/333º) as a uniform stockwork with mutually overprinting vein sets: branching steep veins appear to cross-cut flat veins, but are also cross-cut by the flats (Fig 7.11). Quartz vein stockworks appear to be distributed in spaced clusters of 4-5 m width along the mine wall, and within a preferred unit in the gabbro located above the intrusive contact. Gold-bearing veins occur in all three clusters but are predominant in the steep south-dipping set (Fig 7.11).

Quartz veins are mostly planar to anastomosing, fracture-fill veins with translucent recrystallised quartz and variable amounts of calcite, tourmaline, pyrite and albite(?) lacking any significant wallrock alteration. The veins cut a moderate to intense penetrative chlorite foliation in the gabbro and sedimentary rocks (S3: 85º/086º); strain localisation zones parallel to the foliation have dextral foliation deflection sense with a 35ºN pitching lineation.

7.3.4 Wallrock alteration styles

Silicate alteration in the immediate wallrocks of the K2 and Raleigh veins is dominantly composed of chlorite ± tourmaline ± actinolite, and is accompanied by ore sulphides. Alteration halos are narrow, generally less than 1 m-wide, but up 2 m-wide locally. Chlorite, tourmaline and carbonate crystals (dolomite?) are elongate and aligned within a foliation. Tourmaline is more common in the K2-Line deposits, but is present nonetheless at Raleigh.

Biotite is common in the wallrocks of pre and post ore stage veins, but whether this biotite represents a separate alteration phase is unclear. In drill hole URD054 - 375.1 m there are two phases of biotite: one appears to be part of a pervasive metamorphic assemblage that is ubiquitous in meta-sedimentary rocks, forms a spaced foliation in the quartzofeldspathic rock, and is widespread in its wallrock distribution distal from the high-grade ore veins. A separate phase of coarser grain size, randomly-oriented biotite flakes and calcite crystals, overprints the earlier fabric in the vicinity of ore-stage, V4-flat quartz-calcite veins developed at a high angle to the wallrock foliation.

In some early veins, the development of biotite and Fe-carbonate is particularly strong in the immediate vein halos. Thin sections showing randomly oriented, elongate euhedral biotite crystals overprinting a background wallrock foliation (in drill hole URD069-178 m) suggesting there is more than a single phase of hydrothermal biotite alteration.

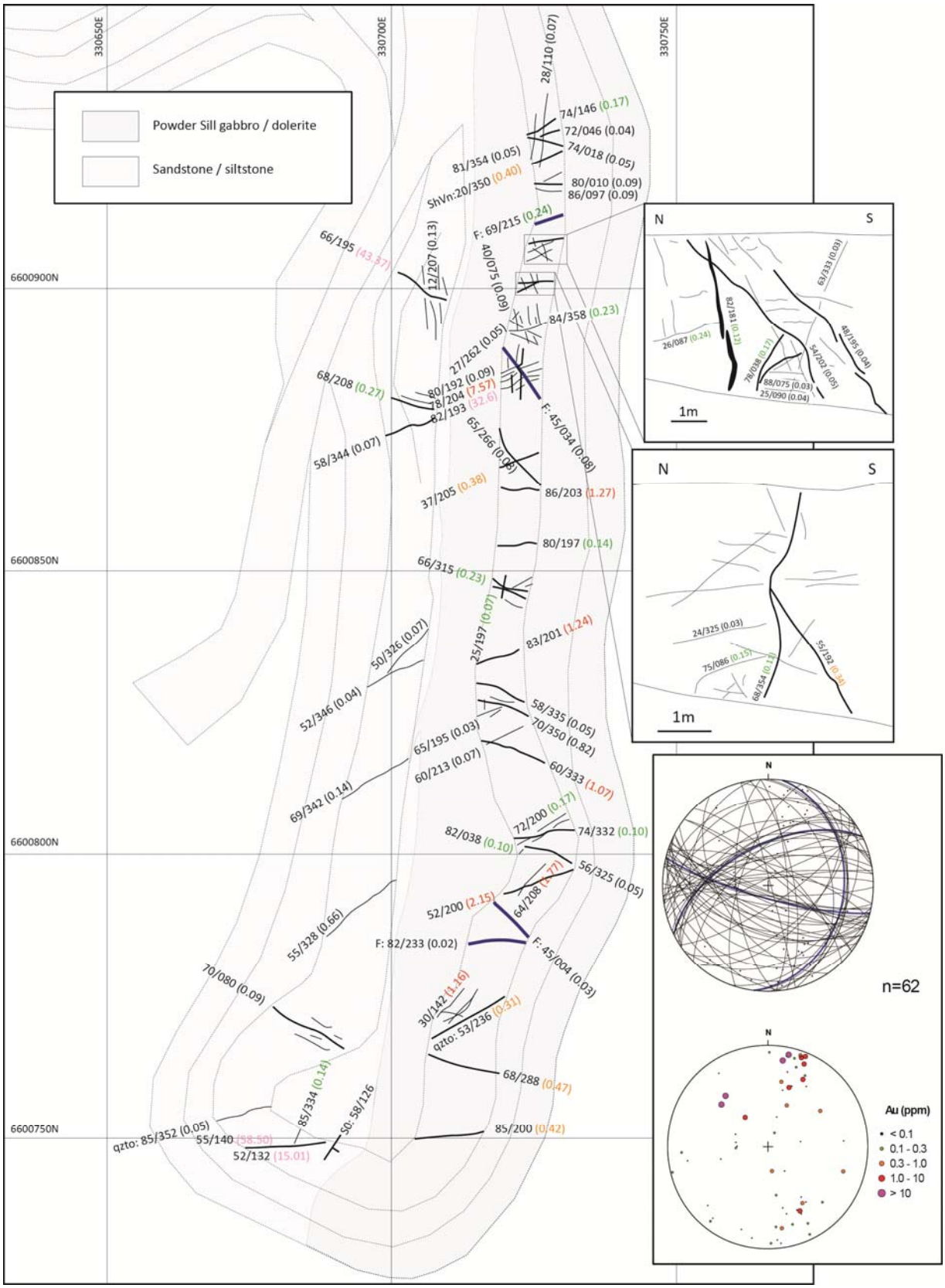

Figure7. 11 - Spatial distribution of gold veins in the 21-Mile gold mine at a contact between metasedimentary rocks and meta-gabbro. Insets show the typical character of stockwork clusters. Grade colours in brackets (ppm Au) match the ranges on the equal area projection where poles to veins are coloured and sized by the Au assay value. Veins cluster into three populations, but the south dipping sets have a dominant control on gold. Assay results are from niche sampled, individual quartz veins to allow an assessment of orientational controls on gold distribution. (See Figure 7.3 for location).

7.3.5 Geochemistry and metal associations

7.3.5.1 Main ore stage veins

Geochemical analyses of the main ore stage veins show a consistent Au-Bi-Cu-Pb-Zn-Te-Sb-W association for the main deposits on the Strzelecki line at Kundana, with low values for Mo, but anomalous As (Table 7.2). Analyses were not collected for the K2 line, but the mineralogy of coarse gold, galena, sphalerite, and abundant arsenopyrite suggests a similar metal association. The main exception to this is elevated arsenic in the carbonaceous-shale related deposits as discussed previously. This suite of metals is consistent with the ore style and metal association of typical lode-gold or 'Orogenic' deposits (Groves et al. 2003). The association of Au with coarse galena is a common observation in lode-gold-style veins throughout the north Kalgoorlie district including the Quarters and Homestead deposits at Mount Pleasant and the WCM veins at Binduli.

7.3.5.2 Multi-element analyses of stockwork veins (Barkers/21-Mile)

Several elements show a correlation with high-grade stockwork veins from the 21-Mile pit including tellurium, tungsten and lead (Table 7.3; Fig 7.12). Other elements including antimony are only weakly anomalous, whereas some such as silver and molybdenum show no relationship to gold bearing veins (Fig 7.12). The occurrence of tungsten and lead in high-grade veins is expected from the known mineralogy of high-grade veins elsewhere in the mining district, and scheelite is a common gangue mineral in veins on both the Strzelecki and K2 trends (Fig 7.9g, h). A lack of correlation with zinc is unexpected since brown sphalerite is commonly observed with visible gold in wallrock flat veins in mines throughout the district.

7.3.5.3 Fluid inclusion studies

Samples constrained by the paragenetic work for this thesis were provided to Dr. S. Hagemann for fluid inclusion analysis under contract to Placer/Barrick. The analysis found three main fluid inclusion groups in the high Au-grade veins from Raleigh:

- Type 1 aqueous, that occur as: (a) two phase, liquid-rich NaCl±KCl inclusions; (b) two-phase, liquid-rich CaCl2±MgCl2±NaCl inclusions; and (c) three-phase, liquid-rich NaCl±KCl inclusions - [Raleigh-RP2].
- Type 2 aqueous-carbonic, that occur as: two- and three-phase, liquid- and vapour-rich H2O-NaCl-CO2±CH4 inclusions - [Rubicon-HK1, Barkers-HK2]; and
- Type 3 carbonic, that occur as mono-phase and two-phase CO2±CH4 inclusions - [Rubicon-HK3, Rubicon-HK12, Rubicon-HK13].

This led to the inference that there is no specific fluid inclusion assemblage that relates to high-grade gold samples (>17ppm Au). There is also no correlation between base-metal content and phase immiscibility in fluid inclusions trapped in the Kundana samples.

Table 7.2 – Multi-element analyses of mineralisation from main-stage ore veins of the Strzelecki Line, in decreasing gold-grade order

Raleigh open pit mine										
Sample#	Au_ppm	As_ppm	Bi_ppm	Cu_ppm	Mo_ppm	Pb_ppm	Sb_ppm	Te_ppm	W_ppm	Zn_ppm
RP4	**579.51**	12	5.54	1323	0.6	2756	19.97	69.5	234.4	2636
RP6	**567.70**	16	5.78	1338	0.6	2829	18.22	68.6	745.2	2623
RP3	**156.93**	4	1.29	276	1.1	398	3.14	55.9	159.3	147
RP1	**103.70**	32	3.33	955	0.5	1219	7.45	48.2	2.4	843
Barkers underground mine										
Sample#	Au_ppm	As_ppm	Bi_ppm	Cu_ppm	Mo_ppm	Pb_ppm	Sb_ppm	Te_ppm	W_ppm	Zn_ppm
B5806S	**158.70**	0.05	21.67	72	0.9	720	1.00	305.3	2.6	181
B5898S	**25.40**	8	0.62	98	4.1	245	3.15	44.6	18.2	169
B6222S	**7.34**	5	0.67	119	2.2	80	1.02	6.7	3.3	228
Strzelecki underground mine										
Sample#	Au_ppm	As_ppm	Bi_ppm	Cu_ppm	Mo_ppm	Pb_ppm	Sb_ppm	Te_ppm	W_ppm	Zn_ppm
S5780	**93.79**	22	2.77	1083	3.0	2914	5.68	29.5	2.3	1411
S5820S	**37.64**	6	0.91	246	1.2	386	1.85	49.1	11.0	116
S5810	**32.84**	5	0.61	508	1.7	342	2.15	10.9	1.2	157
S5780S	**21.18**	54	0.63	81	1.2	204	0.63	6.9	1280.8	506
S5898	**6.94**	1	0.94	160	0.6	273	0.86	7.6	144.3	284

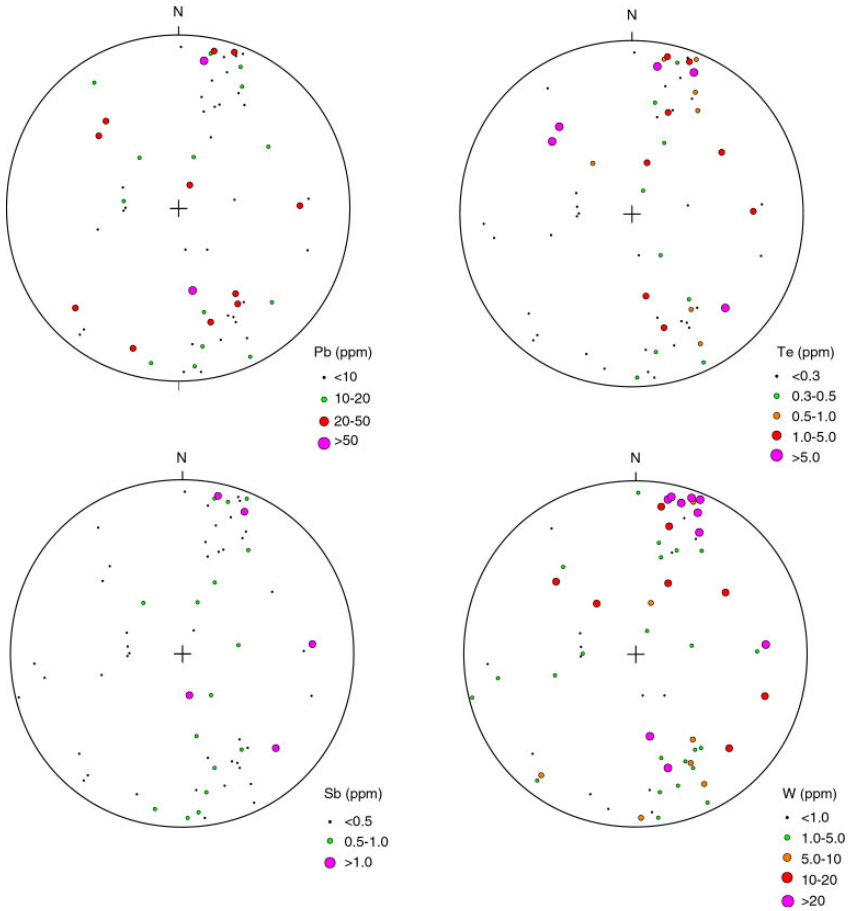

Figure 7.12 – Equal area projections showing comparisons of vein orientations with selected elements related to the observed ore mineralogy of the 21-Mile stockwork veins in the wallrocks of the Barkers main vein. Tellurium, tungsten and lead are elevated in orientations that host high-grade gold.

Table 7.3 – Multi-element analyses of niche sampled stockwork veins from the 21 Mile pit in order of decreasing gold grade.

Sample#	Au	Ag	As	Cu	Mo	Pb	Sb	Te	V	W	Zn
R1481867	**58.50**	0.90	16.70	10.00	2.10	22.00	0.20	7.67	4.00	4.75	21.00
R1481868	**43.37**	3.34	20.80	18.00	2.00	74.00	0.42	63.78	20.00	12.38	238.00
R1481830	**32.57**	0.36	71.10	81.00	2.10	20.00	1.20	2.74	112.00	39.61	59.00
R1481855	**15.01**	0.94	41.30	16.00	2.50	36.00	0.47	8.74	10.00	10.38	30.00
R1481829	**7.57**	0.16	90.00	64.00	2.60	17.00	2.03	5.32	104.00	41.97	53.00
R1481848	**2.15**	0.14	57.70	96.00	2.70	7.00	0.44	3.83	93.00	0.63	43.00
R1481847	**1.77**	0.15	55.10	78.00	1.70	7.00	0.23	0.24	111.00	0.65	63.00
R1481833	**1.27**	0.02	37.90	84.00	2.00	7.00	0.97	0.94	144.00	23.09	60.00
R1481837	**1.24**	0.05	31.50	67.00	2.80	7.00	0.38	3.03	87.00	8.10	89.00
R1481852	**1.16**	0.04	164.10	82.00	1.30	16.00	0.52	0.94	99.00	17.42	177.00
R1481842	**1.07**	0.02	26.40	31.00	4.20	4.00	0.47	0.11	30.00	8.82	32.00
R1481839	0.82	0.03	57.40	59.00	2.40	11.00	0.66	0.46	51.00	4.86	89.00
R1481858	0.66	0.02	106.50	23.00	2.20	36.00	0.60	0.87	19.00	2.04	141.00
R1481853	0.47	0.04	42.30	25.00	1.50	3.00	0.21	0.10	17.00	12.15	12.00
R1481869	0.46	0.18	27.40	17.00	2.30	30.00	0.28	1.24	12.00	2.26	37.00
R1481854	0.42	0.08	200.50	77.00	2.50	30.00	0.46	0.11	74.00	36.21	116.00
R1481808	0.40	0.01	13.80	44.00	0.50	3.00	1.07	0.00	60.00	0.00	44.00
R1481832	0.38	0.04	33.90	47.00	1.60	8.00	0.64	0.36	124.00	10.91	73.00
R1481822	0.34	0.03	21.70	96.00	1.30	6.00	0.47	0.33	125.00	3.20	84.00
R1481851	0.31	0.02	88.80	33.00	1.90	16.00	0.37	1.25	13.00	12.44	12.00
R1481863	0.27	0.10	11.50	16.00	1.30	15.00	0.27	0.73	13.00	41.65	55.00
R1481811	0.24	0.01	21.00	108.00	0.30	11.00	0.69	0.00	101.00	0.00	172.00
R1481812	0.24	0.01	21.80	40.00	0.90	3.00	0.26	0.00	75.00	0.41	98.00
R1481824	0.23	0.06	26.10	94.00	2.40	9.00	0.58	0.33	78.00	8.23	78.00
R1481835	0.23	0.09	92.20	63.00	3.50	19.00	1.05	7.50	107.00	12.17	98.00
R1481817	0.17	0.01	20.30	36.00	2.30	4.00	0.38	0.09	49.00	5.48	68.00
R1481846	0.17	0.05	86.90	156.00	1.30	7.00	0.35	0.19	100.00	0.48	77.00
R1481820	0.15	0.08	10.70	71.00	0.90	5.00	0.48	0.00	143.00	0.42	93.00
R1481834	0.14	0.02	19.00	42.00	4.80	6.00	0.89	0.44	46.00	50.63	24.00
R1481856	0.14	0.04	40.50	10.00	1.50	11.00	0.38	0.31	10.00	2.51	28.00
R1481859	0.14	0.01	11.70	30.00	3.90	4.00	0.22	0.27	15.00	1.17	24.00
R1481864	0.13	0.42	17.00	55.00	1.90	21.00	0.27	0.33	23.00	3.10	117.00
R1481807	0.13	0.04	48.60	96.00	0.40	4.00	0.89	0.00	132.00	-0.05	135.00
R1481813	0.12	0.03	12.80	28.00	4.10	3.00	0.21	0.13	14.00	3.47	18.00
R1481821	0.11	0.09	8.90	45.00	1.80	3.00	0.29	0.23	126.00	0.21	73.00
R1481870	0.11	0.09	138.60	51.00	3.70	125.00	0.87	4.74	19.00	45.87	93.00
R1481844	0.10	0.05	39.00	229.00	1.10	4.00	0.16	0.11	162.00	1.13	73.00
R1481843	0.10	0.01	13.50	30.00	2.20	2.00	0.22	0.53	27.00	7.03	26.00
R1481828	0.09	0.01	50.10	62.00	2.20	10.00	0.79	0.60	99.00	31.22	74.00
R1481809	0.09	0.21	23.20	54.00	2.10	19.00	0.53	0.08	77.00	0.52	93.00
R1481810	0.09	0.01	22.00	53.00	0.80	10.00	0.43	0.00	90.00	0.07	107.00
R1481825	0.09	0.01	20.00	58.00	2.20	5.00	0.44	0.10	116.00	1.28	85.00
R1481866	0.09	0.08	6.20	5.00	1.00	7.00	0.09	0.29	-2.00	4.46	5.00
R1481831	0.08	0.06	30.70	50.00	2.50	8.00	1.10	0.29	49.00	32.71	34.00
R1481827	0.08	0.03	11.50	53.00	1.40	4.00	0.44	0.07	126.00	0.29	76.00
R1481865	0.07	0.03	18.30	9.00	1.20	3.00	0.10	0.41	4.00	7.65	4.00
R1481805	0.07	0.02	21.50	69.00	0.60	5.00	0.33	0.00	107.00	0.00	128.00
R1481836	0.07	0.09	57.50	22.00	3.60	11.00	0.60	3.31	47.00	7.50	41.00
R1481861	0.07	0.10	23.00	31.00	3.40	23.00	0.33	0.42	14.00	5.46	41.00
R1481862	0.07	0.07	29.90	45.00	3.50	20.00	0.97	1.15	10.00	42.67	75.00
R1481841	0.07	0.06	227.70	67.00	4.20	9.00	0.68	0.95	104.00	3.43	81.00
R1481857	0.05	0.02	14.00	7.00	1.30	7.00	0.17	0.19	17.00	2.75	41.00
R1481802	0.05	0.04	31.80	105.00	5.00	39.00	0.48	0.00	110.00	0.00	96.00
R1481845	0.05	0.01	9.10	11.00	2.10	2.00	0.13	0.00	11.00	1.00	9.00
R1481806	0.05	0.02	38.30	71.00	1.90	11.00	0.71	0.00	91.00	0.08	85.00
R1481838	0.05	0.01	12.50	13.00	2.50	3.00	0.16	0.16	11.00	3.49	10.00
R1481826	0.05	0.01	12.40	35.00	4.90	3.00	0.72	0.05	53.00	1.09	45.00
R1481814	0.05	0.01	24.10	43.00	2.60	4.00	0.35	0.05	54.00	2.27	46.00
R1481803	0.04	0.17	23.50	65.00	1.40	14.00	0.34	0.00	100.00	0.06	113.00
R1481815	0.04	0.01	32.40	41.00	3.40	5.00	0.41	0.00	38.00	4.39	38.00
R1481860	0.04	0.01	9.60	19.00	1.50	12.00	0.26	0.08	14.00	3.35	57.00
R1481804	0.04	0.02	31.20	63.00	3.10	24.00	0.43	0.06	81.00	0.00	92.00
R1481818	0.04	0.05	28.20	48.00	1.90	6.00	0.43	0.05	69.00	3.79	87.00
R1481849	0.03	0.01	2.10	98.00	0.80	1.00	0.22	0.07	80.00	0.18	37.00
R1481816	0.03	0.01	32.20	67.00	1.20	6.00	0.37	0.06	83.00	2.48	122.00
R1481823	0.03	0.03	15.20	46.00	2.30	4.00	0.74	0.34	133.00	0.75	88.00
R1481840	0.03	0.19	13.60	17.00	3.70	3.00	0.15	0.08	17.00	10.22	19.00
R1481819	0.03	0.02	24.10	32.00	6.00	3.00	0.45	0.06	25.00	3.98	22.00
R1481850	0.02	0.01	8.00	73.00	0.90	3.00	0.59	0.00	75.00	0.87	47.00

Unmixing (phase immiscibility) in the gold-related quartz vein system was interpreted by Dr. Hagemann at about 253 ±25° C, and 190 ±40 MPa. The T-P conditions were remarkably well constrained in three quartz vein samples (HK3,HK12, and HK13 - all from the Rubicon deposit) where unmixing was established. Depth of vein formation during unmixing was interpreted at between 5 to 8 km assuming lithostatic fluid pressures.

7.3.6 Timing of Mineralisation

The relative timing of mineralisation at Kundana is determined by vein paragenesis and structural cross-cutting (Table 7.4). Paragenesis work mostly comprised drill core re-logging of 13 drill holes from mines on the Strzelecki-line and 12 drill holes on the K2-Line, with mine mapping and polished thin section analysis (Fig. 7.3). Samples of the Rubicon vein were provided to the AMIRA P680 project for SHRIMP U-Pb analysis of hydrothermal phosphate.

7.3.6.1 Vein paragenesis

The earliest veins are crustiform veins (Fig. 7.13a, b, d), with quartz-carbonate-albite-sulphide mineralogy, and deformed quartz-carbonate±albite±pyrite-pyrrhotite veins. Early planar veins were deformed by the regional penetrative fabric-forming event and the veins are commonly folded with an axial planar cleavage, and boudinaged within the foliation (Fig. 7.13a). Since that cleavage is axial planar to the earliest stage of veins in the Kundana corridor, and the regional scale folds, it is possible that those veins are remnants of a hydrothermal system that existed prior to the deformation that formed the current structure of the district.

Ore stage veins occur in three generations that are essentially synchronous: laminated shear veins (Fig. 7.13c); rare conjugate laminated shear veins; and thin flats formed during reverse faulting. Gold mineralisation occurred late in the main vein emplacement event in small-scale fractures and faults related to vein formation and deformation (Fig. 7.8). Reactivation of vein laminations with moderate north-plunging slickenside lineations (defined by gold, related sulphide minerals, and chlorite) indicates a different kinematic event to the vein emplacement. Gold also occurs sited in small-scale faults and fractures that offset and displace the main ore veins (Section 7.3.7).

Gold bearing veins are overprinted by several post-ore vein generations distinguished by the presence of actinolite, tourmaline, or chlorite-hematite (Table 7.4). Tourmaline is a dominant mineral in the main ore-stage veins, but also occurs in planar veins that cut across laminations and is therefore late- to post-ore, since veins of this type occur without gold in areas away from the main ore veins (Table 7.4).

Table 7.4 – Summary of vein paragenesis for the Kundana Mines, the lower replication contains highlighted diagnostic characters for each vein stage.

Stage	Vein Generation	Mineralogy	Texture	Morphology	Alteration	Orientation	Other
Pre - Ore	V1	qz-cb	comb-fibre crustiform	sheared/folded	biotite	2 clusters 84/309; 65/210	ubiquitous
	V2a	qz-cb-ab	euhedral	crack fill planar	carbonate alteration	Variable with common intersection	
	V2b	qz-cb-po-py	recrystallised	planar	bi,cb	variable	
Main Ore - Stage	**V3a**	**qz-py-sph +/-aspy-po-ax**	**laminated**	**sheared / crack fill**	**bi (none)**	**variable dip to 050**	**conjugate to V3b**
	V3b	**qz-sph-ga-Au (to?)**	**laminated**	**shear / breccia**	**(to?) none, locally ch-aspy**	**steep southwest dip 72/235; 84/227**	**Main Ore Stage**
	V4	**qz-sph-Au**	**recrystallised**	**crack fill**	**none**	**shallow stockwork 18/360; 18/180**	**Main / 2nd ore stage**
Post - Ore	V5	qz-act-py-po +/-cpy-aspy	recrystallised	crack fill	bi-cb, ms @ Barkers	variable; strong cluster 66/235	
	V6	qz-cb-to-py-(Kfd?)	recrystallised infill	crack fill	bi-ch	variable; strong cluster 1/360	Commonly overprints V3b
	Other rare veins	qz-ch-ca	infill / cavity	infill / cavity	none	variable	late
		qz-cb-hm	recrystallised	shear / breccia	hematite	variable	localised

Diagnostic properties

Stage	Vein Generation	Mineralogy	Texture	Morphology	Alteration	Orientation	Other
Pre - Ore	V1	**qz-cb**	**comb-fibre crustiform**	sheared/folded	biotite	2 clusters 84/309; 65/210	ubiquitous
	V2a	qz-cb-**ab**	euhedral	crack fill planar	carbonate alteration	Variable with common intersection	
	V2b	qz or qz-cb-po-py	recrystallised	planar	bi,cb	variable	
Main Ore - Stage	**V3a**	qz-py-sph +/-aspy-po-ax	**laminated**	sheared / crack fill	**bi (none)**	**variable dip to 050**	conjugate to V3b
	V3b	**qz-sph-ga-Au (to?)**	**laminated**	shear / breccia	(to?) none, locally ch-aspy	**steep southwest dip 72/235; 84/227**	Main Ore Stage
	V4	**qz-sph-Au**	recrystallised	**crack fill**	none	**shallow stockwork 18/360; 18/180**	Main / 2nd ore stage
Post - Ore	V5	qz-**act**-py-po +/-cpy-aspy	recrystallised	crack fill	bi-cb, ms @ Barkers	variable; strong cluster 66/235	
	V6	qz-cb-**to**-py-(Kfd?)	recrystallised infill	**crack fill**	bi-ch	variable; strong cluster 1/360	Commonly overprints V3b
	Other rare veins	qz-**ch**-ca	infill / cavity	infill / cavity	none	variable	late
		qz-cb-**hm**	recrystallised	shear / breccia	hematite	variable	localised

.

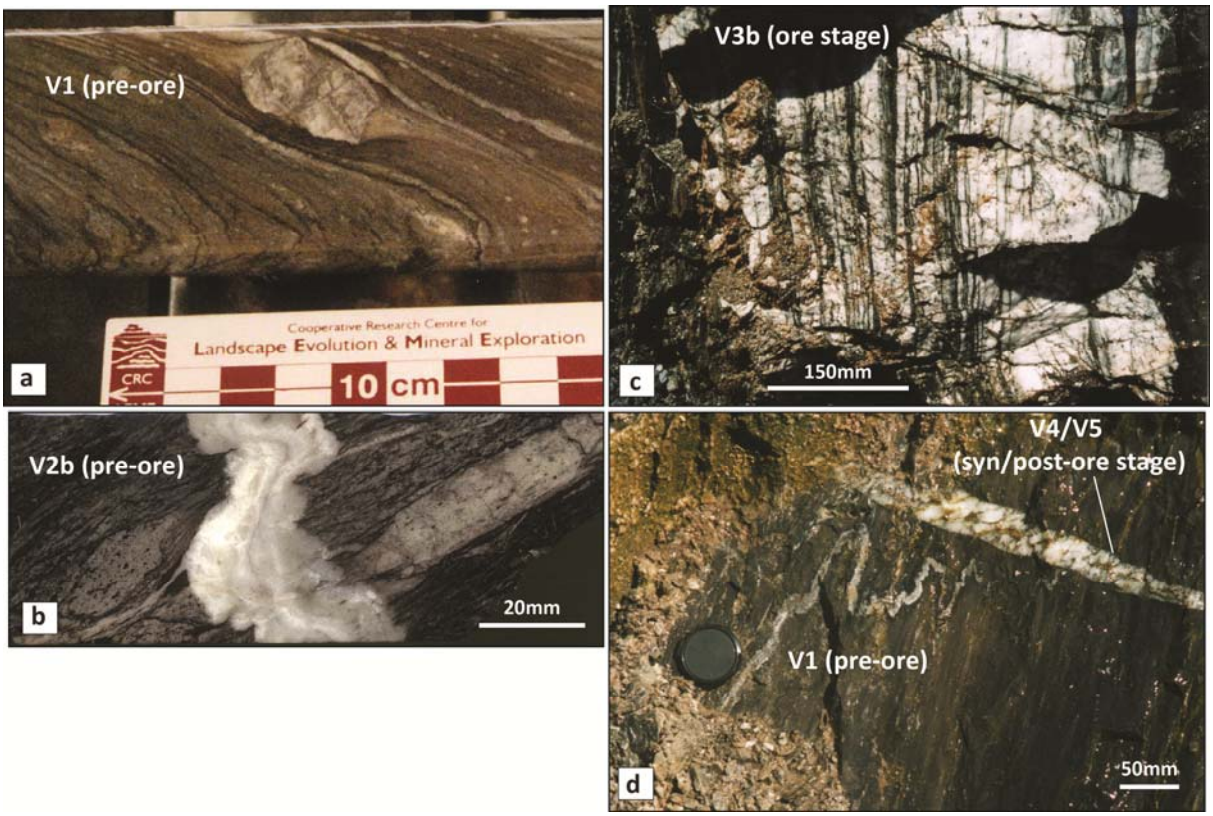

Figure 7.13 – Examples of cross-cutting relationships in pre /syn / post ore stage veins; a) pre-ore sheared and boudinaged crustiform carbonate vein URD069 128 m; b) pre-ore, folded, banded quartz-carbonate sulphide vein cutting lapilli andesite, with axial plane foliation SRD039 269.4 m; c) ore-stage V3b laminated quartz-carbonate shear vein, Rubicon gold mine; d) ptygmatically folded pre-ore crustiform carbonate V1 vein with axial planar foliation cut by late ore-stage V4 or V5 quartz-sulphide post-ore stage vein (no gold or base metal sulphides observed), Rubicon gold mine.

7.3.7 Structural characteristics of the ores

7.3.7.1 Vein thickness, geometry and gold distribution

Veins in the Strzelecki and Barkers mine trend 310° and dip 60°-70° southwest. Underground mine geologists verbally confirmed that the grade of the ore dies out where the strike orientation of the vein moves away from this trend. Small kinks in the vein localised thick vein intersections. The thickest portions of the veins form semi-continuous steeply 60°-65° southeast-pitching pipes, where the veins attains thicknesses of >0.5 m (Fig. 7.14a).

The veins in the Kundana mines display a well-developed shallow north-plunging slip lineation that is manifest as slickenside grooving on the vein surface (Fig. 7.14a). In underground exposures at the Barkers mine the lineation pitches 25°-35°N in the plane of the vein and this orientation is observed everywhere throughout the mines (B. Rayson and H. Hadlow, personal communication). The slip vector of the veins is about orthogonal to the trend of the thickest portion of the veins suggesting the majority of the quartz was emplaced with oblique movement sense. Preferential opening along the fault produced dilational jogs and probably facilitated thick quartz precipitation at 90° to the slip vector, with development of breccia and cataclasite typical of extremely high fluid pressures (e.g. Sibson 1987).

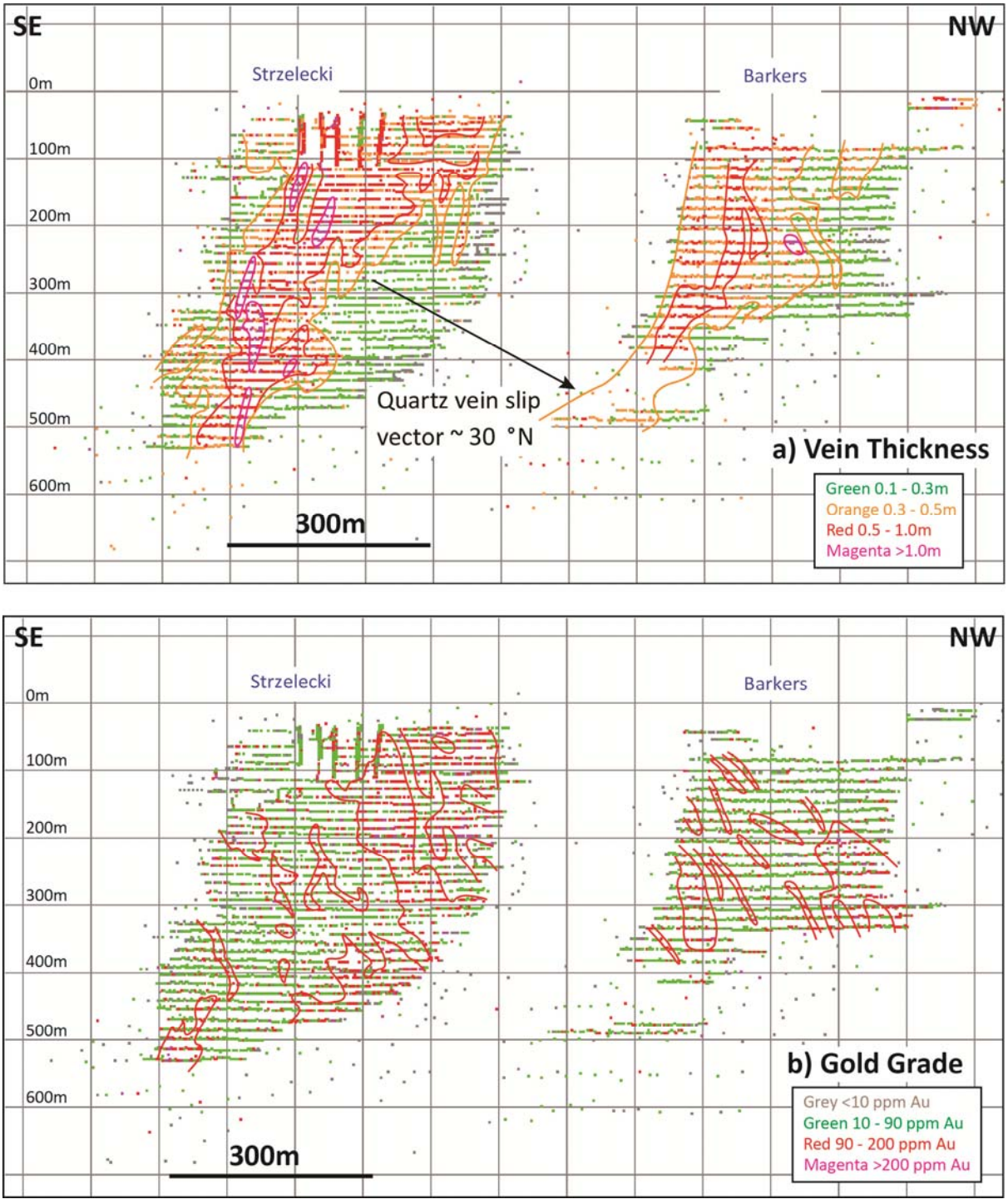

Figure 7.14 – Longitudinal sections through the Strzelecki and Barkers ore bodies from point samples at underground face locations; a) vein thickness showing dominantly steep south plunging zones of greatest veins thickness developed at ~90 to a prominent slickenside lineation on the vein surface, produced by sinistral reverse brittle-ductile shearing during vein emplacement; b) gold grade showing high grade gold ore shoots with a moderate plunge to the north, probably related to late reactivation and vein deformation.

The distribution of gold grades is erratic in the Barkers and Strzelecki veins (Fig. 7.14b) and whereas the very high grades seems to show no direct relationship to vein thickness, the presence of gold grades >10 ppm Au correlates generally with a vein thickness of >0.1 m. Small localised very-high-grade shoots appear in the extreme north and south ends of both ore-bodies that have steep-to-vertical north pitches (Fig. 7.14b). This orientation of the highest grades may be related to brittle-ductile shearing since these high-grade shoots are sub-parallel to the principal stretching lineation of the Zuleika Shear Zone. That orientation is also sub-parallel to lineations on the Raleigh veins defined by coarse native gold and base-metal sulphides (Fig 7.15). At several places in the Barkers gold mine, small thin shear bands transgress the laminations within the ore vein suggesting a later timing for the shear bands.

Stratigraphic horizons would have failed during reactivation (eg. enforced shearing; Robert et al. 1994) and the emplacement of veins during such movements would have produced the characteristic brittle-ductile deformation style. The K2-line South and North ore bodies may have had a closer relationship to the Zuleika Shear Zone since they are developed in veins on sheared carbonaceous shale contacts in the vicinity of the high strain zone. The ore bodies are therefore located on contacts that almost certainly failed during the ductile deformation yet this early failure was not necessarily related to ore formation. A lack of coincidence between the thickest portions of the veins and the highest-grade areas indicates that some other factor controlled the location of the high-grade ore shoots. Later shear laminations that crosscut the veins may provide this connection.

An alternative hypothesis was advanced by Hadlow (1990) who observed that the highest grade portions of the South gold mine were located where 345°-350° trending intense foliation zones intersected the main vein / contact. Those foliation zones appear to be approximately axial planar to shallow, south-plunging tight-to-isoclinal folds in the wallrocks of the South gold mine: a relationship that is repeated at most ore bodies on the K2 line including Rubicon (Fig. 7.4).

Folds in the K2 ore horizon are developed in black shale and chert layers that plunge 20°/150°. This fold orientation is about parallel to regional F3 folds, but is at about 90º to minor folds in the Arctic pit that plunge parallel to the principal stretching lineation in the adjacent Zuleika Shear Zone (Chapter 5). A possible interpretation is that ENE-WSW shortening produced upright F3 folds that were progressively rotated into parallelism with the principal extension direction of the finite strain ellipsoid, as the strain was partitioned into D3 ductile shear zones. The presence of those folds in the ore horizon contact may have induced anisotropy at a mine-scale, which localised high-grade ore shoots in the veins. At a mine camp scale the presence of the small F2 anticline formed in the Powder Sill may have provided an induced anisotropy in which locally-high degrees of pure shear affected regional strain and fluid flow patterns and focussed fluids into the actively deforming stratigraphic horizons at Kundana.

7.3.7.2 Vein kinematics

Structural analysis of the Kundana veins reveals clear kinematic stages in the vein development. Ductile shearing at NW-SE trending lithological (and vein) contacts shows reverse movement sense (Fig. 7.15); this combined with moderately south plunging mica defined stretching lineations, suggests dextral kinematics during vein emplacement. The marginal shear zones of the Raleigh vein preserve the original *dextral* vein emplacement kinematics, whereas later vein deformation has produced a *sinistral* kinematic sense (Fig. 7.15). Similar relationships are observed in oriented drill holes at the Rubicon mine with reverse-sense foliation deflection and a shallow south-plunging mica-sulphide defined stretching lineation, whereas internal vein deformation laminae have moderate north-plunging lineations.

Wallrock shear zones are possibly part of the initial vein emplacement event, characterised by sigmoidal shear vein arrays in multiple hydrothermal episodes, that were deformed during progressive shearing, and resulted in thick (0.5-1.2 m) laminated veins (Fig. 7.7a), with wallrock inclusions (Fig. 7.7b). The pervasive regional fabric is truncated at the margin of ore-stage veins in the Rubicon mine with an incident angle of ~20º (Fig. 7.4), hence the ore-stage veins are considered syn- to post-folding and post the peak of metamorphism. Retrograde hydrothermal wallrock assemblages of chlorite-arsenopyrite on the K2-Line support that timing.

7.3.7.3 Cross-cutting and overprinting relationships

The timing and paragenetic history appears to be one of continuous regional shortening and vein deformation, punctuated by episodes of fluid overpressure. Kinematic interpretations indicate some change in the shear sense on the lodes between deformation and mineralisation increments. At each successive phase of regional shortening it is conceivable that earlier formed structures were reactivated since there appears to have been a broadly consistent shortening direction. This reactivation may include foliation reactivation, fold tightening, fault/shear zone reactivation, and further vein deformation. Table 7.5 summarises the main events in the development of the Kundana deposits, with examples of various paragenetic vein stages in Figure 7.13a-d.

Table 7.5 – Compilation of interpreted stages in the formation of the Kundana vein deposits

	Deformation increment	**Fabric**
1	E-W regional shortening	penetrative foliation/folding
2	fluid overpressure	V1 crustiform veins
3	E-W regional shortening	dextral shearing /thrusting
4	fluid overpressure	main veins on lithologic contacts
5	E-W regional shortening	vein deformation
6	fault valving	flat veins V4/V5?
7	E-W regional shortening	shear vein arrays V6
8		cross faults

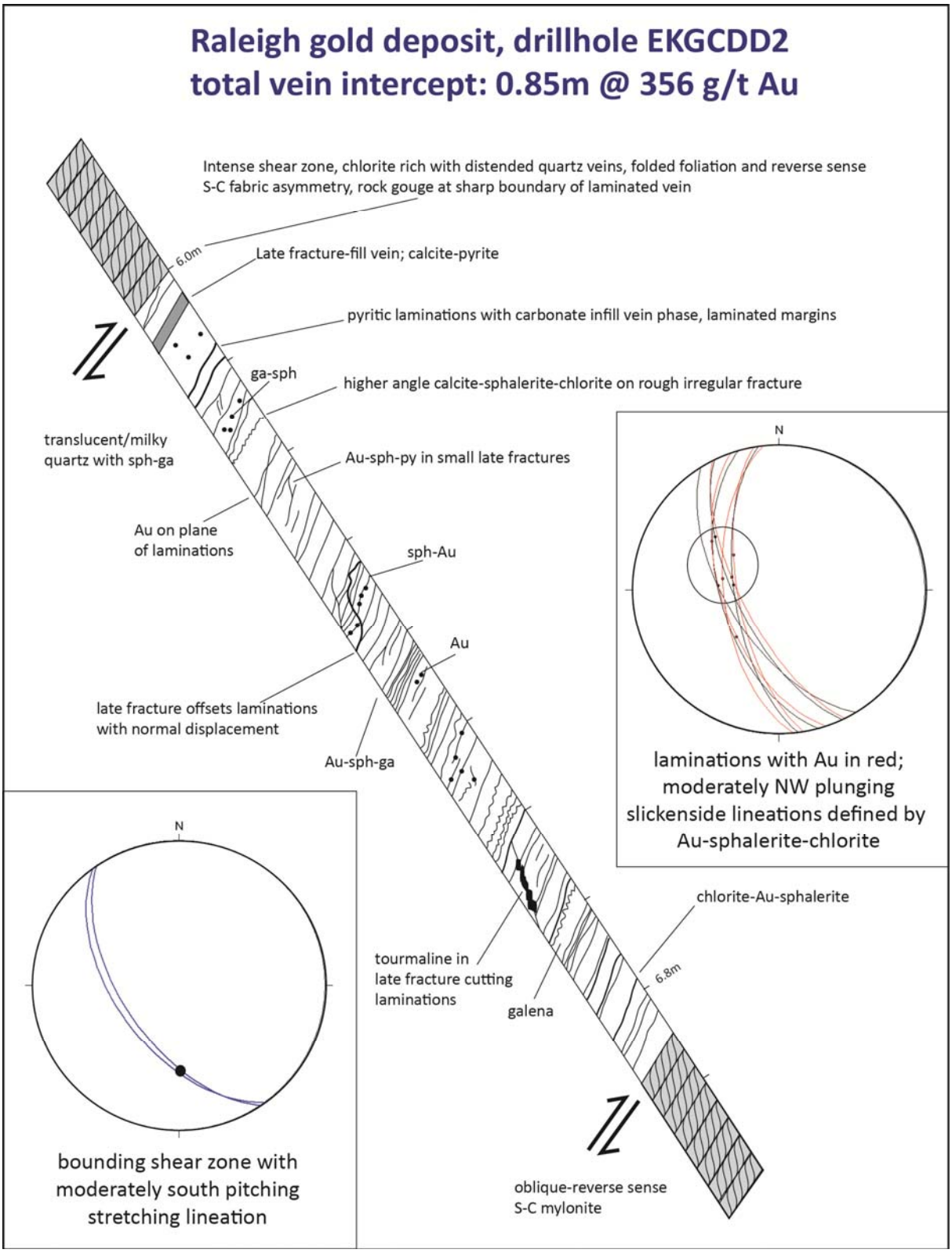

Figure 7.15 – Schematic diagram of high grade quartz-carbonate vein from drill hole EKGCDD2 at the Raleigh gold deposit. Kinematic indicators in the wallrock shear zones show oblique dextral kinematics. The vein was split with a chisel to expose shear lamination planes and allow the orientation and mineralogy of lineations to be recorded. Slip features on the surface of vein laminations are defined by native gold and base metal sulphides that form NW-plunging slickenside lineations, consistent with gold precipitation during sinistral post vein-emplacement, vein deformation events. See Figure 7.3 for drill hole location.

1. E-W regional shortening: interpreted as forming a penetrative foliation S3 and transposition of bedding at a high angle to the principal shortening direction.
2. Fluid overpressure: V1 crustiform vein formation; in most examples V1 veins cut the foliation at some angle with subsequent shortening resulting in the penetrative foliation being oriented as axial planar to folds in V1 veins and sub-parallel to the transposed vein limbs: some V1 veins may be synchronous or pre-dating S3.
3. E-W regional shortening: shear zone development, most V1 veins are sheared and folded, shear zones tend a 10-20° angle with respect to regional foliation.
4. Fluid overpressure: rheological contacts reactivated preferentially over shear zones during main vein emplacement. **Au emplacement**.
5. Subsequent main vein deformation: formation of shear laminations, and minor brecciation of veins. **Au emplacement**.
6. Fault valving: formation of low angle veins; may be synchronous with main vein emplacement, but main veins are cross-cut by low angle fractures and veins of similar morphology and mineralogy as V4/V6. Main vein deformation. **Au emplacement?**
7. E-W regional shortening: V6 vein arrays in conjugate sets indicate E-W shortening, laminations in main veins are folded, micro-faulted and stylolitised. Main vein deformation. **Au emplacement**.
8. E-W shortening: cross-cutting of all other features by late brittle-ductile faults.

A complex sequence of events appears to control the location of the Kundana veins at a local scale, but these events fall into a short time slice when considered in the context of regional deformation events. Significant shortening of the rock sequence and deformation of the K2 horizon predates the emplacement of the main vein, whereas subsequent deformation of the veins appears to coincide with the mineralization events in several stages. Strain localisation and fabric intersection appear to be major controls on the preparation of the ore structures and subsequent location of high-grade ore shoots. Cross faults have a late timing, are lacking in gold/alteration, and hence appear to have no significant influence on the location of the main ore veins. This contrasts with the strike extensions of the same faults, which have ore bodies located where they intersect layers in the mafic volcanic sequence at Mount Pleasant.

7.3.8 Phosphate geochronology of ore components

AMIRA project P680 was a multi-disciplinary university-industry collaborative research project led by Dr. N. Vielreicher. The purpose of that project was to attempt absolute age dating of ore components to better constrain the ages of mineralisation within the EGP. The results of much of that work are published in Vielreicher et al. (2006).

Well field-constrained samples of mineralisation were requested from the industry sponsors by AMIRA P680, and access to the Rubicon pit was provided by Placer/Barrick for that purpose. Polished thin sections of vein samples in the ore zones from this study were used by Dr. Vielreicher for SHRIMP U-Pb analyses of hydrothermal monazite and xenotime. The results returned a robust age of 2639±3 ma for the crystallisation of hydrothermal xenotime in the Rubicon ore vein (Vielreicher et al. 2006; Fig. 7.16).

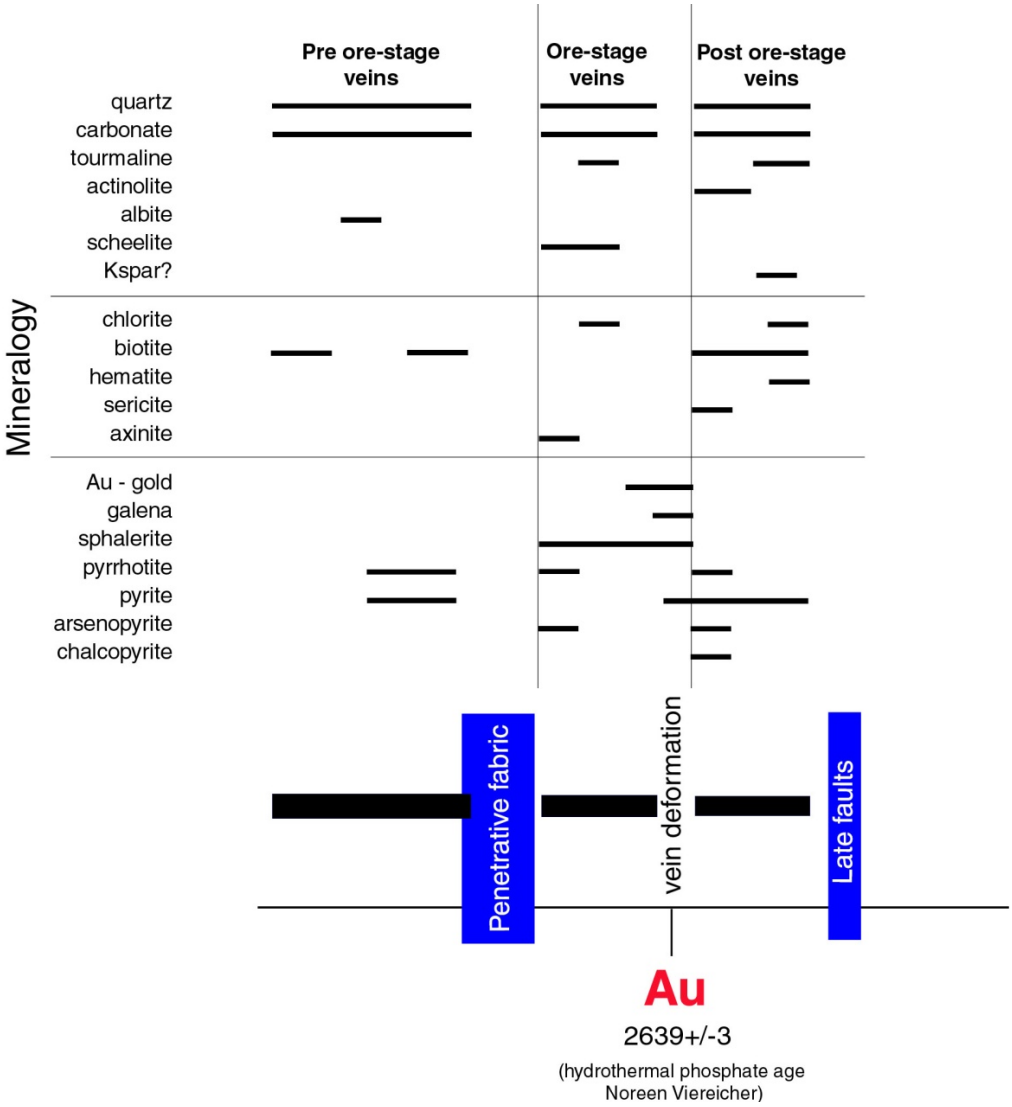

Figure 7.16 - Summary table of mineralogy, vein emplacement and deformation events, and geochronology (hydrothermal phosphate ages from Vielreicher et al. 2006).

7.3.9 Kundana summary

At a mine camp scale, the broad, folded gabbro-dolerite Powder Sill appears to be a major control on the location of mineralisation possibly related to competency contrasts against a dominantly sedimentary sequence of weak rocks along its eastern contact, which favoured sinistral reverse shearing during emplacement of the gold lodes. Quartz-carbonate-Au-base metal mineralisation at Kundana displays a strong structural control during phases of shearing, and later reactivation of shear zones and deformed lithological contacts. Ore zones have strong

internal plunge controls on high gold grades that are primarily related to vein orientation changes.

The ore veins at Kundana are preferentially located on rheological contrasts and at favourable structural sites along contacts. Much of the early ductile deformation appears to be important in setting up the camp-scale structure that provided favourable sites for ore deposition. That camp-scale structure and its fabrics are clearly earlier than the hydrothermal vein systems that host gold deposits. The kinematics of the vein emplacement event is different to that observed in microstructures that host gold, hence gold is late in the paragenetic sequence, but broadly syn- to post-S3 foliation in its timing, and is overprinted by late fault movements (Fig. 7.16).

The characteristics and timing of the Kundana gold deposits would be considered typical of the late ‘Orogenic’ style of mineralisation in that they are closely associated with the latest phases of deformation of the greenstone belts. There are however no particular factors that link the Kundana lode-gold mineralisation style to subduction as a causative ‘orogenic’ process in the deformation; as would be the case for Phanerozoic porphyry and epithermal style deposits (e.g. porphyritic intrusions with anomalous geochemistry indicative of enriched mantle melts emplaced above active subduction zones).

7.4 Centurion gold deposit at Binduli: two timings and styles of gold mineralisation separated by unconformity and deformation

7.4.1 Introduction

Binduli Gold district is located 13 km south west of Kalgoorlie and comprises 10 mined deposits with past production of 5.14 Mt @ 2.36ppm Au for a total 0.39 Moz Au (Table 7.6; Croesus Mining NL. 2006) and recent production of 4.76 Mt @ 1.0ppm Au for a total 0.15 Moz Au (Norton Gold Fields Ltd. public release). Past production plus existing resources and reserves account for a total endowment of ~2.27 Moz Au. The mines are distributed in two linear trends and were described in detail by Ivey et al. (1998); Fowler (1999); Crossing (2001); and Hilyard et al. (2000). The Centurion deposit contained 2.6 Mt at 1.9 ppm Au (157,550 oz Au) endowment.

Several previous studies have focussed on general deposit description (Ivey et al. 1998); lithological characters of the host rocks (Doyle 1999); alteration and mineralisation controls (Mueller 2000; Standing 2000); and timing and depositional settings of the ore deposit (Arnold 1997). Mineralisation models have been strongly biased towards epigenetic, mesothermal orogenic mineralisation for Binduli, whereas Arnold (1997) first documented separate timings for the two main mineralisation styles present at Binduli, and interpreted a syn-genetic exhalative origin for an early disseminated mineralisation style. Those interpretations have been largely ignored or discounted by later workers, but observational data at mine and drill-core scales in this study suggest that a modified version of the model of Arnold (1997) may have validity in the Centurion deposit.

New work in this study is aimed at determining the relative timing of mineralisation styles in the Centurion deposit at Binduli, via mapping, geochemical and petrographic analysis. The primary reasons for selecting this deposit for study are: (1) the presence of two distinct styles of mineralisation; (2) the presence of unconformities; and (3) cross-cutting relationships between the two mineralisation styles and the regional foliation. Criteria from the Centurion deposit are used to assess the regional timing of depositional, mineralisation and deformation events; and in this respect the deposit is a key location for understanding the regional geology of Kalgoorlie.

7.4.2 Lithological and structural setting

Gold deposits at Binduli are localised along two lithological trends separated by the Centurion Fault: a steeply east-dipping reverse shear zone (Standing 2000; Crossing 2001) that separates a western succession of dominantly clastic sedimentary rocks with intercalated felsic porphyritic volcanic rocks and quartz-phyric intrusions, from an eastern succession that comprises dominantly deep-water deposited carbonaceous shales, with sandstone-siltstone and minor conglomerate, intercalated andesite, dacitic volcaniclastic rocks and quartz-feldspar

Table 7.6 – Deposits and production statistics for the Binduli district (Croesus Mining NL. 2006)

DEPOSIT	TONNES	GRADE	CONTAINED GOLD (oz)	RECOVERY	GOLD PRODUCED
Pitman	71,750	2.44	5,629	93.0%	5,235
Centurion	1,944,771	3.05	190,444	92.2%	175,609
Choctaw	73,856	4.29	10,179	94.9%	9,657
Blackfoot	98,503	2.13	6,748	93.0%	6,273
Ben Hur 1	929,433	1.56	46,798	91.0%	42,628
Ben Hur 2	89,922	1.48	4,282	91.6%	3,890
Kaska	312,413	1.49	14,925	90.6%	13,466
Beaver	209,548	2.73	18,368	92.7%	17,033
Navajo Pits	784,448	1.78	44,765	93.5%	41,907
Fort William	622,637	2.38	47,528	93.8%	44,626
TOTAL	**5,137,281**	**2.36**	**389,666**	**92.6%**	**360,324**

porphyry intrusions (Fig. 7.17; Ivey et al 1998). The gross distribution of lithologies was mapped in detail by Crossing (2001) who determined the setting of the rocks as submarine high-level intrusions and extrusive dacite cryptodomes with marginal apron breccia deposits, intercalated with deep-water sediments of fine-medium grained sandstone-siltstone and shale. A conglomeratic unit dominated by feldspar porphyry clasts and sulphide replaced mudstone clasts unconformably overlies the eastern succession at Centurion gold mine (Binduli porphyry conglomerate, Section 3.2.3; Fig. 7.17).

The sequence at Binduli was folded and weakly deformed prior to a major late uplift event resulting in deposition of the Navajo Sandstone and Kurrawang Formation units above a major sub-regional unconformity. At Centurion, the porphyry conglomerate unit is cross-cut by unconformable polymictic conglomerate and quartz-rich cross-bedded sandstone of the Navajo Sandstone member to the north and south of the mine (Fig. 7.17; Fig. 7.18). The Navajo Sandstone member is the dominant coarse-clastic unit in the Ben Hur series of mines south of Centurion gold mine, indicating the Kurrawang unconformity may have removed most of the porphyry conglomerate in that area. The structure of the Centurion mine sequence is a shallow north-west plunging anticline (Ivey et al. 1998) cored by the Centurion Porphyry, which is a crowded feldspar-phyric, aphanitic-groundmass intrusion with an age of 2667±3 Ma determined from SHRIMP U-Pb analyses of zircon (Fletcher et al. 2001). Units east of the Centurion Fault are folded into south plunging major folds of ~1000 m wavelength and dissected by major N-S striking faults that separate the Gibson-Honman Rock sequence from the main Binduli sequence (see Fig. 3.11).

Two main styles of gold mineralisation documented at Binduli include disseminated sulphide replacements and quartz-carbonate-base metal lode-Au veins. The two styles were classified by their geographic development as ECM and WCM (Eastern Contact Mineralisation and Western Contact Mineralisation respectively; Ivey et al. 1998). The ECM is restricted in its exposure whereas the WCM is a late, fault-related event that has a much wider distribution. The ECM was mined between early 1998 to late 1999 and produced 120,000t @ 15ppm Au (57900

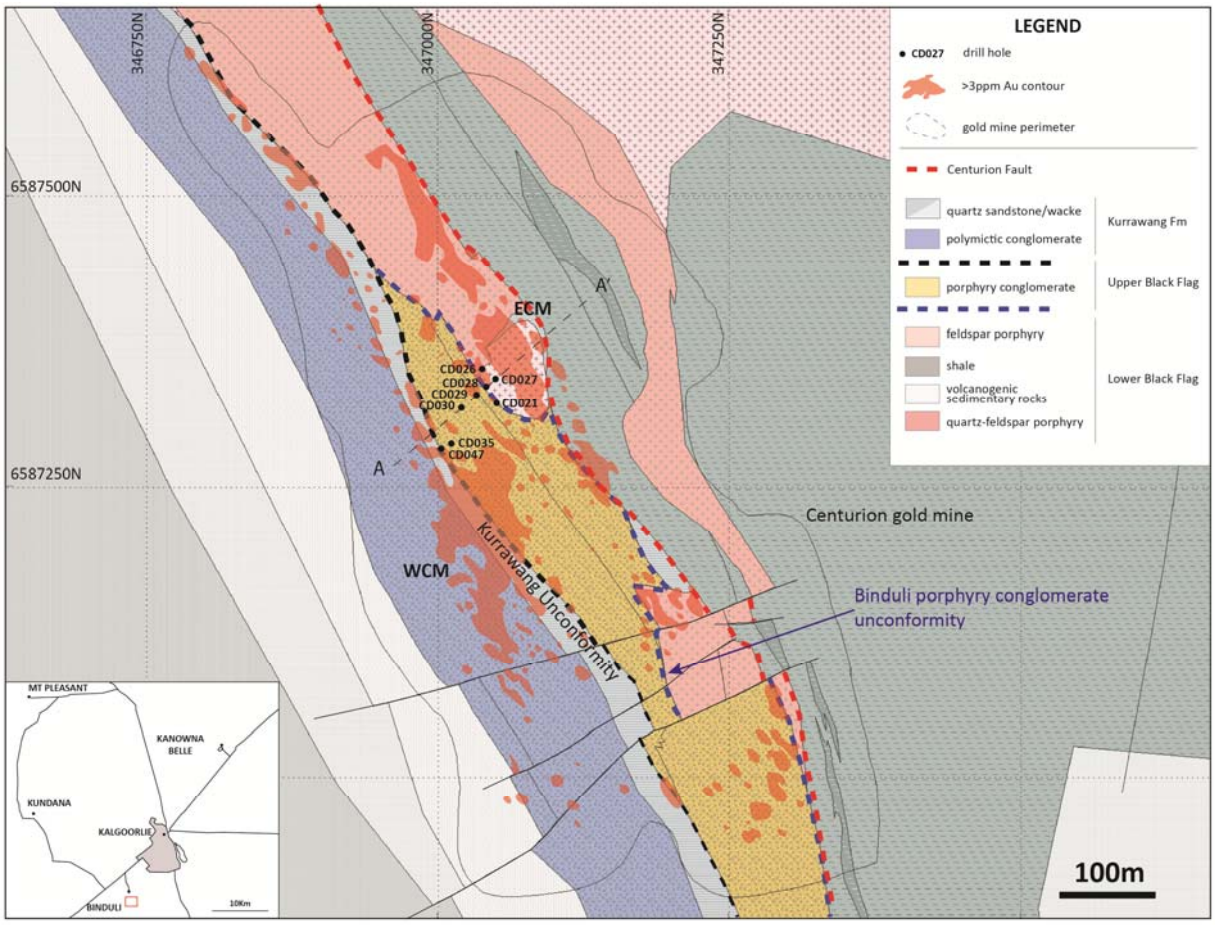

Figure 7.17 – Bedrock geology map of the Centurion gold mine area at Binduli (geology modified from Crossing (2001); grade contours modified from Croesus Mining End of Mine Report (Hillyard 2000); with location of key unconformities, mine outline and drill holes logged in detail in this study. All holes drilled at -60º/060º on average. Gold grades form two irregularly distributed linear zones: a western and eastern zone representing WCM (Western Contact Mineralisation) and ECM (Eastern Contact Mineralisation). The two mineralisation zones represent different styles: WCM orogenic quartz-carbonate lode style; and ECM disseminated sulphide replacement style; but WCM orogenic lode -Au veins are present throughout the mine overprinting the earlier ECM style. Compare with Figure 3.10 for context within the Binduli mine district. Note: contact positions within Centurion gold mine perimeter reflect locations as exposed against the mine topography, whereas drill hole locations are at surface collar positions.

oz Au). In this study, eight diamond drill holes were re-logged and sampled at the Norton Goldfields Core Facility (CD21, CD26,CD27,CD28,CD29,CD30,CD35,CD47); one drill hole at the GSWA Core Library (CD28); and three drill holes at the Bellamel Mining office (KWD007, KWD022, KWD023; Fig. 7.17; Fig. 3.11).

7.4.3 Sulphide replacement style mineralisation (ECM)

7.4.3.1 Host sequence lithology

Host rocks to the ECM comprise very fine-grained, laminated quartzo-feldspathic siltstone-mudstone; very fine-grained quartz-rich siltstone-mudstone; fine-grained laminated sandstone; interbedded coarse-grained intraformational conglomerate and laminated sandstone; interbedded coarse-grained intraformational conglomerate; and intercalated felspathic

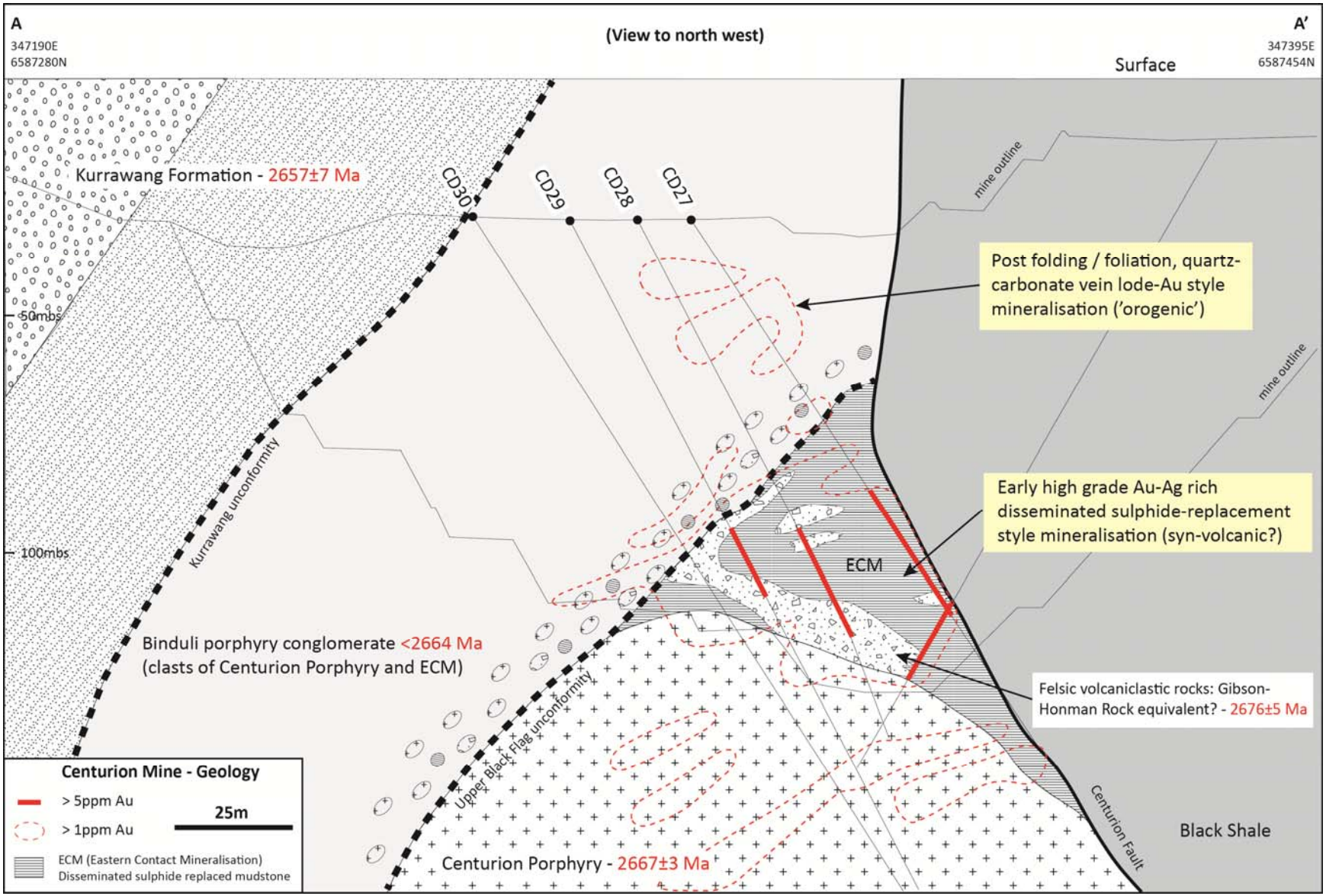

Figure 7.18 – Cross-section A-A' as located on Figure 7.17; re-logged geology significantly modified from a similar cross-section in Croesus Mining N.L. report (Hillyard et al. 2000). Centurion Porphyry age from Fletcher et al. (2001); Gibson–Honman Rock age from Barley et al. (2002).

volcaniclastic grit with pebbly grit, and coherent facies dacitic quartz-rich felsic rocks (Fig. 7.19a). Sedimentary structures in the fine grained rocks include graded bedding with scour and fill structures offset by fine scale normal faults. Undeformed layers in the laminated siltstone and mudstone are crystal-rich units in thin section with a connected matrix network between randomly oriented euhedral feldspar crystals in planar bed forms that may indicate a tuffaceous origin (Fig. 7.19b). The coarse-grained intraformational conglomerate contains mostly mudstone clasts some of which are sulphide replaced, but the unit is lacking porphyritic or volcanic clasts (Fig. 7.19c). Intraformational breccia zones (~10cm thick) contain angular mudstone and feldspathic grit chips interbedded with fine grained mudstone-siltstone. In CD27 beds with clasts of sandstone-mudstone are interbedded with fine-grained layers that have centimetre-scale beds, becoming chaotically broken and deformed against the Centurion Fault (Fig. 7.19d). Interbedded intraformational conglomerate and breccia zones have lower erosional contacts with sulphidised mudstone, and on that basis are interpreted as part of the ECM sedimentary sequence.

Intercalated felsic volcanic and volcaniclastic rocks

Coarse-grained felsic volcaniclastic and volcanic rocks are intercalated with the sedimentary units in the ECM with mixed zones of bedded mudstone, felsic volcaniclastic sandstones, and felsic volcanic rocks with peperitic contacts against shale / mudstone (Fig. 7.19e). The felsic volcaniclastic units are interbedded medium to coarse-grained felsic volcaniclastic grits that are lithic dominated with angular grains of quartz and feldspar; angular mudstone chips; and banded sulphide-replaced mudstone clasts (Fig. 7.19e).

Peperitic textures are interpreted between aphanitic groundmass quartz-feldspar dacite intermixed with wispy mudstone in CD28 where coherent, fine-grained felsic rocks may be intrusions or felsic lava rocks(?) (Fig. 7.19f; Fig. 7.19g). Those rocks are locally mixed with intraformational breccia, with some banded felsic clasts (rhyolite?). In CD28 there is a basal mixed unit that contains: polymictic volcaniclastic breccia (intraformational sedimentary breccia?); sulphide replaced mudstones; siltstone; felsic rocks; and clasts of porphyry. Contacts of felsic volcaniclastic conglomerate with Centurion Porphyry show strong pyrite alteration with mudstone fragments at the contact in CD29.

Centurion Porphyry

Centurion Porphyry is a crowded, aphanitic groundmass biotite-hornblende feldspar porphyry with rare quartz (Fig. 7.20a,b). Euhedral feldspar accounts for ~30% of phenocrysts which are randomly oriented in a fine felsitic groundmass. Contacts with the overlying units are usually sharp, and in CD26 a very fine grained felsic massive rock at the contact may be hornfelsed mudstone.

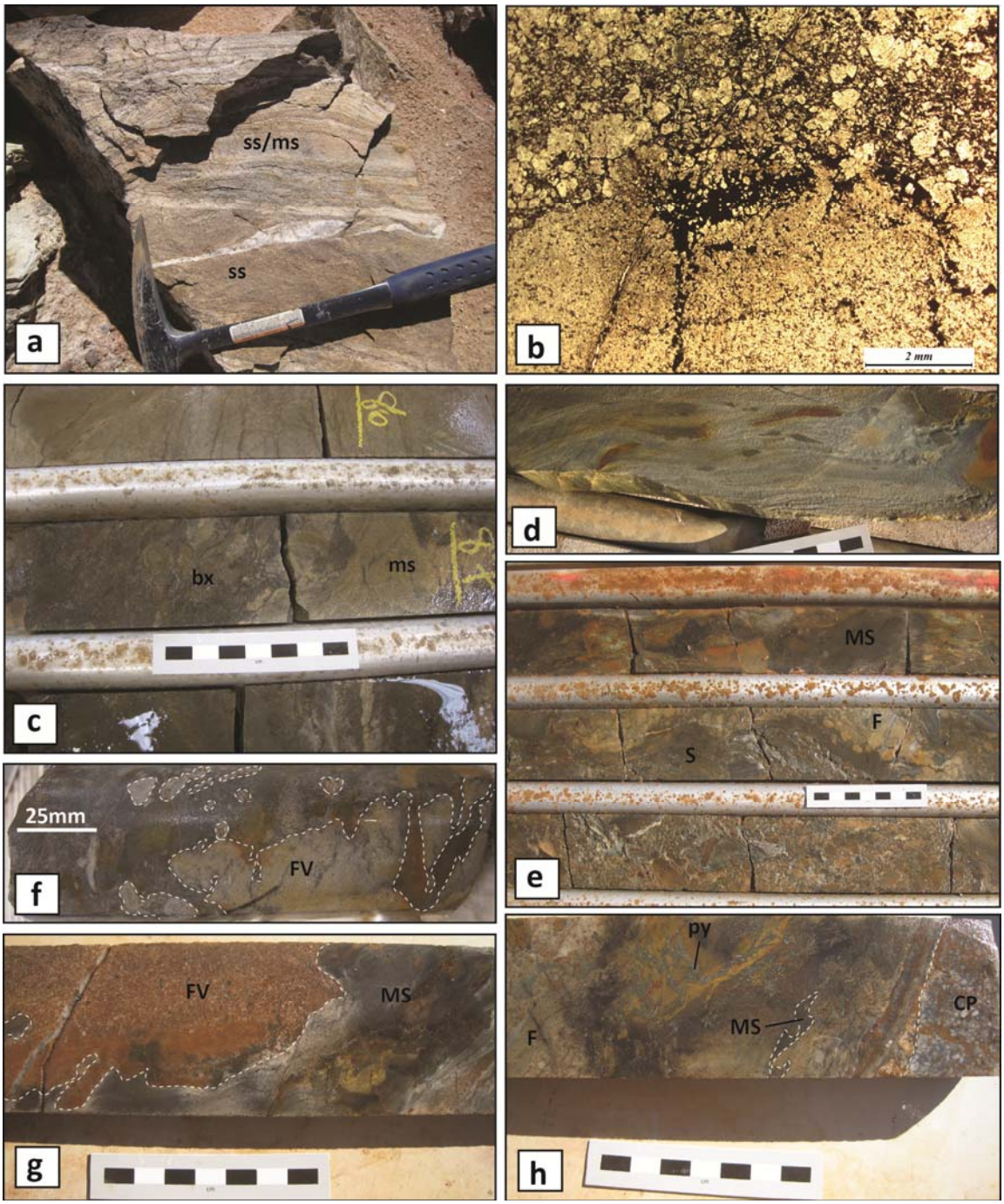

Figure 7.19 – a) interbedded sandstone and laminated mudstone (ECM) with weak sulphide replacement (Centurion gold mine, pit sample); b) PPL photomicrograph of fine grained, feldspathic tuffaceous rocks from a sample of the ECM, black isotropic mineral is replacement pyrite in the tuff matrix and along fractures in more competent beds (Note that fractures are not thoroughgoing; Centurion gold mine, pit sample); c) intraformational breccia (bx) composed of silicic mudstone and sulphidised shale clasts (drill hole CD28; GDA: 347287E; 6587363N); d) finely bedded, sulphide replaced sandstone and mudstone strongly deformed and lensed in proximity to the Centurion Fault (drill hole CD27 115 m; GDA : 347295E; 6587370N); e) intercalated coarse felsic breccia (F), conglomerate (S) and mudstone (MS) within the ECM sedimentary package (drill hole CD26 ~125 m; GDA: 347282E; 6587380N); f) Peperite zone of mixed felsic quartz-feldspar dacitic volcanic (FV) and sedimentary rocks within the ECM (drill hole CD28 90-5 m – 91.9 m); g) Peperite contact of feldspar rich volcanic rocks (FV) with fine bedded mudstone (MS) within the ECM (drill hole CD29 94.4 m; GDA: 347276E; 6587354N); h) intraformational conglomerate composed of felsic volcaniclastic rocks and mudstone fragments at a contact with the Centurion Porphyry (drill hole CD29 99.95 m).

Discussion

The Binduli Porphyry Conglomerate is described in detail in Section 3.2.3 as unconformably overlying the ECM with rip-up clasts at the base of the unit and sulphide replaced mudstone clasts dominant in the lower parts of the unit (Fig. 7.18). Mudstone clasts in the porphyry conglomerate show varying degrees of sulphide replacement ranging from near total replacement to weak or un-sulphidised fine-grained siltstone and mudstone clasts (Fig. 7.20c-f). Binduli Porphyry Conglomerate contains a majority (>90%) of feldspar-porphyry clasts that are indistinguishable from the Centurion Porphyry in their textures and phenocryst populations (compare Fig. 7.20b and f). Previous workers in the Centurion mine considered a possibility that the porphyry conglomerate was a marginal breccia to the Centurion Porphyry (Hillyard 2000).

The probability that epigenetic mineralisation selectively replaced clasts in the porphyry conglomerate is considered unlikely given the presence of weakly sulphide replaced to un-sulphidised siltstone-mudstone fragments in the conglomerate that are identical to stratigraphic units in the ECM, which are also variably mineralised (Fig. 7.20g). Furthermore, the Binduli ECM is not an isolated occurrence localised near vein mineralisation, but may be a stratigraphic unit. It is an important ore host elsewhere in the Binduli mining centre including a significant occurrence at Fort William. The ore at Fort William contains elevated gold and base metals in sulphide replaced, finely-banded mudstones that may be a structural repetition of the Centurion ECM.

7.4.3.2 ECM Mineralisation

Sulphide replacement in the ECM is variably developed in the host sequence. The strongest replacement appears to be localised in mudstone beds, but this is not universal and in some parts of the sequence the intensity can vary from >50% sulphide replacement to weak disseminated pyrite in fine-grained siliceous, bedded siltstone (Fig. 7.20h). Fine grained, laminated sulphide-replaced mudstone usually contains high grades of gold (up to 115.8 ppm Au in CD21). Variation of gold grade with levels of sulphide replacement is well demonstrated in drill hole CD21 with a zone of strong sulphide replacement to 87.5 m down-hole with high Au grades (23.04 ppm) and common white WCM-style quartz veins cross-cutting the ECM (Fig. 7.20h); this is followed by weak to moderate sulphide replacement, which is a lower grade zone (6.07, 1.46 ppm Au), then after 88 m the level of sulphide replacement increases as does the grade (15.9 ppm Au). Weak sulphide replacement of mudstones approaching the contact with Centurion Porphyry is accompanied by typically low gold grades.

Highly sulphidised ECM is characterised by replacement of the groundmass in fine grained tuffaceous sedimentary rocks. In thin section there is a clear relationship of sulphides located in the interstices between feldspar grains, suggesting the possibility for syn-genetic

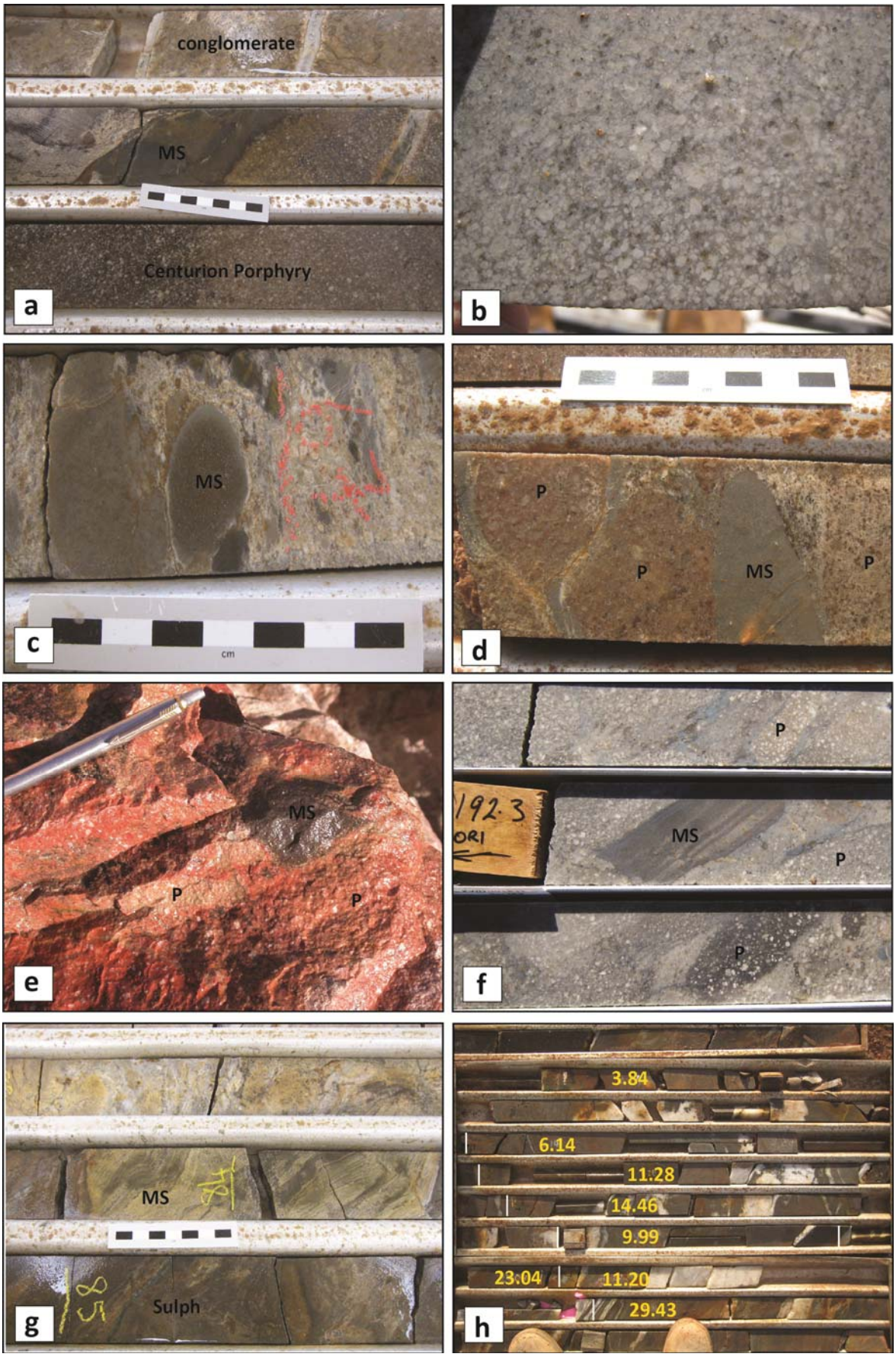
conglomerate
MS
Centurion Porphyry
a
b
MS
c
cm
P
P
MS
P
d
MS
P
P
e
P
MS
P
192.3
ORI
MS
P
P
f
MS
Sulph
g
3.84
6.14
11.28
14.46
9.99
23.04
11.20
29.43
h

Figure 7.20

Captions for figure 7.20

a) Contact of the Centurion Porphyry with overlying ECM sedimentary and volcaniclastic rocks. The contact is a sharp planar margin against dark sulphide replaced and strongly magnetite altered mudstone (MS). The ECM in this area contains a band of intraformational felsic volcaniclastic conglomerate with mudstone fragments. Light coloured areas in the Centurion Porphyry are sericite-carbonate alteration halos around WCM quartz vein arrays (contact at 106.2 m in drill hole CD28; GDA: 347287E; 6587363N).

b) Close up of Centurion Porphyry showing the typical crowded texture produced by abundant (>50%) equant, euhedral plagioclase phenocrysts, minor quartz and ferromagnesians in an aphanitic groundmass. The rock is typically massive and texturally uniform over large areas. Drill core has 50 mm diameter (KWD007 342.5 m; GDA: 347109E; 6587256N)

c) Polymictic Binduli porphyry conglomerate dominated by feldspar porphyritic clasts and rare sulphide replaced mudstone pebbles. Strong sericite-carbonate alteration overprints the rock with late sericite rimming the mudstone pebble marked ‘MS’ and possibly destroying earlier sulphides that have replaced the mudstone (CD28 67.0 m).

d) Porphyry and mudstone clast (MS) dominated Binduli Porphyry Conglomerate with well rounded pebbles of feldspar porphyry (P) and fine grained grey, weakly sulphidised mudstone clasts. The rock is clast supported and typically does not have a high proportion of matrix (<10%). Strong sericite-carbonate alteration overprints the conglomerate (CD35 54.7 m; 347250E; 6587303N).

e) Sulphide replaced mudstone (M) clast within strongly hematite altered porphyry conglomerate. The hematite alteration generally obscured the fragmental texture of the conglomerate but in cut faces, clear pebble-matrix relationships are displayed. Matrices are dominated by millimetre to centimetre sized lithic fragments of porphyry and mudstone (Centurion gold mine sample, Binduli).

f) Drill core intersection of Binduli Porphyry Conglomerate with un-sulphidised clast of bedded mudstone within porphyry clasts dominated conglomerate, locally minor matrix components are composed of very fine grained siltstone and sandstone (KWD007 192.3 m).

g) Variable degrees of sulphide replacement in Binduli ECM unit. Weak sulphide replacement (MS) contains local bands of strong sulphide replacement and is in sharp contact with a thicker zone of strong sulphides (sulph) within the same unit (CD28 84-85 m).

h) Strongly mineralised zone of ECM sulphide replaced mudstone with overprinting WCM-style white quartz-carbonate veins. The grade tenor shows 1:1 relationships with intensity of sulphide replacement in the mudstones over a broader interval than this single photo (CD21 70-78 m; GDA: 347298E; 6587346N).

replacement of matrix minerals, or that there was a primary porosity in the original unconsolidated tuffaceous rocks, which was later partially replaced (Fig. 7.21a-c; Fig. 7.21 d-f). Bedded tuffaceous units with variation of grainsizes show a preference for sulphides to be sited in the (relatively) coarser units with abundant pyrite in the intergranular voids. This would appear at odds with a general relationship of highest gold grade and strongest sulphide replacement in the mudstones, but these observations apply only to thin sections taken from coarser layers in what are typically fine-grained sandstones and siltstones.

Features of the ECM mineralisation style (Fig. 7.22a-h) include weakly laminated sedimentary rocks with comb-textured plagioclase veins and centre-line sulphide bands, whereas others display the sulphide replacements along bedding planes (Fig. 7.22a). Rare examples of pyritic replacements of cross-bedding suggest an early ore timing unrelated to late deformation. In Figure 7.22, a semi-massive band of sulphide replacement extends into fractures (or original voids?) that cross the planes of bedding, whereas these early sulphide bands are cut by a later micaceous foliation plane that has no associated mineralisation.

Sulphide geochemistry

The sulphides comprise amorphous to euhedral pyrite grains of variable grain size from <5 μm to 2 mm, with accessory sphalerite and molybdenite. Pyrite grains in the Centurion deposit have complex morphology with inclusion-rich cores and clean inclusion-free overgrowths, as determined from reflected light petrography. Three samples were selected for LA-ICPMS microprobe analyses, which were completed under contract to Barrick Gold by Dr. D. Mason (Mason 2012; Fig. 7.22c, d).

Inclusion-rich cores have elevated metals compared to rims (Fig 7.23) and show correlations between Au-Ag-Sb-Te-W-Cu (+/-Hg-Zn), particularly Au-Ag-Te-W in both ECM and sulphidised clasts from the Binduli porphyry conglomerate. Good correlations exist between the metal signatures of porphyry conglomerate pebbles and the underlying ECM (Fig. 7.23). A generally low concentration of metals in the pyrite rims is interpreted as a late overprint related to the low-grade WCM quartz-carbonate lode vein event (Fig. 7.23).

Pyrites from the Binduli Porphyry Conglomerate show morphological similarities to pyrites from the Kanowna Belle deposit (Ren and Heithersay 1998; Davis et al. 2000) and several other deposits in the north Kalgoorlie district (e.g. Morey et al. 2008). At Kanowna Belle, early inclusion-rich cores contain Au-Te-base metals and gangue inclusions, with external growth banding of alternating As-rich and As-poor bands, whereas late overprinting events deposited gold in strain shadow fringes on early pyrites (Davis et al. 2000).

Veins

The ECM style is overprinted by crustiform quartz-carbonate-fluorite ± galena veins and

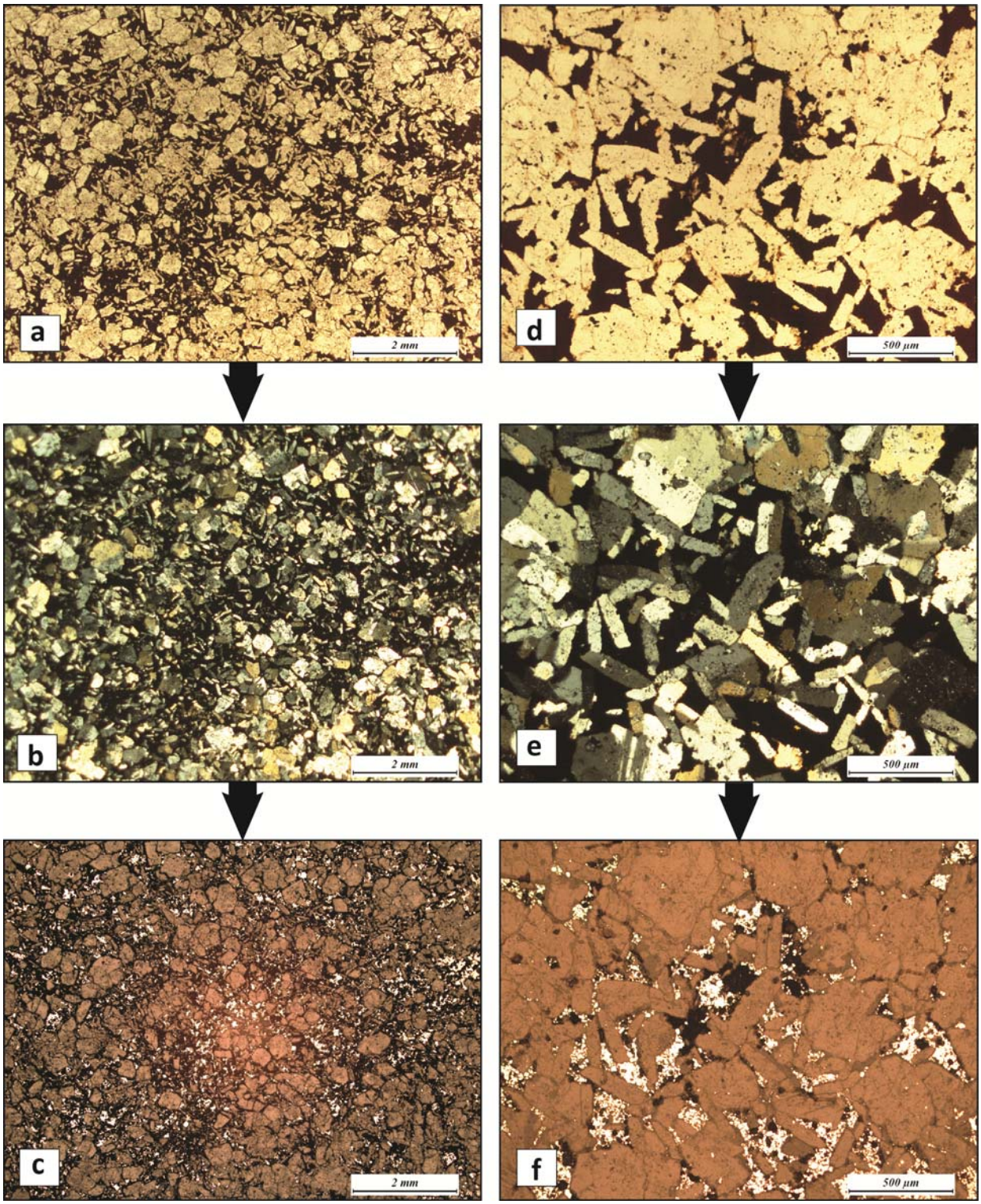

Figure 7.21 – Photomicrographs of ECM sulphide replacement style mineralisation: a),b),c) PPL, XPL and reflected light photomicrographs of the same view showing the crystalline structure of the tuffaceous rocks composed predominantly of fine subhedral equant grains of albite, and possibly K-feldspar. Sample of ECM mineralised sedimentary rocks from Centurion gold mine; d),e), f) PPL, XPL and reflected light views of a detailed area from the same sample showing opaques filling interstitial areas between grains in the feldspathic tuff. The reflected light view shows that pyrite accounts for a major proportion of the opaques: the remainder may be dark carbonaceous sedimentary material. Sulphide replacement occurs mostly in the spaces between grains with only very few pyrite blebs internal to the feldspar grains.

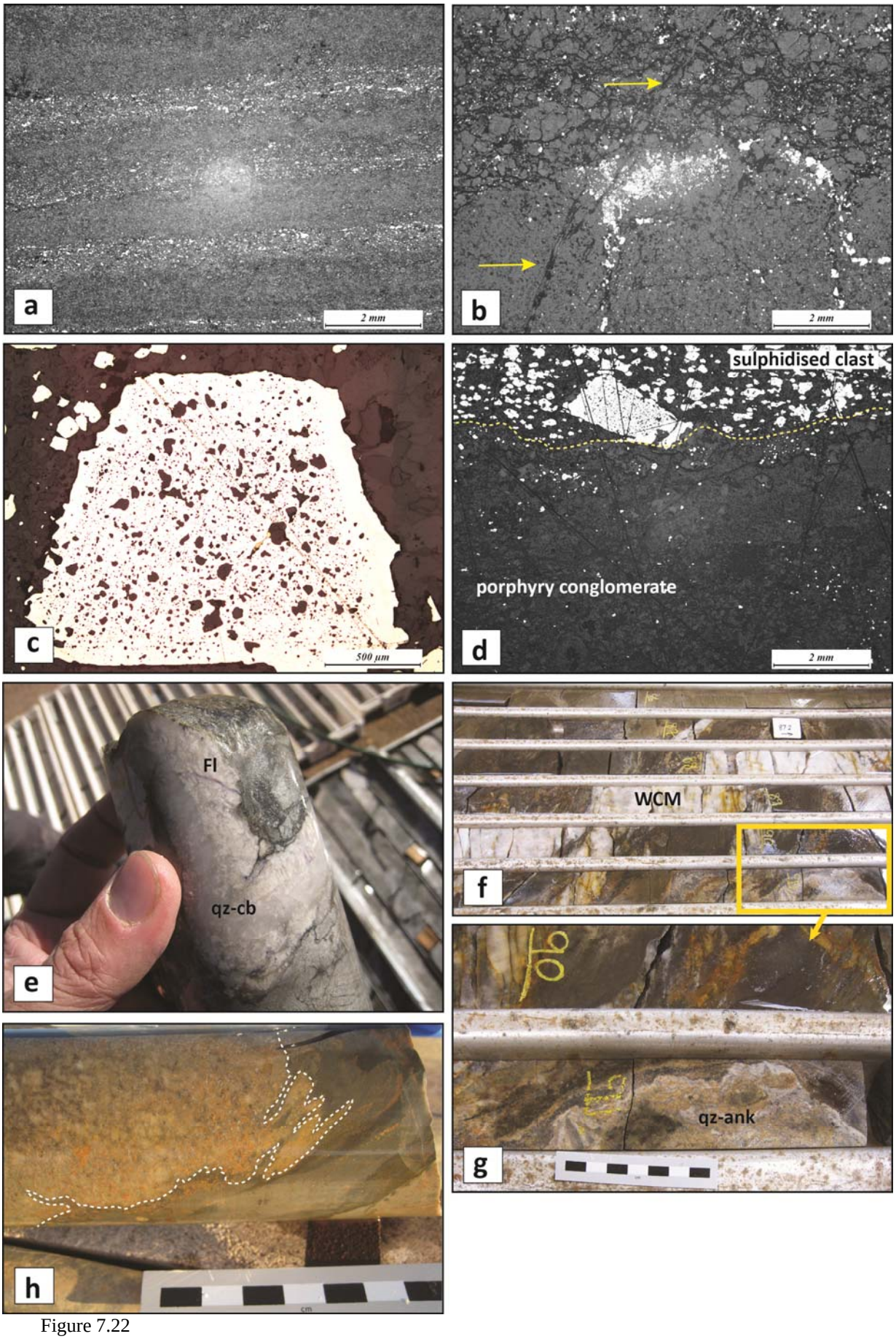
a
2 mm
b
2 mm
c
500 µm
sulphidised clast
porphyry conglomerate
d
2 mm
Fl
qz-cb
e
WCM
f
qz-ank
g
h

Figure 7.22

Captions for Figure 7.22

a) Reflected light photomicrograph of fine grained tuffaceous rocks with pyrite replacement of bedding planes in the silts layers. Sulphides are disseminated throughout the rock, but are concentrated in layers with a connected permeability (Fort William gold mine sample; GDA: 345380E; 6592670N).

b) Reflected light photomicrograph of a pyrite band at a contact between a fine-grained, massive uniform tuff layer (lower) and a coarser grained feldspathic layer (upper). The pyrite is localised at the contact but also in fractures that cut the massive layer that could be interpreted as original fractures in the primary rock sequence. The sulphides are clearly earlier that a later micaceous fracture trending across the bedding that cuts both the sequence and the sulphides (highlighted with yellow arrows (Centurion gold mine ECM sample).

c) Reflected light photomicrograph of a single pyrite crystal etched with HN03 and displaying a complex internal structure of a silicate-inclusion rich core with small blebs of chalcopyrite, and an outer concentric rim of clean inclusion-free pyrite. Ion microprobe analyses show the inclusion rich cores contain most of the metals that are returned from whole rock assays, whereas the rims have generally low concentrations of Au and base metals. The rims are interpreted as a later sulphide precipitation event possibly related to the WCM 'orogenic' vein mineralisation event that overprints early high-grade disseminated sulphide replacement mineralisation (Centurion gold mine ECM sample).

d) Reflected light photomicrograph of the Binduli Porphyry Conglomerate showing a sulphide replaced clast at the edge of the slide within a generally sulphide poor clastic matrix that contains feldspar crystal fragments and lithic clasts of pyrite mineralised feldspar porphyry. The clast section of the slide was etched with HN03 and shows the typical complex internal pyrite structure as observed in (c). Sulphides in the porphyry conglomerate matrix are single stage pyrites that are microscopically associated with lithic fragments of porphyry. Straight dark lines on the photomicrograph are scratches from polishing of the thin section (Centurion gold mine ECM sample).

e) Folded quartz carbonate vein with late fluorite-galena filled fractures. The vein overprints the ECM mudstones and is buckle folded with an axial planar foliation defined by biotite (KWD007 297.7 m; GDA: 347109E; 6587256N).

f) Drill hole intersection of high-grade ECM with overprinting white buck WCM quartz-carbonate veins. The ECM is overprinted by an earlier quartz-ankerite vein set (g) that is folded with the host mudstones; the WCM veins overprint all previous fabrics (CD28 86 - 91 m; GDA: 347287E; 6587363N).

g) Close up of the box marked in (f) showing early folded crustiform quartz-ankerite veins within the ECM.

h) Deformed peperitic contact between felsic porphyritic volcanic unit and the ECM mudstone (CD27 93 – 93.2 m; GDA: 347295E; 6587370N).

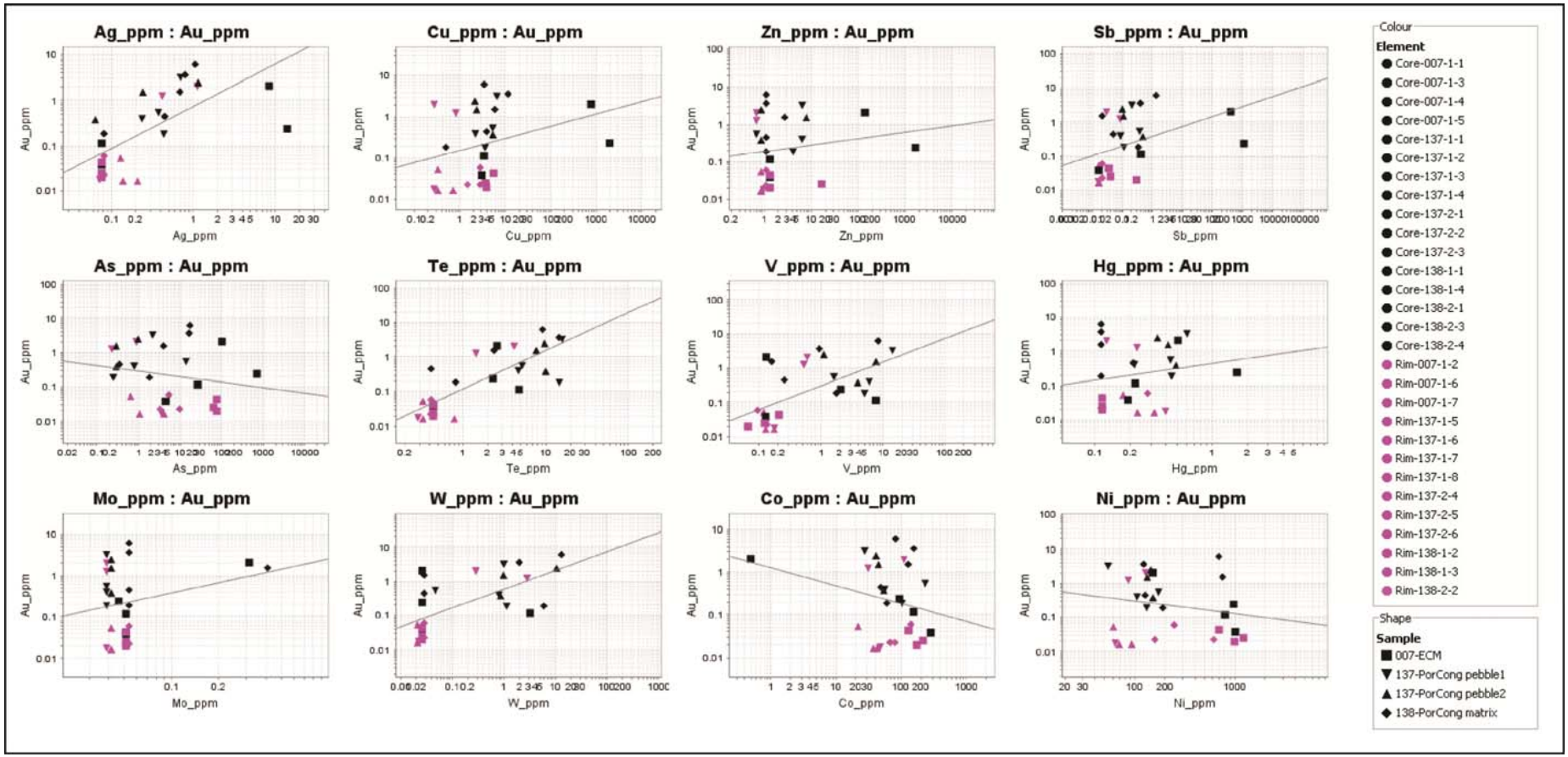

Figure 7.23 – IOGAS log-log plots of various metal contents in pyrite crystals from the Centurion gold mine. The data were determined from LA-ICPMS ion microprobe analyses of rims (purple) and cores (black) of selected pyrite samples by Mason (2012) identified from polished thin sections etched with nitric acid. The samples include ECM sulphidised mudstone; pebbles of sulphide-replaced mudstone from the Binduli porphyry conglomerate; and samples of pyrites from fragments in the matrix sandstone of the Binduli porphyry conglomerate. In most cases, *rims* on the pyrite crystals have low metal concentrations suggesting that a late overprinting pyrite event did not accompany high-grade mineralisation. Generally good correlations exist between the porphyry conglomerate pebbles and the ECM. Pyrite in the porphyry conglomerate matrix shows similar relationships to the ECM and pebble sulphides suggesting these are part of the same mineralisation event. Sulphide analyses from sample #138 are microscopically determined as located within recrystallised detrital lithic fragments of feldspar porphyritic rock, which probably represents pre-conglomerate mineralisation.

breccia zones with peripheral brown biotite alteration that are folded and deformed with an axial planar foliation in CD28 and KWD007 (Fig. 7.22e). This event appears to be the unusual 'pegmatitic quartz' event described by Arnold (1997) who included 'green feldspar', galena and pyrite as minor constituents. Those veins equate with the biotite-calcite-fluorite veining event of Standing (2000). In drill hole KWD007, crustiform textured veins up to 20 mm thick are composed of outer quartz-carbonate bands and inner quartz, with late fracture fills at a moderate angle to the vein margin filled with fluorite, which occur in conjunction with fine grains of galena (Fig. 7.22e). Weakly sulphide-replaced mudstone in CD28 is cut by crustiform carbonate (ankerite) + quartz veins with laminations, which are further cut at a high angle by WCM massive milky, buck quartz veins with local sphalerite-pyrite-galena; these later veins have sericitic haloes that overprint the sulphide replaced mudstone (Fig. 7.22f, g).

Strong deformation overprints the ECM in CD27 (Fig. 7.22h) in which bedding laminae and peperitic contacts between sedimentary units and intercalated felsic volcanic units are strongly deformed. The same upright foliation is axial planar to folds in crustiform ankerite-quartz veins that cut the ECM (Fig. 7.22e). The deformation is not pervasive however, and areas of well-preserved bedding with primary sedimentary structures are preserved.

7.4.4 Quartz-carbonate-Au veins (WCM)

Western Contact Mineralisation (WCM), apart from being located primarily in clastic sedimentary units of the western succession, is distinctive in style from the ECM. In general the WCM is a lower grade style of mineralisation in the Binduli mining district and is particularly well developed in cross-bedded Navajo Sandstone at the contact of a porphyry intrusion in the Navajo mine with an average production grade of 1.78 ppm Au (Table 7.6). The WCM style is otherwise present in nearly all mines in the Binduli mining centre regardless of host rock lithology (Fig. 7.17).

WCM veins are thick, white milky quartz (+carbonate) veins, rarely laminated, with sharp parallel walls and accessory disseminated sulphides that include pyrite with minor sphalerite galena and rare fluorite (Fig. 7.22f). The WCM veins form linking extensional arrays in primarily shallow southwest-dipping clusters associated with competency contrasts in the host rocks they cut (Ivey et al. 1998). Previous studies have described WCM veins as related to reverse movements on the Centurion Fault, which suggests they may be faulting-related flats developed in the wallrocks of the Centurion Fault by fluid pressure cycling during high-angle reverse faulting as envisaged by Sibson et al. (1988). WCM veins appear to be developed pervasively, overprinting all rocks in the succession including the porphyry conglomerate, the ECM sections where intercalated felsic volcaniclastic rocks are present, and the Centurion Porphyry.

In CD29 the ECM is cut by WCM-style quartz veins with angular fragments of the sulphidised mudstone in the veins, which are developed at high angles to the bedding; or may be emplaced parallel to bedding planes in the ECM splitting off several layers as wallrock screens contained within the quartz (Fig. 7.20h). Mudstone fragments contained within WCM veins are generally rotated and strongly sulphide-replaced, but do not show evidence of proximal increasing sulphide replacement as would be expected if the sulphide replacement was related to WCM vein emplacement. Locally, strong sericite-carbonate bleached halos in the wallrocks of the WCM veins suggest the WCM vein alteration post-dates the ECM style mineralisation (CD27). The WCM veins also cross-cut folded sequences, and locally cut a deformation fabric that overprints the ECM, which implies vein emplacement was synchronous with, or later than pervasive fabric-forming D3 deformation.

Centurion Porphyry is cut by WCM quartz veins, where early abundant biotite or hematite alteration was overprinted by light-coloured intense sericite-carbonate halos (Fig. 7.20a). The veins are particularly common at the contact of ECM with Centurion Porphyry and form spaced arrays or weakly developed stockworks in the brittle porphyritic host rock (Fig. 7.18).

7.4.5 Wallrock alteration styles

Alteration in the Binduli mining centre is represented by a complex series of overlapping styles that are variably developed over the entirety of the gold deposit cluster (Fig. 7.24). The alteration map in Figure 7.24 was compiled by Placer Dome geologists from extensive field observations and re-logged drill holes, and as such is a broad summary of a more detailed mesoscopic paragenesis. Detailed alteration studies were conducted by Fowler (1999), Doyle (1999), and Standing (2000).

Two main stages of early alteration include pervasive carbonate (ankerite)-sericite-pyrite alteration of the ECM mudstones (Fig. 7.20g), and pervasive hematite±magnetite±biotite alteration of the Centurion Porphyry and porphyry conglomerate (Fig. 7.20a; Fig. 7.20e-f). The timing of the two events is not well constrained, but sulphide replaced mudstone clasts in the porphyry conglomerate have sericite and hematite replacement of the clast rims suggesting the hematite is a later overprint.

In drill hole CD21 the porphyry conglomerate contains 5-10% mudstone/siltstone pebbles and dark-brown, strongly carbonate-magnetite altered pebbles that have remnant porphyritic texture, implying an early timing for the carbonate and magnetite alteration. Hematite is present throughout the Binduli area, but is not pervasive; and preserved sections of magnetite-biotite altered Binduli Porphyry Conglomerate and Centurion Porphyry indicate that the hematite overprints an earlier magnetite-biotite assemblage. Hematite is also variable in its overprinting of the porphyry conglomerate with adjacent sections of strong hematite and sericite-carbonate alteration.

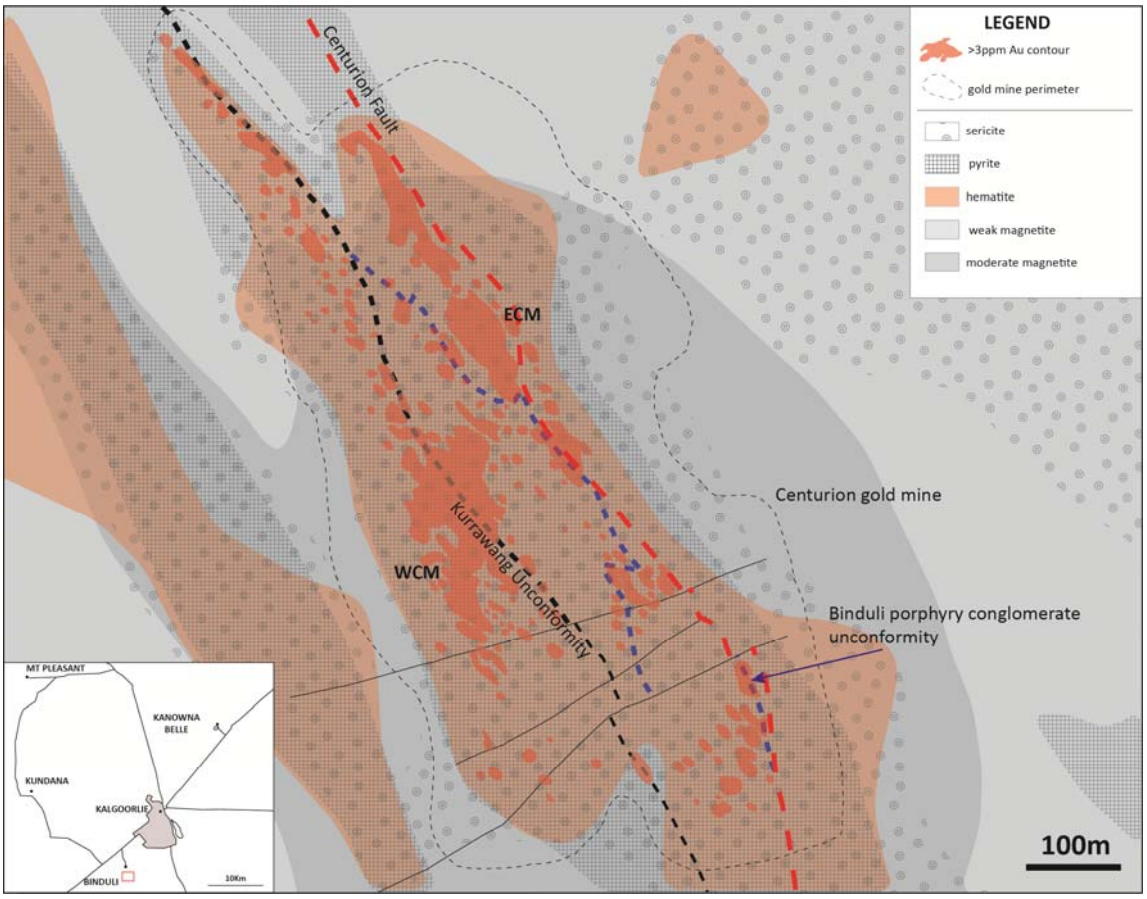

Figure 7.24 – Map of alteration minerals from drill hole relogging and mapping in the Centurion mine area (PDAP). The map is the same scale and area as Figure 7.17.

The Binduli mining district contains abundant quartz-phyric porphyritic intrusions with high magnetic susceptibility, and the observed abundance of hematite and magnetite proximal to the ore indicates a highly oxidised environment of ore formation and alteration (Standing 2000; Gunther 2001; Halley 2010). In CD28 the contact between ECM and the Centurion Porphyry has high magnetite content in a zone of elevated gold grade (Fig. 7.20a; J. Dobe personal communication), suggesting an association of the ore with highly oxidised fluids at the margins of a high level intrusion. Late sericite-carbonate alteration overprints the earlier assemblages in the wallrocks of WCM style veins, and can also have a wider distribution with replacement of the matrix in the porphyry conglomerate and along late fractures. High magnetite content in the volcanic and intrusive rocks at Binduli is also characteristic of the Goldilocks sequence south of Kundana that are correlated with the Binduli sequence.

Standing (2000), documented five alteration assemblages for the Centurion deposit as:

1. Hematite+magnetite±ankerite±pyrite Alteration
2. Hematite+sericite±pyrite±magnetite±ankerite Alteration
3. Quartz+ankerite+pyrite+sericite Alteration (ECM)
4. Biotite+calcite±fluorite Veining and Alteration (Post ECM)

5. Sericite+quartz+pyrite±carbonate Veining and Alteration (WCM)

In contrast to the alteration stages of Standing (2000), re-logging of the Binduli drill core in this study suggests that there is early-stage biotite-magnetite alteration overprinted by hematite. The biotite-magnetite alteration is intense, proximal to high-grade gold zones, as indicated by drill intersections that are hematite-absent. Intermediate-stage crustiform quartz-carbonate-fluorite veins appear to have associated biotite alteration that overprints the hematite-sericite alteration, but this is not widely developed. Late stage sericite is associated with the WCM veins, whereas an earlier stage of sericite may be present with Fe-carbonate alteration of the ECM.

7.4.6 Metal associations

Samples of the rocks and ore styles from the Centurion mine and drill core were collected for whole-rock geochemistry (Table 7.7; Fig. 7.25) to address specific points of enquiry:

1. To characterise the metal association of the Binduli ore styles
2. Assess the possibility that clasts in the Binduli Porphyry Conglomerate are rip-up clasts of underlying ECM high grade mineralisation and,
3. Assess the possibility that clasts of porphyritic intrusive rocks in the porphyry conglomerate are rip-up clasts sourced from the Centurion Porphyry

Sampling from diamond drill holes involved quarter cuts of remaining core at the Norton Goldfields core processing facility, with other samples of ore and waste rock from dumps at the Centurion mine as listed in the Appendix. All of the core samples were from fresh rock drilled several years ago and most of the samples of mineralisation were in high-intensity altered rocks that after exposure to air have a brown rusting from oxidation of sulphides and Fe-carbonates (ankerite).

Twelve samples of mineralisation were collected from a range of grade zones in the ECM ore body; and for comparison, seven individual sulphide replaced pebbles in the Binduli Porphyry Conglomerate were cut from surrounding wall rocks and separately analysed. Care was taken with sampling to avoid areas of WCM style mineralisation and alteration so that the types were not mixed, but the possibility for contamination by micro-veinlets of the later mineralisation style cannot be ruled out, since the WCM overprints the earlier ECM. Given the high-intensity alteration in these rocks, element mobility is variable and only selected immobile trace elements were appropriate for correlation purposes. In general, there is significant and pervasive addition of K, CO2 and S in the rocks at Centurion gold mine; hence typical major element ratio plots for rock type and lithologic association are not appropriate in this instance. Statistical assessment of the trace element analyses indicated wide variability, and non log-normal distribution for a range of trace elements for which no multivariate statistics were attempted (e.g. correlation coefficient, factor analysis); and which were excluded from further assessment.

Table 7.7 – Whole rock geochemical data for samples of ECM mineralisation and niche sampled sulphide-replaced mudstone clasts from the Binduli Porphyry conglomerate. Elements that were below detection limits in all samples are not listed in the table. Full sample details are supplied in Appendix.

Sample#		SG15356	SG15354	SG15367	SG21363	SG15355	SG21374	SG15370	SG15365	SG21364	SG15366	SG21373	SG21375		SG21389	SG15352	SG21358	SG21394	SG15353	SG21393	SG21379	
Lith		ECM	ECM	ECM	ECM	ECM	ECM	ECM	ECM	ECM	ECM	ECM	ECM	**Ave ECM**	Clast	Clast	Clast	Clast	Clast	Clast	Clast	**Ave Clast**
Au	(ppm)	**45.5**	**16.8**	**37.7**	**4.84**	**4.15**	**3.47**	**2.68**	**1.55**	**1.17**	**0.789**	**0.239**	**0.15**	**9.92**	**14.2**	**12.7**	**0.869**	**10.8**	**2.67**	**0.145**	**0.034**	**5.92**
Ag	(ppm)	7.7	13.5	18.5	2.15	1.25	0.55	4.15	0.55	6.35	0.55	0.05	0.5	**4.65**	8.3	5.95	0.15	1.3	0.9	0.05	BD	**2.78**
As	(ppm)	122	35.8	55.6	30.2	14.8	24.8	32.2	6.6	60.6	13.2	42.2	19.2	**38.10**	131	31.6	5.4	3.4	168	5	1.8	**49.46**
Sb	(ppm)	3.58	9.34	4.98	12.2	3.64	1.76	10.4	1.48	148	4.04	3.34	2.72	**17.12**	3.2	2.36	0.7	0.4	4.94	0.46	0.26	**1.76**
Bi	(ppm)	2.18	1.86	2.84	0.48	0.46	0.24	0.86	0.2	0.54	0.34	0.44	0.26	**0.89**	1.88	2.46	0.42	0.14	1.46	1.12	0.3	**1.11**
Mo	(ppm)	27.9	1300	31.9	52.2	39.9	0.2	8.3	345	18.3	9.2	0.2	5.7	**153.23**	1.1	1.9	0.5	0.3	3.1	1.5	0.3	**1.24**
Cu	(ppm)	17	14.5	34.5	144	13	67	21	40.5	208	26.5	118	161	**72.08**	16	21	18	21.5	57	16	6.5	**22.29**
Pb	(ppm)	96	231	242	54	37	31	123	19	83	32	9	53	**84.17**	27	39	5	9	27	15	4	**18.00**
Zn	(ppm)	4060	2480	2610	2150	954	322	886	56	900	268	120	304	**1259.17**	56	16	22	184	70	34	12	**56.29**
Ni	(ppm)	108	138	124	124	50	98	116	86	78	22	114	52	**92.50**	78	104	16	30	96	14	4	**48.86**
Cd	(ppm)	8.4	4.25	5.15	4.1	1.9	0.55	1.6	BD	1.85	0.5	0.2	0.5	**2.64**	0.1	BD	BD	BD	0.1	BD	BD	**0.10**
Tl	(ppm)	0.38	1.11	0.33	0.62	0.21	0.75	0.36	0.03	0.67	0.13	0.51	0.16	**0.44**	0.1	0.29	0.06	0.43	0.1	0.11	0.07	**0.17**
Te	(ppm)	43.8	31.7	46.3	10.2	7.2	2.1	13	3.8	8.2	3	1.4	1.5	**14.35**	15.3	25.6	0.5	4.8	6.4	BD	0.1	**8.78**
Hg	(ppb)	330	360	1060	380	130	100	320	20	270	190	40	60	**271.67**	330	1470	110	200	140	10	BD	**376.67**
Fe	(%)	5.36	8.81	7.1	4.84	3.85	5.64	12.7	3.22	5.05	2.69	5.1	6.31	**5.89**	19.4	21	2.86	7.68	18.4	2.15	0.51	**10.29**
Mn	(ppm)	312	603	1420	443	493	1110	635	563	1000	828	701	2270	**864.83**	2420	664	783	2430	2600	850	198	**1420.71**
Ca	(%)	1.24	2.04	5.44	1.02	1.89	2.15	2.05	2.75	2.02	2.82	1.23	3.91	**2.38**	2.78	1.78	1.27	1.25	2.75	1.42	0.59	**1.69**
Mg	(%)	0.54	1.03	2.85	0.7	0.87	1.65	1.1	1.27	1.02	1.41	1.02	2.06	**1.29**	1.75	0.45	0.32	0.98	2.4	0.18	0.08	**0.88**
Rb	(ppm)	30	9.5	5.5	133	40	174	56	4	83	82	140	55	**67.67**	15	57	66	40	19	103	110	**58.57**
Sr	(ppm)	260	300	440	480	360	380	380	900	480	420	280	420	**425.00**	740	2300	400	260	580	620	700	**800.00**
Th	(ppm)	10.5	6.5	7.5	9.5	12.5	10	7.5	12.5	4	20.5	10.5	7.5	**9.92**	6.5	13	20.5	19	5.5	11.5	8	**12.00**
U	(ppm)	3	2	2.5	2.5	4.5	2.5	2.5	5	1.5	6.5	3	2.5	**3.17**	2	3	5	6.5	1.5	4	3	**3.57**
W	(ppm)	20	40	25	15	20	20	25	30	15	25	20	10	**22.08**	35	15	15	15	BD	10	10	**16.67**
Zr	(ppm)	120	80	100	230	220	150	140	180	90	180	150	110	**145.83**	60	150	220	260	50	170	180	**155.71**
La	(ppm)	34	24.5	19.5	29	26.5	30.5	30.5	41.5	11.5	17	35	23.5	**26.92**	34	51	145	98	16	60	27	**61.57**
Ce	(ppm)	61.5	48	38.5	49.5	47	53.5	58	80	22	32.5	56	43.5	**49.17**	68	100	207	193	30.5	114	57.5	**110.00**
Nd	(ppm)	26	20	17.5	22	21	23	24	32	9.5	15	23.5	17.5	**20.92**	30	41	78.5	81.5	12.5	52	27	**46.07**

Sample#		SG15356	SG15354	SG15367	SG21363	SG15355	SG21374	SG15370	SG15365	SG21364	SG15366	SG21373	SG21375		SG21389	SG15352	SG21358	SG21394	SG15353	SG21393	SG21379	
Lith		ECM	ECM	ECM	ECM	ECM	ECM	ECM	ECM	ECM	ECM	ECM	ECM	**Ave ECM**	Clast	Clast	Clast	Clast	Clast	Clast	Clast	**Ave Clast**
Sm	(ppm)	5	4	3.5	4	4	5	4.5	5	2	3	4.5	3.5	**4.00**	5	6	12	12.5	2.5	7.5	5	**7.21**
Eu	(ppm)	1.4	1.4	1.4	1.2	1.2	1	1.2	1.8	0.4	0.8	1.2	1.2	**1.18**	1.2	1.8	3	2.4	0.6	1.8	1.2	**1.71**
Dy	(ppm)	2.5	2.5	3	2.5	3	3.5	2	2.5	1.5	2.5	4	3.5	**2.75**	3	2	3.5	4	2	2.5	2	**2.71**
Yb	(ppm)	1	1	1.5	2	1.5	2	1	1.5	1	2	1.5	2	**1.50**	1.5	1	1.5	2.5	1	1	1	**1.36**
Y	(ppm)	12	13	17	14	14	20	12	13	8	17	17	16	**14.42**	15	10	15	20	11	12	12	**13.57**
Sc	(ppm)	30	30	30	50	30	50	40	30	40	30	50	50	**38.33**	30	20	40	30	20	40	40	**31.43**
Li	(ppm)	8	7	10	58	8	94	53	20	9	6	64	31	**30.67**	7	28	17	56	16	17	35	**25.14**
Al2O3	(%)	14.9	12.4	10.6	13	15.5	14.2	11	15.2	6.71	14.8	15.1	9.31	**12.73**	2.09	9.59	14.2	15.2	5.41	13.2	11.9	**10.23**
BaO	(%)	0.05	0.027	0.016	0.162	0.051	0.121	0.117	0.016	0.062	0.083	0.137	0.072	**0.08**	0.048	0.098	0.107	0.04	0.046	0.111	0.114	**0.08**
CaO	(%)	1.86	3.09	8.16	1.42	2.63	3.12	2.88	3.95	2.84	3.98	1.77	5.46	**3.43**	5.29	2.75	1.73	1.73	7.19	2.01	0.78	**3.07**
Cr2O3	(%)	0.01	0.018	0.011	0.021	0.005	0.039	0.02	0.01	0.006	0.005	0.043	0.021	**0.02**	0.008	0.007	0.008	BD	0.006	0.006	0.002	**0.01**
Fe2O3	(%)	7.76	12.7	10.3	6.73	5.35	8.21	17.7	4.49	6.86	3.78	7.21	8.93	**8.34**	27.1	30.8	3.99	10.5	28.1	3.98	1.68	**15.16**
K2O	(%)	2.58	0.518	0.187	6.79	3.04	5.8	2.83	0.093	5.17	5.99	5.58	1.64	**3.35**	0.714	1.87	3	1.21	0.541	3.93	4.23	**2.21**
MgO	(%)	0.95	1.81	4.76	1.37	1.48	2.99	1.84	2.19	1.72	2.31	1.91	3.53	**2.24**	2.89	1.14	0.65	1.59	4.32	0.57	0.48	**1.66**
MnO	(%)	0.04	0.08	0.18	0.05	0.05	0.14	0.08	0.07	0.11	0.11	0.08	0.28	**0.11**	0.3	0.09	0.09	0.28	0.36	0.11	0.02	**0.18**
Na2O	(%)	7.07	7.08	6.17	1.89	7.25	2.17	4.66	8.86	0.57	4.88	3.36	2.87	**4.74**	0.74	2.49	5.46	7.6	2.7	2.33	1.76	**3.30**
NiO	(%)	0.013	0.019	0.015	0.014	0.005	0.011	0.017	0.01	0.009	0.002	0.012	0.006	**0.01**	0.013	0.018	0.014	0.004	0.016	BD	BD	**0.01**
P2O5	(%)	0.089	0.133	0.1	0.091	0.094	0.126	0.09	0.153	0.013	0.116	0.091	0.052	**0.10**	0.026	0.113	0.155	0.122	0.056	0.127	0.118	**0.10**
SiO2	(%)	56.86	51.51	42.02	61.3	57.17	54.03	45.84	56.67	67.18	57.26	57.44	54.35	**55.14**	39.42	32.3	65.67	54.68	26.97	68.53	75.83	**51.91**
SO3	(%)	14.25	24.72	16.93	12.26	9.28	7.22	33.35	6.28	12.47	5	9.63	15.22	**13.88**	50.6	56.16	4.63	14.57	53.45	2.48	0.48	**26.05**
TiO2	(%)	0.39	0.37	0.28	0.42	0.38	0.6	0.35	0.37	0.18	0.26	0.63	0.37	**0.38**	0.2	0.27	0.27	0.27	0.11	0.3	0.22	**0.23**
V2O5	(%)	0.01	0.012	0.006	0.062	0.008	0.028	0.014	0.006	0.011	0.007	0.039	0.012	**0.02**	0.01	0.017	0.005	0.014	0.005	0.007	0.009	**0.01**
CO2	(%)	2.53	4.36	12.1	1.83	3.81	4.33	4.33	5.83	4.29	5.83	2.27	8.47	**5.00**	8.51	3.04	2.27	1.98	11.3	2.13	0.73	**4.28**

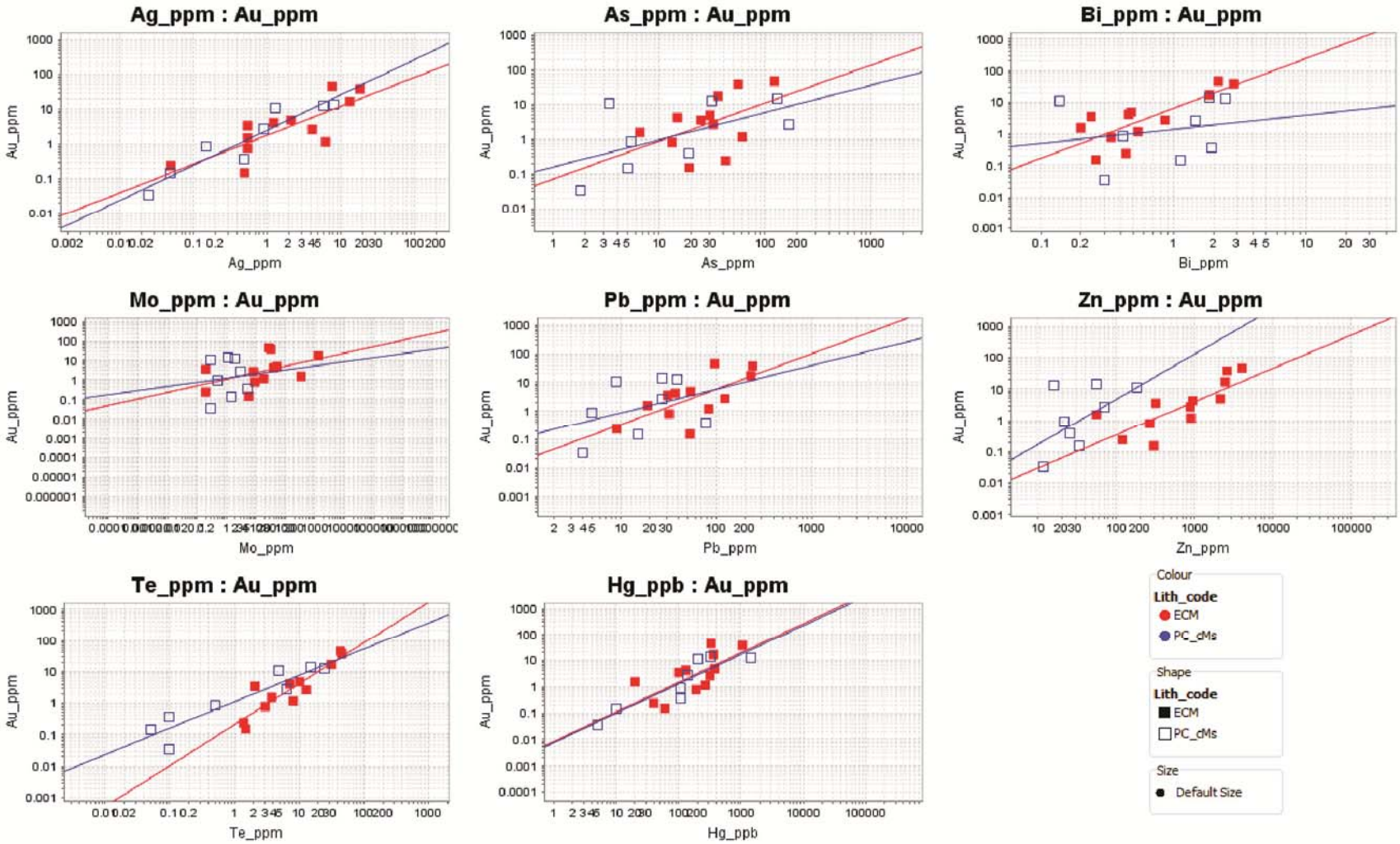

Figure 7.25 – Log normalised plots of selected metals vs. Au in the Binduli Eastern Contact Mineralisation (ECM), and from selectively sampled sulphide replaced mudstone clasts from the Binduli Porphyry Conglomerate (PC_cMs). Regression lines show correlation between the two sample types in a range of metals, which support the field observations that rip-up clasts of ECM are contained in the porphyry conglomerate.

In the ECM, assessment of metal values from the whole rock analyses using ioGAS-64 software shows correlation between high-grade gold with silver, bismuth, tellurium, and zinc, and a lesser positive association of gold with lead and mercury; all of which showed enrichment values above background levels. The ore is low in copper (~72ppm Cu) and has a negative correlation with high gold grade, but has elevated molybdenum (up to 1300 ppm, averaging 153ppm Mo). A summary metal association for the ECM replacement style mineralisation is Au-Ag-Bi-Te-Zn (±Mo, Pb, Hg).

Assessment of the chemistry of sulphide-replaced clasts from the porphyry conglomerate shows generally lower concentrations of metals than the whole rock ECM samples. There may be issues of sample purity and other analytical issues associated with the clast pebbles since they are small, low volume samples (as small as 3cm x 3cm) and may not have true comparative value with the ECM samples, which were up to two metre sections of quartered drill core.

Comparatively, the element association of the ECM mineralisation and sulphidised clasts is the same, regardless of the absolute metal levels. Correlation coefficients for the clasts in the porphyry conglomerate show good correspondence between Au-Ag-Sb-Bi-Te-Hg. Antimony (Sb) correlates strongly with As and Cu as would be expected if the mineralisation contained tennantite or tetrahedrite, but the absolute values of those elements is low. A very strong correlation exists between Te and Hg as for the Fimiston mineralisation at the Golden Mile (Clout 1990; Gauthier et al. 2004a). One major difference in metal signature between ECM and clasts is the consistently low Zn values in the clasts, which may reflect alteration by a later event that overprints the ECM and porphyry conglomerate.

The ECM metal association: Au-Ag-Bi-Te-Zn (±Mo, Pb, Hg) is anomalous for typical orogenic mineralisation: Au-Ag ± As ± B ± Bi ± Sb ± Te ± W as defined by Groves et al. (2003). Anomalous Hg in sulphide-replaced clasts in the porphyry conglomerate (Au-Ag-Sb-Bi-Te-Hg) supports the possibility that the clasts are fragments of a pre-unconformity mineralisation despite the clasts having low concentrations of Zn and Mo. It should be noted that As is a common pathfinder for orogenic gold deposits throughout the Eastern Goldfields Province and, whereas present at moderate levels in the Binduli deposits, does not display the widespread anomalism characteristic of gold camps throughout the district.

7.4.7 Timing of mineralisation

Syn-sedimentary intrusions and volcaniclastic rocks are observed as intercalated with ECM in the Centurion mine and in drill core, which supports the palaeo-depositional model of Crossing (2001). The age of the ECM felsic volcanic rocks is not known, but they may correlate with similar coarse-clastic, dacitic volcaniclastic rocks with intercalated mudstone units, 600 m east of the Centurion Fault; and at Gibson-Honman Rock 2.5 km east of the Centurion deposit (Stage 1 in Fig. 7.26). Sulphide replacement of the interstitial spaces between grains in fine-

grained tuffaceous sedimentary rocks indicates the possibility for syn-genetic replacement during seafloor hydrothermal alteration related to high-level felsic volcanic extrusions; or that post-depositional replacement occurred.

Critically, the siting of sulphides in what was clearly a primary porosity makes it improbable that the sulphide replacement was related to late lode-Au WCM alteration. The ECM mudstones were lithified, and the sequence was folded prior to the D3 folding and foliation that was accompanied by WCM vein mineralisation. Maintaining a primary porosity throughout burial F1 and F2 folding is an unlikely proposition.

Given the Au-Ag metal signature of the ECM (sans base metals), and the unfavourable geochemistry of the Black Flag sequences for VMS mineralisation (Witt et al. 1996), the ECM style at Binduli is probably not of a true VMS association, or exhalite as proposed by Arnold (1997). Nonetheless, the sequence is clearly an early replacement mineralisation that was structurally overprinted by later events, and may have been related to seafloor hydrothermal fluid systems.

Centurion Porphyry intruded the ECM with a crystallisation age of 2667±3 Ma interpreted from SHRIMP U-Pb analysis of zircons (Fletcher et al. 2001), providing a minimum age for the ECM of ~2670 Ma (Stage 2 in Fig. 7.26). This constraint places the ECM volcaniclastic and sedimentary rocks within analytical error of the interpreted SHRIMP U-Pb age of Gibson-Honman Rock at 2675±6 Ma (Krapez et al. 2000).

Field relationships show the Binduli ECM and Centurion Porphyry were ripped-up at the basal unconformity of the distinctive Binduli porphyry conglomerate unit. Inclusion of Centurion Porphyry fragments in the conglomerate provides a maximum age of deposition for the Binduli Porphyry Conglomerate of <2664 Ma (Stage 3 in Fig. 7.26; Section 3.23). A minor (intermediary) mineralisation event overprinted the ECM and porphyry conglomerate with crustiform carbonate-quartz-fluorite-galena veins.

Pre-Kurrawang folding of the lower and upper Black Flag formations is demonstrated by regional mapping and the correlation of the Binduli sequence interpreted at Goldilocks, south of Kundana (Stage 4 in Fig. 7.26; Chapter 3). The gross structure of the Centurion sequence is a shallow to moderate north-plunging anticline, which is unconformably truncated and overlain by units of the Kurrawang Formation to the west of the mine (Stage 5 in Fig. 7.26). Navajo Sandstone at the base of the Kurrawang cuts-out the Binduli Porphyry Conglomerate along strike from Centurion gold mine, but similar units in the Goldilocks area suggests the porphyry conglomerate had a much wider distribution.

Post-Kurrawang F3 folding and metamorphic foliation deformed the F2-folded Binduli sequence with folding of early sulphide-replaced mudstone units and crustiform veins with an axial-planar biotite foliation. Later strain localisation produced shear zones such as the D3 Centurion Fault with concurrent development of late ‘orogenic-style’ quartz-carbonate-Au-base

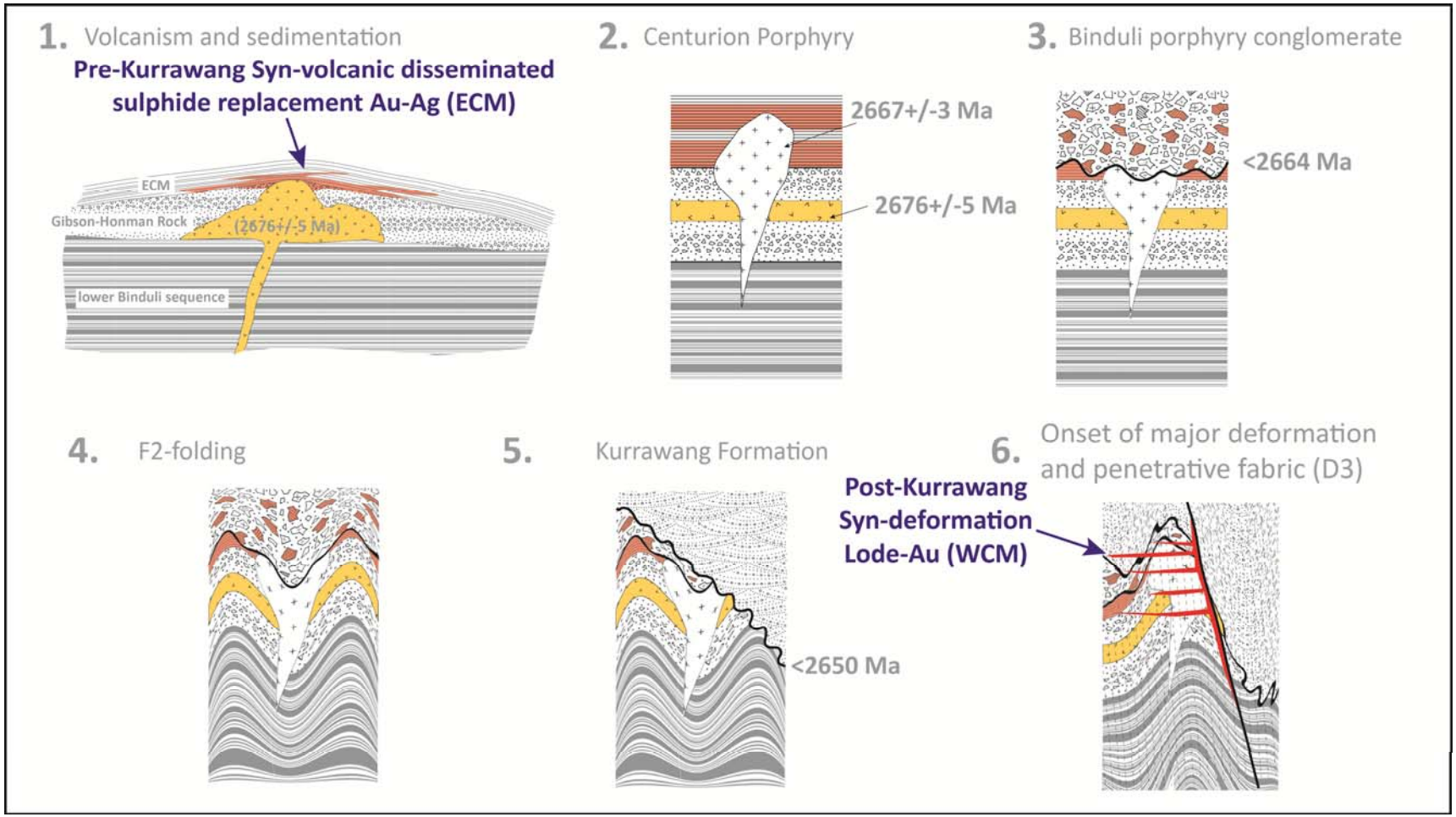

Figure 7.26 – Schematic representation of structural timing of stages in the Binduli mining district leading to two distinct and temporally separate gold mineralisation events. Early ECM replacement-style disseminated mineralisation was intruded by the Centurion porphyry. Erosion of those units produced a distinctive conglomeratic unit that contains clasts of the Centurion Porphyry and the sulphide replaced mudstones. Deformation (D2) produced a folded unconformity and was followed by later exhumation and deposition of the Kurrawang Formation above a second angular unconformity. Deformation (D3) of the Kurrawang Formation and synchronous-late, lode-gold style (WCM) quartz-carbonate-gold vein mineralisation followed Stage 5, with vein emplacement related to reverse fault movements, in which the veins cross-cut all previous fabrics.

metal veins in stacked arrays that appear genetically related to late shear zones and reverse-fault movements (Stage 6 in Fig. 7.26).

This sequence clearly demonstrates there are two separate gold-bearing mineralisation events at Binduli that have distinctive metal associations and styles. Early seafloor hydrothermal alteration and mineralisation is expected in areas where high-level felsic intrusions and extrusions interact with sediments in the seafloor environment. High-level stratiform mineralisation styles are common throughout the district and these occurrences support the contention of an early phase of gold mineralisation prior to the regionally pervasive lode-gold deposits (see also Hutchinson 1987). Early high level mineralisation was demonstrated for the Kanowna Belle district by Ross et al. (2004) who documented epithermal Au-rich vein clasts in the Golden Valley Conglomerate, footwall to the Kanowna Belle Gold Mine. Golden Valley Conglomerate is also folded and foliated by later deformation events that have associated lode gold deposits.

7.4.8 Binduli summary

Centurion gold deposit at Binduli shows evidence of two mineralisation events separated by intrusion, unconformity and deformation. The early event has characters that suggest ECM replacement style mineralisation in a high-level seafloor environment, the later WCM event is typical of deeper crustal levels and related to late deformation and metamorphism, and is time-correlated with the Kundana gold deposits. Gold mineralisation events at Binduli, located close to the major Kurrawang unconformity, provide key constraints on the timing of exhumation, regional folding/foliation, and mineralisation.

7.5 Discussion: timing of mineralisation, unconformity and cross-cutting

Early sulphide-replacement style ECM mineralisation was developed prior to the unconformity that separates the Lower and Upper Black Flag Formations. The Centurion porphyry with an interpreted age of crystallisation at 2667±3 Ma intruded the ECM and provides a minimum age of deposition for the ECM siltstone-mudstone sequence before ~2670-2664 Ma. On Table 6.1, the Binduli ECM is noted as a possible correlative of other sulphide replacement style occurrences in the district (e.g. Spargoville; Lake Yindarlgooda Ministerial Reserve, and potentially Nimbus high-grade Ag-Hg deposit, which is located within the Perkolilli rhyolite unit - 2675±3 Ma; Nelson 1995). The age of mineralisation at Binduli is unknown, but early magnetite-biotite, and hematite alteration suggest a strongly oxidised fluid, and the anomalous metal signature of the ECM is atypical for lode-gold mineralisation elsewhere in the Kalgoorlie district. Given these constraints and the textural characters of the replacement style, the option of a seafloor replacement style deposit, related to high-level

intrusions in the vicinity of submarine felsic lava dome complexes is a possible explanation for the setting of the ECM.

A further possibility is for replacement-style mineralisation related to hydrothermal alteration during the intrusion of the Centurion Porphyry at a later stage. The setting of the Centurion porphyry is not known in detail, but clasts of Centurion Porphyry making up the bulk of the Binduli Porphyry Conglomerate suggest both ECM and Centurion Porphyry were available source rocks to that depositional event. Whether the Centurion Porphyry was a causative intrusion in the mineralisation of the ECM is not resolved with the available data.

Geochronological and structural constraints from Chapter 6 place the deposition of the Binduli Porphyry Conglomerate as post-F1a isoclinal folding, but possibly related to D1b (Table 6.1). Folding (F2) produced the broad Mount Pleasant Anticline and folds in the Binduli felsic volcanic and sedimentary sequences including the Binduli Porphyry Conglomerate, which extend west to the Kundana South/Goldilocks area. This was followed by uplift and erosion and deposition of the Kurrawang/Navajo sequence above a major conglomerate unconformity at <2650 Ma that marks the end of extrusive volcanism in the Kalgoorlie district. The D3 deformation of the Kurrawang sequence was broadly synchronous with the WCM orogenic lode-gold mineralisation style, which occurs primarily in flat veins in the footwall of the Centurion Fault, and as extensional vein arrays that cross cut the folded and S3 foliated eastern limb of the Kurrawang Syncline.

This sequence of cross-cutting implies a gap in timing between ECM replacement style and WCM veins of ~14 Ma if the upper error of the Centurion Porphyry is used (2664 to <2650 Ma), or ~20 Ma for the lower error of the Centurion Porphyry age (2670 to <2650 Ma). Kundana orogenic-style quartz carbonate veins are of a similar style to the WCM veins at Binduli, and are constrained in their timing of development as syn- to post-regional F3 folding and S3 foliation. The age interpreted from SHRIMP U-Pb analysis of hydrothermal phosphate at 2639±3 Ma, is a reasonable estimate of the timing of orogenic lode gold mineralisation and is supported by the available field relationships.

7.6 The conglomerate - gold relationship

Binduli and Kundana mining centres are linked by the fact they both contain gold deposits that expose the Kurrawang unconformity, and that the sequences that host gold deposits at Binduli are also present at Goldilocks to the south of Kundana, and that also host broad areas of weak disseminated replacement-style gold mineralisation. At Binduli the trend of the western line of gold deposits defines the margin of the Kurrawang Formation, whereas at Kundana the ‘Kurrawang gold deposit’ exposes the unconformity (Fig. 7.3). The Kurrawang Formation is also sheared with slivers of the polymictic Kurrawang Conglomerate emplaced into the Zuleika Shear Zone where it outcrops in the North and Arctic mines (Fig. 7.3).

Spatial relationships between late clastic unconformable conglomerates and gold deposits are documented in all Neoarchaean terranes globally, and are particularly evident in the Rouyn-Timmins segment of the Abitibi in Canada, with a strong spatial association of preserved slivers of Timiskaming sedimentary and tuffaceous rocks and gold deposits, along the Porcupine-Destor Fault (Robert et al. 2005; Bateman and Bierlein 2007). A similar relationship exists in the Kambalda-Agnew section of the EGP with major gold deposits spatially associated with late clastic sedimentary rocks at Kambalda, Kalgoorlie, Leonora and Agnew - yet a single fault cannot be demonstrated to have continuity over that region. In the Musoma-Mara region of the Lake Victoria Greenstone Belt in Tanzania, a spatial association of gold occurrences and unconformable late clastic sedimentary rocks along major faults is a clear control on major gold deposits (Tripp et al. 2007c, unpublished data), and similar relationships are demonstrated between gold districts and the Palkanmardi Conglomerate in India (Poulsen 2010).

Late clastic sequences are interpreted to mark the onset of orogenesis in greenstone belts (Robert et al. 2005), and were developed syn-orogenically as demonstrated by strong linear distributions of lithofacies, with major fault controls on at least one margin. In this respect the units are fault-preserved slivers of previous basins or basin segments, but are not themselves basins as such.

Several models have been proposed to explain the spatial association of major gold deposits and late clastic unconformable sequences. An early model (Hall 1998) held that the late clastic sequences covered a much wider lateral area than the present day linear remnants. Given that major gold deposits are located in the upper parts of the greenstone stratigraphy, it was postulated that the sedimentary rocks acted as a sub-regional hydrothermal ‘seal’ that allowed the upper greenstone segments to overpressure, fracture and release magmatic sourced, metal-rich oxidised fluids that would mix with basinal reduced fluids. By a mechanism of mixing fluids of drastically different redox states, voluminous precipitation of metal could be precipitated in the hydro-fractured upper greenstones.

A second hypothesis interpreted that major shear zones controlled the linear distribution of the late clastic rocks, and the conglomerate-gold relationship could be one, in which the fault-preserved conglomerate remnants identify major crustal-tapping structures that were long-lived and controlled major fluid flow and gold precipitation. Linear distribution of gold deposits within a certain proximity to major shear zones is an empirical criterion commonly applied in exploration for gold deposits (Groves 2000; Weinberg et al. 2004). Crustal tapping structures are thought to be a significant control on the location of greenstone-hosted gold deposits where they are intersected by higher order faults and shear zone splays (Groves 1993; Vearncombe et al. 1989; Nguyen 1997).

A third and less speculative explanation for the conglomerate-gold relationship is one of preservation (Dr. H. Poulsen written communication 2003). This concept interprets that areas

with the youngest stratigraphic units have the potential to preserve the thickest sections of greenstone stratigraphy. In many Archaean sequences worldwide, the presence of multiple mineralisation styles and timings is well documented. Since those styles include some syn-genetic deposits and high-level intrusion-related systems, the potential to preserve early mineral systems will require extensive depocentres that were not significantly eroded during the orogenic phase, and the presence of thick sequences of the youngest syn-orogenic sedimentary rocks will identify those areas of preferential preservation.

A recurring theme is that the world-class and giant Archaean greenstone deposits have coincidence of multiple styles and timings of mineralisation (e.g. McIntyre-Hollinger, Canada; Fimiston-Mt Charlotte, WA). Development of early mineral systems during complex deformation phases and intrusive events may result in areas of the crust that were re-activated by later fluid and intrusion events after a period of dormancy.

7.7 New opportunities identified from this work

The recognition of late clastic sequences identifying crustal *regions* of preferential preservation has wide application in area selection for exploration. A critical new understanding from the work here is that a second, and earlier, unconformity between lower and upper Black Flag formations, has a specific and real spatial association with the locations of major gold deposits at Kanowna Belle and Binduli (Fig. 7.27; Fig. 7.28). Recognition of this unconformity as possibly skirting the eastern edge of the Golden Mile district may provide a similar relationship for the largest Archaean greenstone gold deposit.

Kanowna Belle gold mine is understood as a locus of intrusion and mineralisation, and has previously been explained with structural controls on mineralisation (Davis et al. 2000). Work completed here has identified the Grave Dam unconformity located in the mine at Kanowna Belle as representing a ~20 ma time gap (Fig. 7.27) and, as such, a major unconformity within the Kalgoorlie district that is correlated with the Gidji conglomerate unconformity, and the Binduli Porphyry Conglomerate unconformity (Chapter 3; Chapter 4). The presence of this time break suggests that a long period (~20 ma) of quiescence was followed by an orogenic pulse that included rapid exhumation and felsic volcanism (Grave Dam member; Gidji felsic/Gidji Conglomerate; and Upper Black Flag formation dacitic volcanic and sedimentary rocks south of Binduli). The timing of intrusion of the Kanowna Belle Porphyry overlaps this orogenic pulse, and it is possible the fault that controlled the deposition of the Grave Dam member was actively intruded by the high-level Kanowna Belle Porphyry, which was later deformed as documented by Davis (2000).

A sub-regional scale unconformity with a spatial association with major gold deposits presents a significant opportunity for area selection and exploration targeting (Fig. 7.28). Key requirements include detailed maps that portray the correct distribution of stratigraphy; way-up;

structure; and the locations of major unconformities. These data sets are the fundamental tools of exploration that can be enhanced with, but not substituted by, geophysical or geochemical data sets. Use of the latter sub-regional data sets is greatly improved when compared against accurate, basic geological data.

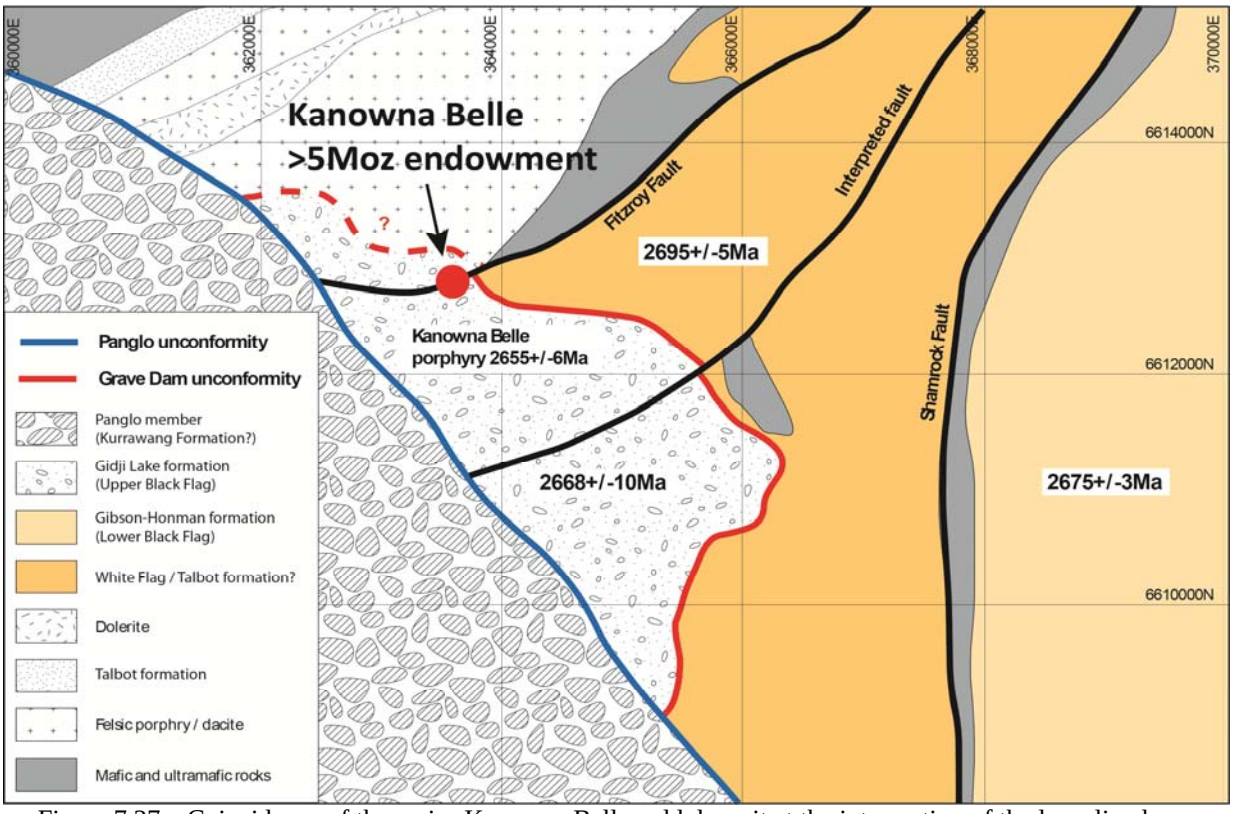

Figure 7.27 – Coincidence of the major Kanowna Belle gold deposit at the intersection of the long-lived Fitzroy Fault with an unconformity between upper Black Flag Gidji Lake formation and folded underlying units

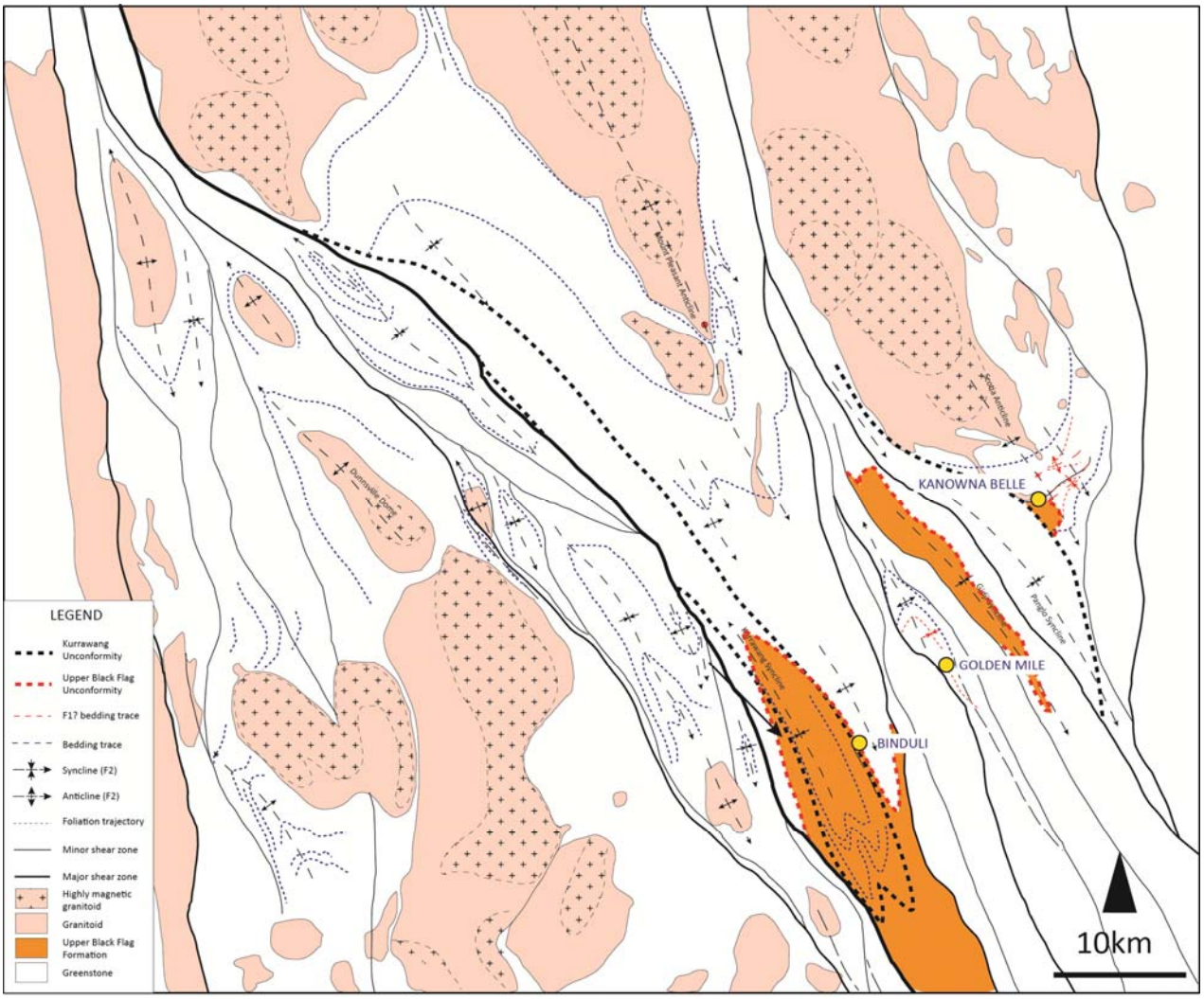

Figure 7.28 – Map showing the regional distribution of the Upper Black Flag unconformity and a spatial association with major gold deposits. In practical terms, identifying long-lived faults and their location and intersection with unconformities provides a key criterion in area selection for major Neoarchaean gold deposits.

8 Discussion and synthesis

8.1 Stratigraphy and structural geology

The approach taken in this study attempts to synthesise stratigraphic, structural and geochronological data to understand the development of the Kalgoorlie greenstones, and by representing those data on maps, to assess the controls on major gold deposits. This approach is less radical than that suggested by Kusky and Vearncombe (1997) who advocated: “The structure and stratigraphy of greenstone belts will only be unravelled when ‘stratigraphic’ methods of mapping are abandoned”. On the contrary, integrated structural and stratigraphic understanding was critically lacking from studies of the Eastern Goldfields Province prior to the AMIRA and pmdCRC projects from 2000 onwards, which advanced the stratigraphic understanding substantially (particularly the work of Krapez et al. 2000). Previous to this, interpretations relied heavily on geophysical interpretation and sparse fabric data, with minimal constraining information from the stratigraphy, since high-quality geochronological data were generally lacking.

In Chapter 3, considerable attention was paid to the mesoscopic textural and compositional characters of coarse clastic units in the study area for the purpose of lithostratigraphic correlation, and to identify units for analysis with SHRIMP geochronology (Chapter 4). A new understanding from this work is the identification of two major formations interpreted as lower and upper ‘Black Flag formations’; or a preferred local terminology of Gibson-Honman formation and Gidji Lake formation, for lower and upper units respectively (Chapter 4). This major subdivision appears to apply well in the study area and accounts for the ‘Black Flag Group’ formations that cover all of the studied tectonostratigraphic domains. Units that correlate with the ~2675 Ma Gibson-Honman formation include Lakewood dacite and Perkolilli rhyolite; units that correlate with ~2660 Ma Gidji Lake formation include Binduli Porphyry Conglomerate, and Grave Dam grit member at Kanowna. The formation map in Chapters 3 and 4, is the first available map that shows a preliminary subdivision of the generalised ‘Black Flag Beds’ and the interpreted spatial location of the major unconformities in the Kalgoorlie district.

The Gibson-Honman formation (GHf) has a gradational lower contact with underlying ~2680 Ma White Flag Formation proximal andesitic volcanic rocks in the Ora Banda Domain, interpreted from a major component of intermediate rocks in the former (GHf). This gradation is indicative of a gradual change from intermediate to felsic volcanism at least in the Ora Banda Domain, but in general terms, the appearance of the White Flag and Gibson-Honman formations overlying Upper Basalt heralds a major change from mafic to felsic volcanism in that domain. In the Kambalda Domain the change is indicated by the Lakewood dacitic felsic volcanics; and in the Boorara Domain, the Perkolilli rhyolitic volcanics.

In the Ora Banda Domain, andesitic and dacitic volcanic rocks are generally composed of stratified volcanic breccia and syn-volcanic coherent sills, gradational and intercalated with below-wave-base deposited turbiditic sedimentary rocks of the Talbot formation at the base, but also with unnamed thick sequences of similar rocks at several levels in the column: field reconnaissance shows that rhyodacitic volcanic rocks at Gibson-Honman Rock sit above a thick sequence of fine-grained sandstone and shale to the north. The volcanic setting for the White Flag and Gibson-Honman formations is sub-marine lava dome complexes typical of silicic lavas extruded into shallow water (Cas and Wright 1987); or sub-aqueous extrusive domes or cryptodomes (McPhie et al. 1993) that reflect a probable continuation of an extensional basin setting that commenced with deposition of the mafic volcanic sequences.

Gidji Lake formation coarse clastic sedimentary and volcanic rocks are thick packages of poorly sorted, to plane-bedded rocks with local evidence of sub-aerial volcanic inputs unconformably overlying the Gibson-Honman formation. Structural characteristics of those units indicate there may have been local fault controls on the deposition of the sequences (Gidji conglomerate; Grave Dam grit; Binduli Porphyry Conglomerate). Interpreting the tectonic controls on the deposition of the Gidji Lake Formation as either extensional or contractional is problematic, since local extensional fault controls could be accommodated in a transpressional contractional setting. The poorly-sorted nature of the Binduli porphyry conglomerate and Grave Dam Grit suggests rapid deposition in proximal fault-controlled half grabens, whereas the Gidji conglomerate is possibly an intermediate to distal equivalent, given a dominance of plane-bedded, well sorted quartzolithic sandstone and shale, with intervals of felsic volcanics.

The Kurrawang Formation records a rapid exhumation of the greenstones in that it contains a diverse provenance indicated by the composition of clasts, and a variety of zircon populations including all major volcanic episodes, but also a >3.0 Ga zircon population unrelated to any volcanic or intrusive units in the EGP. The late clastic sequences are the youngest Neoarchaean rocks, which were followed by orogenic contraction and metamorphism. The youngest rocks in the study area are Proterozoic, in the form of pervasive dyke swarms.

8.2 Structural history

The deformation history presented in Chapter 6 outlines the major deformation episodes in the context of the stratigraphy and considers the sedimentary responses to tectonism. Using the mappable unconformities, granitoid intrusions and cross-cutting relationships, the age of each deformation stage can be estimated, or bracketed as listed in Table 6.1.

Extension of a pre- ~2700 Ma greenstone basement led to the deposition of mafic and ultramafic volcanic rocks, and probably continued up until the deposition of the Gibson-Honman formation (lower Black Flag). Folding of the sequence led to the formation of localised isoclinal F1 folds, but uncertainty surrounds F1 folding and the nature of that deformation.

Three possibilities include: (1) F1 was extensional and developed with an influence from granitoid doming - in which case the F1 folds would be part of a continuous 'DE' extensional episode that terminated with the onset of D2 contraction, (2) F1 was produced during contraction and represents a ‘tectonic mode switch’ (e.g. Czarnota et al. 2010) if followed by resumed extension to accommodate deposition of the Gidji Lake formation, or (3) F1 folds were produced with nappe-style transport marking a major change from extension to contraction. For option (3), Gidji Lake formation sequences that unconformably overlie F1 folds may have been developed as syn-orogenic basins, possibly with a strike-slip control, or as syn-thrusting sedimentary basins (e.g. deWit et al. 1992). No absolute criteria are available to critically assess the merits of the three options presented for F1 folding, but the restricted (non-regional) development of the F1 folding suggests there was non-uniform preservation in a highly dissected terrane.

Second folding F2 is the dominant regional fold-forming event that affected all older sequences, and took place after the deposition of the Gidji Lake formation (youngest sequences in the Black Flag Group). At that stage, the onset of a major ENE-WSW contractional deformation phase was progressing, characterised by fault-bend folding with ramp anticlines, particularly evident in the sedimentary rocks, with a dominance of anticlinal domains separated by major faults, and isolated narrow synclinal domains.

Linear, fault-controlled late clastic sequences of the Kurrawang and Panglo formations are primarily distributed as synclinal remnants of fluvial to marine sequences preserved in the footwalls of west-dipping major faults. This structure is typical of many of the late clastic sequences elsewhere in the EGP and may represent footwall preservation of an originally fault controlled basin, where the rocks in the hangingwall of the controlling fault were removed by syn- to post-inversion exhumation (e.g. Bleeker and van Breemen 2010; Bleeker 2012).

A possible modern analogue for linear, fault-controlled basins is the Markham Valley alluvial / fluvial system in an actively deforming transpressional setting at the Australia-Papua New Guinea margin (Tingey and Grainger 1976; Abbott et al. 1994). In that setting, a >300km long basin is currently developing at up to ~800m elevation above sea level, above the Ramu-Markham Fault Zone, which marks the Australia-Pacific plate boundary. An active braided river system is flanked by mountainous regions that feed the basin with alluvial fans, which source a full age-spectrum of rock types from the New Guinea Mobile Belt to the south (Triassic to Pliocene), and the Finisterre accreted arc terrane to the north (Oligocene-Pliocene). The braided river system becomes a marginal-marine outwash system at the Huon Gulf to the east.

Critical aspects of the Markham Valley setting include the development of a thick accumulation of conglomerate and sandstone >300km long x 10km wide, within an actively uplifting mountain range in a transpressional tectonic setting. The tectonics includes a local, high angle of convergence in a SSW direction perpendicular to regional orogen-parallel

structures (Abers and Mcaffrey 1994). From this example it is clear that bulk extension is not a requirement to develop linear sedimentary basins such as the late clastic sequences in the Eastern Goldfields Province, but that syn-orogenic clastic sequences can readily be formed in contractional or transpressional settings. The lithofacies and sequences of the Kurrawang and Panglo are not directly comparable to the Markham Valley setting: the latter includes meandering river deposits and sedimentological characteristics typical of a modern, very-high rainfall environment. Critically, the modern setting has tropical vegetation, which controls the meandering habit of rivers by bank stabilisation, a characteristic lacking from Precambrian fluvial systems and which leads to a dominance of braided fluvial systems in those settings (Miall 1992).

Deformation and metamorphism of the Kurrawang and earlier greenstone sequences mark the onset of penetrative deformation that was dominantly contractional, with a pervasive regional axial planar foliation to F3 folds. That foliation was accompanied by D3 shear zones, lode-Au mineralisation, and was overprinted by D4 faults and localised intrusions.

8.2.1 Role of granitoid intrusion during deformation

Key to the structural history and tectonic interpretation of the study area is the role played by granitoid doming (if any), versus externally driven contractional and extensional deformation (e.g. Myers and Watkins 1985). 'Doming' here refers to intrusion synchronous with deformation, but can also relate to solid-state diapirism in which magmatism may precede deformation by a significant time interval. The Eastern Goldfields Province is well-known for its strong linear NNW-SSE striking structural grain (e.g. Isles et al. 1989) and was categorised by Kusky and Vearncombe (1987) as "broad greenstone terrains with internally bifurcating lithological domains and irregular granitoid contacts" - one of three end-member regional greenstone outcrop patterns (Fig. 8.1 a-g).

In geophysical images of the EGP a range of granite-greenstone contact relationships is observed including: (1) greenstones with bedding parallel to granite dome contacts (Fig. 8.1 c, f); (2) greenstone fabrics wrapping granite domes in a 'foliation / porphyroblast' type relationship (Fig 8.1 e, g); (3) folded bedding cut by intrusions (Fig. 8.1d); and (4) strike-slip superimposed on doming (Fig 8.1a). The influence of granitoid doming throughout the deformation history is difficult to quantify, but in the study area, an influence from doming is suggested by several key observations including the structural geology of the Magdala Mine in a complex granite contact zone (Chapter 5); regional granite-greenstone contact patterns (e.g. Owen Complex; Fig 8.1); disruption of the F2 fold geometry at Mount Pleasant; and reactivation of the Talbot formation basal decollement fault by the Liberty Granodiorite at Mount Pleasant (Chapter 6).

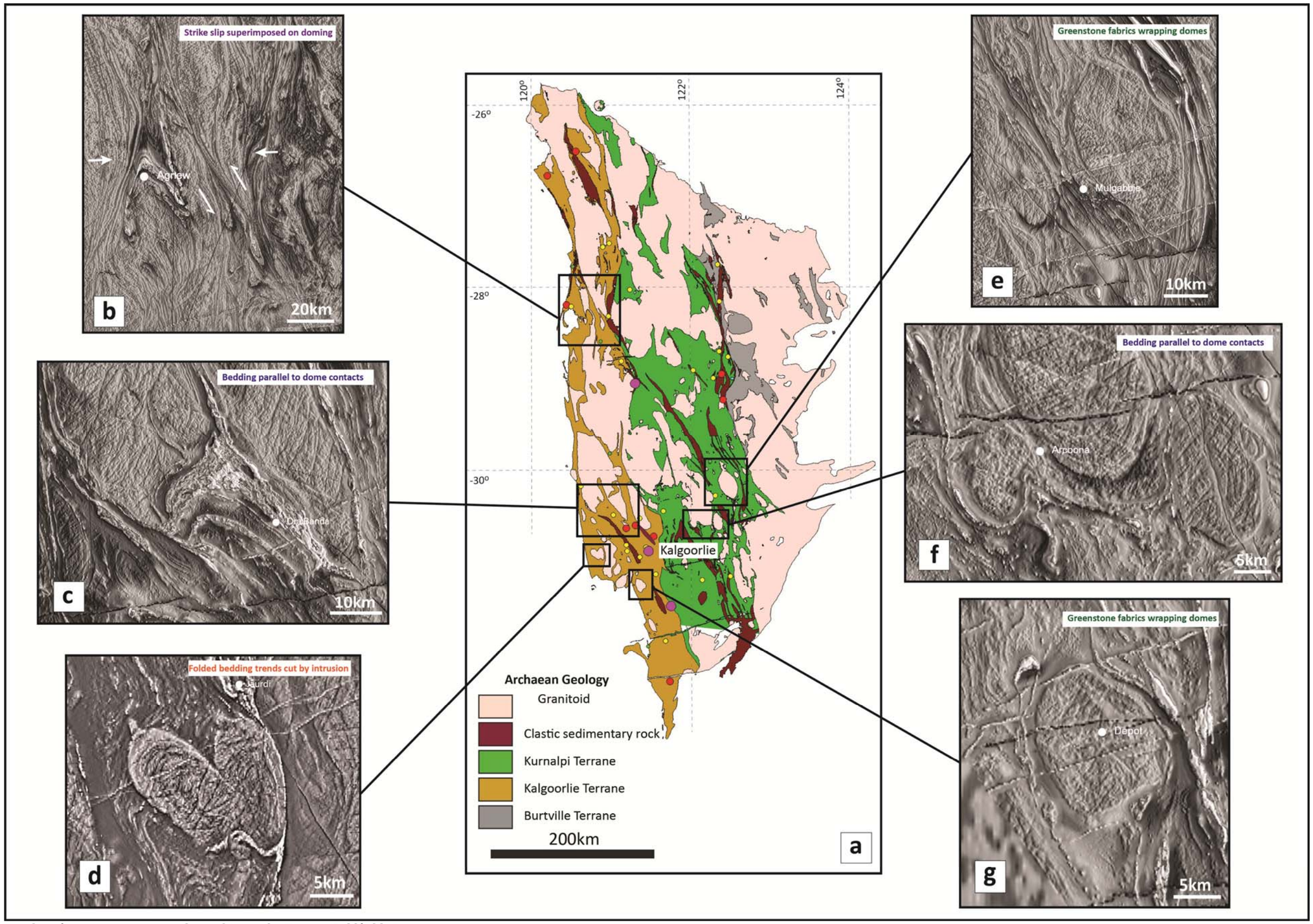

Figure 8.1 – Examples of granite-greenstone relationships in the Eastern Goldfields Province

With two possible inputs (1) intrusion, (magmatic or later diapiric), and (2) far-field shortening, the potential exists for a combination of processes, for example: (a) a granite-greenstone, dome and keel tectonic belt, later deformed by a superimposed contractional deformation event, or (b) an ongoing input from granite doming during externally imposed contractional deformation. Option (a) could be envisaged as a terrain typical of the Mesoarchaean Pilbara Block (Fig. 8.2a) later deformed by a major regional contraction, but a generally shallow depth to the base of the EGP greenstones demonstrated by seismic data, indicates the greenstone belts are not deep 'keels' anchored in the upper to middle crust (Goleby et al. 1998). Option (b) appears to be a better fit given the close correspondence between intrusion and greenstone ages. This may account for the typical form of narrow linear belts of greenstone terrane volcano-sedimentary rocks, interspersed with elongate granitoid batholiths and plutons, and separated by major faults and shear zones (Fig. 8.2b). A mix of vertical and horizontal tectonic influences is a possible explanation for the typical granite-greenstone relationships in the Kalgoorlie district, that suggestsgranitoid doming during active shortening may have been an ongoing process.

8.3 Mineral deposit styles and metallogenic setting

Preservation of early probable VMS-type mineral systems and world-class komatiite hosted Ni-Cu-PGE deposits at Kambalda, that are overprinted by later lode-Au type vein deposits, argues for a rift-related setting for the Kalgoorlie Terrane in at least the earliest stages of development (e.g. Hutchinson et al 1971; Hutchinson 1981; Hutchinson 1987; Groves and Batt 1984; Poulsen et al. 1992; Campbell and Hill 1998; Swager 1997; see also Hannington et al. 2005). VMS-type precious and base-metal systems are also located elsewhere in the Kalgoorlie Terrane and EGP including: Nimbus high-grade Ag VMS (Henderson 2012); Binduli Au-Ag disseminated sulphide replacement (Chapter 7); Yindarlgooda Ministerial Reserve Cu-Zn (Sofoulis et al. 1969); Spargoville (Fehlberg and Giles 1984); syn-volcanic hydrothermal alteration on the Mt Georges Shear Zone at Leonora (H. Poulsen written communication 2012; Witt and Hagemann 2012); and true base-metal (Cu-Zn-Ag-Au) VMS deposits at Teutonic Bore and Jaguar (Hallberg and Thomson 1985). The syn-volcanic VMS-type metallogenic characters of the district are contrasted with a general lack of mineral deposit types that would be expected in convergent margin settings (porphyry Cu-Au and precious metal epithermal; e.g. Seedorff et al. 2005; Hutchinson 1987) notwithstanding a close *spatial* association of lode-Au deposits with hypabyssal porphyry intrusions (Perring et al. 1991).

Given that most EGP research work and available exposure is closely associated with mineral deposits, the paucity of preserved high-level epithermal and porphyry associated systems seriously detracts from arguments in favour of subduction / arc-accretion in the Neoarchaean. If modern-style subduction / arc-accretion could be demonstrated for the EGP and major sutures

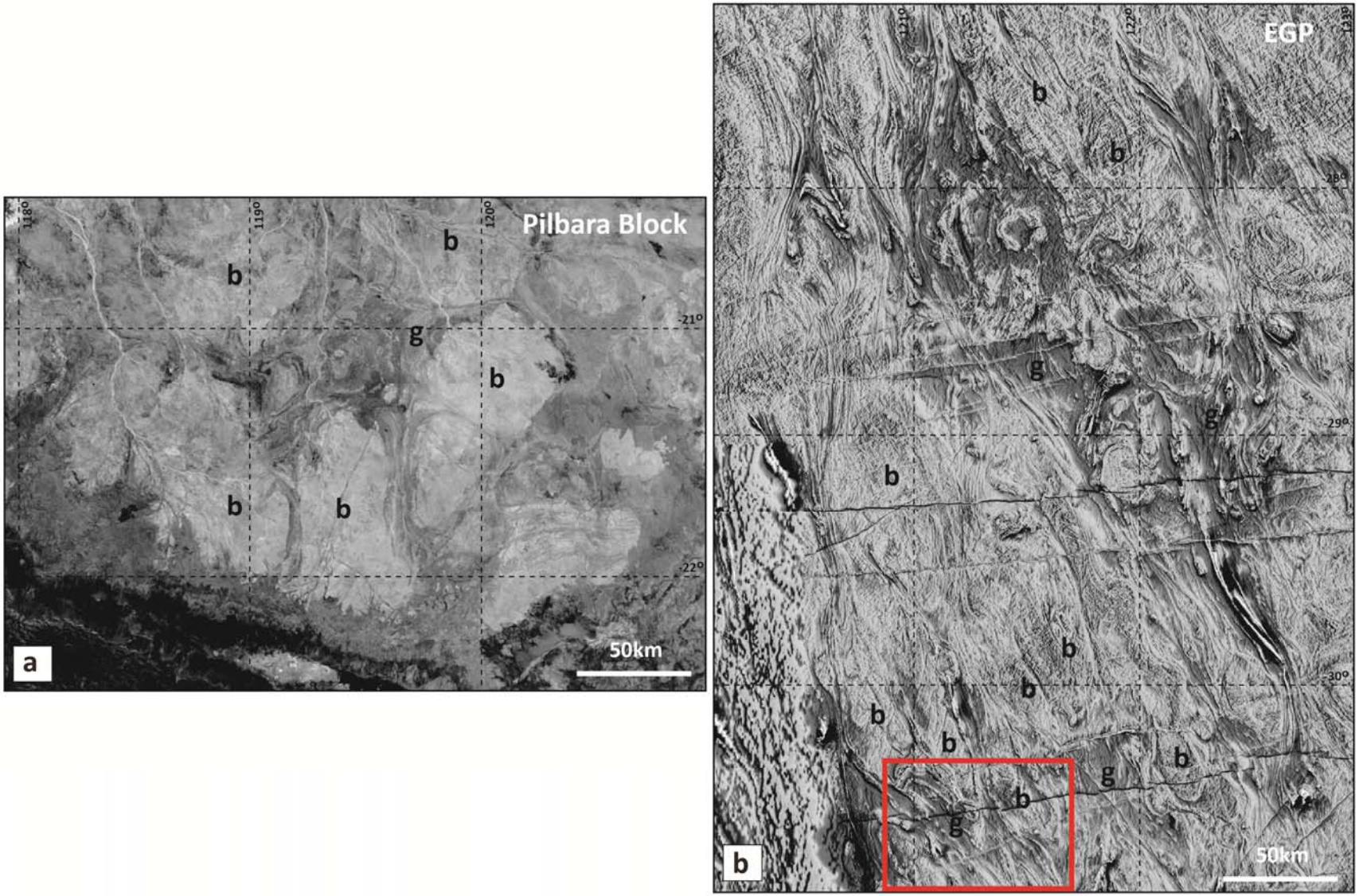

Figure 8.2 – a) Google Earth image of the Mesoarchaean Pilbara Block grey scaled to highlight the dome-basin style granite dome (b) and greenstone keel (g) structure; b) Reduced-to-Pole aeromagnetic image of the Neoarchaean Eastern Goldfields Province grey scaled to highlight the elongate structure of elliptical batholiths (b) and intervening linear greenstone belts (g). The red box marks the study area.

located, the paradigm for Archaean greenstone gold exploration would fundamentally change, as would the prospectivity of those belts.

Late syn-deformation lode-Au deposits are non-specific as to the tectonic setting of the EGP despite their widespread occurrence and close spatial association with mineral deposit camps that contain evidence of early VMS-type mineralisation styles. The categorisation of those Lode-Au deposits as 'Orogenic' appears appropriate since it emphasises the syn-deformational nature of the deposits, however it is problematic when used as prescriptive of active environments of subduction and volcanic arcs (e.g. Groves et al. 2003). Lode-Au deposits are not necessarily associated with subduction/arc environments (e.g. Dube and Gosselin 2007). In this respect the 'Orogenic' classification may oversimplify a deposit style commonly formed in a variety of environments.

8.4 Geotectonic setting

The interpretation of Neoarchaean tectonic settings is controversial. Arguments concerning the validity of applying uniformitarian tectonic models to Archaean rocks centre on issues of: (1) the nature of the basement to greenstone belts, (2) properties and thickness of the continental crust, (3) mantle heat flux, (4) the nature of the Archaean geotherm, and (5) the rigidity of the lithosphere among others (e.g. Archibald et al. 1987; Davies 1992; Brown 2008; Wyman et al. 2008; Hynes 2008). End member models of Archaean tectonics include plume related magmatism and extension, gravity-driven vertical tectonic models, and Uniformitarian plate tectonic models; whereas some authors argue for combinations of plate-plume interaction (e.g. Czarnota et al. 2010).

Critical evidence used to argue for and against end member models is primarily isotope-geochemical (e.g. Mueller and Wooden 1998; Shirey et al. 2008; Foley 2008; Mueller et al. 2011), but arguments are also based on sedimentological and basin analysis inferences (e.g. Fralick et al. 2008). Other authors focus on identifying the key indicators of plate subduction / arc-accretion in the Phanerozoic, and then using the presence or lack of these as critical indicators of the age of onset of modern-style plate tectonics (Kusky and Kidd 1992; Kusky 1998, 2008; Hamilton 2011; Brown 2008; Stern 2005; Cawood et al. 2006). In the Kalgoorlie Terrane, bi-modal magmatism may indicate an extensional rift tectonic setting (Witt et al. 1996; Brewer et al. 2004), whereas rocks of the Gindalbie / Kurnalpi terranes were interpreted as formed in an intra-arc setting by Krapez et al. (1997). Cyclic uplift-subsidence was interpreted as indicative of a transtensional environment that may have been produced by a trench-linked, strike-slip fault zone within a remnant ocean basin (Barley et al. 2002; Krapez and Hand 2008).

Deformation styles and associations provide a second order control on discriminating tectonic setting, but gross tectonic fabric, and distribution and types of structures can provide critical tests of proposed tectonic settings nonetheless (e.g. Pilbara Block vs. Yilgarn Craton;

Platt et al. 1980; Passchier 1994; Van Kranendonk et al. 2004), and their control on stratigraphic distribution may be a key indicator of the relative importance of shear zones in the tectonic history of the Neoarchaean.

8.4.1 Lithotectonic association

A lithotectonic association (or Supersequence) for the southern EGP is defined by the generalised stratigraphy of: voluminous lower sequences of ultramafic and mafic sub-marine volcanic rocks; a middle sequence of intermediate to felsic volcanic and volcaniclastic sequences; and an upper unconformable epiclastic sequence.

In the Kalgoorlie district these assemblages are characterised from oldest to youngest by:

a) Sub-marine mafic, and ultramafic volcanic sequences that have sub-regional strike continuity; with stratigraphic variations in sequence, thickness and geochemistry controlled by major faults that were arguably active at the time of volcanism.
b) Sub-marine to (locally) sub-aerial, felsic and intermediate volcanic sequences with variable lateral distribution probably related to spatially restricted volcanic centres, and with a probable control by localised growth faults.
c) Sedimentation units dominated by below-wave-base deposited turbiditic sandstone, siltstone and shale internal to volcanic packages and sequences.
d) Abundant coarse clastic, submarine volcanic and volcaniclastic sequences in restricted, locally fault-controlled sub-basin remnants lying above angular unconformities.
e) Rare, late-stage alluvial/fluvial to marine, unconformable syn-orogenic clastic sedimentary basins developed as a response to orogenesis, in linear fault-controlled synclines (‘Late Basins’).

Lithotectonic associations in the EGP can be adequately explained by an ensialic rift setting as originally proposed by Groves and Batt (1984) and Swager (1997) despite the widespread popularity of subduction / arc-accretion models in the literature. Of particular note is a range of mineral deposits types and the rift-related metallogenic settings suggested by early styles of mineralisation in the highly endowed EGP (Chapter 2; Chapter 7).

8.4.2 Structural boundaries and terrane ‘sutures’

Throughout the southern EGP the typical lithotectonic association is developed across ‘terranes’ with local differences of sequence and in some instances major age groups. For instance, the age of ultramafic volcanism in the Laverton district is ~100Ma older than for the Kalgoorlie Terrane. Stratigraphic domains separated by major geophysical lineaments, and rare exposures of high strain zones are used to infer the presence of terrane boundary faults or

sutures (e.g. Barley et al. 2008); whereas a review of modern sutures suggests that many of the key criteria are lacking from the Kalgoorlie Neoarchaean.

Sutures are fundamental geologic features that juxtapose pre-existing lithospheric blocks as a result of the consumption of intervening oceanic lithosphere during subduction, and may be modified by post-suturing strike-slip deformation, or obliterated by intrusion (Dewey 1977; Johnson et al. 2002). In a documentation of the Bi'r Umq - Nakasib Shear Zone in Sudan and Saudi Arabia, Johnson et al. (2002) described diagnostic characteristics of sutures as a combination of the following features:

1. The suspected suture should be a zone of high strain.
2. A suture should separate crustal blocks (terranes) with distinct geologic histories and form the boundary between stratigraphic, thermal, metamorphic and structural domains.
3. Deformed rocks in the suture should include those expected to mark the margins of buoyant crustal blocks, such as rift or arc volcanic units and continental rise shelf sequences including carbonates and continental quartzites.
4. The structural history of the suture zone will have an early history with sub-horizontal structures reflecting thrusting during impingement of accreted terranes (low angle reverse faults and reclined folds); and a later stage of rotation and steepening of early-formed structures, and strike-slip shear zones in response to strain partitioning.
5. Kinematics of the suture zone likely involved oblique shear or transpression.
6. The suture zone may include melange, blueschist, and allocthonous ophiolite nappes, and/or lenses of serpentinite, talc schist and gabbro that reasonably proxy for ophiolite.
7. Flanking terranes may include convergent margin igneous suites reflecting subduction prior to collision.
8. The scale of the suture zone should approximate the lateral dimensions of a lithospheric plate (terrane) and be traceable for hundreds or thousands of kilometres.

Melange is a key structural assemblage that accompanies sutures zones and is a recognised criterion for evidence that subduction occurred. The key characters of melange include:

> "landscapes composed of ellipsoidal lumps and lenticular sheets of serpentine, basalt, radiolarian chert, limestone, greywacke, and perhaps greenschist, blueschist, or other metamorphic rocks. Lumps can be any size from mm to multiple kilometres. Large sheets of coherent greywacke or crumpled radiolarian chert, or large fragments of seamounts can be included. Polymict melanges form primarily where subduction is dominated by oceanic materials. Terrigenous clastic sediments

are deposited longitudinally in trenches, and the resulting wedge varies from broken formation (typically greywacke fish in scaly clay) to folded and imbricate, but substantially coherent clastics, depending on the sedimentation/subduction ratio. Broken formation is characterised by infinite shear zones, which can be split down to shiny flakes" – (paraphrased from W. Hamilton, written communication 2011).

Several aspects of the 'classic' suture zone are lacking, or not demonstrated for the domain and 'terrane' boundary shear zones of the EGP. On the second criterion of Johnson et al. (2002), the EGP 'sutures' appear to fail a fundamental test of suture definition, in particular that they should separate "stratigraphic, thermal, metamorphic and structural domains". The same is true of the EGP 'terranes' which also fail a fundamental test: "A tectonostratigraphic terrane is a fault-bounded package of rocks of regional extent characterized by a geologic history which differs from that of neighbouring terranes" (Howell et al. 1985). In the study area, the Mount Monger Fault (also documented as 'Ockerberry Fault' by Goscombe et al. 2009), appears to be a high-strain zone that intervenes adjacent domains of *comparable* stratigraphy, structure and metamorphism (Chapter 5). Shear zones that separate domains in the EGP lack blueschist metamorphic rocks in melange zones, and importantly there are no true ophiolite assemblages that if present, would indicate there was pre-existing oceanic crust and upper mantle rocks (see also Hamilton 1998, Stern 2008). Platt (1980) concluded: "the total tectonic disruption characteristic of subduction complexes or continental collision zones is lacking".

Metamorphic work by the pmdCRC recorded the presence of rare, high-grade metamorphic rocks in a major shear zone at Duketon and in the north Linden Domain of 7.0-8.7 kb and 570-640 ºC with thermal regimes of 18-23ºC / km, interpreted as a result of high advection / conduction ratios and 'sub-subduction zone' conditions (Goscombe et al. 2009). However, similar metamorphic conditions were recorded in the middle crust exposed in the Kapuskasing Structure of Canada, related to post metamorphic uplift on faults (Percival and Card 1983).

The high-P parageneses in the EGP were interpreted by Goscombe et al. (2009) from annealed polygonal granoblastic gneisses in low-strain lenses within lower metamorphic grade high-strain shear zones. These assemblages were interpreted as early-formed, upper amphibolite facies rocks overprinted by later metamorphic stages (Goscombe et al. 2009). Other occurrences of locally elevated-pressure metamorphic minerals in the EGP are scattered, generally within gneiss domains and appear unrelated to major structures with the exception of a few instances including a moderate-to-high pressure belt along the western Ida Fault at north Coolgardie. High pressure minerals were also recorded in arcuate to crescent shaped domains around the lateral terminations of elongate granite-gneiss batholith domes (Goscombe et al. 2009).

The rocks sampled by Goscombe et al. (2009) along the 'major' Kalgoorlie / Gindalbie Terrane boundary recorded low-med peak pressures with anti-clockwise P-T paths. Several

sections were plotted across the ‘terranes’ of the EGP, which showed differences in field gradients across the Kalgoorlie / Kurnalpi terrane boundary that were interpreted as a result of extension for the entire length of that boundary fault (Goscombe et al. 2009).

Notably the final interpretation of Goscombe et al. (2009) presented two end-member scenarios equally likely to explain the metamorphic data from the EGP: (1) asymmetric (subduction), and (2) symmetric (rifting); and they recognised high-pressure rocks with restricted distribution, but lacking a strong correlation with major high strain zones of tectonic interleaving as described previously. It is unlikely that these high-P rocks represent blueschist equivalents in melange zones between arc domains.

8.4.3 Spatial distribution of heat sources

A further important problem for the application of subduction / arc-accretion tectonic models is the geographically random distribution of intrusions and volcanic rocks of a given age group or geochemical type observed throughout the Yilgarn Craton (M. VanKranendonk written communication 2011; Fig. 8.3). A map distribution of the granite groups was compiled by the AMIRA P482 project (Cassidy et al. 2002) and shows that the various geochemical groups are present across broad areas of the Yilgarn Craton and the EGP (Fig. 8.3a); in particular, the High-Ca (‘shallow-subduction slab melts’), which occur across the Yilgarn Craton as does the Low Ca granite group, These were interpreted as a result of post-subduction strike-slip shortening by Czarnota et al. (2010). Mafic granitoids (‘metasomatised asthenosphere melts’ Czarnota et al. 2010), are dominant in the Kalgoorlie district of the EGP and Meekatharra district in the Murchison Province, but present elsewhere; whereas the Syenitic group (‘crust and metasomatised mantle melts’ as interpreted by Czarnota et al. 2010; or extension related high-T partial melts by Cassidy et al. 2002) is present dominantly in the easternmost parts of the EGP.

In modern convergent settings (e.g. Papua New Guinea; Chile), magmatic belts are linear and have consistent ages of volcanic deposits and intrusions separated by major arc-parallel faults (Fig. 8.4a,b). For example, Figure 8.4a (of similar scale to Figure 8.3) shows the detailed distribution of intrusions on mainland PNG, with the structure of that island composed of three major, linear volcano-plutonic belts sub-parallel to the Australia-Pacific plate boundary, spanning ~30Ma. The Miocene Maramuni Arc was produced by active subduction from ~18-12Ma (Hill et al. 2002). Oligocene-Miocene accreted island arc terranes of the Finisterre-Huon were adjoined to the Australian Plate by oblique transpression after about 4 Ma. The Pliocene ‘Medial’ arc is a linear belt of post-subduction porphyritic intrusions lacking significant volumes of co-eval volcanics that were unrelated to any post-Miocene subduction, but were possibly related to decompression melting of enriched underplated crust during delamination (Cloos et al. 2005).

A similar relationship is demonstrated by the age distribution of intrusions in Northern Chile, which span ~200 Ma (Fig. 8.4b; Dallmeyer et al. 1996; Grocott et al. 2009). In the Coastal and western Main Cordillera, suites of Triassic to Palaeocene plutonic complexes are aligned parallel to the continental margin and subduction zone. The intrusions young from west to east in a 700 km-long segment of the Andes (Dallmeyer et al. 1996; Grocott et al. 2009).
Crystallisation age data for the Yilgarn Craton appear to show that magma emplacement occurred across a broad source area unrelated to major linear crustal features. This is in contrast to a widely referenced data set of neodymium model ages calculated from Sm-Nd point data that is used to infer a major N-S discontinuity defined by interpreted mantle extraction ages, contoured to show an interpreted proto-continental boundary at the western margin of the Eastern Goldfields Province (Champion and Cassidy 2007; Czarnota et al. 2010).

If a linear subduction control was the tectonic impetus for formation of the Archaean granite-greenstone terranes of the Yilgarn Craton, a corresponding linear distribution of volcano-plutonic belts would be expected with linear belts of successively accreted crust. This is clearly not demonstrated by the available composition and age data (Fig. 8.3). At a sub-regional scale, arc 'terranes' are also unlikely given the compilation in Section 5.3.2 of existing age and stratigraphic data for the Yindarlgooda Dome in the Gindalbie Terrane, which shows there is no significant difference in sequence or age across an interpreted 'terrane boundary' at the location of the Mount Monger Fault. An alternative model is required to explain the widespread granite intrusions that occur across the entire Yilgarn Craton at any given age range from 2800 - 2650 Ma (Fig. 8.3).

Recent publications have questioned the uncritical application of subduction / arc-accretion models to the Yilgarn and southern Eastern Goldfields Province (Chapter 2; Chapter 5). The work of Barnes et al. (2012) was concerned with scale, among other factors; particularly the size of an interpreted back-arc mantle plume (as proposed by Czarnota et al. 2010) to explain the early part of the volcanic package. The former authors argue that modern LIP (Large Igneous Province) magmatism is a result of mantle plume melting an order of magnitude (or two orders of magnitude) larger than the area covered by the EGP.

The scale of the EGP is compared to three modern areas of active tectonics in Figure 8.5 including rifting (East Africa), compression (South America) and transpression (PNG). In all cases the EGP is several times smaller than the long dimension of major tectonic zones, whereas short axis dimensions of the EGP are comparable to the Cordillera-Domeyko and the PNG Mobile Belt and accreted island arc terranes. Short axis dimensions and the scale of individual belts in the EGP are comparable to the arc components of the New-Guinea mainland, and both the EGP and PNG represent significantly shortened crustal elements. However, if subduction / arc-accretion was a driving force in the EGP, differentiation of linear, age-constrained volcano-plutonic belts would also be expected - but this is not observed. In essence, the scale is 'right',

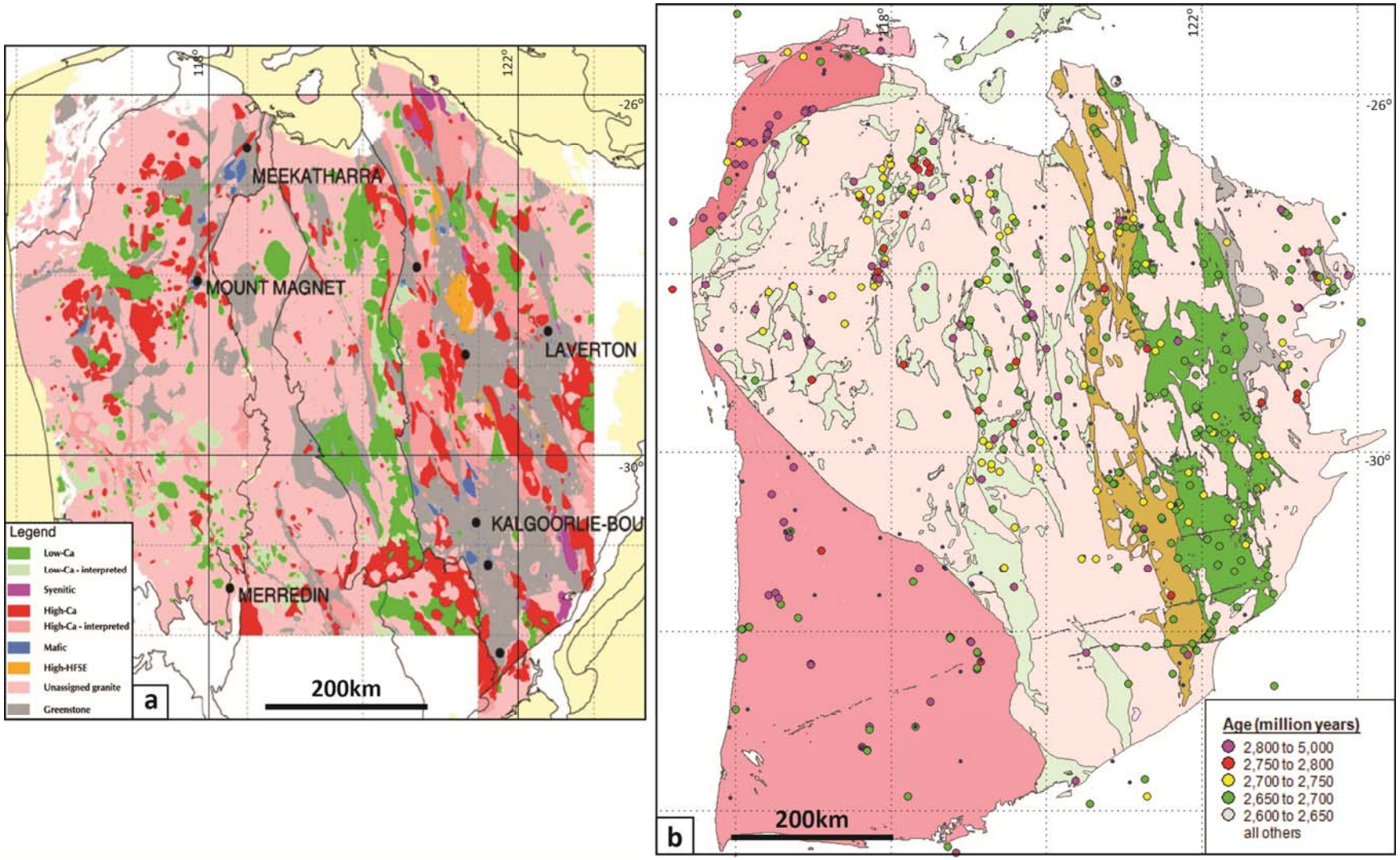

Figure 8.3 – a) Distribution of granitoid groups throughout the Yilgarn Craton from Cassidy et al. (2002), note the craton-wide distribution of most major granitoid types; b) SHRIMP U-Pb zircons ages from granitoids and greenstones showing (1) correspondence of granitoid and greenstone volcanic ages across major tectonic domains, and (2) craton-wide distribution of ages in each of the 50 million year bins indicating there is no linear distribution of intrusions or volcanic rocks as would be expected if there was a linear subduction control on the development of the 'terranes'. Geochronological data from GSWA and GA compilations at http://geodownloads.dmp.wa.gov.au/Downloads/Metadata_Statements/XML/Geochronology_2011.xml.

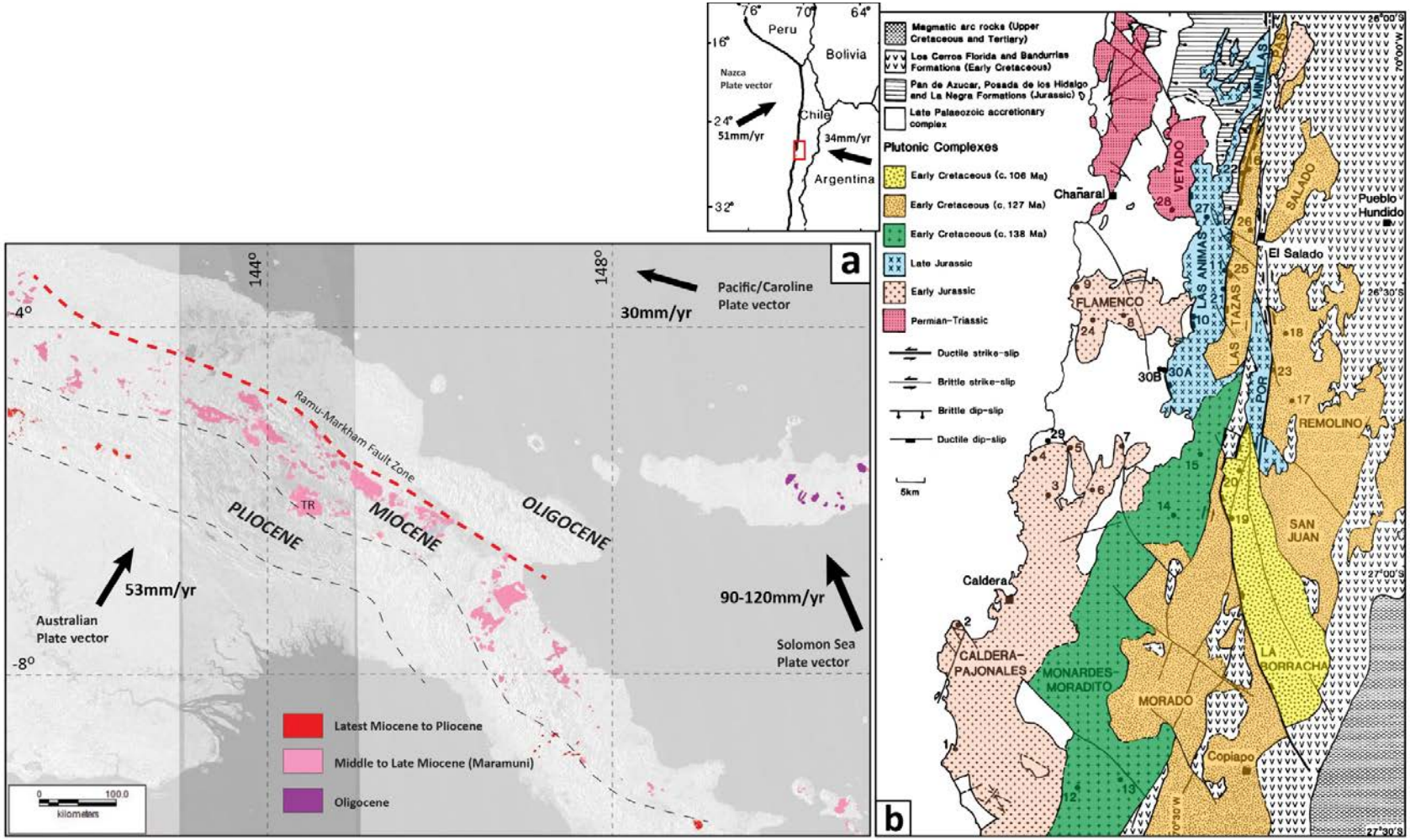

Figure 8.4 – a) SRTM (Shuttle Radar Topography Mission) image of the topography of Papua - New Guinea draped with intrusions coloured by age. The intrusions form three main belts that coincide with the major volcanic belts: (1) Oligocene accreted island arc terranes (2) Miocene Maramuni Arc, and (3) Pliocene post-subduction 'Medial' plutonic arc. The intrusions and volcanics are aligned in age belts parallel to the Australia-Pacific plate boundary, marked by the Ramu-Markham Fault Zone. The intrusion marked "TR" is a Triassic granodiorite intrusion in the Kubor basement uplift (intrusions from Australian Bureau of Mineral resources [BMR] 1:250K geology of PNG references in Rogerson and Williamson 1985; modern day plate vectors from Johnson 1979, Woodhead et al. 1998, and Beavan et al. 2002); b) Geology of an area of Northern Chile with linear belts of intrusions spanning >150Ma from the Triassic to Early Cretaceous and Palaeocene (modified from Dallmeyer et al. (1996).

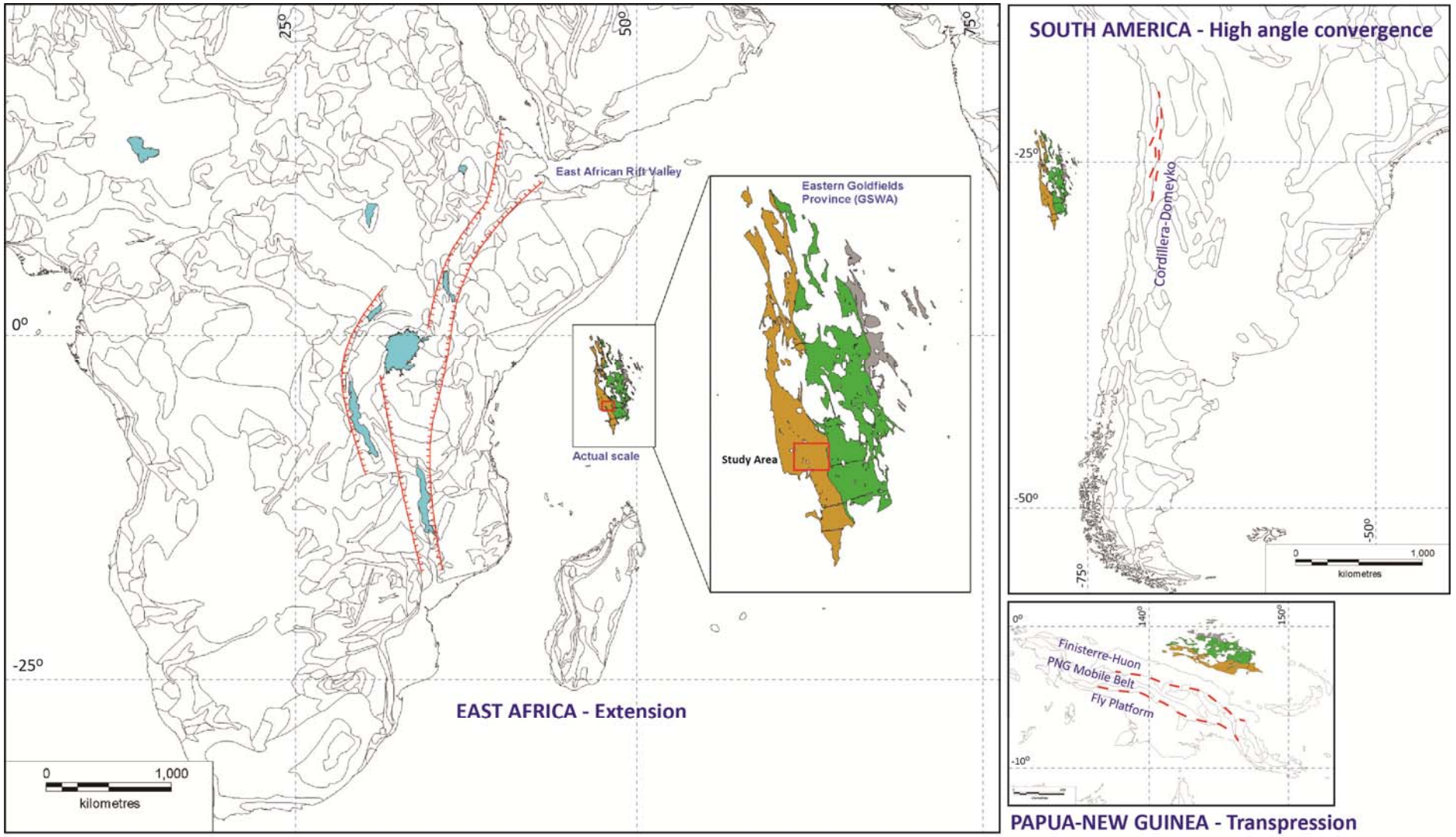

Figure 8.5 – Images of the Eastern Goldfields Province at the same scale, compared with a variety of modern tectonic settings (continent shapes show boundaries of major geological provinces, blanked to highlight structural domains of interest; polygons from Barrick World-GIS). In each case the EGP is several times smaller than the long dimension of major tectonic boundaries, but the EGP terranes have comparable short axis dimensions to the Cordillera-Domeyko in Northern Chile, and the PNG Mobile Belt and accreted island arc terranes.

but the timing is ‘wrong’. A possible alternative is that the EGP ‘terranes’ were originally much wider rift segments that have been later shortened, and the original extensional faults are preserved as ‘terrane’ boundaries.

8.4.4 Basement to the Kalgoorlie greenstones

The distribution of ages in the EGP shows evidence for a pre- ~2700 Ma greenstone basement to the Kalgoorlie succession (Fig. 8.6). Notably most of the pre- ~2700 Ma ages are located at the periphery of the greenstones and near marginal granite-gneiss domains. Many of those ages are from granitic and gneissic rocks, with some exceptions including felsic and ultramafic intrusions and migmatites (Fig. 8.6). Isolated occurrences of pre- ~2700 Ma greenstone include the Noganyer (~2864 Ma) and Penneshaw (~2938 Ma) formations at the southern end of the EGP; sandstones (~2808 Ma) near Laverton at the eastern margin of the EGP; pebble conglomerate (~2870 Ma) in the northern goldfields; and various intrusions into greenstone that may be syn-volcanic sills and dykes, or intrusions into older basement rocks. The red polygons in Figure 8.6 highlight areas of crust greater than ~2700Ma age, which may represent remnants of a rifted basement to younger greenstones (Fig. 8.7); intrusions contemporaneous with rifting; or intrusions that contain a greater than ~2700 Ma inherited component (Compston et al. 1986).

Many of the oldest greenstone ages are located at the extreme margins of the greenstone belts, which may be a result of preservation of the original rifted basement exhumed in the hinterland of a major rift basin; but this relationship remains cryptic given the highly shortened nature of the EGP. There are several possible explanations for the isolated occurrences of significantly older granite-greenstone crust including: (1) that pre- ~2700 Ma ages represent lower parts of a continuous stratigraphy exhumed at the margins of the greenstone belts by granite intrusions, (2) faults have exposed parts of a lower stratigraphy, or (3) the old crustal fragments are cryptic remnants of a pre- Kalgoorlie Sequence, rifted greenstone basement.

Option (3) is a preferred explanation since granite batholiths and major faults are common throughout the EGP granite-greenstone terranes, and if these were the cause of exhuming deep older crust, a broader distribution of those ages might be expected. Additionally, a lack of old crust along major faults, that faces away from the faults into younger crust, suggests that either the faults were not crustal penetrating reverse faults, or that the pre- ~2700 Ma crust was not present immediately below the Kalgoorlie and Kurnalpi ‘terranes’ at the time of faulting.

Chapter 5 presents evidence for Upper Basalt thickness changes across domain boundary faults that were arguably extensional faults at that ‘Upper Basalt time’. The orientation of original extension vectors is unknown, and late ENE-WSW shortening has obscured original relationships, but two possibilities are schematically represented in Figure 8.7.

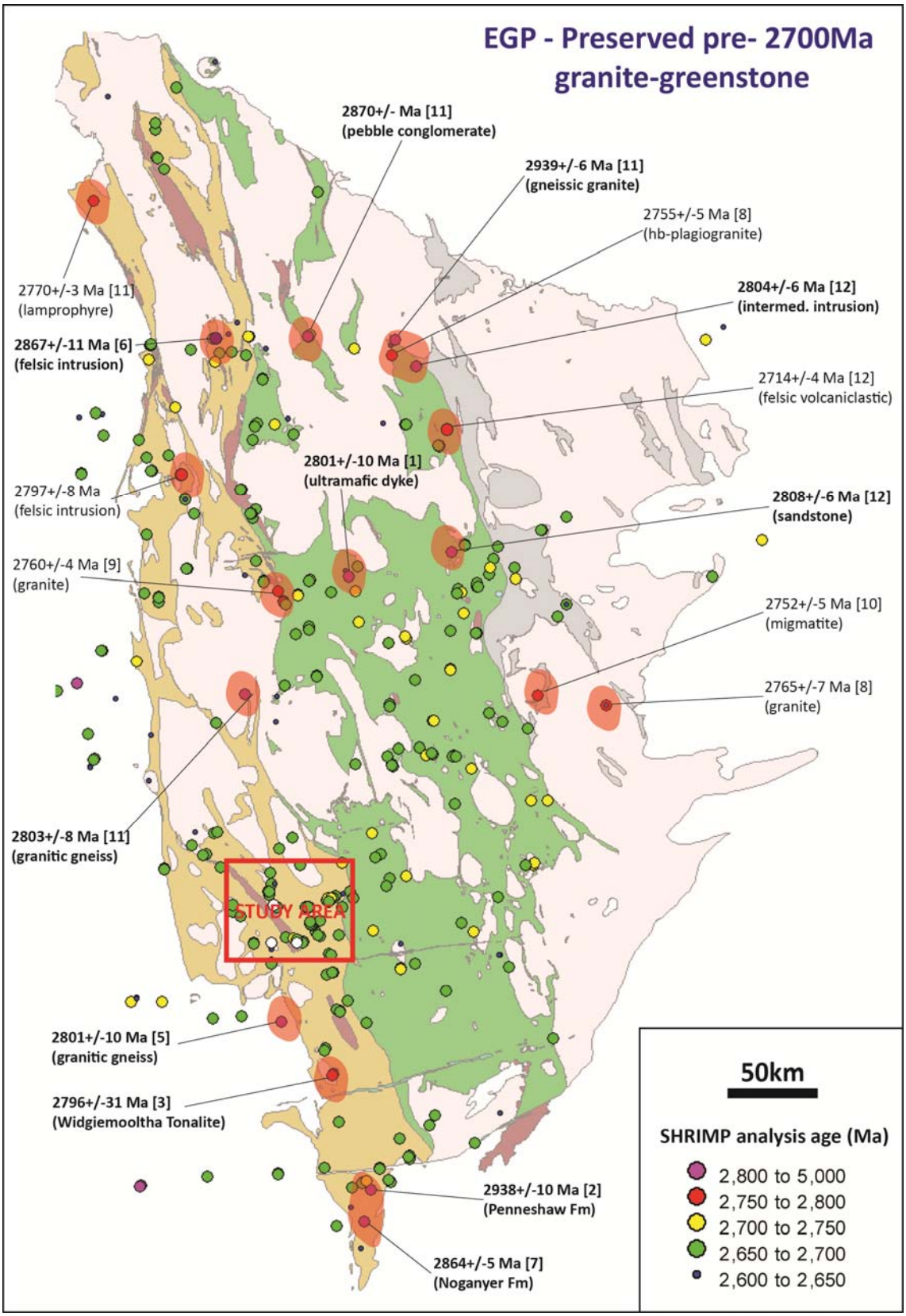

Figure 8.6 – Compilation of SHRIMP U-Pb zircon analyses in the EGP on simplified GSWA geology (See Fig. 8.1 for legend). Red polygons highlight areas of >2700Ma crust, which may represent remnants of a rifted basement to younger greenstones; intrusions contemporaneous with rifting; or intrusions that contain a >2700 Ma inherited component. Ages >2800 Ma are highlighted in bold type. Numbers in brackets for references: [1] Pidgeon et al. (1990); [2] Hill et al. (1992); [3] Hill et al. (1993); [4] Nelson (1995); [5] Nelson (1997); [6] Yeats et al. (1999); [7] Krapez et al. (2000); [8] Fletcher et al. (2001); [9] Black et al. (2002); [10] Cassidy et al. (2002); [11] Dunphy et al. (2002); [12] Kositcin et al. (2008).

Domain boundary faults in the north Kalgoorlie district accommodated stratigraphic thickness changes, which may have resulted from pure extension in a NE-SW rifting, or possibly vertical movements in an EGP-parallel extension, with the domain boundary faults acting as sub-vertical transfer faults between relay ramps. Given the scale of the EGP and the study area compared to the modern, major Gregory Rift system in East Africa (Fig. 8.5), the Kalgoorlie district may represent a small arm of what was an extensive linked rift system.

The major NE-trending geophysical feature in Figure 8.7 has other manifestations including a NE-SW belt of thick, upper late-clastic preservation as documented in Chapters 3 and 4. At a regional scale, Horwitz et al. (1966) also documented a NE-SW trending band of conglomerate preservation from the Southern Cross Province to the Laverton domain in the EGP. These cross-belt trends of stratigraphic preservation may reveal early extensional structural controls on the deposition of clastic sequences that are not obvious due to later obliteration by the ENE-WSW contractional deformation.

8.5 Summary

Key indicators of subduction - including: voluminous andesitic volcanic sequences with evidence of generation from metasomatised mantle melts, paired metamorphic belts and tectonic melange, a linear distribution of intrusive rocks and co-eval volcanic rocks, and the presence of preserved ophiolite - are lacking in the Eastern Goldfields Province.

Arc volcanism is not well demonstrated in the southern Eastern Goldfields Province, with generally low volumes of intermediate volcanic rocks and a relatively restricted distribution of andesitic volcanic centres. The andesitic volcanic rocks have extrusive settings more akin to sub-marine cryptodomes, rather than volcanic island arc or continental margin arc settings. Paired metamorphic belts are not observed in the Eastern Goldfields Province, and evidence for melange, including mixing of exotic blocks and chaotic distribution of lithotypes in a tectonic matrix is entirely lacking. Granitoid intrusion groups show no regularity of distribution, or linear distribution with age as would be expected if these were the products of mantle wedge melting above linear subduction zones. Ophiolitic rocks are not present in the EGP. Kalgoorlie ‘Terrane’ rocks span an age range from ~2710 - 2650 Ma, but are a young phase of greenstone development, possibly within a large rifted greenstone province that includes older basement greenstones more than ~100 Ma older than the Kalgoorlie greenstones.

Critically, the controls on major gold deposits are not contingent on the structural characters of subduction settings, but are closely associated with early greenstone belt controls on high-level, syn-volcanic hydrothermal alteration systems related to major rift axes, and the fundamental structures that controlled early greenstone development. Those structures were zones of repeated structural reactivation and maintained hydrothermal fluid flow, spanning several phases of exhumation with unconformity and late deformation.

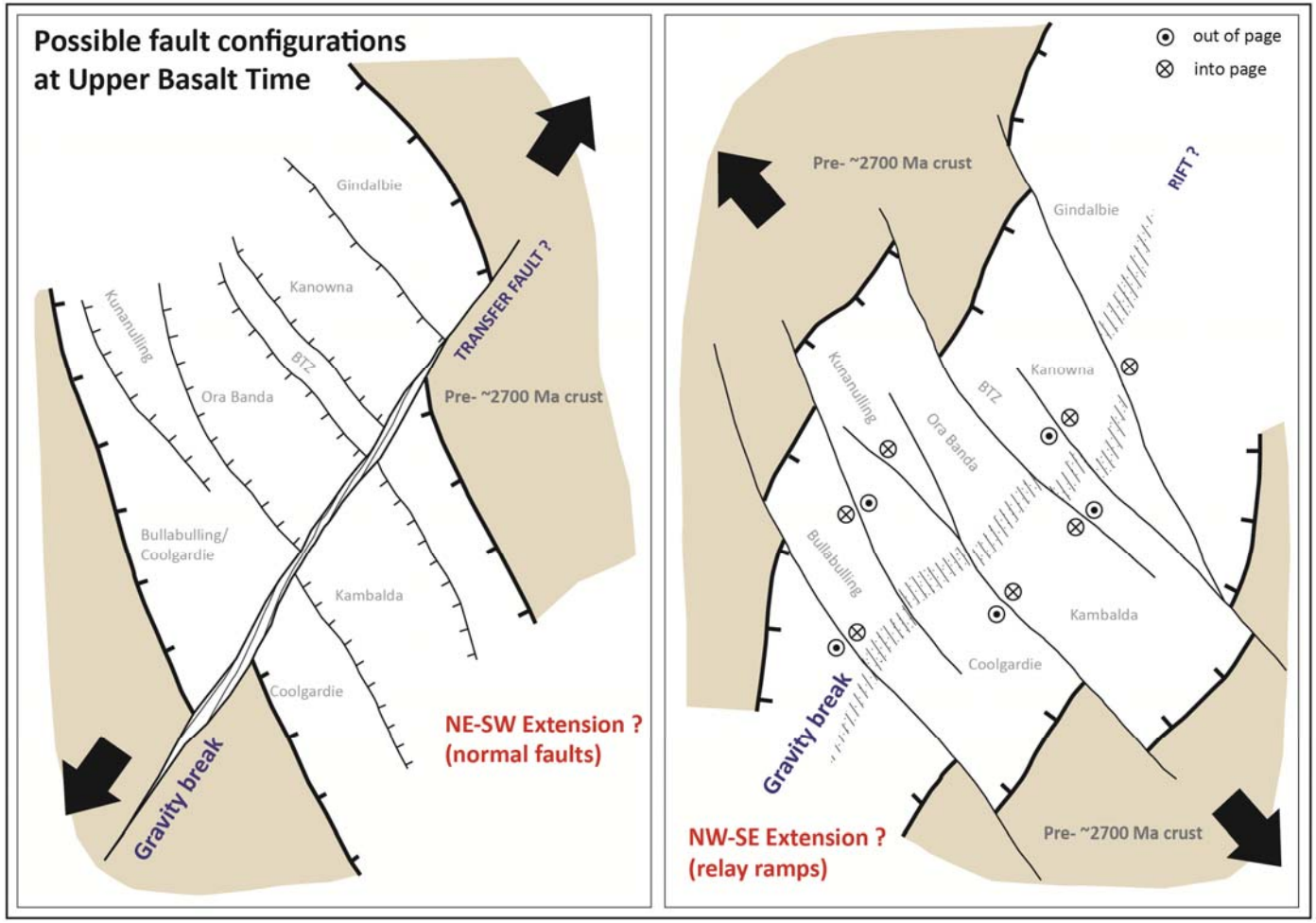

Figure 8.7 – Schematic diagrams of potential fault configurations for a postulated 'Kalgoorlie arm' of a hypothetical major >2700 Ma EGP rift system. The extension vector for the EGP is unknown, but since present faults show a history that extends back to mafic volcanism, there are at least two possible configurations for those faults as (1) conventional extensional faults, or (2) relay ramps during an extension orthogonal to a rift axis. A significant 'gravity ridge' is present in the gravity data for the Kalgoorlie district, and is correlated with a geophysical feature that was previously identified as a major transcrustal lineament (O'Driscoll 1986), and as a palaeo silicification-high by Archibald (1998). This trend is co-linear with trends of preserved late coarse clastic sequences across the EGP as documented by Horwitz et al. (1966).

9 Conclusions

A key goal of this project is to understand aspects of the extraordinary gold endowment that occurs in several Neoarchaean greenstone belts globally, using one of the best known and studied examples in the world at Kalgoorlie in Western Australia. Fundamental structural and stratigraphic problems remain, despite intensive geological research carried out in this district for over 40 years. This thesis brings together extensive (publicly unavailable) data sets of drilling and geophysics with new mapping and geochronology, to assess the stratigraphic and structural controls on major gold deposits, and to speculate about the tectonic controls on Neoarchaean granite-greenstone terranes.

The major conclusions of this thesis include: (1) the role of major faults and implications for the application of subduction / arc-accretion tectonics to the Neoarchaean of Kalgoorlie; (2) identification of the critical controls on major gold deposits; (3) a revision of the stratigraphy of domains in the Kalgoorlie Terrane and proposals for new stratigraphic subdivisions and nomenclature; and (4) a revised structural history that incorporates stratigraphy, unconformities and fabric cross-cutting relationships to provide a robust structural framework for the study area. In the following paragraphs major conclusions are numbered with first level bullet point, supporting statements are marked with letters a, b, c etc.

9.1 Domain / terrane boundaries and the tectonics of greenstone formation

1. The Zuleika Shear Zone marks a domain boundary that juxtaposes crustal blocks with minor stratigraphic differences and thickness of sequences, but does not juxtapose blocks of significantly different geological history. This suggests that fault bounded domains in the Kalgoorlie Terrane were not diverse crustal blocks amalgamated by strike slip or accretion, but they were subjacent depocentres, possibly half-grabens, bounded by early extensional faults such as the Zuleika Shear Zone and Bardoc Tectonic Zone. Differences of stratigraphy across the faults may have been a consequence of relative subsidence and syn-extensional sequence growth.
2. Geological units in the Yindarlgooda Dome show no major differences in lithotectonic assemblages, stratigraphic sequence, or age from formations in the adjacent Boorara Domain of the Kalgoorlie Terrane. On this basis, the allocation of ‘terrane boundary’ status to the Mount Monger Fault as separating a western back-arc (Kalgoorlie Terrane) from an eastern accreted volcanic arc (Gindalbie Terrane; see references in Chapters 2 and 5) is suspect, and indicates the application of subduction / arc-accretion models to greenstones of the southern Eastern Goldfields Province is equally suspect, or may not be correct. Recent published work on the geochemistry of basalt and intermediate to felsic volcanic

rocks, and their isotopic character supports this contention (References in Chapter 2). Earlier models that proposed rifting of a pre- 2700 Ma greenstone basement may be better analogues for the tectonic setting of the greenstones.

9.2 Critical controls on major Neoarchaean gold deposits

1. Major gold deposits in the Kalgoorlie district have variable styles and timings of mineralisation that are spatially coincident, yet separated in time by stratigraphic and deformational events. The largest deposits include early high-level mineralisation styles, later overprinted by lode-Au, vein style mineralisation:
    a) At Binduli, early disseminated sulphide-replacement style Au-Ag mineralisation replaced the matrix of primary tuffaceous volcanic deposits and mudstones, and was overprinted by late, lode-Au veins. Those two mineralisation events are separated by deposition of the unconformable Binduli porphyry conglomerate / F2 folding / and deposition of the Kurrawang Formation. The late lode-Au veins were syn-orogenic, synchronous with late D3 folding and foliation, and the veins cross-cut folded and foliated Kurrawang rocks.
    b) The lode-Au vein style at Kundana mining centre has timing synchronous with D3 deformation. Similar relationships are present at Kanowna Belle where disseminated intrusion-hosted mineralisation is overprinted by syn-to-post deformation Red Hill style lode-Au quartz veins that are locally significant sources of Au mineralisation (Davis et al. 2000). At the Golden Mile, early high-level Fimiston lodes were deformed and subsequently overprinted extensively by post-foliation, Mount Charlotte quartz-gold stockwork veins (Clout 1989; Gauthier et al. 2004).
2. At a *regional* scale, major gold districts in the Eastern Goldfields Province have spatial and temporal relationships with unconformable, late clastic sedimentary sequences. This spatial relationship of late clastic sequences and major gold systems reflects preservation of the thickest parts of originally more extensive greenstone belts, and indicates a preservation of regions where high-level mineralisation styles were developed in the Neoarchaean. The spatial relationship is also an indicator of proximity to major early faults:
    a) Gold deposits are distributed in camps that have a predictable regional association with thick greenstone distribution indicated by the presence of late clastic sequences in the uppermost units of the stratigraphy.
    b) Diversity of mineralisation styles and settings in the largest gold deposits indicates that areas of thick stratigraphic preservation are more favourable

to the perpetuation of hydrothermal mineral systems that are evidently present at camp locations throughout several uplift and deformation events.

3. At a *camp* scale, major gold deposits in the north Kalgoorlie district show a spatial association with unconformable epiclastic and volcaniclastic rocks located above an unconformity internal to the Black Flag Formation:
    a) The Binduli district is spatially associated with the ~2664 Ma Binduli porphyry conglomerate unconformity that is interpreted to separate lower (Gibson-Honman) and upper (Gidji Lake) Black Flag formation sequences.
    b) The Kanowna Belle gold deposit is hosted in hypabyssal porphyritic rocks that have a spatial association with a ~2660 Ma unconformity at the base of the Grave Dam sequence (correlated with upper Black Flag Formation).
    c) Unconformable sedimentary and volcaniclastic rocks of the interpreted upper Black Flag Formation (~2660 Ma) are present in the vicinity of the eastern margin of the world class Mount Charlotte / Fimiston gold camp at Kalgoorlie.
4. The persistence of separate Au events in coincident locations suggests fundamental crustal controls that were primarily structural. Structures that controlled early hydrothermal mineralisation may have provided loci for later syn-orogenic mineralisation.

9.3 Lithostratigraphy and chronostratigraphy

Recent publications dealing with the 'Felsic volcaniclastic and sedimentary unit' overlying the Upper Basalt unit have interpreted multiple unconformable tectonic uplift sequences on the basis of sequence stratigraphic concepts (Barley et al. 2002; Krapez et al. 2000; Barley et al. 2008). In contrast, this thesis takes a more conventional approach using lithostratigraphy and chronostratigraphy, and represents those facets on maps to display the distribution of major formations across fault bounded domains of the Kalgoorlie Terrane.

1. Formations between the Upper Basalt unit and the unconformable late-clastic Kurrawang Formation previously bracketed as 'Black Flag Beds' (Woodall 1965), and 'Spargoville Formation, Black Flag Formation, White Flag Formation' (Barley et al. 2002; Krapez et al. 2000; Barley et al. 2008), are separated on the basis of this work into four units from oldest to youngest: Talbot formation; White Flag Formation; lower Black Flag formation; upper Black Flag formation. The sequence includes unconformities between White Flag Formation and Talbot

formation (locally), and between lower and upper Black Flag formations; but notably offers a new interpretation of the sequence order and regional correlations compared to previous interpretations. In the Coolgardie Domain, the detailed stratigraphy of 'Black Flag Beds' equivalent rocks remains uncertain in the absence of more detailed work.

2. This work makes a general separation into lower and upper Black Flag formations as a working model for assigning rocks in the district to stratigraphic groups, but a more direct nomenclature that identifies the sequences with their areas of best exposure is a more useful way to classify these units. Two major subdivisions of the generic 'Black Flag Group' are proposed as: (1) a lower 'Gibson-Honman formation' (~2675 Ma) including felsic volcanic rocks at Gibson-Honman Rock, Lakewood dacitic volcanics, and Perkolilli rhyolitic volcanics; and (2) an upper 'Gidji Lake formation' (~2660 Ma) including felsic volcaniclastic rocks at Gidji, Binduli Porphyry Conglomerate and Grave Dam Grit. The two formations are separated by an unconformity, with map patterns indicating that the Gibson-Honman formation was folded prior to deposition of the Gidji Lake formation.
3. Ultramafic-dacite association: at Kanowna, dacitic volcaniclastic rocks in the footwall of the Kanowna Belle gold deposit previously had uncertain stratigraphic relationships, and were possibly correlated with younger volcaniclastic sequences based on textural and compositional characters. The age of those rocks is confirmed at 2704±5 Ma from a new U-Pb SHRIMP determination, which places the Kanowna Belle footwall sequence as part of the well-known ultramafic-dacite association of the Boorara Domain, correlative with the time-equivalent Kambalda Komatiite association.
4. The end of mafic volcanism is constrained by a new U-Pb SHRIMP age determination for the Golden Mile Dolerite at 2685±4 Ma (host to the largest Archaean greenstone gold deposit). The new age determination for the Golden Mile Dolerite here indicates a possible three million year time gap between the intrusion of the Golden Mile Dolerite (>2681 Ma) and overlying Lakewood dacite volcanics (<2678 Ma). This suggests the Golden Mile dolerite was a high-level intrusion at the Upper Basalt / Black Flag interface, which accords with local primary amygdaloidal textures in the upper units of the sill.
5. Talbot formation: rocks in the Mount Pleasant area previously correlated with Spargoville Formation are significantly older than the Spargoville type locality, with an original stratigraphic designation of 'Black Flag Series' (Talbot 1934). To avoid nomenclature confusion a new designation 'Talbot formation' is assigned to units stratigraphically above Upper Basalt and below White Flag Formation.

Talbot formation rocks are bracketed in age between 2694 - 2687 Ma on the basis of new SHRIMP U-Pb analyses of detrital zircons in sandstone (2696±2 Ma), and igneous zircons from a cross-cutting sill (2689±2 Ma). The Talbot formation includes below-wave-base deposited, plane-bedded sandstone, siltstone and mudstone, probably deposited as proximal submarine fan turbidites with a conformable lower depositional contact onto pillowed Victorious Basalt.

6. White Flag Formation: a major andesitic volcanic unit present in the Ora Banda Domain of the Kalgoorlie Terrane is demonstrated from field relationships as conformable to locally unconformable on underlying Talbot formation rocks. A new SHRIMP U-Pb age estimate of volcaniclastic breccia at 2690±9 Ma accords with mapped field relationships that place the unit as overlying Talbot formation sedimentary rocks and as gradational with below-wave-base deposited mudstone, sandstone and proximal felsic volcanic rocks of the Binduli sequence up-section (lower Black Flag formation). The nearest units with similar intermediate composition volcanic rocks include andesitic volcanics on the shores of Lake Yindarlgooda, and similar sequences on the northern edge of Lake Lefroy at Kambalda. Intermediate coherent intrusive rocks at Gidji returned a U-Pb SHRIMP age determination at 2682±8 Ma, which is within error of the White Flag Formation and the Gidji rocks are a possible correlative with White Flag Formation on that basis. The detailed distribution of the Gidji sequence is uncertain, and may be restricted to sub-volcanic intrusions that cross-cut the Gidji ultramafic sequence. A 2695±6 Ma age determination for dacitic sandstone intercalated with the Ballarat ultramafic-clast dominated conglomerate can be time correlated with either sedimentary rocks at Mount Pleasant (2694 - 2687 Ma) or White Flag Formation rocks at White Flag Lake (2690±9 Ma). Interpretation of 2695±6 Ma as a maximum depositional age for the Ballarat conglomerate sequence, suggests deposition after ~2689 Ma, and accords with published age determinations for that unit.
7. Gibson-Homan formation: felsic volcaniclastic and sedimentary sequences of the lower Black Flag formation have lithostratigraphic similarities across domains: Ora Banda Domain (Gibson-Honman rhyodacitic volcanics), Kambalda Domain (Lakewood dacitic volcanics), and Boorara Domain (Perkolilli rhyolite sequence). A new U-Pb SHRIMP age determination of 2672±6 Ma constrains the age of the Lakewood sequence as correlating with the Gibson-Honman and Perkollili felsic volcanic sequences.
8. Gidji Lake formation: coarse-clastic sedimentary rocks, correlated with upper Black Flag formation, also show lithostratigraphic similarities across domains in

that they are primarily felsic-volcanic derived conglomerate and sandstone with angular unconformity on underlying rocks. Upper Black Flag formation deposition marks the end of extrusive volcanism in the Kalgoorlie Terrane. At Binduli in the Ora Banda Domain, new mapping and drill core re-logging confirms an unconformable relationship between the Binduli porphyry conglomerate and underlying mudstone (ECM host) and Centurion Porphyry. The age of that unconformity is estimated at <2664 Ma on the basis of published SHRIMP analyses of the Centurion Porphyry. Gidji felsic volcaniclastic rocks and overlying Gidji Lake conglomerate in the Kambalda Domain are constrained by new SHRIMP analyses, which produced an age estimate of 2660±16 Ma with an inherited component at 2682±8 Ma; the latter being identical to the age of underlying coherent intermediate porphyritic rocks dated here also at 2682±8 Ma. An unconformity was defined at the base of the Gidji sequence from new mapping and drill hole re-logging, and this sequence is correlated with intermediate volcaniclastic and sedimentary rocks east of Mount Charlotte, forming a long, linear fault-controlled clastic basin remnant. In the Boorara Domain, the Government Dam member sandstone-siltstone sequence is tentatively correlated as a distal lateral equivalent of the Grave Dam member on the basis of a 2661±11 Ma U-Pb SHRIMP determination (Squire 2007), which compares with published age determinations for the unit. Golden Valley member polymictic and felsic conglomerates and sandstones have an estimated age of 2669±7 Ma from new zircon U-Pb SHRIMP analyses. A marked unconformity at the base of the Grave Dam and Golden Valley members is determined here from new mapping, drill hole intersections and cross-section analysis, and is supported by new and published geochronology.

9. Kurrawang Formation: the Panglo member in the Kanowna district is likely correlative with the Kurrawang Formation, which unconformably overlies all older units in the stratigraphy that were folded prior to deposition of the Panglo member. The Panglo is present as a synclinal remnant preserved in the footwall of the Bardoc Tectonic Zone, which identifies that fault as a domain boundary fault of similar significance to the Zuleika Shear Zone. The Bardoc Tectonic Zone also has early controls on sequence and stratigraphic thickness changes between adjacent domains. Correlation of the Panglo member with Kurrawang Formation is based on contact relationships and descriptive characteristics, but requires further support from detrital zircon geochronology. The Kurrawang Formation is a key stratigraphic time marker in the Kalgoorlie Terrane and is a dominantly alluvial/fluvial to marine sequence of quartz-rich sandstones (Navajo), polymictic

coarse basal conglomerates, thick cross-bedded quartz sandstones, and upper sections of interbedded siltstone. The unit is unconformable on all older granite, greenstone and sedimentary rocks, which were folded prior to the deposition of the Kurrawang. A new SHRIMP U-Pb analysis of detrital zircons with a youngest population at 2657±7 Ma indicates probable deposition after ~2650 Ma.

9.4 Deformation History

1. The Kalgoorlie Terrane records a deformation history with seven stages that can be grouped into five major events, which record a change from bulk extension to bulk contraction - the latter includes syn-orogenic clastic sedimentation. At least three of the seven stages are interpreted as basin development phases:
    a) DE: accounts for deposition of major stratigraphic sequences including the mafic and ultramafic volcanics; Talbot formation, White Flag Formation and lower Black Flag formation. The oldest rocks in the Kalgoorlie Terrane include the Penneshaw Formation at Norseman (~2935 Ma), which may have been a local basement that was extended to allow the deposition of those sequences.
    b) D1a: a first folding event occurred between deposition of the lower and upper Black Flag formations, since the upper Black Flag formation rocks sit unconformably on early isoclinal folds at Kanowna. Major map scale F1 folds are located only at Kanowna and the Golden Mile, Kalgoorlie (also sites of major gold deposits).This restricted distribution reflects either irregular preservation of a contractional deformation that produced F1 folds in the earliest stages of the regional ENE-WSW contraction, or possibly localised controls on early deformation.
    c) D1b: a syn-orogenic extension that accommodated deposition of the upper Black Flag formation, locally in linear fault-controlled half grabens (Gidji) with abundant coarse clastic rocks at the base of upwards and laterally fining sequences. Other units at Kanowna and Binduli, have less-certain controls on the geometry of the basin structure.
    d) D2: the second folding event was a regional contractional deformation that marks the cessation of extrusive volcanism. Fault-bend folding typical of thin-skinned stacking characterises F2 in sedimentary sequences, whereas broad, open and upright, to slightly inclined fold axial planes are typical at a regional scale. Broad-scale granite-cored antiforms and domes have intrusive contacts sub-parallel to bedding in the

greenstones suggesting a granitoid doming influence on the D2 deformation.

e) D3a: syn-contractional deposition, resulting in long, linear fault-controlled, late-clastic sedimentary sequences at <2650 Ma, unconformably overlying F2 folded rocks (Kurrawang, Panglo). The deposition of these sequences occurred over a relatively short time period (about 2650 – 2639 Ma).

f) D3b: major deformation resulting in burial, metamorphism, folding and foliation of all sequences. Regionally pervasive S3 foliations trend uniformly over the district and form axial planar foliations to F3 folds with inclined axial planes in the late clastic sequences, which are generally preserved in the footwalls of major domain boundary faults. S3 transects earlier F1 and F2 fold axial planes. The maximum age of the regional foliation is timed by the <2650 Ma rocks that are folded and foliated by it; the minimum age is placed at around 2639±3 Ma by lode-Au veins that were broadly synchronous with, and overprinting, the regional foliation.

g) D4: late brittle-ductile faults that cut all earlier units and fabrics, timed as occurring after 2636Ma

2. The deformation history of the north Kalgoorlie district indicates a complex interplay of tectonism and sedimentation, rather than a simple sequence of deformation phases that entirely post-dated the formation of a greenstone belt. Similar tectono-stratigraphic controls are typical in modern contractional tectonic environments, particularly where rapid uplift is associated with active volcanism and sedimentation.

References

Abbott, L.D., Silver, E.A., Thompson, P. R., Filewicz, M.V., Schneider, C., and Abdoerrias, 1994. Stratigraphic constraints on the development and timing of arc-continent collision in northern Papua New Guinea, Journal of Sedimentary Research, Vol. B64, No.2, p. 169-183.

Abers, G.A., and Mcaffrey, R., 1994. Active arc-continent collision: Earthquakes, gravity anomalies, and fault kinematics in the Huon-Finisterre collision zone, Papua New Guinea, Tectonics, Vol. 13, No. 2, p. 227-245.

Ahmat, A.L., 1995a. Kanowna, Geological Survey of Western Australia. 1:100 000. series Explanatory Notes, 28p.

Ahmat, A.L., 1995b. Gindalbie, Geological Survey of Western Australia. 1:I00 000 series Geological. Map.

Angerer, T., Kerrich, R., Hagemann, S.G., 2013. Geochemistry of a komatiitic, boninitic, and tholeiitic basalt association in the Mesoarchean Koolyanobbing greenstone belt, Southern Cross Domain, Yilgarn craton: Implications for mantle sources and geodynamic setting of banded iron formation, Precambrian Research 224 p. 110–128.

Archibald, N.J., Bettenay, L.F., Binns, R.A., Groves, D.I., and Gunthorpe, R.J., 1978, The evolution of Archaean greenstone terrains, Eastern Goldfields Province, Western Australia, Precambrian Research, v. 6, p. 103-131.

Archibald, N.J., 1979. Tectonic-metamorphic evolution of an Archaean terrain: A study of the Norseman-Widgiemooltha granitoid-greenstone belt, Eastern Goldfields Province, Western Australia, Unpublished PhD thesis, University of Western Australia, 440p.

Archibald, N.J., Bettenay, L.F., 1977. Indirect evidence for tectonic reactivation of a pre-greenstone sialic basement in Western Australia, Earth Planet. Sci. Lett. 33, 370-378.

Archibald, N.J., Bettenay, L.F., Bickle, M.J., and Groves, D.I., 1981, Evolution of Archaean crust in the Eastern Goldfields Province of the Yilgarn Block, Western Australia, in Archaean Geology edited by J.E.Glover and D.I Groves: International Archaean Symposium, 2nd, Perth, W.A., 1980, Proceedings: Geological Society of Australia, Special Publication no. 7, p. 491-504.

Archibald, N.J., 1987. Geology of the Norseman-Kambalda area, in Second Edition Eastern Goldfields geological field conference, abstracts and excursion guide, (Eastern Goldfields Discussion Group, Kalgoorlie and Geological Society of Australia, Western Australian Division, Perth, p. 13-14).

Archibald, N.J., 1993. Stratigraphy structure and mineralisation, Kanowna Area, A summary report detailing mapping methodology, results and potential gold targets, unpublished consulting report to Delta Gold.

Archibald, N.J., 1998. 3D geology and tectonic synthesis of the Kalgoorlie Terrane, in Geodynamics and Gold Exploration in the Yilgarn, Australian Geodynamics Cooperative Research Centre workshop abstracts, p. 17-22.

Arnold, G.O., 1997. Report on high grade exhalite-hosted gold mineralization at Binduli, G.O.Arnold Ore Search Consulting. Unpublished consulting report to Croesus Mining NL. 27p.

Bader, K., 1994, Geology of the Merougil Formation, Unpublished Honours Thesis, Monash University.

Barley, M.E., 1982. Porphyry-style mineralisation associated with early Archean calcalkaline igneous activity, Eastern Pilbara, Western Australia. Economic Geology, 77, p. 1230-1236.

Barley, M.E., Brown, S.J.A, Krapez, B., and Cas, R.A.F., 2002. Tectonostratigraphic analysis of the Eastern Yilgarn Craton: an improved geological framework for exploration in Archaean Terranes. AMIRA Project P437a, Final Report.

Barley, M.E., Eisenlohr, B.N., Groves, D.I., Perring, C.S., and Vearncombe, J.R, 1989, Late Archaean convergent margin tectonics and gold mineralisation: a new look at the Norseman-Wiluna Belt: Geology, v. 17, p. 826-829

Barley, M.E., Brown, S.J.A., Krapez, B., and Kositcin, N., 2008. Physical volcanology and geochemistry of a Late Archaean volcanic arc: Kurnalpi and Gindalbie Terranes, Eastern Goldfields Superterrane, Western Australia, Precambrian Research 161 p. 53–76.

Barnes, S. J., Van Kranendonk, M.J., and Sonntag D.I., 2012. Geochemistry and tectonic setting of basalts from theEastern Goldfields Superterrane, Australian Journal of Earth Sciences 59, p. 707–735.

Bateman, R., and Bierlein, F.P. , 2007. On Kalgoorlie (Australia), Timmins–Porcupine (Canada), and factors in intense gold mineralisation, Ore Geology Reviews, Vol. 32, p. 187–206.

Bateman, R. J., Hagemann, S. G., McCuaig, T. C., and Swager, C. P. , 2001a. Protracted gold mineralization throughout Archaean orogenesis in the Kalgoorlie camp, Yilgarn Craton, Western Australia: structural, mineralogical, and geochemical evolution. In World-class gold camps and deposits in the Eastern Yilgarn Craton, Western Australia, with special emphasis on the Eastern Goldfields Province (edited by S. G. Hagemann, P. Neumayr, and W. K. Witt), Geological Survey of Western Australia, Record 2001/17, p. 63-98.

Bateman, R., Costa, S., Swe, T., Lambert, D., 2001b. Archaean mafic magmatism in the Kalgoorlie area of the Yilgarn Craton, Western Australia: a geochemical and Nd isotopic study of the petrogenetic and tectonic evolution of a greenstone belt, Precambrian Research 108, p. 75–112.

Bateman, R., and Hagemann, S.G., 2004. Gold mineralisation throughout about 45 Ma of Archaean orogenesis: protracted flux of gold in the Golden Mile, Yilgarn craton, Western Australia, Mineralium Deposita, 39, p. 536-559.

Beavan, J., Tregoning, P. , Bevis, M., Kato, T., and Meertens, C., 2002. Motion and rigidity of the Pacific Plate and implications for plate boundary deformation, Journal of Geophysical Research, Vol.107, no. B10, 2261, p. 19-1 – 19-15.

Beckett, T.S., Fahey, G.J., Sage, P. W., Wilson, G.M., 1998. Kanowna Belle gold deposit: *in* Geology of Australian and Papua New Guinean Mineral Deposits, (edited by D.A. Berkman, and D.H. Mackenzie), The Australian Institute of Mining and Metallurgy, Melbourne: Monograph 22 p. 201-206.

Bedard, J.H., Brouillette, P. , Madore, L., Berclaz, A., 2003. Archaean cratonization and deformation in the northern Superior Province, Canada: an evaluation of plate tectonic versus vertical tectonic models, Precambrian Research, 127, p. 61–87.

Bedard, J.H., 2010. Falsification of the plate tectonic hypothesis for genesis of Archaean volcanic and plutonic rocks, and an outline of possible alternative mechanisms, in Fifth International Archaean Symposium Abstracts (edited by I.M.Tyler and C.M. Knox-Robinson), Geological Survey of Western Australia, Record 2010/18, p. 151-152.

Begg, G. C., Griffin, W.L., O'Reilly, S.Y., and Natapov, L., 2010. The lithosphere, geodynamics and metallogeny of early earth, in Fifth International Archaean Symposium Abstracts (edited by I.M.Tyler and C.M. Knox-Robinson), Geological Survey of Western Australia, Record 2010/18, p. 253-25.

Bell, T.H., 1981. Foliation development – the contribution, geometry and significance of progressive, bulk, inhomogeneous shortening, Tectonophysics, v. 75, p. 273-296.

Belousova, E.A., Griffin, W.L., Begg, G., O'Reilly, S.Y., 2010. The Terranechron® approach to crustal evolution studies and implications for continental growth, in Fifth International Archaean Symposium Abstracts (edited by I.M.Tyler and C.M. Knox-Robinson), Geological Survey of Western Australia, Record 2010/18, p. 44-46.

Bickle, M.J., Nisbet, E.G., and Martin, A., 1994. Archean Greenstone Belts Are Not Oceanic Crust, Journal of Geology, Vol. 102, p. 121-138.

Black, L.P. , Champion, D.C., and Cassidy, K.F., 2002. Compilation of SHRIMP U-Pb geochronology data, Yilgarn Craton, Western Australia, 1996-2000: Geoscience Australia Record.

Black, L.P. , Kamo, S.L., Allen, C.M., Aleinikoff, J.N., Davis, D.W., Korsch, R.J., 2003. TEMORA 1: a new zircon standard for Phanerozoic U–Pb geochronology, Chemical Geology 200, p. 155–170.

Bleeker, W., and van Breemen, O., 2010. The fundamental architecture of the south-central Abitibi Greenstone Belt, Superior Craton, Canada, and the localization of world-class Au

deposits, in Fifth International Archaean Symposium Abstracts: Geological Survey of Western Australia, Record 2010/18, p. 153-154.

Bleeker, W. 2012. Targeted Geoscience Initiave 4. Lode gold deposits in ancients deformed and metamorphosed terranes: The role of extension in the formation of Timiskaming Basins and large gold deposits, Abitibi Greenstone Belt - A Discussion; in Summary of Field Work and Other Activities 2012, Ontario Geological Survey, Open File Report 6280, p. 47-1 to 47-12.

Blenkinsop, T.G, Martin, A., Jelsma, H.A., and Vinyu, M.L., 1997. The Zimbabwe Craton, in Greenstone Belts, (edited by M. deWit and L.D. Ashwal), Oxford Monographs on Geology and Geophysics, 35, p. 567-580.

Blenkinsop, T.G., 2004. Pure and Simple: A Practical Guide to Predicting Ore Body Geometry in Shear Zones, in Mining and Resource Geology Symposium, Economic Geology Research Unit, James Cook University, Contribution No 62.

Blewett, R.S., 2005, An assessment of the utility of the new 3D data versus the 2D data at a regional scale: geodynamic insights. In 3D Geological Models of the Eastern Yilgarn Craton, pmd*CRC Project Y2, Final Report, p 139-161.

Blewett, R.S., Czarnota, K., Henson, P. A., 2010a. Structural-event framework for the eastern Yilgarn Craton, Western Australia, and its implications for orogenic gold, Precambrian Research, 183 p. 203–229.

Blewett, R.S., Henson, P. A., Roy, I.G., Champion, D.C., and Cassidy, K.F., 2010b. Scale-integrated architecture of a world-class gold mineral system: The Archaean eastern Yilgarn Craton, Western Australia, Precambrian Research, 183, p. 230–250.

Blewett, R.S., Cassidy, K.F., Champion, D.C., Henson, P. A., Goleby, B.R., Jones, L. and Groenewald, P. B., 2004. The Wangkathaa Orogeny: an example of episodic regional ‘D2’ in the late Archaean Eastern Goldfields Province, Western Australia. Precambrian Research 130, 139-159.

Borrodaile, G.J., 1976. "Structural facing" (Shackleton's Rule) and the Palaeozoic rocks of the Malaguide Complex near Velez Rubio, SE Spain. In Proceedings of the Koninklijke Nederlandse Akademie van Wetenschappen, Amsterdam, series B, vol. 79 (5), p. 330-336.

Brewer, T.S., Ahall, K-L., Menuge, J.F., Storey, C.D., and Parrish, R.R., 2004. Mesoproterozoic bimodal volcanism in SW Norway, evidence for recurring pre-Sveconorwegian continental margin tectonism, Precambrian Research, 134, p. 249-273.

Brown, M., 2008. Characteristic thermal regimes of plate tectonics and their metamorphic imprint throughout Earth history: When did Earth first adopt a plate tectonics mode of behaviour? In When Did Plate Tectonics Begin on Planet Earth? (edited by K.C.Condie and V. Pease), Geological Society of America, Special Paper, 440, p. 97-128.

Brown, M.A.N., Jolly, R.J.H., Stone, W., and Coward, M.P. , 1999. Nickel ore troughs in Archaean volcanic rocks, Kambalda, Western Australia: indicators of early extension. In McCaffrey, K.W.J., Lonergan, L., and Wilkinson, J., (eds), Fractures, fluid flow and mineralization. Geological Society Special Publications. 155, p. 197-211.

Brown, S.J.A., Krapez, B., Beresford, S.W., Cassidy, K.F., Champion, D.C., Barley, M.E., Cas, R.A.F, 2001. Archaean Volcanic and Sedimentary Environments of the Eastern Goldfields Province Western Australia, Fourth International Archaean Symposium, A Field Guide, GSWA Record 2001/13, 66p.

Cameron, E.M., and Hattori, K., 1987. Archean gold mineralization and oxidized hydrothermal fluids, Economic Geology, Vol. 82, p. 1177-1191.

Campbell, I.H., and Hill, R.I., 1988. A two-stage model for the formation of the granite-greenstone terrains of the Kalgoorlie-Norseman area, Western Australia, Earth and Planetary Science Letters, 90, p. 11-25.

Card, K.D., 1990. A review of the Superior Province of the Canadian Shield, a product of Archean accretion, Precambrian Research, 48, p. 99-156.

Carey, M.L., 1994. Petrography and Geochemistry of Selected Sills from the Kambalda-Kalgoorlie Region, W.A., Australian National University, upublished B.Sc. Thesis, 110p.

Cas, R.A.F., and Wright, J.V., 1987. Volcanic successions moderns and ancient, a geological approach to products, processes and successions, Chapman and Hall, 528p.

Cassidy, K.F., Champion, D.C., Krapez, B., Barley, M.E., Brown, S.J.A., Blewett, R.S., Groenewald, P. B., and Tyler, I.M., 2006. A revised geological framework for the Yilgarn Craton Western Australia, Geological Survey of Western Australia, Record 2006/8, 8p.

Cassidy, K.F., Champion, D.C., McNaughton, N.J., Fletcher, I.R., Whitaker, A.J., Bastrakova., I.V., and Budd, A.R., 2002. Characterisation and metallogenic significance of Archaean granitoids of the Yilgarn Craton, Western Australia. Minerals and Energy Research Institute of Western Australia (MERIWA), Report No. 222, 514p.

Cawood, P. A., Kroner, A., and Pisarevsky, S., 2006. Precambrian plate tectonics: Criteria and evidence, Geological Society of America, GSA Today: v. 16, no. 7, p. 4-11.

Champion, D.C., and Cassidy, K.F., 2007. An overview of the Yilgarn Craton and its crustal evolution. In Kalgoorlie '07 Conference (edited by F.P. Bierlein and C.M. Knox-Robinson), Proceedings of Geoconferences (WA) Inc., 25-27 September 2007, Kalgoorlie, Western Australia. Geoscience Australia Record 2007/14, p. 8-13.

Chen, S.F., Libby, J.W., Greenfield, J.E., Wyche, S., Riganti, A., 2001. Geometry and kinematics of large arcuate structures formed by impingement of rigid graitoids into greenstone belts during progressive shortening. Geology 29, p. 283–286.

Christensen, U., 1985. Thermal evolution models for the Earth: Journal of Geophysical Research, Vol. 90B, p. 2995-3007.

Chorowicz, J., 2005. The East African rift system, Journal of African Earth Sciences, 43, p. 379–410.

Christie, D., 1975. Scotia nickel sulphide deposit, in Economic Geology of Australia and Papua New Guinea, Volume 1, Metals, edited by C. L. KNIGHT: Australasian Institute of Mining and Metallurgy, Monograph 5, p. 121–124.

Claoue-Long , J.C., Compston, W., and Cowden, A., 1988. The age of the Kambalda greenstones resolved by ion-microprobe: implications for Archaean dating methods, Earth and Planetary Science Letters, 89, p. 239-259.

Clement, S.W.J., and Compston, W., 1994. Ion probe parameters for very high resolution without loss of sensitivity, U.S. Geological Survey Circular, 1107, p. 62.

Cloos, M., Sapiie, B., van Ufford, A.Q., Weiland , R.J., Warren, P. Q., and McMahon, T.P. , 2005. Collisional delamination in New Guinea: the geotectonics of subducting slab breakoff, Geological Society of America, Special Paper 400, 51p.

Clout, J.M.F., 1991. Geochronology of the Kambalda-Kalgoorlie area: a review, Western Mining Corporation (Kambalda Nickel Operations), unpub. technical report no. 187, 13p.

Clout, J.M.F., 1989. Structural and isotopic studies of the Golden Mile gold-telluride deposit, Kalgoorlie, W.A.: Unpublished Ph.D. thesis, Clayton, Australia, Monash University, 352 p.

Clout, J.M.F., Cleghorn, J.H., and Eaton, P. C., 1990. Geology of the Kalgoorlie Goldfield, in Geology and Mineral Deposits of Australia and Papua New Guinea, (edited by F.Hughes), Australian Institute of Mining and Metallurgy: Monograph 14, p. 411-431.

Colvine, A.C., Fyon, J.A., Heather, K.B., Marmont, S., Smith, P. M., And Troop, D.G., 1988, Archaean lode gold deposits in Ontario, Part I a depositional model Part II a genetic model, Ontario Geological Survey, Miscellaneous Paper 139.

Colvine, A.C., Andrews, A.J., Cherry, M.E., Durocher, M.E., Fyon, A.J., Lavigne, Jr., M.J., Macdonald, A.J., Marmont, S., Poulsen, K.H., Springer, J.S. and Troop, D.G., 1984. An integrated model for the origin of Archaean lode gold deposits. Ontario Geological Survey, Open File Report 5524, 100p.

Compston, W., Williams, I.S., Campbell, I.H., Gresham, J.J., 1986. Zircon xenocrysts from the Kambalda volcanics: age constraints and direct evidence for older continental crust below the Kambalda-Norseman greenstones, Earth and Planetary Science Letters, 76, p. 299-311.

Condie, K.C., 1986. Origin and early growth rate of continents, Precambrian Research, 32, p. 261-278.

Condie, K.C., 2000. Episodic continental growth models: Afterthoughts and extensions: Tectonophysics, Vol. 322, p. 153–162.

Condie, K.C., and Benn, K., 2006. Archean geodynamics: Similar to or different from modern geodynamics?, inBenn, K., et al., eds., Archean geodynamics and environments: American Geophysical Union Geophysical Monograph 164, p. 47–59.

Condie, K.C., and Kroner, A., 2008. When did plate tectonics begin? Evidence from the geologic record, in When did plate tectonics begin on planet Earth? (edited by K.C. Condie and V. Pease), Geological Society of America Special Paper 440, p. 281-294.

Condie, K.C., 1997. Plate tectonics and crustal evolution, Butterworth-Heinemann, 282p.

Connors, K.C., Donaldson, J., Morrison, B., and Davy's, C., 2003. The Stratigraphy of the Kambalda-St Ives district: Workshop Notes, unpubilished Gold Fields Australia Technical Note No: TN SIG0329, 94p.

Corbett, G.J., and Leach, T.M., 1998.Southwest Pacific rim gold-copper systems: Structure, alteration and mineralisation: Economic Geology, Society of Economic Geologists Special Publication 6, 238 p.

Cornejo, P. , Tosdal, R.M., Mpodozis, C., Tomlinson, A., Rivera, O., and Fanning, M.C., 1997. El Salvador, Chile, porphyry copper deposit revisited: Geologic and geochronologic framework: International Geology Review, v. 39, p 22–54.

Cowden, A., and Roberts, D.E., 1990. Komatiite hosted nickel sulphide deposits, Kambalda, in Geology and Mineral Deposits of Australia and Papua New Guinea, (edited by F.Hughes), Australian Institute of Mining and Metallurgy: Monograph 14, p. 567-581.

Crossing, J., 2001. Geological Re-Assessment of the Binduli Area – Supplementary Report. Compass Geological Report for Placer Dome Asia Pacific, Unpublished Internal Report.

Crossing, J., 2003. Detailed mapping of the Kalgoorlie area, unpublished technical report prepared for Placer Dome Asia Pacific, 87p.

Czarnota, K. Blewett, R.S., 2007. Don’t hang it on a foliation to unravel a structural event sequence: an example from the Eastern Goldfields Superterrane, in Specialist Group in Tectonics and Structural Geology, Geological Society of Australia Abstracts, Deformation In the Desert, Alice Springs, 9–13 July 2007, 75.

Czarnota, K., Champion, D.C., Goscombe, B., Blewett, R.S., Cassidy, K.F., Henson, P. A., Groenewald, P. B., 210. Geodynamics of the eastern Yilgarn Craton, Precambrian Research, 183 p. 175–202.

Dallmeyer, D.R., Brown, M., Grocott, J., Taylor, G.K., and Treloar, P. J., 1996. Mesozoic Magmatic and Tectonic Events within the Andean Plate Boundary Zone, 26º-27º.30'S, North Chile: Constraints from 40Ar/39Ar Mineral Ages, Journal of Geology, 104, p. 19-40.

Davies, G.F., 1992. On the emergence of plate tectonics, Geology, Vol. 20, p. 963-966.

Davis, B.K., 2002. The Scotia-Kanowna Dome, Kalgoorlie Terrane: Deformational History, Structural Architecture and controls on Mineralisation, In: Applied Structural Geology for Mineral Exploration and Mining: Excursion Guide. Australian Institute of Geoscientists.

Davis, B.K., and Maidens, E., 2003. Archaean orogen-parallel extension: evidence from the northern Eastern Goldfields Province, Yilgarn Craton, Precambrian Research, Vol. 127, p. 229–248.

Davis, B.K., Archibald, N.J., Aaltonen, A., 2000. Kanowna Belle Gold Mine-Anatomy and history of a plumbing system. 15th Australian Geological Convention, Sydney, July 3–7.

Davis, B.K., Blewett, R.S., Squire, R., Champion, D.C., Henson, P. A., 2010. Granite-cored domes and gold mineralisation: Architectural and geodynamic controls around the Archaean Scotia-Kanowna Dome, Kalgoorlie Terrane, Western Australia Precambrian Research, Vol. 183, p. 316–337.

Davis, B.K., 1998. Report on structural geology of the Kanowna Belle deposit. Unpublished Report to Golden Valley Joint Venture, November 1998 (Delta Gold Report no. WA98.066).

de Wit, M.J., 1998. On Archean granites, greenstones, cratons and tectonics: does the evidence demand a verdict? Precambrian Research, 91, p. 181-226.

de Wit, M.J., Armstrong, R.A., Kamo, S.L., and Erlank, A.J., 1992. Gold-Bearing Sediments in The Pietersburg Greenstone Belt: Age Equivalents Of The Witwatersrand Supergroup Sediments, South Africa, Economic Geology, Vol. 88, p. 1242-1252.

deLaeter, J.R., and Martyn, J.E., 1986. Age of molybdenum-copper mineralization at Coppin Gap, Western Australia, Australian Journal of Earth Sciences, Vol. 33, p. 65-71.

DeSitter, L.U., 1956. Structural Geology, McGraw-Hill Series in the Geological Sciences, McGraw-Hill Book Company, 552p.

Dewey, J., and Spall, H., 1975. Pre-Mesozoic plate tectonics: How far can the back in Earth history Wilson Cycle be extended? Penrose Conference Report, Geology, Vol. 3, p. 422-425.

Dewey, J., 1977. Suture Zone Complexities: a review, Tectonophysics, Vol. 40, 53-67.

Doyle, M.G., 1999. Volcano-sedimentary facies analysis in the Binduli area, Western Australia, Centre for Teaching and Research in Strategic Mineral deposits, University of Western Australia, unpublished report prepared for Croesus Mining N.L.

Drummond, B.J., Goleby, B.R., Swager, C.P. , Williams, P. R., 1993. Constraints on Archaean crustal composition and structure provided by deep seismic sounding in the Yilgarn Block. Ore Geol. Rev. 8, 17 124.

Dubé, B., and Gosselin, P. , 2007. Greenstone-hosted quartz-carbonate vein deposits, in Goodfellow, W.D., ed., Mineral Deposits of Canada: A Synthesis of Major Deposit-Types, District Metallogeny, the Evolution of Geological Provinces, and Exploration Methods: Geological Association of Canada, Mineral Deposits Division, Special Publication No. 5, p. 49-73.

Dunphy, J.M., Fletcher, I.R., Cassidy, K.F., and Champion, D.C., 2003. Compilation of SHRIMP U-Pb geochronology data, Yilgarn Craton, Western Australia, 2001–02. Geoscience Australia Record, 2003/15.

Duuring, P. , Cassidy, K.F., and Hagemann, S.G., 2007. Granitoid-associated orogenic, intrusion-related, and porphyry style metal deposits in the Archean Yilgarn Craton, Western Australia, Ore Geology Reviews, 32 p. 157–186.

Eisenlohr, B.N., Groves, D., and Partington, G.A., 1989. Crustal-scale shear zones and their significance to Archaean gold mineralisation in Western Australia, Mineralium Deposita, v. 24, p. 1-8.

Fehlberg, B., and Giles, C. W., 1984, Archaean volcanic exhalative gold mineralization at Spargoville, Western Australia, in Gold ’82 - The Geology, Geochemistry and Genesis of Gold Deposits edited by R. P. FOSTER: Rotterdam, A.A. Bakema Publ.; Geological Society of Zimbabwe, Special Publication, no. 1, p. 285-303.

Feldtmann, F.R., 1936. Contributions to the study of the geology and ore deposits of Kalgoorlie, East Coolgardie Goldfield, Part IV, unpublished GSWA Report, 302p.

Fletcher, I.R., Dunphy, J.M., Cassidy, K.F., and Champion, D.C., 2001. Compilation of SHRIMP U-Pb geochronological data, Yilgarn Craton, Western Australia, 2000-2001. Geoscience Australia Record 2001/47, 111p.

Foley, S., 2008. A trace element perspective on Archean crust formation and on the presence or absence of Archean subduction: in When Did Plate Tectonics Begin on Planet Earth? (edited by K.C.Condie and V. Pease), Geological Society of America, Special Paper, 440, p. 31-50.

Forman, F.G., 1937, A contribution to our knowledge of the Pre-Cambrian in some parts of Western Australia, Royal Society of Western Australia Journal, v. 23, p. 17-27.

Forman, F.G., 1953. The geological structure of the shield in southern Western Australia in relation to mineralization, in Geology of Australian Ore Deposits, edited by A.B. Edwards; Australian Institute of Mining and Metallurgy, v., p. 65-78.

Fowler, M.J., 1999. Centurion Gold Deposit, Binduli, Western Australia: From Geology to exploitation. MSc in Ore Deposit Geology and Evaluation Thesis (unpublished). University of Western Australia, 124p.

Fralick, P. , Hollings, P. , and King, D., 2008. Stratigraphy, geochemistry, and depositional environments of Mesoarchean sedimentary units in western Superior Province: Implications for generation of early crust: in When Did Plate Tectonics Begin on Planet Earth? (edited by K.C.Condie and V. Pease), Geological Society of America, Special Paper, 440, p. 77-96.

Gauthier, L., Hagemann, S.G., Robert, F. and Pickens, G., 2004a. New constraints on the architecture and timing of the giant Golden Mile gold deposit, Kalgoorlie, Western

Australia, in Predictive Mineral Discovery Under Cover, edited by J. Muhling et al., SEG 2004 Extended Abstracts, Centre for Global Metallogeny, The University of Western Australia, v. 33 p. 353-356.

Gauthier, L., Hagemann, S.G., Robert, F. and Pickens, G., 2004b. Structural architecture and relative timing of Fimiston gold mineralization at the Golden Mile deposit, Kalgoorlie, in Gold And Nickel Deposits In The Archaean Norseman-Wiluna Greenstone Belt, Yilgarn Craton, Western Australia — A Field Guide (edited by P. Neumayr, M. Harris and S. W. Beresford), Geological Survey Of Western Australia, Record 2004/16, p. 54-60.

Gee, R.D., Baxter, J.L., Wilde, S.A., and Williams, I.R., 1981. Crustal development in the Archaean Yilgarn Block, Western Australia, Geological Society of Australia, in Archaean Geology edited by J.E.Glover and D.I.Groves: International Archaean Symposium, 2nd, Perth, W.A., 1980, Proceedings: Geological Society of Australia, Special Publication no. 7, p 43-56.

Gebre-Mariam, M., Groves, D.I., Mcnaughton, N.J., Mikucki, E.J., and Vearncombe, J.R., 1993. Archaean Au-Ag mineralisation at Racetrack, near Kalgoorlie, Western Australia: a high crustal-level expression of the Archaean composite lode-gold system, Mineralium Deposita, v. 28, p. 375-387.

Gebre-Mariam, M., Hagemann, S.G., Groves, D.I. 1995. A classification scheme for epigenetic Archaean lode-gold deposits, Mineralium Deposita, 30, p. 408-410.

Gemuts, I., and Theron, A., 1975. The Archaean between Coolgardie and Norseman – stratigraphy and mineralisation, In: Economic Geology of Australia and Papua New Guinea, Volume 1. Metals (Ed.) Knight, C.L. Australia Institute of Mining and Metallurgy, Monograph 5, p. 66-74.

Giles, C.W., 1981. Archaean calc-alkaline volcanism in the Eastern Goldfields Province, Western Australia. In: Glover, J.E., Groves, D.I. (Eds.), Archaean Geology Second International Symposium Perth 1980, Geol. Soc. Aust., Spec. Publ. 7, p. 275-286.

Glikson, A. Y., 1968: The Archaean geosynclinals succession between Coolgardie and Kurrawang, near Kalgoorlie, Western Australia. Ph.D. Thesis, Univ. West Aust. (unpublished).

Glikson, A.Y., 1971a. Archaean geosynclinal sedimentation near Kalgoorlie, Western Australia, in J.E. Glover, ed., Symposium on Archaean Rocks: Geological Society of Australia, Special Publication, v. 3, p. 443-460.

Godfrey, M., 2004. Provenance and tectonic setting of Late Archaean metasedimentary rocks in the Eastern Goldfields of Western Australia, The University of Western Australia, unpublished PhD thesis, 247p.

Goldfarb, R.J., Groves, D.I., and Gardoll, S., 2001. Orogenic gold and geologic time: A global synthesis, Ore Geology Reviews, Vol. 18, p. 1–75.

Goldie, R., Kotila, B., and Seward, D., 1979. The Don Rouyn Mine: An Archean porphyry copper deposit near Noranda, Quebec, Economic Geology, Vol. 74, p. 1680-1683.

Golding, L.Y., 1985. The nature of the Golden Mile Dolerite southeast of Kalgoorlie, Western Australia, Australian Journal of Earth Sciences, v.32, p. 655-63.

Goleby, B. R., Korsch, R. J., Fomin, T., Owen, A. J., and Bell, B., 2000. Preliminary interpretation of results from the 1999 Yilgarn deep seismic survey, Eastern Goldfields, W.A. In: Goleby B. R., Bell B., Korsch R. J., Sorjonen-Ward P. , Groenewald P. B., Wyche S., Bateman R., Fomin T., Witt W., Walshe J., Drummond B. J. & Owen A. J. eds. Crustal Structure and Fluid Flow in the Eastern Goldfields, Western Australia, Australian Geological Survey Organisation Record 2000/34, p. 58–73.

Goleby, B.R., Rattenbury, M.S., Swager, C.P. , Drummond, B.J., Williams, P. R., Sheraton, J.W., and Heinrich, C.A., 1993. Archaean crustal structure from seismic reflection profiling, Eastern Goldfields: results from the Kalgoorlie seismic transect: Australian Geological Survey Organisation, Record 1993/15, 54p.

Goleby, B.R., Blewett, R.S., Korsch, R.J., Champion, D.C., Cassidy, K.F., Jones, L.E.A., Groenewald, P. B., and Henson, P. , 2004. Deep seismic reflection profiling in the Archaean northeastern Yilgarn Craton, Western Australia: implications for crustal architecture and mineral potential, Tectonophysics, 388, p. 119–133.

Goodwin, L.B., and Williams, P. F., 1996, Deformation path partitioning within a transpressive shear zone, Marble Cove, Newfoundland, Journal of Structural Geology, v. 18, no. 8, p. 975-990.

Goscombe, B., Blewett, R.S., Czarnota, K., Groenewald, P. B., and Maas, R., 2009. Metamorphic evolution and integrated terrane analysis of the Eastern Yilgarn Craton: rationale, methods, outcomes and interpretation, Geoscience Australia Record, 2009/23, 269p.

Goscombe, B., Blewett, R.S., Czarnota, K., Foster, D., and Wade, B., 2010. Thermobarometric evolution of east Yilgarn crust: constraints on Neoarchaean tectonics and gold mineralization, in Fifth International Archaean Symposium Abstracts (edited by I.M.Tyler and C.M. Knox-Robinson), Geological Survey of Western Australia, Record 2010/18, p. 184-185.

Gresham, J. J., and Loftus-Hills, G. D., 1981. The geology of the Kambalda nickel field, Western Australia: Economic Geology, Vol. 76, p. 1373-1416.

Griffin, T. J., 1990. Geology of the granite-greenstone terrain of the Lake Lefroy and Cowan 1:100,000 sheets, Western Australia: Western Australia Geological Survey, Report 32.

Grocott, J., Arevalo, C., Welkner, D., and Cruden, A., 2009. Fault-assisted vertical pluton growth: Coastal Cordillera, north Chilean Andes, Journal of the Geological Society, London, Vol. 166, p. 295–301.

Groves, D.I., 1993, The crustal continuum model for late-Archaean lode-gold deposits of the Yilgarn Block, Western Australia, Mineralium Deposita, v. 28, p. 366-374.

Groves, D.I., and Batt, W.D., 1984, Spatial and temporal variations of Archaean metallogenic associations in terms of evolution of granitoid-greenstone terrains with particular emphasis on Western Australia, in Archaean Geochemistry edited by A. Kroner, G.N. Hanson and A.M. Goodwin: Berlin, Springer-Verlag, p. 73-98.

Groves, D.I., and Phillips, G.N., 1987, The genesis and tectonic control on Archaean gold deposits of the Western Australian shield – a metamorphic replacement model, Ore Geology Reviews, v. 2, p. 287-322.

Groves, D.I., and Bierlein, F.P. , 2007. Geodynamic settings of mineral deposit systems, in Bicentennial Review, Jounral of the Geological Society of London, v. 164, p. 19-30.

Groves, D.I., Goldfarb, R.J., Robert, F., and Hart, C.J.R., 2003. Gold deposits in metamorphic belts: Overview of current understanding, outstanding problems, future research, and exploration significance: Economic Geology, v. 98, p. 1–29.

Gunther, M., 2001. Binduli Project annual report for the period 01/07/2000 to 30/06/2001, Placer Dome Asia Pacific Ltd. Unpublished technical report, 62p.

Gustafson, J. K., and Miller, F. S., 1937, Kalgoorlie geology reinterpreted: Australasian Institute of Mining and Metallurgy, Proceedings, Vol. 106, p. 93-125.

Hadlow, H.R., 1990. Structural controls on mineralization in the Kundana South Pit, Coolgardie Goldfield, WA, MSc (Prelim) thesis (unpublished), The University of Western Australia, Perth.

Hall, G., 1998, Autochthonous model for gold metallogenesis and exploration in the Yilgarn, in Geodynamics and Gold Exploration in the Yilgarn, Australian Geodynamics Cooperative Research Centre workshop abstracts, p. 32-35.

Hall, I. E., and Bekker, C., 1965. Gold deposits of Norseman, in Geology of Australian ore deposits (2nd edition) edited by J. McAndrew: Commonwealth Mining and Metallurgical Congress, 8th, Australia and New Zealand, 1965, Publication 1, p. 101–107.

Hallberg, J.A., and Thomson, J.F.H., 1985. Geologic Setting of the Teutonic Bore Massive Sulfide Deposit, Archean Yilgarn Block, Western Australia Economic Geology Vol. 80, p. 1953-1964.

Halley, S.W., 2010. Mapping the footprints of hydrothermal systems, in Fifth International Archaean Symposium Abstracts (edited by I.M.Tyler and C.M. Knox-Robinson), Geological Survey of Western Australia, Record 2010/18, p. 264-265.

Hamilton, W.B., 1998. Archean magmatism and tectonics were not products of plate tectonics. Precambrian Research, Vol. 91, 143–179.

Hamilton, W.B., 2011. Plate tectonics began in Neoproterozoic time, and plumes from deep mantle have never operated, Lithos, Vol. 123, p. 1–20.

Hammond, R.L., and Nisbet, B.W., 1992, Towards a structural and tectonic framework for the central Norseman-Wiluna greenstone belt, Western Australia, in The Archaean: terranes, processes and metallogeny, edited by J.E. Glover and S.E.Ho, Geology Department (Key Centre) and University Extension, University of Western Australia, Publication 22, p. 39-50.

Hand, J.L., 1998. The sedimentological and stratigraphic evolution of the Archaean Black Flag Beds, Kalgoorlie Western Australia: Implications for regional stratigraphy and basin setting of the Kalgoorlie Terrane. Unpub. PhD thesis. Monash University, Australia.

Hanmer, S., and Passchier, C., 1991, Shear-sense indicators: a review, Geological Survey of Canada Paper, 90-17, 72 p.

Hannington, M.D., de Ronde, C.E.J., and Petersen, S., 2005. Sea-floor tectonics and submarine hydrothermal systems, in Hedenquist, J.W., Thompson, J.F.H., Goldfarb, R.J., and Richards, J.P. , eds., Economic Geology 100th Anniversary Volume, Society of Economic Geologists, p. 111-141.

Harrison, N., Bailey, A., Shaw, J.D., Petersen, G.N., and Allen, C.A., 1990, Ora Banda gold deposits, in Geology and mineral deposits of Australia and Papua New Guinea, edited by F.E.Hughes, Australasian Institute of Mining and Metallurgy, Monograph 14, p. 389-394.

Haughton, S.H., 1969. Geological history of southern Africa, Geological Society of South Africa, p. 30-32.

Hedenquist, J.W., Arribas R., A., Jr., and Gonzalez-Urien, E., 2000. Exploration for epithermal gold deposits: Reviews in Economic Geology, v. 13, p. 245–277.

Hewitt, D.F., 1963. The Timiskaming Series of the Kirkland Lake area Canadian Mineralogist, v. 7, pt. 3, p. 497 523,

Hill, R.I., and Campbell, I.H., 1989. A post-metamorphic age for gold mineralization at Lady Bountiful, Yilgarn Block, Western Australia, Australian Journal of Earth Sciences, Vol. 36, p. 313-316.

Hill, R.E.T., Barnes, S.J., Gole, M.J., Dowling, S.E., 1995. The volcanology of komatiites as deduced from field relationships in the Norseman Wiluna Greenstone Belt, Western Australia. Lithos, 34, p. 159-188.

Hill, R.I., Chappell, B.W., and Campbell, I.H., 1992. Late Archaean granites of the southeastern Yilgarn Block, Western Australia, age, geochemistry and origin, Transactions of the Royal Society of Edinburgh: Earth Sciences, Vol. 83, p. 211-226.

Hill, R.I. and Campbell, I.H., 1993. Age of granite emplacement in the Norseman region of Western Australia, Australian Journal of Earth Sciences, Vol. 40, p. 559-574.

Hill, K.C, Kendrick, R.D., Crowhurst, P. V., and Gow, P. A., 2002, Copper–gold mineralisation in New Guinea: tectonics, lineaments, thermochronology and structure, Australian Journal of Earth Sciences, Vol. 49, p. 737-752.

Hillyard, S., Schon, A., and Price, D., 2000. Report summarising the mining of the Centurion cutback by Croesus Mining at its Binduli operation, unpublished technical report, 69p.

Ho, S. E., 1987. Fluid inclusions: their potential as an exploration tool for Archaean gold deposits, in Recent advances in understanding Precambrian gold deposits edited by S. E. Ho and D. I. Groves: University of Western Australia, Department of Geology and Extension Service, Publication no. 11, p. 239-264.

Ho, S.E., Bennett, J.M., Cassidy, K.F., Hronsky, J.M.A., Mikucki, E.I., and Sang, J.H., 1990. Fluid inclusion studies, in Gold deposits of the Archaean Yilgarn Block, Western Australia: nature, genesis and exploration guides edited by S. E. Ho, D. I. Groves, and J. M. Bennett: University of Western Australia, Department of Geology and University Extension Service, Publication no. 20, p. 198-21.

Hobbs, R.W., Drummond, B.J., Goleby, B.R., 2006. The effects of three-dimensional structure on two-dimensional images of crustal seismic sections and on the interpretation of shear zone morphology. Geophysical Journal International Vol. 164, p. 490–500.

Hodgson, C.J., 1989, The structure of shear-related, vein-type gold deposits: a review, Ore Geology Reviews, v. 4 p. 231-273.

Honman, C.S., 1914. The geology of the country between Kalgoorlie and Coolgardie, Western Australia Geological Survey Bulletin, v. 56, 83p.

Honman, C.S., 1916. The geology of the country to the south of Kalgoorlie including mining centres of Golden Ridge and Feysville, Geological Survey of Western Australia Bulletin, v. 66, 75p.

Horwitz, R. C., Kriewaldt, M. J. B., Williams, K. R., and Docpel, J. J. G., 1967. A zone of Archaean conglomerates in the Eastern Goldfields of Western Australia: Western Australia Geological Survey Ann. Rept. 1966, p. 53-56.

Howe, D., 1999. Sedimentology and stratigraphy of the Kurrawang Formation, the Merougil Formation and the Black Flag Group, Kalgoorlie Terrane, Western Australia, unpublished B.Sc. thesis, Curtin University of Technology, 159p.

Howell, D.G., Jones, D.L., and Schermer, E.R. 1985. Tectonostratigraphic terranes of the Circum-Pacific region, in Tectonostratigraphic Terranes of the Circum-Pacific Region (edited by D.G. Howell), Circum-Pacific Council for Energy and Mineral Resources, Earth Science Series No. 1., p. 3-30.

Hunter, W.M., 1993. Geology of the granite-greenstone terrane of the Kalgoorlie and Yilmia 1:100,000 sheets, Western Australia, Geological Survey of Western Australia, Report 35, 80p.

Hutchinson, R., Ridler, R., and Suffel, G., 1971. Metallogenetic relationships in the Abitibi belt, Canada: A model for Archean metallogeny: Canadian Institute of Mining and Metallurgy, Trans., v. 74, p. 106-115.

Hutchinson, R.W., 1981. Metallogenic evolution and Precambrian tectonics, in: Precambrian plate tectonics (edited by A. Kroner). Elsevier, Amsterdam, pp 733-760.

Hutchinson, R.W., 1987. Metallogeny of Precambrian gold deposits: space and time relationships, Economic Geology, Vol. 82, p. 1993-2007.

Hyde, R.S., 1980. Sedimentary facies in the Archean Timiskaming Group and their tectonic implications, Abitibi Greenstone Belt, northeastern Ontario, Canada, Precambrian Research, 12 (1980) 161--195

Hynes, A., 2008. Effects of a warmer mantle on the characteristics of Archean passive margins, in When Did Plate Tectonics Begin on Planet Earth? (edited by K.C.Condie and V. Pease), Geological Society of America, Special Paper, 440, p. 149-156.

Ireland, T.R., and Williams, I.S., 2003. Considerations in zircon geochronology by SIMS, Reviews in Mineralogy and Geochemistry, v. 53, p. 215-241, Hanchar, J.M. and Hoskin, W.O., editors.

Isles, D.J., Harman, P. G. and Cunnenn, J.P. , 1989. The contribution of high resolution aeromagnetics to Archean gold exploration in the Kalgoorlie region, Western Australia, Economic Geology, Monograph 6, p. 389-397.

Ivanic, T.J., Wingate, M.T., Van Kranendonk, M.J., Kirkland, C.L., and S. Wyche, 2010. Age and significance of voluminous mafic–ultramafic magmatic events in the Murchison domain, Yilgarn Craton, in Fifth International Archaean Symposium Abstracts (edited by I.M.Tyler and C.M. Knox-Robinson), Geological Survey of Western Australia, Record 2010/18, p. 75-77.

Ivey, M.E., Fowler, M.J., Gent, P. G., and Barker, A.J., 1998. Centurion gold deposit, Binduli, in Geology of Australian and Papua New Guinean Mineral Deposits, (edited by D.A. Berkman, and D.H. Mackenzie), The Australian Institute of Mining and Metallurgy, Melbourne: Monograph 22 p. 215-218.

Jensen, E.P. , and Barton, M.D., 2000. Gold Deposits Related to Alkaline Magmatism, SEG Reviews, Vol. 13, 2000, p. 279–314.

Johnson, P. R., Abdelsalam, M., Stern, R.J., 2002. The Bir Umq-Nakasib shear zone: geology and structure of a Neoproterozoic suture, Saudi Geological Survey, Technical Report SGS-TR-2002-1, 33p.

Keats, W., 1987. Regional geology of the Kalgoorlie-Boulder mining district. Geological Survey of Western Australia, Report 21, 44p.

Knight, J.T., Ridley, J.R., and Groves, D.I., 2000. The Archaean amphibolite facies Coolgardie goldfield, Yilgarn Craton, Western Australia: nature, controls and gold field-scale patterns of hydrothermal wallrock alteration, Economic Geology, 95, p 49-84.

Kositcin, N., Brown, S.J.A., Barley, M.E. Krapez, B., Cassidy, K.F., Champion, D.C., 2008. SHRIMP U-Pb zircon age constraints on the Late Archaean tectonostratigraphic architecture of the Eastern Goldfields Superterrane, Yilgarn Craton, Western Australia

Krapez, B., 1996. Sequence-stratigraphic concepts applied to the identification of basin-filling rhythms in Precambrian successions. Aust. J. Earth Sci. 43, 355–380.

Krapez, B., 1997. Sequence-stratigraphic concepts applied to the identification of depositional basins and global tectonic cycles. Aust. J. Earth Sci. 44, 1–36.

Krapez, B., Brown, S., Hand, J., 1997. Stratigraphic signatures of depositional basins in Archaean volcanosedimentary successions of the Eastern Goldfields Province. Aust. Geol. Surv. Org. Rec. 1997 (41), 33–38.

Krapez, B., Brown, S.J.A., Hand, J., Barley, M.E., and Cas, R.A.F., 2000. Age constraints on recycled crustal material and supracrustal sources of Archaean metasedimentary sequences, Eastern Goldfields Province, Western Australia: evidence from SHRIMP zircon dating. Tectonophysics, 322, 89-133.

Krapez, B., and Barley, M.E., 2008. Late Archaean synorogenic basins of the Eastern Goldfields Superterrane, Yilgarn Craton, Western Australia, Part III. Signatures of tectonic escape in an arc-continent collision zone. Precambrian Research 161, p. 183-199.

Krapez, B., and Hand, J.L., 2008. Late Archaean deep-marine volcaniclastic sedimentation in an arc-related basin: The Kalgoorlie Sequence of the Eastern Goldfields Superterrane, Yilgarn Craton, Western Australia. Precambrian Research, 161, p. 89-113.

Krapez, B., and Pickard, A.L., 2010. Detrital-zircon age-spectra for Late Archaean synorogenic basins of the Eastern Goldfields Superterrane, Western Australia. Precambrian Research, 178, p. 91-118.

Krapez, B., Barley, M.E., Brown, S.J.A., 2008a. Late Archaean synorogenic basins of the Eastern Goldfields Superterrane, Yilgarn Craton, Western Australia Part I. Kalgoorlie and Gindalbie Terranes. Precambrian Research, 161, p. 135-153.

Krapez, B.,Standing, J.G., Brown, S.J.A., and Barley, M.E., 2008b. Late Archaean synorogenic basins of the Eastern Goldfields Superterrane, Yilgarn Craton, Western Australia Part II. Kurnalpi Terrane, Precambrian Research, 161, p. 154–182

Kroner, A., 1977. Precambrian mobile belts of southern and eastern Africa-ancient sutures or sites of ensialic mobility? A case for crustal evolution towards plate tectonics, Tectonophysics, 40, p. 101-135.

Kroner, A., 1979: Pan-African mobile belts as evidence for a transitional tectonic regime from intraplate orogeny to plate margin orogeny. King Abdulaziz University Jeddah, Saudi Arabia, Institute of Applied Geology Bulletin (3): 21-37.

Kusky, T.M., 1998. Tectonic setting and terrane accretion of the Archean Zimbabwe craton, Geology, Vol. 26; no. 2; p. 163–166.

Kusky, T. M., and Kidd, W.S.F., 1992. Remnants of an Archean oceanic plateau, Belingwe greenstone belt, Zimbabwe, Geology, Vol. 20, p. 43-46.

Kusky, T.M., and Vearncombe, J.R., 1997. Structural Aspects, in Greenstone Belts, (edited by M. deWit and L.D. Ashwal), Oxford Monographs on Geology and Geophysics, 35, p. 91-124.

Langsford, N., 1989. The stratigraphy of Locations 48 and 50, in The 1989 Kalgoorlie Gold Workshops (field volume) edited by I. M. Glacken: Australasian Institute of Mining and Metallurgy, Annual Conference, and Eastern Goldfields Geological Discussion Group, Kalgoorlie, WA, 1989, p. B1–B8.

Lea, J.R., 1998. Kundana gold deposits, in Geology of Australian and Papua New Guinean Mineral Deposits (Eds: D.A. Berkman and D.H. Mackenzie), Australian Institute of Mining and Metallurgy, Monograph 22. pp207-210

Libby, J.W., Barley, M.E., Eisenlohr, B.N., Groves, D.I., Hronsky, J.M.A., and Vearncombe, J.R., 1990, Craton-scale deformation zones, in Gold deposits of the Archaean Yilgarn Block, Western Australia,

Ludwig, K.R., 2001, Squid (1.13b), A user's manual, Berkeley Geochronology Center Special Publication No. 2.

MacLaren, M., and Thomson, J.A., 1913. The geology of the Kalgoorlie goldfield I-V, Mining and Scientific Press, p. 45-48, 95-99, 187-190, 228-232, 374-379.

Martin, H., 1986. Effect of steeper Archean geothermal gradient on geochemistry of subduction-zone magmas, Geology, Vol. 14. p. 753-756.

Martin, H., Smithies, R.H., Rapp, R., Moyen, J.-F., and Champion, D., 2005, An overview of adakite, tonalite-trondhjemite-granodiorite (TTG), and sanukitoid - Relationships and some implications for crustal evolution, Lithos, v. 79, p. 1–24.

Martyn, J.E., 1987. Evidence for structural repetition in the greenstones of the Kalgoorlie district, Western Australia, Precambrian Research, 37, p. 1-18.

Mason, D.R., 2006. Petrographic descriptions for rock samples from drill holes UMD06-202 and 204 at the Kundana north project (Kalgoorlie Region Western Australia), Repost no 3247, consulting report to Barrick Gold Corporation, 40p.

Mason, D.R., 2012. Analysis of Pyrites by LA-ICP-MS, Centurion Gold Deposit, Binduli Area, Western Australia, unpublished consulting report to Barrick Gold, Report No. MG3823, 17p.

Mazdab, F.K., and Wooden, J.L., 2006. Trace element analysis in zircon by ion microprobe (SHRIMP-RG): technique and applications, Geochimica et Cosmochemica Acta Supplement, 70 (18), A405

McCall, G. J. H., 1969. The Archaean succession west of Lake Lefroy: Royal Society of Western Australia, Journal, v. 53, p. 119–128.

McMath, J.C., Gray, N.M, and Ward, H.W., 1953. The geology of the country about Coolgardie, Coolgardie Goldfield W.A., Geological Survey of Western Australia, Bulletin No. 107, 365p.

McNaughton, N.J., Mueller, A.G., and Groves, D.I., 2005. The age of the giant Golden Mile Deposit, Kalgoorlie, Western Australia: ion-microprobe zircon and monazite U-Pb geochronology of a syn-mineralization lampro-phyre dike: Economic Geology, v. 100, p. 1427−1440.

McPhie, J., Doyle, M. and Allen, R., 1993. VolcanicTextures: a guide to the interpretation of textures in volcanic rocks; Centre for Ore Deposit and Exploration Studies, University of Tasmania, Hobart, Tasmania, 196p.

Miall, A.D., 1992. Alluvial Deposits, in Facies Models response to sea level change, (edited by R.G. Walker and N.P. James), Geological Association of Canada, p. 119-142.

Micklethwaite, S., and Cox, S.F., 2004. Fault-segment rupture, aftershock-zone fluid flow, and mineralization, Geology, v. 32, p. 813–816.

Micklethwaite, S., 2007. The significance of linear trends and clusters of fault-related mesothermal lode gold mineralization, Economic Geology, v. 102, p. 1157–1164.

Mikucki, E.J., and Roberts, F.I., 2003. Metamorphic petrography of the Kalgoorlie region, Eastern Goldfields Granite-Greenstone Terrane: METPET database, Western Australia Geological Survey Record, 2003/12.

Miller, J.M., 2006. Linking structure and mineralisation in Laverton, with specific reference to Sunrise Dam and Wallaby, in: Barnicoat, A.C., Korsch, R.J., (Eds.). Predictive Mineral Discovery CRC-Extended Abstracts for the April 2006 Conference. Geoscience Australia Record 2006/7, 62–67.

Molnar, P. , 1992, Brace-Goetz strength profiles, the partitioning of strike-slip and thrust faulting at zones of oblique convergence, and the stress-heat flow paradox of the San Andreas Fault, in Fault Mechanics and Transport Properties of Rocks, edited by B. Evans And T. Wong, Academic Press, p. 434-459.

Moores, E.M., 2002. Pre–1 Ga (pre-Rodinian) ophiolites: Their tectonic and environmental implications, Geological Society of America Bulletin, v. 114, no. 1, p. 80–95

Morey, A.A., Tomkins, A.G., Bierlien, F.P. , Weinberg, R.F., Davidson, G.J., 2008. Bimodal Distribution of Gold in Pyrite and Arsenopyrite: Examples from the Archean Boorara and Bardoc Shear Systems, Yilgarn Craton, Western Australia, Economic Geology, v.103, p. 599-614.

Morris, P. A., 1993. Archaean mafic and ultramafic volcanic rocks, Menzies to Norseman, Western Australia, Western Australia Geological Survey, Report 36, 107p.

Morris, P. A., 1998. Archaean felsic volcanism in parts of the Eastern Goldfields region, Western Australia, Geological Survey of Western Australia, Report 55, 80p.

Morris, P. A., and Witt. W.K., 1997. Geochemistry and tectonic setting of two contrasting Archaean felsic volcanic associations in the Eastern Goldfields, Western Australia, Precambrian Research, v. 83, p. 83-107.

Mueller, A.G., and Harris, L.B., 1987, An application of wrench tectonic models to mineralised structures in the Golden Mile district, Kalgoorlie, Western Australia, in Recent Advances in Understanding Precambrian Gold Deposits, edited by S.E. HO and D.I.GROVES, University of Western Australia Department of Geology and University Extension Service, Publication 11, p. 97-107.

Mueller, A.G., Harris, L.B., and Lungan, A. 1988a, Structural control of greenstone-hosted gold mineralisation by transcurrent shearing: a new interpretation of the Kalgoorlie mining district, Western Australia, Ore Geology Reviews, v. 3, p. 359-387.

Mueller, P. A., and Wooden, J.L., 1988. Evidence for Archean subduction and crustal recycling: Wyoming Province, Geology, Vol. 16, p. 871-874.

Mueller, P. A., Wooden, J.L., Mogk, D.W., Henry, D.J., and Bowes, D.R., 2010. Rapid growth of an Archean continent by arc magmatism, Precambrian Research, Vol. 183, p. 70–88

Mueller, A.G., 2000. Petrography of wall-rock alteration in feldspar porphyry and meta-sediments from the Binduli mining district, Eastern Goldfields Province, Western Australia, unpublished consulting report to Placer Dome Exploration Ltd., 18p.

Myers, J.S., 1993. Precambrian history of the West Australian Craton and adjacent orogens. Annual Reviews in Earth and Planetary Science, Vol. 21, p. 453-485.

Myers, J.S., and Watkins, K.P. , 1985. Origin of granite-greenstone patterns, Yilgarn Block, Western Australia, Geology, Vol. 13, p. 778-780.

Nelson, D.R., 1995. Compilation of SHRIMP U-Pb zircon geochronology data, 1994, Geolological Survey of Western Australia, Record 1995/3, p. 244.

Nelson, D.R., 1997. Evolution of Archaean granite-greenstone terranes of the Eastern Goldfields, Western Australia: SHRIMP U-Pb zircon constraints, Precambrian Research, Vol. 83, p. 57-81.

Nelson, D. R., 2004, Compilation of geochronology data 2003: Western Australia Geological Survey, Record 2004/2.

Nguyen, P. T., 1997. Structural controls on gold mineralisation at the Revenge mine and its tectonic setting in the Lake Lefroy area, Kambalda, Western Australia. Unpublished Ph.D Thesis, University of Western Australia.

Norris, R.J., and Henley, R.W., 1976. Dewatering of a metamorphic pile, Geology Vol. 4, p. 333-336.

Oliver, N.H.S., Rubenach, M.R.J., and Valenta, R.K., 1998, Precambrian metamorphism, fluid-flow and metallogeny of Australia, AGSO Journal of Australian Geology and Geophysics, v. 17, p. 31-53.

Oliver, N.H.S., 1996, Review and classification of structural controls on fluid flow during metamorphism, Journal of Metamorphic Geology, v. 14, p. 477-492.

Oliveira, M.A., Dall'Agnol, R., Scaillet B., Almeida, J.A.C., Althoff, F.J., and Leite1, A.A.S., 2010. Mesoarchean sanukitoid rocks of the Rio Maria Terrane, Brazil, in Fifth International Archaean Symposium Abstracts (edited by I.M.Tyler and C.M. Knox-Robinson), Geological Survey of Western Australia, Record 2010/18, p. 109-111.

Oversby, B., 1994. A proposed extensional transfer structure in the Archaean of the Eastern Goldfields, AGSO Research Newsletter, 21, p 11-12.

Park, R.G., 1981. Origin of horizontal structure in high-grade Archaean terrains, in Archaean Geology edited by J.E.Glover and D.I.Groves: 2nd International Archaean Symposium, Perth, W.A., 1980, Proceedings: Geological Society of Australia, Special Publication no. 7, p. 481-490.

Passchier, C.W., 1994. Structural geology across a proposed Archaean terrane boundary in the eastern Yilgarn Craton, Western Australia, Precambrian Research, 68, p 43-64.

Percival, J.A., 2010. A 4-D, Craton-scale framework for the Superior Province, Canada, in Fifth International Archaean Symposium Abstracts (edited by I.M.Tyler and C.M. Knox-Robinson), Geological Survey of Western Australia, Record 2010/18, p. 145-147.

Percival J.A., Stern R.A. & Skulski T., 2001, Crustal growth through successive arc magmatism: Reconnaissance U-Pb SHRIMP data from the northeastern Superior Province, Canada, Precambrian Research, Vol. 109, p. 203-238.

Percival, J.A., and Card, K.D., 1983. Archean crust as revealed in the Kapuskasing uplift, Superior province, Canada, Geology 1983, Vol. 11, p. 323-326

Perring, C.S., Groves, D.I., Shellabear, J.N., and Hallberg, J.A., 1991. The "porphyry-gold" association in the Norseman-Wiluna Belt of Western Australia: implications for models of Archaean gold metallogeny, Precambrian Research, Vol. 51, p. 85-113.

Phillips, G.N., 1986. Geology and Alteration in the Golden Mile, Kalgoorlie, Economic Geology, Vol. 81, p. 779-808.

Phillips, G.N., and Groves, D.I., 1983. The nature of Archaean gold-bearing fluids as deduced from gold deposits of Western Australia, Journal of the Geological Society of Australia, Vol. 30, p. 25-39.

Phillips, G.N., Groves, D.I., and Brown, I.J., 1987. Source requirements for the Golden Mile, Kalgoorlie: significance to the metamorphic replacement model for Archaean gold deposits, Canadian Journal of Earth Sciences, v. 24, p. 1643-1651.

Phillips, D., and Miller, J.M., 2004. 40Ar/39Ar dating of mica-bearing pyrite from thermally overprinted Archean gold deposits, Geology, v. 34; no. 5; p. 397–400

Phillips, G.N., and Zhou, T., 1999. Gold-only deposits and Archaean granite, SEG Newsletter, Society of Economic Geologists, no. 37, p. 1, 8-13.

Pidgeon R.T., Wilde S.A., Compston W. and Shield M.W., 1990. Archaean evolution of the Wongan Hills Greenstone Belt, Yilgarn Craton, Western Australia, Australian Journal of Earth Sciences, 37, p. 279-292.

Platt, J.P. , 1980. Archaean greenstone belts: a structural test of tectonic hypotheses, Tectonophysics, Vol.65, p. 127-150.

Pollack, H.N., 1997. Thermal characteristics of the Archaean, in Greenstone Belts, (edited by M. deWit and L.D. Ashwal), Oxford Monographs on Geology and Geophysics, 35, p. 223-233.

Poulsen, K.H., 2010. Polymictic conglomerate as a guide to gold in Archean greenstone belts with reference to Hutti and Kolar, Eastern Dharwar Craton, India; in Gold Metallogeny, India and Beyond, edited by M. Deb and R. Goldfarb; Alpha Science International, p. 83-94.

Poulsen, K.H., Card, K.D., and Franklin, J.M., 1992. Archean tectonic and metallogenic evolution of the Superior Province of the Canadian Shield, Precambrian Research, Vol. 58, p. 25-54.

Poulsen, K.H., Robert, F., and Dubé, B., 2000, Geological classification of Canadian gold deposits: Geological Survey of Canada, Bulletin 540, 106p.

Powell, R., Will, T.M., and Phillips, G.N., 1991, Metamorphism of Archaean greenstone belts: Calculated fluid compositions and implications for gold mineralisation, Journal of Metamorphic Geology, v. 9, p. 141-150.

Preston, N.,W., 2008. Links between the stratigraphic and structural architecture and distribution of gold in the northern Kanowna Belle region, Western Australia, unpublished BSc. Thesis, School of Geosciences, Monash University, 187p.

Rasmussen, B., Mueller, A.G., Fletcher, I.R., 2010. Zirconolite and xenotime U–Pb age constraints on the emplacement of the Golden Mile Dolerite sill and gold mineralization at the Mt Charlotte mine, Eastern Goldfields Province, Yilgarn Craton, Western Australia Contributions to Mineralogy and Petrology, Vol. 157, p. 559–572.

Ren, S.K. and Heithersay, P. S., 1998. The Kanowna Belle gold deposit and its implications to Archaean metallogeny of the Yilgarn Craton, Western Australia, Proceedings of the Ninth Quadrennial International Association on the Genesis of Ore Deposits Symposium, p. 303-318.

Richter, F. M., 1985. Models for the Archean thermal regime: Earth and Planetary Science Letters, Vol. 73, p. 350-360.

Robert, F., and Brown, A.C., 1986. Archaean gold-bearing quartz veins at the Sigma mine, Abitibi greenstone belt, Quebec: Part I. geologic relations and formation of the vein system, Economic Geology, v. 81, p 578-592.

Robert, F., Poulsen, K.H., and Dubé, B., 1994, Structural analysis of lode gold deposits in deformed terranes, Geological Survey of Canada, open file 2850, 140p.

Robert F., 2001, Syenite-associated disseminated gold deposits in the Abitibi greenstone belt, Canada, Mineralium Deposita, Vol. 36, p. 503-516.

Robert, F., and Poulsen, K.H., 1997, World-class Archaean gold deposits in Canada: An overview: Australian Journal of Earth Sciences, v. 44, p. 329–351.

Robert, F., and Poulsen, K.H., 2001. Vein Formation and Deformation in Greenstone Gold Deposits, Society of Economic Geologists Reviews, Vol. 14, p. 111–155.

Robert, F., Brommecker, R., Bourne, B.T., Dobak, P. J., McEwan, C.J., Rowe, R.R., and Zhou, X., 2007. Models and Exploration Methods for Major Gold Deposit Types In "Proceedings of Exploration 07: Fifth Decennial International Conference on Mineral Exploration" edited by B. Milkereit, 2007, p. 691-711.

Robert, F., Poulsen, K.H., Cassidy, K.F., and Hodgson, C.J., 2005, Gold metallogeny of the Superior and Yilgarn Cratons, Economic Geology 100th Anniversary Volume, p. 1001–1033.

Ross, A.A., Barley, M.E., Brown, S.J.A., McNaughton, N.J., Ridley, J.R and Fletcher, I.R. 2004. Young porphyries, old zircons: new constraints on the timing of deformation and gold mineralisation in the Eastern Goldfields from SHRIMP U–Pb zircon dating at the Kanowna Belle Gold Mine, Western Australia. Precambrian Res., 128, p. 105–142.

Seedorff, E., Dilles, J.H., Proffett, J.M., Einaudi, M.T., 2005. Porphyry Deposits: characteristics and origin of hypogene features, Economic Geology 100th Anniversary Volume, p. 251–298.

Shackleton, R.M., 1946. Geology of the Migori Gold Belt and adjoining areas, Geological Survey of Kenya, Report No. 10, 77p.

Shirey S.B., Kamber B.S., Whitehouse M.J., Mueller P. A. and Basu A.R., 2008. A review of the isotopic and trace element evidence for mantle and crustal processes in the Hadean and Archean: Implications for the onset of plate tectonic subduction, in When Did Plate Tectonics Begin on Earth? (edited by K. Condie and V. Pease), Geological Society of America, Special Paper 440, 1–29.

Shirey, S.B., and Carlson, R.W., 2010. Isotopic constraints on formation of Hadean-Archean mantle and crust, in Fifth International Archaean Symposium Abstracts (edited by I.M.Tyler and C.M. Knox-Robinson), Geological Survey of Western Australia, Record 2010/18, p. 25-28.

Sibson, R.H., 1987. Earthquake rupturing as a mineralizing agent in hydrothermal systems: Geology, v. 15, p. 701–704.

Sibson, R.H., 1987, Earthquake rupturing as a mineralizing agent in hydrothermal systems, Geology, v. 15, p. 701-704.

Sibson, R.H., Robert, F., and Poulsen, K.H., 1988, High-angle reverse faults, fluid-pressure cycling and mesothermal gold-quartz deposits, Geology, v. 16, p. 551-555.

Sircombe, K.N., Cassidy, K.F., Champion, D.C., Tripp, G.I., Rogers, J., 2007. Compilation of SHRIMP U-Pb geochronological data, Yilgarn Craton, Western Australia, 2004-2006, Geoscience Australia Record (In press)

Smithies, R.H., Champion, D.C., and Cassidy, K.F., 2003. Formation of Earth's early Archaean continental crust, Precambrian Research, Vol. 127, p. 89–101.

Smithies, R.H., Champion, D.C., Sun, S., 2004. The case for Archaean boninites. Contributions to Mineralogy and Petrology, Vol. 147, p. 705–721.

Sofoulis, J., Williams, X. K., and Rowston, D. L., 1968. Investigation of Ministerial Reserve 4538H, Lake Yindarlgooda, Bulong District, W.A.: West. Australia Geol. Survey Record 1968/17, 43p.

Sofoulis, J., Williams, X. K., and Rowston, D. L., 1969. Investigation of Ministerial Reserve 4538H, Lake Yindarlgooda, Bulong District, W.A.: West. Australia Geol. Survey Ann. Rept, 1968, p. 42-46.

Sparks, M.A., Needy, S.K., Roell, J.L., Carter, C.A., Geyer, M., Barth, A.P. , Wooden, J.L., and Mazdab, F., 2008, Geologic history of a gneissic suite from southeastern California: GSA Abstracts with Programs 40, no. 5, 28p.

Squire, R.J., Allen, C.M., Cas, R.A.F, Campbell, I.H., Blewett, R.S., and Nemchin, A., 2010. Two cycles of voluminous pyroclastic volcanism and sedimentation related to episodic granite emplacement during the late Archean: Eastern Yilgarn Craton, Western Australia, Precambrian Research, Vol. 183, p. 251–274.

Squire, R.J., and Cas, R.A.F, 2006. Project M376 – Stratigraphic and structural architecture of late-basin depositional systems in the Eastern Goldfields province, Yilgarn Craton, Final meeting and Field Workshop, 7-8 June, 2006.

Standing, J.G., 2000. The nature of hydrothermal alteration at the Centurion gold deposit, Binduli gold mine WA, unpublished consulting report to Placer Dome Exploration Asia Pacific Ltd 16p.

Standing, J.G., 2004a. Results of geological mapping for the Kanowna Belle West geological review and target generation project, Kalgoorlie district, W.A., unpublished consulting report to Placer Dome Asia Pacific. 18p.

Standing, J.G., 2004b. Results of geological mapping forming part of the Gidji – Abattoir geological review and target generation project, Kalgoorlie district, WA, unpublished consulting report to Placer Dome Asia Pacific. 18p.

Standing, J.G., and Castleden, N., 2002. A new view of Coolgardie: implications for correlations within the Kalgoorlie terrane, in Applied Structural Geology for Mineral Exploration and Mining, International Symposium, (edited by S.Vearncombe, S. Reddy, C.

Swager, F. Tabeart, J. Thomson), Australian Institute of Geoscientists, Bulletin 36, p. 248-251.

Stern, R.J., 2005. Evidence from ophiolites, blueschists, and ultra-high pressure metamorphic terranes that the modern episode of subduction tectonics began in Neoproterozoic time. Geology 33, 557–560.

Stern, R.J., 2008. Modern-style plate tectonics began in Neoproterozoic time: an alternative interpretation of Earth's tectonic history, in When did plate tectonics begin on planet Earth? Geological Society of America Special Paper 440, 265–280.

Stewart, A.J., 1998. Recognition, structural significance, and prospectivity of early F1 folds in the Minerie 1:100,000 sheet area, Eastern Goldfields, Western Australia, Australian Geological Survey Organisation, Res. Newsletter, 29, p4–6.

Stidolph., P. A., 1977. The geology of the country around Shamva, Rhodesia Geological Survey, Bulletin No. 78, 249p.

Stillwell, F.L., 1929. Geology and ore deposits of the Boulder belt, Kalgoorlie, Geological Survey of Western Australia, Bulletin 94, 122p.

Suppe. J. 1983. Geometry and kinematics of fault bend folding. American Journal of Science, 283, 684-721.

Swager, C.P. and Nelson, D.R., 1997. Extensional emplacement of a high-grade granite gneiss complex into low-grade greenstones, Eastern Goldfields, Yilgarn Craton, Western Australia, Precambrian Research, Vol. 83, p. 203-219.

Swager, C.P. 1989. Structure of the Kalgoorlie greenstones – regional deformation history and implications for the structural setting of the Golden Mile gold deposits, Western Australia Geological Survey, Report 25, Professional Papers, p. 59-84.

Swager, C.P. , 1994, Geology of the Dunnsville 1:100,000 sheet, Western Australia Geological Survey, Record no. 1990/2, 35p.

Swager, C.P. , 1995, Geology of the greenstone terranes in the Kurnalpi-Edjudina region, Southeastern Yilgarn Craton: Western Australia Geological Survey, Report 47, 31p.

Swager, C.P. , Griffin, T.J., Witt, W.K., Wyche, S., Ahmat, A.L., Hunter, W.M., and Mcgoldrick, P. J., 1990, Geology of the Archaean Kalgoorlie Terrane – an explanatory note: Western Australia Geological Survey, Report 48, 26p.

Swager, C.P. , 1997. Tectonostratigraphy of late Archaean greenstone terranes in the Southeastern Goldfields, Western Australia, Precambrian Research, 83, 11-42.

Swager, C., and Griffin, T.J., 1990. An early thrust duplex in the Kalgoorlie-Kambalda greenstone belt, Eastern Goldfields Province, Western Australia, Precambrian Research, v. 48, p. 63-73.

Swager, C.P. , Griffin, T.J., Witt, W.K., Wyche, S., Ahmat, A.L., Hunter, W.M., and McGoldrick, P. J., 1990. Geology of the Archaean Kalgoorlie Terrane – an explanatory note: Western Australia Geological Survey, Report 48, 26p

Talbot, H.W.B., 1934. The country north and west from Kalgoorlie, Western Mining Corporation Limited, Technical Report 72 T/1, unpublished, 37p.

Talbot, C., 1973. A plate tectonic model for the Archaean crust, Philosophical Transactions of the Royal Society of London, Vol. 173, p. 413-428.

Tarney, J., Dalziel, I.W.D., and de Wit, M.J., 1976. Marginal basin "Rocas Verdes" complex from Southern Chile: a model for Archaean greenstone belt formation, in The Early History of the Earth (edited by B.F.Windley), Wiley, London, p. 131-146.

Taylor, T., 1984. The Palaeoenvironmental and tectonic setting of Archaean volcanogenic rocks in the Kanowna district, near Kalgoorlie, Western Australia, University of Western Australia unpubl. MSc thesis.

Tingey, R.J., and Grainger, D.J., 1976. Markham Papua New Guinea, 1:250,000 Geological Series Explanatory Notes, Department of National Resources Bureau of Mineral Resources, Geology and Geophysics, Geological Survey of Papua New Guinea, 51p.

Tomich, S. A., 1974, A new look at Kalgoorlie Golden Mile geology: Australasian Inst. Min. Metall., Proc. 251, p. 27-35.

Tomich, S. A., 1976, Further thoughts on the application of the volcanogenic theory to the Golden Mile ores at Kalgoorlie: Australasian Inst. Min. Metall., Proc. 258, 19-29.

Travis, G. A., Woodall, R. and Bartram, G. D., 1971, The geology of the Kalgoorlie Goldfield, in Symposium on Archaean rocks, edited by J. E. Glover: Geological Society of Australia, Special Publication, 3, p. 175-190.

Tripp, G. I., 2000. Structural geology and gold mineralisation of the Ora Banda and Zuleika districts, Eastern Goldfields, Western Australia, Curtin University of Technology, unpublished MSc Thesis, 378p.

Tripp, G.I., and Vearncombe, J., 2000. Gold mineralised Archaean fault-fracture networks, Ora Banda, Western Australia, Geological Society of Australia, 15th Australian Geological Convention, Abstracts.

Tripp, G.I., 2002a. Structural Geology in Mineral Exploration; Enterprise Gold Deposit, Ora Banda, Western Australia, in Applied Structural Geology for Mineral Exploration and Mining, International Symposium, (edited by S.Vearncombe, S. Reddy, C. Swager, F. Tabeart, J. Thomson), Australian Institute of Geoscientists, Bulletin 36, p. 216-219.

Tripp, G.I., 2002b. Nature of the Archaean Zuleika Shear Zone, Kalgoorlie, Western Australia, in Applied Structural Geology for Mineral Exploration and Mining, International Symposium, (edited by S.Vearncombe, S. Reddy, C. Swager, F. Tabeart, J. Thomson), Australian Institute of Geoscientists, Bulletin 36, p. 212-215.

Tripp, G.I., 2002c. Zuleika Shear Zone: Kinematic History, Tectonic Significance and Gold Mineralization, Field Guide in Applied Structural Geology for Mineral Exploration and Mining, International Symposium, Australian Institute of Geoscientists, 45p.

Tripp, G.I., 2004. Rubicon gold mine, Kundana mining centre, in Gold And Nickel Deposits In The Archaean Norseman–Wiluna Greenstone Belt, Yilgarn Craton, Western Australia - A Field Guide (edited by P. Neumayr, M. Harris and S. W. Beresford), Geological Survey Of Western Australia, Record 2004/16, p. 61-73.

Tripp, G.I., and Rogers, J. 2005. North Kalgoorlie region geological traverse, Field Guide, Placer Dome Asia Pacific, unpublished, 57p.

Tripp, G.I. and Vearncombe, J.R. 2004. Fault/fracture density and mineralization: a contouring method for targeting in gold exploration, Journal of Structural Geology, Vol. 26, 1087-1108.

Tripp, G.I., Poulsen, K.H., Pueschel, C., Boyd, D., Dalla-Costa, H., Outhwaite, M. & Millin, S. 2007a. Stratigraphy of coarse clastic rocks in the Kalgoorlie district and applications to gold exploration, unpublished internal report, Barrick Australia-Pacific, 115p.

Tripp, G.I., Cassidy, K.F., Rogers, J., Sircombe, K., and Willson, M., 2007b. Stratigraphy and structural geology of the Kalgoorlie greenstones: key criteria for gold exploration, In Kalgoorlie ’07 Conference (edited by F.P. Bierlein and C.M. Knox-Robinson), Proceedings of Geoconferences (WA) Inc., 25-27 September 2007, Kalgoorlie, Western Australia, Geoscience Australia Record 2007/14, p. 203-208.

Tripp, G.I., Dobe, J.T., and Mason, D.R., 2007c. Geological Assessment of the Gokona - Nyabigena Gold Deposit, North Mara Tanzania, and Targets for Gold Exploration, unpublished report to Barrick Gold, 86p.

Trofimovs, J., 2003. Tectonostratigraphic evolution of the Archaean volcanic-intrusive-sedimentary Boorara Domain succession, Eastern Goldfields, Western Australia. Unpublished, Ph.D. thesis, Monash University, Australia.

Trofimovs, J., Davis, B.K. and Cas, R.A.F., 2004. Contemporaneous ultramafic and felsic intrusive and extrusive magmatism in the Archaean Boorara Domain, Eastern Goldfields Superterrane, Western Australia, and its implications, Precambrian Research, v. 131, p. 283-304.

Trofimovs, J., Davis, B., Cas, R.A.F., Barley, M., and Tripp, G.I. 2006. Reconstructing the event stratigraphy from the complex structural-stratigraphic architecture of an Archaean volcanic-intrusive-sedimentary succession: the Boorara Domain, Eastern Goldfields Superterrane, Western Australia. Aust. J. Earth. Sci. 53, 347-371

Turek, A., and Compston, W., 1971. Rubidium-Strontium geochronology in the Kalgoorlie region, in Symposium on Archaean rocks, edited by J. E. Glover: Geological Society of Australia, Special Publication, 3, p. 72.

Van Kranendonk, M.J., Hickman, A. H., Smithies, R H., Nelson, D. N., and Pike, G., 2002. Geology and tectonic evolution of the Archaean North Pilbara terrain, Pilbara Craton, Western Australia: Economic Geology, v. 97, p. 695-732

Van Kranendonk, M.J., Collins, W.J., Hickman, A., and Pawley, M.J., 2004. Critical tests of vertical vs. horizontal tectonic models for the Archaean East Pilbara Granite–Greenstone Terrane, Pilbara Craton, Western Australia Precambrian Research, Vol. 131, p. 173–211.

Van Kranendonk, M.J., 2007. Tectonics of early Earth, *in* Van Kranendonk, M. j., Smithies, R. H., and Bennett, V., editors, Earth's Oldest Rocks: Amsterdam, Elsevier, Developments in Precambrian Geology, v. 15, p. 1105-1116,

Van Kranendonk, M. J., & Ivanic, T. J. 2009. A new lithostratigraphic scheme for the northeastern Murchison Domain, Yilgarn Craton: Geological Survey of Western Australia, Annual Review 2007–08, 34–53.

Van Kranendonk, M.J., 2010. Two types of Archean continental crust: plume *and* plate tectonics on early earth, American Journal of Science, Vol. 310, p. 1187-1209.

Vanderhor, E, Witt, W.K., 1992. Strain partitioning near the Keith- Kilkenny fault zone in the central Norseman- Wiluna Belt, Western Australia. BMR Record 1992/68, p. 13.

Vearncombe, J.R., 1998, Shear zones, fault networks, and Archaean gold, Geology, v.26, no. 9, p. 855-858.

Vearncombe, J.R., Barley, M.E., Eisenlohr, B.N., Groves, D.I., Houstoun, S.M., Skwarnecki, M.S., Grigson, M.W., and Partington, G.A., 1989, Structural controls on mesothermal gold mineralisation: examples from the Archaean terranes of southern Africa and Western Australia, Economic Geology, Monograph 6, p. 124-134.

Vielreicher, N.M., Baggott, M.S., Groves, D.I., McNaughton, N.J., and Snee, L., 2006. AMIRA P680 Chronology of Deformation, Metamorphism and Gold Mineralisation in the Eastern Goldfields Province, Western Australia: An Improved Framework for Exploration, 457p.

Vielreicher, N.M., Groves, D.I., Snee, L., Fletcher, I.R., and Mcnaughton, N.J., 2010. Broad synchroneity of three gold mineralization styles in the Kalgoorlie Gold Field: SHRIMP, U-Pb, and 40Ar/39Ar geochronological evidence, Economic Geology, v. 105, p. 187–227

Weinberg, R.F., and Van der Borgh, P. , 2008. Extension and gold mineralization in the Archean Kalgoorlie Terrane, Yilgarn Craton. Precambrian Research, 161, P. 77-88.

Weinberg, R.F., van der Borgh, P. , Moresi, L., 2003. Timing of deformation in the Norseman-Wiluna Belt, Yilgarn Craton, Western Australia. Precambrian Research, 120, p. 219- 239.

Weinberg. R.F. , Hodkiewicz. P. , Groves, OJ., 2004. What controls gold distribution in Archean Terranes? Geology 32, p. 545- 548.

Weinberg, R.E, van der Borgh. P. , Bateman, RJ., Groves, D.1., 2005. Kinematic history of the Boulder- Lefroy Shear Zone and controls on associated gold mineralization, Yilgarn Craton, Western Australia. Economic Geology, Vol. 100, p. 1407- 1426.

Western Mining Corporation, 1966. Surface plan of Kalgoorlie showing sample locations for arsenic abundance study, Plan No. 201-651, unpublished.

Whitaker, A.J., 2001. Components and structure of the Yilgarn Craton, as interpreted from aeromagnetic data, in Cassidy, K.F. et al., editors, 4th International Archaean Symposium 2001, Extended Abstracts, Geoscience Australia Record 2001/37, 536-538.

Whitaker, A.J., 2004. The geophysical characteristics of granites and shear zones in the Yilgarn Craton, and their implications for gold mineralisation, in The Ishihara Symposium: Granites and Associated Metallogenesis, Geoscience Australia, p. 129-143.

Williams, P. R., and Currie, K.L., 1993. Character and regional implications of the sheared Archaean granite-greenstone contact near Leonora, Western Australia Precambrian Research, Vol. 62, p. 343-365.

Williams, P. R., and Whitaker, A.J., 1993, Gneiss domes and extensional deformation in the highly mineralised Archaean Eastern Goldfields Province, Western Australia, Ore Geology Reviews, v. 8, p. 141-162.

Williams, I. R., 1969, Structural layering in the Archaean of the Kurnalpi 1:250 000 sheet area, Kalgoorlie region: Western Australia Geological Survey, Annual Report 1968, p. 40–41.

Williams, I.R., 1970, Explanatory notes on the Kurnalpi 1:250,000 geological sheet, Western Australia, Geological Survey of Western Australia, Record 1970/1 (unpublished).

Williams, 1. R., 1976, Regional interpretation map of the Archaean geology, southeast part of the Yilgarn Block: West. Australia Geol. Survey.

Witt, W.K., 1990, Geology of the Bardoc 1:100,000 sheet, Western Australia Geological Survey, Record 1990/14. 50p.

Witt, W.K., 1991, Regional metamorphic controls on alteration associated with gold mineralisation in the Eastern Goldfields Province, Western Australia: implications for the timing and origin of Archaean lode-gold deposits, Geology v. 19, p. 982-985.

Witt, W.K., 1993. Gold mineralisation in the Menzies-Kambalda region, Eastern Goldfields, Western Australia, Geological Survey of Western Australia, Report 39, 165p.

Witt, W.K., 2001. Tower Hill gold deposit, Western Australia: An atypical, multiply deformed Archaean gold-quartz vein deposit, Australian Journal of Earth Sciences, 48:1, 81-99

Witt, W.K., and Hagemann, S., 2012. Syn-volcanic hydrothermal alteration in Yilgarn Craton greenstones, University of Western Australia, Centre for Exploration Targeting Newsletter, Issue 22, 12p.

Witt, W.K., and Davy, R., 1997. Geology and geochemistry of granitoid rocks in the southwest Eastern Goldfields Province: Western Australia Geological Survey, Report 49, 137p.

Witt, W.K., and Hammond, D.P. , 2008. Archean gold mineralisation in an intrusions-related, geochemically zoned district-scale alteration system in the Carosue Basin, Western Australia. Economic Geology, v. 103, p. 445–454.

Witt, W. K., and Harrison, N., 1989, Volcanic rocks and bounding shear zones of the Ora Banda greenstone sequence, in The 1989 Kalgoorlie Gold Workshops (field volume) edited by I. M. Glacken: Australasian Institute of Mining and Metallurgy, Annual Conference, and Eastern Goldfields Geological Discussion Group, Kalgoorlie, W.A., p. A2–A7.

Witt, W.K., Morris, P. A., Wyche, S., and Neslon, D.R., 1996. The Gindalbie Terrane as a target for VMS-style mineralization in the Eastern Goldfields Province of the Yilgarn Craton, Geological Survey of Western Australia 1995-96 Annual Review, 41-47.

Witt, W.K., Knight, J.T., and Mikucki, E.J., 1997, A synmetamorphic lateral fluid-flow model for gold mineralisation in the Archaean southern Kalgoorlie and Norseman terranes, Western Australia, Economic Geology, v. 92, p. 407-437.

Witt, W.K., and Vanderhor, F., 1998. Diversity within a unified model for Archaean gold mineralization in the Yilgarn Craton of Western Australia: An overview of the late-orogenic, structurally-controlled gold deposits, Ore Geology Reviews, Vol. 13, p. 29–64.

Woodall, R. W., 1965, Structure of the Kalgoorlie goldfield, in Geology of Australian ore deposits, v. I , Commonwealth Mining & Metallurgical Congress, 8th, Australia ad New Zealand, edited by J. McAndrew (2nd edition): Australasian Inst. Min. Metall., p. 71-79.

Woods, B.K., 1997. Petrogenesis and Geochronology of felsic porphyry dykes in the Kalgoorlie Terrane, Kalgoorlie, Western Australia Curtin University of Technology, unpublished B.Sc. thesis, 165p.

Woodhead, J. D., Eggins, S.M., and Johnson, R.W., 1998. Magma Genesis in the New Britain Island Arc: Further Insights into Melting and Mass Transfer Processes, Journal Of Petrology, Vol. 39 No. 9, p. 1641–1668

Wyche, S., and Witt, W.K., 1994. Geology of the Daveyhurst 1:100,000 sheet, Geological Survey of Western Australia, Explanatory notes, 21p.

Wyche, S., Kirkland, C.L., Riganti, A., Pawley, M.J., Belousova, E., and Wingate, M.T.D., 2012. Isotopic constraints on stratigraphy in the central and eastern Yilgarn Craton, Western Australia, Australian Journal of Earth Sciences, Vol. 59, p. 657–670.

Wyman, D.A., O'Neill, C., Ayer, J.A., 2008. Evidence for Modern-Style Subduction to 3.1Ga: APlateau–Adakite–Gold(Diamond)Association, in When Did Plate Tectonics Begin on Planet Earth?)(edited by K.C. Condie and V. Pease),GSA Special Paper 440, p. 129–148.

Yeats, C.J., McNaughton, N.J., Ruettger, D., Bateman, R.J., Groves, D.I., Harris, J.L., and Kohler, E., 1999. Evidence for diachronous Archean lode gold mineralization in the Yilgarn craton, Western Australia: A SHRIMP U-Pb study of intrusive rocks: Economic Geology, v. 94, p. 1259−1276.

Appendices